ISSN 0003-2670

ANALYTICA CHIMICA ACTA

International monthly devoted to all branches of analytical chemistry
Revue mensuelle internationale consacrée à tous les domaines de la chimie analytique
Internationale Monatsschrift für alle Gebiete der analytischen Chemie

ELSEVIER SCIENTIFIC PUBLISHING COMPANY

AMSTERDAM

Anal. Chim. Acta, Vol. 91, 87–435, July 1977

Published monthly

Completing Volume 91

ANALYTICA CHIMICA ACTA

Publication Schedule for 1977

Vol. 88, No. 1	January 1977	
Vol. 88, No. 2	February 1977	(completing Vol. 88)
Vol. 89, No. 1	March 1977	
Vol. 89, No. 2	April 1977	(completing Vol. 89)
Vol. 90	May 1977	(complete in one issue)
Vol. 91, No. 1	June 1977	
Vol. 91, No. 2	July 1977	(completing Vol. 91)
Vol. 92, No. 1	August 1977	
Vol. 92, No. 2	September 1977	(completing Vol. 92)
Vol. 93	October 1977	(complete in one issue)
Vol. 94, No. 1	November 1977	
Vol. 94, No. 2	December 1977	(completing Vol. 94)

Subscription price for 1977 (Vols. 88–95): Dfl. 920.00 plus Dfl. 112.00 postage (approx. U.S.$421.22 inclusive of postage). Claims for issues not received should be made within three months of publication of the issues; if not, they cannot be honoured free of charge. Subscribers in the U.S.A. and Canada receive their copies by airmail. Additional charges for airmail to other countries are available on request. For advertising rates apply to the publishers.

Subscriptions should be sent to:
Elsevier Scientific Publishing Company, P.O. Box 211, Amsterdam, The Netherlands.

GENERAL INFORMATION

Languages

Papers will be published in English, French or German.

Detailed information

Authors should consult Vol. 73, p. 435 for detailed instructions. Reprints of this information are obtainable from Dr. Macdonald or from: Elsevier Editorial Services Ltd., Mayfield House, 256 Banbury Road, Oxford (Great Britain).

Submission of papers

Papers should be sent to:

Prof. Philip W. West,
Chemistry Department,
College of Chemistry and Physics,
Louisiana State University,
Baton Rouge,
La. 70803 (U.S.A.)

or to:

Dr. A. M. G. Macdonald,
Department of Chemistry,
The University,
P.O. Box 363
Birmingham B15 2TT (Great Britain)

Reprints

Fifty reprints will be supplied free of charge. Additional reprints (minimum 100) can be ordered at quoted prices. They must be ordered on order forms which are sent together with the proofs.

CHROMATOGRAPHY '77

INTERNATIONAL SYMPOSIUM ON ADVANCES IN CHROMATOGRAPHY

The 12th International Symposium on Advances in Chromatography will be held in November 7-10, 1977 at the International Congress Centre RAI in Amsterdam, The Netherlands.

The scope of the meeting will cover papers and informal discussion groups by outstanding researchers from throughout the world in all fields of chromatography. In particular, new developments in gas, liquid and high performance thin-layer chromatography will be included.

A total of 84 papers will be presented at the Symposium representing contributions from 20 countries. A special feature of the meeting will be an exposition of the latest instrumentation and books.

Registration should be made in advance. The programs, registration forms and hotel reservation cards can be obtained from:

Organisatie Bureau Amsterdam b.v.
International Congress Centre RAI
P.O. Box 7205
Europaplein 14
Amsterdam, The Netherlands

or

Prof. A. Zlatkis
Chemistry Department
University of Houston
Houston, Texas 77004
U.S.A.

541 GVa

HPTLC High Performance Thin-Layer Chromatography

edited by **A. ZLATKIS,** University of Houston Houston, Texas, and **R.E. KAISER,** Institute o Chromatography, Bad Dürkheim

JOURNAL OF CHROMATOGRAPHY LIBRARY Vol. 9

1976. 240 pages. US $43.95/Dfl. 110.00.
ISBN 0-444-41525-4

HPTLC is the advanced technology of TLC an is defined as the combined action of severa variables which include: an optimized coatin material with a separation power superior t the best high performance liquid chromato graphic separation material - a new method o feeding the mobile phase - a novel procedur for layer conditioning - a considerabl improved dosage method and a competen data acquisition and processing system The potential and scope of this new technique is discussed and specific example of biological samples are given. Speed precision, quantitation, sensitivity an automation are described in detail.
The contributors to this book have demon strated that HPTLC, as a new competitiv analytical method, is able to provide solution for complex separation problems.

CONTENTS: Simplified theory of TLC. Th separation number in linear and circular TLC Advantages, limits and disadvantages of th ring development technique. The U-chamber Dosage techniques in HPTLC. HPTLC development, data and results. Consideration on the reproducibility of TLC. Potential an experience in quantitative HPTLC. Applicatio of a new high performance layer in quan titative TLC. Appendix. Subject Index.

ELSEVIER SCIENTIFIC PUBLISHING COMPANY
P.O.Box 211, Amsterdam,
The Netherlands

Distributor in the U.S.A. and Canada:
ELSEVIER NORTH-HOLLAND, INC.,
52 Vanderbilt Ave., New York, N.Y. 10017

The Dutch guilder price is definitive.
US $ prices are subject to exchange rate fluctuations.

2087 E

Analytica Chimica Acta, 91 (1977) 87—96

A NOVEL TITRATION TECHNIQUE FOR THE ANALYSIS OF STREAMED SAMPLES — THE TRIANGLE-PROGRAMMED TITRATION TECHNIQUE

Part I. General Considerations

G. NAGY and ZS. FEHÉR
EGYT Pharmacochemical Works, Budapest (Hungary)
K. TÓTH and E. PUNGOR
Institute for General and Analytical Chemistry, Technical University, Budapest (Hungary)
(Received 17th January 1977)

SUMMARY

The principle of a novel continuous titration technique with triangle-programmed reagent addition is described. The advantages of titration techniques, i.e. high precision, reliability, etc., are combined with the convenience and fast sample handling of mechanized analyzers of the flow-through type. The theoretical titration curves are discussed for detectors with logarithmic and linear signal conversion characteristics. The possibilities of different types of programmed reagent addition are summarized.

The use of instrumental end-point detection offers several advantages in the practical application of different analytical titrations. However, as far as time consumption is concerned, there is generally no improvement unless titration curves are recorded automatically. The first approach to the development of automatic chemical analyzers was the construction of the so-called mechanized titrators. Titrators belonging to this group can be used with different end-point detection techniques and are generally accepted as accurate tools. The various titrators may differ from each other in the manner of their operation (e.g. coulometric or volumetric reagent addition, the method of end-point location) and in the level of their automation, but common to all is a relatively low rate of analysis.

As the continuous improvement of titrators has proceeded, new types of analyzer allowing high speeds of analysis and based on the direct signal transformation principle have appeared. Analyzers of this type employ the flow-through channel principle, the sample preparation, the detection, and the cleaning of the system being done continuously. By constructing an appropriate pattern of the flow system, a large number of samples can be analyzed for one or several components in a short period of time. Therefore, such analyzers have achieved an almost monopolistic position in analytical practice, especially where many similar samples must be analyzed. Since analysis

in commercial flow-through channel analyzers is based on evaluation of a steady-state signal, the accuracy of the results is far less favourable than that of titration procedures. This is obvious, for the steady-state signal can be affected severely by many factors, such as temperature, sample composition (matrix effects), etc.

The above summary indicates that further efforts to improve mechanized analytical systems will result in analyzers containing flow-through analysis channels, yet operating on the basis of titrations. Apparatus of this kind should combine the advantages of both titrators and flow-through mechanized analyzers, i.e. high precision and high speed sample handling.

The aim of this series of papers is to introduce and describe the new concept of carrying out titrations in flowing solutions. The principle of the technique is that discrete samples of small volume can be analyzed in a short time with high precision. Both theory and practice will be described. This work can be related closely to two main fields of instrumental analytical research, i.e. mechanized titrators and flow-through analysis. These areas have been reviewed comprehensively [1, 2], so that a further survey is unnecessary here. Very few attempts have been made to develop analytical methods based on complete titrations in flowing solutions.

The so-called continuous titrators which are capable of analyzing flowing solutions are considered to be outside this group, because they mainly involve balancing a preselected end-point by varying the speed of the sample or reagent addition [3, 4]. Therefore, all the uncertainties of direct sensor signal transformation are generally incorporated in the results obtained. Moreover, it is difficult to imagine how a continuous titrator could be used to analyze rapidly discrete samples of small volume. In connection with continuous titrators, the remarkable pioneering work of Blaedel and Laessig [5] must be mentioned.

Appropriately, the first report of an analytical method based on recording of a complete titration curve obtained in a flow-through system was made at a Technicon Symposium [6]. Later, Fleet and Ho [7] worked out a titration method further developing Eichler's principle, the gradient titration technique. In their method, constant flow rates of both the reagent and sample are mixed; this operational mode is very favourable if the apparatus is to be assembled from modules of the Technicon type. The mixture passes through a homogenizer coil and enters a flow-through potentiometric detector section. The reagent solution of continuously increasing concentration is prepared by a gradient technique. The titration curve recorded is evaluated by plotting time intervals from the beginning of the titration to the end-point against concentration. However, this highly original technique still has several drawbacks which must be overcome before the method can achieve widespread applicability. The inconvenience of gradient preparation, and the uncertainty in determining the starting point of the titration curve, seem to be the most serious. Some preliminary work on these problems, involving argentimetric titrations of chloride-containing samples in flowing solutions, has been reported [8].

In this paper, the entire theory and some important factors governing the practice of the programmed titration technique are discussed. Further papers will show in detail its practical aspects according to the type of titration used.

THEORETICAL CONSIDERATIONS

If a continuous stream of a reagent (titrant) and a sample solution are mixed and homogenized in a certain section of a tube, the degree of titration in the outflow solution depends on the rate of input of the two masses. By changing this rate, the degree of titration can be altered. The degree of titration can be followed by an appropriate sensor placed in a flow-through detector; the reaction must be completed before the mixture of reagent and sample reaches the detector.

For a conventional titration curve, the signal provided by the detector is plotted against the whole amount of titrant added. However, if the points of a titration curve are to be produced in flow-through conditions, then a constant mass flow of sample and a variable mass flow of titrant are essential. With a conventional titrator, the automatic recording of the titration curve is generally done with an X-Y recorder, which provides the possibility of a time-independent reagent addition. However, in some cases, special advantages can be gained by employing a constant rate of addition; a simple signal—time recording gives the titration curve itself. Looking at this problem in the case of flow-through titrations, it is clear that continuous automatic recording of the titration curve can be accomplished only by employing a strict time-dependent reagent addition program and a detector signal—time recording. Since the detector is always in delay to the reagent addition, it would be inconsistent to plot the instantaneous detector signal against the simultaneous addition rate of the titrant. If we assume (a) a constant mass flow (V_s) of a sample of constant concentration (c_s), (b) a linear increase in the reagent addition (from zero) with time ($V_R = tn$, where V_R is the mass flow of the reagent, t is time, n is a constant), and (c) an immediate titration reaction

$$aS + bR \rightarrow dP_1 + gP_2 \qquad (1)$$

then a certain degree of titration will correspond to a given time period (t). This is true at the point where the reagent and sample flows come together, if their mixing at that point is instantaneous and complete.

The reaction mixture flows continuously in the tube behind the point of confluence; thus, after a certain delay, the solution segment with a titration degree corresponding to the t period of reagent addition rate will pass through the system. The delay in detection will depend linearly on the flow-rate in the tube and on the distance between the point of detection and the point of confluence. At a certain point of time, t, the channel behind the mixing point contains a solution of continuously changing

titration degree. If tailing is not significant, i.e. the concentration in an individual segment is constant during its passage through the tube, and if the reagent addition—time program

$$V_R = nt \tag{2}$$

is employed, then at a given instant each infinitesimal cross-section of the solution in the channel can be characterized by a V_R reagent addition rate as well as by the corresponding degree of titration. In other words, each section of the tube belongs, or can be related, to a given point of a titration curve. Accordingly, the titration curve itself can easily be recorded; and from this curve, the V_R value corresponding to the equivalence point and thus the sample concentration (for a known flow rate) can be determined. However, the determination of the reagent addition rate at the equivalence point from the recording is not free from uncertainties. The above-mentioned sources of errors, the delay in detection, the tailing, and the dilution caused by the increasing rate of addition all cause difficulties in the accurate determination of the $t = 0$ point from the recording. Consequently, it is obvious that, for evaluation of V_R, two distinct points are needed, one of which must be the equivalence point itself; the latter point is generally obvious on a titration curve. The accuracy of the determination can be improved greatly if two equivalence points serve as the basis of evaluation. A recording with two equivalence points can be obtained by means of a reagent triangle addition program. The introduction of this novel concept greatly improves the capability and analytical value of the continuous titration technique in flowing sample solutions.

The reagent addition program employing the triangle technique is shown in Fig. 1; the rate of reagent addition increases in the first part of the program according to eqn. (2). After $t = \tau$, the rate of addition decreases at the same rate; in this range the rate of addition changes according to the equation

$$V_R = (2\tau - t)n \tag{3}$$

where 2τ is the duration of the whole program. Considering a constant flow of sample solution of a certain concentration and appropriate n and τ values, the mass flow of the reagent and sample will achieve chemical equivalence twice. Above V_R values corresponding to the equivalence point, the stage of overtitration exists.

For a defined reagent addition program, the time interval between the appearance of the two equivalence points is highly dependent on the mass flow of the sample solution (V_S), which can be expressed by the equation

$$V_S = c_S v \tag{4}$$

where c_S is the concentration and v the flow rate of the sample solution. According to this, if the flow rate is constant, the time interval mentioned is affected by the concentration of the flowing solution, as shown in Fig. 2,

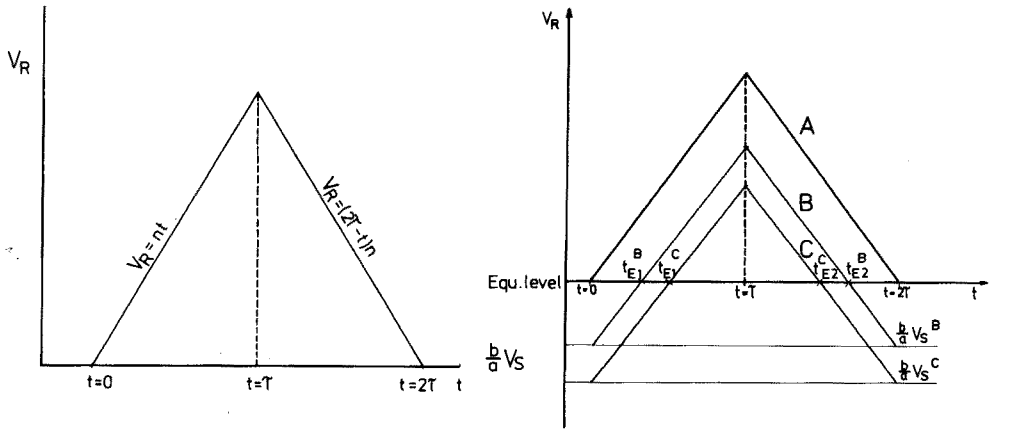

Fig. 1. Triangular reagent addition program for continuous titration in streamed samples.

Fig. 2. The time dependence of the reagent mass flow during a triangle-programmed continuous titration. See text for explanation.

where the reagent mass flow (V_R) is plotted against time (t). The negative values of V_R represent the excess of the sample mass flow with respect to the stoichiometry of the chemical reaction (eqn. 1). In Fig. 2, the difference of the reagent and sample flows is converted to the V_R scale according to the stoichiometry of the chemical reaction, which is represented by a solid continuous line. Three different cases are shown in Fig. 2; line A shows the case when $V_S = 0$, whereas for line B the sample mass flow is smaller than it is in the case of C. It is obvious that $V_R = 0$ corresponds to the chemical equivalence, and that the 2τ time interval of the reagent addition program (case A) is delineated by two equivalence stages. Moreover, it can readily be concluded from Fig. 2 that the higher the sample mass flow, the shorter the section defined by the two equivalence points

($t_{E2}^B - t_{E1}^B$, or $t_{E2}^C - t_{E1}^C$).

This time period can be expressed quantitatively by introducing the following simplifying conditions: (1) the mixing of the sample and the reagent is complete and instantaneous at the point of confluence; (2) the confluence occurs in a section of infinitesimal thickness; (3) the chemical reaction (eqn. 1) is instantaneous and quantitative.

At the equivalence point the reagent mass flow (V_{RE}) equals the constant sample flow, i.e. from eqns. (1) and (4)

$$V_{RE} = \frac{a}{b} V_S = \frac{a}{b} c_s v \tag{5}$$

However, during the total reagent addition program, there are two equivalence points appearing at times t_{E1} and t_{E2}. From eqns. (2) and (3), it follows that

$$V_{RE} = n t_{E1} = \frac{a}{b} c_s v \tag{6}$$

and

$$V_{RE} = n(2\tau - t_{E2}) = \frac{a}{b} c_s v \qquad (7)$$

If Q is defined as $(t_{E2} - t_{E1})$, i.e. the time between the appearance of the two equivalence states, then eqns. (6) and (7) give

$$Q = t_{E2} - t_{E1} = 2\tau - 2\frac{a}{bn} c_s v$$

As can be seen, the Q value is related linearly to the concentration of the sample solution. Accordingly, if the detection of t_{E1} and t_{E2} end-points is possible, then by measuring the Q value and knowing all the other parameters or keeping them constant, the concentration of the flowing solution can easily be determined. It must be mentioned that the slope of the Q vs. c_s function, and therefore the sensitivity of the determination of c_s is strongly dependent on the values of τ, n, v.

On the basis of this principle of triangle-programmed reagent addition, analytical procedures can theoretically be developed for the titrimetric concentration measurement of flowing sample solutions.

PRACTICAL ASPECTS

There are two important practical problems connected with this principle. First, an appropriate reagent addition program must be achieved; secondly, the best continuously operating technique for the detection must be selected.

The programmed reagent mass flow is most easily obtained with a reagent solution. Either the volume or the concentration of the reagent solution can then be changed according to the triangle program. Some commercially available instruments are suitable either for direct use or after only minor alterations. The application of the concentration programmed method looks more favourable but requires more sophisticated instrumentation.

Another convenient method of programmed reagent addition involves electrolytic generation of the reagent, by a current-programmed electrolysis of 100% current efficiency. We propose that if the triangle programmed titration is accomplished with an electrically generated reagent, then the method should be named triangle-programmed coulometric titration. The coulometric reagent addition — similarly to the classical coulometric titration — can be done by electrolysis in the sample flow (internal reagent generation) or separately in a generator cell (external reagent generation).

As far as the continuous detection of different species in flowing solutions is concerned, many well known methods and instruments are available [9, 10]. However, depending on the concentration—signal conversion equation for different detectors, the titration curves recorded will differ in shape. Specific differences may also arise depending on the individual characteristics of the

detector and of the titration reaction employed. Accordingly, a great variety of recordings with different shapes can be expected with the continuous triangle titration technique, analogously to the great variety of titration curves obtained oscillometrically, potentiometrically, amperometrically, biamperometrically, conductometrically, etc.

The applicability and advantages of the continuous titration technique with programmed reagent addition can be explained by selecting two different types of titration curve. In potentiometric titrations, the concentration—signal conversion equation is logarithmic, whereas this equation is linear in amperometric titrations.

Curves obtained for logarithmic concentration—signal conversion

If the detector gives a logarithmic signal, and is equally sensitive to the reagent and sample concentration, the appropriate titration curve (A) is given in Fig. 3. In the case shown, it is assumed that the flow rate of the solution in the flow-through detector is constant. Figure 3 also shows the equivalence level. From the theoretical titration curve, the expected recordings can easily be derived if the data of the reagent addition program and the sample flow are known. The expected recordings have been drawn for four different sample concentrations, a constant reagent addition program being assumed. To explain these curves, it is obvious that during the reagent addition program as V_R increases linearly in time, the detector signal (which is initially equal to the value corresponding to the c_s concentration)

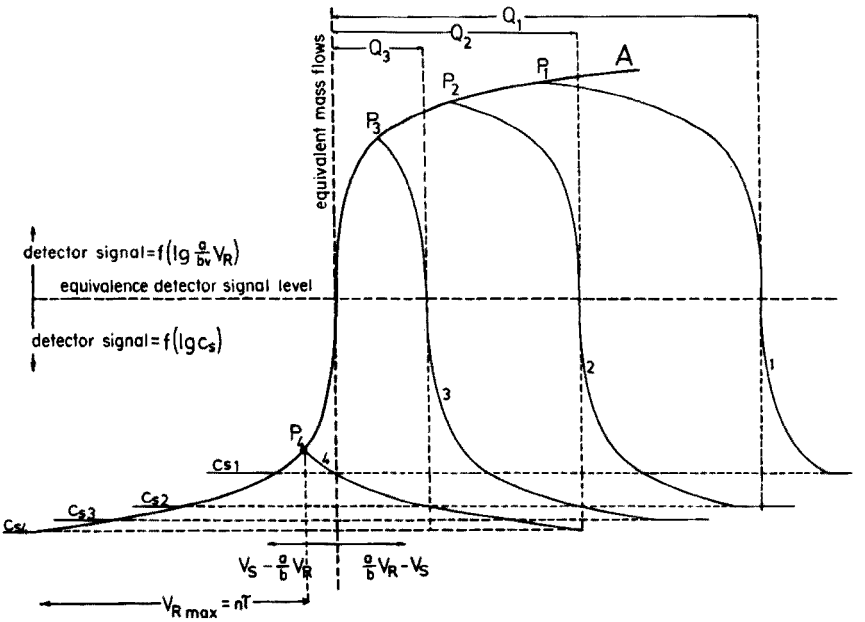

Fig. 3. Theoretical triangle-programmed titration curves on a mass flow scale with a logarithmic detector.

changes continuously following the titration curve. At instant $t = \tau$, however, V_R reaches its maximum and starts to decrease. Consequently, the detector signal also achieves a maximum value ($P_1 \ldots P_4$), so that the V_S vs. V_R a/b recording would come down on the same track from point P if a signal vs. $V_S - V_R$ a/b function were recorded. However, since a signal vs. time curve is recorded, the part of the recording after $t = \tau$, or the appearance of point P, will appear as a mirror image of the first part.

In Fig. 3, the Q values are also indicated. It must be noted that there is no Q value for the highest concentration of sample (c_{s4}). The reason for this is obvious: the reagent mass flow with the program employed is not high enough to achieve equivalence even at the instant $t = \tau$.

The superiority of the triangle titration method over the direct measurement is obvious from Fig. 3. For example, if a logarithmic detector is used, detector drift, which is a serious source of error in direct measurements, is avoided. And, a small signal difference corresponding to a small concentration difference can be converted to a huge change in Q values by applying a suitable program.

To give the theoretically expected recordings in their real form for the detector signal vs. time function, a few curves of this kind are shown in Fig. 4.

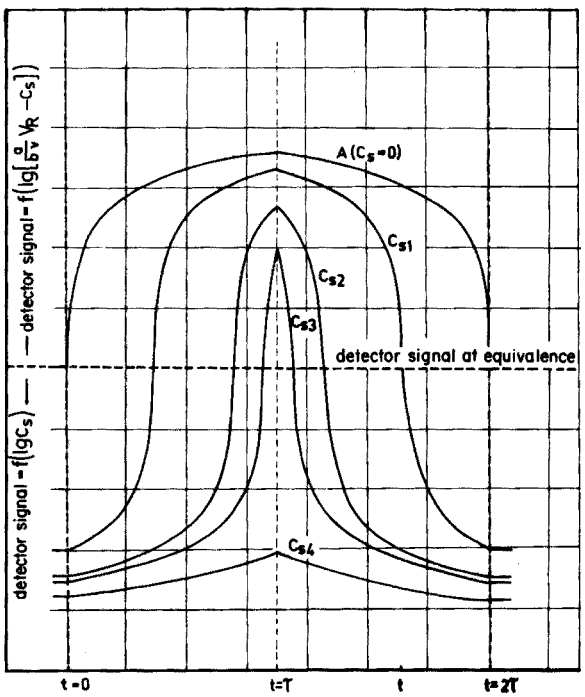

Fig. 4. Theoretical triangle-programmed titration curves on a time scale with a logarithmic detector.

Curves obtained with linear concentration—signal conversion

The theoretically expected recordings will also be discussed for a special case, where a linear signal-converting detector is used in connection with the triangle programmed technique. It is assumed that the excess of the titrant is related linearly to the detector signal, and that neither the product nor the sample affects the detection. Figure 5 shows such a titration curve (A); after the equivalence point the detector signal increases proportionally to the reagent concentration. c_{s1} ... c_{s4} represent the concentrations of four different sample solutions and mark the starting point of the corresponding titration curves. When the same reagent addition program is used, the detector signal achieves its maximum (P_1 ... P_4) at instant $t = \tau$ and then starts to decrease. Since the recording is time-based, after point P the mirror image of the previous recording appears (shown by thin lines in Fig. 5). The ends of each reagent addition program in the mirror image are marked by L_1 ... L_4. The Q values corresponding to the different sample concentrations are also indicated.

In Fig. 6 the theoretically expected curves of this nature are shown on a time-based scale. Curve A in this case is the recording expected in the absence of a sample ($c_s = 0$). The sample concentration for curve c_{s2} is higher than that for curve c_{s1}, hence $Q_2 < Q_1$, because a higher reagent mass flow is needed to overtitrate a solution of higher sample mass flow. Thus if the same triangle reagent addition program is employed, the higher the sample mass flow, then the shorter will be the part of the program falling under the region of overtitration.

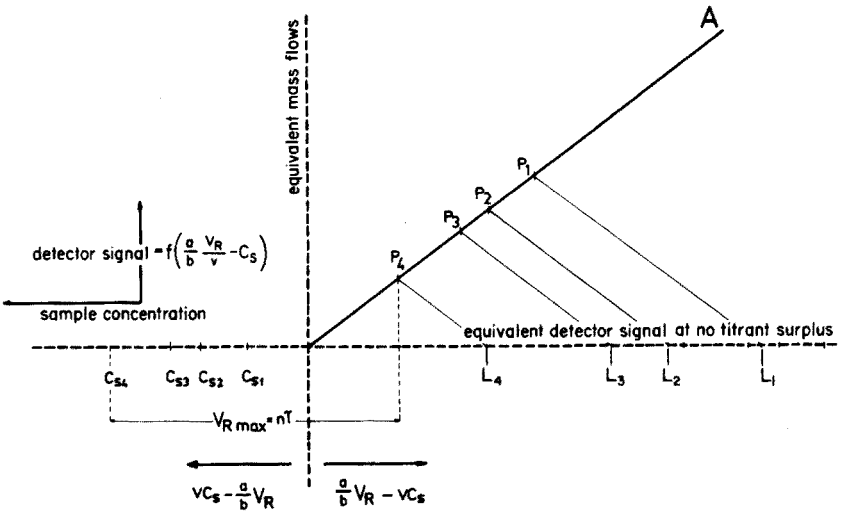

Fig. 5. Theoretical triangle-programmed titration curves on a mass flow scale with a detector of linear characteristics.

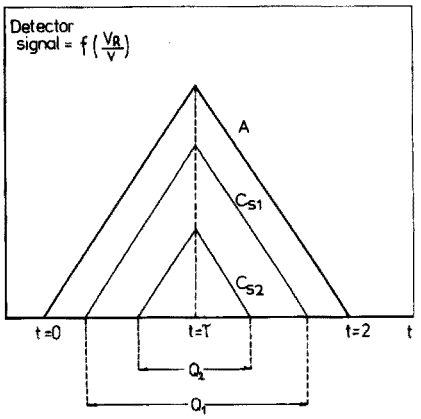

Fig. 6. Theoretical triangle-programmed titration curves on a time scale with a detector of linear characteristics.

CONCLUSIONS

The programmed reagent addition titration technique has obvious advantages over the direct methods in analyzing flowing individual samples. Since the titration method is based on a chemical equivalence, neither a base-line drift nor a change in the slope of the linear signal-converting function of the detector will affect the value Q which serves as the basis for evaluation. These factors are serious sources of error when methods based on direct evaluation of the detector signals are employed.

In this first paper of the series, only the principles of the triangle-programmed reagent addition method have been described in detail, and the expected recordings have been shown and explained for two types of detector. The practice of the technique based on various acid—base, complexiметric, iodimetric and other titration methods, with different potentiometric, amperometric and other detectors for applied analysis, will be reported in later papers.

REFERENCES

1 J. P. Phillips, Automatic Titrators, Academic Press, New York, 1959; J. K. Foreman and P. B. Stockwell, Automatic Chemical Analysis, Ellis Horwood, Chichester, 1975.
2 W. J. Blaedel and R. H. Laessig, Adv. Anal. Chem. Instrum., 5 (1966) 69.
3 K. E. Hallikainen and D. J. Pompeo, Instruments, 25 (1952) 335.
4 M. M. Nicholson, Anal. Chem., 33 (1961) 1328.
5 W. J. Blaedel and R. H. Laessig, Anal. Chem., 36 (1964) 1617; 37, (1965) 332, 1255, 1650.
6 D. L. Eichler, Technicon Symposium, 1969, Vol. 1, Mediad, New York, 1970, p. 51.
7 B. Fleet and A. Y. W. Ho, Anal. Chem., 46 (1974) 9.
8 G. Nagy, K. Tóth and E. Pungor, Anal. Chem., 47 (1975) 1460.
9 Zs. Fehér, G. Nagy, K. Tóth and E. Pungor, Analyst (London), 99 (1974) 699.
10 E. Pungor, Zs. Fehér and G. Nagy, Pure Appl. Chem., 44 (1975) 595.

Analytica Chimica Acta, 91 (1977) 97—106

A NOVEL TITRATION TECHNIQUE FOR THE ANALYSIS OF STREAMED SAMPLES — THE TRIANGLE-PROGRAMMED TITRATION TECHNIQUE

Part II. Argentimetric Titrations

G. NAGY and Zs. FEHÉR

EGYT Pharmacochemical Works, Budapest (Hungary)

K. TÓTH and E. PUNGOR

Institute for General and Analytical Chemistry, Technical University, Budapest (Hungary)

(Received 17th January 1977)

SUMMARY

An apparatus is described for carrying out triangle-programmed titrations with coulometric reagent generation. Different halides and pseudohalides can be determined by titration with silver(I). Both voltammetric and potentiometric detection systems are discussed, but emphasis is placed on potentiometric detection with ion-selective electrodes. The proposed technique can be used for accurate determinations of flowing samples of halides and pseudohalides at low concentrations. The simultaneous determination of two-component mixtures is discussed.

Recently a novel quantitative analytical technique has been developed in this laboratory. The method is based on titrations in continuously flowing solutions, and combines the advantages of titrimetric methods (precision and reliability) with the convenience and rapidity of flow-stream analysis. The method employs a programmed reagent addition, a constant sample flow rate and a flow-through detector for end-point determination. The program on which the addition process is based is an isosceles triangle, with the reagent addition rate varying as a function of time; because of this program, the results can be evaluated on the basis of the time interval between the two easily detected end-points corresponding to the two sections of the reagent addition program.

A survey of the literature on related topics and a detailed theoretical description of the method have been given in Part I [1]. This paper describes the practice of the method, illustrated by applications of argentimetric titrations to particular analytical problems.

Argentimetric titrations have been widely used for the determination of halides, pseudohalides and many organic compounds. For the end-point detection of such titrations, almost all the electroanalytical techniques (potentiometry [2], oscillometry [3], amperometry [4]) can be advantageously

used in preference to visual indicators. Because of their structure, the simple silver halide-based ion-selective membranes show a reversible response to both the silver titrant and the appropriate anion. Accordingly, the interpretation of a recorded argentimetric titration curve is relatively easy if the appropriate precipitate-based ion-selective electrode is used.

As far as reagent addition is concerned in the practice of argentimetric titrations, the coulometric method has distinct advantages and has achieved widespread application [5—7].

EXPERIMENTAL

Apparatus

A schematic design of the apparatus is shown in Fig. 1. The main part is a solution-carrying channel comprising different sections. In manufacturing the apparatus, great care must be taken to avoid mixing in the direction of the flow. The first part of the channel (A) is a flow-through electrolysis cell serving for reagent generation. The cell has two compartments separated by a dialysis membrane. During operation the electrolyte flows in parallel in the two compartments. In the anode compartment silver reagent is generated by polarizing a silver electrode (4-mm diameter silver rod); the cathode is a platinum electrode. This arrangement avoids any mixing of the products of the electrolysis process.

Section C of the flow-through channel is the detector cell containing the appropriate voltammetric or potentiometric electrodes. The anode compartment of the generating cell is connected to the detector section through a drip vessel of very small volume, which holds no more than 0.1 ml of

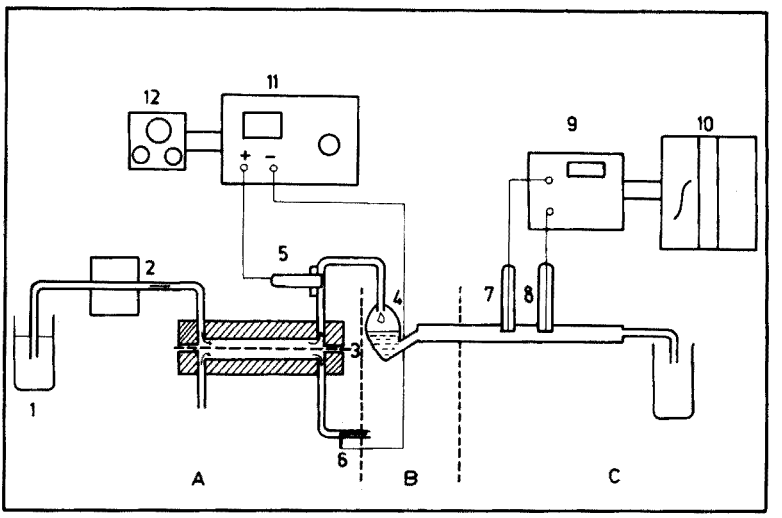

Fig. 1. Experimental set-up for the triangle-programmed titration technique. 1. Solution reservoir. 2. Peristaltic pump. 3. Dialysis membrane. 4. Drip vessel. 5. Generating electrode. 6. Counter electrode. 7. Indicator electrode. 8. Reference electrode. 9. Measuring instrument. 10. Recorder. 11. Current generator. 12 Signal generator.

solution. This drip vessel has two functions: it insulates the electrolysis cell and the detector electrically, and it serves as a mixer to homogenize the reagent and the sample in a direction perpendicular to the flow.

The solution was streamed at a constant volumetric flow rate with a peristaltic pump (LKB Varioperpex 12000). The reagent generating current was provided by a current generator (Tacussel Type ASA 100-1). A function generator (Philips PM 5168) was employed as programmer in the single-shot triangular mode. For potential measurements, a Keithley differential electrometer Type 604 was used with a Bryans recorder Type 2600 A 3. Voltammetric measurements were done with a Radelkis polarograph OH-102, which served to record the current at a constant electrode potential selected in the limiting current range of the component to be determined.

For potentiometric detection, the indicator electrodes were silicone rubber-based chloride, bromide and iodide ion-selective electrodes, specially made in this laboratory, and silver—silver halide electrodes. A saturated calomel reference electrode (OP-810, Radelkis) placed in a separate chamber, was connected by an agar-agar salt bridge.

For voltammetric detection, a silicone rubber-based graphite electrode [8] was used as indicator electrode; the saturated calomel reference electrode (OH-907) was placed in the flow-through detector cell directly behind the indicator electrode.

Chemicals

All the chemicals were of analytical grade.

To all the flowing solutions potassium nitrate and nitric acid were added in amounts sufficient to provide concentrations of 10^{-1} M in KNO_3 and 10^{-2} M in HNO_3. These ensured low resistance in the generating circuit, and then served for ionic strength adjustment or as background electrolyte to provide trouble-free detection.

RESULTS AND DISCUSSION

Coulometric generation of silver(I)

The silver ion is one of the most frequently employed coulometrically generated titrants in analytical practice [9]. However, when the triangle-programmed titration technique is used, the current density for the generation is of great importance, and it cannot be chosen in the most favourable range. Two practical difficulties may arise in this connection. First, to achieve the required degree of overtitration, the intensity of the generating current employed must be high, and consequently a high IR drop can appear. The high cell voltage sometimes required is not provided by any variety of instrument. Secondly, in the case of high generating current densities, the polarization of the silver anode may result in a change of current efficiency during the program. To avoid possible complications from these factors during the titrations, the generation process had to be studied separately in the same system over a relatively wide current range.

For this study, 50 ml of the flowing solution passing through the generating cell were collected. During the time of collection, a constant intensity of the generating current was applied for a precisely determined time period, and great care was taken to collect all the solution containing the silver ion generated. A classical titrimetric method — with a Radiometer automatic titrator, a silver indicator electrode and potassium iodide titrant — was used to determine the amount of silver generated. It was found that the current efficiency up to a current intensity of 100 mA was 100% within ±1%, which was accepted as an experimental error. However, the cell voltage even at the maximal current intensity fell far beyond the range of the Tacussel generator (200 V). Accordingly, it was clear that a wide range of current intensities is available for electrochemical generation of the reagent by the triangle programmed method.

These results were supported by other findings obtained by generating silver and using voltammetric detection. When current—time programs of different slopes and i_{max} were examined over a very wide range, sharp isosceles triangles were obtained on the voltammetric limiting current—time recordings. The voltammetric current intensity was recorded at a constant potential of +0.1 V (vs. SCE).

Titration of chloride and other single species

Sample solutions of different chloride concentrations gave the recordings shown in Fig. 2 when potentiometric end-point detection was used; Fig. 2 also gives the generating current—time curve. It can be seen that the recordings for each sample solution appear as two potentiometric titration curves which are almost mirror images. This is in good agreement with the

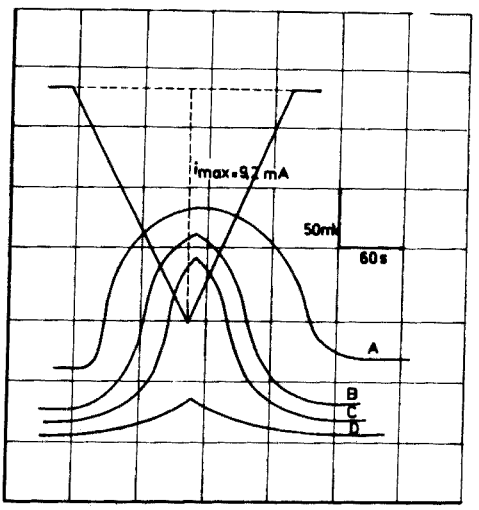

Fig. 2. Programmed coulometric titration curves for chloride. Chloride concentration: (A), $2 \cdot 10^{-4}$ M; (B), $4.5 \cdot 10^{-4}$ M; (C), $6 \cdot 10^{-4}$ M; (D), 10^{-3} M.

theoretical expectations. The equivalence points of the titration on the basis of the titration curves can easily be determined by any classical method. With appropriate electronic devices, it is not difficult to imagine how the equivalence points and the time interval between their appearance can be determined and displayed or printed out automatically by more sophisticated instrumentation. However, the determination of the equivalence points with the same instrumentation can be facilitated by using two identical ion-selective electrodes placed at a certain distance from each other and then recording the potential difference between them. Such differential potentiometric titration curves — together with the current program and the original titration curve — are shown in Fig. 3.

The concentration of the sample solution can be calculated from the equation derived previously [1]:

$$Q = 2\tau - 2\frac{a}{bn} c_s v \qquad (1)$$

(where Q is the time interval between the appearance of the two equivalence points, 2τ the time interval of the triangle current program, a, b are stoichiometric constants, n is a constant, characteristic of the slope of the current program, c_s is the concentration of the sample solution and v is the flow rate). The Q values are measured and the other parameters are known. However, in deriving this equation, some assumptions were made, and for example the tailing effect was completely ignored. Therefore, from the theoretical aspect, it is advisable to calibrate the system for Q values by titrating standard solutions flowing in the same system at the same flow rate with the same reagent generation program. Plotting the Q values against the concentration gives suitable calibration curves, such as that presented in Fig. 4 for chloride-containing solutions. As can be seen, the plot is linear over a reasonable range and extrapolation to $c = 0$ yields the experimentally applied 2τ value (212 s). However, at low concentrations, there are deviations from the theoretical line in the direction of higher Q values. The tailing effect is most probably responsible for this. Since there is apparently a range where eqn. (1) is not completely valid, the use of calibration curves is recommended for the determination of individual species.

Similar calibration curves can be obtained for argentimetric titrations of flowing sample solutions containing bromide, iodide and cyanide when the appropriate ion-selective electrode is used as detector.

Many organic compounds, e.g. those containing —SH groups, ionically bound halides, etc., can be titrated with silver(I). All these compounds may be determined by the triangle programmed technique. This may be illustrated by the calibration curve for papaverine · HCl shown in Fig. 5.

Generally speaking two important observations must be emphasized. First, varying the τ, n and v values produces different $Q - c$ calibration curves. Obviously, the narrower the range to be measured, the more

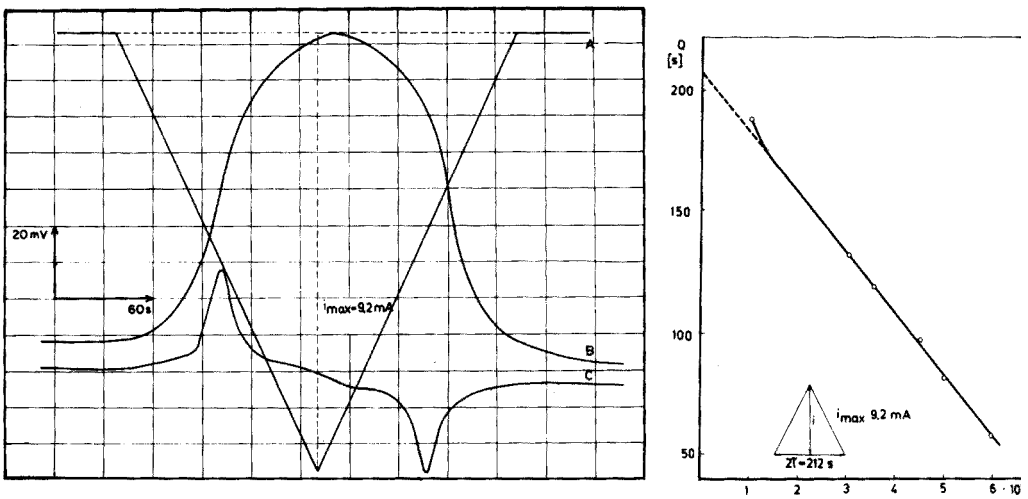

Fig. 3. Differential potentiometric titration curves for chloride ($3.5 \cdot 10^{-4}$ M). (A) Current program. (B) Normal titration curve. (C) Differential titration curve.

Fig. 4. Calibration curve for the determination of chloride samples with the programmed coulometric titration. Flow rate, 5.3 ml min^{-1}; i_{max}, 9.2 mA; 2τ, 212 s.

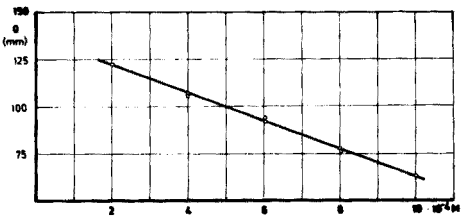

Fig. 5. Calibration curve for the determination of papaverine hydrochloride samples. Flow rate, 5.3 ml min^{-1}; i_{max}, 9.2 mA; 2τ, 212 s.

precise the determination with the calibration curve. With a correct choice of τ, n, v values, calibration curves can be either prepared for rough estimations in wide ranges or precise determinations in narrow concentration ranges. Secondly, it must be emphasized that the triangle-programmed argentimetric titration technique permits the titration of samples at concentrations very much lower than those titratable by the classical potentiometric techniques. This advantage arises from the generally accepted benefits of coulometric titrant addition, and also from the commonly known properties of flow-through potentiometric detection [10].

Simultaneous titration of two species

In the theory and practice of titrations, it is of great importance to know if determinations are possible when two or more species reacting with the titrant are present in the sample. In argentimetric titrations, this problem

has been studied very frequently, especially when an ion-selective electrode is used as detector. However, if an indicator electrode responds to two components in the sample, direct potentiometric determination of the individual components can be very difficult. Therefore, the applicability of the triangle-programmed titration technique was studied for samples containing more than one component reacting with silver ion.

Recordings obtained for samples containing cyanide and chloride, and chloride and iodide can be seen in Figs. 6 and 7, respectively. In these cases, the recording consists of two almost symmetrical parts in two well defined sections, which obviously correspond to the two-step titration process. Accordingly, there are two Q values, on the basis of which the individual concentrations can be determined. However, the relationships between the Q values and the individual concentrations must always be studied. To illustrate this, the simultaneous determination of chloride and iodide will be discussed.

In accordance with the difference of almost six orders of magnitude between the solubility products of silver chloride and silver iodide, the simultaneous potentiometric titration of chloride and iodide is possible over certain ranges and concentration ratios. When the triangle programmed technique is used, the equivalence points observed on the titration curve can be dealt with as follows. At the first inflection point, the mass flow of the reagent is considered to be equal to the mass flow of the iodide content of the sample. (It is assumed that up to this point the chloride does not consume reagent.) Thus, mass balance requires

$$nt_{E_1} - [c_I - (L_{AgI})^{\frac{1}{2}}]\, v = (L_{AgI})^{\frac{1}{2}}\, v \qquad (2)$$

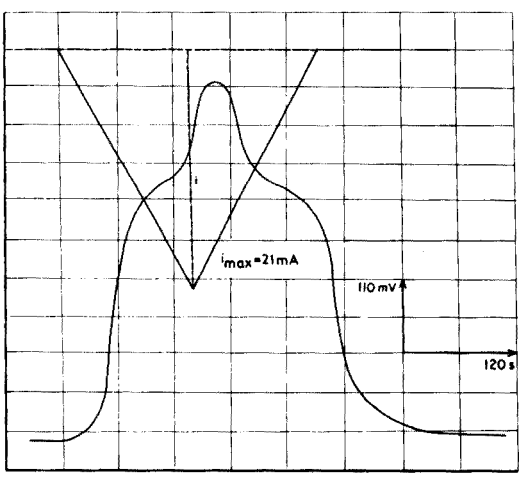

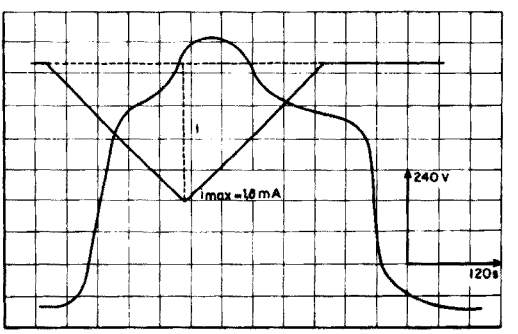

Fig. 6. Programmed coulometric titration curve of a streaming sample containing chloride and cyanide. $c_{Cl^-} = c_{CN^-} = 1.5 \cdot 10^{-3}$ M; i_{max}, 21 mA; 2τ, 272 s.

Fig. 7. Programmed coulometric titration curve of a streaming sample containing chloride and iodide. $c_{Cl^-} = 6 \cdot 10^{-4}$ M; $c_{I^-} = 10^{-4}$ M; i_{max}, 1.8 mA; 2τ, 352 s.

where c_I is the iodide concentration of the solution, and L_{AgI} is the solubility product of the silver iodide precipitate. Thus the first equivalence point appears at time

$$t_{E_1} = c_I \, v/n \tag{3}$$

At the second equivalence point (t_{E_2}), mass balance requires

$$nt_{E_2} - \left[c_{Cl} - (L_{AgCl})^{\frac{1}{2}} + c_I - \frac{L_{AgI}}{(L_{AgCl})^{\frac{1}{2}}}\right] v = (L_{AgCl})^{\frac{1}{2}} v \tag{4}$$

since both halides in the sample consume the reagent. Obviously, it was assumed in the derivation of eqn. (4) that at the second equivalence point, the concentration of free reagent is equal to the square root of the solubility product of silver chloride.

For the mirror image of the two equivalence points, the following equations can be derived

$$n(2\tau - t_{E_1'}) = c_I \, v \tag{5}$$

$$t_{E_1'} = 2\tau - c_I \, v/n \tag{6}$$

and

$$n(2\tau - t_{E_2'}) = v\left[c_{Cl} - (L_{AgCl})^{\frac{1}{2}} + c_I - \frac{L_{AgI}}{(L_{AgCl})^{\frac{1}{2}}} + (L_{AgCl})^{\frac{1}{2}}\right] \tag{7}$$

$$t_{E_2'} = 2\tau - \frac{v}{n}\left[c_{Cl} + c_I - \frac{L_{AgI}}{(L_{AgCl})^{\frac{1}{2}}}\right] \tag{8}$$

The Q values can therefore be expressed by

$$Q_1 = t_{E_1} - t_{E_1'} = 2\tau - 2 \, c_I \, v/n \tag{9}$$

and

$$Q_2 = t_{E_2} - t_{E_2'} = 2\tau - 2\frac{v}{n}\left(c_{Cl} + c_I - \frac{L_{AgI}}{(L_{AgCl})^{\frac{1}{2}}}\right) \tag{10}$$

The equation describing the first Q value (Q_1) is very similar to eqn. 1, which means that the presence of chloride does not affect the value of Q_1. However, the value of Q_2 depends on the concentration of both components. The chloride concentration can be determined separately on the basis of the difference ($Q_1 - Q_2$) since

$$Q_1 - Q_2 = -2\frac{c_{Cl} v}{n} + 2\frac{v}{n}\frac{L_{AgI}}{(L_{AgCl})^{\frac{1}{2}}} \tag{11}$$

The experimental results for the simultaneous determination of chloride–iodide mixtures were in good agreement with the above considerations. To illustrate this, Fig. 8 shows the $Q_1 - c_I$ curve for different chloride concentrations; while in Fig. 9 the experimental ($Q_2 - Q_1$) values are plotted against the chloride concentration. For this experiment, care was taken to use solutions with a constant total concentration of halide ($6 \cdot 10^{-4}$ M).

Table 1 shows the Q_2 values for different iodide and chloride concentrations. The Q_2 values show moderate constancy, which provides some further support for eqn. (10).

Voltammetric end-point detection

As indicated earlier, voltammetric detection was also employed. The graphite indicator electrode was polarized to + 0.1 V vs. SCE, so that the silver(I) concentration was followed on the basis of its reduction to the metal. Accordingly, the titration curves for the halides should have the shape of the amperometric titration curves generally found for an electroactive titrant.

With the new technique, the titration curves for different halide determinations appeared as two curves of the above-described type connected

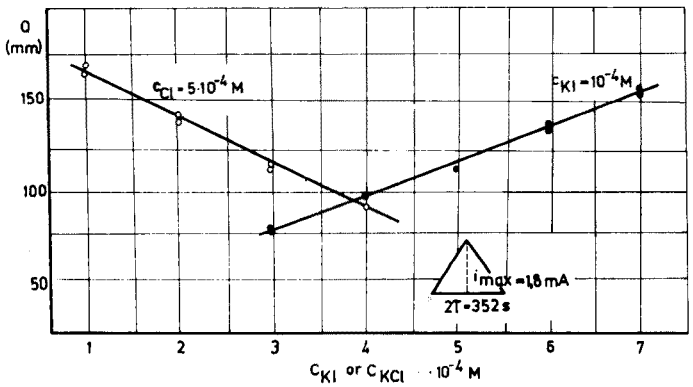

Fig. 8. Relationship between the Q values and the appropriate halide concentration established on the basis of titration curves recorded in samples containing chloride and iodide. ○ Q_1 vs. c_{I^-}. ● $Q_1 - Q_2$ vs. c_{Cl^-}. i_{max}, 1.8 mA; 2τ, 352 s.

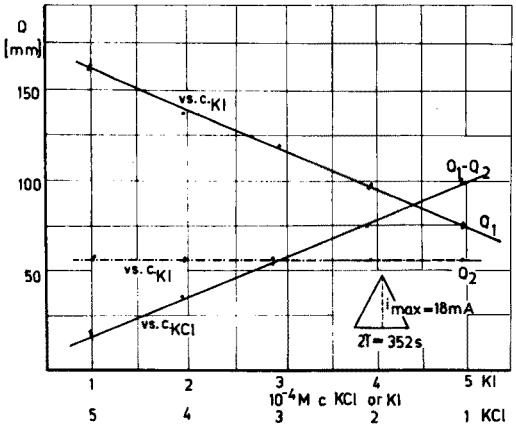

Fig. 9. Relationship between the Q values and the appropriate halide concentration established on the basis of titration curves recorded in samples containing chloride and iodide at a total constant concentration of $6 \cdot 10^{-4}$ M. i_{max}, 1.8 mA; 2τ, 352 s.

TABLE 1

Comparison of the values of Q_1 and Q_2 obtained with mixed solutions of constant total halide concentration
(Flow rate, 5.0 ml min^{-1}; i_{max}, 1.8 mA; 2τ, 704 s.)

Sample	Q_2 [mm]	Q_1 [mm]	$Q_1 - Q_2$ [mm]
10^{-4} M KI $5 \cdot 10^{-4}$ M KCl $5 \cdot 10^{-1}$ M $NaNO_3$	61	163	102
$2 \cdot 10^{-4}$ M KI $4 \cdot 10^{-4}$ M KCl $5 \cdot 10^{-1}$ M $NaNO_3$	60	133	73
$3 \cdot 10^{-4}$ M KI $3 \cdot 10^{-4}$ M KCl $5 \cdot 10^{-1}$ M $NaNO_3$	61	120	59
$4 \cdot 10^{-4}$ M KI $2 \cdot 10^{-4}$ M KCl $5 \cdot 10^{-1}$ M $NaNO_3$	59	99	40

to each other and almost symmetrical. The determination of the equivalence points and the Q value can therefore be done easily.

Because of the reduction of silver(I) on the graphite electrode surface, a change in the electrode activity is to be expected, but this would not change the Q value determined on the basis of chemical equivalence.

For an electrode of higher activity, the same reagent addition program will result in a triangular titration curve of greater height, but the Q value determined from titration curves recorded for different electrodes will not differ theoretically. Thus the advantage of the triangle programmed reagent addition technique over the simple direct amperometric method is obvious. During the present measurements, only a slight change in the indicating electrode activity was observed.

REFERENCES

1 G. Nagy, Zs. Fehér, K. Tóth and E. Pungor, Anal. Chim. Acta, 91 (1977) 87.
2 I. M. Kolthoff and N. H. Furman, Potentiometric Titrations, J. Wiley, London, 1949.
3 E. Pungor, Oszcillometria és konduktometria, Akadémiai Kiadó, Budapest, 1963; Oscillometry and Conductometry, Pergamon, London, 1966.
4 J. T. Stock, Amperometric Titrations, Interscience, New York, 1965.
5 J. J. Lingane, Anal. Chem., 26 (1954) 622.
6 D. D. DeFord and H. Horn, Anal. Chem., 28 (1956) 797.
7 E. P. Przybylowicz and L. B. Rogers, Anal. Chem., 28 (1956) 799.
8 E. Pungor, Zs. Fehér and G. Nagy, Pure Appl. Chem., 44 (1975) 595.
9 G. W. C. Milner and G. Phillips, Coulometry in Analytical Chemistry, Pergamon, Oxford, 1967.
10 Zs. Fehér, G. Nagy, K. Tóth and E. Pungor, Analyst, 99 (1974) 699.

Analytica Chimica Acta, 91 (1977) 107—112

A BARIUM ION-SELECTIVE ELECTRODE BASED ON THE NEUTRAL CARRIER *N,N,N',N'*-TETRAPHENYL-3,6,9-TRIOXAUNDECANE DIAMIDE

M. GÜGGI, E. PRETSCH and W. SIMON

Department of Organic Chemistry, Swiss Federal Institute of Technology, Universitäts strasse 16, CH-8092 Zürich (Switzerland)

(Received 24th January 1977)

SUMMARY

A barium-selective liquid membrane electrode based on a neutral carrier — *N,N,N',N'*-tetraphenyl-3,6,9-trioxaundecane diamide — in a poly(vinyl chloride) matrix is described. The sensor discriminates against alkali and alkaline earth metal cations by factors in the range of approximately 10^2—10^3 and 30—10^5, respectively. In contrast to earlier systems, the electrode shows an excellent e.m.f. stability (the drift is less than 0.8 mV/d) and an operational lifetime of more than two years.

Electrically neutral, lipophilic organic complexing agents are widely used as components for ion-selective electrodes [1—4]. Sensors for Li^+ [5, 6], Na^+ [6, 7], K^+ [4, 6, 8, 9, 10], NH_4^+ [6, 11, 12], Ca^{2+} [6, 13], Sr^{2+} [14], and Ba^{2+} [6, 15, 16] have been based on such molecules. Because of their analytical potential, considerable effort has been directed towards the design of selective and stable electrodes for barium(II) [6, 15, 16]. The first such sensors were based on solutions of nonylphenoxypolyoxyethylene ethanol (Igepal CO-880) complexes of Ba^{2+} on a porous polyvinylidene fluoride membrane [15]. Through the incorporation of similar complexes in poly(vinyl chloride) (PVC) matrices, together with appropriate plasticizers, solvent polymeric membranes [17] of higher e.m.f. stability and lifetimes up to 30 d were obtained [16]. On the basis of model calculations [18], a series of neutral lipophilic complexing agents (neutral carriers) for alkali and alkaline earth metal cations have been prepared (see [6]). The structure of the most useful carrier for Ba^{2+} found so far is shown in the upper corner of Fig. 1 [6]. The present paper reports the preparation of the neutral carrier as well as the properties and uses of sensors based on it.

EXPERIMENTAL

Synthesis of ligand

3,6,9-Trioxaundecane diacid was prepared from tetraethylene glycol and nitric acid [19]. The 3,6,9-trioxaundecanedioyl dichloride was prepared from this diacid and oxalyl chloride in dry benzene [20].

For preparation of *N,N,N',N'*-tetraphenyl-3,6,9-trioxaundecane diamide, the acid chloride (1 equivalent, generally 1 g) in dry benzene (15 ml) was added to a solution of the amine (2 eq) plus triethylamine (4 eq) in benzene (15 ml) to give the amide, which was purified by crystallization from chloroform—ether.

The analytical results were as follows. I.r. in $CDCl_3$ (Perkin-Elmer infracord 157 G): the positions of the strongest bands were 1680, 1595, 1495 cm^{-1}. ^{1}H-n.m.r. (signals in p.p.m. relative to TMS; solvent, $CDCl_3$; Hitachi Perkin-Elmer R24): 3.65 (singlet, 8 protons), 4.05 (singlet, 4 protons), 7.35 (singlet, 20 protons). M.s. (*m/e* values of M^+ and most intense signals; Hitachi Perkin-Elmer RMU-6M): M^+ 524, 268, 255, 254 (base peak), 240, 210, 182, 169, 168, 167, 91, 77. Elemental analysis: calculated for $C_{32}H_{32}N_2O_5$, 73.3%C, 6.2%H, 5.3%N; found, 73.3%C, 6.2%H, 5.5%N.

Electrode system

The measurements were performed on cells of the type

$$\text{Hg; } Hg_2Cl_2\text{, KCl (satd.)/0.1 M } NH_4NO_3\text{/sample solution//membrane//0.01 M } BaCl_2\text{, AgCl; Ag} \qquad (I)$$

The sensor systems discussed here are based on PVC membranes of the type described by Moody et al. [21]. The membrane composition is: the $Ba(SCN)_2$ complex of the Ba^{2+}-selective ligand (crystallized from a solution of $Ba(SCN)_2$ and ligand in a 1:1 molar ratio (ethyl acetate)), 1.1% by weight, *o*-nitrophenyl-n-octyl ether (*o*-NPOE), 65.9% by weight; and PVC (SDP, hochmolekular, Lonza AG, Visp, Switzerland), 33.0% by weight.

The membranes were about 0.2 mm thick, and were incorporated into electrode bodies Philips IS-560 (N.V. Philips' Gloeilampenfabrieken, Eindhoven, Holland). They were used in combination with calomel electrodes as described earlier [22].

E.m.f. Measurements

Measurements were made at 22 ± 2°C, the standard deviation from the measuring equipment was < 0.1 mV for single determinations (see [22]).

Selectivity factors

These were determined by the separate solutions technique on aqueous 0.1 M solutions of the chlorides from the following relationships

$$\text{E.m.f.} = \text{constant} + \frac{2.303RT}{2F} \log (a_{Ba^{2+}} + k_{BaM}\, a_{M^{z+}}{}^{2/z}) \qquad (1)$$

$$\log k_{BaM} = \frac{(E_2 - E_1)\, 2F}{2.303RT} - \log a_{M^{z+}}{}^{2/z} + \log a_{Ba^{2+}} \qquad (2)$$

where a are ion activities; z is the charge of the interfering ion; E_1 is the e.m.f. of the cell assembly (I), the sample being a 0.1 M solution of $BaCl_2$; E_2 is the e.m.f. of the cell assembly (I), the sample being a 0.1 M solution of the chloride of the interfering ion; and R, T, F, have their usual meanings.

Ion Activities

The fundamental values set forth by Bates [23] were employed as activity standards. The activity coefficients γ_{Ca} for Ca^{2+} were found to be related to the ionic strength I by

$$\log \gamma_{Ca} = \frac{-2.04 I^{\frac{1}{2}}}{1 + 1.55 I^{\frac{1}{2}}} + 0.2I$$

The activity coefficients proposed by Bates [23] for Na^+ are described by

$$\log \gamma_{Na} = \frac{-0.51 I^{\frac{1}{2}}}{1 + 1.30 I^{\frac{1}{2}}} + 0.06I$$

For all other alkali and alkaline earth metal cations the activity coefficients γ_i were calculated by the Debye—Hückel method [24]; thus,

$$-\log \gamma_i = A z^2 \frac{I^{\frac{1}{2}}}{1 + BbI^{\frac{1}{2}}}$$

where A and B were taken to be 0.509 and 0.328, respectively (T = 25°C, H_2O).

Reagents

Doubly distilled water (quartz apparatus) and chemicals from Fluka, (puriss. p. a.), Merck or Dixa (Zürich) (pro analysi) were used throughout.

RESULTS AND DISCUSSION

The response of the neutral carrier electrode assembly (I) is linear in the range 10^{-1}—$8 \cdot 10^{-6}$ M $BaCl_2$ (Fig. 1) giving a slope of 32.5 ± 1.0 mV (standard deviation; theoretical, 29.28 mV, 22°C) for the linear regression. In unbuffered Ba^{2+} systems, the detection limit is well below 10^{-6} M. Except for the discrimination against Cs^+, Sr^{2+} and Mg^{2+}, the selectivities are comparable to those obtained with other neutral carrier systems (Fig. 2) [15, 16]. The electrode presented here shows a substantially higher discrimination against Cs^+ and Mg^{2+} and a poorer selectivity with respect to Sr^{2+} (Fig. 2). In 10^{-3} M $BaCl_2$ solutions, the uncorrected e.m.f. of cell (I) is only slightly affected by changes in the pH of the sample solution between 2 and 8 (Fig. 3). Although no quantitative statements were made, a pH range of 1.5—10 at 10^{-3} M Ba^{2+} was claimed earlier [16]. If the existence of certain associated species of the carrier—cation complex with anions in the membrane phase is assumed [25, 26], the deviation towards positive e.m.f. values at a high pH of the sample solution (Fig. 3) may be rationalized by model calculations as being due to hydroxyl ions.

When the final Ba^{2+} concentration is increased by factors of 10 in the range 10^{-4}—10^{-1} M, the final e.m.f. of the cell is reached (within 0.3 mV) in less than 1 min. The speed of response is therefore comparable to one of the other systems described [16].

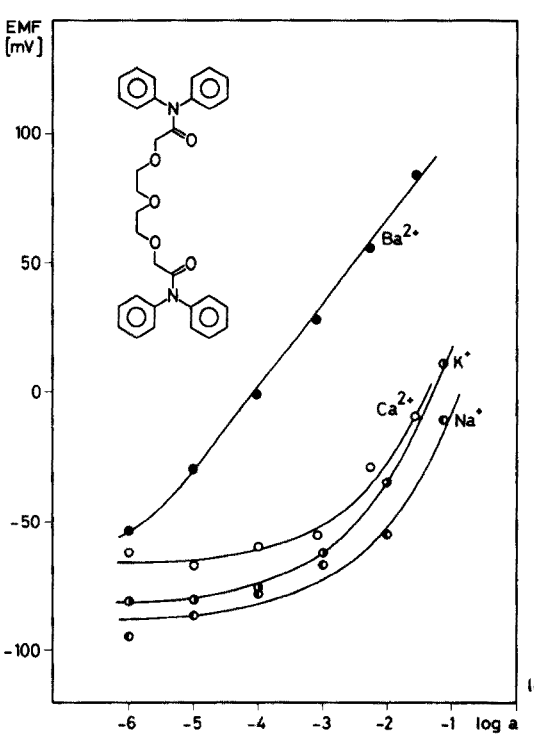

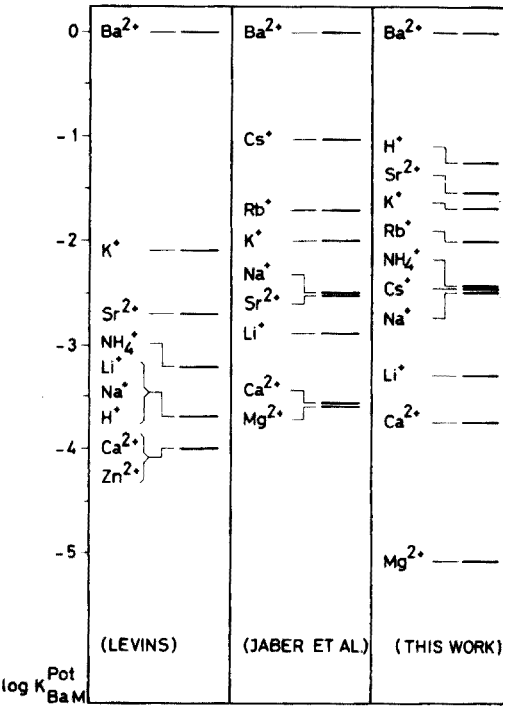

Fig. 1. E.m.f. response for cell (I) to aqueous solutions of the chlorides of Ba^{2+}, Ca^{2+}, Na^{+}, and K^{+}. The e.m.f. readings were corrected for changes in the liquid junction potential using the Henderson equation [29].

Fig. 2. Comparison of the selectivity coefficients obtained with 0.1 M solutions of the chlorides. Left: Ba^{2+}-electrode described by Levins [15]. Middle: Ba^{2+}-electrode described by Jaber et al. [16]. Right: Selectivity coefficients obtained by the separate solution technique on the electrode described here.

Because of the high lipophilicity of the carrier and plasticizer used [27], the electrodes described here have a very long lifetime. For a typical electrode, which was in permanent use and contained the initial internal filling solution, the e.m.f. values of cell (I) measured (10^{-1} M $BaCl_2$, 22 ± 2°C) were 146.0, 138.1, 126.0, 148.2 and 149.3 mV on the 7th, 36th, 77th, 105th and 164th day of operation, respectively. This corresponds to drifts of less than 0.8 mV per day. Table 1 shows the e.m.f. values obtained on 0.1 M solutions of different chlorides relative to the values of a 0.1 M $BaCl_2$ solution. It becomes obvious that the selectivities are changed only slightly even over periods exceeding a year (457 days). This is consistent with the extremely high lifetimes reported for neutral carrier electrodes selective for K^{+} [9].

As shown earlier [16], Ba^{2+}-selective electrodes are of interest for potentiometric titrations of sulphate with Ba^{2+} solutions. In such titrations, barium

TABLE 1

E.m.f. values (mV) at 22 ± 2° C measured for cell (I) and aqueous 0.1 M solutions of the chlorides before and after ageing of the membrane (days after preparation of the electrode)

Ion	7th day	457th day	Ion	7th day	457th day
Li^+	−124.2	−108.5	Mg^{2+}	−151.1	−130.3
Na^+	−86.2	−102.0	Ca^{2+}	−98.0	−86.5
K^+	−60.4	−89.6	Sr^{2+}	−38.2	−40.8
Rb^+	−73.6	−96.4	Ba^{2+}	−0	−0
NH_4^+	−96.2	−109.4			

perchlorate in nonaqueous solvents, e.g. 80% ethanol, has previously been recommended [28]. A curve obtained in the automatic potentiometric titration of a 10^{-3} M solution of K_2SO_4 in 30% (w/w) isopropanol with 10^{-2} M $Ba(ClO_4)_2$ in isopropanol is shown in Fig. 4. In ten such titrations of sulphate, the standard deviation was 0.4%. The characteristics of the electrode, including the selectivities, were unchanged even after four weeks of its permanent use in titrations in the solvent system mentioned. The results obtained here as well as the findings reported earlier [16] indicate that neutral carrier-based Ba^{2+}-selective electrodes are attractive candidates for an automatic determination of sulphur in organic compounds with sample sizes below 4 mg.

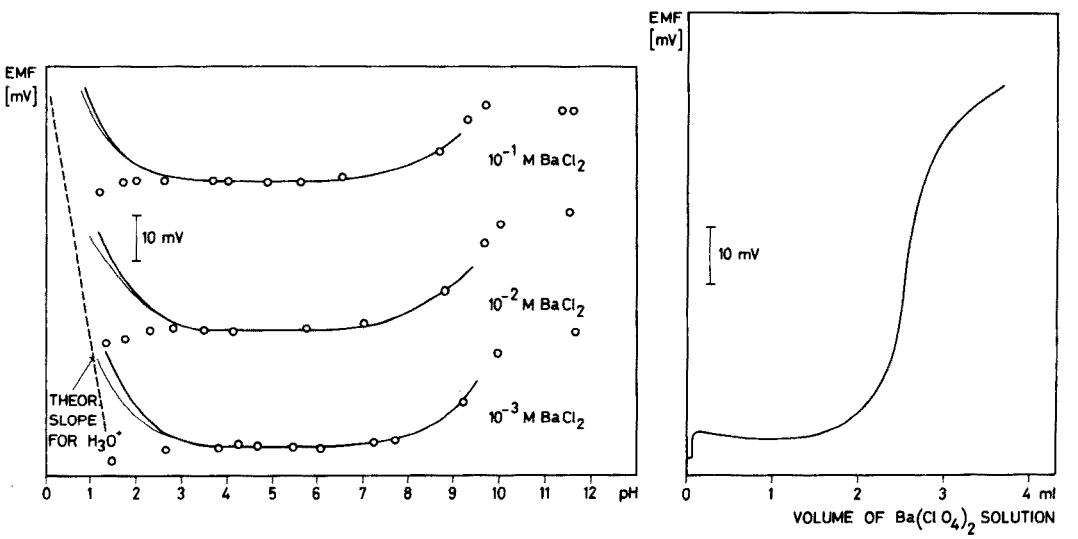

Fig. 3. Dependence of the e.m.f. of cell (I) on the pH of the sample solution for different $BaCl_2$ concentrations. Points, experimental values (uncorrected). Thin lines, experimental values in the region pH 1—3 corrected for liquid junction potentials [29]. Thick lines, experimental values corrected for liquid junction potentials and activity changes caused by addition of HCl or NaOH to the $BaCl_2$ sample solutions.

Fig. 4. Titration of 25 ml of $1.0 \cdot 10^{-3}$ M K_2SO_4 added to 15 ml of water and 12 ml of isopropanol with $Ba(ClO_4)_2$ in isopropanol ($1.0 \cdot 10^{-2}$ M), on an automatic titrator (Metrohm E 436). Titration speed: auto 8 ($\leq$ 2 ml min^{-1}).

REFERENCES

1 J. Koryta, Ion-selective Electrodes, Cambridge University Press, London, 1975.
2 K. Cammann, Das Arbeiten mit ionenselektiven Elektroden, Springer-Verlag, Berlin, 1973.
3 R. P. Buck, Anal. Chem., 48 (1976) 23R.
4 Z. Stefanac and W. Simon, Chimia, 20 (1966) 436; Microchem. J., 12 (1967) 125.
5 M. Güggi, U. Fiedler, E. Pretsch and W. Simon, Anal. Lett., 8 (1975) 857.
6 D. Ammann, R. Bissig, Z. Cimerman, U. Fiedler, M. Güggi, W. E. Morf, M. Oehme, H. Osswald, E. Pretsch and W. Simon in M. Kessler, L. C. Clark, Jr., D. W. Lübbers, I. A. Silver and W. Simon (Eds.), Ion and Enzyme Electrodes in Biology and Medicine, Urban and Schwarzenberg, Munich, 1976.
7 M. Güggi, M. Oehme, E. Pretsch and W. Simon, Helv. Chim. Acta, 59 (1976) 2417.
8 U. Fiedler and J. Růžička, Anal. Chim. Acta, 67 (1973) 179.
9 O. H. LeBlanc, Jr., and W. T. Grubb, Anal. Chem., 48 (1976) 1658.
10 J. Petránek and O. Ryba, Anal. Chim. Acta, 72 (1974) 375.
11 I. H. Krull, C. A. Mask and R. E. Cosgrove, Anal. Lett., 3 (1970) 43.
12 R. P. Scholer and W. Simon, Chimia, 24 (1970) 372.
13 D. Ammann, M. Güggi, E. Pretsch and W. Simon, Anal. Lett., 8 (1975) 709.
14 E. W. Baumann, Anal. Chem., 47 (1975) 959.
15 R. J. Levins, Anal. Chem., 43 (1971) 1045; 44 (1972) 1544.
16 A. M. Y. Jaber, G. J. Moody and J. D. R. Thomas, Analyst, 101 (1976) 179.
17 R. Bloch, A. Shatkay and H. A. Saroff, Biophys. J., 7 (1967) 865.
18 W. Simon, W. E. Morf and P. C. Meier in J. D. Dunitz, P. Hemmerich, J. A. Ibers, C. K. Jørgensen, J. B. Neilands, D. Reinen and R. J. P. Williams (Eds.), Structure and Bonding, Vol. 16, Springer-Verlag, Berlin, 1973.
19 J. P. Sauvage, Diss. Université Louis Pasteur, Strasbourg, 1971.
20 D. Ammann, R. Bissig, M. Güggi, E. Pretsch, W. Simon, I. J. Borowitz and L. Weiss, Helv. Chim. Acta, 58 (1975) 1535.
21 G. J. Moody, R. B. Oke and J. D. R. Thomas, Analyst, 95 (1970) 910.
22 D. Ammann, E. Pretsch and W. Simon, Anal. Lett., 7 (1974) 23.
23 R. G. Bates and M. Alfenaar in R. A. Durst (Ed.), Ion-selective Electrodes, National Bureau of Standards, Spec. Publ. 314, Washington, 1969.
24 J. N. Butler, Ionic Equilibria, Addison-Wesley Series in Chemistry, Reading, Mass., Palo Alto, London, 1964.
25 W. E. Morf and W. Simon, in H. Freiser (Ed.), Recent Advances in Ion Selective Electrodes, Plenum Press, New York, 1978, in press.
26 W. E. Morf and W. Simon, Symposium Mátrafüred (Hungary), October 1976.
27 E. Pretsch, R. Büchi, D. Ammann and W. Simon, in Essays on Analytical Chemistry, E. Wänninnen (Ed.), Pergamon Press, in press.
28 J. S. Fritz and S. S. Yamamura, Anal. Chem., 27 (1955) 1461.
29 P. Henderson, Z. Phys. Chem., 59 (1907) 118; 63 (1908) 325.

Analytica Chimica Acta, 91 (1977) 113—120

THE USE OF A CHLORIDE-SELECTIVE COMBINATION ELECTRODE IN AN AUTOMATED CONTINUOUS POTENTIOMETRIC SYSTEM

M. VANDEPUTTE, L. DRYON and D. L. MASSART

Farmaceutisch Instituut, Vrije Universiteit Brussel, Paardenstraat 67, B-1640 Sint Genesius-Rode (Belgium)

(Received 10th January 1977)

SUMMARY

The use of a combination chloride-selective electrode is proposed for potentiometric automated measurements. With this type of electrode, potential oscillations can be completely eliminated by earthing the flow-through cell, even at high flow rates. With the chloride electrode, sample rates up to 50 samples/h can be reached. The system has been tested for carry-over at high and low concentration ranges. Accuracy and precision of the system are determined by chloride measurements in mineral water samples.

Ion-selective electrodes seem to be very suitable for use in automated systems. They have been applied for on-line continuous monitoring of several anions in power station waters. Off-line methods, however, seem to be less successful. Although the use of some electrodes, e.g. the calcium [1] or the sulfide [2] electrode, in a Technicon system allows analysis rates of up to 60 samples/h, other electrodes, e.g. the chloride or fluoride electrode, allow rates of only 10, 20 or 30 samples/h [3—6]. These rates contrast unfavourably with those obtained (60 samples/h) in classical colorimetric systems with, for example, a Technicon AutoAnalyzer.

At first sight, this appears surprising, for the response of solid-state ion-selective electrodes is very fast. Mertens et al. [5] concluded that the discrepancy between the fast response of the electrode and the slow response of an automated system incorporating such an electrode is due to film diffusion. For this reason, faster responses of the automated systems should be obtained either by stirring the cell solution or increasing the flow rate.

Potentiometric automated systems are subject to potential oscillations caused by the peristaltic pump. Van den Winkel et al. [7] showed that base-line shifts and oscillations are caused by changes in streaming potential in the connecting tube between indicator and reference flow-through electrodes, and proposed methods of eliminating such effects. But at the high flow rates needed to reduce the diffusion phenomenon at the indicator electrode surface [7], these effects persist. Accordingly, attempts were made to incorporate a combination electrode in a Technicon system, so that

only one flow-through cell would be needed, thereby eliminating the major cause of potential oscillations, i.e. the plastic connection between the two electrodes.

Combination electrodes have not been used very often in automated systems. Berthier [8] used them in an on-line system for the continuous monitoring of fluoride and chloride in rain waters, and Oliver et al. [6] for the determination of fluoride in vegetation and gases. Oliver et al. reached an analysis rate of only 10 samples/h. In the present work, combination electrodes were tested in stirred and unstirred cells for the measurement of chloride and fluoride; the chloride results are reported below.

An automated potentiometric chloride instrument has been produced by Orion (model 99-17); reportedly, this is no longer commercially available, although its use has been discussed [9]. Automated discontinuous potentiometric systems are also available [10—12]. The Technicon three-channel potentiometric apparatus (Stat/Ion) measures chloride samples at a rate of 48 samples/h, and its use for clinical purposes has been evaluated by Lustgarten et al. [11] and by Fleisher et al. [12]. Another potentiometric system is the Orion Space Stat [13] which determines Cl^-, Na^+ and 4 other parameters but needs 10 min for each sample; it was designed for application in space research.

EXPERIMENTAL

The flow diagram (Fig. 1) is derived from that of Van den Winkel et al. [7].

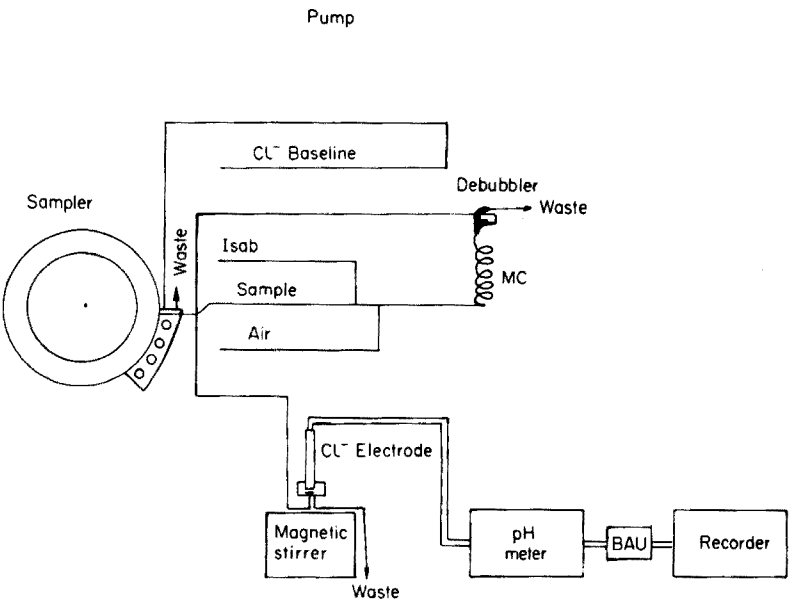

Fig. 1. Flow scheme of the automated system. BAU: Base-line adjustment unit.

The apparatus was constructed from the following parts: Technicon sampler AutoAnalyzer 1 with 1:1 cam; Gilson Minipulse proportioning pump with a continuously adjustable flow rate (the highest flow rate allowed by the debubbling system (5.8 ml min^{-1}) was employed); digital pH meter Orion model 601; home-made baseline adjustment unit [14]; Perkin-Elmer recorder model 56. A combination chloride electrode (Orion model 96-17) was used with filling solution 90 00 17 in the outer chamber. The flow-through cell is a hollow perspex cylinder provided with metallic inlet and outlet nipples. The cell is placed on a magnetic stirrer so that stirring bars can be employed to stir the internal solution.

All chemicals were of analytical grade. Ionic Strength Adjustment Buffer as proposed by Parthasarathy et al. [15] was used to avoid effects of variable ionic strength.

RESULTS AND DISCUSSION

Despite the combination electrode, base-line shift and oscillations increasing with the flow rate were observed (Fig. 2), but they were much less important than those reported earlier [7]. Earthing both nipples eliminated all base-line oscillations, even at the highest flow rate reached with the peristaltic pump. This contrasts with the findings of Van den Winkel et al. [7], who could not suppress these oscillations completely when two separated cells were used; under such conditions, streaming potentials are much higher, being proportional to the length of the connecting tube. It can be concluded that combination electrodes offer the advantage of eliminating interferences from streaming potentials.

Since the literature indicates that only rather small sample rates can be obtained, and since it was shown that stirring the cell increases the possible sample rate, it was decided initially to measure only under stirred-cell conditions. The linear range of the calibration curve of the chloride electrode starts at about $5 \cdot 10^{-4}$ M Cl^- [16], hence the range 10^{-3}—10^{-2} M Cl^- was investigated first. A manual calibration curve showed a slope of 56.8 mV. To investigate the time—response relationship of the electrode in the Technicon system, the time needed to reach 90% of the equilibrium reading was determined for different ten-fold concentration jumps in the direction

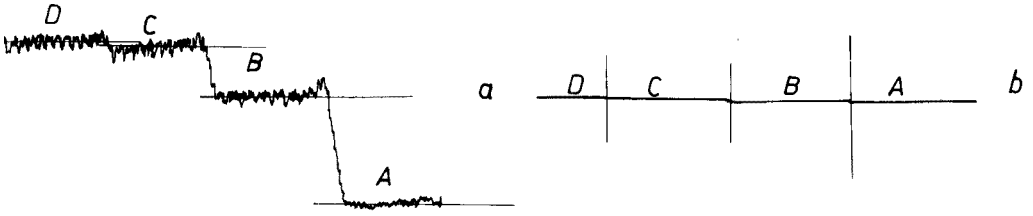

Fig. 2. (a) Base-line shift and oscillations obtained without earthing inlet and outlet nipples of the flow-through cell. (b) Base-line with earthed flow-through cell. Flow rate (ml min^{-1}): A, 1.6; B, 5.8; C, 9.3; D, 11.2.

of increasing concentration. The results obtained (Table 1) show that in all cases the time needed was below 36 s, the sampling time for a sample probe with a 50 (1:1) cam. An analysis rate of 50 samples/h should therefore be possible. Calibration curves obtained by the automatic system at that rate of analysis indeed showed slopes of 56.6 mV for the 10^{-2}—10^{-3} M range, which is in good agreement with the manual measurements.

One method of evaluating the behaviour of an automated system of this type is to determine the carry-over, i.e. the degree to which a result is influenced by the concentration of the preceding sample. The total carry-over was determined as recommended by Broughton et al. [17]: three samples of high concentration (A) are measured successively followed immediately by three samples of low concentration (B), yielding the sequence $A_1A_2A_3B_1B_2B_3$. The corresponding recorded values are $a_1a_2a_3b_1b_2b_3$, and the carry-over between sample A_3 and sample B_1 is given by $K = (b_1 - b_3)/(a_3 - b_3)$. The "true" value of B is assumed to be b_3, because it is preceded by two samples of equal concentration. Of course, there is no carry-over if b_1 is equal to b_3. Therefore, the statistical significance of any differences between the recorded b_1 and b_3 values was first investigated. The 10^{-3}—10^{-2} M range was studied with a base line of 10^{-3} M, $A = 10^{-2}$ M and $B = 3 \cdot 10^{-3}$ M. The results obtained (Table 2) showed no significant difference between the b_1 and b_3 values, so that one can state that there is no carry-over in this concentration range. A lower concentration range (1—10 ppm Cl^-) was then studied similarly. The % equilibrium reached for an analysis rate of 50 samples/h is given in Table 3. The measurements were carried out with and without stirring. It can be seen that the final potential (Table 3) is higher when the cell solution is not stirred. To understand this, one should note that very low concentrations near the detection limit were used. The limit of detection for a chloride electrode is determined by the solubility of the silver halide sensing element. Chloride ion activity in distilled water arising from the solubility of silver chloride at 25°C is $1.4 \cdot 10^{-5}$ M [16]. That the phenomenon noted is due to the low concentration was proved as follows. The steady state recorded when going from 1 to 10 ppm Cl^- is given in Fig. 3, which shows clearly the difference in potential obtained for stirred and unstirred working conditions. The effect increases when going from 1 to 100 ppm Cl^- (Fig. 3), which is in agreement with the proposed hypothesis. Clearly, the turbulent streaming conditions on stirring remove halide ions from the membrane more quickly. This was confirmed by the difference in slope obtained between stirred and unstirred manual measurements (Table 4); moreover, the difference disappeared at a

TABLE 1

Response time in the automated continuous potentiometric system

Cl^- jump (M)	$10^{-5} \rightarrow 10^{-4}$	$10^{-4} \rightarrow 10^{-3}$	$10^{-3} \rightarrow 10^{-2}$	$10^{-2} \rightarrow 10^{-1}$
T 90% (s)	16.5	10.4	9.3	10.4

TABLE 2

Peak heights in a carry-over experiment
(Concentration $A = 10^{-2}$ M, $B = 3 \cdot 10^{-3}$ M. Sample rate, 50 samples/h. Peak heights in cm.)

	b_1 (cm)	b_2 (cm)	b_3 (cm)	a_3 (cm)	K
	6.90	6.85	6.80	14.40	0.013
	6.80	6.85	6.85	14.40	0
	6.85	6.85	6.85	14.45	0
	6.80	6.85	6.85	14.40	0
	6.85	6.85	6.85	14.45	0
	6.85	6.85	6.90	14.50	0
	6.90	6.90	6.90	14.55	0
	6.90	6.85	6.90	14.45	0
	6.90	6.90	6.90	14.60	0
	6.90	6.85	6.90	14.50	0
Mean	6.87	6.86	6.87	14.47	
S.d.	0.04	0.02	0.04	0.07	

TABLE 3

Percentage equilibrium obtained for several concentrations
(Base-line, 1 ppm Cl^-. Sample rate, 50 samples/h.)

Stirred solution				Unstirred solution			
Cl^- (ppm)	Peak height (cm)	Equil. (cm)	% Equil. reached	Cl^- (ppm)	Peak height (cm)	Equil. (cm)	% Equil. reached
1.5	1.05	1.10	95.5	1.5	1.15	1.20	95.8
2	1.75	1.80	97.2	2	1.95	1.95	100.0
4	4.00	4.20	95.2	4	4.30	4.35	98.9
6	5.80	5.90	98.3	6	6.05	6.10	99.2
8	7.20	7.30	98.6	8	7.45	7.45	100.0
10	8.35	8.45	98.8	10	8.60	8.60	100.0

higher concentration range (Fig. 4). This phenomenon, of course, affects the slope of the calibration lines, but the detection limit is only slightly lower in unstirred solutions. In both stirred and unstirred solutions, more than 90% equilibrium is attained (Table 3).

Carry-over tests were then done at the low concentration range with 1 ppm Cl^- as the base-line, 8 ppm as the A value and 2 ppm as the B value. Both with stirring and without, the values obtained for b_1 and b_3 differ significantly at the 5% level of significance based on the nonparametric test of Mann and Whitney. The mean values, standard deviations and average differences are listed in Table 5.

The K values listed in Table 6 were compared by the nonparametric test. They did not differ significantly at the 5% level, and this was confirmed

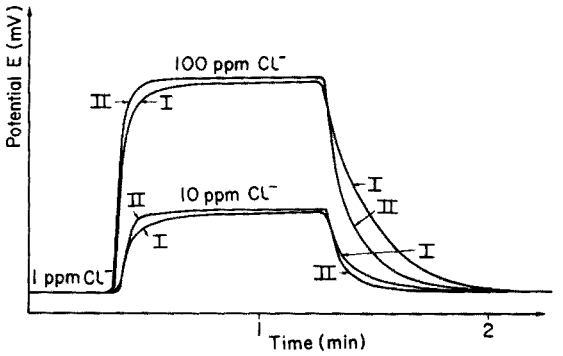

Fig. 3. Output for the stirred (I) and unstirred (II) cell solution at low chloride concentration.

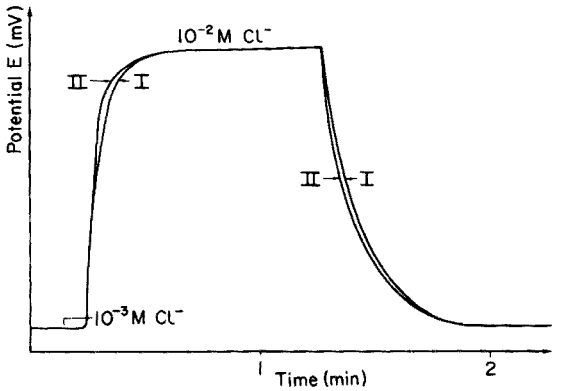

Fig. 4. Output for the stirred (I) and unstirred (II) cell solution at high chloride concentration.

TABLE 4

Comparison of manual stirred and unstirred measurements for the 1—100 ppm range

Concentration (ppm)	Stirred (mV)	Unstirred (mV)	Concentration (ppm)	Stirred (mV)	Unstirred (mV)
1	+141.4	+146.0	20	+94.4	+96.6
2	+139.9	+144.1	40	+80.3	+81.7
4	+134.3	+136.6	60	+71.4	+71.7
6	+126.5	+130.7	80	+64.8	+63.9
8	+120.8	+127.3	100	+59.1	+58.6
10	+107.1	+109.6			

by the sign test. It can be concluded that in this instance, stirring the cell solution has no advantageous effect on the response kinetics of the electrode. Since carry-over occurred, it was decided to use a base-line value from the upper end of the range studied. Carry-over should then be lower because of a faster return to the base-line; electrode responses are faster at higher concentrations. The recorder output is shown in Fig. 5. For a base-line of 8 ppm,

TABLE 5

Values obtained in the carry-over experiment at low concentrations
(Base-line, 1 ppm Cl^-; *A* value, 8 ppm Cl^-; *B* value, 2 ppm Cl^-. Sample rate, 50 samples/h.)

	Stirred solution			Unstirred solution		
	b_1	b_2	b_3	b_1	b_2	b_3
Mean[a] (cm)	2.12	1.95	1.94	2.26	2.09	2.03
S.d.	0.17	0.10	0.07	0.13	0.06	0.04
% Difference $(b_1 - b_3)$		8.50			10.2	

[a]Mean of 10 replicates.

TABLE 6

Values of *K* for stirred and unstirred solutions
(Base-line, 1 ppm Cl^-; *A* value, 8 ppm Cl^-; *B* value, 2 ppm Cl^-. Sample rate, 50 samples/h.)

Stirred	0.080	0.191	0.008	0.016	0.016	0.024	0.016	0	0.024
Unstirred	0.032	0.024	0.039	0.031	0.024	0.024	0.019	0.072	0.072

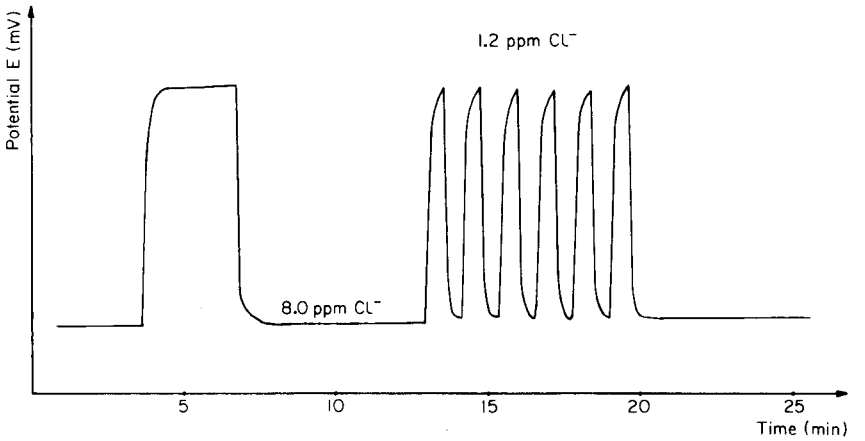

Fig. 5. Steady state and replicates for chloride analysis. Rate: 50 samples/h.

the mean value of the equilibrium reached 96.8%. A carry-over test was done with this base-line value, an *A* concentration of 6 ppm and a *B* concentration of 1.2 ppm, without stirring; stirring had little or no effect. The b_1 and b_3 values were significantly different at the 5% level of significance, but not at the 1% level. Therefore, it can be concluded that there is a slight carry-over.

The precision and accuracy of the system were studied by measuring the chloride content of mineral waters; the analysis rate was 50 samples/h and stirring was not used. Samples of high chloride content were diluted with

distilled water. The determinations were also done manually. The results are compared in Table 7. Both the accuracy and the precision of the automated method are good. For sample 1 the relative standard deviation was 1.1%.

In analyses for fluoride, the combination electrode allowed a sampling rate of 50 samples/h without carry-over when the concentration exceeded 0.5 ppm. Below this concentration, some carry-over occurred.

TABLE 7

Comparison of manual and automated chloride methods

Sample	Manual method (ppm)	Automated method (ppm)	Sample	Manual method (ppm)	Automated method (ppm)
1	3.73	3.68	5	11.60	11.20
2	2.08	2.25	6	36.00	33.00
3	5.90	5.86	7	349.00	351.00
4	4.33	4.72			

The authors thank FGWO for financial assistance, P. Van den Winkel for advice, and J. Lambrecht and G. Wuestenberg for technical assistance.

REFERENCES

1 J. Růžička and J. C. Tjell, Anal. Chim. Acta, 47 (1969) 475.
2 P. W. Alexander and G. A. Rechnitz, Anal. Chem., 46 (1974) 860.
3 J. Mertens, P. Van den Winkel, A. Henrion-Boeckstijns and D. L. Massart, J. Pharm. Belg., 2 (1974) 181.
4 E. D. Erdmann, Environ. Sci. Tech., 9 (1975) 252.
5 J. Mertens, P. Van den Winkel and D. L. Massart, Anal. Chem., 48 (1976) 272.
6 R. T. Oliver, G. F. Lenz and W. P. Frederick, Advances in Automated Analyses, Volume II, Technicon International Congress, 1969, p. 309.
7 P. Van den Winkel, J. Mertens and D. L. Massart, Anal. Chem., 46 (1974) 1765.
8 P. Berthier, Analusis, 2 (1973–1974) 722.
9 C. Fuchs, D. Dorn and C. McIntosh, Z. Anal. Chem., 279 (1976) 150.
10 H. Dahms, Clin. Chem., 13 (1967) 437.
11 J. A. Lustgarten, R. E. Wenk, C. Byrd and B. Hall, Clin. Chem., 20 (1974) 1217.
12 M. Fleisher, V. G. Bethune, G. Pennacchia and M. K. Schwartz, Clin. Chem., 21 (1975) 980, Abstracts.
13 Orion Research Newsletter, 6 (1974) 7.
14 J. Mertens, Ph.D. Vrije Universiteit Brussel, 1976.
15 N. Parthasarathy, J. Buffle and D. Monnier, Anal. Chim. Acta, 59 (1972) 447.
16 Instruction Manual for Halide Electrodes, Orion Research, Cambridge, Mass., 1974.
17 P. M. G. Broughton, M. A. Buttolph, A. H. Gowenlock, D. W. Neill and R. G. Skentelbery, J. Clin. Path., 22 (1969) 278.

Analytica Chimica Acta, 91 (1977) 121—128

DETERMINATION OF BACITRACIN BY DIFFERENTIAL PULSE POLAROGRAPHY

E. JACOBSEN and J. H. PEDERSTAD

University of Oslo, Institute of Pharmacy, P.O. Box 1068 Blindern, Oslo 3 (Norway)

B. ØYSTESE

A/S Apothekernes Laboratorium for Specialpraeparater, Skøyen, Oslo 2 (Norway)

(Received 12th January 1977)

SUMMARY

Differential pulse polarograms of pharmaceutical-grade bacitracin exhibit a well-defined double wave at the dropping mercury electrode over the entire pH range 1—8. The current is diffusion-controlled and proportional to the concentration as well as to the biological activity of the sample. The concentration of bacitracin and of zinc—bacitracin can be determined by pulse polarography with a standard deviation less than 2%. The biologically inactive oxidation product (bacitracin F) is reduced at less negative potentials and can easily be determined in the presence of the biologically active components of bacitracin.

Bacitracin is a polypeptide produced by strains of *Bacillus licheniformis*. Pharmaceutical-grade bacitracin is a family of polypeptides of which the main component, bacitracin A (I), also possesses the major microbiological activity [1, 2]. The commercial product also contains a biologically inactive component, bacitracin F, which is derived from bacitracin A by oxidation (reaction 1) [3].

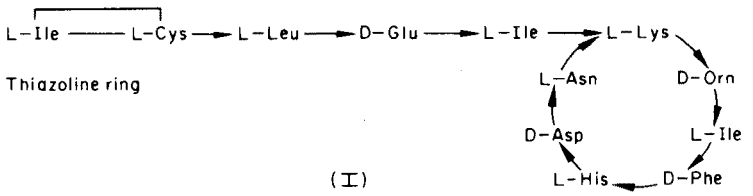

(I)

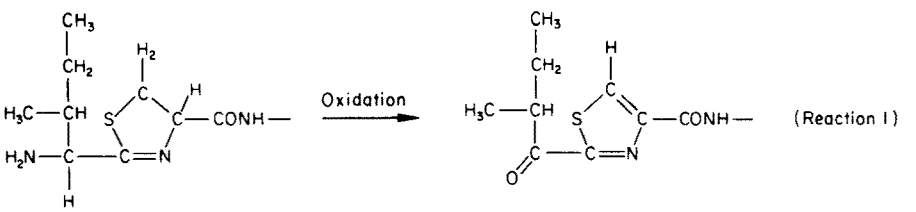

(Reaction 1)

Thiazoline ring of bacitracin A

Ketothiazole in bacitracin F

The concentration of bacitracin is usually determined by the agar diffusion method [4, 5]. The various components of bacitracin can be separated by counter-current distribution [6] or by h.p.l.c. [2] and the concentration of each component determined by u.v. spectrophotometry. However, all these methods are time-consuming and unsuitable for routine analysis. According to Purkaystha and Riedel [7] bacitracin is reduced at the dropping mercury electrode in the pH range 3—11. They recommend phosphate buffer pH 9.8 as supporting electrolyte and claim that 25—300 ppm of bacitracin can be determined by d.c. polarography [7]. Moreover, they observed a very good correlation between the polarographic and the microbiological methods.

The object of the present work was to study the electro-reduction of biologically active and inactive components of bacitracin and to investigate the application of differential pulse polarography to rapid analysis of the antibiotic.

EXPERIMENTAL

The differential pulse polarograms were obtained with a Princeton Applied Research Model 174 Polarographic Analyzer. A Houston Omnigraph 2000 XY recorder was used to record the polarograms. A Metrohm EA 427 Ag/AgCl (saturated KCl) electrode was used as reference electrode and a platinum coil served as auxiliary electrode. Dissolved oxygen was removed from the solutions by bubbling oxygen-free nitrogen through the cell for 5 min and passing it over the solution during the electrolysis. All experiments were performed at 25 ± 0.1°C.

Pharmaceutical-grade bacitracin (designated in this paper as bacitracin A*), zinc—bacitracin A* and a purified bacitracin F fraction (A/S Apothekernes laboratorium for Specialpraeparater, Oslo) were studied. Stock solutions were prepared by dissolving the appropriate amount of the drug in methanol or in 0.1 M sulphuric acid. Only freshly prepared stock solutions were used, and all acidic solutions were discarded after 45 min. Cyclohexanediamine tetraacetic acid (CDTA; 99.9% pure; Fluka) was used. A CDTA—phosphate buffer of pH 5.5 was prepared by dissolving 1.5 g of CDTA in 112 ml of 0.1 M sodium hydroxide and diluting to 1 l with 0.1 M potassium dihydrogen-phopshate. All other chemicals were of reagent grade and were used without further purification.

RESULTS AND DISCUSSION

Preliminary experiments showed that differential pulse polarograms of bacitracin A* recorded from acidic or neutral media exhibit two well-defined peaks. At pH values above 8 the peaks were only poorly defined and the following experiments were restricted to lower pH values. A typical polarogram of bacitracin A* is given in Fig. 1 (curve A*).

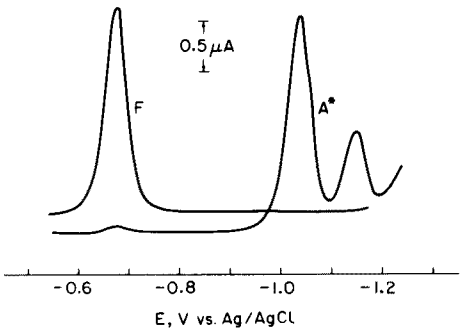

Fig. 1. Differential pulse polarograms of 50 μg ml^{-1} solutions of bacitracin F (curve F) and of bacitracin A* (curve A*) in phosphate buffer pH 6. Drop time 0.5 s, scan rate 2 mV s^{-1} and pulse amplitude 50 mV.

The greatest peak height was observed at slow scan rates, long drop times and large pulse amplitudes. However, the separation of the two peaks decreased with increasing drop time and increasing pulse amplitude. Hence, to obtain high sensitivity and, at the same time, sufficient separation of the two peaks, the instrumental settings: drop time 0.5 s, pulse amplitude 50 mV and scan rate 2 mV s^{-1} were used in the following experiments.

Polarograms of bacitracin F exhibit only one peak at all pH values. The peak potential of this wave is about 0.4 V less negative than the first bacitracin A* peak (Fig. 1, curve F).

The effect of pH on the current—voltage curve was investigated by recording polarograms of bacitracin A* (100 μg ml^{-1}) in various supporting electrolytes. Well-defined waves were observed in the pH range 1—8. As indicated in Table 1, the peak height of the first wave decreases and the half-width increases with increasing pH of the electrolyte, indicating a more irreversible electrode reaction in slightly acidic and neutral media. The peak

TABLE 1

Effect of pH on differential pulse polarograms of bacitracin A* (100 μg ml^{-1}) in various supporting electrolytes

Buffer	pH	First wave			Second wave	
		$-E_p$ (mV)	i_p (μA)	Half-width (mV)	$-E_p$ (mV)	i_p (μA)
Sulphuric acid	1	763	4.29	48	935	—
KCl/HCl	2	810	4.19	48	957	1.85
Phthalate	3	898	4.56	50	1042	1.95
Phthalate	4	957	4.29	50	1085	1.70
Phosphate	5	1033	3.91	52	1144	1.80
Phosphate	6	1057	3.74	53	1197	1.80
Phosphate	7	1156	3.33	56	1266	2.35
Borate	8	1219	2.67	67	1325	2.45

potential of both waves is shifted to more negative values with increasing pH, which implies that hydrogen ions are consumed in the electrode reactions.

The peak current of the first peak is greater than that of the second and consequently more suitable for quantitative work. As indicated in Table 1, the highest peak current and the best separation of the two peaks are obtained at pH values less than 5. At pH values less than 2 the second peak is partly masked by the hydrogen wave and the peak height cannot be measured.

Polarograms recorded from 0.1 M sulphuric acid and from phosphate buffer pH 6 with various amounts of bacitracin A* and F present, showed that the peak current increases linearly with the concentration in the range 5—100 $\mu g\ ml^{-1}$. At higher concentrations, the standard curve is slightly curved and the peak potential is shifted to more negative values. The peak potential for 1000 $\mu g\ ml^{-1}$ is about 0.1 V more negative than at 100 $\mu g\ ml^{-1}$. However, the polarograms were perfectly reproducible and indicate that bacitracin can be determined by differential pulse polarography in the entire concentration range 5—1000 $\mu g\ ml^{-1}$. The best results (standard deviation of the peak current less than 2%) were obtained when the current was measured from the foot of the wave rather than by the "base-line method". Bacitracin A* is most easily determined in 0.1 M sulphuric acid, because the two peaks are well separated at this pH value. However, fairly good results were obtained also at higher pH values. A few data obtained from phosphate buffer pH 6 are given in Table 2.

Polarograms of bacitracin A* recorded at various time intervals after mixing the solution, showed that the drug is decomposed in acidic media and that the rate of decomposition increases rapidly with increasing

TABLE 2

Differential pulse polarographic data for the reduction of various amounts of bacitracin in phosphate buffer pH 6
(Drop time 0.5 s, pulse amplitude 50 mV and scan rate 2 mV s^{-1})

Bacitracin A*				Bacitracin F		
Conc. ($\mu g\ ml^{-1}$)	$-E_p$ (V)	i_p (μA)	i_p/C ($\mu A\ \mu g^{-1}\ ml$)	$-E_p$ (V)	i_p (μA)	i_p/C ($\mu A\ \mu g^{-1}\ ml$)
5	1.100	0.250	0.050	0.750	0.250	0.050
10	1.100	0.455	0.046	0.750	0.540	0.054
20	1.100	0.980	0.049	0.745	1.07	0.054
30	1.100	1.57	0.052	0.742	1.60	0.053
40	1.100	2.03	0.051	0.740	2.15	0.054
50	1.105	2.60	0.052	0.735	2.73	0.055
60	1.105	3.08	0.051	0.730	3.13	0.052
70	1.105	3.50	0.050	0.730	3.73	0.053
80	1.105	4.01	0.050	0.725	4.43	0.055
90	1.107	4.34	0.048	0.730	4.73	0.053
100	1.110	4.60	0.046	0.729	5.33	0.053

temperature and decreasing pH of the electrolyte. Polarograms recorded at 25°C showed that the peak height decreased about 2% at pH 5, 17% at pH 2.5 and 80% at pH 1 in 3 days after mixing the solution. When the temperature was raised to 37°C, the decomposition was complete after two days in 0.1 M sulphuric acid and the peak height had decreased by 60% in phosphate buffer pH 6. However, no decrease in peak height was observed at any pH during the first hour after mixing the solution. Hence, when acidic electrolytes are used, the solutions should be discarded after 45 min. Following this procedure excellent results were obtained even at very low pH values (Table 3).

The effect of drop time was investigated by recording d.c. polarograms of bacitracin (100 μg ml^{-1}) in phosphate buffer pH 6 at various heights of the mercury column. The value $ih^{-\frac{1}{2}}$, where h is the height of the column after correction for the "back-pressure", was constant, indicating that the current is diffusion-controlled. The temperature coefficient (determined in the range 20—45°C) of the d.c. current, 1.6% per degree, also indicates that the current is controlled by diffusion.

Bacitracin forms stable complexes with metal ions such as cadmium, manganese and zinc [8] and the drug is usually produced as a zinc—bacitracin complex. This complex is almost insoluble in water and slightly acidic buffers, but dissolves easily in 0.1 M sulphuric acid. A differential pulse polarogram of zinc—bacitracin recorded from 0.1 M sulphuric acid is given in Fig. 2, curve A. The second peak is the reduction wave of zinc and the first and third are due to the reduction of bacitracin. Experiments showed that the height of the first bacitracin peak increases linearly with increasing concentration of the drug in the range 5—90 μg ml^{-1}. Further experiments showed that zinc—bacitracin is decomposed in 0.1 M sulphuric acid (about 60% in one day at room temperature) and the height of the bacitracin peak decreases rapidly with the time elapsed after mixing the solution. However, reproducible results and no decrease in peak current were observed during the first 45 min after mixing the solution.

Although zinc—bacitracin may be determined in 0.1 M sulphuric acid it would be advantageous to use a supporting electrolyte in which the drug is

TABLE 3

Polarographic determination of bacitracin in 0.1 M sulphuric acid (Drop time 0.5 s, pulse amplitude 50 mV and scan rate 2 mV s^{-1})

Sample No.	Biol. activity (IU/mg)	Peak current, μA				Mean	S.d. (%)
1	49.0	2.56	2.58	2.53	2.55	2.55	0.8
2	57.3	2.78	2.77	2.79	2.76	2.77	0.5
3	57.3	2.73	2.73	2.73	2.71	2.72	0.4
4	59.5	2.91	2.93	2.93	2.91	2.91	0.4

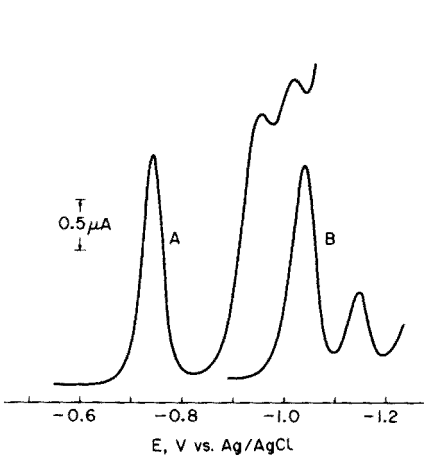

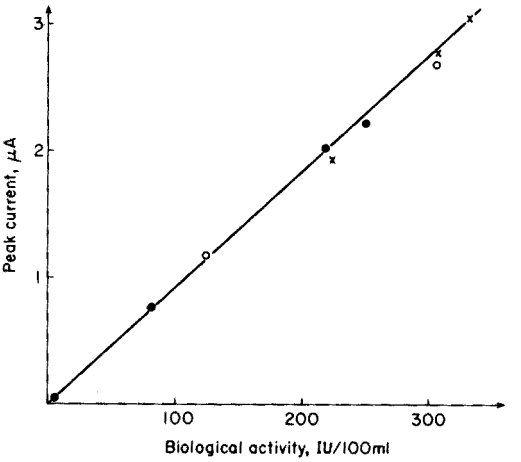

Fig. 2. Differential pulse polarograms of zinc—bacitracin (50 μg ml^{-1}) recorded from 0.1 M sulphuric acid (curve A) and from CDTA—phosphate buffer pH 5.5 (curve B). Drop time 0.5 s, scan rate 2 mV s^{-1} and pulse amplitude 50 mV.

Fig. 3. Correlation between biological activity and polarographic peak current of 50 μg ml^{-1} samples of bacitracin. The drug was decomposed at 37 °C in 0.1 M sulphuric acid (•), phosphate buffer pH 6 (○) and distilled water (×) in 0—7 days.

more stable. Cyclohexanediaminetetraacetic acid (CDTA) is a complexing agent which forms a more stable complex with zinc (formation constant pK_c = 18.7) than bacitracin ($pK_c \approx 14$) [8]. Hence, in the presence of excess of CDTA, the drug is liberated from the zinc—bacitracin complex and the drug dissolves easily.

A differential pulse polarogram of zinc—bacitracin recorded from a CDTA—phosphate buffer with pH 5.5 is given in Fig. 2, curve B. No decrease in peak current was observed after several hours in this electrolyte, and the height of the first bacitracin peak still increases linearly with concentration in the range 5—90 μg ml^{-1}. Based on the above experiments the following procedure is suggested.

Recommended procedure

Dissolve the sample containing 0.5—90 mg of zinc—bacitracin in $5 \cdot 10^{-5}$ M CDTA—0.1 M phosphate buffer pH 5.5 and dilute to 100.00 ml with the same buffer. Dilute 10.00 ml of the solution to 100 ml with the buffer and transfer a suitable amount of the solution to a polarographic cell. Remove dissolved air with pure nitrogen, and record a differential pulse polarogram with drop time 0.5 s, pulse amplitude 50 mV and scan rate 2 mV s^{-1} in the potential range −0.8 to −1.2 V. Measure the peak current of the first wave and determine the amount of zinc—bacitracin from a standard curve or by the standard addition method. If zinc is not present in the sample, the CDTA in the buffer can be omitted.

Provided that the determination is completed within 45 min, 0.1 M sulphuric acid is preferable as supporting electrolyte for bacitracin as well as

TABLE 4

Microbiological and polarographic measurements of bacitracin (50 μg ml^{-1})

Sample No.	Biol. activity (IU/mg)	S.d. (%)	Peak current (μA)	S.d. (%)	Peak current/Biol. activity (μA mg/IU)
1	46.3	1.6	2.46	2.3	0.053
2	49.0	1.9	2.56	0.8	0.052
3	57.3	3.1	2.78	0.5	0.049
4	57.3	5.3	2.75	0.4	0.048
5	59.5	0.8	2.92	0.4	0.049
6	61.7	3.5	3.00	0.6	0.049
7	61.7	1.7	3.05	2.3	0.049

for zinc—bacitracin. The polarogram is then recorded in the potential range −0.6 to −0.1 V with the same instrumental parameters as above.

A few samples of bacitracin of various biological activity were analysed by the proposed polarographic method. The results are given in Table 4. It is interesting to note from the last column that the ratio peak current/biological activity is constant, which implies that the height of the first polarographic peak increases linearly with the biological activity of the sample. In order to verify that the polarographic method does not measure inactive products along with the biologically active molecules, bacitracin was dissolved in 0.1 M sulphuric acid, distilled water and in phosphate buffer, respectively, and stored at 37°C. After various time intervals a sample was analysed by polarography and the biological activity of the same sample was determined by the agar diffusion method [4, 5]. As indicated in Fig. 3, there is a very good correlation between the height of the polarographic peak and the biological activity of the sample, and it is obvious that when bacitracin is completely decomposed in 0.1 M sulphuric acid and the biological activity has decreased to zero, no polarographic wave is observed. Consequently, the proposed polarographic method is a very simple and rapid method for the determination of the concentration which is correlated to the biological activity of the sample.

Bacitracin is decomposed also in alkaline media. Experiments showed that although the polarographic current decreases with increasing decomposition of the drug in alkaline buffers, a polarographic wave is still observed even after the biological activity had decreased to zero.

The polarographic wave is probably due to reduction of the >C=N group in the thiazoline ring which is easily hydrolysed in acidic media, causing a decrease in biological activity and in polarographic current. Experiments in alkaline media indicated that the biological activity of the drug depends not only on the thiazoline ring, but also on other (polarographically inactive) groups which are deaminated in alkaline media [3]. Hence, the proposed polarographic method cannot be used for the determination of bacitracin A* samples which have been decomposed in alkaline solutions.

Bacitracin F is an oxidation product of bacitracin and the commercial

product always contains a small amount of bacitracin F. Experiments showed that the concentration of bacitracin F in neutral and slightly acidic solutions of the drug, increases with increasing temperature and the time elapsed after mixing the solution. Because bacitracin F is reduced at less negative potentials than the biologically active drug (Fig. 1), the two forms can easily be determined in the presence of each other. The concentration of bacitracin F (in the range 5—100 μg ml^{-1}) can be determined from a standard curve or by the standard addition method. As indicated in Table 2, the value i_p/C is the same for both bacitracin A* and F. Hence, the percentage of bacitracin F in the commercial product can be determined by simply measuring the ratio of the two peaks.

The bacitracin F content in a few samples of bacitracin was determined by polarography and by thin-layer chromatography by visual comparison of the area of the spots. Samples (50 mg) were dissolved in 50 ml of methanol, 5.00 ml of the solution was diluted to 100 ml with phosphate buffer pH 6, and a polarogram was recorded in the potential range −0.5 to −1.1 V. The results are given in Table 5. Both methods give concordant results, but the proposed polarographic method is considerably faster and more convenient for routine analysis.

TABLE 5

Determination of bacitracin F in bacitracin A* by differential pulse polarography (d.p.p.) and thin layer chromatography (t.l.c.)

Sample	Biol. activity (IU/mg)	Bacitracin F, (%)	
		D.p.p.	T.l.c.
1	38.8	11.9	12.5—15
2	43.5	13.2	10—12.5
3	51.0	5.5	5
4	51.3	7.7	5
5	59.8	5.5	6—7
6	61.0	3.6	4
7	64.0	4.2	4
8	64.0	6.4	4—5
9	65.0	6.0	4

REFERENCES

1 G. G. F. Newton and E. P. Abraham, Biochem. J., 53 (1953) 597 and 604.
2 K. Tsuji and J. H. Robertson, J. Chromatogr., 112 (1975) 663.
3 W. Konigsberg and L. C. Craig, J. Org. Chem., 27 (1962) 934.
4 D. C. Grove and W. A. Randall, Assay methods of antibiotics, a laboratory manual, Medical Encyclopedia, New York, 1955.
5 S. G. Dahl, T. Waaler, S. Thomassen, B. Øystese and T. Høyland, Pharm. Acta Helv., 47 (1972) 424.
6 G. G. F. Newton and E. P. Abraham, Biochem. J., 53 (1953) 597.
7 A. R. Purkaystha and B. E. Riedel, Dacca Univ. Stud., 18 (1970) 89.
8 R. E. Wasylishen and M. R. Graham, Can. J. Biochem., 53 (1975) 1250.

Analytica Chimica Acta, 91 (1977) 129—138

ANODIC STRIPPING COULOMETRY AT A THIN-FILM MERCURY ELECTRODE

RUEDI EGGLI
Institute of Inorganic Chemistry, University of Zürich, CH-8001 Zürich (Switzerland)
(Received 29th November 1976)

SUMMARY

Primary coulometric versions of d.c. anodic stripping voltammetry, performed in a microcell at a mercury-plated rotating glassy carbon electrode, are applied to the determination of cadmium and lead. With exhaustive preelectrolysis of the sample solution, 5—100 ng of the metal can be determined from the charge contained in the stripping signal; precision and accuracy are in the 5% range. An extrapolation procedure that requires only partial metal deposition is evaluated.

Several different techniques of anodic stripping analysis are currently used in trace metal determinations [1]. The characteristic common to most of these techniques is that they are applied in a voltammetric mode such that only a small fraction of the metal contained in the sample solution is actually used in the analytical deposition and stripping process. This has the disadvantages that the stripping signal is sensitive to the preelectrolysis conditions [2, 3] and that a calibration step is required. Both drawbacks can be avoided by application of coulometric methods. In the basic version of such a procedure, the metal is completely deposited on the working electrode and Faraday's law is used to calculate its amount from the measured charge used in the subsequent dissolution step. It requires a stripping procedure that provides for complete and uniform metal dissolution and that yields a signal which permits easy determination of faradaic charge. Further, a cell with a high ratio of electrode area to sample volume is needed to keep the preelectrolysis time small.

Stripping coulometry is not a new method. It was applied many years ago by Rogers and co-workers, who used the conventional linear potential-sweep stripping method to determine trace amounts of silver at a platinum electrode [4] and, less successfully, cadmium and zinc at mercury-plated platinum electrodes [5]. But since then, very few reports dealing with true coulometric versions of anodic stripping analysis seem to have been published. Meites [6] proposed a controlled-potential stripping procedure for the determination of zinc at a mercury pool, and Gründler [7] determined gold at a carbon paste electrode by a chronopotentiometric stripping method.

The present work was designed to evaluate coulometric stripping procedures at thin-film mercury electrodes. A microcell with a rotating mercury-covered glassy carbon electrode was used to determine trace amounts of cadmium and lead by potentiostatic deposition and linear potential-sweep stripping of the metal. Coulometric analyses were carried out by the basic procedure involving an exhaustive preelectrolysis step and by an extrapolation method that requires only partial depletion of the sample.

EXPERIMENTAL

Cell and electrodes

Figure 1 shows the cell which is a three-electrode system designed to be used with solution volumes of 100—600 μl. Its center body is made from Plexiglas

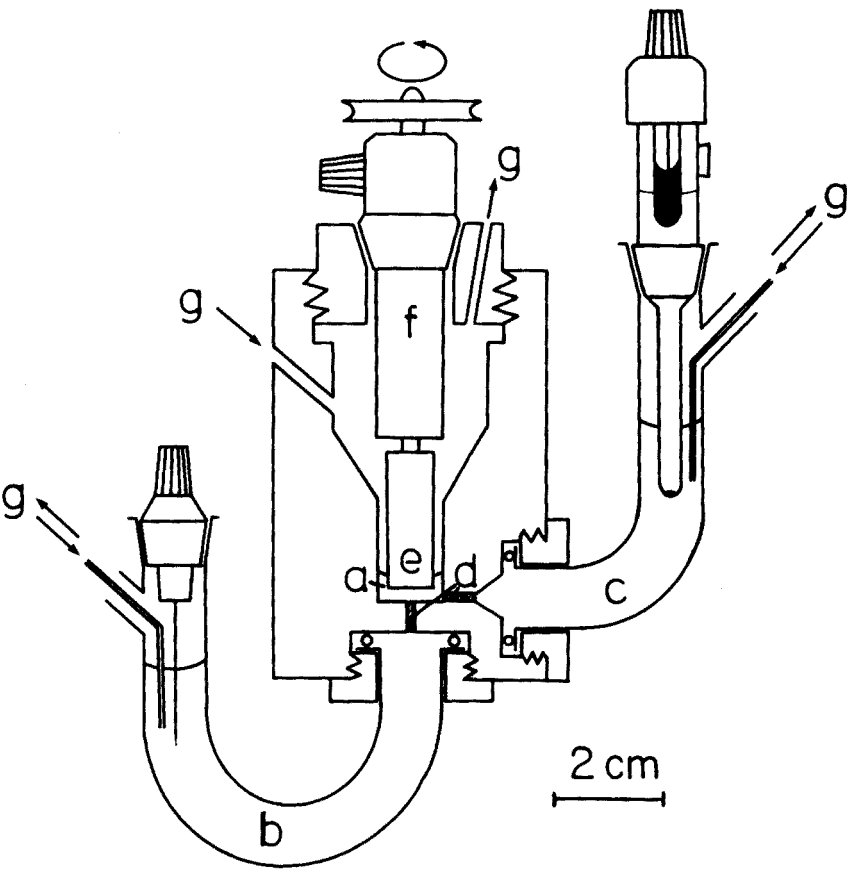

Fig. 1. Coulometric microcell with rotating disk electrode. (a) Working electrode compartment; (b) counter electrode compartment with platinum counter electrode; (c) side compartment with reference half-cell; (d) ceramic plug liquid junctions; (e) tip of rotating electrode; (f) jacket of belt-driven rotating shaft; (g) nitrogen inlet or outlet.

and contains the cylindrically shaped working electrode compartment which has an inner diameter of 12 mm. The reference half-cell (a saturated calomel electrode (SCE) with a ceramic plug) and the platinum wire counter electrode are each placed in side compartments of borosilicate glass which are attached to the main cell body by screw connections with O-ring-tightened flanges. The two liquid junctions are porous ceramic plugs (diameter 0.8 mm) which are glued in the Plexiglas with epoxy resin. The rotating electrode consists of a Plexiglas jacket serving as a holder for the rotating shaft and an interchangeable Plexiglas tip containing the glassy carbon disk. The jacket fits in a cone screwed into the cell allowing easy adjustment of electrode position. A belt, driven by a tachogenerator-regulated motor, was used to rotate the shaft; the rate was adjustable between 10 and 110 r.p.s. with a precision of 0.5%. The glassy carbon disk (Tokay GC-A, 6-mm diameter) was glued into the Plexiglas tip (10-mm diameter) with epoxy resin. Its surface was first ground with carborundum paper (Buehler Carbimet 600) and then polished successively with diamond pastes of grain sizes 6, 3 and 1 μm.

The working electrode compartment was deaerated by a stream of nitrogen (oxygen content below 3 p.p.m., flow rate 0.2 l min^{-1}) that was first passed through a wash bottle filled with water to prevent evaporation losses of the sample solution. Oxygen was also excluded from the side compartments of the cell, which were always filled with the supporting electrolyte used in the sample. All measurements were carried out at ambient temperature (26—27°C).

Instrumentation

Potentiostatic deposition and linear potential-sweep stripping were done with a potentiostat (AMEL 551) driven by a linear sweep generator (AMEL 566). Cell currents were measured with a zero-resistance ammeter (AMEL 668/RM), and a Houston 2002 X-Y recorder was used to record the current—time/potential curves. The amount of mercury used to plate the electrode was measured with a PAR 379 current integrator.

Chemicals

All reagents used were of highest purity (Merck Suprapur) and doubly distilled water was used throughout. A 0.05 M acetate buffer (0.05 M HAc—0.05 M NaAc) was used as supporting electrolyte. Sample solutions of lead and cadmium were prepared daily by dilution of standardized 0.01 M stock solutions prepared from lead acetate and cadmium sulfate. The mercury plating solution was a 0.05 M acetate buffer containing 32 p.p.m. of mercury.

General procedure

Electrode preplating. In a separate conventional three-electrode cell containing 25 ml of deaerated mercury plating solution, the rotating glassy

carbon electrode was held at a potential of −0.4 V vs. SCE until a charge of 0.035 C had been used up; then the potential was set to +0.15 V during 1 min to strip deposited trace metals. This electrode was used in anodic stripping experiments during one day, regardless of the number of runs performed. After use, the mercury film was wiped off with clean filter paper.

Anodic stripping experiments. After initiation of the deaeration process, which was continued throughout the whole experiment, an aliquot of the supporting electrolyte (usually 200 μl) was placed in the working electrode compartment and spiked with metal solution of the appropriate concentration from a calibrated 3-μl pipette (Oxford ultramicro pipette). The electrode was then inserted and positioned in such a way that the disk remained about 1 mm below the surface of the sample solution. After deaeration for 3 min deposition and stripping under continuous rotation of the electrode (usually 45 r.p.s.) were started. No deaeration interval was required between subsequent measurements carried out with the same sample in the closed cell. In any experiment performed to evaluate precision and accuracy at charge levels below 20 μC, the supporting electrolyte was cleaned electrolytically in situ before the metal solution was introduced. For this cleaning the rotating electrode was held at −1 V vs. SCE for a sufficient period (10 min with a solution volume of 200 μl); the electrode was then transferred to the plating cell and stripped by scanning the potential from −1 to +0.15 V at a rate of 10 mV s^{-1}.

Determination of charge. The peaks in the stripping current—time curves were integrated by counting area elements of 1 mm^2. The precision was better than 1% if the area exceeded 300 mm^2. The baseline of a stripping voltammogram was defined by the stripping curve of a blank recorded under equal conditions.

RESULTS AND DISCUSSION

Dependence of stripping peak charge on deposition time

For a diffusion-controlled reduction of metal ions, performed at constant potential under conditions of forced convection, the time dependence of the current is given by the Lingane equation [8] which can be written in the integrated form

$$Q = Q_0 \cdot (1 - e^{-kt}) \tag{1}$$

where Q denotes the charge transferred after deposition time t, and Q_0 is the charge used for complete reduction of the metal ions present in the solution. The rate constant k is determined by the diffusion coefficient D of the reacting ion, the thickness δ of the diffusion layer and the ratio of electrode area A to solution volume V

$$k = (D/\delta) \cdot (A/V) \tag{2}$$

When the process is carried out at a rotating disk electrode under limiting current flow, D/δ can be calculated from the Levich equation [9], introducing the dependence of k on the angular velocity ω of the disk and the kinematic viscosity ν of the solution

$$k = (0.62 \cdot D^{2/3} \cdot \nu^{-1/6} \cdot \omega^{1/2})\,(A/V) \tag{3}$$

In anodic stripping coulometry as done in this work, the quantity measured is the charge Q obtained by stripping an amount of metal that has been deposited during a time, t_d, at constant deposition potential and, additionally, during the first period of the potential-sweep process. The dependence of Q on t_d can be described approximately by eqn. (1) if the total deposition time, t, is expressed by

$$t = t_d + t' \tag{4}$$

where t' accounts for the additional metal deposition after the time t_d. As the rate constant k decreases with increasing potential, this approximation is valid only if the time interval where k decreases is sufficiently small. For experimental verification, it is convenient to combine eqns. (1) and (4) in the form

$$-\ln (1 - Q/Q_0) = k\, t_d + k\, t' \tag{5}$$

Thus, a plot of $-\ln (1 - Q/Q_0)$ versus t_d should yield a straight line of slope k, intersecting the abscissa at $t_d = -t'$.

In separate experiments with the same mercury film, the dependence of Q on the deposition time, t_d, was determined for cadmium and lead at a deposition potential of -1.0 V vs. SCE. The results shown in Figs. 2 and 3 indicate that the above description conforms well to the experimental data. The rate constants, determined from the slopes of the linear plots of Fig. 3 were 0.0072 s^{-1} for Cd^{2+} and 0.0097 s^{-1} for Pb^{2+}. Equation (3) was used to calculate the rate constants from the experimental conditions (ω = 283 s^{-1}, A/V = 1.42 cm^{-1}); a value of 0.010 $cm^2\ s^{-1}$ was used for ν, and, as an approximation, the diffusion coefficients of Cd^{2+} and Pb^{2+} in 0.1 M KNO_3 ($0.73 \cdot 10^{-5}$ and $1.0 \cdot 10^{-5}$ $cm^2\ s^{-1}$, respectively [9], were taken. The resulting rate constants were 0.012 s^{-1} for Cd^{2+} and 0.015 s^{-1} for Pb^{2+}; each is about 50% higher than the observed value, indicating that the effective electrode area exposed by the mercury droplets is smaller than the geometrical area of the carbon disk which was used in the calculation. The difference between the two rate constants can be attributed largely to the difference between the diffusion coefficients of the two metal ions, the calculated ratio $k_{Pb^{2+}}/k_{Cd^{2+}}$ of 1.23 being only slightly lower than the ratio of the observed constants — which is 1.35. A further factor accounting for the difference between the two rate constants is that at a deposition potential of -1.0 V, the rate constant for lead deposition is at its limiting value, whereas the corresponding value for cadmium is slightly below it. This is indicated by the measurements shown in Fig. 4.

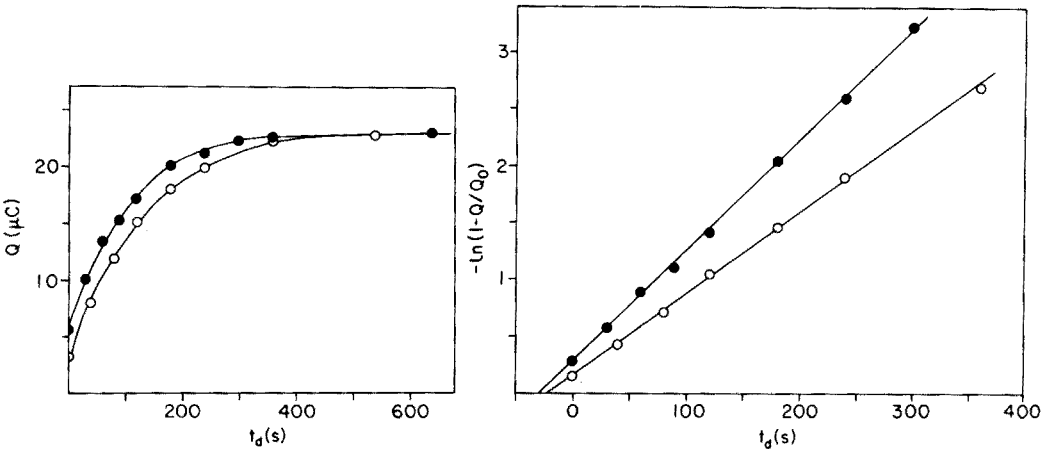

Fig. 2. Dependence of stripping peak charge Q on deposition time, t_d, for cadmium (○) and lead (●). Total charge taken of each metal 23.2 μC; solution volume 200 μl; deposition potential −1 V vs. SCE; scan rate 10 mV s^{-1}, electrode rotation rate 45 r.p.s.

Fig. 3. $-\ln(1 - Q/Q_0)$ plotted versus deposition time, t_d, for cadmium (○) and lead (●). Values for Q and Q_0 were taken from the measurements of Fig. 2.

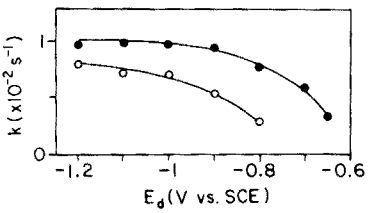

Fig. 4. Variation of deposition rate constant k with deposition potential E_d for cadmium (○) and lead (●). Experimental conditions as noted in Fig. 2.

In mixtures containing equal amounts of both metals, the observed rate constants had the same ratio as those determined in separate solutions of lead and cadmium with the same mercury film electrode. However, the absolute values of the constants showed variations of up to 20% when different mercury films were used, all being plated under equal conditions. This is probably due to the low reproducibility of the effective electrode area.

The dependence of the lead deposition rate constant on the rotation rate of the electrode was determined between 10.8 and 103 r.p.s. for the experimental conditions noted in Fig. 2. As expected from eqn. (3), k increased linearly with the square root of the angular velocity ω; the observed slope was $5.2 \cdot 10^{-4}$ $s^{-1/2}$.

Coulometric stripping analysis with exhaustive preelectrolysis

According to eqn. (5), the time required for the deposition step of such an analysis depends on the deposition rate constant and the desired degree of exhaustion, Q/Q_0. When the term $k \cdot t'$ in eqn. (5) is neglected, the deposition time is given by $-(1/k)\ \ln\ (1 - Q/Q_0)$. Satisfactory results were obtained when deposition times corresponding to $Q/Q_0 = 0.999$ were used.

Analysis of solutions containing only one metal species. To evaluate precision and accuracy, separate analyses for lead and cadmium were carried out with amounts of metal equivalent to charges of 4.63—116 μC. As a solution volume of 200 μl was used, the corresponding concentration ranges are 25—622 p.p.b. for lead and 13—338 p.p.b. for cadmium. The experimental conditions were the same as used in previous experiments, and the rate constants found there were used to calculate the deposition times required for 99.9% depletion of the sample solutions. The respective values for cadmium and lead were 16 and 12 min. The results (Table 1) prove that the procedure allows accurate analyses to be performed at a comparably high precision level. Under the experimental conditions applied, the limit of detection was attained at a charge level of about 0.3 μC.

Analysis of mixtures. When mixtures of lead and cadmium were analysed, the accuracy and precision obtained in the determination of each metal were the same as those achieved in the analysis of solutions containing only a single metal species, provided that the peaks were completely resolved, i.e. the current minimum between the two peaks touched the baseline defined by the stripping curve of the respective blank. The width of the stripping peaks is affected mainly by the scan rate and, to a lesser extent, by the amount of deposited metal. Both factors cause peak broadening when they are increased, as is illustrated by the stripping curves shown in Fig. 5. To fix the limits of conditions that yield complete peak resolution,

TABLE 1

Determination of cadmium or lead by anodic stripping coulometry with exhaustive preelectrolysis
(Solution volume, 200 μl; deposition potential, −1.0 V vs. SCE; electrode rotation rate, 45 r.p.s.; deposition time, 16 min for cadmium and 12 min for lead; scan rate, 10 mV s^{-1}.)

Given		Found					
Pb or Cd		Pb			Cd		
Concn. ($\cdot 10^{-7}$ M)	Q_0 (μC)	Q_0[a] (μC)	s_r[a] (%)	f[b] (%)	Q_0[a] (μC)	s_r[a] (%)	f[b] (%)
1.20	4.63	4.73	5.0	+2.2	4.50	2.1	−2.8
6.01	23.2	23.4	2.0	+0.9	23.1	4.3	−0.4
30.1	116	114	1.7	−1.7	120	1.0	+3.4

[a] Average and relative standard deviation of 3 determinations.
[b] Relative accuracy of mean.

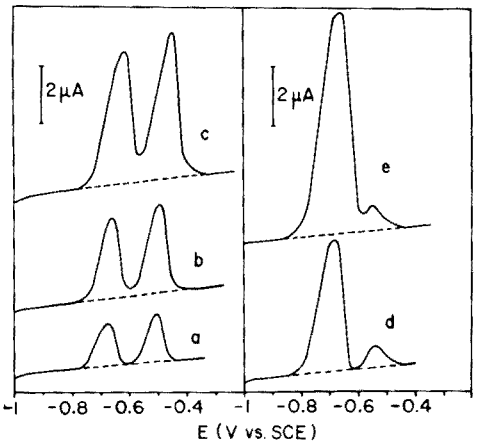

Fig. 5. Influence of scan rate and peak charge on resolution of stripping curves (solution volume 200 μl, electrode rotation rate 45 r.p.s., deposition time 17 min). Equal amounts (23.2 μC) of cadmium and lead, stripped with scan rates of 5 (a), 10 (b) and 20 mV s^{-1} (c). 5.5 μC of lead, stripped with 10 mV s^{-1}, in the presence of 43.5 μC (d) and 87 μC (e) of cadmium. Dashed lines are baselines.

mixtures containing various amounts of lead and cadmium were analysed at scan rates of 2, 5, 10, 20, 50, and 100 mV s^{-1}. When equal molar amounts of both metals were present, each equivalent to 57.5, 23.2, 10.2 and 4.63 μC, the respective highest scan rates yielding completely resolved stripping curves were 2, 5, 10 and 50 mV s^{-1}. For the accurate determination of an amount of lead corresponding to 5.5 μC in the presence of excess quantities of cadmium equivalent to 43.5 and 142 μC, the highest permissible scan rates were 10 and 5 mV s^{-1}, respectively.

Predictive stripping coulometry

In controlled-potential coulometry, several time-saving procedures are known that permit the charge Q_0 to be calculated from data measured in a non-exhaustive electrolysis process [10]. One of these methods, introduced by Meites [11], is based on eqn. (1) and can accordingly be applied to stripping coulometry of metals conforming to the related eqn. (5). To perform such an analysis, three non-exhaustive deposition steps, each followed by stripping at equal scan rates, must be done consecutively with deposition times $t_{d1} < t_{d2} < t_{d3}$ which satisfy the condition $t_{d3} - t_{d2} = t_{d2} - t_{d1} = \Delta t_d$. The total charge Q_0 can then be calculated from the charges Q_1, Q_2 and Q_3 obtained by stripping after the respective deposition times t_{d1}, t_{d2} and t_{d3}, by means of the following eqn. [11], which can be derived from eqn. (5)

$$Q_0 = \frac{Q_2^2 - Q_1 \cdot Q_3}{2Q_2 - (Q_1 + Q_3)} \qquad (6)$$

Succesful application of this procedure, leading to errors of the same order of magnitude as obtained in the exhaustive preelectrolysis method, has two prerequisites. The first, imposed by the law of error propagation, requires that Q_3/Q_0 and Δt_d are both sufficiently high; the second demands that Q_1 is large enough to be determined with a precision comparable to that obtained in the measurement of Q_2 and Q_3. Experiments with total metal charges between 10 and 120 μC showed that satisfactory results are obtained when Δt_d is larger than $0.2/k$ and Q_1 amounts at least to 0.1 Q_0. Data of two predictive analyses are listed in Tables 2 and 3. In each of these examples the total time of analysis was considerably shorter than the time required to analyse the respective samples by the conventional technique using exhaustive preelectrolysis. However, a saving of time can be realized only under certain experimental conditions, as is shown by the following considerations. The time required to perform a predictive stripping analysis is given by $t_{de} + t_{d1} + t_{d2} + t_{d3} + 3t_{sc}$ where t_{de} denotes the deaeration time

TABLE 2

Determination of cadmium by predictive anodic stripping coulometry
(The solution taken (200 μl) contained 67.6 p.p.b. of cadmium. Electrode rotation rate, 45 r.p.s.; deposition potential, −1.0 V vs. SCE; potential sweep from −1 to −0.5 V at 10 mV s^{-1}.)

i	t_{di} (s)	Q_i (μC)	Q_0 Given (μC)	Q_0 Found (μC)	Relative accuracy (%)	t_p[a] (s)	t_e[b] (s)
1	0	3.18					
2	40	8.13	23.2	23.9	+3.0	450	1190
3	80	11.9					

[a]Time for predictive analysis including 180 s for deaeration.
[b]Time for analysis with exhaustive preelectrolysis, calculated for $Q/Q_0 = 0.999$ and $k = 0.0072\ s^{-1}$, including 180 s for deaeration.

TABLE 3

Determination of cadmium and lead in a mixture by predictive anodic stripping coulometry
(The solution taken (300 μl) contained 41.5 p.p.b. of lead and 22.5 p.p.b. of cadmium. Potential sweep from −1 to −0.3 V at 5 mV s^{-1}; other conditions as noted in Table 2.)

i	t_{di} (s)	Q_i (μC) Pb	Cd		Q_0 Given (μC)	Q_0 Found (μC)	Relative accuracy (%)	t_p[a] (s)	t_e[b] (s)
1	60	5.98	3.62						
2	180	9.35	7.11	Pb	11.6	12.2	+5.2	1140	1760
3	300	10.9	8.78	Cd	11.6	10.3	−11.2		

[a]Time for predictive analysis including 180 s for deaeration.
[b]Time for analysis with exhaustive preelectrolysis, calculated for $Q/Q_0 = 0.999$ and $k_{Cd^{2+}} = 0.0048\ s^{-1}$, including 180 s for deaeration.

and t_{sc} is the scanning time. The minimum analysis time t_{pmin} is obtained by calculation of the deposition times from eqn. (5) and the above-mentioned conditions $\Delta t_d = 0.2/k$ and $Q_1 = 0.1\ Q_0$, thus

$$t_{pmin} = t_{de} + 0.9/k - 3t' + 3t_{sc} \quad (7)$$

The corresponding time necessary for a conventional coulometric stripping analysis with 99.9% depletion of the sample is given by

$$t_{emin} = t_{de} + 6.9/k - t' + t_{sc} \quad (8)$$

A comparison of these expressions, neglecting the influence of t', shows that the minimum time necessary for a predictive analysis is shorter than the time required for the exhaustive preelectrolysis method, only if k is smaller than $3/t_{sc}$. As the scanning time, given by the ratio of the potential range swept to scan rate, is usually fixed, the predictive method will only find meaningful application in cases where the rate constant of metal deposition is comparably low, i.e. when a cell with a low ratio of electrode area to sample volume is used.

A disadvantage of the predictive method is that perfectly reproducible deposition conditions (i.e. hydrodynamic conditions and electrode area) are required, whereas the signal obtained in the conventional exhaustive electrolysis procedure is not affected by small variations of the preelectrolysis conditions.

REFERENCES

1 T. R. Copeland and R. Skogerboe, Anal. Chem., 46 (1974) 1257A.
2 L. Huderová and K. Štulík, Talanta, 19 (1972) 1285.
3 H. E. Allen, W. R. Matson and K. H. Mancy, J. Water Pollut. Contr. Fed., 42 (1970) 573.
4 S. S. Lord, R. C. O'Neill and L. B. Rogers, Anal. Chem., 24 (1952) 209.
5 K. W. Gardiner and L. B. Rogers, Anal. Chem., 25 (1953) 1393.
6 L. Meites, Anal. Chim. Acta, 20 (1959) 456.
7 P. Gründler, J. Electroanal. Chem. Interfacial Electrochem., 52 (1974) 269.
8 J. J. Lingane, J. Am. Chem. Soc., 67 (1945) 1916.
9 R. N. Adams, Electrochemistry at Solid Electrodes, Marcel Dekker, New York, 1969.
10 J. E. Harrar, in A. J. Bard (Ed.), Electroanalytical Chemistry, Vol. 8, Marcel Dekker, New York, 1975, p. 18.
11 L. Meites, Anal. Chem., 31 (1959) 1285.

Analytica Chimica Acta, 91 (1977) 139—142

CONTROLLED-POTENTIAL COULOMETRIC DETERMINATION OF PLATINUM IN AMERICIUM—PLATINUM ALLOYS

W. BARTSCHER and B. GIOVANNONE

European Institute for Transuranium Elements, (EURATOM) P.O. Box 2266, D-7500 Karlsruhe (Federal Republic of Germany)

(Received 28th October 1976)

SUMMARY

A controlled-potential coulometric method for the determination of platinum in americium—platinum alloys is described. Platinum in the hexachloroplatinate complex is reduced to the metal at —0.3 V vs. the saturated silver chloride electrode on a mercury pool electrode. For quantities up to 5 mg, the standard deviation was 6.4 μg.

Actinide—platinum intermetallic compounds are of interest because of their chemical stability and their rôle as intermediate products in the preparation of pure actinide metals [1]. Furthermore, studies of their physical properties should give information on electronic configuration in actinide compounds. Chemical analysis is needed to check the composition of these materials.

Whilst americium can be determined by EDTA titration [2], where platinum does not interfere, the precise determination of milligram amounts of platinum is more difficult. Gravimetric methods based on precipitation [3] or electrode deposition [4] are not sensitive enough. Spectrophotometric [5, 6] and polarographic [7] methods have standard deviations of 1% or more. A coulometric method [8], based on the reduction of platinum(IV) to the divalent state by galvanostatically generated tin(II) chloride, gave errors of about 5%.

Controlled-potential coulometry is precise and sensitive. Takata and Muto [9] reported a method of this kind for the simultaneous determination of gold, platinum and palladium at a mercury electrode in phosphate medium. Because of difficulties in the recovery of americium, this medium was inconvenient for the present purpose, and a method in a less powerful complexing medium was developed. Conventionally, the first step in coulometric reduction is pre-electrolysis at a potential which is sufficiently high to reduce impurities without reduction of the element to be determined. Then the potential is lowered to give complete reduction of this element. Because of the irreversibility of all platinum redox couples, this range of potential is very large. The reduction of the $PtCl_6^{2-}$ complex starts at about 0.8 V vs. NHE,

and complete reduction requires a potential of −0.1 V vs. NHE. At −0.1 V, hydrogen ions are reduced on platinum electrodes in acidic solution, whereas a mercury pool electrode is oxidized at potentials above 0.5 V; and the mercury reacts with the platinum complex to give platinum metal and insoluble mercury(I) chloride. These problems can be overcome by adding the platinum solution to a mercury pool electrode, to which the potential has already been applied. Impurities are not eliminated by pre-electrolysis, but are determined in a special blank.

EXPERIMENTAL

Apparatus

The controlled-potential coulometer with electronic integrator used was the ORNL-2005-X50 model (Indiana Instruments). The electrolysis cell with the mercury pool electrode was fitted with a stirrer, saturated silver chloride reference electrode and counter electrode, separated by a Vycor glass tube [10]. All manipulations were done in glove boxes.

Procedure

Dissolve 10—20 mg of the intermetallic compound in a mixture of 3 ml of concentrated hydrochloric acid and 1.5 ml of concentrated nitric acid. Add 20 mg of sodium chloride, and evaporate to dryness. Dissolve the residue in 2 ml of concentrated hydrochloric acid, and evaporate again. Finally, dissolve the residue in 2 ml of concentrated hydrochloric acid and dilute with water to 25 ml in a volumetric flask.

Transfer 2.5 ml of mercury, 5 ml of 1 M sulfuric acid and 0.1 ml of 1 M sulphamic acid to the electrolysis cell. Pass a stream of nitrogen through the solution and pre-electrolyse at a potential of −0.3 V vs. the saturated silver chloride electrode until a constant residual current of about 30 μA has been reached. Then switch on the integrator and add an aliquot of the sample solution containing up to 5 mg of platinum. Continue the electrolysis until the residual current is constant again. The quantity of electricity (Q_1 coulomb) which passed after addition of the sample, the residual current (i_1 A), and the electrolysis time (t_1 s) are measured.

Analyse a blank solution containing all reagents in the same way, and measure the quantity of electricity passed (Q_2), the residual current (i_2), and the electrolysis time (t_2).

The quantity of platinum in the electrolytic cell is calculated from the equation $(Q_1 - i_1 \cdot t_1) - (Q_2 - i_2 \cdot t_2) \cdot 0.5054$ = mg Pt, where 0.5054 is the electrochemical equivalent of platinum for reduction from the quadrivalent state to the metal.

The integrator is calibrated electrically as described in the operation manual.

RESULTS AND DISCUSSION

Reduction potential

For the following investigations a platinum solution was prepared from Specpure platinum metal by the above procedure. The conditions for complete recovery were established for aliquots containing 4 mg of platinum. The results reported in Table 1 indicate that a potential of −0.3 V vs. a saturated silver chloride electrode is most satisfactory.

TABLE 1

Recovery of platinum

Potential (V vs. sat. AgCl)	Electrolysis time (min)	Recovery (%)
+0.1	45	89.4
−0.1	18	98.6
−0.2	13	99.9
−0.3	10	99.8
−0.4	10	100.1

Standard deviation and accuracy

When 8 aliquots each containing 5 mg of platinum were analysed, the standard deviation was 6.4 μg. The mean recovery was 99.94% with a limit of confidence of ±0.09% at the 68% level when the standard deviation, the number of determinations and the possible errors of the integrator calibration and the balance were taken into account.

Influence of americium

Solutions of pure ^{241}Am gave high blanks, which increased with the age of the solution. However, after addition of a known amount of platinum to these solutions, the difference between found and expected platinum values diminished with time and became zero after 1 week. The high blanks of the americium solution are ascribed to the hydrogen peroxide formed by radiolysis. Addition of titanium(IV) sulfate to the americium solution gave

TABLE 2

Analysis of $AmPt_5$

	Preparation 1	Preparation 2
% Am	19.47	21.73
% Pt	80.05	77.83
% O	0.38	0.60
Total	99.90	100.16

the typical coloration of titanium peroxide. Platinum is known to catalyse the decomposition of hydrogen peroxide. The decrease in the blank in the presence of platinum demonstrates that the speed of decomposition of hydrogen peroxide is faster than that of its formation, so that no interference is to be expected in solutions of americium—platinum compounds. This is proved by the results for the total analysis of two different products with the nominal composition Am Pt_5 (Table 2).

The americium was determined by titration with EDTA [2] and the oxygen content was measured by hot extraction [11].

REFERENCES

1 W. Müller, J. Fuger and J. C. Spirlet, J. Inorg. Nucl. Chem., Supplement (1976) p. 139.
2 K. Buijs and W. Bartscher, Anal. Chim. Acta, 88 (1977) 403.
3 A. P. Blackmore, M. A. Marks, R. R. Barefoot and F. E. Beamish, Anal. Chem., 24 (1952) 1815.
4 R. G. Gardner, C. H. Ward and W. H. Ashley, LA-3176 (1965).
5 F. E. Beamish and W. A. E. McBryde, Anal. Chim. Acta, 9 (1953) 349.
6 W. Bartscher and W. Kramer, Anal. Chim. Acta, 63 (1973) 216.
7 F. E. Beamish, Anal. Chim. Acta, 44 (1969) 253.
8 A. J. Bard, Anal. Chem., 32 (1960) 623.
9 Y. Takata and G. Muto, Bunseki Kagaku, 15 (1966) 862.
10 L. M. Angeletti, W. J. Bartscher and M. J. Maurice, Z. Anal. Chem., 246 (1969) 297.
11 Comm. European Commun., Communication 3115, TUSR 16 (1973) p. 33.

Analytica Chimica Acta, 91 (1977) 143—148

DÉTERMINATION DU CADMIUM, DE L'INDIUM ET DU TELLURE PAR POLAROGRAPHIE IMPULSIONNELLE SANS SÉPARATION PRÉALABLE

SUON KIM NUOR et OLIVIER VITTORI

Laboratoire de Chimie Analytique III, Université de Lyon I, 43 Boulevard du 11 Novembre 1918, 69621 Villeurbanne (France)

(Reçu le 14 decembre 1976)

RÉSUMÉ

On propose une méthode de détermination du cadmium, de l'indium et du tellure par polarographie impulsionnelle différentielle. L'électrolyte support requis est KI 0,1 M dans l'acide tartrique saturé et doit être préparé sous azote. Dans ce milieu les pics de Cd, In et Te sont bien séparés et se prêtent au dosage sans séparation préalable. Le cadmium et le tellure présentent des interférences mutuelles mais le dosage reste précis. L'indium n'interfère pas. Une application au composé $CdIn_2Te_4$ est décrite.

SUMMARY

Cadmium, indium and tellurium can be determined without preliminary separation by differential pulse polarography in a specially prepared supporting electrolyte of 0.1 M KI saturated with tartaric acid. In this medium the three peaks are well separated. There is no interference for Cd—In and In—Te mixtures, but Cd—Te mixtures can prove difficult. However, the peak intensity of tellurium is over ten times that of cadmium for the same concentration, and it is possible to determine tellurium near the limit of detection. Cadmium is determined afterwards in more concentrated solution. Indium does not interfere. An application to $CdIn_2Te_4$ is reported.

Le dosage simultané du cadmium et de l'indium par les méthodes polarographiques n'est possible que dans peu de milieux car les potentiels de demi-vague de ces deux éléments sont en général très voisins. Un milieu composé selon: N_2H_4 3 M—NaOH 1 M a été décrit comme permettant une bonne séparation [1]. Cependant KI 0,1 M peut également être utilisé bien que le cadmium présente alors un maximum important [2—4]. Le tellure(IV) est réductible en milieu acide, neutre ou basique et la vague est déformée sur son plateau par un maximum très intense, sauf dans NaOH 1 M [5, 6]. Ce maximum peut être utilisé à des fins analytiques en polarographie à tension alternative surimposé et en polarographie à impulsions surimposées (p.i.s.) [7, 8]. Dans le présent article nous décrivons le dosage simultané de cadmium, de l'indium et du tellure dans un électrolyte support composé de KI 0,1 M et d'acide tartrique saturé à 25°C, sans recourir à une séparation préalable des trois éléments. Un exemple d'application à la détermination de la composition stoechiométrique du composé $CdIn_2Te_4$ est donné.

PARTIE EXPÉRIMENTALE

Appareillage et réactifs

Les polarogrammes sont obtenus avec l'ensemble PRG 4 Soléa-Tacussel. Le débit du capillaire, mesuré en circuit ouvert dans l'eau est de 0,388 mg s^{-1}. Les paramètres importants sont fixés aux valeurs suivantes: durée de l'impulsion 60 ms, mesure du courant entre 30 et 42 ms, durée de vie de goutte 3 s, amplitude de l'impulsion 20 mV.

Les étalons sont réalisés avec $InCl_3$, $3CdSO_4 \cdot 8H_2O$ et TeO_2 (Merck). L'acide tartrique et l'iodure de potassium sont de qualité Normapur (Prolabo). L'eau est déionisée puis bidistillée.

Préparation de l'électrolyte support. L'électrolyte support requiert certaines précautions lors de sa préparation car KI dans l'acide tartrique se colore rapidement en jaune indiquant l'apparition d'iode. Ainsi à une solution de KI de concentration supérieure à 0,1 M, soumise pendant 1 h à un barbottage d'azote pour éviter la présence d'oxygène, on ajoute progressivement, sous agitation magnétique l'acide tartrique solide. Après 3 h la saturation est considérée comme complète et la concentration en KI est ajustée à 0,1 M par addition d'une solution d'acide tartrique saturée et désoxygénée. Ainsi préparée et conservée sous azote la solution ne prend une légère teinte jaune qu'après 12 h environ. De plus il n'a pas été constaté de réelles différences dans les polarogrammes avec un électrolyte support légèrement coloré.

Solutions étalons. Les solutions étalons de In, Cd et Te sont préparées dans KI 0,1 M pour In et Cd et dans HCl 1 M pour Te, aux concentrations de 10^{-2} M. Les essais d'étalonnage par ajouts dosés avec une micropipette Eppendorf (10 μl) pour diluer au minimum l'électrolyte support, ont montré une reproductibilité de l'ordre de 1%.

Mise en solution de $CdIn_2Te_4$

La synthèse du composé $CdIn_2Te_4$ a été réalisée au laboratoire de chimie minérale III de l'Université Lyon 1. Le mélange homogène de CdO, In_2O_3 et Te est préparé dans la stoechiométrie Cd:In:Te = 1:2:4. Puis le mélange est placé dans une nacelle et porté progressivement à 600°C sous atmosphère d'hydrogène. Le produit obtenu est caractérisé par diffraction —X.

Le composé $CdIn_2Te_4$ dont nous disposons se présente sous forme d'une poudre fine de couleur grise. La dissolution d'une masse connue est faite avec 1 ml d'acide nitrique 12 M. Pour initier la réaction un chauffage très léger est nécessaire mais lorsque celle-ci a débuté elle se poursuit aisément et complètement hors de la flamme. Un dégagement de vapeurs rousses indique la présence de NO_2. La dissolution est totale quand ces vapeurs ont disparu. Les solutions des échantillons sont alors étendues à 10 ml par l'eau.

RÉSULTATS ET DISCUSSION

L'acide méso-tartrique utilisé dans la présente étude a une solubilité de 20 g l^{-1} environ à température ordinaire [9]. Compte tenu des valeurs des pK_a des deux acidités de l'acide tartrique (respectivement pK_{a_1} = 3,22 et pK_{a_2} = 4,82) un calcul montre que le pH doit être de 1,76 et la concentration en ion H_3O^+ de $1{,}74 \cdot 10^{-2}$ M. En présence de KI 0,1 M ces valeurs sont assez bien confirmées, le pH étant de 1,8—1,9. La présence de KI fait regresser un peu la solubilité de l'acide tartrique et ceci se constate expérimentalement quand nous préparons l'électrolyte support.

La forte dissociation de cet acide nous place à l'abri de variations légères du pH qu'auraient pu provoquer les ajouts dosés de tellure en solution chlorhydrique ou des échantillons dissous de $CdIn_2Te_4$.

Dans l'électrolyte support KI 0,1 M—acide tartrique saturé, les potentiels des pics de réduction de l'indium et du cadmium sont réspectivement à —0,54 et —0,64 V vs. ECS, c'est à dire environ 10 mV plus anodique que les $E_{1/2}$ ce qui est inhérent à l'usage de la p.i.s. La réduction du tellure est plus complexe. Le tellure(IV) en solution sous forme d'acide tellureux H_2TeO_3 se réduit d'abord en Te(0) adsorbé sur la goutte de mercure [7, 8] puis en tellurure (Te(—II)) selon un processus sans doute catalytique et dépendant du pH [5]. Sur la vague polarographique classique ceci se traduit par un maximum situé sur le plateau et très intense. En p.i.s. nous observons un pic, déformé dans sa partie cathodique pour les concentrations supérieures à 10^{-5} M, et dont nous avons rapporté antérieurement la variation linéaire avec la concentration [7]. Dans la présente communication les dosages du tellure sont faits sur le pic observé à —0,82 V vs. ECS qui correspond à la réduction Te(0) → Te(—II) compte-tenu du rapport élevé de l'intensité sur la concentration d'une part, et de la valeur assez négative du potentiel d'autre part. La première étape Te(IV) → Te(0) est alors confondue avec le tracé de l'électrolyte support antérieurement à —0,35 V vs. ECS ce qui serait conforme avec le comportement du tellure en milieu acide (Fig. 1).

La première partie de notre étude a porté sur la recherche des interférences mutuelles des trois éléments pris séparément deux à deux. Dans le Tableau 1 nous rapportons quelques essais typiques sur les couples In—Cd et In—Te. Il s'est avéré que ces couples avaient un comportement électrochimique normal et qu'un large excès d'un constituant par rapport à l'autre ne permettait pas l'observation d'une interférence. Les variations des intensités des pics des éléments dont la concentration varie ici de 0 à 10^{-4} M indiquent que les rapports $i/[M]$ sont constants (M = In, Cd, Te).

Par contre l'étude du couple Cd—Te est plus complexe car chaque élément influe nettement sur la détermination de l'autre. L'addition de tellure entre 0 et 10^{-4} M à une solution de cadmium montre que l'intensité i_{Te} du pic croît d'abord linéairement avec la concentration mais à partir de [Cd] ≈ [Te] cette intensité évolue beaucoup moins rapidement. Enfin si [Te] > 10[Cd], i_{Te} croît à nouveau (Fig. 2). Similairement l'addition de Cd

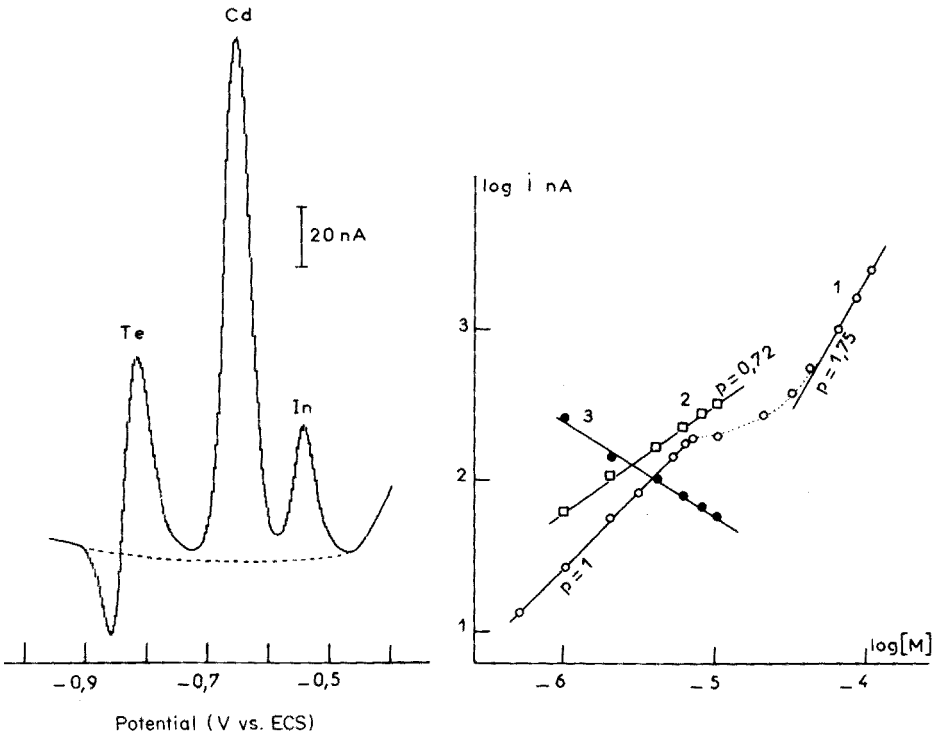

Fig. 1. Polarogramme en p.i.s. de In, Cd et Te aux concentrations: $[In^{3+}] = 10^{-5}$ M, $[Cd^{2+}] = 3 \cdot 10^{-6}$ M, $[Te^{IV}] = 2 \cdot 10^{-6}$ M.

Fig. 2. Interférences mutuelles du cadmium et du tellure. Courbe 1, évolution de l'intensité du pic du tellure en présence de cadmium $2{,}5 \cdot 10^{-6}$ M. Courbe 2, évolution de l'intensité du pic du cadmium en présence de tellure 10^{-5} M. Courbe 3, influence de l'addition du cadmium (courbe 2) sur l'intensité du pic du tellure 10^{-5} M.

TABLEAU 1

Variation de l'intensité du pic de Cd, In, Te à concentration constante

Couple	Elément à concentration constante	Elément à concentration variable	Nombre de mesures	Intensité du pic de l'élément à concentration fixe (nA)
Cd—In	$2{,}5 \cdot 10^{-6}$ M Cd	$0 \rightarrow 10^{-4}$ M In	13	$i_{Cd} = 129 \pm 1$
Cd—In	$2{,}5 \cdot 10^{-5}$ M In	$0 \rightarrow 10^{-4}$ M Cd	12	$i_{In} = 108 \pm 2$
In—Te	$2{,}5 \cdot 10^{-6}$ M Te	$0 \rightarrow 10^{-4}$ M In	13	$i_{Te} = 130 \pm 1$
In—Te	10^{-5} M In	$0 \rightarrow 10^{-4}$ M Te	12	$i_{In} = 50 \pm 2$

à une solution de tellure 10^{-5} M montre une relation entre i_{Cd} et [Cd] selon une puissance 0,72, tandis que le pic du tellure diminue. Il semble que le Te(0) adsorbé sur l'électrode joue un rôle vis à vis du cadmium, soit en inhibant partiellement la réduction ce qui expliquerait la pente de 0,72 soit en formant un composé intermétallique en surface du mercure. Bien qu'aucune

preuve de cette seconde hypothèse ne puisse être avancée ici, il faut signaler que Brainina a déjà cité plusieurs exemples similaires [10]. De plus dans le cas du couple In—Te la réduction de l'indium qui n'est pas affectée fait davantage incliner vers cette seconde hypothèse, aucun composé intermétallique entre Te et In ne se formant alors qu'une inhibition antérieure devrait aussi affecter i_{In}.

La déformation du pic du cadmium devient nette dès que la concentration en tellure est environ dix fois supérieure (Fig. 3).

Nous avons observé aussi les variations de i_{In}, i_{Cd} et i_{Te} dans le mélange ternaire. Nous retrouvons assez bien les comportements précédemment signalés notamment la courbe en trois segments pour le tellure et une pente de 0,63 pour i_{Cd} (Fig. 4). Il apparait surtout dans ce qui suit que la mesure du tellure est difficile dans une zone où $[Cd] < [Te] \leqslant 10[Cd]$, or le composé $CdIn_2Te_4$ nous place dans ce domaine.

Cependant ce domaine est beaucoup plus simple à traiter quand [Cd] est faible. Comme par ailleurs le pic du tellure est, à concentrations semblables, beaucoup plus intense que celui du cadmium, nous avons été conduit à la procédure qui suit. En premier lieu nous déterminons le tellure très près de

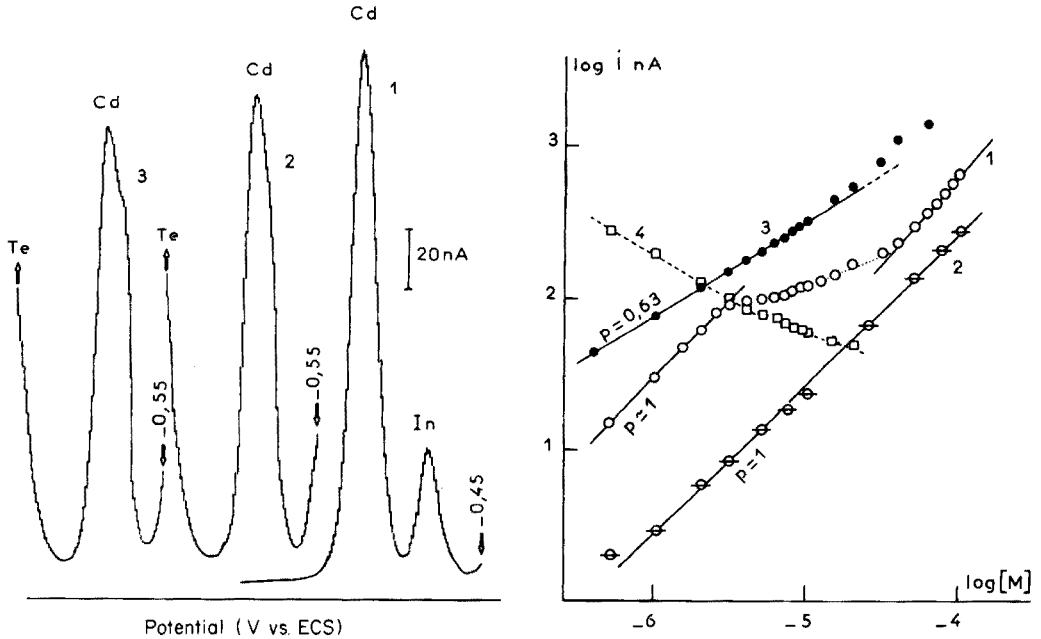

Fig. 3. Déformation progressive du pic cadmium $2{,}5 \cdot 10^{-6}$ M lors de l'addition de tellure. 1, 0; 2, $1{,}5 \cdot 10^{-5}$ M; 3, $3{,}2 \cdot 10^{-5}$ M.

Fig. 4. Interférences mutuelles du cadmium, de l'indium et du tellure. Courbe 1, évolution de l'intensité du pic du tellure en présence de cadmium $3 \cdot 10^{-6}$ M et d'indium 10^{-5} M. Courbe 2, évolution du pic de l'indium en présence de cadmium $5 \cdot 10^{-6}$ M et du tellure $5 \cdot 10^{-6}$ M. Courbe 3, évolution du pic du cadmium en présence d'indium 10^{-5} M et de tellure 10^{-5} M. Courbe 4, variation du pic du tellure 10^{-5} M lors de l'addition de cadmium (conditions de la courbe 3).

la limite de détection ($5 \cdot 10^{-7}$—10^{-6} M). Puis sur une solution plus concentrée du composé $CdIn_2Te_4$ le cadmium est déterminé en tenant compte de la pente apparente inférieure à l'unité du graphique i_{Cd} en fonction de [Cd] qui se déduit des variations dues à des ajouts dosés. Les résultats se sont révélés satisfaisants (Tableau 2). La détermination de l'indium ne pose pas de problèmes.

TABLEAU 2

Dosage de In, Cd, Te dans le composé $CdIn_2Te_4$

Échantillon	Masse (mg)	Te (mg)		In (mg)		Cd (mg)	
		Théor.	Expér.	Théor.	Expér.	Théor.	Expér.
1	115,20	69,20	69,45	31,00	30,85	15,20	15,07
2	61,80	37,14	36,98	16,62	16,65	8,16	7,89
3	41,60	25,00	25,00	11,19	11,20	5,49	5,43
4	38,00	22,84	22,60	10,22	9,80	5,02	5,17
5	21,00	12,62	11,15	5,65	5,40	2,77	2,77
6	15,40	9,26	8,93	4,14	3,95	2,03	1,92

Nous tenons à remercier M. Roubin Maître-Assistant, pour la fourniture des échantillons.

BIBLIOGRAPHIE

1 C. Pecker, M. Herlem et J. Badoz-Lambling, Fresenius Z. Anal. Chem., 224 (1967) 302.
2 P. Zuman, Collect. Czech. Chem. Commun., 15 (1950) 1111.
3 I. M. Kolthoff et J. J. Lingane, Polarography, Interscience, New York, 1952.
4 R. Pointeau et J. Bonastre, Eléments de Polarographie, Masson, Paris, 1970.
5 J. J. Lingane et L. W. Niedrach, J. Am. Chem. Soc., 70 (1948) 4115; 71 (1949) 196.
6 I. I. Nazarenko et A. N. Ermakov, Selenium and Tellurium, Wiley, New York, 1972.
7 M. Volaire, O. Vittori et M. Porthault, Anal. Chim. Acta, 71 (1974) 185.
8 M. Volaire, O. Vittori et M. Porthault, Bull. Soc. Chim. Fr., (1974) 823.
9 F. C. Whitmore, Organic Chemistry, Dover, New York, 1961.
10 Kh. Z. Brainina, Stripping Voltammetry in Chemical Analysis, Wiley, New York, 1974.

Analytica Chimica Acta, 91 (1977) 149—156

A SELF-GENERATING THIRD-ORDER ELECTRODE

Part II. Analytical Applications of the Silver—Silver Sulphide Electrode

JØRGEN BIRGER JENSEN

Fysisk-Kemisk Institut, Danmarks Tekniske Højskole, DK-2800 Lyngby (Denmark)

(Received 27th September 1976)

SUMMARY

Analytical applications of the silver—silver sulphide electrode are illustrated by potentiometric determinations of Cd(II) and Pb(II) ions. The stability of the electrode potential in the presence of oxidizing agents is demonstrated by various titrations with silver(I) solutions. The influence of pH on the electrode potential in pure acidic solutions is noted. The electrode used was prepared by electrolytic deposition of silver sulphide on a silver rod; after 2 years, it remained reliable, and was unaffected by light under normal laboratory conditions.

Several types of ion-selective electrode sensitive to Cd(II) and Pb(II) have been reported [1—4]; some of these electrodes are commercially available. In the present paper it is shown that potentiometric titrations of Cd(II) and Pb(II) can be done just as well with a silver—silver sulphide electrode. For such determinations, this electrode can be regarded as a reliable, rapid, simple and inexpensive alternative to the more complicated and expensive commercial solid-state electrodes.

It has already been shown [5] that the silver—silver sulphide electrode probably acts as a self-generating third-order electrode, and can be treated mathematically on this assumption. Accordingly emphasis in [5] was placed on the agreement between theoretical expectations and experimental performance, rather than on practical applications. The applicability of the electrode is proved by potentiometric titrations of Cd(II) and Pb(II), usually with an automatic titrator suitable for routine work. The titrants selected are either stable or very easily restandardized. The pH and redox sensitivity of the silver—silver sulphide electrode is discussed.

EXPERIMENTAL

Apparatus and reagents

All the instruments were obtained from Radiometer, Copenhagen. An expanded-scale pH meter (PHM26) was used with an automatic titrator (ABU1, TTT11, SBR2) and a Servograph recorder (REC51). The indicator

electrode was a silver metal electrode (P4011) on which silver sulphide was electrolyzed. The reference electrode was either a Hg/Hg_2SO_4, K_2SO_4 (sat.) electrode (K601) or a Hg/Hg_2Cl_2, KCl (sat.), $NaNO_3$ (1 M) electrode (K701). The $NaNO_3$ solution was renewed daily to avoid diffusion of KCl into the solution. The pH was measured with a glass electrode (G202C) and one of the above reference electrodes. Measurements were made in a thermostatted cell at 25 ± 0.1 °C. Where relevant, the ionic strength was kept constant with sodium nitrate.

All the chemicals were of analytical grade and were used without further purification.

Characteristics of the silver—silver sulphide electrode

The electrode employed for the measurements reported here was identical to the electrode described previously [5]; it was prepared and stored in the same way. The electrodes used have functioned for over two years without any indications of ageing, i.e. erroneous results, decrease in response time or unstable potentials. When the electrode was stored in distilled water, practically no memory effect was observed, and the electrode was ready for use almost instantly. When stored in 0.1 M sodium sulphide, the electrode must be rinsed thoroughly with distilled water; even then there was a drift in the electrode potential towards positive values, showing that it is difficult to remove all the sulphide ions from the surface of the electrode. The concentration of the residual sulphide was of course very small and without analytical significance. After about 30 min a stable electrode potential was established, and the titrations could be carried out without problems.

THEORY

Consider an aqueous solution of metal ions, Me^{2+}, which form a metal sulphide with a very low solubility product. A stable electrode potential is observed on a silver—silver sulphide electrode immersed in such a solution provided that MeS is formed on the electrode surface [5]. The electrode potential can be calculated from the Nernst equation

$$E = E^0 + \frac{RT}{2F} \ln \frac{a_{Me^{2+}}}{a_{Me}} \tag{1}$$

Normally E^0 is known, and to predict the electrode potential the unknown term a_{Me} must be evaluated. The deviation from stoichiometry of silver sulphide is very small [6—9]. If this is also true for MeS, and if MeS and Ag_2S can be considered to behave as two thermodynamically separate phases without any tendency to mix, then it can be shown that

$$\mu_{Me} = \mu^0_{MeS} - \mu^0_{Ag_2S} = RT \ln a_{Me} \tag{2}$$

The Nernst equation valid for the potential of the silver—silver sulphide electrode measuring metal ions can then be expressed as:

$$E = E^0 - \frac{(\mu^0_{MeS} - \mu^0_{Ag_2S})}{2F} + \frac{RT}{2F} \ln a_{Me^{2+}} \quad (3)$$

or

$$E = E^{0'} + \frac{RT}{2F} \ln a_{Me^{2+}} \quad (4)$$

When the values of μ^0_{MeS} and $\mu^0_{Ag_2S}$ from Latimer [10] are used at zero ionic strength, the $E^{0'}$ value for Cd(II) is found to be 122 mV, and the value for Pb(II) is 151 mV.

Three conclusions can be drawn from the above. First it is possible to explain thermodynamically the potential stability of the Ag/Ag_2S electrode when the electrode measures metal ions which form insoluble metal sulphides. Secondly, the potential of the Ag/Ag_2S electrode measuring metal ions in aqueous solutions can be predicted from the Nernst equation. This potential is always more positive than that obtained with a metal rod in the same solution, hence the Ag/Ag_2S electrode acts as the more noble electrode. Thirdly, only if pure silver metal is present in the equilibria at the surface of the Ag/Ag_2S electrode would the potential be expected to be stable for long periods. If μ_{Ag} is not zero, then $E^{0'}$ would have a value differing from that calculated above. This alone would not affect the electrode function, but if the value of μ_{Ag} varies in an uncontrolled manner, a drift or fluctuation in potential would be recognized. If only a mixture of metal sulphide and silver sulphide were used as electroactive material, then μ_{Ag} would have no fixed value but would vary from zero (where silver metal is present in the mixture) to the value of μ_{Ag_2S} (where sulphur is formed in the mixture). This behaviour of sulphide mixtures may perhaps explain the drift in electrode potentials which are sometimes reported for solid-state electrodes based on Ag_2S/Mes mixtures. Occasionally, electrical disturbances would change the value of μ_{Ag} — and thus also of μ_{Me} and a_{Me} — in such electrodes.

RESULTS AND DISCUSSION

Potentiometric titrations of cadmium(II)

Sodium hydroxide and sodium oxalate were examined as titrants. Cadmium hydroxide shows no amphoteric properties [11]; the solubility product is $2 \cdot 10^{-14}$ $(mol\ l^{-1})^3$ at zero ionic strength [10]. To estimate the accuracy of Cd(II) titrations with sodium hydroxide, weighed amounts of cadmium(II) nitrate were dissolved in 20 ml of water and titrated with a NaOH solution which had been freshly standardized against a Fixanal nitric acid solution. The results are summarized in Table 1. Aliquots of a stock 0.1 M cadmium(II) nitrate solution were also titrated; one such titration is shown in Fig. 1A. In all titrations, precipitation of the hydroxide was quick, and there was no tendency to form supersaturated solutions.

Figure 1B shows a titration curve of $Cd(NO_3)_2$ with a saturated solution of sodium oxalate. To estimate the accuracy of the titrations, aliquots of

TABLE 1

Summary of the data from Cd(II) and Pb(II) titrations

Amount taken (mmol)	Amount found, mean (mmol)	Relative error (%)	No. of detns.
$Cd(NO_3)_2 \cdot 4\ H_2O$ titrated with 0.1 M NaOH			
0.211	0.213	0.9	1
0.136	0.134	1.5	1
0.228	0.232	1.7	1
0.217	0.219	0.9	1
0.304	0.302	0.7	1
$Cd(NO_3)_2 \cdot 4\ H_2O$ titrated with Na oxalate (saturated)			
0.1	0.097	3	3
0.2	0.198	1	4
0.3	0.307	3.5	4
0.4	0.410	2.5	3
$Pb(NO_3)_2$ titrated with Na oxalate			
0.1	0.102	2	3
0.2	0.197	1.5	4
0.3	0.295	1.7	4
0.4	0.396	1	3
$Pb(NO_3)_2$ titrated with Na_2SO_4			
1.0	0.975	2.5	6
1.5	1.475	1.7	6
2.0[a]	1.98	1	5
3.3[a]	3.500	0.7	5

[a]In a 1:1:2 ethanol—acetone—water medium.

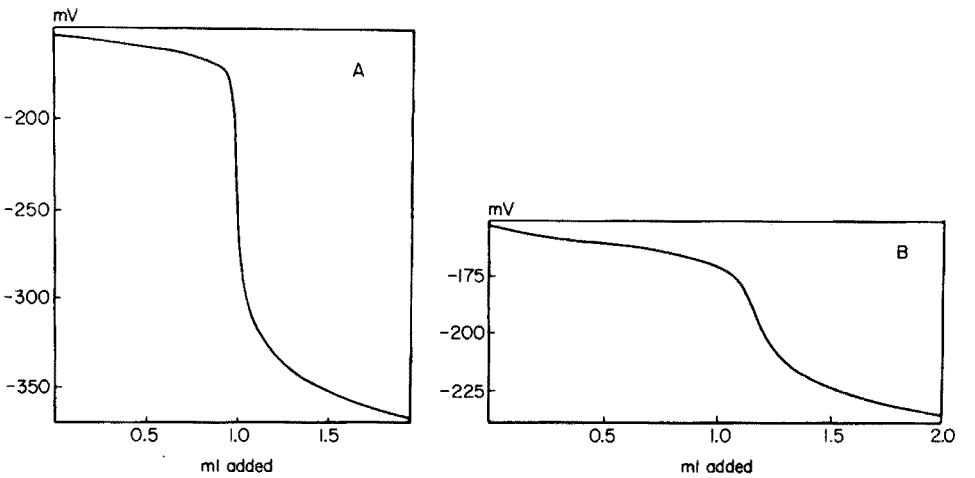

Fig. 1. (A) Titration of 5 ml of 0.1 M $Cd(NO_3)_2$ + 15 ml of water with 1.0 M NaOH. (B) Titration of 3 ml of 0.1 M $Cd(NO_3)_2$ + 17 ml of water with a saturated $Na_2C_2O_4$ solution. Indicator electrode Ag/Ag_2S. Reference electrode Hg/Hg_2Cl_2, KCl (sat.), $NaNO_3$ (1.0 M). Potentials relative to the reference electrode.

0.1 M $Cd(NO_3)$ were titrated after dilution with water to 20 ml. No problems were encountered. The results are summarized in Table 1.

The solubility product of $CdCO_3$ is about $5 \cdot 10^{-12}$ $(mol\ l^{-1})^2$ [10]. The titration of $Cd(NO_3)_2$ with Na_2CO_3 was carried out manually so that the pH variation could also be followed (Fig. 2). In the pure 0.01 M $Cd(NO_3)_2$ solution, the pH is about 5.3; when Na_2CO_3 is added, the pH is raised to about 6.1, and then $CdCO_3$ precipitates. The consumption of carbonate in increasing the pH from 5.3 to 6.1 has, of course, no analytical significance. Figure 2 suggests that carbonate could also be titrated.

Potentiometric titrations of lead (II)

The automatic titration equipment was used with sodium oxalate and sodium sulphate as titrants. The following values have been reported [12]

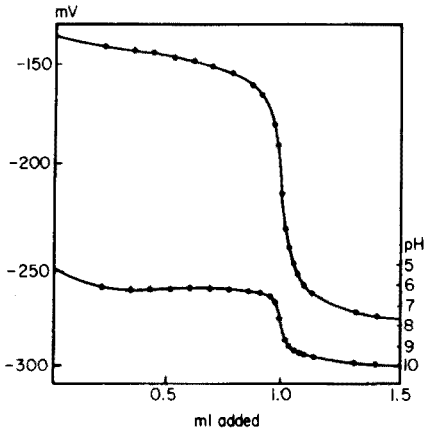

Fig. 2. Upper curve: titration of 10 ml of 0.01 M $Cd(NO_3)_2$ with 0.1 M Na_2CO_3 (Ag/Ag_2S electrode). Lower curve: pH variation during the titration (glass electrode). Reference electrode for both, Hg/Hg_2SO_4, K_2SO_4 (sat.). Potentials calculated relative to SCE.

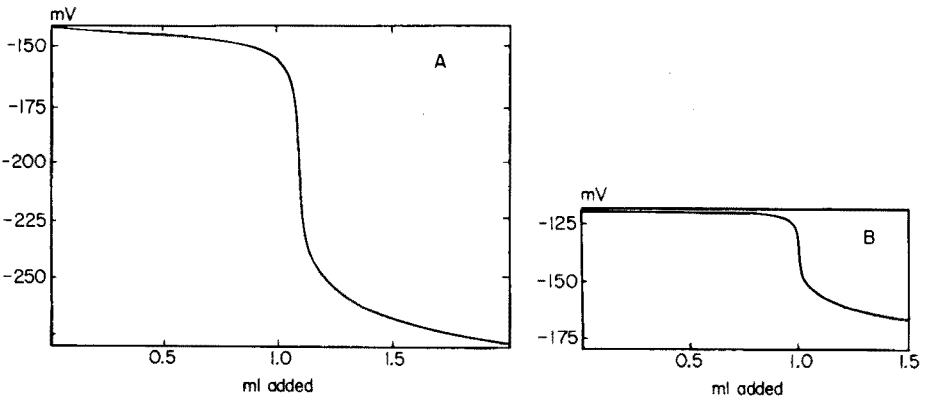

Fig. 3. (A) Titration of 3 ml of 0.1 M $Pb(NO_3)_2$ + 17 ml of water with a saturated solution of $Na_2C_2O_4$. (B) Titration of 10 ml of 0.1 M $Pb(NO_3)_2$ + 5 ml of acetone + 5 ml of ethanol with 1.0 M Na_2SO_4. Electrode system as for Fig. 1.

for the solubility products: $S_{PbC_2O_4} = 2.74 \cdot 10^{-11}$ (mol l^{-1})^2 and $S_{PbSO_4} = 1.06 \cdot 10^{-8}$ (mol l^{-1})^2 (18°C). A typical titration curve with oxalate as titrant is shown in Fig. 3A. The titration was carried out similarly to the Cd—oxalate titration. The results are summarized in Table 1.

Various potentiometric titrations and measurements of sulphate ions with ion-selective electrodes as monitoring devices have been reported; iron-selective electrodes [13], sodium-selective glass electrodes [14], and coated-wire ion-selective electrodes [15] have been used. In relation to the present work, the sulphate-selective membrane electrode of Mohan and Rechnitz [16] is interesting. This electrode is based on a four-component mixture of $PbSO_4$, PbS, Ag_2S, and Cu_2S; Cu_2S was incorporated to improve the dynamic properties of the electrode, and did not affect the value of the equilibrium potential [16]. It seems reasonable to suggest that similar electrode reactions occur with the membrane electrode and with the Ag/Ag_2S electrode, the theory outlined above being applicable in both cases. As mentioned earlier [5], PbS must be formed at the surface of the Ag/Ag_2S electrode; thus if solid $PbSO_4$ is added to the solution, it should be possible to measure sulphate with the Ag/Ag_2S electrode. Accordingly, titrations of Pb(II) with sulphate solution are possible if the lead(II) activity in the solutions exceeds about 10^{-12} mol l^{-1}. Figure 3B shows a titration curve of lead nitrate with sodium sulphate. To improve the potential jump at the equivalence point the titration was carried out in a 1:1:2 acetone—ethanol—water mixture, in which lead sulphate is less soluble than in pure water. To estimate the accuracy of the titrations with sulphate samples of lead nitrate solution varying from 0.05 mol l^{-1} to 0.33 mol l^{-1} were titrated with 1.0 M Na_2SO_4; the results are summarized in Table 1.

Sensitivity of the Ag/Ag_2S electrode to acids and oxidizing agents

Light and Swartz [17] have expressed doubts about the reliability of the Ag/Ag_2S electrode for measurements under highly oxidizing conditions. They titrated chloride with silver(I) solution in the presence of strong oxidants (1 M nitric acid plus 0.1 M iron(III)), measuring the potential variation during the titration with an Orion homogeneous Ag_2S membrane electrode and with a conventional Ag/Ag_2S electrode. They found that while the membrane electrode was unaffected by the oxidizing conditions and indicated the expected titration curve, the Ag/Ag_2S electrode gave misleading results. Attempts to reproduce these results in the present work failed. Figure 4 shows titration curves for chloride under acidic, oxidizing and normal conditions; the titration curves are very much alike, and the results were found to be very reliable under all conditions tested. These results do not support the statement that Ag/Ag_2S electrodes give erroneous results under oxidizing conditions. When the titrations were attempted in 1 M HNO_3, a slight smell of H_2S appeared, and the titrations were therefore not completed.

Potentiometric acid—base titrations

The pH dependence of the potential of the Ag/Ag_2S electrode has been evaluated by Mirna [18], and used in a calibration procedure by Crombie et al. [19]. If the total amount of sulphur is constant, then the pH dependence can be written [18]

$$E = \text{const} + \frac{RT}{2F} \ln\left(1 + \frac{a_{H^+}}{K_2} + \frac{a_{H^+}^2}{K_1 K_2}\right) \quad (5)$$

where K_1 and K_2 are the dissociation constants of hydrogen sulphide. The values of pK_1 and pK_2 are close to 7.0 and 13.0, respectively, hence it should be possible, in the normal pH range in aqueous solutions, to carry out pH titrations with an Ag/Ag_2S indicator electrode. This was verified (Fig. 5) for the titration of perchloric acid with sodium hydroxide; the equivalence point was found to be the same in an identical titration with a glass indicator electrode. Difficulties occurred in obtaining stable and reproducible potentials in the initial phase of the titration, but there were no later complications; the fluctuation of the initial potentials made it impossible to precalculate these potentials or the magnitude of the potential jump. With regard to analytical applications, the titrations can be done quickly and accurately. As well as perchloric acid, nitric acid can be titrated; chloric acid presents difficulties because of chloride ions, but even this titration is possible if some sodium sulphide (10^{-5}—10^{-4} M) is added to the chloric acid solution.

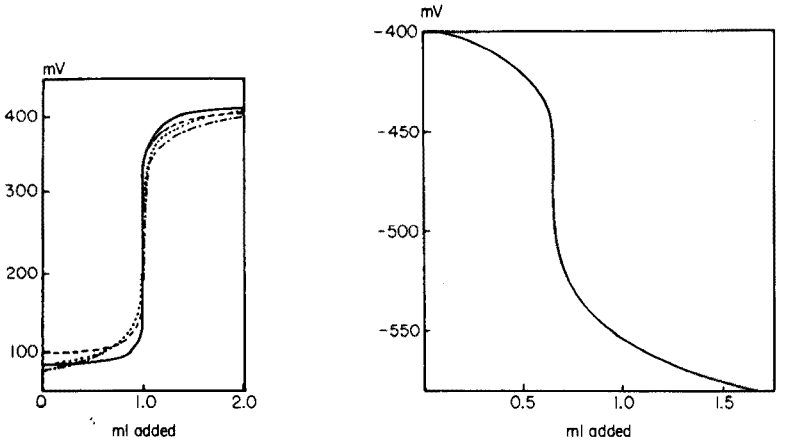

Fig. 4. Titrations of 1 ml of 1.0 M NaCl and 50 ml of 1.0 M $NaNO_3$ with silver(I) solutions under varying acidic and oxidizing conditions. Normal conditions, (——) i.e. pH 4.9; (--------) acidic conditions, pH 0.5 (HNO_3); (·····) pH 0.5 (HNO_3) but oxygen was bubbled through the solution; (—·—·—) pH 0.5 (HNO_3) with 1 ml of 0.1 M $Ce_2(SO_4)_3$ added. Electrode system as for Fig. 1.

Fig. 5. Titration of 0.25 ml of 1.0 M $HClO_4$ and 20 ml of water with 0.385 M NaOH. Indicator electrode, Ag/Ag_2S. Reference electrode, Hg/Hg_2SO_4, K_2SO_4 (sat.). Potentials relative to the reference electrode.

The author thanks his colleagues at Fysisk-Kemisk Institut for advice, encouraging discussions, and linguistic criticism, and Jette Klausen for skilled technical assistance.

REFERENCES

1 J. W. Rose, in R. A. Durst (Ed.), Ion-Selective Electrodes, N.B.S. Monograph 3, Washington, 1969.
2 J. Růžička and C. G. Lamm, Anal. Chim. Acta, 53 (1971) 206; 63 (1973) 115.
3 M. Mascini and A. Liberti, Anal. Chim. Acta, 60 (1970) 405; 64 (1973) 63.
4 H. Hirata and K. Higashiyama, Anal. Chim. Acta, 54 (1971) 414; Z. Anal. Chem., 257 (1971) 104.
5 J. B. Jensen, Anal. Chim. Acta, 76 (1975) 279 (Part I).
6 C. Wagner, J. Chem. Phys., 21 (1953) 1819.
7 H. Rickert, Einfuhrung in die Electrochemie fester Stoffe, Springer-Verlag, Berlin, 1973.
8 B. Hartmann, H. Rickert and W. Schendler, Electrochim. Acta, 21 (1976) 319.
9 M. Koebel, Anal. Chem., 46 (1974) 1559.
10 W. M. Latimer, The Oxidation States of the Elements and their Potentials in Aqueous Solutions, Prentice-Hall, New York, 2nd edn. 1952.
11 J. B. Jensen, Acta Chem. Scand., 26 (1972) 4031.
12 Handbook of Chemistry and Physics, 50th edn. (1969—1970) B252.
13 R. Jasinski and I. Trachtenberg, Anal. Chem., 44 (1972) 2373.
14 N. Akimoto and K. Hozomi, Anal. Chem., 46 (1974) 766.
15 H. James, G. Carmack and H. Freiser, Anal. Chem., 44 (1972) 856.
16 M. S. Mohan and G. A. Rechnitz, Anal. Chem., 45 (1973) 1323.
17 T. S. Light and J. L. Swartz, Anal. Lett., 1 (1968) 825.
18 A. Mirna, Z. Anal. Chem., 254 (1971) 114.
19 D. J. Crombie, G. J. Moody and J. D. R. Thomas, Anal. Chim. Acta, 80 (1975) 1.

Analytica Chimica Acta, 91 (1977) 157—163

CELLULE À CIRCULATION POUR DES MESURES ÉLECTROCHIMIQUES ET SPECTROPHOTOMÉTRIQUES SIMULTANÉES

M. SOULARD, F. BLOC et A. HATTERER

Laboratoire de Chimie Minérale Appliquée, École Supérieure de Chimie de Mulhouse, 3, rue Alfred Werner, 68093 Mulhouse Cedex (France)

(Reçu le 24 octobre 1976)

RÉSUMÉ

Une cellule à circulation ouverte, couplant des mesures électrochimiques et spectrophotométriques, est décrite. Elle permet l'identification de composés instables et l'étude de leur cinétique de décomposition. Les caractéristiques de cette cellule ont été examinées, en particulier, l'influence de différents paramètres hydrodynamiques sur le courant limite de diffusion.

SUMMARY

An open flow cell, for simultaneous electrochemical and spectrophotometric measurements, is described. It can be used in the identification of unstable compounds and in studies of their kinetics of decomposition. The characteristics of this cell have been examined, especially the effect of different hydrodynamic parameters on the limiting diffusion current.

L'analyse qualitative et quantitative d'espèces instables en solution, pour préciser les cinétiques et les mécanismes d'évolution, peut être facilitée par le couplage de techniques basées sur des propriétés différentes. Pour l'étude des systèmes Br_2, Cl_2—NH_3—H_2O, nous avons réalisé une cellule à circulation ouverte assurant des concentrations locales constantes en composants avec couplage de mesures électrochimiques (voltampérométrie) et spectrophotométriques (absorption optique).

PRINCIPE — DESCRIPTION

En circuit ouvert, un flux de réactif A (solution Br_2) et un flux de réactif B (solution NH_4^+) se mélangent et forment des composés C_i instables (bromamines). Ces derniers sont à concentration c_i fixes à une distance x de l'injecteur correspondant à un temps de contact $t = x/V$ pour une vitesse moyenne constante V du mélange [1]. Un capteur optique à la distance $x—\epsilon$ et un capteur électrochimique à la distance $x + \epsilon$ (ϵ négligeable devant x) permettent l'identification et le dosage simultanés des espèces A et C_i par deux techniques complémentaires.

La cellule (Fig. 1) comprend un tube cylindrique en silice avec deux fenêtres planes parallèles (tétrasil quartex). A sa base un injecteur est relié à deux pompes péristaltiques pour introduire les solutions A et B stockées en réservoirs thermostatés. L'électrode indicatrice tournante, dont l'élément sensible est un disque de carbone vitreux, est fixée à un arbre guidé dans un

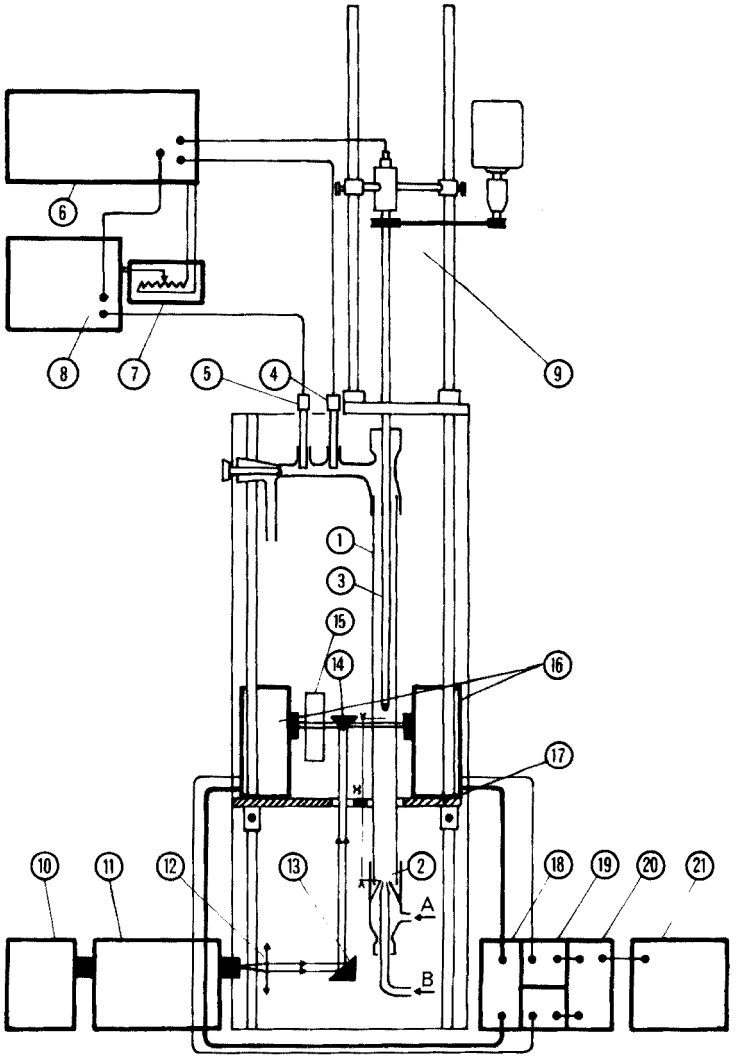

Fig. 1. Schéma du montage. (1) Tube de mesure; (2) injecteur; (3) électrode de travail; (4) électrode de référence; (5) électrode auxiliaire; (6) potentiostat; (7) potentiomètre; (8) enregistreur; (9) dispositif de guidage; (10) source lumineuse; (11) monochromateur; (12) lentille; (13) miroir; (14) prisme; (15) référence; (16) photomultiplicateurs; (17) chariot; (18) alimentation haute tension; (19) amplificateurs opérationnels; (20) amplificateur logarithmique de rapport; (21) enregistreur.

palier étanche. Au-dessus un dispositif mécanique assure la rotation et la translation verticale de l'électrode. La liaison électrique est réalisée par un fil métallique en contact avec une goutte de mercure. Sur un tube latéral, les électrodes de référence (calomel : ECS) et auxiliaire (Pt) sont branchées au potentiostat (Tacussel type PRT 20) avec pilote externe (Tacussel type Synchroscript) couplé à l'enregistreur (Tacussel type EPL 1). Pour les mesures optiques (DO = $f(\lambda)$) à divers niveaux x, un montage différentiel est réalisé à partir d'éléments M.P.I. (MacKee Pedersen Instruments). Le faisceau lumineux issu du monochromateur, renvoyé verticalement par un miroir, est dédoublé par un prisme solidaire d'un chariot; fixés sur celui-ci deux photomultiplicateurs reçoivent respectivement les faisceaux d'analyse et de référence.

Par ailleurs, divers montages de mesures d'absorption optique sont proposés pour des dosages catalytiques [2, 3], pour l'analyse de composés injectés dans un flux de solution [4] et pour l'étude de cinétiques rapides par la méthode du "flux stoppé" [5, 6].

MESURES ÉLECTROCHIMIQUES ET SPECTROPHOTOMÉTRIQUES

Obtention du régime de diffusion stationnaire

Le tracé des courbes $i = f(E)$ nécessite un régime de diffusion stationnaire à la surface de l'électrode, obtenu en provoquant un déplacement de l'électrode par rapport à la solution. Pour une électrode à disque tournant, selon Levich [7], le courant limite de diffusion s'exprime

$$i_L = knFAD^{2/3}\,\nu^{-1/6}\omega^{1/2}C.$$

(les abréviations utilisées correspondent à la notation habituelle, en particulier ω est la vitesse angulaire et ν la viscosité cinématique).

Dans les systèmes à circulation, l'influence des paramètres hydrodynamiques sur le courant de diffusion a été étudiée [8, 9]. Pour une électrode dont la surface est perpendiculaire à la direction d'un courant laminaire, Matsuda [10] exprime le courant limite de diffusion par

$$i_L = knFAD^{2/3}\,\nu^{-1/6}L^{-1/2}V^{1/2}C$$

où V est la vitesse de l'écoulement et L une caractéristique d'électrode.

Récemment, divers auteurs [11—14] ont appliqué la voltampérométrie hydrodynamique à diverses cellules pour l'étude analytique de systèmes variés. Dans notre cellule, le régime de diffusion stationnaire est établi à la fois par l'écoulement de la solution et la rotation de l'électrode; la simple circulation de réactifs dans une large gamme de débits entraînerait des variations importantes du courant limite.

Essais voltampérométriques

Nous avons testé la cellule en étudiant la réduction de HBrO en présence de Br^- suivant la réaction

$HBrO + H^+ + 2\,e^- \rightleftharpoons Br^- + H_2O$

Les courbes $i = f(E)$ (Fig. 2) concernent des solutions tamponnées et désoxygénées de Br^- et de HBrO en présence de K_2SO_4 à 25°C dans l'obscurité. L'évolution du courant limite de réduction de HBrO est suivie en fonction des vitesses angulaire ω et linéaire V, sous potentiel fixe (−0,5 V/ECS). En solution statique (électrode tournante) les courbes $i_L = f(\omega)$ obtenues pour trois concentrations de HBrO, vérifient l'équation de Levich, tandis qu'en régime dynamique (électrode fixe), les courbes $i_L = f(V)$ suivent la relation de Matsuda.

Les courbes $i_L = f(V)$ de la Fig. 3 sont tracées pour diverses valeurs de ω, avec simultanément rotation de l'électrode et écoulement de la solution. Dans le domaine de ω et V étudié, i_L peut se mettre sous la forme: $i_L = K\omega^{1/2} + aV$ avec $K = knFAD^{2/3}\nu^{-1/6}C$. La pente des droites diminue lorsque ω croît. Pour $\omega \geqslant 200$ rad s^{-1}, le second terme dans l'expression de i_L devient négligeable. L'erreur introduite est alors d'environ 3,5% pour des vitesses linéaires maximales autorisées par la cellule (17 cm s^{-1}). Ainsi, le courant limite est indépendant de la vitesse d'écoulement pour une vitesse de rotation suffisamment élevée de l'électrode.

D'autres vérifications montrent que la position de l'électrode indicatrice, définie par la distance x, n'affecte pas les courbes $i = f(E)$ relatives aux espèces stables ($HBrO—Br^-$).

Mesures spectrophotométriques

Le montage spectrophotométrique de la cellule a été testé, entre 200 et 450 nm, sur des solutions de brome en circulation. Les spectres sont identiques à ceux obtenus sur des solutions statiques et présentent des bandes d'absorption attribuables à Br_2, Br_3^-, HBrO et BrO^-, suivant le pH et la concentration en bromure.

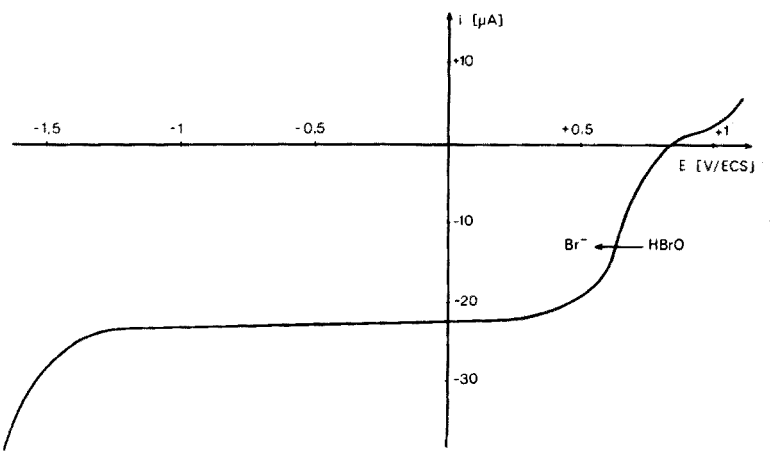

Fig. 2. Courbe $i = f(E)$. Electrode en carbone vitreux; pH 6,8; $[K_2SO_4] = 0{,}1$ M; $[HBrO] = 2 \cdot 10^{-4}$ M; $[Br^-] = 5 \cdot 10^{-3}$ M.

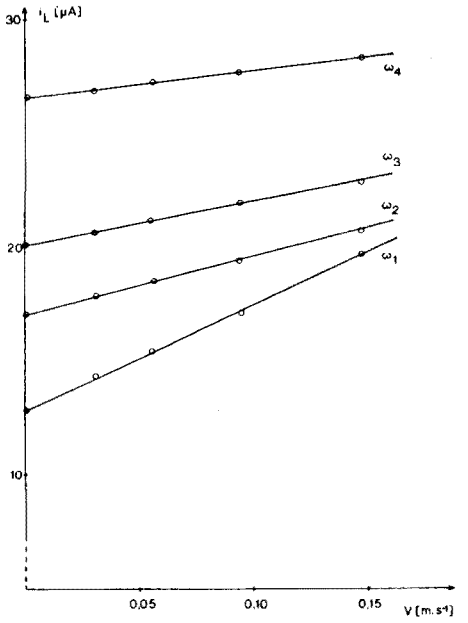

Fig. 3. Courbes $i_L = f(V, \omega)$. [HBrO] = $2 \cdot 10^{-4}$ M; ω_1 = 43 rad s^{-1}; ω_2 = 84 rad s^{-1}; ω_3 = 125 rad s^{-1}; ω_4 = 220 rad s^{-1}.

CONTROLE DE LA CELLULE EN VUE D'ÉTUDES DE CINÉTIQUE

Toute étude de cinétique par la méthode du flux continu implique des composés C_i d'âge t constant à une distance x de l'injecteur. La vitesse d'écoulement doit donc être constante en tous points du tube de mesure. Cette condition est sensiblement réalisée sur le front d'un écoulement turbulent stationnaire. La cellule ayant des vitesses moyennes comprises entre 0,0088 m s^{-1} et 0,176 m s^{-1}, le nombre de Reynolds R varie de 300 à 3350; dans la majorité des cas, le régime serait alors laminaire. En fait, les solutions sortent de l'injecteur en régime turbulent et s'écoulent dans le tube où le régime laminaire pour $R < 2000$, est atteint pour une distance ℓ définie par: $\ell = 0{,}028\, Rd$ (d = 1,9 cm diamètre interne du tube). De plus, la vitesse de rotation élevée de l'électrode perturbe le régime laminaire éventuellement établi, en provoquant un tourbillon. La loi de distribution des vitesses n'a pu être établie expérimentalement au moyen d'un tube de Pitot (trop faibles vitesses d'écoulement). Des contrôles qualitatifs par injection discontinue d'un colorant dans l'injecteur ou à la base du tube, montrent une bonne homogénéité dans tous les cas (coloration uniforme 1 à 2 cm avant l'électrode tournante).

Ces résultats sont complétés par l'étude de la cinétique d'une réaction chimique de constante de vitesse connue. En effet, la concentration en composés C_i, mesurée au centre du tube par le capteur électrochimique, doit être

comparée à celle mesurée par le capteur optique suivant un diamètre de la section du tube. Par ailleurs, il faut vérifier si des écarts éventuels entre les deux types de mesure dépendent de la vitesse d'écoulement.

Divers impératifs entraînent le choix de la réaction d'oxydo—réduction hypochlorite—iodure en milieu alcalin: $ClO^- + I^- \rightarrow IO^- + Cl^-$. L'évolution de ce système est suivie par spectrophotométrie d'absorption u.v. et par ampérométrie. En effet, ClO^- et IO^- ont des spectres D.O. = $f(\lambda)$ différents [15, 16] et les vagues de réduction des courbes $i = f(E)$ sont distinctes. IO^- formé est instable et se dismute en IO_3^- et I^-; mais à 25° C cette dismutation, lente devant l'oxydation de l'iodure par l'hypochlorite [17], est négligée dans les calculs. Selon Chia et Connick [18] la vitesse de la réaction s'exprime par

$$\frac{d[IO^-]}{dt} = k \frac{[I^-]\,[ClO^-]}{[OH^-]}$$

Au moyen de la cellule, nous avons enregistré simultanément l'absorbance à 372 nm et l'intensité limite du courant de réduction à — 0,9 V/ECS pour une distance x de 25 cm entre l'injecteur et les capteurs sur des solutions désoxygénées de concentration initiale connue en ClO^- et I^-, circulant à différentes vitesses, c'est-à-dire après des temps de contact différents.

Les mesures obtenues (Tableau 1) permettent le calcul de la concentration d'hypoiodite en fonction du temps et de la constante de vitesse.

Les deux techniques conduisent à deux valeurs moyennes k_m concordantes, malgré une dispersion dans les mesures. Cependant, la valeur de k diffère de celle obtenue par Chia et Connick ($k = 60\ s^{-1}$) au moyen d'une cellule à régime statique, mais rejoint celle déterminée par Lister et Rosenblum [19]

TABLEAU 1

Étude de la cinétique de l'oxydation de l'iodure par l'hypochlorite, à 25° C, au moyen de la cellule à circulation (Force ionique μ = 1,03 M)

						Mesures voltampérom.		Mesures spectrophotom.	
$[ClO^-]$ (10^{-3} M)	$[I^-]$ (10^{-3} M)	$[OH^-]$ (M)	V_m (10^{-2} m s^{-1})	R	t (s)	$[IO^-]$ (10^{-3} M)	k (s^{-1})	$[IO^-]$ (10^{-3} M)	k (s^{-1})
3,60	6,13	1,027	4,55	865	5,50	3,053	88,3	3,074	90,6
5,70	3,87	1,024	4,55	865	5,50	3,242	99,4	3,271	103,0
4,65	5,00	1,026	11,49	2183	2,18	2,493	104,6	2,589	113,3
4,65	5,00	1,026	9,45	1795	2,65	2,708	103,0	2,775	109,0
4,65	5,00	1,026	7,52	1428	3,33	2,939	99,9	2,936	99,7
4,65	5,00	1,026	5,59	1062	4,48	3,245	98,1	3,247	98,2
4,65	5,00	1,026	3,53	670	7,10	3,730	103,1	3,743	104,8
4,65	5,00	1,026	1,58	301	15,80	4,266	106,7	4,216	96,2
						k_m = 100,4 ± 12,1		k_m = 101,9 ± 11,4	

(k = 91,3 s^{-1}) en cellule à régime dynamique. Ces vérifications satisfaisantes permettent donc l'utilisation de la cellule pour des études de cinétique.

En conclusion, cet appareillage de mesures électrochimiques et spectrophotométriques doit permettre l'identification ainsi que la détermination des cinétiques de décomposition et des conditions d'existence de produits instables en solution. L'étude se poursuit en particulier sur les bromamines dans le système Br_2—NH_3—H_2O.

Les auteurs remercient le Professeur J. P. Schwing de Strasbourg qui a suggéré les vérifications cinétiques, et les Mines de Potasse d'Alsace (M.D.P.A.) pour leur aide matérielle.

BIBLIOGRAPHIE

1 E. F. Caldin, Fast Reactions in Solution, Blackwell Scientific Publications, Oxford, 1964.
2 H. Weisz, Angew. Chem., 6 (1976) 177.
3 A. M. Wilson, Anal. Chem., 38 (1966) 1784.
4 J. W. B. Stewart, J. Růžička et Coll., Anal. Chim. Acta, 78 (1975) 145; 79 (1975) 79; 81 (1976) 371; 81 (1976) 387; 82 (1976) 137; 87 (1976) 353; 88 (1977) 1.
5 F. J. W. Roughton et B. Chance, Technique of Organic Chemistry, vol. VIII, 2° Part, Interscience, New York, 1963.
6 R. B. Coolen, N. Papadakis, J. L. Dye et Coll., Anal. Chem., 47 (1975) 1644; 47 (1975) 1649.
7 V. G. Levich, Acta Physicochim. URSS, 17 (1942) 257.
8 V. G. Levich, Physicochemical Hydrodynamics, Prentice-Hall, Englewood Cliffs, New Jersey, 1962.
9 R. N. Adams, Electrochemistry at Solid electrodes, M. Dekker, New York, 1969.
10 H. Matsuda, J. Electroanal. Chem., 15 (1967) 109.
11 W. J. Blaedel et G. W. Schieffer, Anal. Chem., 46 (1974) 1564.
12 E. Pungor, Zs. Feher et G. Nagy, Pure Appl. Chem., 44 (1975) 595.
13 M. Varadi et E. Pungor, Anal. Chim. Acta, 80 (1975) 31.
14 A. M. Gary, M. Roynette et J. P. Schwing, Bull. Soc. Chim. Fr., (1971) 3779; (1972) 3654.
15 J. C. Morris, J. Phys. Chem., 70 (1966) 3798.
16 O. Haimovich et A. Treinin, Nature (London), 207 (1965) 185.
17 O. Haimovich et A. Treinin, J. Phys. Chem., 71 (1967) 1941.
18 Y. Chia et R. E. Connick, J. Phys. Chem., 63 (1959) 1518.
19 M. W. Lister et P. Rosenblum, Can. J. Chem., 41 (1963) 3013.

Analytica Chimica Acta, 91 (1977) 165—173

POLAROGRAPHY OF TIN(II) CHLORIDE IN ACETONITRILE

A. R. BRAJER*, T. E. FARLEY*, J. W. KAUFFMAN*, L. K. YOUNG*, R. J. WILLIAMS and J. W. ROGERS**

Department of Chemistry, Midwestern State University, Wichita Falls, Texas 76308 (U.S.A.)

(Received 8th December 1976)

SUMMARY

Polarographic and spectrophotometric data show that tin(II) chloride is a weak electrolyte in dilute acetonitrile solutions. The dominant species, $SnCl_2$, exists in a labile equilibrium with the ions $SnCl^+$ and $SnCl_3^-$. Oxidation and reduction of these ionic species is responsible for all observed polarographic plateaux. The dichloro—tin(II) molecule is shown to be a good acceptor species in acetonitrile solution, readily forming 1:1 complexes with ligands such as 4-picoline *N*-oxide.

Donaldson has discussed comprehensively the role of covalent tin(II) compounds as acceptor species in complex formation [1]. A considerable number of complexes prepared from tin(II) salts and various organic ligands is known [1]. A series of Sn(II) complexes has recently been prepared in these laboratories by reaction of anhydrous tin(II) chloride ($SnCl_2$) with substituted pyridine *N*-oxides (pno) in acetonitrile and tetrahydrofuran solvents [2, 3]. Elemental analysis of each crystalline solid prepared in this manner showed a general stoichiometry of the type, $SnCl_2 \cdot$ pno.

Although a significant number of Sn(II) addition compounds and complexes has now been prepared, relatively few have been characterized as to stability, bonding and structure. Such a characterization of the complexes of tin(II) chloride with pyridine *N*-oxides has now been undertaken. Part of this investigation has been devoted to the application of electrochemical techniques to a study of the solution chemistry of these complexes in acetonitrile. The advantages of aprotic solvents in electrochemical studies of organic and inorganic systems is well known [4, 5]. Owing to their lack of acidity, relatively low basicity and solvating characteristics, aprotic solvents have proved to be an excellent medium in which to prepare and study complexes of Sn(II) with weak and strong donors.

The application of polarography to the study of the redox properties of many inorganic complexes, as well as the study of complexation equilibria,

*Robert A. Welch Foundation Undergraduate Scholars.

**To whom correspondence should be directed.

involves commonly known procedures and techniques. However, it has been necessary to characterize the basic electrochemical and electrolyte characteristics of tin(II) chloride in acetonitrile in order to establish the feasibility of application of such methods to the study of tin(II) complexes in aprotic media. The results of this portion of the total study are reported here.

POLAROGRAPHIC DATA

Tin(II) chloride exhibits two well-defined polarographic waves at negative potentials and two anodic waves with an ill-defined point of separation in acetonitrile containing tetra-*N*-propylammonium perchlorate (TPAP) as a supporting electrolyte (Fig. 1 curve a). The separate cathodic waves vary slightly, but systematically, with the square root of the corrected height of the mercury column ($h^{1/2}$) above the dropping mercury electrode (d.m.e.) (Table 1). The sum of the cathodic currents is directly proportional to $h^{1/2}$ as is the total anodic current. The slopes of log plots for both the first and second cathodic waves are 67 and 71 mV, respectively (Table 1). These values suggest some irreversibility in the electrode mechanism resulting from coupled homogeneous chemical reactions or a slow heterogeneous electron-transfer step.

The second cathodic plateau (most negative) exhibits a diffusion current nearly twice that of the first, but with the ratios of diffusion currents dependent upon h (Table 1). The second polarographic wave grows at the expense of the first on addition of measured quantities of tetra-*N*-methylammonium chloride (TMAC) as a source of uncomplexed chloride ion (Table 2). At a ratio of 1:1 TMAC to tin(II) chloride, only a remnant of the first cathodic plateau is observed (Table 2; Fig. 1, curve b). No polaro-

TABLE 1

Polarographic data for reduction of tin(II) chloride in acetonitrile[a]
(Sn(II) chloride (1.0 mM) in acetonitrile containing 0.1 M TPAP. DME characteristics at open circuit and 50-cm Hg head: m = 0.0067 g, t = 5.83 s.)

$h_{corr}^{1/2}$ ($cm^{1/2}$)	Cathodic wave 1[a]		Cathodic wave 2[b]		Total cathodic		Anodic wave[c]	
	i_d (μA)	$i_d/h_{corr}^{1/2}$ ($\mu A/cm^{1/2}$)	i_d (μA)	$i_d/h_{corr}^{1/2}$ ($\mu A/cm^{1/2}$)	i_d (μA)	$i_d/h_{corr}^{1/2}$ ($\mu A/cm^{1/2}$)	i_d (μA)	$i_d/h_{corr}^{1/2}$ ($\mu A/cm^{1/2}$)
9.40	3.25	0.35	7.59	0.81	10.84	1.15	11.58	1.23
8.85	3.16	0.36	6.60	0.75	9.76	1.10	10.92	1.23
8.27	2.97	0.36	6.16	0.74	9.03	1.10	10.18	1.23
7.64	2.79	0.37	5.36	0.73	8.05	1.05	9.35	1.22
6.95	2.72	0.39	5.00	0.72	7.72	1.11	8.61	1.24
6.19	2.52	0.41	4.54	0.73	7.06	1.14	7.70	1.24
5.32	2.16	0.41	3.74	0.70	5.90	1.11	6.68	1.25

[a] $E_{1/2}$ = −0.06 V. Slope of log $(i_d - i)/i$ vs. E(d.m.e.) = 67 mV.
[b] $E_{1/2}$ = −0.70 V. Slope of log $(i_d - i)/i$ vs. E(d.m.e.) = 71 mV.
[c] Two polarographic waves with ill-defined point of separation.

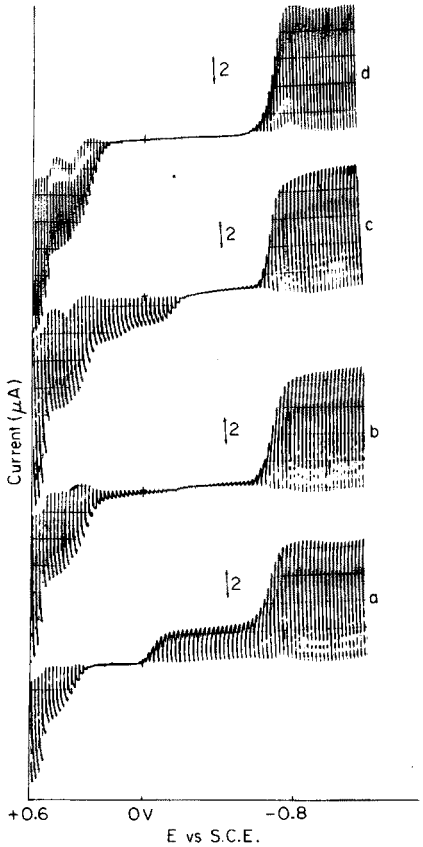

Fig. 1. Polarographic waves in acetonitrile solvent of (a) tin(II) chloride (1 mM), (b) tin(II) chloride (1 mM) with 1 mM TMAC present, (c) tin(II) chloride (1 mM) with 2 mM TMAC present, and (d) tetramethylammonium trichlorostannate (1 mM).

TABLE 2

Polarographic data for reduction of tin(II) chloride in acetonitrile—tetramethylammonium chloride mixtures[a]

$[Cl^-]$ (mM)	Cathodic wave 1		Cathodic wave 2		Total cathodic current
	$-E_{1/2}$ (V)	i_d (μA)	$-E_{1/2}$ (V)	i_d (μA)	i_d (μA)
0.00	0.06	2.67	0.70	5.45	8.12
0.25	0.09	2.09	0.70	5.97	8.06
0.50	0.10	1.79	0.70	6.11	7.90
0.75	0.12	1.32	0.70	6.44	7.76
1.00	0.17	0.69	0.70	7.04	7.73
1.25	—	0.00	0.70	7.76	7.76
1.50	—	0.00	0.70	7.65	7.65

[a]See Table 1.

graphic wave associated with the oxidation of chloride in acetonitrile is observed at this ratio. The sum of the cathodic diffusion currents remains approximately constant at all ratios (Table 2). The $E_{1/2}$ of the first wave is shifted in a negative direction by increasing quantities of TMAC; the $E_{1/2}$ of the second wave is unperturbed by addition of TMAC in concentrations up to 1.5 mM (Table 2). A wave attributable to the oxidation of chloride on mercury in acetonitrile is observed in polarograms of solutions containing TMAC to tin(II) chloride ratios greater than 1.0 (Fig. 1, curve c). The diffusion current of the second cathodic wave is not significantly altered by the addition of TMAC in any amount above a 1:1 ratio with tin(II) chloride. However, the slope of the log plot of the wave is systematically diminished by added quantities of TMAC in excess of 5 mM. A slope of 37 mV was observed for the second cathodic wave in polarograms of solutions containing 1 mM tin(II) chloride and 50 mM TMAC. This value is very near that expected for the reversible, two-electron formation of Sn(Hg).

These data show that free chloride reacts with some form of Sn(II), converting it to a higher complexed form which is reduced at the second cathodic wave. The growth of the second wave at the direct expense of the first, at a near constant total diffusion current (Fig. 1, Table 2) suggests that both waves result from the transfer of an equal number of electrons (n_{app}) and that the species reduced in each step exhibit similar diffusion coefficients. The insensitivity of the diffusion current — but sensitivity of the slope of the second wave — to excess of free chloride suggests that only the reversibility or mechanism of the electrode process is altered by excess of chloride.

These results are in general agreement with the data presented by Thomas and Kolthoff in a survey of the polarographic behavior of group-IV metal halides in acetonitrile [6]. They suggest a disproportionation of the type

$$2SnCl_2 \rightleftarrows SnCl^+ + SnCl_3^-$$

to explain the existence of more than one type of tin(II) chloride complex and the absence of free chloride in dilute solutions of tin(II) chloride in acetonitrile.

In an attempt to confirm this statement of electrolyte behavior and to assign specific polarographic steps to the oxidation and/or reduction of specific Sn(II) species, a polarogram of tetramethylammonium trichlorostannate [$(CH_3)_4N^+SnCl_3^-$] was recorded in acetonitrile—TPAP solution. The observed polarogram (Fig. 1, curve d), corresponds exactly to that recorded in a 1:1 tin(II) chloride—TMAC solution. The single reduction plateau of the trichlorostannate ion ($SnCl_3^-$) exhibits the same polarographic characteristics as the second reduction plateau observed in tin(II) chloride polarograms, (Tables 1—3). These data confirm that the oxidation and reduction of $SnCl_3^-$ are responsible, respectively, for both anodic waves and the second cathodic wave in polarograms of tin(II) chloride in acetonitrile solutions.

TABLE 3

Polarographic data for 1 mM tetramethylammonium trichlorostannate in acetonitrile containing 0.1 M TPAP
($E_{1/2}$ = −0.06 V. Slope of log $(i_d - i)/i$ vs. E(d.m.e.) = 70 mV.)

$h_{corr}^{1/2}$ ($cm^{1/2}$)	i_d (μA)	$i_d/h_{corr}^{1/2}$ ($\mu A/cm^{1/2}$)
8.85	11.94	1.49
8.27	11.39	1.49
7.64	10.62	1.43
6.95	9.93	1.39
6.19	9.24	1.38
5.32	7.92	1.35

Polarograms of anhydrous tin(II) perchlorate—TPAP solutions in acetonitrile exhibit one reversible 2e, wave with $E_{1/2}$ = +0.02 V compared to $E_{1/2}$ = −0.06 V for the first wave in tin(II) chloride solutions. This behavior demonstrates that the first plateau observed in the polarographic reduction of tin(II) chloride in acetonitrile is not the result of reduction of Sn(II)—acetonitrile or Sn(II)—perchlorate complexes.

Addition of a pyridine *N*-oxide ligand such as 4-picoline *N*-oxide (4-pno) to 1.0 mM solutions of tin(II) chloride alters only the structure of the first cathodic wave. The wave splits on addition of 4-pno in concentrations less than 1.0 mM (Fig. 2). The new cathodic plateau apparently associated with a tin(II) 4-pno complex completely replaces the original wave at 4-pno—tin(II) chloride ratios of 1:1 or greater (Fig. 2). A plateau associated with the reduction of free 4-pno is only observed in solutions containing 4-pno to tin(II) chloride ratios greater than 1.0. Addition of excess of 4-pno shifts the complex wave anodically. Addition of 0.5 mM TMAC to a solution containing 1.0 mM tin(II) chloride and 0.5 mM 4-pno destroys the low-potential wave and enhances the diffusion current of the $SnCl_3^-$ reduction wave by a proportional amount without altering the complex wave (Fig. 3). Continued addition of TMAC destroys the complex, producing $SnCl_3^-$ and releasing free 4-pno, detectable by its known reduction wave observed in polarograms taken to potentials near the background of the solvent—TPAP medium.

The polarographic behavior of tin(II) chloride in the presence of controlled quantities of TMAC and 4-pno demonstrates that chloride ion is a strong ligand toward tin(II) in acetonitrile. Trichlorostannate ion is formed quantitatively in solutions containing chloride in a 1:1 ratio with tin(II) chloride. Pyridine *N*-oxide ligands, such as 4-pno, form complexes with Sn(II) in a 1:1 ratio of ligand—tin(II) chloride. This ratio and the three-fold coordination of Sn(II) by the strong chloride ligand strongly suggest a solution stoichiometry of the type $SnCl_2 \cdot L$, for complexes of tin(II) chloride with monodentate ligands such as 4-pno.

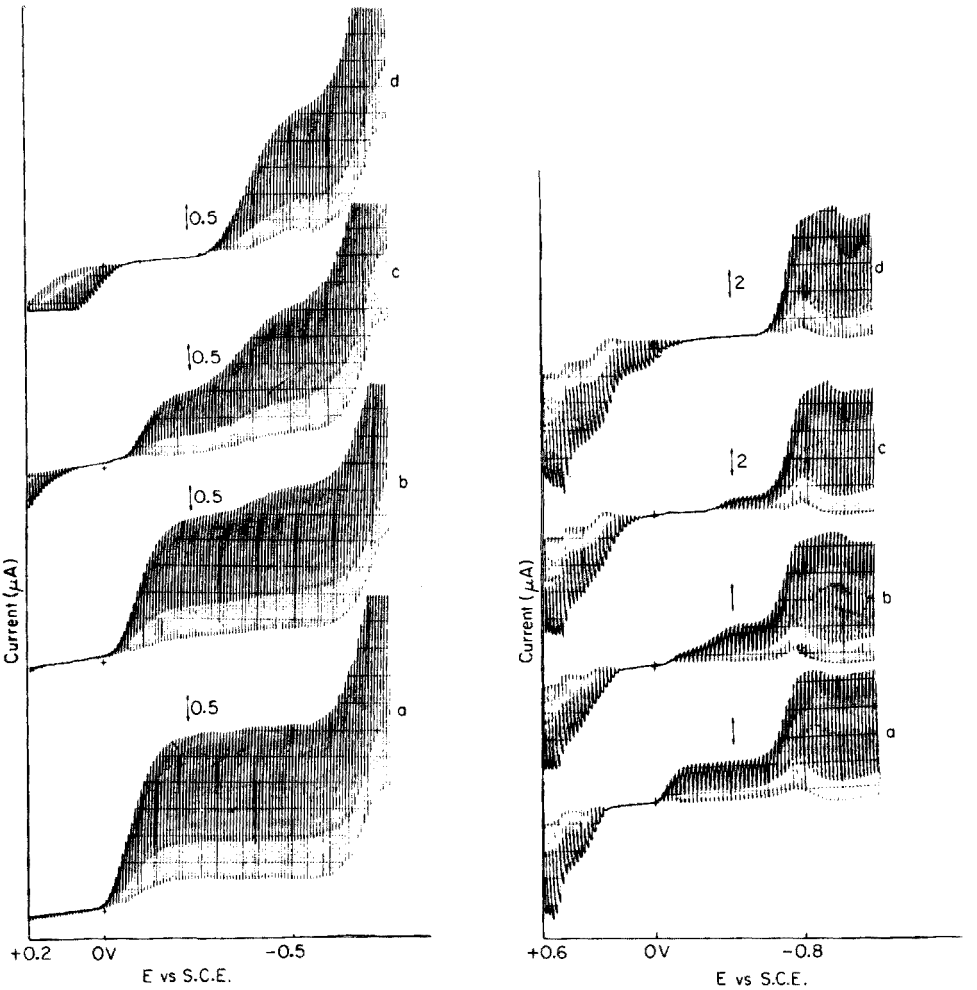

Fig. 2. Low-potential cathodic wave of 1 mM tin(II) chloride in acetonitrile containing (a) no 4-pno, (b) 0.25 mM 4-pno, (c) 0.5 mM 4-pno and (d) 1 mM 4-pno.

Fig. 3. Polarographic waves of 1 mM tin(II) chloride in acetonitrile containing (a) no TMAC or 4-pno, (b) 0.5 mM 4-pno, (c) 0.5 mM 4-pno and 0.5 mM TMAC and (d) 0.5 mM 4-pno and 1 mM TMAC.

Even though complexation of tin(II) chloride with chloride ion in a 1:1 ratio apparently consumes all the available Sn(II) forming only $SnCl_3^-$, only the cathodic wave at lower potential is diminished by addition of chloride or 4-pno to 1.0 mM solutions of tin(II) chloride. The polarographic plateaux associated with the reduction and oxidation of $SnCl_3^-$ are observed in all polarograms of tin(II) chloride, tin(II) chloride—TMAC, and tin(II) chloride—4-pno mixtures. These polarographic data are consistent with the postulated electrolyte behavior of tin(II) chloride only if it is assumed that the

disproportionation equilibrium exists greatly in favor of the $SnCl_2$ species and that it shifts rapidly to the right during reduction or oxidation of $SnCl_3^-$. The diffusion current of the cathodic wave at lower potential relative to that of the wave at higher potential resulting from the two-electron reduction of $SnCl_3^-$, appears to be inconsistent with the expected behavior of a single wave resulting from a diffusion-controlled reduction of 1.0 mM tin(II) chloride existing primarily as $SnCl_2$ molecules. However, since the wave cannot be attributed to the reduction of solvated Sn(II) ion or a Sn(II) perchlorate complex, it must be assumed that it results from the reduction of the $SnCl^+$ species in equilibrium with $SnCl_2$, or $SnCl_2$.

U.V. DATA

U.v. spectra of tin(II) chloride, tin(II) chloride—TMAC mixtures and $SnCl_3^-$ in acetonitrile were recorded to establish independent evidence of the postulated disproportionation equilibrium and its relative position. The spectrum of a 1.0 mM solution of tin(II) chloride in acetonitrile is characterized by a dominant absorption peak at 213 nm (A = 1.6) with well defined shoulders at 203 and 226 nm (Fig. 4). A small peak at 255 nm (A = 0.15) is also observed. Addition of controlled quantities of TMAC causes the disappearance of the band at 213 nm, the appearance of two strong absorption peaks at 226.5 and 236.3 nm and two weak peaks at 272.4 and 291.5 nm. The four peaks grow in intensity with increasing quantities of TMAC (Fig. 5). However, addition of TMAC beyond a 1:1 ratio with tin(II) chloride causes no significant change in these absorbance bands (Fig. 4). Only a band at 198 nm attributable to free chloride grows in intensity. The spectrum of a 1.0 mM solution of tetramethylammonium trichlorostannate in acetonitrile is identical to that of a 1:1 mixture of Sn(II) chloride and TMAC in acetonitrile (Fig. 5).

The spectrum of a 1.0 mM Sn(II) chloride—0.5 mM TMAC solution can be duplicated to within ±0.04 absorbance units by a linear combination of the absorbances of a 1.0 mM Sn(II) chloride—1.0 mM TMAC solution using 0.5 as a combination coefficient. These data and the absence of bands in the spectrum of a 1.0 mM tin(II) chloride solution that correspond to those observed in the spectra of 1.0 mM tetramethylammonium trichlorostannate solutions, show that the predominant species in tin(II) chloride solutions in acetonitrile is the neutral Sn(II) chloride complex, $SnCl_2$. Thomas and Kolthoff have also presented conductivity data consistent with these findings [6].

CONCLUSIONS

The polarographic and spectrophotometric behavior of tin(II) chloride solutions show that chloride ion and the monodentate ligand 4-pno, must react with $SnCl_2$ in equilibria of the type $SnCl_2 + Cl^- \rightleftarrows SnCl_3^-$ and

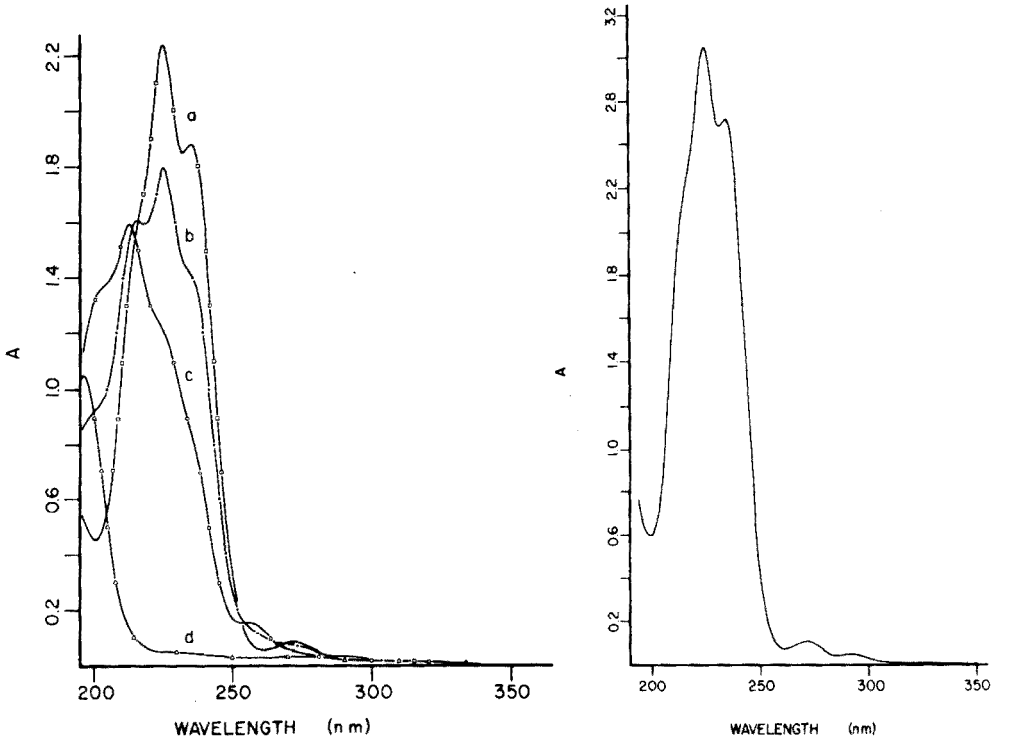

Fig. 4. U.v. spectra in acetonitrile of (a) 1 mM tetramethylammonium chloride, (b) 1 mM tin(II) chloride, (c) 1 mM tin(II) chloride with 0.5 mM tetramethylammonium chloride, (d) 1 mM tin(II) chloride with 1 mM tetramethylammonium chloride.

Fig. 5. U.v. spectrum of tetramethylammonium trichlorostannate (1 mM) in acetonitrile.

$SnCl_2$ + 4-pno $\rightleftarrows$ $SnCl_2 \cdot$ 4-pno, and that $SnCl_2$ in acetonitrile also exists in a labile disproportionation equilibrium of the type $2SnCl_2 \rightleftarrows SnCl^+ + SnCl_3^-$.

The cathodic polarographic plateaux at low and higher potential may be attributed to the two-electron reduction of $SnCl^+$ or $SnCl_2$ and $SnCl_3^-$, respectively. The disappearance of the low-potential wave and the build-up of the higher potential wave on addition of chloride must therefore be attributed to the removal of $SnCl_2$ and $SnCl^+$ and formation of $SnCl_3^-$ via the sequence

$$2SnCl_2 \rightleftarrows SnCl^+ + SnCl_3^-$$
$$\uparrow \quad\quad\quad\quad\quad\quad \uparrow$$
$$+Cl^- \quad\quad\quad\quad\quad\quad$$

The relative heights of approximately 2:1 for the second (reduction of $SnCl_3^-$) to the first cathodic plateau may be explained by a reaction sequence in which either $SnCl^+$ or $SnCl_2$ is reduced at the electrode surface at potentials of the first wave, releasing free chloride ion which subsequently

forms complexes with all forms of Sn(II) at the electrode surface to form $SnCl_3^-$ which is not reducible at potentials of the first wave. In effect, the current of the first wave is limited by both diffusion and the production of chloride. The quantitative production of $SnCl_3^-$ and $SnCl_2 \cdot$ 4-pno on respective additions of 1.0 mM Cl^- and 1.0 mM 4-pno to 1.0 mM solutions of tin(II) chloride, suggests that the first cathodic plateau results from the reduction of $SnCl_2$. In summary, the polarographic processes occurring at cathodic potentials may be generally represented: First wave: $SnCl_2 + 2e^- \rightarrow Sn(Hg) + 2Cl^-$; $SnCl_2 + Cl^- \rightarrow SnCl_3^-$. Second wave: $SnCl_3^- + 2e^- \rightarrow Sn(Hg) + 3Cl^-$.

EXPERIMENTAL

Apparatus

The instrumentation and polarographic cells were of a conventional design and have been described elsewhere [7]. All u.v. spectra were recorded on a Cary 118C u.v.—visible spectrophotometer with Quarasil 1-mm pathlength stoppered cells.

Chemicals

Spectroquality acetonitrile containing less than 0.03% water (Aldrich), polarographic-grade tetramethylammonium chloride (Southwestern Analytical Chemicals) and anhydrous tin(II) chloride containing less than 1% Sn(IV) (Alpha Products) were used. Tetramethylammonium trichlorostannate was prepared by the method of Haight et al. [8]. Analysis of the prepared salt showed 39.00% Sn(II) (calculated 39.67%). Tin(II) perchlorate was prepared by the method of Davies and Donaldson [9]. Analysis of the prepared salt showed 27% Sn(II) (calculated 32%).

All polarographic and spectrophotometric solutions were prepared and transferred under a nitrogen atmosphere in a Dri-Lab glove box (Vacuum Atmospheres Corp.).

The authors gratefully acknowledge the financial support of the Robert A. Welch Foundation [R. J. Williams (AO-557), J. W. Rogers (AO-337)].

REFERENCES

1 J. D. Donaldson, Progress in Inorganic Chemistry, Vol. 8, Interscience, New York, 1967.
2 J. W. Kauffman, D. H. Moor and R. J. Williams, J. Inorg. Nucl. Chem., 39 (1977) 000.
3 P. Scott, J. Kauffman, J. W. Rogers and R. J. Williams, in preparation.
4 S. Wawzonek and M. E. Runner, J. Electrochem. Soc., 99 (1952) 457.
5 C. K. Mann, Nonaqueous Solvents for Electrochemical Use, in A. J. Bard (Ed.), Electroanalytical Chemistry, Vol. III, Dekker, New York, 1968.
6 F. G. Thomas and I. M. Kolthoff, J. Electroanal. Chem. Interfacial Electrochem., 31 (1971) 423.
7 W. N. Greig and J. W. Rogers, J. Electrochem. Soc., 117 (1970) 1141.
8 G. P. Haight, J. Zoltewiez and W. Evans, Acta Chem. Scand., 16 (1962) 311.
9 C. G. Davies and J. D. Donaldson, J. Inorg. Nucl. Chem., 30 (1968) 2635.

Analytica Chimica Acta, 91 (1977) 175—180

A SIMPLE AUTOMATIC PHOTOTITRATOR FOR THE DETERMINATION OF TOTAL CARBONATE AND TOTAL ALKALINITY OF SEA WATER

ANDERS GRANÉLI and TORBJÖRN ANFÄLT

Department of Analytical Chemistry, University of Gothenburg, Fack, S-402 20 Göteborg 5 (Sweden)

(Received 30th December 1976)

SUMMARY

An automatic photometric analyser based on the reversed use of a conventional motor syringe buret and modern optoelectronic components is described. The buret serves as a photometric titration vessel into which sample and reagents are selectively drawn through a set of solenoid valves. It has been applied to the photometric titration of total alkalinity and total carbonate concentration of sea water, giving precisions of 0.10% and 0.13%, respectively.

Photometric titrations are often superior to potentiometric since electrodes react sluggishly to temperature changes and are often slow in their response to concentration shifts, whereas photometers give stable signals instantaneously upon mixing. However, since photometric titrations often involve the addition of several reagents, e.g. buffering substances, masking agents and indicators, a completely automatic titration procedure with motor syringe burets can be very complicated. For instance, the semi-automatic, high-precision successive titration of alkaline earth metals in sea water described by Anfält and Granéli [1] utilizes four burets, but the sample solution has still to be weighed, and the buffer and indicator pipetted. This paper describes a phototitrator which automatically measures the sample and titrant volumes, and the volumes of all other reagents involved, and also changes the sample. This is accomplished by using a motor syringe buret as titration vessel, i.e. instead of delivering reagents from several burets into a separate titration vessel, the reagents are drawn into the buret from reagent bottles.

THEORY

The acidimetric titration of sea water has two equivalence points corresponding mainly to the formation of hydrogencarbonate (v_1) and carbonic acid (v_2). In the volume range $v_1 < v < v_2$ the main reaction is

$$HCO_3^- + H^+ \rightleftharpoons H_2CO_3$$

In this volume range, v_1 and v_2 can be evaluated, respectively, from the two

Gran functions [2]

$$F_1 = (v_2 - v)\,[H^+] = K(v - v_1) \quad (1)$$

and

$$F_2 = (v - v_1)/[H^+] = K(v_2 - v) \quad (2)$$

where v is the volume of titrant and $[H^+]$ is obtained from the absorbance of an indicator. However, in many coastal waters there is almost no free carbonate and thus the Gran function F_2 can be approximated to $v/[H^+]$ for the determination of the total alkalinity [3].

The indicator should of course be chosen so that its transition interval occurs in the volume range $v_1 < v < v_2$ [4]. Bromothymol blue is suitable in this case. The indicator reaction of the titration is I^{2-} (blue) + $H^+ \rightleftharpoons HI^-$ (yellow). Therefore

$$[H^+] = K_1\,[HI^-]/[I^{2-}] \quad (3)$$

where K_1 is the stability constant of the indicator. The total absorbance is

$$A = a_I[I^{2-}] + a_{HI}[HI^-] \quad (4)$$

where a_I and a_{HI} are the molar absorptivities of I^{2-} and HI^-, respectively. The absorbance is measured at 615 nm which means that the absorption maximum is

$$A_{max} = a_I[I]_{tot} \quad (5)$$

and the absorption minimum is

$$A_{min} = a_{HI}[I]_{tot} \quad (6)$$

The total indicator concentration is

$$[I]_{tot} = [I^{2-}] + [HI^-] \quad (7)$$

Combining eqns. (4), (5), (6) and (7) gives

$$A_{max} - A = (a_I - a_{HI})[HI^-] \quad (8)$$

and

$$A - A_{min} = (a_I - a_{HI})[I^{2-}] \quad (9)$$

From eqns. (3), (8) and (9)

$$[H^+] = K_1\,(A_{max} - A)/(A - A_{min})$$

which can be inserted into eqns. (1) and (2). However, A_{max} and A_{min} must be corrected for dilution.

Since v_1 must be known in order to obtain v_2 and vice versa, v_2 is calculated by an iterative procedure: a guessed value of v_2 is inserted in the Gran function F_1. The value of v_1 obtained is used to calculate a new value of v_2 from the Gran function F_2. The procedure is repeated using the method of

chords until the difference between two consecutive v_2 values is less than 10^{-5} ml. At the same time, v_1 is obtained.

EXPERIMENTAL

Titrator

The design of the titrator is shown in Fig. 1. It consists of a motor syringe buret (Metrohm Dosimat E 412), which is modified, so that accurate volume increments can be either pushed out of or drawn into the buret by the piston. The ordinary two-way stopcock of the buret is replaced by a Teflon lid with five separate 0.7-mm bore holes. Each hole is connected to a solenoid valve with Teflon tubing. The number of solenoid valves can, of course, be increased, but more than eight to ten seems to be unnecessary. The valve in the centre of the lid is used to empty the buret of waste. The others are used for reagents and sample. Thorough and instantaneous mixing of the solution is accomplished by means of a Teflon-clad magnetic ball. The ball is rotated at a very high speed by an ordinary magnetic stirrer placed at right angles to

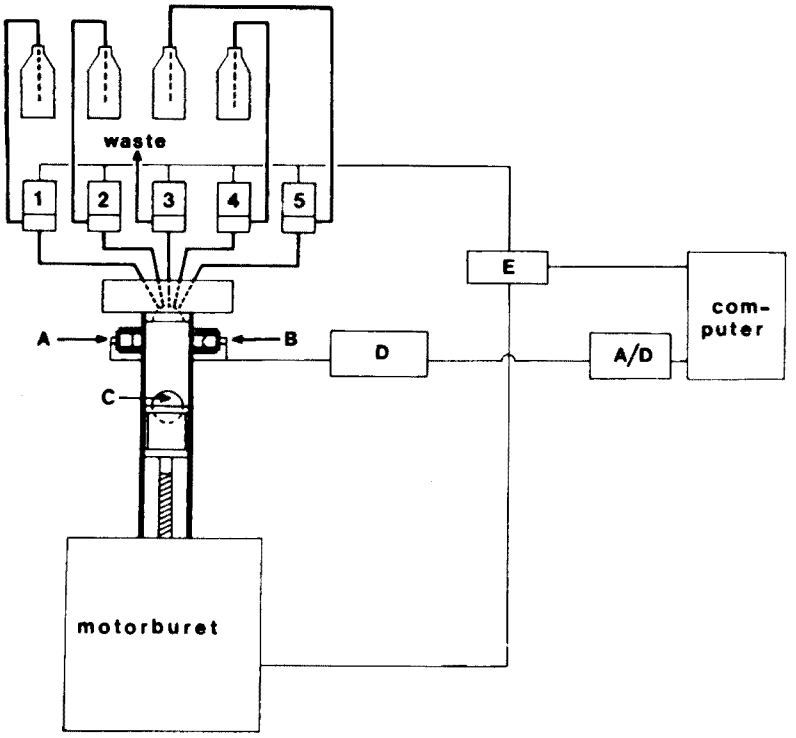

Fig. 1. Automatic phototitrator. (A) Photodiode. (B) Light emitting diode. (C) Teflon-clad stirrer ball. (D) Photometer electronics. (E) Relays. The stirrer motor is placed at right angles to the buret.

the buret. The magnetic ball fits exactly into half-spheres in the buret piston and the lid respectively. The piston can therefore be pushed all the way to the top of the buret, thus completely emptying it of solution.

The photometer unit is incorporated into the titrator. It is based on opto-electronic components and has been described previously [1, 3]. The radiation source is a light-emitting diode (LED) with a peak wavelength of 615 nm. The light emitted is electronically chopped and detected phase-selectively by a photodiode. The LED and the photodiode are placed diametrically on either side of the buret giving a path length equal to the diameter of the buret. The phototitrator is controlled by a minicomputer processing system consisting of a CAI ALPHA LSI-2/20 computer with 16 K memory, a 100-Hz real-time clock, a 12-bit A/D converter and 12 relays. The programming language is BASIC.

Reagents

0.005 M hydrochloric acid was prepared from ampoules (Merck). Sodium chloride and sodium sulfate were added to give an ionic strength of 0.6 M. A 0.1% solution of bromothymol blue was prepared by dissolving the indicator acid in 20% ethanol.

Procedure

Test tubes with sea water and indicator were connected to solenoid valves with Teflon tubing. A bottle of hydrochloric acid was connected with Teflon tubing to a third valve. The bottle with acid was kept 0.5 m above the buret in order to provide a slight over-pressure during the titration; this held the carbon dioxide formed in solution.

The buret was first rinsed three times with 2-ml portions of sea water. A voltage corresponding to zero transmittance was read by the A/D while the light path was blocked with the buret piston. A sample (12 ml) of sea water was drawn into the buret and an approximate voltage corresponding to 100% transmittance was read. Then 0.3 ml of bromothymol blue was added and A_{max} measured. Acid was added to the sample until the absorbance was equal to $0.65 \times A_{max}$. The absorbance was then measured after every 0.2-ml addition of acid until it was $0.08 \times A_{max}$. This proved to give a suitable volume range for v. Finally an excess of acid was added and the minimum absorbance was measured. However, since the difference between 100% transmittance and A_{min} is small, A_{min} was set to zero, i.e. a new value for 100% transmittance was obtained and all absorbance values were recalculated accordingly. The equivalence volumes v_1 and v_2 were calculated and also corrected for the systematic error caused by the indicator acid. The density of the sea water had previously been determined and therefore the total carbonate concentration (C_t) and the total alkalinity (A_t) could be calculated on the mol/kg scale (M_w).

RESULTS AND DISCUSSION

Buret

The many advantages of using the buret as titration vessel are obvious. First of all, the cost is reduced since only one buret is necessary for any kind of photometric titration. Secondly, the buret is very suitable as a completely automatic instrument for photometric analysis, because it can be emptied of waste, rinsed and filled with new sample without any intervention by an operator. Thirdly, it is possible to perform several different analyses successively, just by connecting reagent bottles to the number of solenoid valves necessary. Fourthly, one of the main advantages of the buret when it is used in a photometric titration, is the possibility of back-titrating with sample. For instance, if the titration curve cannot be evaluated by the linear regression method described above, the breakpoint may be determined with increasing accuracy simply by alternating titration back and forth with sample and titrant around the equivalence point [5].

Precision

The precision of the volume measurements with the buret was found to be ± 0.03%, which is of the same order of magnitude as the value determined by Jagner and Årén [6]. Ten consecutive titrations of surface sea water were performed on board R/V Akademik Kurchatov during its 22nd cruise in the Indian ocean. The salinity of the sample was 34.736‰ and the mean total alkalinity and mean total carbonate concentration were found to be 2.255 mM_w and 1.955 mM_w, respectively. The relative standard deviations were 0.10% and 0.13%, respectively. The precision is thus practically the same as that obtained by Almgren et al. [7] for the potentiometric titration of A_t and C_t.

Accuracy

To test the accuracy of the method, HALTAFALL [8] calculations were performed where all the species involved were accounted for, as described by Hansson and Jagner [9]. The resulting equivalence volumes v_1 and v_2 were corrected for the indicator species. The amount of acid corresponding to the unprotonated indicator in the first equivalence volume was added to v_1, while the amount of acid corresponding to the total indicator concentration was subtracted from v_2. The systematic error thus obtained was −0.15% for the total alkalinity and +0.40% for the total carbonate concentration. The accuracy of the method also depends on how accurately the standard hydrochloric acid can be prepared and on the total concentration of indicator. The manufacturer of the acid states that it is accurate to within 0.1%, i.e. of the same order of magnitude as the precision of the method.

The time required for one complete titration is 15 min, i.e. approximately half the time required for the potentiometric titration.

The authors are indebted to Professor David Dyrssen for general discussions

and to Dr. Mats Strandberg for valuable co-operation. Grants from Knut och Alice Wallenbergs Stiftelse and the Swedish Natural Sciences Research Council are gratefully acknowledged.

REFERENCES

1 T. Anfält and A. Granéli, Anal. Chim. Acta, 86 (1976) 13.
2 D. Dyrssen and L. G. Sillén, Tellus, 19 (1967) 113.
3 T. Anfält, A. Granéli and M. Strandberg, Anal. Chem., 48 (1976) 357.
4 A. Johansson, Anal. Chim. Acta, 61 (1972) 285.
5 D. Jagner and K. Årén, Anal. Chim. Acta, 57 (1971) 185.
6 D. Jagner and K. Årén, Anal. Chim. Acta, 52 (1970) 491.
7 T. Almgren, D. Dyrssen and M. Strandberg, Deep-Sea Research, in press.
8 N. Ingri, W. Kakolowicz, L. G. Sillén and B. Warnqvist, Talanta, 14 (1967) 1261.
9 I. Hansson and D. Jagner, Anal. Chim. Acta, 65 (1973) 363.

Analytica Chimica Acta, 91 (1977) 181—187

RAPID DETERMINATION OF THE "TITRATION ALKALINITY" OF SEA WATER BY EQUILIBRATION WITH CO_2

ROBIN S. KEIR*, SAM P. KOUNAVES and ALBERTO ZIRINO

Chemistry and Environmental Sciences Group, Naval Ocean Systems Center, San Diego, CA 92152 (U.S.A.)

(Received 8th December 1976)

SUMMARY

Sea-water samples of salinities 31.88, 35.84, and 39.87°/$_{oo}$ were acidified and then titrated with HCO_3^- under 1 atm. pressure of CO_2. The resulting pH—HCO_3^- titration plots were interpreted in terms of an ion pairing model, and an equation relating pH and alkalinity was derived. This expression was used to develop a rapid, volume-independent technique to measure alkalinity. The method has an accuracy of ±1% and a precision of ±0.35% (one σ), and lends itself to the analysis of flowing samples and to samples of small volume.

Studies of marine environments require rapid, precise determinations of the titration alkalinity of sea water [1], and such determinations should be amenable to continuous shipboard monitoring. Present methods [2, 3], which require titration of the sample with HCl, are not readily adaptable to continuous flow analysis because sample and acid volumes need to be known accurately. Titration with CO_2, however, is volume-independent, and lends itself readily to the analysis of flowing samples. Although this method is inherently less precise than the HCl titration, it may be useful in the study of estuaries where variable surface alkalinities require collection of numerous data. Additionally, the method may be used for samples of very small volume. This paper describes the CO_2 titration method and discusses the pH—alkalinity titration curve of sea water using a model of the Garrels and Thompson type [4].

THEORY

"Titration alkalinity" can be defined as the number of equivalents of hydrogencarbonate plus the equivalents of bases stronger than hydrogencarbonate in 1 l of sea water at constant temperature [3]. When sea water is equilibrated with CO_2 at 1 atm. pressure the equilibrium

$$CO_2(aq) + H_2O + B^{n-} \rightleftarrows HCO_3^- + BH^{1-n} \quad (1)$$

*Current Address: Department of Geology, Yale University, New Haven, CT, U.S.A.

where B is any base stronger than hydrogencarbonate, is shifted far to the right. The pH of the resulting solution at constant temperature is a function of the hydrogencarbonate concentration. Hence, the "titration alkalinity" can be measured by equilibrating sea water at constant temperature with 1 atm. pressure of CO_2 and measuring the pH.

For a sea-water solution in equilibrium with 1 atm. pressure of CO_2 at 25°C, the hydrogencarbonate range of 0—4.5 meq l^{-1} corresponds to a pH range of 3.7—5.2. In this pH range, the free ion species which exist in significant amounts are H^+, Na^+, K^+, Mg^{2+}, Ca^{2+}, HCO_3^-, SO_4^{2-}, Cl^-, and F^-. To solve for the hydrogencarbonate concentration as a function of pH, the above ions are considered in equilibrium with H_2O, CO_2, HSO_4^-, HF and the possible ion pairs formed by association of the above ions. The ion pairs present are considered to be $NaSO_4^-$, KSO_4^-, $MgSO_4$, $CaSO_4$, $NaHCO_3$, $MgHCO_3^+$, $CaHCO_3^+$, MgF^+, and CaF^+. This sea-water solution can be represented by a model system composed of a solution of NaCl, $NaHCO_3$, KCl, KF, $MgCl_2$, $MgSO_4$, and $CaCl_2$. The relationship between pH and titration alkalinity can then be derived on the basis of this model by use of appropriate equilibrium expressions, mass balances, and the electroneutrality condition. These equations are listed in Table 1.

Reaction (1) shows that $C_{HCO_3} = A$, the titration alkalinity, and in the model system under consideration $C_{HCO_3} = C_{NaHCO_3}$. Substituting the appropriate mass balance equations into the electroneutrality expression gives

$$A = [HCO_3^-] + [NaHCO_3] + [MgHCO_3^+] + [CaHCO_3^+] - [HSO_4^-] - [HF] - [H^+] \quad (2)$$

Insertion of the equilibrium expressions into eqn. (2) yields

$$A = \frac{\alpha P_{CO_2} K'_{CO_2}}{[H^+]} \left\{1 + \frac{[Na^+]}{K'_{NaHCO_3^+}} + \frac{[Mg^{2+}]}{K'_{MgHCO_3^+}} + \frac{[Ca^{2+}]}{K'_{CaHCO_3^+}}\right\} - \left\{\frac{C_{SO_4}}{1 + \frac{K'_{HSO_4^-}}{[H^+]}\left\{1 + \frac{[Na^+]}{K'_{NaSO_4^-}} + \frac{[K^+]}{K'_{KSO_4^-}} + \frac{[Mg^{2+}]}{K'_{MgSO_4}} + \frac{[Ca^{2+}]}{K'_{CaSO_4}}\right\}}\right\} - \left\{\frac{C_F}{1 + \frac{K'_{HF}}{[H^+]}\left\{1 + \frac{[Mg^{2+}]}{K'_{MgF^+}} + \frac{[Ca^{2+}]}{K'_{CaF^+}}\right\}}\right\} - [H^+] \quad (3)$$

Equation (3) can then be expressed in terms of the apparent dissociation constant which is defined as $K''_{HL} = a_H [L]_T / [HL]$, where L = HCO_3^-, SO_4^{2-}, or F^-; a_H = hydrogen ion activity (as measured by the pH electrode, here); and $[L]_T$ is the sum of the free ligand and metal ion pair concentrations [5]. K''_{HL} can also be written as

$$K''_{HL} = \gamma_H K'_{HL} \left\{1 + \sum_i \frac{[M_i]}{K'_{M_iL}}\right\}$$

TABLE 1

Equilibria, mass balances and electroneutrality conditions
(Square brackets denote molar concentrations.)

Equilibria

$$K'_{CO_2} = \frac{[H^+]\,[HCO_3^-]}{\alpha P_{CO_2}}$$

where α is the solubility of CO_2 in sea water.

$$K'_{ML} = \frac{[M]\,[L]}{[ML]}$$

where K'_{ML} is the stoichiometric equilibrium constant for ML with free ions M (H^+, Na^+, Mg^{2+}, or Ca^{2+}) and L (HCO_3^-, SO_4^{2-}, or F^-).

Mass balances (Salts: NaCl, $NaHCO_3$, KCl, KF, $MgCl_2$, $MgSO_4$, $CaCl_2$. C_i denotes total concentration.)

$$C_{Na} = C_{NaCl} + C_{NaHCO_3} = [Na^+] + [NaHCO_3] + [NaSO_4^-]$$

$$C_K = C_{KCl} + C_{KF} = [K^+] + [KSO_4^-]$$

$$C_{Mg} = C_{MgCl_2} + C_{MgSO_4} = [Mg^{2+}] + [MgHCO_3] + [MgSO_4] + [MgF^+]$$

$$C_{Ca} = C_{CaCl_2} = [Ca^{2+}] + [CaHCO_3^+] + [CaSO_4] + [CaF^+]$$

$$C_{Cl} = C_{NaCl} + C_{KCl} + 2C_{MgCl_2} + 2C_{CaCl_2} = [Cl^-]$$

$$C_{SO_4} = C_{MgSO_4} = [SO_4^{2-}] + [HSO_4^-] + [KSO_4^-] + [NaSO_4^-] + [MgSO_4] + [CaSO_4]$$

$$C_F = C_{KF} = [F^-] + [HF] + [MgF^+] + [CaF^+]$$

Electroneutrality condition

$$[H^+] + [Na^+] + [K^+] + 2[Mg^{2+}] + 2[Ca^{2+}] + [MgHCO_3^+] + [CaHCO_3^+] + [MgF^+] + [CaF^+] = [Cl^-] + [F^-] + 2[SO_4^{2-}] + [HCO_3^-] + [HSO_4^-] + [NaSO_4^-] + [KSO_4^-]$$

where γ_H is the free hydrogen ion activity coefficient and M_i = Na^+, K^+, Mg^{2+} and Ca^{2+}. When written in terms of the apparent dissociation constants, eqn. (3) becomes

$$A = \frac{\alpha P_{CO_2} K''_{CO_2}}{a_H} - a_H \left\{ \frac{1}{\gamma_H} + \frac{C_{SO_4}}{a_H + K''_{HSO_4^-}} + \frac{C_F}{a_H + K''_{HF}} \right\} \qquad (4)$$

This equation describes the pH—alkalinity curve of sea water in the range pH 3—5 and can be simplified as follows. The term in parentheses can be considered as a constant (k); it varies by less than 1% over the pH range 3.7—5.2 because [2] $K''_{HSO_4^-} \gg a_H$ and $\frac{1}{\gamma_H} + \frac{C_{SO_4}}{a_H + K''_{HSO_4^-}} \gg \frac{C_F}{a_H + K''_{HF}}$

Hence eqn. (4) can be rewritten as

$$A = \frac{\alpha P_{CO_2} K''_{CO_2}}{a_H} - k\, a_H \qquad (5)$$

When $k\,a_H \ll \alpha P_{CO_2} K''_{CO_2}/a_H$, eqn. (5) reduces to $A = \alpha P_{CO_2} K''_{CO_2}/a_H$, or

$$\log A = \text{pH} + \log (\alpha P_{CO_2} K''_{CO_2}) \quad (6)$$

Thus at constant temperature and high alkalinity, a linear relationship exists between log (alkalinity) and pH. The line has unit slope and an intercept equal to $\log \alpha P_{CO_2} K''_{CO_2}$. Because α and K''_{CO_2} vary with salinity, a family of parallel lines is needed to describe fully the log (alkalinity)—pH field at all salinities. As log (alkalinity) approaches infinity, the plot becomes curvilinear. Competition for H^+ by SO_4^{2-} and F^- will shift this portion of the plot toward higher pH values.

EXPERIMENTAL

Equipment and chemicals

A diagram of the apparatus is shown in Fig. 1. A Corning combination electrode (No. 476050) was connected to an Orion 801 digital pH meter. The electrode was calibrated before each determination with Beckman buffers.

A Gilmont microburette, 2.5-ml capacity, was used for all titrations. A stock HCO_3^- solution was made by drying A.R. sodium carbonate [6], dissolving ca. 1.3 g (accurately weighed) in distilled water and diluting to 100 ml. The CO_2 employed was of at least 99.5% purity.

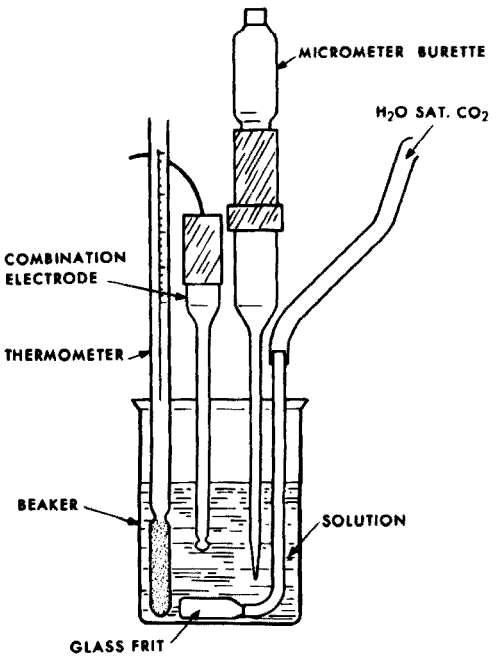

Fig. 1. Diagram of apparatus.

Determination of pH—log (alkalinity) standard curve

Alkalinity-free sea-water was prepared from San Diego Bay water which had been filtered (0.47-μm Millipore filter), acidified with HCl to pH 2 to remove HCO_3^-, and evaporated to give a stock solution with a salinity of 41.2 °/₀₀. This stock was subsequently diluted with distilled water to give samples of 39.87, 35.84, and 31.88 °/₀₀ salinity. To obtain a titration curve for each salinity, a 50-ml sample was placed in the thermostated cell (25°C) and water-saturated CO_2 was bubbled continuously through it at a rate of ca. 1.2 l min^{-1}. Increments (0.005 ml) of the standardized Na_2CO_3 solution were then added with the microburette. The volume of standard and the potential of the electrode were recorded. The equivalence point (i.e. $A = 0$) was determined from a derivative plot of $\Delta mV/\Delta ml$ vs. ml of standard carbonate. A was then calculated from $A = (V - V_0)N/50 \text{ ml} + V$, where V = ml of standard carbonate added, V_0 = ml of carbonate added to equivalence point, and N = meq l^{-1} of the standard carbonate. The pH was calculated from $\text{pH} = 4.008 + [(E_{cell} - E_{4.008})/\Delta mV/\Delta pH]$ where E_{cell} = potential produced by electrode, $E_{4.008}$ = potential of the 4.008 pH buffer, and $\Delta mV/\Delta pH$ = experimentally determined electrode response.

RESULTS

Figure 2 presents the obtained log (alkalinity) vs. pH plots with the 35.84 °/₀₀ curve omitted for clarity. An enlargement of the plots for alkalinities between 1.7 and 2.7 meq l^{-1} is shown in Fig. 3. The slopes and intercepts of these plots were calculated by linear regression (Table 2). Table 2 also shows the values of $\alpha K''_{CO_2}$ calculated from the values tabulated in Riley and Skirrow [7]. A quick inspection of the data shows that the values of $\alpha K''_{CO_2}$ obtained by the proposed method are only approximations of the literature values. The proposed technique fails to yield good absolute values because there is too much experimental error in the slopes to yield good intercepts at pH 0 and because the true value of P_{CO_2} in the solution is unknown. However, in the alkalinity range 1.7—2.7 meq l^{-1} the technique yields a good linear correlation between log (alkalinity) and pH ($r^2 = 0.999$) and is suitable for quantitative analysis. Thus it is possible to bracket a sample with appropriately prepared standards and then analyse a large number of samples by titration with CO_2 (if a salinity correction is to be avoided, standards should be within 0.05 °/₀₀ of the sample). The accuracy of this method was determined by preparing three sets of five standard solutions of known alkalinities by the procedure described for the preparation of the titration curves. The solutions were made up at salinities 38.92, 36.71, and 33.51 °/₀₀, and for each salinity, the solutions of lowest and highest alkalinity were considered as "standards". All fifteen solutions were titrated with CO_2 in random order. For each sample, a stable pH was reached within 2 min and then the equilibrium pH values were plotted vs. log (alkalinity). For each salinity, a straight line was drawn between the "standards" and

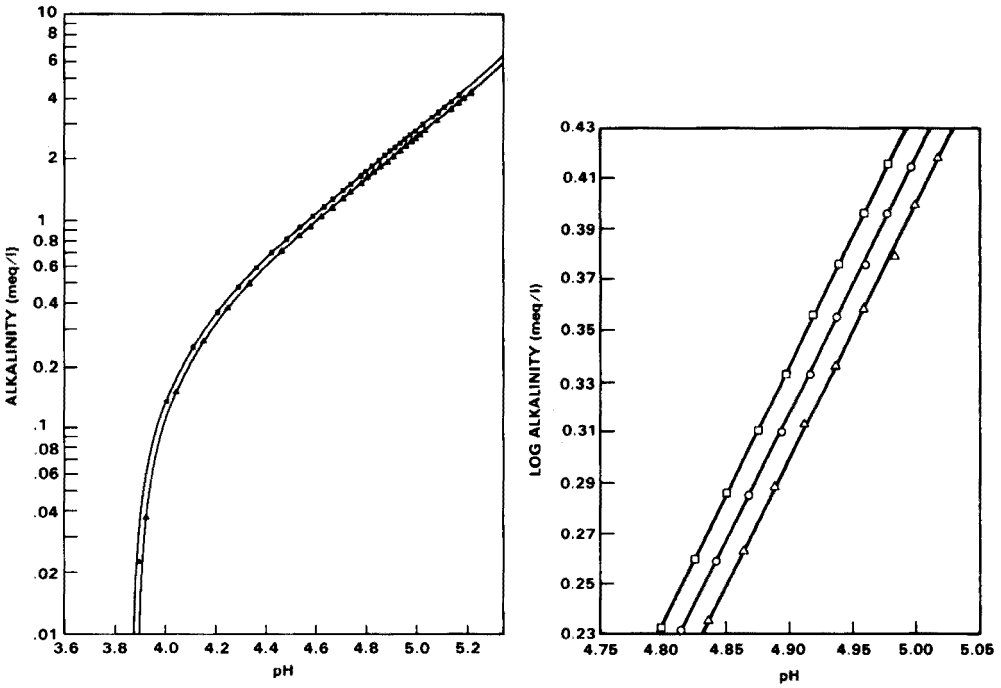

Fig. 2. Experimental log A vs. pH plot for S = 31.88 °/₀₀ (▲) and S = 39.87 °/₀₀ (■).

Fig. 3. Experimental log A vs. pH plots for alkalinities between 1.7 and 2.7 meq l^{-1} at three salinities. △ 31.88 °/₀₀. ○ 35.84 °/₀₀. □ 39.87 °/₀₀.

TABLE 2

Values of log $\alpha K''_{CO_2}$ obtained by titration with CO_2 and from the literature

Salinity (°/₀₀)	log A − log $\alpha K''_{CO_2}$	log $\alpha K''_{CO_2}$ at 1 atm. and 25°C	
	pH	Experimental	Ref. 7
31.88	1.003	−4.615	−4.545
35.84	1.018	−4.669	−4.531
39.87	1.019	−4.658	−4.515

the alkalinities of the 3 remaining solutions were computed from the plots. The results are presented in Table 3. Although the average recovery was 99.9%, the error was ±0.96 (one σ). Similarly, the relative precision of the technique — established by titrating 10 replicate samples of filtered San Diego Bay water — was found to be ±0.36% (one σ).

TABLE 3

Accuracy of the CO_2 titration

Salinity (‰)	Expected	Found	Recovery (%)
38.92	2.404	2.388	99.3
	2.188	2.200	100.5
	1.968	1.949	99.0
35.71	2.404	2.366	98.4
	2.188	2.205	100.8
	1.968	1.959	99.5
33.51	2.404	2.409	100.2
	2.188	2.221	101.5
	1.968	1.969	99.9

REFERENCES

1 N. R. Anderson, Chemical Oceanographic Research: Present Status and Future Direction, Office of Naval Research ACR 190 (1973).
2 C. Culbertson, R. M. Pytkowicz and J. E. Hawley, J. Mar. Res., 28 (1970) 15.
3 J. M. Edmond, Deep-Sea Res., 17 (1970) 737.
4 R. M. Garrels and M. E. Thompson, Am. J. Sci., 260 (1962) 57.
5 L. G. Sillen, Master Variables and Activity Scales, in R. F. Gould (Ed.), Equilibrium Concepts in Natural Water Systems, A.C.S. Publications, 1967, pp. 45—56.
6 A. E. Vogel, A text book of Quantitative Inorganic Analysis, Longmans Green, London, 1957.
7 J. P. Riley and G. Skirrow (Eds.), Chemical Oceanography, Vol. 2, 2nd edn., Academic Press, 1975.

Analytica Chimica Acta, 91 (1977) 189—197

DETERMINATION OF COPPER, NICKEL, AND CADMIUM IN SEA WATER BY APDC CHELATE COPRECIPITATION AND FLAMELESS ATOMIC ABSORPTION SPECTROMETRY

EDWARD A. BOYLE and JOHN M. EDMOND

Department of Earth and Planetary Sciences, Massachusetts Institute of Technology, Cambridge, MA 02139 (U.S.A.)

(Received 1st November 1976)

SUMMARY

Copper, nickel, and cadmium can be determined in 100 ml of sea water by coprecipitation with cobalt pyrrolidinedithiocarbamate and graphite atomizer atomic absorption spectrometry. Concentration ranges likely to be encountered and estimated (1 σ) analytical precisions are 1—6 nmol kg^{-1} (±0.1) for copper, 3—12 nmol kg^{-1} (±0.3) for nickel and 0.0—1.1 nmol kg^{-1} (±0.1) for cadmium. The technique may be applied to fresh-water samples with slight modification.

This report describes a technique for the determination of copper, nickel, and cadmium in sea water. The metals are concentrated from a 100-ml sample by cobalt pyrrolidinedithiocarbamate coprecipitation [1]. The precipitate is redissolved in an organic solvent and digested to simplify the sample matrix. The resulting solution is analyzed by atomic absorption spectrometry with heated graphite atomization. Extension of the method to fresh-water samples is discussed briefly.

EXPERIMENTAL

Prevention of contamination

Quantitative methods for elements at very low concentration levels must preclude contamination of the sample, as well as satisfy accuracy and sensitivity requirements. Elaborate clean-room techniques entail considerable inconvenience in terms of cost and availability and do not entirely eliminate introduction of contamination by the analyst. For this reason the method was designed for use in an ordinary laboratory with the precautions outlined below.

Reagents are stored in polyethylene or polypropylene bottles and leached in 1 M hydrochloric acid for at least one day. For acid storage, bottles are leached in 6 M hydrochloric acid at 80°C for 2 h. When not in use, bottles are covered with plastic bags.

All glassware and plastic ware are stored in a covered bath with a leaching solution consisting of 0.1 M hydrochloric acid and 0.1 M nitric acid. Immediately prior to use, the glassware is rinsed with high-purity distilled water and used without drying. The distilled water should be of sufficient purity to give no detectable blank if treated as a sample.

Other precautions are that: disposable polyethylene gloves are used for critical handling steps; samples are allowed minimal exposure to open laboratory air; microliter pipette tips are flushed several times with 0.1 M hydrochloric acid before each use; and silicone rubber stoppers are kept in 2% EDTA solution between each use. Other precautions are mentioned in the Procedure. Although not used here, a laminar-flow clean bench would help ensure integrity of the sample during manipulation steps and is recommended.

Equipment

Two special items are illustrated in Fig. 1. The filtration funnel (A) is made by joining a 15-ml fine sintered glass frit to the bottom of a tall-form 200-ml pyrex beaker. The redissolution apparatus (B) is made from plexiglass and silicone rubber stoppers. A frame for securing the filtration funnel into a 250-ml filter flask is necessary; this frame may be constructed from plexiglass with 1/8-in o.d. tygon tubing straps with glass hooks.

Reagents

Cobalt chloride solution. Dissolve 0.2 g of ultrapure $CoCl_2 \cdot 6H_2O$ (Spex Industries) in 250 ml of distilled water.

APDC solution. Purify a 2% ammonium pyrrolidinedithiocarbamate solution in water by repeated extraction with carbon tetrachloride [2].

Acid—acetone mixture. Prepare a (95 + 5) solution of acetone and 0.1 M hydrochloric acid; dispense from a 250-ml polyethylene squeeze bottle.

Nitric—perchloric acid mixture. Prepare 6 M nitric acid, redistilled in a vycor glass still, containing 1% (v/v) ultrapure perchloric acid.

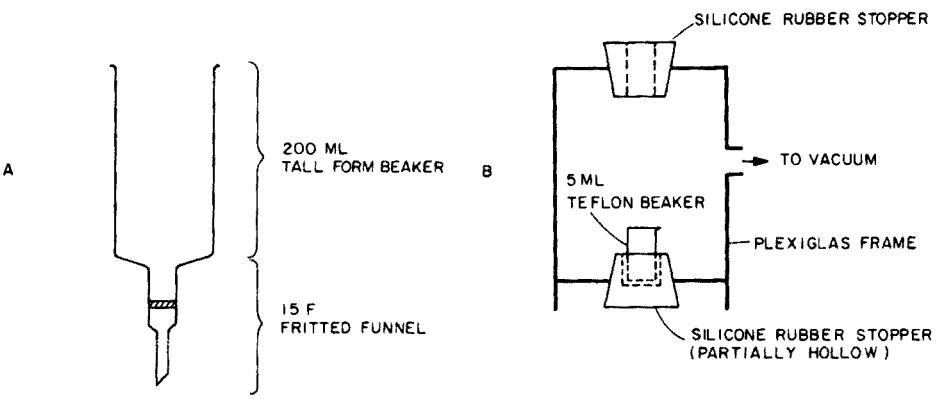

Fig. 1. (A) Filtration funnel. (B) Dissolution apparatus.

Ammonium sulfate solution. Prepare $3 \cdot 10^{-2}$ M ammonium sulfate (reagent grade) in $1.5 \cdot 10^{-2}$ M sulfuric acid (reagent grade).

Hydrochloric acid (6 M). Prepare from acid redistilled in a vycor glass still.

Standards. Prepare nickel and copper standards (20 μmol ml^{-1}) and cadmium standard (10 μmol ml^{-1}) in 0.1 M hydrochloric acid.

Procedure

Samples should be acidified to pH 2 by addition of 6 M hydrochloric acid immediately after collection. This procedure minimizes adsorption on to container walls [3].

Weigh out approximately 100 g of sample into a 200-ml tall-form beaker. Add 250 μl of cobalt chloride solution and swirl gently to mix thoroughly. Add 500 μl of APDC solution, swirl gently to mix thoroughly, and allow the precipitation to proceed for 5 min before filtration. During this waiting period, remove the filtration funnel from the acid bath, rinse with distilled water, and strap into the filtration rig. Apply full vacuum and rinse the interior of the filtration funnel with two portions of 6 M hydrochloric acid followed by two portions of distilled water. Then filter the sample using full vacuum. Rinse the interior of the funnel with a small portion of distilled water to remove the last traces of sea salt. Release the vacuum slowly by means of a stopcock valve with an in-line air filter.

Remove a 5-ml Teflon beaker from the acid bath and rinse with distilled water. Place it into the dissolution apparatus. Rinse the tip of the filtration funnel with acid—acetone solution and place the funnel into the top of the dissolution apparatus. Rinse through several small portions of acid—acetone mixture by applying a gentle vacuum. This procedure dissolves the precipitate and washes it into the beaker. Release the vacuum; remove the beaker, and carefully remove the filter funnel from the dissolution apparatus. Remove the traces of the chelate from the tip of the filter funnel by washing with acid—acetone mixture and collecting the wash in the Teflon beaker.

Cover a hot plate with a glass fiber filter. Place the beaker on the hot plate at very low heat (to avoid bumping) and cover with an inverted 20-ml pyrex beaker; the glass fiber minimizes spattering of condensate running down the inside of the cover. Tilt the beaker by placing one edge on a glass rod, to prevent condensation from falling back into the beaker. Evaporate to dryness. Add 500 μl of nitric—perchloric acid mixture and evaporate to dryness at slightly higher heat. Avoid charring the residual organic material by overheating. After cooling, the beaker may be covered with Parafilm and stored indefinitely.

Along with the samples, prepare a matrix for standards by pipetting 250 μl of cobalt chloride solution into each of three 5-ml beakers, adding 10 μl of APDC solution to each, and evaporating and treating with acid mixture as in the preceding paragraph. Determine blanks by running high-purity water as a sample. The water may be tested for traces of the metals by varying the volume of several blank samples.

About one hour before the atomic absorption analysis, pipette 2000 μl of 0.1 M hydrochloric acid into each sample and standard matrix beaker. While allowing 15 min for the residue to dissolve, prepare a secondary mixed standard by diluting 10 μl of cadmium standard plus 50 μl of copper standard and 100 μl of nickel standard to 100.0 ml with distilled water. Mix thoroughly and pipette 50 μl into one of the standard matrix beakers and 100 μl into another; the third matrix beaker is used for a matrix blank. After the dissolution period, swirl each beaker gently to mix the solution and rinse the sides of the beaker. This solution is used for the copper and nickel determinations.

Prepare a diluted solution for the cadmium determinations by pipetting 250 μl from each concentrated sample and standard into dry 5-ml Teflon beakers. Add 750 μl of ammonium sulfate solution and mix by gentle swirling. Cover all beakers with Parafilm and analyze immediately to minimize evaporation.

Determinations were made with a Perkin-Elmer HGA 2100 graphite furnace, model 403 atomic absorption spectrophotometer and model 56 chart recorder. Manufacturer's recommended operating conditions for wavelength, slit and lamp current were followed. Instrumental parameters for the graphite furnace are given in Table 1. Deuterium arc background correction was applied, with the deuterium arc beam aligned to coincide with the hollow-cathode beam at the center of the graphite tube. Optical windows were kept clean by recommended procedures and were masked outside the optical path to minimize light scattering in the optics. The chart recorder was set to 0.5 absorbance full scale with minimum pen damping. Typical peak height output is illustrated in Fig. 2. A 100-g sample with 1 nmol kg^{-1} of each element processed as described above should give peak absorbances of approximately 0.02 for copper, 0.01 for nickel, and 0.1 for cadmium.

TABLE 1

Instrumental parameters for HGA 2100

Element	Sample volume (μl)	Gas flow continuous (cm^3 min^{-1})	Dry cycle	Char cycle	Atomization cycle
Cu	50	30	20 s 110°C	25 s 850°C	10 s 2400°C
Ni	100	30	35 s 110°C	20 1150°C	12 s 2600°C
Cd	50	20	25 s 110°C	20 s 500°C	5 s 1600°C[a]

[a] For Cd, this was followed by cleaning for 5 s at 2600°C.

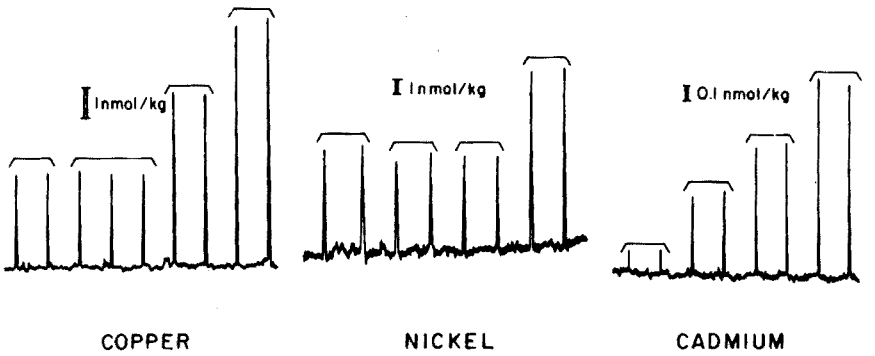

Fig. 2. Representative peak height output for copper, nickel, and cadmium. Duplicate injections are indicated by brackets. Peak height expected for 1 nmol kg^{-1} (Cu, Ni) and 0.1 nmol kg^{-1} (Cd) in a 100-g sample is indicated by bar.

All samples and standards should be injected in duplicate, or more if duplicates disagree significantly. Standards spanning the sample absorbance range are run before and after each series of about five samples and a drift correction is applied. The volumes and standard concentrations are chosen to remain within the linear range, which should be checked regularly. Experience suggests that the calibration plots are reliably linear below an absorbance of 0.15.

The cobalt chloride should be sufficiently pure that the standard matrix blank gives a peak height below $5 \cdot 10^{-4}$ absorbance units. Where a small matrix blank is observed, this value is subtracted from the peak heights of the standards. With some instruments a small ($<1 \cdot 10^{-3}$ absorbance units) baseline shift occurs on atomization; if necessary this correction should also be applied to the peak signals.

The reproducibility of pipetting into the furnace is important; satisfactory results can be obtained by gently inserting Brinkmann pipette tips into the graphite tube as far as possible, i.e. the position is the same for each injection.

It is advisable to monitor the recovery periodically by standard additions. The recovery is quite reproducible, however, and need not be determined for each sample.

RESULTS

Two standard addition plots for a deep Sargasso Sea water sample are shown in Fig. 3. Experience from a large number of such plots indicates that copper and nickel recoveries are essentially quantitative, whereas cadmium recovery is about 10% lower. Table 2 gives the results of duplicate analyses on water samples taken from a profile at a station south of New Zealand (GEOSECS station 293). The pooled standard deviations are: copper, ± 0.13 nmol kg^{-1}; nickel, ± 0.28 nmol kg^{-1}; and cadmium, ± 0.10 nmol kg^{-1}.

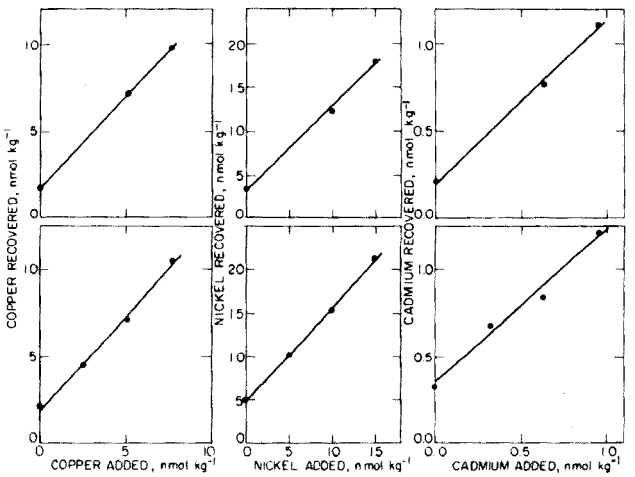

Fig. 3. Standard additions plot for a sea-water sample. Best-fit lines are indicated.

TABLE 2

Replicate sea-water analysis
(Results are given as nmol kg^{-1}.)

Sample depth (m)	Copper	Nickel	Cadmium
216	1.28	4.5	0.31
	1.14	4.7	0.38
916	2.48	5.8	0.71
	2.17	6.2	0.73
1733	2.25	7.2	0.87
	2.19	7.1	—
2326	2.85	7.8	1.07
	2.63	7.0	1.12
	2.74	7.1	1.29
4926	4.55	8.2	0.98
	4.08	7.8	1.26

A comparison of copper analyses by this technique with flame atomic absorption analyses after a similar coprecipitation technique [1, 4] is given in Table 3. Individual results from the two methods agree within the estimated errors. The systematic difference is due to propagation of the standardization and blank errors and is within the stated precision. A significant systematic error unique to either flame or flameless analysis is ruled out.

The accuracy of the analyses is estimated to be similar to the precision. The results of the standard additions tests suggest an accuracy better than 10%

TABLE 3

Comparison of flame and flameless atomic absorption analyses of sea-water samples for copper

Sample No.[a]	Flameless (nmol kg^{-1})	Flame (nmol kg^{-1})	Difference[b]
284	1.80	1.80	0.00
290	1.99	1.87	0.12
292	1.35	0.98	0.37
293	1.50	1.33	0.17
294	1.39	1.28	0.11

[a]See ref. 4 for description of samples.
[b]The average difference is 0.15, which is consistent with the estimated precisions of 0.13 (flameless) and 0.15 (flame).

for the determination of added Cu, Ni and Cd. No suitable reference standard sea-water samples are available for comparison, however.

The limiting factor in the precision is not the atomic absorption determination; this is indicated by a comparison of the pooled precision of replicate injections with the overall precision (Table 4). For copper and nickel the limiting factor is probably quantitative transfer of the precipitate to the final solution. For cadmium the additional error is probably associated with the slightly lower (and therefore potentially more variable) precipitation efficiency. Improvements in precision require improved sample handling procedures rather than instrumentation.

DISCUSSION

The method described resulted from various optimization experiments. Preliminary work with cadmium is described below to illustrate the methodology. Cadmium is used as the example because it exhibited the largest variations with respect to changes in analytical conditions.

Initial work showed that cobalt interfered with the determination of cadmium. Injection of a standard into a cobalt chloride matrix resulted in rapidly decreasing peak absorbance on successive injections, with a char

TABLE 4

Comparison of precision for replicate samples with replicate injections

Element	Pooled standard deviations (nmol kg^{-1})			
	Samples	n	Injections	n
Cu	0.13	6	0.04	25
Ni	0.28	6	0.10	19
Cd	0.10	5	0.03	22

temperature of 300°C and an atomization temperature of 1600°C. When this series of injections was followed by a high-temperature (2600°C) tube cleaning cycle for 10 s, the sensitivity was restored to its initial level. Apparently, cobalt coats the graphite surface and retards reduction of cadmium to the atomic state. The cleaning cycle removes cobalt and allows reduction to proceed unhindered. Similar coating effects have been used to minimize carbide formation [5]. In addition to this cumulative coating effect, cobalt also affects the peak height of cadmium in a cleaned tube (Fig. 4 A, B). Use of a higher atomization temperature does not eliminate this effect (Fig. 4C). Such errors can be eliminated by using standards containing the same cobalt concentration as the samples. Sensitivity is enhanced by minimizing the amount of cobalt used for coprecipitation and by dilution of the final concentrate. Finally, addition of ammonium sulfate to the matrix allows the use of a higher charring temperature [6] and minimizes interferences.

The coprecipitation procedure is applicable to fresh water samples, with the following modifications. Organic material dissolved in fresh water often precipitates on acidification and clogs the fritted glass discs. To avoid this problem, a filter rig with disposable acid-leached glass fiber filters should be substituted for the filtration funnels. For some highly colored water samples, the organic material inhibits precipitation at the reagent levels recommended above. If this effect is observed, the cobalt and APDC levels should be increased until the chelate does not pass through the filter. The recovery efficiency should be monitored for each different type of sample.

Conclusions

APDC chelate coprecipitation coupled with flameless atomic absorption provides a simple and precise method for the determination of nanomol kg^{-1} levels of copper, nickel, and cadmium in sea water. With practice, the method is not overly time-consuming. It is reasonable to expect to complete sample

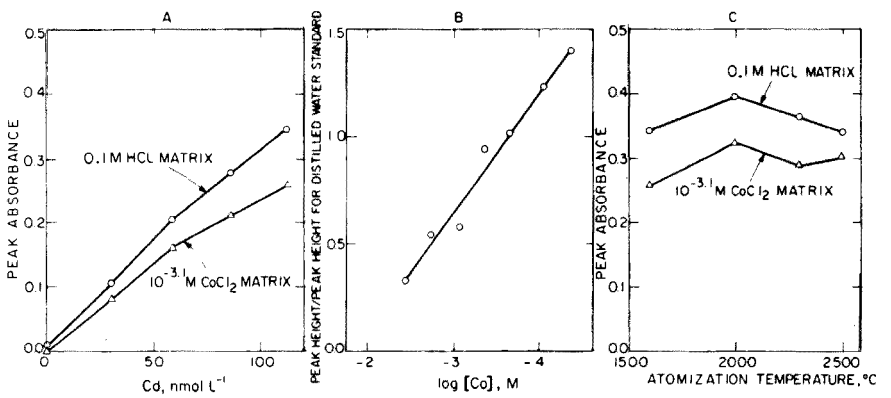

Fig. 4. (A) Effect of $10^{-3.1}$ M Co on a cadmium standard curve. (B) Effect of cobalt concentration on cadmium peak height at 1600°C atomization temperature. (C) Effect of atomization temperature on cobalt interference, [Co] = $10^{-3.1}$ M, [Cd] = 115 $nmol^{-1}$.

concentration in less than 20 min, digestion in about 4 h, and sample preparation in another hour; atomic absorption time should average about 5 min per element. Excellent results have been obtained on the distribution of nickel and cadmium in the ocean by this technique [7, 8].

REFERENCES

1 E. A. Boyle and J. M. Edmond, in T. R. P. Gibb (Ed.), Analytical Methods in Oceanography, Advances in Chemistry Series, No. 147, American Chemical Society, Washington D.C., 1975, p. 44.
2 W. Slavin, Atomic Absorption Spectroscopy, Interscience-Wiley, New York, 1968, p. 75.
3 D. E. Robertson, Anal. Chim. Acta, 42 (1968) 533.
4 E. A. Boyle and J. M. Edmond, Nature (London), 253 (1975) 107.
5 J. H. Runnels, R. Merryfield and H. B. Fisher, Anal. Chem., 47 (1975) 1258.
6 R. D. Ediger, At. Absorpt. Newsl., 14 (1975) 127.
7 F. R. Sclater, E. A. Boyle and J. M. Edmond, Earth Planet. Sci. Lett., 31 (1976) 129.
8 E. A. Boyle, F. R. Sclater and J. M. Edmond, Nature (London), 263 (1976) 42.

Analytica Chimica Acta, 91 (1977) 199—209

DETERMINATION OF TRACE IMPURITIES IN IRON AND NICKEL-BASE ALLOYS BY GRAPHITE FURNACE ATOMIC ABSORPTION SPECTROMETRY

T. R. DULSKI and R. R. BIXLER

Carpenter Technology Corporation, R&D Center, P.O. Box 662, Reading, Pennsylvania 19603 (U.S.A.)

(Received 26th July 1976)

SUMMARY

Five approaches to the determination of trace amounts of lead, bismuth, thallium, selenium, tellurium, and silver in iron and nickel-based alloys were investigated. While all procedures produced satisfactory results, direct techniques yielded a significant time advantage over separation schemes. Matrix effects made calibration curves an impractical approach. A spiking technique was used to generate data on a wide range of standard alloy samples.

The need for trace element analysis of ferrous and nickel-based alloys derives from three sources. The first is in primary processing where trace levels of certain elements can affect both the hot and cold working properties of many steels and alloys deleteriously because of their tendency to accumulate in grain boundaries, weakening the microstructure. Secondly, in customer processing of finished steel, such as in forming and stamping operations, problems traceable to low level "tramps" may occur. Finally, in end-use applications, catastrophic failure of critical components in high stress, high temperature, high corrosion, or high radiation applications can often be directly related to trace levels of certain impurities.

At the 1—10 p.p.m. level, various techniques are available for the determination of common tramp elements, e.g. dithizone is commonly applied in the spectrophotometric determination of lead, bismuth, and zinc. Selenium and tellurium may be precipitated as metals with a carrier [1] or a spike and collected on a membrane filter for x-ray fluorescence analysis. Lead, bismuth, tin, antimony, thallium, and silver may be extracted into a methyl isobutyl ketone solution of tri-n-octylphosphine oxide (TOPO—MIBK) and the organic layer read out by flame atomic absorption [2—5]. Alternatively, ion exchange may be employed to concentrate the tramp elements for atomic absorption [6]; point-to-plane d.c. arc emission techniques are also useful in this concentration range and many other techniques are available.

At the 0.1—1.0 p.p.m. level the number of available techniques is much lower; most are relatively new. Polarography — especially cathode ray [7],

differential pulse, and anodic stripping voltammetry [8] — has been applied to the determination of tramp elements in alloys. Preconcentration [9] and carrier distillation [10] techniques for emission spectroscopy and spark-source mass spectrometry [11] have been applied to the problem. One of the newer techniques is graphite-furnace atomic absorption spectrometry.

Five techniques of sample preparation for the graphite furnace, including two separation techniques and three direct acid dissolution techniques, have been compared. This study was necessary because many of the conventional methods of sample dissolution thwarted early efforts with the graphite furnace.

EXPERIMENTAL

Equipment

A Perkin-Elmer Model 503 atomic absorption spectrophotometer, equipped with a Model HGA2000 graphite furnace, was used. The instrument was fitted with a smoke removal device which consisted of two glass tubes mounted out of the light path at each end of the furnace housing and connected with flexible tubing through a "Y" joint to a water aspirator. In addition, an overhead exhaust system was used.

Simultaneous deuterium arc background correction was used. Careful alignment of hollow cathode or electrodeless discharge lamps with the background continuum source was accomplished with a center-zero strip chart recorder, as described by the instrument manufacturer.

The analytical peaks were recorded on a strip chart recorder capable of 10, 5, 4, 3, 2, and 1 mV full scale response. Samples were introduced into the furnace by means of Eppendorf micropipets. Electrodeless discharge lamps were used for all elements except silver, for which a hollow cathode lamp was employed. The purge gas was argon.

Standard solutions

Stock standard solutions were prepared from high-purity metals or oxides. In some cases commercially available standard solutions were employed. Working standard solutions of 10 μg ml^{-1} or less were prepared daily from stock standard solutions.

Reagents

Nitric acid of the highest available purity (J. T. Baker, Ultrex) was used for the analysis for lead of NBS 360 series iron and steel standards. Other work was performed with ACS certified grade acids. Water for the final dilution of samples was distilled, and then passed through three ion-exchange resin beds and a microfiltration column. Other reagents were ACS certified.

Sample preparation

Manganese dioxide separation. The procedure described by Vassilaros [9]

was modified as follows: samples (2 g) of high temperature alloys were dissolved in 70 ml of water + 30 ml of hydrochloric acid + 10 ml of sulfuric acid, with low heat, overnight. The solutions were reduced to fumes and light salts, and cooled; 200 ml of 1.2 M nitric acid and 200 ml of water were added. Manganese(II) sulfate solution (5 ml of 5% w/v) was added, the samples were heated to boiling and removed from heat, and 20 ml of 0.25 M potassium permanganate solution was added with stirring. The samples were allowed to stand overnight, then filtered on low porosity paper and washed with water and with 1.5 M nitric acid. Papers were transferred to the original vessels and the filter paper was wet-ashed with nitric, hydrochloric, and sulfuric acids. Samples were cooled and diluted to 50 ml in volumetric flasks.

TOPO—MIBK separation. The procedure described by Burke [2] was followed. Many superalloys yielded to hydrochloric acid dissolution, given sufficient time, making the nitric acid destruction step unnecessary. When nitric acid was used, formic acid or urea was employed to destroy the excess of nitric acid. Alloy samples (2 g) were extracted from 100 ml of aqueous solution into 10 ml of TOPO—MIBK solution. A grooved graphite tube was employed to prevent excessive spreading of the solvent in the furnace.

Direct: nitric acid medium. As described by Shaw and Ottaway [12], iron-base samples were dissolved in dilute nitric acid; as much as 2 g of mild steel could be readily contained in a final dilution volume of 50 ml when 20% (v/v) nitric acid was employed.

Direct: hydrofluoric acid—nitric acid medium. As described by Welcher et al. [13] high temperature alloys were dissolved in hydrofluoric acid—nitric acid, but the relative acid volumes were changed to 20 ml of hydrofluoric acid + 10 ml of nitric acid + 10 ml of water; this mixture readily dissolved a wider variety of high alloy materials, including nickel—chromium base alloys.

Direct: hydrochloric acid medium and hydrochloric acid—nitric acid medium. The severe interference of chloride was studied from two directions. An attempt was made to apply the work of Ediger et al. [14] on copper in sea water to the chloride system with an alloy matrix, and char temperatures were investigated in an attempt to duplicate the work of Frech [15].

RESULTS AND DISCUSSION

Table 1 shows the base composition of the samples used; they include N.B.S. "benchmark" standards, secondary standards developed for intra-company use, and standards developed for industry cooperative testing programs.

Separation procedures

When the investigation of the graphite furnace technique began, the severe interference problems from chloride anion in direct procedures led to a study of two separation procedures chosen to allow the maximum number of "tramp" elements to be determined from a single separation.

TABLE 1

Base compositions of samples

Sample code	Grade or type	Matrix
NBS 361-364	Low alloy steel	Fe
NBS 365	Electrolytic iron	Fe
NBS 1206-2	Rene 41	53 Ni/19 Cr/12 Co/10 Mo/3 Ti
NBS 1207-1 and 1207-2	Waspaloy	56 Ni/19 Cr/13 Co/5 Mo/3 Ti
NBS 1208-1 and 1208-2	Inco 718	52 Ni/19 Fe/17 Cr/5 Nb/3 Mo
Tramp #1-#4	Pyromet 600	74 Ni/15 Cr/9 Fe
Tramp #5	—	70 Ni/17 Cr/4 Fe/2 Nb
Tracealloy 5911-5913	—	68 Ni/12 Cr/9 Co/2 Al/2 Ti/2 Mo/2 W/2 Ta
609-1, 611-1, 627-1	Nichrome-type	80 Ni/20 Cr
P-293	Pure nickel	Ni

The manganese dioxide separation had been applied by Vassilaros [9] to both emission spectrographic and flame atomic absorption determination of bismuth and lead in iron and nickel-base alloys. In this approach the "tramp" constituents are carried down by adsorption on the massive manganese dioxide precipitate. By using the dissolved manganese dioxide residue for graphite furnace work, the complete separation of lead and bismuth from complex alloy matrices was confirmed. Thallium was also carried down quantitatively by the manganese dioxide. The smoke was considerable, but the deuterium arc corrected for it completely.

The TOPO—MIBK separation of Burke [2] has been employed for some time at this laboratory in the flame atomic absorption determination of lead, tin, and thallium. (Silver, bismuth, and antimony are also obtained in the TOPO—MIBK extract but are determined by other techniques.) It was decided to use the extract in graphite furnace work. Good sensitivity was obtained for a variety of elements, once the furnace program parameters were established.

The parameters used for the extracts from these two separation procedures (Table 2) are the result of a lengthy series of determinations in which the dry—char—atomize parameters were varied by increments.

Direct procedure

Lead, bismuth, silver, and thallium could be determined at low and sub-p.p.m. levels in mild steels and iron by direct introduction into the furnace of a dilute nitric acid solution of the sample. Samples (2.000 g) of NBS 360 series standards were dissolved in 20% (v/v) nitric acid and diluted to 50 ml. Once the linear range for each element had been established — by calibration curves prepared from pure iron and the element of interest — a spiking

TABLE 2

Instrument parameters for separation methods
(Aliquot volume: 5.0—20.0 μl.)

Parameter	MnO_2 Separation			TOPO—MIBK Separation[a]		
	Pb	Bi	Tl	Pb	Bi	Tl
Wavelength (nm)	283.3	223.1	276.8	283.3	223.1	276.8
Bandwidth (nm)	0.7	0.2	0.7	0.7	0.2	0.7
Drying temp. (°C)	250	250	250	120	100	100
Drying time (s)	40	40	40	50	50	50
Charring temp. (°C)	1000	1000	1000	250	300	125
Charring time (s)	60[b]	60[b]	60[b]	20	40	60
Atomizing temp. (°C)[c]	2000	2000	2000	2000	2000	2100

[a]Grooved tube. [b]Gas interrupt for first 30 s of char cycle. [c]The atomization time was 8 s in all cases.

technique could be used. Spikes were added directly to a second sample (2.000 g) which was treated identically. A spike that would yield an absorbance ca. 0.5 times that of the sample alone and also remain in the linear range (the final aliquot size was adjusted accordingly) was chosen. At extremely low concentration levels, spikes were chosen to yield an absorbance at least 0.040 absorbance units above the absorbance of the sample.

This technique was preferable to the use of calibration curves because, as other investigators have also found [16], inter-element effects become important in certain alloy matrices. It is clearly impractical to set up calibration curves for each alloy matrix encountered. A single-point spiking technique, such as that used in these studies, is a satisfactory substitute for, and involves less time than, the multipoint method-of-additions. Several important precautions must be taken, however. A precise knowledge of the linear range of each element in a given acid medium must be obtained so that spiked and unspiked samples are adjusted to fall in the linear absorbance range; a good estimate of the reagent blank must also be obtained.

The same approach was used for high-alloy materials, including nickel-base alloys, except that they were dissolved in hydrofluoric acid—nitric acid. The parameters used for these direct methods are given in Table 3.

Results of direct nitric acid dissolution and direct hydrofluoric acid—nitric acid dissolution are compared with the extraction procedures in Table 4.

Table 5 presents data obtained from NBS 360 series standard reference materials (SRM's) with the nitric acid dissolution; Table 6 illustrates the data from hydrofluoric acid—nitric acid dissolution of different high alloy standards. Results are compared with NBS provisional data in the case of the 1206-1208 SRM's when such data were available. The "Tracealloy" and Cr/Ni sample data were obtained during this laboratory's participation in two round-robin testing programs. For these two series of samples the values for

TABLE 3

Instrument parameters for direct HNO_3 and direct $HF—HNO_3$ methods (Aliquot volume: 5.0—20.0 μl.)

Parameter	Pb	Bi	Tl[a]	Se	Te[a]	Ag
Wavelength (nm)	283.3	223.1	276.8	196.0	214.3	328
Bandwidth (nm)	0.7	0.2	0.7	2.0	0.2	0.7
Drying temp. (°C)	150	150	150	150	150	100
Drying time (s)	20	20	20	20	20	60
Charring temp. (°C)	400	800	500	350	500	150
Charring time (s)	60	60[b]	60[b]	60	60[b]	60
Atomizing temp. (°C)	2000	2200	2000	2400	2000	2400
Atomizing time (s)	8	8	8	10	8	8

[a]Maximum temperature for 30 s after each measurement.
[b]Gas interrupt for first 30 s of char cycle.

TABLE 4

Comparison of results from direct and separation methods (values in p.p.m.)

Sample	Element	Direct	TOPO—MIBK Sep.	MnO_2 Sep.	Given Value
Tramp #5	Pb	6.3	5.3	6.2	6[a]
	Bi	4.4	3.6	4.4	
	Tl	4.8	4.9	4.6	7[a]
NBS 361	Pb	0.2	0.6		0.25
	Bi	4.5	3.5		4
	Ag	4.4	4.6		4
NBS 365	Pb	0.1	0.3		0.1_5
	Bi	<0.02	<0.5		N.D. (<0.1)
	Ag	0.02	<0.1		(0.02)[b]

[a]MIBK—TOPO separation—flame a.a.s. finish.
[b]Not certified by NBS.

selenium and tellurium are compared with results obtained by cathode ray polarography. The remaining samples coded "tramp 1" through "tramp 6" are intralaboratory standards prepared for emission and x-ray spectrographic calibration. For these samples data are compared with results from other techniques (as noted).

Lead contamination

The determination of lead at less than 0.5 p.p.m. proved to be difficult because of an erratic blank. Acids, water, and airborne particulate contamination were contributing factors. As a result, "ACS certified" grade nitric

TABLE 5

Analysis of low alloy steels and iron by the direct HNO_3 method
(Values in parentheses are not certified by N.B.S. Except where noted, all values are in p.p.m.)

Sample	Pb		Bi		Ag	
	Found	Certified	Found	Certified	Found	Certified
NBS 361	0.10 0.20	0.25	4.0 4.9	4	3.8 5.0	4
NBS 362	4.2 5.5	4.3	35	(0.002%)	13	11
NBS 363	20 26 25	22	6.4	(8)	33	37
NBS 364	273	0.024%	14	(9)		
NBS 365	0.1 0.12	0.15	N.D. (<0.05) N.D. (<0.05)	N.D. (<0.1)	0.02 0.02 0.02	(~0.02)

acid was replaced by ultrapurity (J. T. Baker "Ultrex") grade reagent; distilled water was replaced by water which was distilled, then passed through three ion-exchange resin beds and one ultrafiltration bed. Special air filters were installed in the laboratory rooms where samples were prepared and analyzed. While these measures reduced the lead blank, it remained somewhat erratic, and the plastic tips for the Eppendorf pipets were found to contain a measurable quantity of nitric acid-leachable lead. Rather than batch-treat the tips to remove the lead, a procedure was established to pipet the dilute acid blank successively until two successive blanks show the same peak height (in practise the first four aliquots are discarded). The same tip is then used for subsequent samples (rinsing four times before placing an aliquot in the furnace) until solution adhesion begins to occur in the tip. Then a new tip is similarly treated. These measures resulted in a consistent lead blank.

Use of hydrochloric acid

The interference of halogen ions in graphite furnace analysis has been well documented [16—19]. The interference has been attributed to molecular absorption of volatile chloride, bromide, and iodide compounds. Table 7 shows the boiling points of several metal halide salts and the boiling points of the corresponding elemental metals. An examination of Table 7 shows that, at the temperatures commonly used in the "char" cycle (200—1000°C), many metal chlorides would boil and many fluorides would not. This suggests a possible means for the removal of chloride, but does not explain the apparent lack of interference from metal fluorides in the direct hydrofluoric

TABLE 6

Analysis of high-alloy samples by the direct $HF—HNO_3$ method
(All values are in p.p.m)

Sample	Pb		Bi		Ag		Tl		Se		Te	
	Found	Given	Found	Given	Found	Given	Found	Given	Found	Given	Found	Given
NBS 1206-2	29	27[a]	1.5	0.6[a]								
	39		0.9									
NBS 1207-1	19	12[a]	0.25	0.38								
	13		0.35									
NBS 1207-2	22	22[a]	0.43	0.47[a]								
	22		0.95									
NBS 1208-1	6.8	5.4[a]	0.42	0.78[a]								
	8.0		0.63									
			0.50									
NBS 1208-2	26	22[a]	0.17	0.84[a]								
	27		0.19									
Tramp #1									76	77[b]	66	79[b]
											94	
Tramp #2			5.1	4[c]			40	38[c]	9.0	15[b]	175	185[b]
			4.3								159	
Tramp #3			5.5	4[c]					1.2	0.9[b]	30	22[b]
											34	
Tramp #4			1.8	2[c]			2.8	2[c,d]	22.9	23[b]	1.4	1.9[b]
			1.7				1.0					
Tramp #5	6.3	6[d]	4.4	—			5.6	7[d]				
	6.2		4.4				4.6					
							4.0					
Tracealloy 5911	4.1		0.4	<0.5[c]			0.3	<1[d]	9.8		1.1	
	2.2		0.4									
	4.1		0.3									
Tracealloy 5912	3.1	2[d]	1.0	<1[c]			3.1	6[d]	1.1		<1	
	3.8		1.0				4.0		1.3		<1	
	2.8								0.6			
Tracealloy 5913	5.2	4[d]	0.3	<0.5[c]			0.3	<1[d]	9.8		4.2	
			0.3						7.8		6.0	
									9.1			
607-1	17		12		28		2.8		47	46[b]	34	35[b]
609-1	25		24		33		6.4		66	49[b]	25	32[b]
611-1	11		6.1		23		1.6		88	53[b]	36	40[b]
627-1	4.3		1.4		11		0.25		73	46[b]	14	11[b]
P-293	2.3		<0.4		<0.1		<0.2		1.1	<1[b]	<0.2	<0.1[b]

TABLE 7

Estimates of boiling points for certain metals and compounds[a]

Species	Fe	FeF_2	FeF_3	$FeCl_2$	$FeCl_3$
B.p. (°C)	3000	(melts at 1020)	(melts at >1000)	(sublimes above 670)	(decomposes at 315)
Species	Ni	NiF_2	$NiCl_2$	Pb	PbF_2	$PbCl_2$
B.p. (°C)	2840	(sublimes above 1450)	(sublimes at 973)	1751	1290	950
Species	Bi	BiF_3	$BiCl_3$			
B.p. (°C)	1560	(1027)	447			

[a]J. A. Dean (Ed.), Lange's Handbook of Chemistry, 11th edn., McGraw-Hill, New York, 1973.

acid—nitric acid procedure. It may be extrapolated, however, from the work of Culver and Surles [18] that the molecular absorbance by metallic fluorides at many of the common analytical wavelengths is sufficiently low to allow correction by a properly aligned deuterium arc, whereas that from a similar concentration of metallic chlorides is not.

It would, however, be convenient to use hydrochloric acid in the dissolution of certain alloys for graphite furnace work. The method described by Ediger et al. [14] utilizes the addition of ammonium nitrate to eliminate the interference of chloride. Essentially, the ammonium nitrate reacts with the sample to form volatile ammonium chloride which is driven out of the furnace during the char cycle. The application of this technique to steel and alloy samples in chloride and chloride—nitrate media, however, showed no distinct advantage. The work of Frech [15], suggested that char cycle conditions could be chosen to eliminate or minimize chloride interference in lead determinations of steel. Table 8 lists the parameters found to produce the best data for samples dissolved in hydrochloric acid or in hydrochloric acid—nitric acid. Table 9 summarizes the work with chloride-containing samples.

Conclusions

Routine sub-p.p.m. determinations of a number of "tramp" elements in iron and nickel-base alloys appear to be possible with the graphite furnace technique. Exact detection limits are often a function of the alloy system and acids used in dissolution. The standard materials available in this range have been analyzed successfully. Higher concentrations are also readily determined, although dilution errors become important at above 20 p.p.m.

Reproducibility is dependent largely on the selection of appropriate instrument parameters which differ for certain classes of anion matrix. While

TABLE 8

Instrument parameters for direct HCl and direct HCl—HNO_3 methods (Aliquot volume: 5.0—20.0 μl)

Parameter	Pb	Bi	Se	Te[b]
Wavelength (nm)	283.3	223.1	196.0	214.3
Bandwidth (nm)	0.7	0.2	2.0	0.2
Drying temp. (°C)	150	150	150	150
Drying time (s)	20	20	20	20
Charring temp. (°C)	650	800	1000	800
Charring time (s)	60[a]	60[a]	60	60[a]
Atomizing temp. (°C)	2400	2400	2400	2400
Atomizing time (s)	8	8	10	8

[a]Gas interrupt for first 30 s of char cycle.
[b]Maximum temperature for 30 s after each measurement.

TABLE 9

Analysis of low and high alloys by the direct HCl method (Values in p.p.m.)

Sample	Pb		Bi		Se		Te	
	Found	Given	Found	Given	Found	Given	Found	Given
NBS 362	4.8	4.3	42	0.002%[a]	14	12[a]	10	5[a]
Tramp #4	7.4	6[b]	1.5	2[c]	18	23[d]	3.2	1.9[d]
Tramp #5	5.1	6[b]	2.4	—	2.0	5.3[d]	9.7	5.2[d]
NBS 1208-1	6.7	5.4[a]	N.D.	0.78[a]	N.D.	—	—	—
627-1	3.8	4.3[e]	1.5	1.4[e]	17	46[d]	27	11[d]

[a]Not certified by NBS. [b]Flame a.a.s.—MIBK—TOPO extract. [c]Emission spectrometry carrier distillation. [d]Cathode ray polarography. [e]Graphite furnace — HF—HNO_3 direct value.

the use of calibration curves is possible, the sample mix ordinarily encountered in a specialty steel laboratory strongly suggests the use of the spiking technique, since alloy matrix effects are very important.

The authors wish to thank Charles T. Polinko, who performed the polarographic work; C. Lee Thompson, who performed the emission spectrography; and the Carpenter Technology Corporation for permission to publish this paper.

REFERENCES

1 G. L. Vassilaros, Talanta, 18 (1971) 1057.
2 K. E. Burke, Analyst (London), 97 (1972) 19.

3 K. E. Burke, Talanta, 21 (1974) 417.
4 K. E. Burke, Appl. Spectrosc., 28 (1974) 234.
5 K. Thornton and K. E. Burke, Analyst (London), 99 (1974) 469.
6 M. Kirk, E. G. Perry and J. M. Arritt, Anal. Chim. Acta, 80 (1975) 163.
7 P. H. Sholes, Analyst (London), 86 (1961) 392.
8 B. Metters and B. G. Cooksey, Analyst (London), 99 (1974) 457.
9 G. L. Vassilaros, Talanta, 21 (1974) 803.
10 M. G. Atwell and G. S. Golden, Appl. Spectrosc., 24 (1970) 362.
11 C. A. Evans, Jr., R. J. Guidoboni and F. D. Leipziger, Appl. Spectrosc., 24 (1970) 85.
12 F. Shaw and J. M. Ottaway, Analyst (London), 99 (1974) 184.
13 G. G. Welcher, O. H. Kriege and J. Y. Marks, Anal. Chem., 46 (1974) 1227.
14 R. D. Ediger, G. E. Peterson and J. D. Kerber, At. Absorpt. Newsl., 13 (1974) 61.
15 W. Frech, Anal. Chim. Acta, 77 (1975) 43.
16 W. B. Barnett and E. A. McLaughlin, Jr., Anal. Chim. Acta, 80 (1975) 285.
17 W. C. Campbell and J. M. Ottaway, Talanta, 21 (1974) 837.
18 B. R. Culver and T. Surles, Anal. Chem., 47 (1975) 920.
19 M. J. Adams, G. F. Kirkbright and P. Rienvatana, At. Absorpt. Newsl., 14 (1975) 105.

Analytica Chimica Acta, 91 (1977) 211—219

THE DETERMINATION OF TELLURIUM IN WEATHERED OUTCROP, MINERALIZED AND BARREN ROCK

J. A. CORBETT and W. C. GODBEER

CSIRO Division of Mineralogy, North Ryde, New South Wales 2113 (Australia)

(Received 26th January 1977)

SUMMARY

Sensitive and specific methods have been developed for the determination of tellurium in a wide variety of rocks and minerals. X-ray fluorescence is used for concentrations above 1 $\mu g\ g^{-1}$ and carbon furnace atomization a.a.s. for concentrations of 0.01—1 $\mu g\ g^{-1}$. The tellurium is separated by precipitation as elemental tellurium after dissolution in acid; alternative dissolution procedures have been investigated.

Tellurium is an element of considerable geochemical interest; it can have significance as an indicator element, and may also be of interest in ore genesis studies. Little is known of its distribution because of a lack of versatile analytical methods to determine the element at low concentrations in various matrices.

Watterson and Neuerburg [1] and Nakagawa and Thompson [2] have described similar methods for the determination of tellurium in soils and rocks. Dissolution is made in hydrobromic acid and bromine and, after co-precipitation with arsenic, the tellurium is extracted with methyl isobutyl ketone and determined by a.a.s. The method uses a large sample weight (12.5 g), does not provide for complete dissolution and uses a very small aliquot (0.6 ml) of solvent to spray into the atomic absorption flame. Hubert [3] uses the same dissolution and separation techniques, but tellurium is determined by an indirect catalytic reaction. This method uses a 5-g sample without complete dissolution; the catalytic reaction depends upon very careful temperature control.

Beaty [4] and Beaty and Manuel [5] use a tantalum boat or a carbon tube furnace with atomic absorption after co-precipitation of the tellurium with selenium and extraction with methyl isobutyl ketone. The recovery from the extraction is poor and variable because of the presence of other elements; a standard addition must be taken through the whole extraction procedure.

Severne and Brooks [6] have described a method in which soils and rocks are dissolved in nitric and hydrofluoric acids, the selenium and tellurium are co-precipitated with arsenic and, after dissolution in acid, the

tellurium is determined by a.a.s. Greenland and Campbell [7] describe the use of hydride generation to determine tellurium in silicate rocks at very low concentrations.

Many of these methods are designed for a limited, very low, tellurium concentration range; some are suspect in regard to the possible loss of tellurium during the dissolution step, and none offers a method for handling large numbers of samples with tellurium concentrations ranging from 0.01 to 50 $\mu g\ g^{-1}$ in varying matrices.

Burke et al. [8] have described the determination of tellurium in alloys by x-ray spectrometry after a chemical separation with tin(II) chloride. It was considered that this method could be the basis of a method for ores and minerals, and in cases where the amount of tellurium recovered was too small to be measured by x.r.f., the tellurium could be dissolved and measured by a more sensitive technique such as hydride evolution or carbon furnace a.a.s.

PRELIMINARY STUDIES

X-ray fluorescence

A Siemens SRS Sequential x-ray spectrometer with register control and PDP-8 computer was used. With parameters based on those of Burke et al. [8] (see Procedure), tellurium precipitated with tin(II) chloride and filtered on to a Millipore polyvinyl chloride filter (2-μm pore size) gave a detection limit of 0.5 μg. A linear calibration up to 25 μg can be extended to 200 μg by means of a shorter counting time. The presence of up to 100 μg of selenium, bismuth and arsenic, and up to 5 μg of gold and palladium, which are co-precipitated with tellurium, had no effect on the background or peak count.

Carbon-furnace atomic absorption spectrometry

A Varian-Techtron AA5 with a Model 63 Carbon Furnace and BC-6 Simultaneous Background Corrector was used. With 3 μl of tellurium solution (tellurium metal dissolved in nitric acid as in Procedure), a calibration range of 0.1—1 $\mu g\ ml^{-1}$, with a detection limit of 0.005 $\mu g\ ml^{-1}$, was achieved.

The behaviour of tellurium redissolved after precipitation by tin(II) chloride and collected on a Millipore filter was studied. To obtain a high concentration of tellurium, 1 ml of acid was used for dissolution. Of the various acids tested, nitric acid proved the most suitable. Tellurium can be dissolved at 65°C in a stoppered glass vial; the drying characteristics in the carbon furnace were good. Trouble caused by the dispersion of the filter on standing in acid was eliminated by using a Polyvic polyvinyl chloride filter, which is not attacked by nitric acid; a clear solution is obtained.

The presence of tin in the redissolved tellurium solution caused a large non-atomic absorption peak when the tellurium was atomized. Use of a sufficiently high ashing temperature to remove the tin prior to atomization

caused a considerable loss of tellurium. This was overcome by adding phosphoric acid; the resulting tellurium phosphate is not decomposed at the ashing temperature necessary to volatilize the tin.

Other elements which are precipitated with tellurium, e.g. bismuth, palladium and gold, do not interfere up to a 10-fold excess over the tellurium content. However, as a 10-fold excess of selenium causes a 40% drop in absorbance, a standard addition technique was necessary.

Hydride evolution atomic absorption

The technique described by Greenland and Campbell [7] was studied with a Varian-Techtron vapour generator model 64, designed to permit injection of borohydride solutions, and apparatus built in this laboratory designed to use sodium borohydride pellets.

Table 1 lists the results obtained; in both cases there is considerable interference from the hydrides of other elements, all of which could be present in minerals and rocks. It would be necessary to isolate the tellurium by a number of chemical separations in order to use the hydride technique. Table 1 also demonstrates the greatly increased sensitivity obtained with a borohydride solution, although the reproducibility is not as good as with pellets unless special apparatus is designed to give a rapid reproducible rate of addition of solution. Because of the interference problem, work on the hydride evolution method was not continued.

Separation of tellurium

In view of the requirement of obtaining the tellurium in a form suitable for x.r.f. measurement, and for carbon furnace a.a.s. measurement, precipitation methods which reduce tellurium to an elemental form were studied.

Tellurium can be reduced to Te(0) with sulphur dioxide [9], sodium hypophosphite [10], and tin(II) chloride [8]. For small amounts of tellurium, co-precipitants such as selenium and arsenic are used. Tin(II) chloride precipitates tellurium without a carrier [8], although there is some disagreement in the literature as to whether this is possible. Co-precipitation with other elements was avoided as they would interfere with the atomic absorption measurement; the stated conditions [8] were used to precipitate tellurium without co-precipitation.

TABLE 1

Interference from other elements forming hydrides

$NaBH_4$ pellets		$NaBH_4$ solution, 5% (w/v)	
Sample	$A_{214.3}$	Sample	$A_{214.3}$
2.5 μg Te	0.430	1.5 μg Te	0.59(
2.5 μg Te + 10 μg As + 10 μg Sb	0.170	1.5 μg Te + 10 μg As + 10 μg Sb	0.47[
2.5 μg Te + 10 μg As + 10 μg Sb + 10 μg Se	0.140	+ 10 μg Se	
		1.5 μg Te + 10 μg As + 10 μg Sb + 10 μg Se + 50 μg Sn	0.38(

In 3—4 M hydrochloric acid and a volume of 40 ml, known amounts of tellurium were precipitated with 10 ml of tin(II) chloride (1 g ml^{-1}). The solutions were stirred, left for 10 min, and filtered onto 2-μm Millipore Polyvic filters as in Experimental. The solutions, treated as listed in Table 2, were refiltered after standing overnight. The precipitates were dissolved in nitric acid, diluted where necessary, and the tellurium content determined with the carbon furnace as outlined under Experimental.

The results demonstrate that the short standing time is satisfactory for 20 μg of tellurium but standing overnight is necessary to recover 1 μg. The absorbance of a redissolved precipitated solution containing phosphoric acid is different from a solution of tellurium alone in nitric acid; absolute recoveries cannot be calculated. However, as no tellurium was recovered after a third precipitation it is assumed that complete recovery was obtained. Standing overnight was adopted; it appears that the disagreement in the literature over whether tellurium can be completely precipitated with tin(II) chloride without a carrier arises from the use of different temperatures and tin(II) concentrations.

Table 3 shows typical calibration data for the carbon tube furnace and x.r.f. measurements with the precipitation technique adopted. Although the graphs are linear, the calibration procedure cannot be used for the carbon tube furnace in analyses because of interference problems.

Carbon furnace atomization without separation

As a result of the experience gained with the carbon furnace, some work was done on solutions obtained without any separation of the tellurium. Aliquots of solutions prepared as in Experimental were atomized directly by the standard addition technique. Other aliquots from the same solution were treated by precipitation and x.r.f. In this case suitable ashing conditions were established at 325°C for 20 s. Table 4 lists the results obtained; the method can be used in these concentration ranges (5—20 μg g^{-1}).

TABLE 2

Recovery of tellurium by tin(II) chloride
(Conditions as stated in Experimental and measured with the carbon furnace. A. Filtered after 10 min. B. Refiltered after standing overnight. C. Filtered after standing overnight. D. Refiltered after standing over second night.)

Amount of Te (μg)	Temp. (°C)	Recovery[a]			
		A	B	C	D
20	20	19.2	0.8		
20	90	19.8	0.2		
1	20	0.75	0.25		
1	90	0.86	0.14		
1	20			0.98	0.02

[a] Recoveries calculated assuming all Te recovered with two filtrations; on standing for a further 24 h, tellurium was not recovered from any of the above solutions.

TABLE 3

Calibration for tellurium by carbon-furnace a.a.s. after precipitation and dissolution, and by x.r.f. after precipitation

A.a.s.			X.r.f.	
Te (μg)	Abs. × 2	Abs. × 5	Te (μg)	Counts
Blank[a]	0	0	Blank	500
0.05	0.05	0.13	1	935
0.10	0.10	0.26	5	2635
0.15	—	0.39	10	4977
0.20	0.21	0.50	15	7452
0.25	—	0.66	20	9598
0.30	0.32	—	—	—
0.40	0.44	—	—	—
0.50	0.53	—	—	—

[a]With simultaneous background corrector.

TABLE 4

Comparison of direct carbon-furnace method without precipitation and x-ray fluorescence on precipitated tellurium

Sample	A.a.s. (μg g^{-1})	X.r.f. (μg g^{-1})
2	7.8	8
26	16.7	16
50	10.4	10, 10
58	16.7	15.0, 15.0

Dissolution procedure

The form in which the tellurium exists in a material is important in deciding a suitable dissolution procedure. In mineralized material the tellurium of interest will be readily available and complete dissolution of the whole material is not necessary. Where the tellurium is in the crystal lattice of rock-forming minerals a complete dissolution is required. With any acid dissolution procedure there is always a danger of tellurium loss by volatilization.

The partial acid digestion method with perchloric acid and nitric acid, described under Experimental, was tested with known amounts of tellurium and the standard SRM 361 sample of steel. The recoveries from the "spiked" samples ranged from 95—100%, and the values obtained by x.r.f. and a.a.s. indicated no loss of tellurium.

Table 5 compares the results obtained by a complete dissolution with hydrofluoric acid and a partial attack by nitric—perchloric acids (see Experimental). To recover all the tellurium, hydrofluoric acid is necessary.

TABLE 5

Comparison of results (in μg Te g^{-1}) from different acid treatments

Sample	HNO_3—$HClO_4$	HF—HNO_3
8	1.68[a]	1.66
23	0.16, 0.18	0.29, 0.32
GSP-1	<0.01	0.017, 0.019[b]

[a]Mean of 5 results.
[b]0.02 ± 0.003 [5]; 0.021 $\mu g\ g^{-1}$ [1].

This is to be expected for the rock sample GSP-1. However, in weathered outcrop samples, and for geochemical purposes, the nitric acid—perchloric acid attack could be satisfactory (see results for sample 8).

EXPERIMENTAL

Dissolution

The method is suited to any dissolution procedure in which the tellurium can be brought to a final volume of 40—50 ml of 3—4 M HCl. The two procedures used by us were:

(1) Weigh the sample (1 g) into a 100-ml beaker. Carefully add 15 ml of a mixture of nitric—perchloric acid (4 + 1). Heat gently, and evaporate to fumes of perchloric acid. Cool, add 10 ml of hydrochloric acid (s.g. 1.16) and warm to dissolve salts. Add 5 ml of water and filter hot into a 100-ml beaker. Wash with hot 3 M hydrochloric acid, keeping the final volume to 40—50 ml.

(2) Weigh 1 g of sample into a suitable Teflon vessel and thoroughly wet with 1 ml of aqua regia. Add 15 ml of hydrofluoric acid (40%). Stand for 2 h, or overnight, before evaporating to dryness on a hotplate at 100—110°C. Wet the residue with aqua regia, and repeat the hydrofluoric acid treatment. Add 10 ml of hydrochloric acid and warm to dissolve salts (do not boil). If the solution is clear add 3 M hydrochloric acid to bring the volume to 40—50 ml. If necessary, filter the solution as in (1).

Precipitation

Add 10 ml of tin(II) chloride solution (1 g ml^{-1}), stir, and stand overnight. Filter through a 25-mm, 2-μm Polyvic Millipore filter (gentle suction) and wash with 45 ml of 3 M hydrochloric acid and 45 ml of water. Dry the filter at room temperature and proceed with the x.r.f. measurement.

X-ray fluorescence

Standard tellurium solution (0.1 g l^{-1}). Dissolve 0.100 g of pure tellurium in 10 ml of aqua regia, cool, and make up to 1 l with water.

The filters are mounted in a suitable sample holder, so that the whole precipitated area is exposed to the x-ray beam. The parameters are: chromium target at 40 kV and 50 mA, LiF 100 crystal, flow counter, vacuum and a 0.15° collimator with a small aperture, count time 100 s, L_α radiation at 109.53°2θ.

Measure the count for a blank taken through the whole procedure.

Prepare a calibration graph for 0, 1, 5, 10, 15, 20 μg of tellurium precipitated from the tellurium calibration solution. Calibration standards should be counted with each batch of analyses. Deduct the blank reading from the standards and the sample count.

If the tellurium content by x.r.f. is <1 μg, the determination is continued by a.a.s.

Atomic absorption spectrometry

Precipitated standard tellurium solutions. Measure an aliquot of the standard tellurium solution to give 1 μg of tellurium. Make up to 40 ml in 3—4 M hydrochloric acid and continue as described in the precipitation step. Other amounts of tellurium can be prepared to suit the concentrations required.

Trim down the filter to 21-mm (a 21-mm cork borer is convenient). Place the filter in the bottom of a 25 × 50-mm glass vial. Add 1 ml of nitric acid containing 25 μl ml^{-1} of phosphoric acid (0.5 ml of nitric—phosphoric acid can be used for samples containing <0.05 μg Te g^{-1}). Cap the tube, and heat to 70°C in an air oven for 2 h. Cool, and place 3 μl in the carbon furnace of the Varian-Techtron Model 63, fitted with a simultaneous background corrector, and atomize to establish an approximate tellurium content for standard addition purposes.

Measure three 100-μl aliquots of the solution, one into each of three small specimen tubes (diam. 10 mm). To one tube add 10 μl of the nitric—phosphoric acid mixture, to another add 10 μl of tellurium standard solution containing an amount of tellurium equivalent to that expected in the sample, and to the third tube add an amount calculated to be twice that of the sample. These amounts can be measured with Eppendorf or other pipettes.

The atomization parameters are: wavelength, 214.3 nm; lamp current, 8 mA; slit, 1 nm; nitrogen flow; 3.5 l min^{-1}; drying time, 40 s; ashing time, 20 s; atomizing time, 2 s at 2100°C.

DISCUSSION AND RESULTS

Tellurium is atomized in the carbon furnace at temperatures as low as 1600°C, but best repeatability was achieved at temperatures above 2000°C; a fast rate of atomization produces more uniform peak heights. The temperatures for drying and ashing are a function of individual instruments and are found by examining the recorder trace during trials. Consistent

readings are obtained by controlling closely the technique of adding the solution to the furnace by Oxford Ultra micropipettes with flexible plastic tips; the tips always enter the furnace at the same angle and just touch the far side of the furnace.

When the work head reached an equilibrium temperature, a time cycle of 60 s was adopted between sample atomization and the introduction of the next sample.

Repeatability tests were performed on the precipitation separation step. Ten separate aliquots containing 1 μg of tellurium were precipitated and dissolved as described in Experimental. A mean absorbance of 0.154 with s = 0.0132 was obtained. When ten repeat atomizations of one aliquot were made, a mean absorbance of 0.157 with s = 0.0062 was obtained.

It is difficult to obtain samples of known tellurium content to establish accuracy. The results obtained for the steel sample SRM 361 (reported value 5 μg g^{-1}) in Table 6 by both methods and on the rock sample GSP-1 at the low level of 0.02 μg g^{-1} (Table 5) are consistent. Other "spiking" tests always gave satisfactory recoveries.

The precision obtained by the two methods is shown in Table 6; the standard deviation (0.08) at the low level of 1.66 μg g^{-1} is satisfactory.

The methods, developed to determine tellurium in a wide range of materials, have proved successful in handling tellurium contents from 30—<0.01 μg g^{-1} in materials varying from high iron content gossans to high silicate contents, with the nickel, arsenic, selenium, and palladium contents varying considerably. Sulphides and laterites are being studied.

Some work was done on Teflon-lined bomb digestions with hydrofluoric and nitric acids, with subsequent addition of boric acid to form fluoroboric acid. The precipitation of tellurium by tin(II) chloride was not affected by the presence of fluoroboric acid; this method should be satisfactory.

TABLE 6

Precision of results (in μg Te g^{-1}) by x.r.f. and a.a.s. methods

Sample	A.a.s.	X.r.f.	Sample	A.a.s.	X.r.f.
23	0.16, 0.18, 0.13, 0.16	—	15	6.9[c]	5
33	0.22, 0.16	—	25	2.27	2
64	0.06, 0.05	—	12	1.00	1
SRM 361	5.0, 4.1[a]	5, 5	13	1.00	1.5
8	1.68, 1.54, 1.79,	2	2	9.4[c]	8, 9
	1.68, 1.73, 1.66[b]		50	8.9[c]	10, 10
9	1.07	1			

[a]Reported value 5 μg g^{-1}. [b]s = 0.0839. [c]Large dilutions were required for a.a.s.

The authors thank S. C. Goadby for providing the x-ray fluorescence results.

REFERENCES

1 J. R. Watterson and G. J. Neuerburg, J. Res. U.S. Geol. Surv., 3 (1975) 191.
2 H. M. Nakagawa and C. E. Thompson, U. S. Geol. Surv. Prof. paper 600-B (1968) B123.
3 A. E. Hubert, U.S. Geol. Surv. Prof. paper 750-B (1971) B188.
4 R. D. Beaty, Anal. Chem., 45 (1973) 234.
5 R. D. Beaty and O. K. Manuel, Chem. Geol., 12 (1973) 155.
6 B. C. Severne and R. R. Brooks, Talanta, 19 (1972) 1467.
7 L. P. Greenland and E. Y. Campbell, Anal. Chim. Acta, 87 (1976) 323.
8 K. E. Burke, M. M. Yanak and C. H. Albright, Anal. Chem., 39 (1967) 14.
9 W. F. Hillebrand, G. F. Lundell, J. I. Hoffman and H. A. Bright, Applied Inorganic Analysis, 2nd edn., J. Wiley, New York, 1953.
10 B. S. Evans, Analyst, 71 (1946) 68.

Analytica Chimica Acta, 91 (1977) 221—228

COMPARISON OF DISSOLUTION METHODS FOR THE DETERMINATION OF POTASSIUM IN ROCKS AND MINERALS BY ATOMIC ABSORPTION SPECTROMETRY

T. D. RICE

Chemical Laboratory, New South Wales Department of Mines, 36 George Street, Sydney 2000 (Australia)

(Received 10th August 1976)

SUMMARY

Lithium metaborate fusion and hydrofluoric acid dissolution methods used before the flame emission or atomic absorption spectrometric determination of potassium in rocks and minerals are compared with regard to accuracy and precision. Possible contamination by potassium in borosilicate glassware was avoided by the use of platinum or polyethylene vessels; solutions were prepared and measured by weight instead of volume. Separation of potassium by cation-exchange chromatography enabled potassium in all solutions of a given sample to be measured against one set of standard solutions. When the various dissolution methods were used carefully, the results did not differ in precision. Significant systematic errors were not detected; in particular, potassium was not lost by volatilization during fusion for 15 min with lithium metaborate at 900°C.

The possibility that small systematic errors occur during the sample dissolution step of flame-spectrometric procedures for determination of potassium in rocks and minerals is worth investigating. This is particularly important when potassium has to be determined in studies of geological age by the potassium—argon method; it has been stated [1] that if potassium—argon age data are to be useful stratigraphically, the total relative error should not exceed about 0.5%. Therefore the potassium determination has to be sufficiently precise and accurate.

The aim of the present work was to compare different methods of sample dissolution with regard to their precision and freedom from systematic errors. Potassium concentrations of sample solutions were measured by atomic absorption with a precision of ± 0.2% relative at the 95% confidence level.

Potassium was determined after a lithium metaborate fusion procedure and after at least one of three hydrofluoric acid dissolution procedures in the following five samples: the U.S.G.S. basalt BCR-1 [2]; three U.S.G.S. reference minerals for potassium—argon dating, viz. the orthoclase PSU Or-1, biotite LP-6 Bio (40-60) and the Engels amphibole; the New South Wales chlorite rock NSWMD-1 [3].

When lithium metaborate fusions are done above 900°C, there is a danger

of loss by volatilization of some elements, notably the alkali metals [4]. The possibility of volatilization of potassium, even during fusion at 900°C, is suggested by the volatility of inorganic potassium compounds at somewhat lower temperatures. For example, when 20 μg of potassium (as potassium chloride) were added as an aqueous solution to a platinum crucible, evaporated to dryness and heated for 1 h at 600°C, only 9 μg of potassium remained in the residue [5]. Loss of potassium during sample decomposition with hydrofluoric and other acids in an open vessel is probably due to spattering. Volatilization losses of potassium during such decompositions were not observed in the present study; this agrees with earlier findings [6—9].

Solutions were prepared gravimetrically instead of volumetrically, and came in contact with platinum or polyethylene vessels only; numerous experiments involving leaching with caesium chloride solutions showed that there was no detectable adsorption of potassium onto these vessels [10]. Polyethylene dispensing bottles were used; the possibility of contamination of solutions by potassium in borosilicate volumetric glassware, especially in the case of samples low in potassium, was thus eliminated.

Potassium was separated from aliquots of sample solutions by cation-exchange chromatography; the small-scale version of the procedure of Strelow et al. [11] was developed primarily for a study of interferences in the determination of potassium in rocks and minerals by atomic absorption in an air—acetylene flame [3, 10].

About 20% of the sodium remained with the potassium in the above separation procedure; caesium chloride was added to the potassium fractions to eliminate ionization interference by sodium in the air—acetylene flame [12] and this addition gave more than a two-fold increase in atomic absorption sensitivity. For the two dissolution methods involving hydrofluoric acid in open vessels described here, some of the titanium remained with the potassium but did not interfere with the measurement of potassium.

Because of the cation-exchange separation of potassium, only one set of standard solutions was required to match the matrix of all solutions of a given sample. Thus any observed differences in results would involve errors in method(s) of sample dissolution and not difficult-to-detect errors in the preparation of several sets of standard solutions.

EXPERIMENTAL

Polyethylene dispensing bottles

Polyethylene bottles (up to 500-ml capacity with unlined caps) were converted to dispensing bottles as follows: through the centre of the top of the cap drill a hole (2.08 mm) and enlarge the hole with an awl so that a suitable length of polyethylene tubing (Portex brand, bore 1.57 mm, ext. diam. 2.08 mm) can be forced through. Make a closure for this dispensing tube by heat-sealing one end of a ca. 50-mm length of polyethylene tubing (Portex brand, bore 2.00 mm, ext. diam. 3.00 mm). Check that, with the closure fitted to the top of the dispensing tube and the cap screwed on tightly, air cannot be squeezed out.

Subsampling

Each of the coarse-grained samples was poured from its glass container onto a sheet of smooth, unfilled paper, hand-rolled and spread out; subsamples were taken with a small nickel spatula. Finely ground samples were subsampled directly from the container with the same spatula. Coarse-grained samples, especially those containing biotite and other micas, cannot be subsampled directly from the container because of the need to eliminate segregation caused by static electricity [13].

Methods of sample dissolution

In each of the four sample dissolution methods summarized below, a blank was included in every batch; 500-mg or 200-mg subsamples were taken as shown in Table 1; subsamples to be decomposed by acid in open vessels were initially wetted with several drops of water in order to avoid "dusting"; 2 drops of 100-vol hydrogen peroxide were added to each sample solution to avoid possible hydrolytic precipitation of titanium and subsequent coprecipitation of some potassium; with the aid of a top-loading balance (weighing to the nearest 0.01 g), solutions were diluted in 280-ml polyethylene dispensing bottles to a final weight of 250.0 g and mixed well.

Method 1: HF—HNO_3 dissolution in a sealed polyethylene bottle. This procedure was based on Method 1 of Langmyhr and Paus [14]. The weighed subsample was transferred to a 280-ml polyethylene dispensing bottle (containing about 0.5 ml of water and with closure on dispensing tube); 10 ml of 48—51% hydrofluoric acid and 1.5 ml of nitric acid (1 + 2) were added and the bottle, sealed with sides slightly depressed to allow for expansion during heating, was let stand overnight and then heated on a water bath for 3 h with occasional swirling. (Dispensing bottles lost less than 0.01 g in weight during this heating: this showed that they were sealed effectively.) Saturated boric acid (125 ml) was added to the bottle when cool; a clear solution was obtained

TABLE 1

Weights of subsamples and aliquots, and concentration of a.a.s. standard solutions

Sample	Subsample weight[a] (mg)	Aliquot weight (g)	K^+ in a.a.s. standards ($\mu g\ g^{-1}$)
BCR-1	500	12.5	6.9, 7.1, 7.3
Or-1	200	3.54[b]	as above
LP-6 Bio (40-60)	200	5.30[b]	as above
Engels amphibole	200	12.5	1.33, 1.50, 1.66
NSWMD-1	500	20.0	0.58, 0.67, 0.75

[a]Made up to a total solution weight of 250 g.

[b]The difference between this figure and 12.5 is the weight of blank solution added to the column immediately before the aliquot of sample solution.

after heating the sealed bottle for 1 h on the water bath.

Method 2: HF—HNO_3 dissolution. This procedure, in which all heating was done on a water bath, was based on that of McCabe [9]. The sample was digested in a covered 100-ml platinum dish with 10 ml of hydrofluoric acid and 3 ml of nitric acid (1 + 2); after evaporation to dryness and repetition of the digestion and evaporation, the residue was dissolved by warming with 36.4 g of a nitric—boric acid mixture (prepared by mixing 200 ml of nitric acid (1 + 2) with 280 ml of saturated boric acid in a 500-ml polyethylene dispensing bottle).

Method 3: HF—HNO_3—H_2SO_4 dissolution. This was similar to the procedure recommended by Cooper [1] except that 4 ml instead of 6 ml of sulphuric acid (1 + 1) were used.

Method 4: $LiBO_2$ fusion. This method was also used for the determination of potassium in 10 samples in an interlaboratory study [3]. Lithium metaborate was prepared and purified by the method of Ingamells [4]. The fusion procedure was based on that of Boar and Ingram [15]. The subsample was mixed with four times its weight of lithium metaborate in a 30-ml platinum crucible and fused at 900°C for 15 min in a Heraeus TiK 11/12 crucible furnace with the door ajar. A dilute nitric acid solution of the melt was prepared in a 250-ml polyethylene beaker. With orthoclase PSU Or-1, a 7:1 instead of a 4:1 flux-to-sample ratio was necessary for complete decomposition.

As suggested by Ingamells [4], the indicated furnace temperature during lithium metaborate fusions was higher than the temperature of the melt: in the present study, determinations of the melting point of pure sodium fluoride indicated that a fusion temperature of 900°C was achieved when the furnace temperature indicator read 940—950°C.

Cation-exchange separation

A 110-mm high column of Dowex 50W-X8, 100—200 mesh, resin (Baker Analysed) was supported by a plug of ca. 100 mg of 4-denier Terylene fibre [16] near the tapered end of a length of polyethylene tube (bore 6.0 mm, ext. diam. 10.0 mm). The untapered tube length was ca. 180 mm; a polyethylene funnel, with stem shortened to 11 mm, served as a reservoir and was sealed, by pressure only, to the untapered end of the tube. Airborne contamination was excluded by covering the funnel with a Petri dish and by collecting eluates in 50-ml polyethylene bottles attached to the column by a suitably holed cap attached permanently to the polyethylene tube near its tapered end. The resin column did not dry out when not in use for extended periods, provided that a 50-ml polyethylene bottle almost filled with water was attached to the column.

Before use, a set of columns was regenerated with 3.5 M hydrochloric acid and washed with water to remove the excess of acid. Solutions were always transferred to columns from polyethylene dispensing bottles.

Each aliquot of sample solution was transferred to a column assembly detached from its stand and supported in a beaker on a tared top-loading balance;

the dispensing bottle plus sample solution was weighed on an analytical balance before and after this transfer, to obtain the weight to the nearest milligram. For the orthoclase PSU Or-1 and the biotite LP-6 Bio, a definite weight of blank solution (indicated in Table 1) was added immediately before the aliquot of sample solution so that the potassium fraction could be collected at the same stage of the elution as for the basalt BCR-1.

After the aliquot had drained from above the column, 2 portions (ca. 10 ml) of 0.01 M nitric acid containing 0.03% (w/v) hydrogen peroxide were passed through. Potassium was then eluted with weighed amounts of 0.50 M nitric acid and the potassium fraction (11—38 g for a 12.5-g aliquot, 8—38.5 g for a 20-g aliquot) was collected.

The potassium fraction was diluted to 50.00 g with a solution containing sufficient caesium chloride (Merck Suprapur) to give a concentration of 1.20 mg of caesium chloride per g of final solution; the potassium fraction for sample NSWMD-1 was diluted to 35.00 g with a caesium chloride solution giving the same final caesium chloride concentration as above.

The solutions passed through the columns at about 13 ml h^{-1}. The columns required only occasional attention during the complete 2-d cycle of separation and regeneration.

The 3-g fractions of 0.50 M HNO_3 immediately before and after the potassium fraction, were collected, buffered with caesium as described above, and tested for potassium by atomic absorption with scale expansion. In all cases, these headings and tailings did not contain more than 0.1% of the potassium in the potassium fraction.

Standard solutions

The standard solutions listed in Table 1 (450-g batches) were prepared in 500-ml polyethylene dispensing bottles from more concentrated aqueous standard solutions of potassium chloride (Specpure) previously heated at 550°C for 4 h. Standard blank solutions and low standards with potassium concentrations of 0.05 and 0.10 $\mu g\ g^{-1}$ were also prepared. All standard solutions contained the same concentrations of nitric acid and caesium chloride as the sample solutions.

Atomic absorption measurement

Standard and sample solutions, in 50-ml polyethylene bottles, were analysed with a Varian-Techtron Model AA-5 atomic absorption spectrometer with DI-30 digital indicator; each standard solution was replenished as necessary to keep its level within 15 mm of that of the sample solution. All solutions of a given sample were measured on the same day and in random order.

The highest and lowest standards of each set listed in Table 1 were measured with the appropriate sample solutions by a bracketing technique similar to that of Langmyhr and Paus [14]. The concentration of the middle standard of each set in Table 1 was close to that of the sample solution, and, when measured as

a sample, this standard enabled correction to be made for slight non-linearity of instrument response. Such corrections were always negative and less than 0.5%. For measurements with the highest set of standards, the burner was rotated so that the absorbance of the lowest standard was about 0.35. The digital indicator was adjusted to give a reading of about 2.2 times the absorbance.

A small piece of Wratten gelatin filter (Kodak 89B) covered the entrance to the monochromator to block higher order background radiation from the lamp, and thus give better linearity of response.

Other operating conditions were: wavelength 766.5 nm; air pressure 16.0 p.s.i.g., acetylene flow adjusted to give maximum sensitivity; grooved burner with 10-cm slit, Varian Techtron Type AB-51, positioned to give maximum sensitivity; potassium hollow-cathode lamp current 9 mA; Hamamatsu R-136 photomultiplier; spectral bandwidth 1.0 nm.

RESULTS AND DISCUSSION

Table 2 lists the results from four dissolution methods for the basalt BCR-1. This sample was analysed three times by each method (Runs 1—3 in Table 2). The mean results for Methods 2 and 3 agree well, as do those for Methods 1 and 4. Analysis of variance of the results shows that there is about a 95% chance that Methods 2 and 3 give results significantly lower than Methods 1 and 4; the pooled relative standard deviation of a single result by each of the four methods is 0.22%. If it is assumed that the results of Methods 1 and 4 are accurate, the results of Method 3 could be low because of slight spattering during heating in an uncovered platinum dish to sulphuric acid fumes; the results of Method 2 could be low because of the ejection of a few minute particles on the addition of acid to the dried residues. The possibility of such losses in Method 2 was subsequently eliminated by wetting the dried residues carefully with a few drops of water before adding acid.

TABLE 2

Potassium results for U.S. Geological Survey basalt BCR-1, Split 80 Position 9[a]

	Dissolution method	% K (dry basis[b])			
		Run 1	Run 2	Run 3	Mean
1.	$HF—HNO_3$ in sealed bottle	1.423	1.424	1.432	1.426
2.	$HF—HNO_3$	1.416	1.420	1.418	1.418
3.	$HF—H_2SO_4$	1.421	1.415	1.419	1.418
4.	$LiBO_2$ fusion	1.423	1.425	1.426	1.425

[a]Three laboratories obtained an overall mean of 1.426% K when this portion of BCR-1 was analysed in an interlaboratory study [3].
[b]The moisture content of this sample was 0.82%.

TABLE 3

Potassium results for three reference samples

Sample	% K (dry basis)		% H_2O (at 105°C)
	Method 1	Method 4	
Orthoclase	12.43	12.37	<0.02
PSU Or-1[a]	12.40	12.42	
Biotite LP-6	8.33	8.35	0.13
Bio (40-60)[b]	8.31	8.34	
Engels	0.745	0.748	0.03
amphibole[c]	0.746	0.748	

[a]12.39% potassium [17].
[b]8.34% potassium [17].
[c]0.758 ± 0.002% potassium [13].

Table 3 gives the results of duplicate analyses (by Methods 1 and 4) of the orthoclase, the biotite and the Engels amphibole. The relative mean difference between the results of Methods 1 and 4 for these samples does not exceed 0.4%. The results of Method 1 for the biotite LP-6 Bio seem to be slightly low; this may be explained by the presence of two incompletely attacked grains in each solution of this sample. If a Teflon-lined bomb [18—20] had been available, the results of Methods 1 and 4 for the biotite LP-6 Bio would probably have agreed better.

The results in Table 3 agree with previous values [13, 17], except for the amphibole, for which the value reported is higher by about 1% relative. The reason for this is unknown.

The low-potassium chlorite rock sample NSWMD-1 was analysed in duplicate, in each of two runs, by Methods 2, 3 and 4. Table 4 shows that the mean results of each method agree to within 0.4% relative. Analysis of variance shows that between-method differences are insignificant. Table 4 shows blank values for each method and run. The variation in blank values between runs for a given method underlines the importance of the blank determination.

Conclusions

When rock or mineral samples are decomposed by fusion for 15 min with lithium metaborate at 900°C, in platinum crucibles in a furnace as described in Method 4, the results for potassium agree (within experimental error) with those obtained after decomposition of the sample with hydrofluoric acid. When performed with due care, the dissolution methods studied seemed to be of the same precision and free from significant systematic errors.

TABLE 4

Potassium results for chlorite rock sample NSWMD-1

	Dissolution method	K, p.p.m.[a] (dry basis[b])		
		Run 1	Run 2	Mean
2.	$HF—HNO_3$	$\frac{567}{560}(8)$	$\frac{561}{560}(5)$	562
3.	$HF—H_2SO_4$	$\frac{559}{561}(22)$	$\frac{559}{559}(15)$	560
4.	$LiBO_2$ fusion	$\frac{570}{560}(30)$	$\frac{560}{559}(25)$	562

[a]Blank values (p.p.m. K) given in parentheses.
[b]Moisture content, 0.19%.

Permission to publish this paper was given by the Under Secretary, New South Wales Department of Mines. The author thanks Drs. F. J. Flanagan and C. O. Ingamells for supplying some of the samples used.

REFERENCES

1 J. A. Cooper, Geochim. Cosmochim. Acta, 27 (1963) 525.
2 F. J. Flanagan, Geochim. Cosmochim. Acta, 31 (1967) 289.
3 T. D. Rice, Talanta, 23 (1976) 359.
4 C. O. Ingamells, Anal. Chim. Acta, 52 (1970) 323.
5 T. Y. Kometani, Anal. Chem., 38 (1966) 1596.
6 W. Geilmann and A. Ganssle, Glastech. Ber., 27 (1954) 80.
7 W. H. Pinson, Ann. N.Y. Acad. Sci., 91 (1961) 221.
8 F. W. E. Strelow, C. J. Liebenberg and F. Von S. Toerien, Anal. Chim. Acta, 47 (1969) 251.
9 W. J. McCabe, Analysis of Potassium and Other Alkali Metals in Rocks, Institute of Nuclear Sciences, D.S.I.R., Lower Hutt, New Zealand, Contribution No. 473, 1971.
10 T. D. Rice, M.Sc. Thesis, University of Sydney, 1975.
11 F. W. E. Strelow, F. Von S. Toerien and C. H. S. W. Weinert, Anal. Chim. Acta, 50 (1970) 399.
12 E. Althaus, Neues Jahrb. Mineral., Monatsh., 9 (1966) 259.
13 C. O. Ingamells, personal communication.
14 F. J. Langmyhr and P. E. Paus, Anal. Chim. Acta., 43 (1968) 397.
15 P. L. Boar and L. K. Ingram, Analyst (London), 95 (1970) 124.
16 R. A. Edge, Chemist-Analyst, 47 (1958) 17.
17 C. O. Ingamells, Talanta, 21 (1974) 141.
18 J. Dolezal, J. Lenc and Z. Sulcek, Anal. Chim. Acta, 47 (1969) 517.
19 F. J. Langmyhr and P. E. Paus, Anal. Chim. Acta, 49 (1970) 358.
20 Y. Hendel, Analyst (London), 98 (1973) 450.

Analytica Chimica Acta, 91 (1977) 229—241

APPLICATIONS OF THE RING OVEN METHOD IN ENZYMATIC ANALYSIS

HERBERT WEISZ and INGOLF VERENO

Lehrstuhl für Analytische Chemie, Chemisches Laboratorium der Universität Freiburg i.Br. (Federal Republic of Germany)

(Received 29th December 1976)

SUMMARY

The use of the ring oven technique in enzymatic analysis is described. The "segment technique" for catalyzed reactions is applied for the determination of enzymes, inhibitors and substrates. Three different methods have been worked out for this purpose; none of them needs a stable standard scale. These methods are illustrated by various examples: determinations of the enzymes acid and alkaline phosphatase, hyaluronidase, acetylcholinesterase, lipase and alcohol dehydrogenase; indirect determinations of the inhibitors copper, beryllium, molybdenum, the insecticides carbaryl and paraoxon, the herbicides 2, 4-D, mecoprop and bentazon, and the fungicide phenylmercury acetate; and determinations of the substrates ethanol and glucose.

In recent years, enzymatic reactions have found an increasingly important rôle in analytical chemistry [1]. The reasons are obvious: in many cases enzymes are substrate-specific, so that one substance can be determined even in the presence of very similar compounds, and they exhibit high sensitivity as catalysts, so that very small amounts of enzymes suffice to produce high conversion. It seemed interesting to investigate how far such enzymatic analytical methods can be carried out with the aid of the ring oven technique [2, 3]. The possibility of using catalytic reactions with this technique has already been described [4]: the advantage of ring oven spot-colorimetry — i.e., the concentration of the substance to be determined in a sharply outlined ring zone — was combined with the simultaneous comparison method [5, 6]: one drop each of the unknown catalyst sample solution and of two standard solutions were concentrated on the ring oven in three sharply outlined circular segments. The filter paper was then sprayed with a solution of the two reactants for the reaction catalyzed, and the changes (e.g. colouration, bleaching, fluorescence) in the three segments were observed. From the order of these changes the concentration of the unknown catalyst solution can be estimated. This is possible because the reaction within the three segments always takes place under identical conditions.

To apply this "segment technique" for enzymes, it is necessary to overcome the difficulty that enzymes cannot be transferred to the ring zone at

the usual temperature of the ring oven (110°C) without being deactivated. Three different methods have been developed to determine enzymes, inhibitors and substrates. In accordance with the several conditions of the respective enzymatic reactions, one of the three techniques described below may be applied.

Adsorption zone method (method A)

The usual application of the ring oven technique is based on the use of the "heat barrier", at which the solvent evaporates leaving behind the substance to be determined in the form of a sharply defined ring. This is possible only with substances which are sufficiently stable at the operating temperature of the ring oven, and this is obviously not the case with enzymes. A possibility of avoiding the "heat barrier" is offered by an "adsorption barrier" [7, 8]. Here the ring oven itself is used only for the preparation on the filter paper of a narrow ring zone consisting of a suitable adsorbent; the enzyme itself is then transferred with a suitable solvent to the adsorption zone without the use of the ring oven, but on a suitable support (e.g. on a washing ring [9]). After three enzyme solutions — one drop each of the unknown solution and of two standard solutions — have been concentrated in three segments of the "adsorption zone" (see Fig. 1), a solution of the necessary substrate — e.g. indoxyl acetate for the determination of hyaluronidase — is sprayed on to the filter paper, so that the reaction is started simultaneously in all three segments under identical conditions. The order of the changes of colour or fluorescence in the three segments is observed. In most cases, after two further steps with logically selected concentrations of standard solutions it is possible to evaluate the concentration of the unknown solution. To achieve higher accuracy, two more determinations with different drop numbers of the unknown enzyme solution are required. Instead of spraying the substrate on the paper, it is better to press it on with a paper ring (5 mm width of a suitable diameter) moistened with about 100 μl of the substrate solution fully covering the three segments (cf. Fig. 3, but for the substrate). This is more economic (less reagent is needed) and also avoids the danger of blurring the sharply defined segments.

This method is used primarily for the determination of enzymes. It can

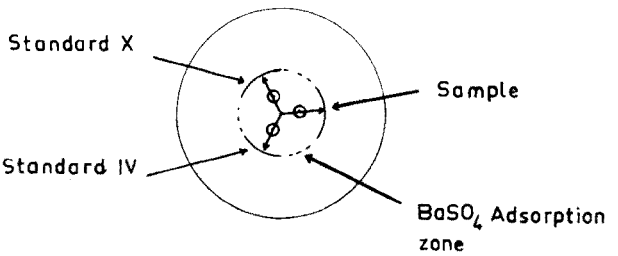

Fig. 1. Method A: adsorption zone.

also be used for the determination of inhibitors, if the inhibition of the enzyme is "irreversible", i.e. if the inhibited enzyme arrives in the adsorption zone, as for inhibition of hyaluronidase by copper. Only if this condition is fulfilled will the conversion of the substrate in the three segments depend on the amount of inhibitor, so that the unknown inhibitor concentration can be determined.

Reaction inside the ring zone (method B)

Method A can be applied only if the enzyme to be determined can be transferred to the adsorption barrier by migration with the solvent through the fibers of the paper. If this is impossible, the reaction between this enzyme and the substrate must be done in the middle part of the filter paper. Enzyme and substrate (and any other necessary substance) — e.g. acetylcholinesterase and indoxylacetate — are placed on three points concentric around the middle of the round filter. If the three spots contain three different amounts of the enzyme under otherwise identical conditions, different amounts of substrate will have reacted when the paper is finally dried (about 5 min) and the reaction stops. The different amounts of reaction product thus formed are concentrated in three segments on the ring oven with a suitable solvent (see Fig. 2). From the different intensities of the three segments, the concentration of the unknown enzyme solution can be evaluated. This technique is an example of a fixed time method [10].

This method also allows inhibitors to be determined. The difficulties mentioned for method A play no rôle, because inhibitor and enzyme — e.g. carbaryl and acetylcholinesterase — remain together in the same place on the filter paper for the full reaction time. The activity of the enzyme, reduced by the amount of inhibitor, produces a corresponding conversion of the substrate, and this conversion provides a measure for the inhibitor.

Particularly for the determination of inhibitors, the order of addition of the various substances on the paper — enzyme, inhibitor, substrate, etc. — may be very important. For example, results may differ when the inhibitor or the enzyme is spotted first, and the best sequence must always be established experimentally.

Substrates can also be determined by this technique. If the enzyme

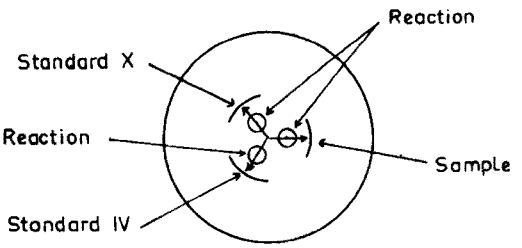

Fig. 2. Method B: reaction inside the ring zone of the filter paper.

activity applied is sufficiently high, a complete conversion of the substrate can be achieved during the reaction time, e.g. until the spots dry out; the amount of reaction product formed is of course a measure of the concentration of the substrate. Different amounts of reaction product are also formed during a given reaction time if the conversion of the substrate is not complete; the substrate originally present can still be determined, because higher concentrations of substrate under otherwise equal conditions yield higher reaction rates. In both cases different concentrations of substrate cause different conversions. As an example of this technique the determination of ethanol with alcohol dehydrogenase in the presence of NAD^+ will be described.

Thus method B allows the determination of enzymes, inhibitors and substrates. The only necessary condition is a sufficient thermal stability of the reaction product.

Direct addition of enzyme to the segments (method C)

Method A (adsorption zone) is applicable only if the enzyme can be eluted into the adsorption zone, and method B when a thermally stable product is formed. If neither of these conditions is fulfilled in a certain enzymatic system, the enzyme itself cannot be determined by the ring oven technique. Nevertheless, inhibitors and substrates can be determined if the enzyme is added directly to the segments within the ring zone. The substance to be determined is transferred to the ring zone on the ring oven. An enzyme solution is sprayed on all three segments simultaneously to start the reaction. Instead of spraying, it is more economic to use a 5-mm wide paper ring (as used for the application of substrate in method A) moistened with about 100 μl of the enzyme solution; the ring is pressed on the filter paper with the three segments (see Fig. 3).

The inhibitor to be determined is transferred together with the substrate into three segments of the ring zone; three different amounts of inhibitor — the unknown and two standards — are used with equal amounts of substrate. The enzyme is applied to the three segments with the paper ring and the reaction starts immediately. The reaction product is either visible (coloured or fluorescent) or made visible with a suitable indicator. This method can of course be used only if no incubation time for the inhibition of the enzyme is

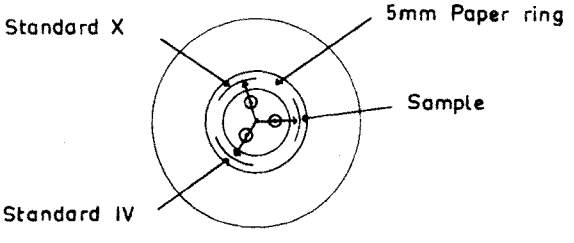

Fig. 3. Method C: addition of enzyme directly to the segments.

necessary, because the reaction starts immediately when the substrate and the enzyme are brought together in the presence of the inhibitor. An example of this type is the determination of beryllium with alkaline phosphatase.

If inhibitors are to be determined with an enzyme which requires an incubation time, the substrate can be added only after inhibitor and enzyme have been in contact for a sufficient time. Therefore the substrate cannot be transferred to the ring zone with the inhibitor, but must be applied some time after the enzyme has been added (sprayed or pressed on with a moistened paper ring) to the segments containing the inhibitor. However, if the inhibitor is concentrated in the ring zone and the segments are pressed with the enzyme-moistened paper ring and the filter is finally sprayed after the incubation time with the substrate, then the enzymatic reaction takes place wherever enzyme and substrate meet, i.e. in the 5-mm wide zone. The inhibitor can be recognized in this case only by the fact that in the three segments the colour (or fluorescence) appears a little later; this is not observed readily.

It is, however, possible to achieve sharply defined and readily visible segments if the enzymatic reaction used produces a more or less colourless product that must be made visible by a suitable indicator. Three different amounts of the inhibitor (unknown and two standards) and an appropriate indicator are concentrated on the ring oven in three segments, the enzyme is added with the aid of the paper ring, and after a suitable incubation period the filter paper is sprayed with the substrate; the reaction product is visible only in the three segments in the form of sharp arcs, the speed of appearance of which depends on the amount of inhibitor in each segment. An example may illustrate this procedure (for details, see below). Urease is inhibited by the fungicide phenylmercury acetate: various amounts of the latter together with equal amounts of bromothymol blue are concentrated in three segments, and urease is applied with the paper ring; when the paper is sprayed with a solution of urea, the yellow segments turn blue sooner or later depending on the concentration of the fungicide in each segment.

Substrates can be determined likewise by method C. As with method B, various amounts of substrate (unknown and standards) are concentrated in three segments and treated with the enzyme solution. The amounts of reaction product can be compared with each other, if necessary after having been made visible with a suitable indicator or with a catalyzed indication system. The well known determination of glucose [11] with glucose oxidase may serve as an example. The enzymatic reaction produces hydrogen peroxide which is made visible by a secondary reaction, e.g. the molybdenum-catalyzed oxidation of iodide. Various amounts of glucose (1 μl each of the unknown and two standards) are transferred to the three segments of the ring zone together with equal amounts of molybdenum and starch (1 μl each); glucose oxidase is applied to the three segments with the paper ring, and after about 30 s the filter is sprayed with iodide solution. Blue colours of various intensities appear in the segments.

The possibilities of applying these three techniques are illustrated by some determinations of enzymes, inhibitors and substrates.

DETERMINATION OF ENZYMES

Determination of acid and alkaline phosphatase (EC 3.1.3.2 and EC 3.1.3.1) by cleavage of 4-methylumbelliferyl phosphate [12]

Acid as well as alkaline phosphatase cleaves 4-methylumbelliferyl phosphate thus forming strongly fluorescent 4-methylumbelliferone.

For the determination of an enzyme six standard solutions are always needed, their concentrations being related in the ratio 1:2:4:6:8:10. Standard solutions of enzymes are usually only stable for a short time and should therefore be prepared in small amounts. With the aid of micropipettes (Eppendorf) standard solutions can be prepared from 5, 10, 20, 30, 40 and 50 μl of the enzyme stock solution and made up to 50 μl with a suitable buffer solution in little PVC vessels.

In the determination of acid phosphatase by method A, a stock solution (40 mU μl^{-1}) in 0.1 M acetate buffer (pH 5.0) is used to prepare the following standard solutions:

Standard solution no.	I	II	IV	VI	VIII	X
Acid phosphatase (mU μl^{-1})	4	8	16	24	32	40

A sufficient number of round filter papers with an adsorption zone is prepared. A barium sulphate adsorption zone proved best for the present purpose: 350 μg of barium (as $BaCl_2$) are washed with water on the ring oven into the ring zone. The filter paper is bathed in 0.05 M sulphuric acid, rinsed in running water for about 30 min and then in distilled water, and dried. The filter papers thus prepared can be stored for a long time and have proved useful for all determinations carried out by method A.

Procedure. On three points concentric around the middle of the filter paper bearing the $BaSO_4$-adsorption zone, place one drop each (1 μl) of the sample solution and of the two standard solutions IV and X, to form an equilateral triangle. Place the filter paper on a suitable support, e.g. a washing ring, and wash the three spots without the use of the ring oven into the adsorption zone with a suitable solvent. In the case of acid phosphatase, wash first with physiological salt solution and then with 0.1 M acetate buffer pH 5.0. Three well defined 10—20-mm long ring segments are thus formed in the adsorption zone. Dry the filter paper with cold air. Moisten a 5-mm wide filter paper ring (15 mm i.d., 25 mm o.d.) with about 100 μl of 0.02 M 4-methylumbelliferyl phosphate in 0.1 M acetate buffer pH 5.0 and press for about 10 s on the filter paper, so that all three segments are covered. This is best done by placing the round filter and the filter paper ring between two glass plates and applying gentle pressure by hand. Then immediately place the round filter under a u.v. lamp and observe the appearance of sharp green fluorescence in the three segments. The order of the appearance allows the

enzyme activity in the sample solution to be assessed.

In further steps, place the sample drop and one drop each of two logically selected standard solutions on new filter papers bearing adsorption zones and proceed as just described. Generally, after the third step a final coordination of the concentration of the unknown sample solution to a corresponding standard solution is possible.

To achieve higher accuracy, it is necessary to carry out two more determinations with different numbers of drops (or different concentrations) of the original sample solution.

In this segment technique [4] as in ring colorimetry [2, 3], the unknown sample is always coordinated to a certain standard solution (number) or in case of doubt a value is selected which is the exact mean of two neighbouring standard values — there is no need for more precise guessing. The following example demonstrates the technique used in all calculations by the weighted average method.

Single coordinations (comparisons) gave the following results (1 S = a segment containing one drop of the original sample solution; roman figures are segments bearing one drop each of the corresponding standard solution):

orientation IV . . 1 S . . X; 1 S nearer to IV
1st determination IV . . 1 S . . VI; 1 S between IV and VI, thus 1 S = V
2nd determination VIII . . 2 S . . X; 2 S nearer to VIII, thus 2 S = VIII
3rd determination II . . S/2 . . IV; S/2 nearer to II, thus S/2 = II.

The concentration of the sample solution is then found by averaging and multiplying the value by the standard concentration of solution I (4 mU μl^{-1}):

1 S = V
2 S = VIII
S/2 = II
7/2 S = XV

S = XV/7/2 = 4.29, and 4.29 · 4 = 17.16 mU μl^{-1} acid phosphatase.

Table 1 gives some results. The range of error was about the same for all determinations of other enzymes described in the present paper, therefore no further detailed results are given.

Alkaline phosphatase. This can be determined analogously. The stock solution contains 3.5 mU μl^{-1} alkaline phosphatase in 0.1 M borate buffer pH 9.4. Standard solutions (0.35—3.5 mU μl^{-1} alkaline phosphatase) are prepared corresponding to Nos. I, II, IV, VI, VIII, X. The substrate is 0.02 M

TABLE 1

Determination of acid phosphatase
(Results are given as mU μl^{-1})

Present	21.6	32.6	7.2	32.0	34.4	5.6	20.0	15.2	28.0
Found	20.0	34.3	7.6	29.7	34.3	5.6	19.4	17.9	29.6

4-methylumbelliferyl phosphate in borate buffer pH 9.4. Alkaline phosphatase is transferred with borate buffer pH 9.4 to the $BaSO_4$ adsorption zone.

Determination of hyaluronidase (EC 3.2.1.35) with indoxyl acetate [13]

Indoxyl acetate is cleaved to fluorescent indoxyl which is converted only slowly to blue indigo. The determination of hyaluronidase is carried out by method A, similarly to the procedure for phosphatase.

The stock solution (5 U μl^{-1} hyaluronidase) is prepared in 0.025 M phosphate buffer pH 6.9. The standard solutions are 0.5—5 U μl^{-1} hyaluronidase corresponding to Nos. I, II, IV, VI, VIII, X. The substrate is 0.1 M indoxyl acetate in ethanol.

Hyaluronidase is transferred to the adsorption zone ($BaSO_4$) with phosphate buffer pH 6.9 and immediately the 5-mm filter paper ring moistened with indoxyl acetate is pressed for some seconds onto the three segments. The filter paper is observed under a u.v. lamp.

Determination of acetylcholinesterase (EC 3.1.1.7) by cleavage of indoxyl acetate [14]

The enzymes so far mentioned could be determined by method A, because these enzymes could be eluted on the filter paper. For the next three determinations, this was not possible, and method B had to be applied.

The enzyme splits indoxyl acetate to indoxyl which gives indigo at the heat of the ring oven.

The stock solution contains 5 mU μl^{-1} acetylcholinesterase in 0.025 M phosphate buffer pH 6.85. The standard solutions are 0.5—5 mU μl^{-1} acetylcholinesterase corresponding to Nos. I, II, IV, VI, VIII, X. The substrate is 0.1 M indoxyl acetate in ethanol.

On three points concentric around the middle of the round filter paper, are placed 1-μl portions of indoxyl acetate solution, and the ethanol is evaporated (ethanol deactivates the enzyme). To the three indoxyl acetate spots the enzyme solution is added: 1 μl each of the sample solution and of two standards. The spots are allowed to dry. The indoxyl formed is washed with ethanol to the ring zone on the ring oven at about 90°C. Instantaneously, sharply defined blue segments of different intensities appear (no fluorescence).

Determination of lipase (EC 3.1.1.3) by cleavage of 4-methylumbelliferone heptanoate [15]

Lipase hydrolyzes 4-methylumbelliferone heptanoate to fluorescent 4-methylumbelliferone.

The stock solution contains 400 mU μl^{-1} lipase in 0.1 M phosphate buffer pH 7.4. The standard solutions are 40—400 mU μl^{-1} corresponding to Nos. I, II, IV, VI, VIII, X. The substrate is 0.01 M 4-methylumbelliferone heptanoate as a suspension in phosphate buffer pH 7.4 (dissolved first in a little methyl cellosolve and made up to volume with phosphate buffer).

Portions (1 μl) of 4-methylumbelliferone heptanoate and lipase solutions (sample and two standards) are placed on three points of the filter paper and allowed to react until dry. The 4-methylumbelliferone formed is then washed to the ring zone on the ring oven. The three fluorescent segments are observed under u.v. light.

Determination of alcohol dehydrogenase (ADH, EC 1.1.1.1) by oxidation of ethanol in the presence of NAD^+ [16]

Ethanol is oxidized to acetaldehyde and nicotinamide adenine dinucleotide (NAD^+) is reduced to fluorescent NADH.

The stock solution contains 20 mU μl^{-1} ADH in 0.1 M Tris buffer pH 9.0. The standard solutions are 2—20 mU μl^{-1} ADH corresponding to Nos. I, II, IV, VI, VIII, X. The substrate is 1 M ethanol in Tris buffer pH 9.0. The coenzyme is used as a 0.01 M NAD^+ solution in water.

NAD^+ solution (1 μl) is placed on the three spots of the filter paper and dried; then 1-μl portions of ADH (sample and two standards) and of ethanol are added to the three spots. The reaction proceeds until the spots dry. The NADH formed is washed with water to the ring zone on the ring oven. The fluorescence in the three segments is observed under u.v. light.

DETERMINATION OF INHIBITORS

All three methods (A, B, C) can be utilized for the determination of inhibitors. As always in the determination of inhibitors, equal enzyme activities are applied and the residual activity is evaluated.

Indirect determination of the insecticide carbaryl [17] and paraoxon [18] with acetylcholinesterase

Carbaryl (1-naphthyl-*N*-methylcarbamate) and paraoxon (*O*,*O*-diethyl-*o*,*p*-nitrophenylphosphate) and some other insecticides inhibit acetylcholinesterase. They can be determined by following method B, as just described for the determination of acetylcholinesterase.

The stock solutions contain 1 $\mu g\ \mu l^{-1}$ carbaryl in ethanol, and 0.1 $\mu g\ \mu l^{-1}$ paraoxon in ethanol. The standard solutions are 0.1—1 $\mu g\ \mu l^{-1}$ carbaryl or 10—100 ng μl^{-1} paraoxon, corresponding to Nos. I, II, IV, VI, VIII, X. The acetylcholinesterase solution (5 mU μl^{-1}) is prepared in phosphate buffer pH 6.85, and the substrate is 0.1 M indoxyl acetate in benzene.

On three concentric points on the filter paper are placed one drop of the unknown solution of the insecticide (carbaryl or paraoxon) and two standard solutions (IV and X). The spots are dried, and each is treated with 1 μl of the enzyme solution (5 mU μl^{-1}). After incubation for 1 min (not to dryness!), 1 μl of indoxyl acetate solution in benzene (not in ethanol which would deactivate the enzyme) is added. After the reaction has proceeded to dryness, the indoxyl formed is washed to the ring zone on the hot ring oven; the intensities of the blue colour of the indigo formed in the three segments are

compared. A higher intensity means a higher activity of the remaining enzyme and consequently a lower concentration of the inhibitor. By further suitably chosen steps (see the detailed description for acid phosphatase), the concentration of the unknown inhibitor (carbaryl, paraoxon) can be evaluated with reasonable accuracy.

Table 2 gives some results for the determination of nanogram amounts of carbaryl. For paraoxon and the other inhibitors (herbicides, fungicides and metal ions) discussed below the range of error is similar, therefore no other results for the determination of inhibitors are tabulated.

Indirect determination of the herbicides 2,4-D, mecoprop, bentazon, and of the fungicide phenylmercury acetate by inhibition of urease (EC 3.5.1.5) [19]

Urea is decomposed by urease to form ammonia which can be measured with a pH indicator, e.g. bromothymol blue (pH 6.0—7.6; yellow → blue). 2,4-D (2,4-dichlorophenoxyacetic acid), mecoprop (2-(2-methyl-4-chlorophenoxy)-propionic acid), bentazon (3-isopropyl-2,1,3-benzothiadiazinone-4-2,2-dioxide) and phenylmercury acetate inhibit urease. Only method C can be used here because the reaction product (ammonia) is volatile.

The following stock solutions were used: 30 $\mu g\ \mu l^{-1}$ bentazon in ethanol; 20 $\mu g\ \mu l^{-1}$ 2,4-D in water; 10 $\mu g\ \mu l^{-1}$ mecoprop in ethanol; 1 $\mu g\ \mu l^{-1}$ phenylmercury acetate in methyl cellosolve. The standard solutions contain 3—30 $\mu g\ \mu l^{-1}$ bentazon, 2—20 $\mu g\ \mu l^{-1}$ 2,4-D, 1—10 $\mu g\ \mu l^{-1}$ mecoprop, or 0.1—1 $\mu g\ \mu l^{-1}$ phenylmercury acetate, corresponding to Nos. I, II, IV, VI, VIII, X. The urease solution (25 U ml^{-1}) is prepared in 10^{-6} M phosphate buffer pH 7.0. The substrate is a 5% urea solution in phosphate buffer pH 7.0, and the indicator is an aqueous 0.01% bromothymol blue solution (exactly neutralized).

On the three spots are added 1 μl of the inhibitor to be determined (one drop each of the unknown and two standards) and one drop of bromothymol blue solution. These are washed with ethanol into the three segments of the ring zone (temperature of the ring oven about 90°C). A 5-mm paper ring moistened with 100 μl of urease solution is pressed on the filter paper covering the three segments for 2 min. The filter paper is then sprayed with urea solution and stored in a glass vessel over water in order to avoid drying. The order of appearance of the blue colour in the three segments is observed. As in all other determinations of enzymes and inhibitors, suitably chosen further steps and a simple calculation follow.

TABLE 2

Determination of carbaryl
(Results are given as ng μl^{-1})

Present	740	350	620	575	955	250	445	155	665
Found	800	428	600	600	914	233	457	150	742

Indirect determination of molybdenum [20] or beryllium [21] by inhibition of acid or alkaline phosphatase

Acid and alkaline phosphatase hydrolyze naphthyl-1-phosphate to phosphoric acid and naphthol, and the latter couples with fast blue salt B (bis diazotized *o*-dianisidine) to a red-violet azo dye. Molybdenum(VI) inhibits the acid phosphatase and beryllium(II) the alkaline phosphatase. Because the reaction product (azo dye) is not thermally stable, only method C can be used for the determinations.

The stock solutions contained 10 ng Mo μl^{-1} as $(NH_4)_6Mo_7O_{24}$ in aqueous solution, or 100 ng Be μl^{-1} as $BeSO_4 \cdot 4H_2O$ in aqueous solution. The standard solutions are 1—10 ng Mo μl^{-1} or 10—100 ng Be μl^{-1}, corresponding to Nos. I, II, IV, VI, VIII, X. The enzyme solutions are 40 U ml^{-1} acid phosphatase in acetate buffer pH 5.0, or 3.5 U ml^{-1} alkaline phosphatase in borate buffer pH 9.4. The substrate is naphthyl-1-phosphate (0.2 mg ml^{-1}) in water, and the indicator is a 1 mg ml^{-1} solution of fast blue salt B in water.

Molybdenum(VI) or beryllium(II) (one 1-μl drop each of the unknown and two standards) are spotted on three points of the filter paper followed by one drop (1 μl) of naphthyl-1-phosphate. The spots are washed with water on the ring oven into the ring zone. A filter paper ring moistened with about 100 μl of acid (for Mo) or alkaline phosphatase (for Be) is pressed on the filter paper (no incubation time!). After spraying with fast blue salt B, within the three segments, sharply outlined red-violet colourations appear with different velocities depending on the inhibitor concentration.

It is of interest that even 10 ng of beryllium gives a distinct inhibitory effect, whereas the inhibition with aluminium begins at about 500 ng.

Indirect determination of copper(II) by inhibition of hyaluronidase [13]

This determination can be done by method A (adsorption zone, see above) because copper(II) inhibits hyaluronidase "irreversibly".

The aqueous stock solution contained 0.5 μg Cu μl^{-1} as $CuSO_4$. The standard solutions are 50—500 ng Cu μl^{-1}, corresponding to Nos. I, II, IV, VI, VIII, X. The enzyme solution is 5 U μl^{-1} hyaluronidase in phosphate buffer pH 6.9. The substrate is 0.1 M indoxyl acetate in ethanol.

A filter paper with an adsorption zone ($BaSO_4$) is spotted with three equal drops of hyaluronidase, followed by three drops of copper(II) (unknown and two standards). After incubation for about 30 s, the inhibited enzyme is washed to the adsorption zone with phosphate buffer pH 6.9, without use of a ring oven, of course. A 5-mm filter paper ring impregnated with 100 μl of indoxyl acetate solution is pressed on the still moist filter paper for 10 s. The order of appearance of the fluorescence within the three segments is observed.

DETERMINATION OF SUBSTRATES

Determination of ethanol with alcohol dehydrogenase (ADH) [22]

The determination is carried out by method B as described above for the determination of the enzyme (ADH) itself.

The stock solution contained 3 $\mu g\ \mu l^{-1}$ (3‰) ethanol in Tris buffer pH 9.0. The standard solutions are 0.3—3 $\mu g\ \mu l^{-1}$ (0.3—3‰) ethanol corresponding to Nos. I, II, IV, VI, VIII, X. The enzyme is ADH (0.2 U μl^{-1}) in Tris buffer pH 9.0; the coenzyme is NAD^+ (0.01 M) in water.

The three concentric points on the filter paper are spotted with 1 μl each of NAD^+, ADH and ethanol (unknown and standards IV and X). After drying, the NADH formed is eluted into the three segments of the ring zone with water on the ring oven. The segments are then compared under a u.v. lamp. As for all the other determinations of enzymes and inhibitors, further steps with suitably chosen standard solutions and different numbers of drops of sample solution (see the detailed description of the determination of phosphatase) are needed for the final evaluation.

Table 3 gives some results.

Determination of glucose with glucose oxidase (GOD, EC 1.1.3.4) [11]

Glucose oxidase oxidizes glucose to gluconic acid and hydrogen peroxide; in the presence of molybdenum(VI), hydrogen peroxide oxidizes iodide to iodine which finally is made visible with starch. Method C must be used because the final product of reaction (iodine) cannot be reasonably washed into the ring zone.

The stock solution contained 2 $\mu g\ \mu l^{-1}$ (D+)-glucose in water. The standard solutions are 0.2—2 $\mu g\ \mu l^{-1}$ (D+)-glucose, corresponding to Nos. I, II, IV, VI, VIII, X. The GOD solution (300 U ml^{-1}) is prepared in acetate buffer pH 5.0. The other reagent solutions required are 10 ng Mo μl^{-1} (as Na_2MoO_4 in water), 0.02 M KI in acetate buffer pH 5.0, and 1% starch in water.

Glucose, molybdenum(VI) and starch solutions (1 μl each on the three concentric points on the filter paper) are washed with water on the ring oven into the ring zone and dried. A 5-mm filter paper ring moistened with 100 μl of GOD solution is pressed on the three segments for 30 s and then the paper is sprayed with the solution of potassium iodide. The order of the appearance of the intense blue colour within the three segments is observed. The further steps are carried out as in all other determinations described here. The results were not quite as good as for the determination of ethanol.

DISCUSSION

All the experiments described here in very concise form show that the ring oven technique can be applied in the field of enzymatic analysis. These very simple techniques are, however, not as sensitive as many other enzymatic

TABLE 3

Determination of ethanol
(Results are given as $\mu g\ \mu l^{-1}$)

Present	0.75	2.92	2.19	1.51	1.03	1.08	0.67	2.10	1.56
Found	0.75	2.91	2.00	1.45	1.00	1.05	0.65	2.00	1.70

analytical methods, although in some cases, e.g. in the determination of ethanol, the sensitivity is quite satisfactory. In the further development of this combination of methods, the sensitivity can perhaps be enhanced, possibly by variation of the capillary support (e.g., t.l.c. plates).

REFERENCES

1 G. G. Guilbault, Enzymatic Methods of Analysis, Pergamon Press, Oxford, 1970.
2 H. Weisz, Mikrochim. Acta (Wien), (1954) 785.
3 H. Weisz, Microanalysis by the Ring Oven technique, 2nd edn., Pergamon Press, Oxford, 1970.
4 H. Weisz, S. Pantel and I. Vereno, Mikrochim. Acta (Wien), (1975 II) 287.
5 F. L. Hahn and G. Leimbach, Ber. Dtsch., Chem. Ges., 55 (1922) 3070.
6 J. Bognár, Mikrochim. Acta (Wien), (1963) 397.
7 H. Weisz and S. Abe, Mikrochim. Acta (Wien), (1970) 1054.
8 H. Weisz, Proc. Soc. Anal. Chem., (1974) 319.
9 P. W. West, A. J. Llacer and Ch. Cimerman, Mikrochim. Acta (Wien), (1962) 1165.
10 K. B. Yatsimirskii, Kinetic Methods of Analysis, Pergamon Press, Oxford, 1966.
11 H. V. Malmstadt and H. L. Pardue, Anal. Chem., (33) (1961) 1040.
12 H. N. Fernley and P. G. Walker, Biochem. J., 97 (1965) 95.
13 G. G. Guilbault, D. N. Kramer and E. Hackley, Anal. Biochem., 18 (1967) 241.
14 G. G. Guilbault and D. N. Kramer, Anal. Chem., 37 (1965) 120.
15 T. J. Jacks and H. W. Kircher, Anal. Biochem., 21 (1967) 270.
16 H. U. Bergmeyer, Methoden der enzymatischen Analyse, 3. Aufl. Verlag Chemie Weinheim/Bergstr., 1974, Vol. I, p. 459.
17 C. E. Mendoza, P. J. Wales, H. A. McLeod and W. McKinley, Analyst (London), 93 (1968) 34.
18 P. A. Giang and S. A. Hall, Anal. Chem., 23 (1951) 1830.
19 F. Geike and I. Schuphan, J. Chromatogr., 72 (1972) 153.
20 F. Geike, Z. Anal. Chem., 255 (1971) 134.
21 G. G. Guilbault, M. H. Sadar and M. Zimmer, Anal. Chim. Acta, 44 (1969) 361.
22 H. O. Bergmeyer, Methoden der enzymatischen Analyse, 3. Aufl. Verlag Chemie Weinheim/Bergstr., 1974, Vol. II, p. 1545.

Analytica Chimica Acta, 91 (1977) 243—250

THE ENTHALPIMETRIC DETERMINATION OF THE MICHAELIS CONSTANT OF THE α-CHYMOTRYPSIN-CATALYSED HYDROLYSIS OF *N*-ACETYL-L-TYROSINE ETHYL ESTER BASED ON THE INTEGRATED MICHAELIS—MENTEN EQUATION

J. K. GRIME*, K. LOCKHART and B. TAN

Department of Chemistry, University of Otago, P.O. Box 56, Dunedin (New Zealand)

(Received 22nd November 1976)

SUMMARY

An enthalpimetric method is discussed for the determination of the Michaelis constant (K_m) for the α-chymotrypsin-catalysed hydrolysis of *N*-acetyl-L-tyrosine ethyl ester (ATEE). The integrated form of the Michaelis—Menten equation is used to achieve a graphical determination of K_m in a single experiment (s_r = 7.6%). The inhibitory effect of ethanol is briefly described.

The Michaelis—Menten theory [1] postulates that the reaction of an enzyme (E) with a substrate (S) to form a product (P), takes place via the formation of an enzyme—substrate complex:

$$E + S \underset{k_{-1}}{\overset{k_1}{\rightleftharpoons}} ES \overset{k_2}{\rightarrow} P + E \qquad (1)$$

The velocity (v) of such a reaction is described by the hyperbolic equation

$$v = \frac{V_{max}\,[S]}{K_m + [S]} \qquad (2)$$

where [S] is the substrate concentration, V_{max} the maximum velocity and K_m is the Michaelis constant.

Originally this equation was derived on the assumption that $k_2 \ll k_{-1}$, i.e. that the first step in the process could be regarded as a simple equilibrium. Thus $K_m = K_s = k_1/k_{-1}$, where K_s is the dissociation constant of the enzyme—substrate complex. Experimental evidence has since indicated that K_m can be given this particular significance in only a limited number of cases. The "equilibrium theory" was later revised [2] to include assumptions that are valid regardless of the relative magnitudes of k_{-1} and k_2 and still permit derivation of an explicit rate equation. This "steady-state theory" assumes that after a short period of time $d[ES]/dt \approx 0$. With this approximation, a

*To whom correspondence should be addressed.

rate equation identical to eqn. (2) can be derived. In this equation, which includes the equilibrium assumption as a special case, K_m is simply the ratio of three velocity constants:

$$K_m = \frac{k_{-1} + k_2}{k_1} \tag{3}$$

where K_m = [S], then $v = V_{max}/2$. Thus, K_m is numerically equal to the concentration of the substrate (usually expressed in mol dm^{-3}) when the reaction proceeds at half its maximum velocity. The numerical value of K_m, which is characteristic for a particular enzyme–substrate combination, is independent of enzyme concentration, but may depend on pH, temperature and other extrinsic parameters. K_m values defined in this manner are often used to compare the relative affinities of a series of substrates for a particular enzyme.

It is apparent from eqn. 2 that, whether or not K_m has any significance as a dissociation constant, its value is essential in defining the rate law for an enzyme-catalysed reaction. Furthermore, the factors that affect the velocity of such a reaction, viz. the formation of the ES complex and its breakdown, will be reflected in the values of K_m and V_{max}, respectively. Accurate methods for the determination of these parameters are obviously needed.

Since the relationship between the independent variable [S] and the dependent variable v is represented by an asymptotic curve approaching V_{max}, K_m and V_{max} are usually determined by a linear transformation. The three most commonly used transformations and the appropriate graphical manipulations are shown in Table 1. Although these equations are all variants of eqn. (2), they do not provide equally accurate estimates of K_m and V_{max}. Equations (4) and (5) (see Table 1), which both involve the reciprocal of v, distribute weight inappropriately on the smallest values of v. Indeed eqn. (4) has been shown to be significantly less accurate than eqns. (5) and (6) when subjected to quantitative error analysis [3]. Furthermore, all these plots are based on initial velocity measurements made at several substrate concentrations and therefore each plot necessitates at least four experiments.

TABLE 1

Linear transformations of Michaelis–Menten equation

Equation	Extrapolation		
	Ordinate	Abscissa	Slope
(4) $\frac{1}{v} = \frac{1}{V_{max}} + \frac{K_m}{V_{max}}\frac{1}{[S]}$	$\frac{1}{V_{max}}$	$\frac{-1}{K_m}$	$\frac{K_m}{V_{max}}$
(5) $\frac{[S]}{v} = \frac{K_m}{V_{max}} + \frac{1}{V_{max}}[S]$	$\frac{K_m}{V_{max}}$	$-K_m$	$\frac{1}{V_{max}}$
(6) $v = V_{max} - K_m\frac{v}{[S]}$	V_{max}	$\frac{V_{max}}{K_m}$	$-K_m$

An alternative approach is to determine the progress curve of a reaction at a single substrate concentration and to apply the integrated form of eqn. (2) to the experimental data. Thus, the same kinetic parameters can be determined from a single experiment.

THEORY

For a simple irreversible uninhibited enzyme-catalysed reaction, eqn. (2) can be written in the form

$$\frac{dp}{dt} = \frac{V_{max}\,(S_0 - p_{(t)})}{K_m + (S_0 - p_{(t)})} \tag{7}$$

where $p_{(t)}$ is the number of moles of substrate consumed at time t, and S_0 is the initial number of moles of substrate ($p_{(t)} = 0$, when $t = 0$). Integrating and rearranging gives the equation of the progress curve

$$\frac{2.303}{t} \log_{10} \frac{S_0}{S_0 - p_{(t)}} = \frac{V_{max}}{K_m} - \frac{1}{K_m} \cdot \frac{p_{(t)}}{t} \tag{8}$$

Thus a plot of the left-hand side of eqn. (8) versus $p_{(t)}$ will be linear with a negative slope equal to the reciprocal of K_m and an intercept on the abscissa equal to V_{max}. In the absence of a systematic error, progress curve data plotted thus will produce unbiased estimates of K_m and V_{max}, provided that the initial substrate concentration is greater than K_m [4].

It has been shown recently that the progress of an enzyme-catalyzed reaction can be monitored enthalpimetrically with both zero and first-order kinetics prevailing [5], although the work reported hitherto has been predominantly analytical in nature. However, an enthalpimetric determination of K_m for the enzymatic reduction of pyruvate to lactate has been reported [6]. In a "kinetic d.i.e." experiment, reaction velocities, calculated by tangential extrapolation at selected points on the enthalpogram, were plotted according to eqn. (4). The disadvantages of utilizing this transformation have already been discussed.

Adopting the terminology of eqn. (7) and substituting into the "working equation" of kinetic enthalpimetry gives $q_{(t)} = -p_{(t)}\,\Delta H$. Obviously, in the absence of any extraneous thermal effects, the heat output at any instant, $q_{(t)}$, is a direct measure of the extent of reaction, as represented by $p_{(t)}$, the number of moles of substrate consumed at time t. Clearly, for a reaction proceeding to completion, the total heat effect, q, is related to the initial number of moles, S_0. Thus the dependent variable in the integrated rate equation, $p_{(t)}$, can be determined directly from a kinetic enthalpogram from the relationship

$$p_{(t)} = \frac{q_{(t)}}{q} \cdot S_0 \tag{9}$$

A typical corrected enthalpimetric progress curve is represented in Fig. 1.

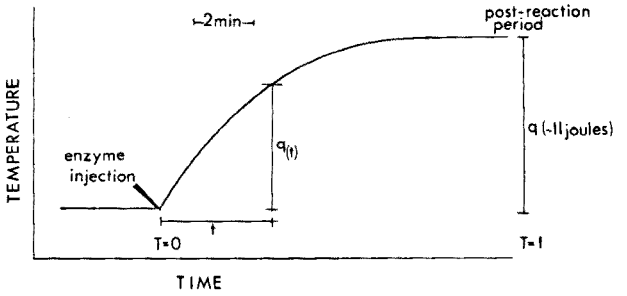

Fig. 1. Enthalpimetric reaction progress curve. Corrected for heat loss from $T = 0.5—1.0$.

To assess the potential of the technique, the well-documented hydrolysis of *N*-acetyl-L-tyrosine ethyl ester (ATEE) in the presence of the proteolytic enzyme α-chymotrypsin was studied.

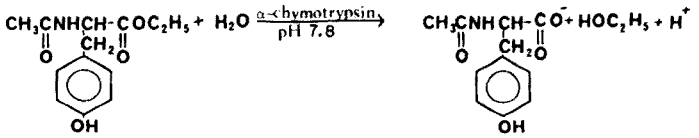

The reaction was buffered at pH 7.8 with a suitable Tris solution. Accordingly the reaction, Buffer—NH_2 + H^+ → Buffer—NH_3^+ occurs concurrently with the ATEE hydrolysis reaction. The function of the buffer is two-fold: not only does it provide constant pH, but its enthalpy of protonation amplifies the observed heat change. In practice, a buffer concentration of 0.2 mol dm^{-3} proved adequate for these purposes.

A reaction pathway more complex than sequence (1) has long been established for chymotrypsin reactions. The sequence involves the formation of a covalent acyl—enzyme intermediate ES′, in addition to the normal noncovalent Michaelis complex ES. The situation can be represented as follows

$$E + S \underset{k_{-1}}{\overset{k_1}{\rightleftharpoons}} ES \underset{P_1}{\overset{k_2}{\searrow}} ES' \xrightarrow{k_3} E + P_2$$

where $K_m = K_s k_3/(k_2 + k_3)$ and $K_s = (k_2 + k_{-1})/k_1$. The numerical value of K_m still has the same significance with regard to substrate affinity.

EXPERIMENTAL

Reagents

Bovine pancreas α-chymotrypsin and ATEE were obtained from the Sigma Chemical Co., St. Louis, Missouri, 63178. Elemental microanalysis showed that the ATEE was more than 99% pure. Both substances were stored, desiccated, below 0°C.

Tris(hydroxymethyl)aminomethane (Tris) buffer pH 7.8 was adjusted with hydrochloric acid.

Solutions of ATEE were prepared by dissolving the solid in a minimal amount of ethanol and subsequent dilution in Tris buffer. In order to reduce errors from non-enzymatic hydrolysis, substrate solutions were prepared in the reaction cell immediately before the experiment. Ethanol exhibits competitive inhibition on the enzymatic action of proteinases [7], consequently affecting the value of K_m. Accordingly, the amount of ethanol added to the substrate was minimized and standardized at 3%. Heats of mixing between non-aqueous and aqueous solutions were precluded by the addition of an equal amount of ethanol to the enzyme solution. Ethanol should not be added directly to the enzyme as it may cause denaturation. Enzyme solutions, also diluted with Tris buffer, were prepared before each set of experiments. Reagent blanks showed no observable heat effects. In practice, approximately 1000 I.U. of enzyme solution were injected into 200 μmol of substrate.

Apparatus

The heat changes during the reaction were monitored by measuring the imbalance potential of a d.c. Wheatstone bridge circuit incorporating a 10,000-ohm thermistor as one arm of the bridge. The signal was amplified by a variable gain, null detector—microvoltmeter (Model 155, Keighley Instrument Co., Cleveland, Ohio) and recorded on a strip-chart potentiometer. All components of the temperature-measuring circuitry were adequately grounded. Caloric calibration of the enthalpograms was achieved in situ, by the joule heating of a 0.25-W carbon resistor (100 ohms nominal). An accurate measurement of the current flowing through the heater was obtained by the measurement of the potential drop across a precision resistor (10 ohms, ± 0.1%) wired in series with the calibration heater. The temperature-measuring and heating circuitry are represented in Fig. 2.

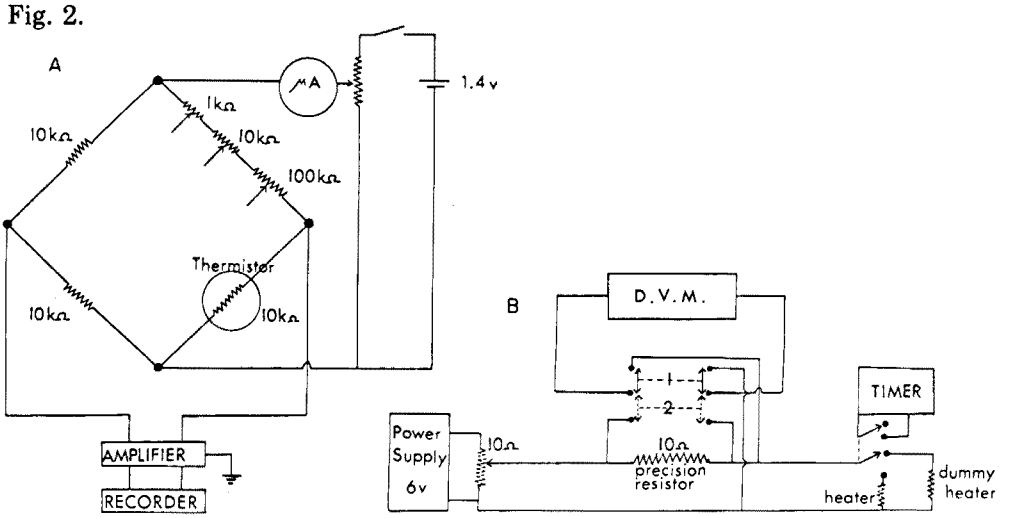

Fig. 2. Apparatus. A. Temperature measuring circuitry. B. Heating circuitry. 1 and 2: alternative switch positions.

Preliminary calibration experiments indicated that the design of the adiabatic cell and its environment were critical to the analytical and calorimetric accuracy and precision of the experiments. Optimum results were obtained with a cylindrical Dewar cell, capacity 15 cm^3, with an inner wall of very thin glass (ca. 0.1 mm). Reagents were injected into the reaction mixture from a 0.5-cm^3 syringe with Chaney adaptor, via polythene delivery lines. Stirring was provided by a motor-driven polythene disc rotating at 600 r.p.m. Temperature mismatch between substrate and enzyme solution was minimized by immersion of the reaction cell and syringe in a water-bath maintained at 25.00 ± 0.01 °C

Procedure

To reduce experimental error, the enzyme solution, the concentration of which is not critical to the accuracy of the experiment, was injected into a quantitatively measured amount of substrate. In practice, about 0.05 g of ATEE was weighed accurately into the reaction cell; 0.3 cm^3 of ethanol and 10.00 cm^3 of Tris were then added by pipette. The syringe was loaded with ca. 1000 I.U. of enzyme and the tip of the delivery line inserted into the reaction cell. The syringe and assembly were then immersed in the water-bath and allowed to come to thermal equilibrium with the environment. The time necessary for this operation can be considerably reduced by intermittent activation of the heating circuitry. On attainment of equilibrium, as evidenced by an isothermal baseline, the enzyme was quickly injected into the substrate solution and the resultant heat effect monitored. After an appropriate post-reaction period, the effective heat capacity of the cell and its contents was determined electrically. This procedure was repeated for reaction solutions containing 5% and 7% ethanol to assess the inhibitory effect of ethanol as manifested by the value of K_m.

RESULTS AND DISCUSSION

Assignment of reaction enthalpies

The overall reaction enthalpy for the ATEE reaction and the buffer reaction was determined to be 48.4 ± 0.4 kJ mol^{-1}. Previous calibration experiments showed the heat change accompanying the protonation of Tris buffer to be 47.7 ± 0.4 kJ mol^{-1}. The enthalpy change associated with the enzymatic hydrolysis alone is obviously small compared with the concurrent protonation reaction and, indeed, falls almost within the limits of experimental error. Accordingly, a numerical value cannot be assigned to the enthalpy change of the enzymatic hydrolysis. This limitation does not, however, hinder the determination of K_m for the enzymatic reaction. The progress curve can be recorded adequately by observing the heat effect of the attendant protonation reaction.

The determination of K_m

A small, but finite, heat loss was observed in the post-reaction period of the experimental enthalpograms. A correction factor was therefore applied to the enthalpograms based on the approximation that the significant heat loss occurs at a constant rate in the second half of the enthalpogram (i.e. $0.5 \leqslant T \leqslant 1$) and is equal in magnitude to the heat loss in the post-reaction period.

Data were not extracted from the first 25% of the progress curve where the substrate concentration is greater than K_m and consequently $dp_{(t)}/dt \approx 0$, as evidenced by the linearity of the enthalpogram. Under the prevailing conditions, the reaction proceeds effectively at V_{max} during this period of time. Values of q, $q_{(t)}$ and t were determined from the corrected enthalpograms. The usual time period between measurements was 6 s. $p_{(t)}$ was then calculated in accordance with eqn. (8) and the results were plotted (Fig. 3). The pertinent results are summarized in Table 2. The K_m for the reaction in 3% ethanol was determined to be $14.3 \cdot 10^{-4}$ mol dm^{-3} (s_r = 7.6%). This compares with literature values of $7-8 \cdot 10^{-4}$ mol dm^{-3} in the absence of alcohol, at various pH values. The inhibitory effect of alcohol on the enzymatic hydrolysis of ATEE is reflected in the increased values of K_m at 5% and 7% ethanolic

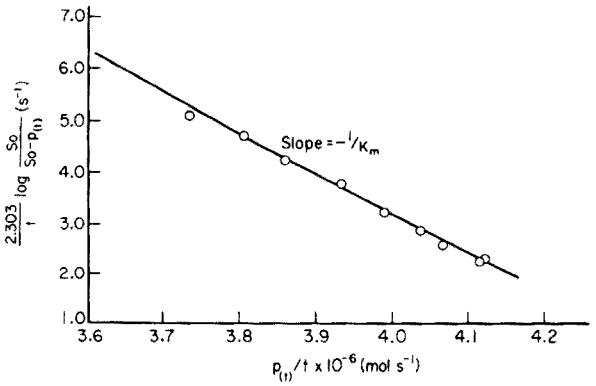

Fig. 3. Graphical determination of K_m — typical results.

TABLE 2

Results

Experiment	ΔH (kJ mol^{-1})	$K_m \cdot 10^{-4}$ (mol dm^{-3})	Initial amount of substrate (mol $\cdot 10^{-6}$)	%EtOH (v/v)
1	48.5	15.2	190.9	3
2	47.7	13.3	181.8	3
3	48.1	15.6	180.2	3
4	48.5	13.3	180.5	3
5	48.1	13.9	174.4	3
6	49.4	15.4	189.0	5
7	48.5	24.4	188.1	7

solution. The precision compares favorably with other methods, which usually quote a precision in determining the slope of ca. ±10%.

Conclusion

The enthalpimetric approach is obviously a realistic alternative method for the determination of kinetic parameters for enzymatic reactions. The universal nature of the enthalpy change means that, in contrast with many methods, the primary catalytic reaction can be observed. The need for a coupling reaction with its own specific prerequisites of pH, substrate concentration, activators etc., in order to produce an analytically measurable entity is obviated, resulting in a reduction in both experimental error and time. Furthermore, the use of a progress curve in lieu of initial rate measurements results in a single experiment determination of K_m and V_{max}.

In these experiments, the kinetic data were taken manually. Computerization of this procedure is in progress.

REFERENCES

1 L. Michaelis and M. L. Menten, Biochem. Z., 49 (1913) 333.
2 G. E. Briggs and J. B. L. Haldane, Biochem. J., 19 (1925) 338.
3 J. E. Dowd and D. S. Riggs, J. Biol. Chem., 240 (1965) 863.
4 G. L. Atkins and I. A. Nimmo, Biochem. J., 135 (1973) 779.
5 C. D. McGlothlin, J. K. Grime and J. Jordan, Enzymatic Enthalpimetry for Clinical Analysis, Symposium of New Approaches to the Routine Determination of Serum Enzymes, Paper No. 71, A.C.S. New York, April 1976.
6 N. Jespersen and K. Barclay, Anal. Lett., 8 (1975) 33.
7 G. Danno, Agric. Biol. Chem., 37 (1973) 445.

Analytica Chimica Acta, 91 (1977) 251—258

CORRECTIONS TO ELECTROPHORETIC DATA OBTAINED IN POROUS SUPPORTING MEDIA

ZVONIMIR PUČAR, BISERKA POKRIĆ and MARIJAN PETEK
Laboratory of Electrophoresis, "Rudjer Bošković" Institute, Zagreb (Yugoslavia)
(Received 7th January 1977)

SUMMARY

To obtain electrophoretic mobilities referring to free solution, relative or absolute correction factors should be used to correct apparent mobility data obtained in a porous supporting medium. The absolute correction factor gives a direct measure of the texture or porosity of the support. The significance and determination of the correction factors are explained in detail, theoretically and experimentally. Another important characteristic of the porous supporting medium is the acid—base dissociation at its interface, resulting in electroosmotic flow dependent on pH. Filter paper cellulose is dissociated, through at least three dissociation constants, over the entire pH range except at the isoelectric point, pH 1.10.

When Michl [1] introduced the technique of high-voltage electrophoresis which involved a water immiscible cooling liquid to dissipate the Joule's heat and avoid evaporation from filter paper strips or porous supporting media of any kind, it became possible to correct the apparent electrophoretic data and obtain reasonably dependable electrophoretic mobilities related to those in free solution. Kunkel and Tiselius [2] were the first to relate the real displacement of the substance during electrophoresis through the structure of the porous support (L) to the apparent displacement (L'), as a correction parameter for the texture or porosity of the support.

Later, in 1957, Pučar [3] proposed a complete formula for the conversion of apparent electrophoretic mobilities into true electrophoretic mobilities in free solution with respect to: (i) texture or porosity of the support; (ii) adsorption chromatographic effects of the substance investigated on the material of the support; and (iii) electroosmotic effects of the support under given experimental conditions. Of these, it is evident that (i) refers to the texture or microscopic structure, (ii) refers to the interaction of the ionic species in solution with the material and (iii) refers to the characteristic of the material in terms of acid—base dissociation constants of active groups at the interstitial surface of the support.

Hence, besides their use in the separation and analysis of mixtures, electrophoretic techniques may be used in at least four ways:

(1) to ascertain molar ionic conductivities or electrophoretic mobilities in free solution, for studies of the complexation of ions in dissolved ionic systems [3—11], of the speciation of ions in solution [11, 12], and of mutual interactions of ions in concentrated electrolytic solutions [13];

(2) to study the processes of hydrolysis of metal ionic species in solution [11, 14—16] through interaction of the —OH groups of the metal hydrolytic species with the =CHOH groups of the cellulosic support. The hydrogen bonds involved give an adsorption chromatographic effect on cellulose which is partly broken at electric field strengths between 0.38 and 0.75 V cm^{-1} and completely broken at higher electric field strengths [15]. When apparent electrophoretic mobilities are corrected with respect to the chromatographic effect, very high "quasi electrophoretic mobilities" result and give a sensitive measure of the extent of the hydrolysis [11, 14, 15];

(3) to obtain a measure of the texture density parallel with the surface of any kind of paper, textile, membrane, or gel, through measuring the L/L' ratio in any direction;

(4) apart from texture, characteristics of the material of the supporting medium may also be ascertained through appropriate electroosmotic measurements in a wide pH range, e.g., pH 0.5—13. This would enable the dissociation of the support material at its interstitial surface to be determined.

The aim of the present paper is to elucidate points 3 and 4. Experiments made with Munktel 20/100, 20/150 and 20/250 filter paper were compared with Munktel 302 filter paper, which is a more recent product. The present results will also enable dependable measurements of molar ionic conductivities corrected to free solution to be made by using the absolute value of the correction factor instead of the relative value. This principle has already been used in two papers [12, 13] without satisfactory explanations being given.

The correction formula

To correct the apparent electrophoretic mobilities (u') of an ionic species obtained in a porous supporting medium into true electrophoretic mobilities (u) in free solution, the following formula is used [3]

$$u = K^2 \left(\frac{u'}{R_F} - \frac{u'_e}{R_{Fe}} \right) \tag{1}$$

where

$$u' = \frac{s'}{H'\tau} \text{ (in mm } h^{-1} \text{ } V^{-1} \text{ cm)} \tag{2}$$

and s' is the apparent displacement of an electrophoretic zone (mm); H' the apparent electrical field strength (V cm^{-1}) in the direction of the electrophoretic displacement of the zone; τ the time of the electrophoretic displacement (h); R_F the chromatographic adsorption factor of the zone on the supporting medium; u'_e the apparent electroosmotic mobility of an

electroneutral substance under given experimental conditions; R_{Fe} the chromatographic adsorption factor on the supporting medium of the zone of the neutral substance used to determine the apparent electroosmotic mobility (this will, in most cases, equal 1); and K is a dimensionless correction factor pertaining to the texture or porosity of the supporting medium in the direction of flow of the electric current. This factor K is independent of the thickness of the support (filter paper).

The corrected electrophoretic mobilities have the dimension mm V^{-1} h^{-1} cm, which represents the electrophoretic displacement of a moving zone in mm h^{-1} at an electric field strength of 1 V cm^{-1}. This mobility value can easily be transformed into the usual units (cm^2 V^{-1} s^{-1}) by multiplying by the factor $0.278 \cdot 10^{-4}$, or into molar ionic conductivity (S cm^2 mol^{-1}) by multiplying by the factor 2.68.

The correction factor K

A column of a homogeneous solution of an electrolyte with a constant area of cross-section q cm^2 and length L' cm may be investigated. The conductivity of the electrolytic solution at the temperature t °C is κ S cm^{-1}. At both ends of the column, an electric potential U V is applied. Hence, a constant potential gradient, or electric field strength, $H' = U/L'$ V cm^{-1}, exists across the column. The electric current (in A) across the column is:

$$I' = \frac{q \kappa U}{L'} \quad \text{or} \quad I' = q \kappa H' \tag{3}$$

Suppose that fibers or particles of non-conducting material are introduced so that a porous column is formed. Although the area of cross-section of the porous column may increase to $q + \Delta q$, the free area of the cross-section available to the electric current will retain the value q. Applying again the electric potential U across the column, the current will be

$$I = \frac{q \kappa U}{L} \quad \text{or} \quad I = q \kappa H \tag{4}$$

This is because the actual length is greater than the apparent length of the column $L > L'$. Hence, $H < H'$, $I < I'$, and every displacement $s > s'$. (In this notation apparent quantities are dashed and actual quantities are undashed.)

From eqns. 3 and 4 it follows that

$$\frac{H'}{H} = \frac{I'}{I} = \frac{q \kappa U}{L' I} = \frac{L}{L'} = \frac{s}{s'} = K \tag{5}$$

The correction factor K represents the ratio of the actual to the apparent electrophoretic displacement of an ion in a porous support.

Equation 2 can be written separately for apparent and actual electrophoretic mobility, u' and u, and by combining both equations the actual mobility u is obtained

$$u = \frac{s}{s'} \frac{H'}{H} u' \quad \text{or} \quad u = K^2 u' \tag{6}$$

The correction factor can be obtained experimentally from $K = q \kappa U/L'I$ (eqn. 5) with a standard electrolytic solution of known conductivity κ at a given temperature (e.g. KCl solution). The free area of the cross-section q may be found from the difference in weight of the wet and dry column, filter paper, gel, membrane, etc.

EXPERIMENTAL AND RESULTS

Determination of relative values of K in filter paper strips

The apparatus for high-voltage electrophoresis was described earlier [3]. Better thermostating was achieved by circulating the cooling and sealing liquid (white spirit) through an ultrathermostat and maintaining the temperature at 20 ± 0.1°C. Two filter paper strips of the same kind (70 cm × 1.5 cm) were uniformly saturated with 0.1 mol dm^{-3} KCl solution and placed horizontally between the electrode vessels (600 cm^3 each) filled with the same salt solution. The dimensions of the strips not immersed in the electrode vessels were 66 cm × 1.5 cm. The filter paper strips were immersed directly in circulating white spirit and kept at 20°C.

When the electric potential (U) at the electrodes is raised gradually and the corresponding current (I) measured, the ratio U/I and K will diminish because of the Joule's heat generated in the strips. A temperature difference Δt is established between the thermostated circulating white spirit and the filter paper strips, depending on the electric effect (UI) applied per cm^2 of the surface of the strips (specific electric effect in V A cm^{-2}; only one surface area of the strips was taken into account here).

The increase in temperature increases the conductivity of the KCl solution and the electric current at the same time

$$\frac{\kappa_{t+\Delta t}}{\kappa_t} = \frac{I_{t+\Delta t}}{I_t} \tag{7}$$

The relative value of K is therefore the function of the specific electric effect applied (V A cm^{-2}). If used for correction of electrophoretic mobilities, all the apparent electrophoretic mobilities must be measured strictly at the same specific electric effect used to determine the relative value of K. Equation 1 will give the correct electrophoretic mobilities for temperature t of the thermostated cooling liquid, although the actual electrophoresis was carried out at $(t + \Delta t)$.

As an example, the relative value of K for Munktel 20/100 paper can be determined from previous experimental data [3]. Two paper strips were wetted appropriately with 0.1 mol dm^{-3} KCl; for each strip, free length L' = 66 cm, width = 1.5 cm; surface area = 198 cm^2; area of cross-section q = 0.108 cm^2; d.c. voltage applied U = 2030 V; current I = 0.0355 A; the power applied to the two strips = 72 V A; the specific electric effect = 0.36 V A cm^{-2}; the temperature of the coolant was 20°C; the conductivity of the KCl solution at 20°C was κ = 0.01169 S cm^{-1}. From eqn. 5, the

relative correction factor was $K = 1.094$ and $K^2 = 1.20$. When inserted into eqn. 1, this correction factor gives electrophoretic mobilities for any reasonable temperature of the coolant if Munktel 20/100 is the filter paper used, and the specific electric effect is kept at 0.36 V A cm^{-2}, although, as will be shown later (Fig. 2), the actual temperature of the strips will be 9°C higher than that of the coolant. The same value of K was also obtained later with Munktel 20/150 and 20/250 papers although these have greater thickness and weight (20/100, 100 g m^{-2}; 20/150, 150 g m^{-2}; 20/250, 250 g m^{-2}).

Determination of absolute value of K

From the preceding section it can be inferred that the relative value of K will approximate to the absolute value at very low specific electric effects. The criterion for the choice of the specific electric effect used in the determination of the absolute value of K is that the change in electric potential at the ends of the strips U should not influence the U/I ratio considerably.

The absolute value of K for Munktel 20/100 was found with the same experimental parameters as before, with the following exceptions: $U = 50$ V, $I = 0.54 \cdot 10^{-3}$ A, the power applied = 0.027 V A, and the specific electric effect = $0.136 \cdot 10^{-3}$ V A cm^{-2}. Inserting the values of U and I into eqn. 5, the absolute value of K for Munktel 20/100 was $K = 1.33$ ($K^2 = 1.77$). This means that the real displacement of ions through the texture of the support is 33% higher than the apparent displacement. The same absolute value of K was found for Munktel 20/150 and 20/250. For Munktel 302 the absolute value found $K = 1.42$ ($K^2 = 2.01$) gives evidence of denser texture, since the real displacement through the texture is 42% higher than the apparent displacement.

Temperature correction of electrophoretic mobilities or molar ionic conductivities when the absolute value of K is used

Since the electrophoretic conductivity of a reference solution of an electrolyte, e.g., 0.1 mol dm^{-3} KCl, is a function of the temperature (Fig. 1), eqn. 7 may be written in the form

$$\kappa_{t+\Delta t} = \kappa_t \frac{I_{t+\Delta t}}{I_t} \tag{8}$$

If the temperature of the circulating white spirit coolant is kept constant at different temperatures t, and U at the end of the strips is changed, the current I_t (at the moment of switching on the current) and the current $I_{t+\Delta t}$ (when equilibrium is reached after a few minutes) can be measured. Inserting κ_t, the corresponding values of $\kappa_{t+\Delta t}$ are calculated. From Fig. 1, or appropriate tables giving $\kappa = f(t)$, the values of Δt, i.e., the difference in temperature in the strips under the electric current and the thermostated circulating coolant can be found. Figure 2 gives Δt vs. the specific electric effect $UI_{t+\Delta t}$ V A cm^{-2}.

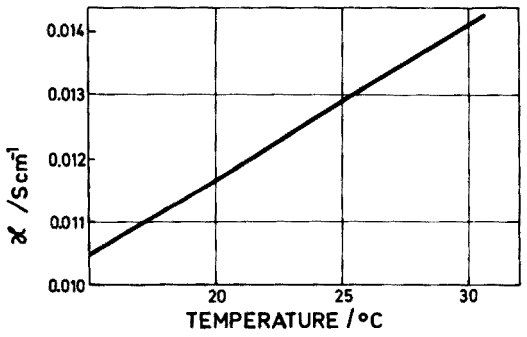

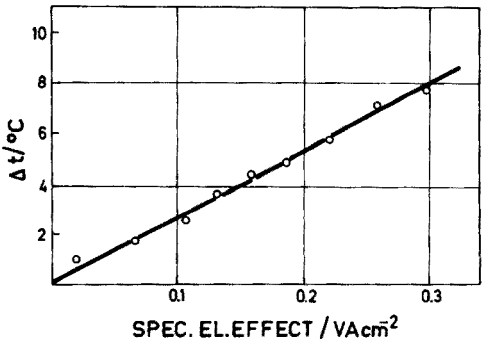

Fig. 1. Dependence on temperature of conductivity of 0.1 mol dm^{-3} KCl solution.

Fig. 2. Dependence on the applied electric power of the difference in temperature of the strips over that of the circulating thermostated coolant (white spirit). Munktel 302 filter paper.

Assuming for example that electrophoretic mobilities should be measured at 25°C while the cooling white spirit is thermostated at 20°C, U should be adjusted so that the specific electric effect amounts to 0.185 V A cm^{-2} (Fig. 2); this corresponds to a power of 36.6 V A applied to the strips of dimensions 66 cm × 1.5 cm [12, 13]. This will ensure that the paper strips are at 25°C during electrophoresis.

Correction for electroosmosis in the support

Electroneutral substances, e.g. hydrogen peroxide in the acid pH region, glucose and dextran, were commonly used to find the electroosmotic mobility in the support under given experimental conditions. If experiments are done in filter paper strips over a wide pH range, e.g., pH 0.5—13.5, the electroosmotic flow is invariable to pH change if glucose or dextran is used as an indicator substance. The electroosmotic mobility in cellulose at ionic strength 0.1 amounts to -0.70 ± 0.08 mm V^{-1} h^{-1} cm or $(-0.19 \pm 0.02) \cdot 10^{-4}$ cm^2 V^{-1} s^{-1}, indicating that, at least in strongly alkaline media, the effect of dissociation of the =CHOH groups of the amorphous part of the cellulose is compensated by the dissociation of similar groups belonging to glucose (=CHOH $\rightleftharpoons$ =CHO^- + H^+). The same also holds for possible dissociation in strongly acidic media (=CHOH $\rightleftharpoons$ CH^+ + OH^-).

It is evident that a single indicator substance, regardless of its electrical inertness, could not be used throughout the pH range 0—14. For pH 0—7, phenolphthalein, ($pK = 9.5$) can be used; for pH 7—14, pyrrolidine ($pK = 2.9$) can be used. After electrophoresis, the wet acidic paper strips are exposed to ammonia vapour to make the phenolphthalein zone visible; the dried alkaline strips are simply heated to reveal the pyrrolidine zone (brownish spot).

The results of electroosmotic mobilities in Munktel 302 paper at 25°C and ionic strength 0.1 in the pH range 0.7—12.9 are given in Fig. 3. It is

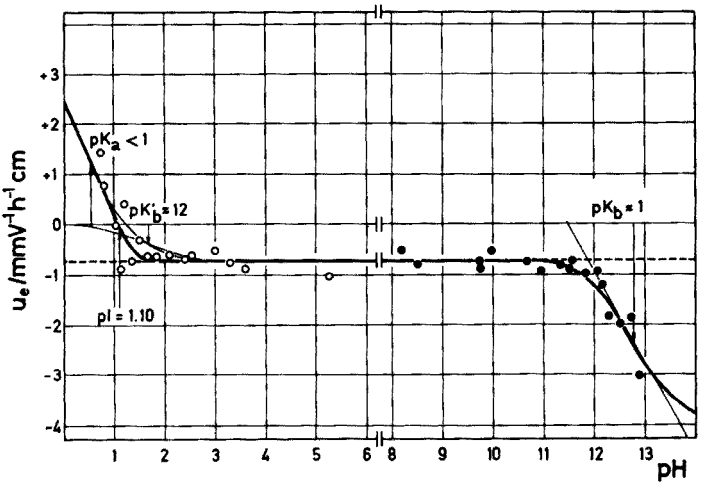

Fig. 3. Dependence of electroosmotic mobility on pH for Munktel 302 filter paper at 25 °C and ionic strength 0.1. Open dots indicate the results obtained with phenolphthalein; full dots represent the results obtained with pyrrolidine indicator. The full curve may serve to correct electrophoretic mobilities with respect to electroosmotic mobility $u_e = K^2 u'_e$ mm V^{-1} h^{-1} cm in Munktel 302 filter paper. Apart from the isoelectric point (pH 1.10) two dissociable acid groups are evident (dissociation constants pK_b at about 12 and 1); one dissociable basic group is evident (pK_a < 1). The horizontal dotted line represents false results obtained with glucose as indicator.

evident that cellulose is dissociated at all pH values except at the isoelectric point, pH 1.10. Two dissociable acidic groups (dissociation constants pK_b at ca. 12 and 1) and one dissociable basic group (pK_a < 1) are evident. The theoretical treatment and results for the dissociation constants of filter paper cellulose will be discussed elsewhere. The full line in Fig. 3 may serve as a dependable correction of electrophoretic mobilities with respect to electroosmotic mobility $u_e = K^2 u'_e$ mm V^{-1} h^{-1} cm in filter paper cellulose over the range pH 0—14 at 25 °C and for ionic strength 0.1. The chromatographic adsorption factor on filter paper cellulose R_{Fe} for both indicator substances was 1.0.

DISCUSSION

The relative values of the correction factor K, inserted into eqn. 1, give correct values of electrophoretic mobilities in free solution for a constant specific electric effect UI V A cm^{-2}. The resulting mobilities refer to the actual temperature of the thermostated cooling liquid regardless of the temperature of the cooling liquid at which the relative value of K had been established. The absolute value of K (and not the relative value) is a direct measure of the texture or porosity of the support and can be used to characterize the texture of papers, textiles, membranes, gels, etc. When inserted into eqn. 1 the absolute value of K gives correct values of electrophoretic mobilities in

free solution for any reasonable specific electric effect. The resulting electrophoretic mobilities refer to a temperature higher than that of the thermostated cooling liquid. Diagrams giving the temperature difference (Δt) as a function of the specific electric effect can be constructed for any purpose in a similar way to Fig. 2.

Care should be taken in determining electroosmotic mobilities in a porous support, especially in the choice of an appropriate indicator. Instead of glucose or dextran, phenolphthalein (for values up to pH 7) and pyrrolidine (for higher pH values) were found to be appropriate indicators. Glucose may only be used in the pH range 2—11.

REFERENCES

1 H. Michl, Monatsh. Chem., 82 (1951) 489.
2 H. G. Kunkel and A. Tiselius, J. Gen. Physiol., 35 (1951) 89.
3 Z. Pučar, Anal. Chim. Acta, 17 (1957) 476.
4 Z. Pučar, Anal. Chim. Acta, 17 (1957) 485.
5 Z. Pučar, Anal. Chim. Acta, 18 (1958) 290.
6 Z. Pučar and Z. Jakovac, J. Chromatogr., 2 (1959) 320.
7 H. Bilinski, B. Pokrić and Z. Pučar, J. Inorg. Nucl. Chem., 33 (1971) 3409.
8 Z. Pučar, Thalassia Jugosl., 7 (1971) 639.
9 Lj. Marazović and Z. Pučar, Rapp. Comm. Int. Mer Médit., 20 (1972) 701.
10 Lj. Musani-Marazović and Z. Pučar, Thalassia Jugosl., 9 (1973) 101.
11 B. Pokrić and Z. Pučar, Anal. Chem., 47 (1975) 1970.
12 M. Ishikawa and Z. Pučar, J. Radioanal. Chem., 11 (1972) 197.
13 Z. Knicwald and Z. Pučar, J. Chem. Soc. Faraday Trans. 1, 72 (1976) 987.
14 B. Pokrić and Z. Pučar, J. Inorg. Nucl. Chem., 33 (1971) 445.
15 B. Pokrić and Z. Pučar, J. Inorg. Nucl. Chem., 35 (1973) 1987.
16 B. Pokrić and Z. Pučar, J. Inorg. Nucl. Chem., 35 (1973) 3287.

Analytica Chimica Acta, 91 (1977) 259—266

DETERMINATION OF CHLOROPHENOXY ACID HERBICIDES BY DENSITOMETRY ON THIN LAYER CHROMATOGRAMS

JOSEPH SHERMA and JOHN KOROPCHACK*

Chemistry Department, Lafayette College, Easton, Pa. 18042 (U.S.A.)

(Received 11th October 1976)

SUMMARY

A quantitative in situ t.l.c. method for the determination of chlorophenoxy acid herbicides and their salts in waters is described. The detection limit (1 ppb) is similar to that obtainable by gas chromatography, but no derivatization is needed. Silica gel G plates are pre-impregnated with a sensitized silver nitrate reagent, and the spots are scanned with a densitometer after u.v. irradiation. Linear calibration graphs were obtained in the range 100—1000 ng for most of the herbicides studied. Preliminary cleanup methods are discussed.

2,4-Dichlorophenoxyacetic acid (2,4-D) and related phenoxy acids and their salts are widely used as herbicides for control of broadleaf weeds in cereal crops, sugar cane, turf, pastures, lawns, and other non-crop land; aquatic weeds; brushes; and woody plants [1, 2]. These acids are also applied for the prevention of preharvest fruit drop, the production of seedless fruit, and regulation of plant growth [3].

Rapid, sensitive, and reliable methods are required for the determination of these herbicides in water supplies. The major method for this purpose is a gas chromatographic procedure requiring methylation of the free acids before chromatography [4]. With one exception, all t.l.c. methods for chlorophenoxy acids reported so far [e.g., 5, 6] have been only roughly quantitative, relying on visual comparison of sample and standard zones; one procedure involves scraping, elution from the adsorbent, and photometry after treatment with chromotropic acid [7].

The standard visual comparison t.l.c. procedures have been worked out for food and crop samples [8, 9], although papers on the examination of water samples have appeared [10—12]. This paper reports a quantitative, in situ t.l.c. method for the determination of the herbicide acids and salts in water samples as an alternative to gas chromatography. It does not require derivatization and has a sensitivity level (1 ppb) comparable with g.l.c. and adequate for environmental monitoring of agricultural, marine, and potable water supplies.

*Present address: Chemistry Department, University of Georgia, Athens, GA 30602 (U.S.A.).

EXPERIMENTAL

Materials

The herbicides studied were 2,4-D and its methyl and butyl esters, 2-(2,4,5-trichlorophenoxy)propionic acid (silvex) and its methyl and isooctyl esters, (2,4,5-trichlorophenoxy) acetic acid (2,4,5-T) and its methyl ester, and [(4-chloro-*o*-tolyl)oxy] acetic acid (MCPA). Stock solutions (1 mg ml^{-1}) were prepared in isooctane (for the esters) or in diethyl ether—hexane (60:40 v/v) (for the acids). Quantitative dilutions were made to yield a solution of each pesticide (100 ng μl^{-1}) for spotting with Drummond microcap pipettes, and a series of standards of each pesticide ranging from 50 ng ml^{-1} to 500 ng ml^{-1} for use with the Kontes automatic spotter. Pesticide-grade solvents were used in all cases, and solutions were refrigerated when not in use.

Preparation of t.l.c. plates

Several brands and types of pre-coated thin layer plates were tested; Analtech Uniplate silica gel G layers (20 × 20 cm) were chosen for use. Plates were pre-impregnated with silver nitrate detection reagent by dipping in a metal Thomas—Mitchell dip tank (A. H. Thomas Co.). The reagent was made by pipetting 8 ml of silver nitrate solution (20 g per 100 ml of distilled water, stored in a dark bottle) into 200 ml of acetone; 20 ml of distilled water, 12 ml of concentrated ammonia liquor, and 16 drops of 2-phenoxyethanol were added with mixing. The phenoxyethanol sensitizes the silver nitrate and retards darkening of the background. Plates were dipped in the reagent for 30 s, drained, and dried in a hood in the absence of direct light for 30 min. Impregnated plates were stored in the dark and used within 24 h. The dip tank should be rinsed out immediately after use.

Procedures

For preliminary studies of the separations, detection, and calibration curves, solutions were spotted with 1-μl microcap pipettes. In multiple applications to the same origin, each application was allowed to dry individually. Sample extracts and standards for comparison were spotted by pipetting volumes (2 ml) into the tubes of a Kontes automatic spotting device, as designed by Getz [13]. Spotting should be carried out, wherever possible, in the absence of light.

Spotted plates were developed in paper-lined, saturated, rectangular N-tanks covered with aluminium foil to protect the impregnated layer from light. Of the various solvent systems tested (Table 1), hexane—glacial acetic acid—ethyl ether (72:30:18, v/v) was the most satisfactory.

After development, the layer was dried in a dark hood for 5 min and then exposed to ultraviolet light from a Hanovia 679A 176W germicidal lamp for 30 min in a hood to exhaust ozone. The lamp was warmed-up for 30 min prior to use and was set at 4 A after warm-up. When positioned

25 cm below the lamp, the layer received a uniform exposure of u.v. radiation. Black pesticide spots against a light grey or tan background appeared after 3 to 4 min and reached maximum contrast with the background after about 30 min.

The spots were scanned with a Kontes Chromaflex fiber optics densitometer in the double-beam, visible (reflection) mode with no filter over the light source. A Bausch and Lomb recorder Model VOM 6 set at 0.025 V was connected to the densitometer. The layer was covered with a clean glass cover plate, and the plate was inserted into the densitometer with the spots facing upward. The glass backing the layer was also thoroughly cleaned. The scan speed was 10 cm min^{-1}, and the direction of scan for each spot was parallel to the direction of solvent development. The use of the Kontes densitometer has been detailed [14, 15].

Each pesticide spot was scanned in the direction of solvent flow and reverse directions, and the calculated areas were averaged. Calculations were based on the product of the peak height and the width at half height. The average area multiplied by the attenuation setting of the scanner was plotted vs. ng per spot to obtain calibration curves. To correct for slight day-to-day variation in these curves, three bracketing standards were chromatographed on each plate along with the water extract samples. The amount (ng) of pesticide in the samples was interpolated from the calibration line constructed from these standards.

The following procedures were used to extract the pesticides from fortified samples and cleanup (purify) the extracts prior to spotting. Pesticide-grade solvents were used in all cases.

Natural water samples (500 ml) not requiring cleanup were placed in a 1-l separatory funnel, the pH was adjusted (pH paper) to pH 2 with concentrated sulfuric acid, and extraction of acids and esters was carried out with 3 × 50 ml portions of benzene, shaking for 2 min each time. The organic phases were combined in a 250-ml beaker, and 7 g of sodium sulfate were added to remove traces of water. The sodium sulfate was pre-extracted with 3 × 15 ml of benzene and then dried before use. The benzene extract was filtered through a sintered glass funnel, washing the sodium sulfate in the beaker with 20 ml of benzene. The filtrate was collected in a 100-ml beaker and evaporated almost to dryness over a hot plate at ca. 60°C, or a rotary evaporator was used after transfer to a round bottom flask. The evaporation container was rinsed with several small portions of benzene, which were transferred by pipette to a tube of the Kontes automatic spotter. The total solvent used for rinsing was ca. 2 ml. Appropriate standards were pipetted into adjacent tubes. For example, a sample fortified at 1 ppb would contain 500 ng in the 500-ml sample. Standards containing 150, 250, and 350 ng ml^{-1} would therefore be used (2 ml of each).

Tap water, and other samples too contaminated for the direct procedure, were extracted and the extract cleaned up by solvent partitioning. The above directions were followed until the three 50-ml extracts were combined,

and then this solution was shaken with 35 ml of ethanol plus 50 ml of 4% aqueous $NaHCO_3$ solution for 2 min. After separation, the aqueous layer was drained off and saved, and the organic layer was extracted twice more with 15 ml of ethanol plus 40 ml of 4% $NaHCO_3$. The aqueous phases, now containing the salts, were combined and extracted further with 2 × 25-ml portions of benzene. All benzene solutions were discarded unless esters were to be determined, in which case they were combined and treated as in the next paragraph. The aqueous solution was acidified with 25 ml of 10% sulfuric acid, and the pesticides, again in their free acid form, were extracted with 3 × 50-ml portions of benzene. The combined benzene layers were dried over sodium sulfate, filtered and concentrated; samples and standards were spotted for t.l.c. as described above.

For esters, the combined benzene extracts of the original water sample plus the hydrogencarbonate solutions (above) were dried over sodium sulfate, filtered, and evaporated just to dryness. A 25-ml portion of isooctane—hexane (1:1, v/v) was added, and this solution was extracted in a 125-ml separatory funnel with 3 × 25-ml portions of 80% acetonitrile in water. The combined acetonitrile phases were placed in a 1-l separatory funnel with 75 ml of water, 30 g of sodium chloride, and 80 ml of isooctane—hexane (1:1, v/v), and shaken vigorously for 2 min. The salt and water were pre-extracted with pesticide grade benzene, and the salt was dried in an oven before use. The organic phase was drained off, washed with 100 ml of water, and dried over sodium sulfate. The solution was filtered, evaporated to dryness, and the residue was transferrred into a tube of the Kontes spotter with ca. 2 ml of benzene. These solvent-partition cleanup procedures for acids and esters are modifications of methods [16] for animal tissues, dairy products, and oils.

RESULTS AND DISCUSSION

Several chromogenic reagents and different methods for application of silver nitrate were studied before the optimum procedure detailed in the last section was selected. Rhodamine B [17] and bromocresol green [6] spray reagents lacked the required sensitivity. A 1% solution of the leuco base of malachite green [*p,p'*-benzylidenebis-(*N,N*-dimethylaniline)] in benzene, used by Getz [18] for the detection of chlorinated insecticides, was applied as a spray after development and drying of the layer. Blue spots on a light blue background appeared after exposure to short wave u.v. light, but the contrast was poor even for spots containing as much as 500 ng of pesticide. Upon standing, the spots eventually faded and became white. Spray application of silver nitrate reagents after plate development gave less uniform detection than dipping, and dip application of the reagent after development was not as successful as pre-impregnation by dipping. Other possible formulations of the reagent contain different concentrations of silver nitrate, ammonia, or phenoxyethanol; or have no ammonia; or also

contain dichlorofluorescein and hydroquinone [19]. These formulations gave weaker spots or backgrounds which darkened more readily, or required very long irradiation times to produce the spots. A lamp (type C-81 in Chromato-Vue model C-5 viewing box) emitting only 254 nm radiation required a longer irradiation time than the germicidal lamp but gave a somewhat whiter background. The dip time (30 s) was selected after evaluating scan areas for a series of concentrations of 2,4-D butyl ester. For example, an increase in dip time from 5 to 30 s produced a calibration curve (peak area vs. ng of pesticide) with a slope 2.6 times as great.

Uniplate silica gel G layers in combination with the silver nitrate reagent described earlier and irradiation with the germicidal lamp gave the best overall results in terms of sensitivity and speed. Baker-flex alumina 1B foils provided a light background and good sensitivity when the 254 nm source was used for irradiation, but, as mentioned before, the irradiation time was excessive. Quantum Q-5 and Q-3 layers and Baker silica gel 1B foils did not give good results. A few runs with Quantum Q-4 layers indicated that these were equivalent to Uniplates.

A time study was carried out on a developed 500 ng spot of 2,4-D butyl ester to determine the optimum time of irradiation with the germicidal lamp. A Uniplate chromatogram was irradiated repeatedly for periods of 5 min up to a total of 45 min, with scanning after each exposure. Maximum sensitivity (peak area) was obtained after about 20 min, but an additional 10-min exposure gave a more even baseline without significant reduction in sensitivity. Exposure for 30 min was therefore used for all analyses.

Hexane—glacial acetic acid—ethyl ether (72:30:18, v/v) was the best general solvent in terms of spot size, intensity, and R_F values for the herbicides studied. Most solvents provided adequate migration of the esters, but solvents without acetic acid did not move the acids far enough and caused spots which were either extremely dark and compact, weak and streaked, or not detected at all. R_F values between 0.3 and 0.7 are optimum for accurate quantification by densitometry [20]. As the acetic acid concentration was increased, the intensity and size of the acid spots increased, while increases in ether concentration increased the R_F values of acids and ethers. The solvent chosen caused two secondary fronts on the chromatogram which did not affect the scans of the herbicide spots. These fronts, especially the top one, became more prominent several hours after u.v. irradiation. The background was light grey below the first front ($R_F \simeq 0.35$) and tan above. The background color of the layer was lighter in color when hexane was used as the non-polar solvent of the mixture in place of cyclohexane or benzene. Table 1 shows R_F values in selected chromatographic systems. Confirmation of the identity of unknown herbicides detected in samples can be made by co-chromatography of purified extracts with known standards in a number of different solvent systems providing diverse R_F values.

All mode options available on the Kontes densitometer were evaluated, including combinations of double beam and single, with the reference

TABLE 1

R_F Values of herbicide acids and esters in different chromatographic systems

Compound	$R_F \times 100$									
	Systems[a]									
	1	2	3	4	5	6	7	8	9	10
2,4-D		1	52	23	25	15	54	3	5	9
2,4,5-T		1	57	27	29	17	62	3	5	10
MCPA			58	31	32	21	61		9	
Silvex			63	35	39	30	68		18	3
Silvex methyl ester	30	36						53		
Silvex isooctyl ester	44	42						66		
2,4-D methyl ester	15	20	78	61	45	38	67	39	78	80
2,4-D butyl ester			84	72	62	49	82		81	81
2,4-5-T methyl ester	71	22						41		

[a]Silica gel layer. 1. Hexane saturated with acetonitrile. 2. Cyclohexane—glacial acetic acid (9:1, v/v). 3. Benzene—glacial acetic acid—acetone (8:1:2). 4. Benzene—glacial acetic acid—chloroform (8:1:1). 5. Hexane—glacial acetic acid—acetone (8:1:1). 6. Hexane—glacial acetic acid—ether (8:1:1). 7. Hexane—glacial acetic acid—ether (72:30:18). Alumina layer. 8. Cyclohexane—glacial acetic acid (9:1). 9. Benzene—glacial acetic acid (9:1). 10. Benzene—glacial acetic acid—ethanol (8:1:1).

or read head, visible reflection source, short wave u.v. transmission source, and long wave u.v. transmission source. Different colored filters were also tested for the sources; they had no advantage. The long wave u.v. source was the most sensitive, as is often the case when colored spots are scanned with this instrument [15], because of its strong emission of visible wavelengths as well as ultraviolet. The visible mode was chosen, however, because of the smoother baselines of the resulting scans of the spots on the plates. The smaller reference light beam, which potentially can increase sensitivity, could not be used to scan in either the double or single beam modes because many spots were wider than the 1-cm length of this beam.

All compounds gave very similar calibration curves which differed only slightly in slope and intercept from one plate to another. The average values calculated by regression analysis for four different compounds, each run in duplicate between 100 and 1000 ng, were slope = 0.079, y-intercept = 7.56, and degree of linearity = 0.994. As a precaution against variation in results, standards were chromatographed on the same plate with samples as described earlier. The reproducibility of the procedure was indicated by applying six spots containing 500 ng each of MCPA with the automatic spotter to the same layer, and scanning the spots after solvent development and detection. The relative standard deviation (s_r) of the peak areas was 5.3%. When the experiment was repeated on three different plates (total of 18 spots), the s_r value was 7.8%.

To demonstrate the effectiveness of the proposed quantitative methods, various water samples were fortified to 1 ng ml^{-1} with different herbicides, and recoveries were determined. River and lake water samples collected in the Easton, Pa. area were fortified with 2,4-D and carried through the direct, non-cleanup procedure. Interferences were not encountered on the chromatogram in the region of the herbicide spot; recoveries for duplicate samples were 97.5 and 102% (river water) and 98.9 and 100.5% (lake water). Attempts to determine herbicides in Easton, Pa. tap water without cleanup of extracts were unsuccessful, as the chromatogram contained large streaks of contamination from the origin to the solvent front. However, any type of water might be analyzed without cleanup if the herbicide level is high enough (e.g. 50—100 ppb), in which case a 50—100 times smaller sample can be taken, which will contribute proportionately less interfering material in the extract. However, some natural water samples required partition cleanup to remove extraneous streaked zones. Recoveries from tap water fortified with silvex at 1 ppb and carried through the extraction and partition cleanup procedure described for acids were 93.4 and 98.0% for duplicate samples. Two other faint zones above silvex plus a residue at the origin appeared in the chromatogram of the sample but were well resolved and did not interfere with quantification. Tap water was also fortified with 1 ppb of the butyl ester of 2,4-D and analyzed by the procedure described for esters. The chromatogram contained two spots below and one above the herbicide, but again the scan was not affected. Recoveries from duplicate samples were 75.1 and 77.8%.

The purpose of this study was to develop a primary quantitative method, for herbicide acids and esters in water, based on thin-layer chromatography with densitometry. Great effort was not expended to optimize the extraction and isolation steps, which were adapted from previously described, standard procedures, to demonstrate the efficacy of densitometry on actual samples. Other substrates (e.g. foods or soils) could be analyzed for residues of the herbicides if appropriate extraction and cleanup steps were included; qualitative t.l.c. procedures [8, 9] with silver nitrate—u.v. detection can be made quantitative in this way. Herbicides should be extracted from the sample with the least polar solvent providing complete recovery so that co-extraction of polar impurities is kept to a minimum. If direct spotting of the concentrated extract does not provide a sufficiently clean chromatogram, solvent partitioning is the first stage of cleanup recommended. If the herbicide of interest is still not resolved, a different t.l.c. solvent system or further cleanup e.g. by chromatography on conventional silica gel [21] or the new, re-useable SI-200 macroporous silica gel [22] is needed. Prior experience indicates that the esters will probably be eluted from a column of the latter adsorbent with the fraction containing a low to moderate percentage of acetone in hexane, while free acids will require a solvent with a high percentage of acetone or some methanol. Since the water samples used did not require column cleanup, elution patterns of the herbicides were

not investigated. Once a sufficiently pure extract has been prepared, by whatever means, densitometry can be used as a sensitive, reproducible, simple, and reliable method for residue quantification.

REFERENCES

1 Herbicide Handbook of the Weed Science Society of America, 3rd edn., 1974.
2 Home and Garden Bulletin No. 51, United States Department of Agriculture, Washington, D.C., 1975, pp. 14—18.
3 R. P. Marquardt, H. P. Burchfield, E. E. Storrs and A. Bevenue, in G. Zweig (Ed.), Analytical Methods for Pesticides and Plant Growth Regulators, Vol. IV, Academic Press, N.Y., 1964, Ch. 11, p. 95.
4 J. M. Devine and G. Zweig, J. Assoc. Off. Anal. Chem., 15 (1969) 187.
5 H. Thielemann, Z. Anal. Chem., 272 (1974) 286.
6 H. Thielemann, Z. Chem., 13 (1973) 226.
7 K. Erne, Acta Vet. Scand., 7 (1966) 77.
8 Methylated Chlorophenoxy Acids, in Pesticide Analytical Manual, United States Food and Drug Administration. Sect. 421, July 1, 1969.
9 Free Chlorophenoxy Acids, in Pesticide Analytical Manual, United States Food and Drug Administration, Sect. 422, July 1, 1969.
10 T. Bogacka and R. Taylor, Chem. Anal. (Warsaw), 15 (1970) 143.
11 H. Zawadzka, H. Elbanowska and M. Adamczewska, Chem. Anal. (Warsaw), 18 (1973) 943.
12 V. D. Chmil, Gig. Sanit., (4), 66 (1976).
13 M. E. Getz, J. Assoc. Off. Anal. Chem., 54 (1971) 982.
14 J. Sherma and G. Marzoni, Am. Lab., October, 1974, p. 21.
15 J. Sherma and L. Dorflinger, Am. Lab., January, 1976, p. 63.
16 General Method for Chlorophenoxy Acids in Fatty Foods, in Pesticide Analytical Manual, United States Food and Drug Administration, Sect. 221.13b, 221.14, and 221.16a, January 1, 1968.
17 H. Thielemann, Z. Anal. Chem., 262 (1972) 192.
18 M. E. Getz, private communication.
19 N. V. Fehringer and J. D. Ogger, J. Chromatogr., 25 (1966) 95.
20 J. C. Touchstone, S. S. Levin and T. Murawec, in J. C. Touchstone (Ed.), Quantitative Thin Layer Chromatography, Wiley-Interscience, N.Y., 1973, Ch. 1.
21 J. Sherma and T. M. Shafik, Arch. Environ. Contam. Toxicol., 3 (1975) 55.
22 M. E. Getz, Talanta, 22 (1975) 935.

Analytica Chimica Acta, 91 (1977) 267—272

ISOTOPIC COMPOSITION MEASUREMENT ON SUB-PICOGRAM AMOUNTS OF PLUTONIUM

R. S. STREBIN, JR. and D. M. ROBERTSON

Battelle, Pacific Northwest Laboratories, Richland, Washington 99352 (U.S.A.)

(Received 15th November 1976)

SUMMARY

Thermal ionization mass spectrometry is a sensitive means of measuring plutonium isotopic composition. Spectral background and chemical interaction of the sample solution with the ionizing filament cause loss of sensitivity when the plutonium sample is in the picogram range. Techniques for background evaluation and reduction and for sample purification are presented. A method incorporating these developments is demonstrated to yield reliable isotopic composition measurements on sub-picogram amounts of plutonium.

Plutonium in the environment is of concern as a potential hazard to man even though it occurs in very low to trace concentrations. Both total concentration and isotopic composition are required in ecological research and in assessment and control of hazards. Determination of concentration and composition at trace concentrations requires chemical separation of the plutonium, usually from large samples. As much as 5-kg samples [1] have been used to obtain composition measurement.

Thermal ionization mass spectrometry is a sensitive measurement method for plutonium [2]. However, the spectrometer ionizing filament is very sensitive to impurity. Thus spectral backgrounds arising from contaminants in the filament or its immediate environment, and chemical interaction of sample solution containing the separated plutonium and traces of process contaminants, operate to reduce measurement sensitivity.

Techniques for evaluation and reduction of spectral background and for sample purification more compatible with the ionizing filament are presented in this paper.

EXPERIMENTAL

Equipment and reagents

Equipment included a three-stage thermal ionization mass spectrometer [3] with an ion-electron-scintillation converter for ion detection; a vacuum chamber for heating and carburizing spectrometer filaments; and a 2Π alpha proportional counter.

A hydrochloric acid solution of ^{239}Pu isotopic spike (99.978 atom-% ^{239}Pu;

Oak Ridge National Laboratory, Isotopes Division) and a hydrochloric acid solution of National Bureau of Standards plutonium isotopic standard (NBS-948) were used. Other chemicals were ACS reagent grade.

Spectral background

A technique utilizing plutonium isotopically enriched to 99.978 atom-% ^{239}Pu was employed to evaluate spectral background in the plutonium mass region (masses 239, 240, 241, and 242). The term, background, refers to ions that are produced by the filament from materials other than plutonium but that have the appropriate mass/charge ratio to be collected at plutonium mass positions.

The spectral background varies with changes in spectrometer operating conditions. The background of concern is the one that occurs when operating conditions are adjusted to maximize plutonium ion collection. Thus background tests are performed by placing plutonium on the filament, adjusting the spectrometer to optimum conditions and measuring backgrounds at the plutonium minor isotope mass positions where the effect of background is the most significant. Use of a plutonium source with little if any of the minor isotopes clearly permits a more accurate determination of background levels at minor isotope positions. The 99.978 atom-% ^{239}Pu plutonium source provided an excellent means for making the background measurements.

With that source, the background in the plutonium mass region was found to exhibit a typical hydrocarbon pattern. Additional tests with the ^{239}Pu spike in different solution matrices showed no alteration in background pattern. From these experimental observations and the observations of others [4] that carburization often produces a hydrocarbon background, it was concluded that the background resulted from the carburization of filaments. Consequently, filament treatments were sought to minimize the background.

A vacuum test-bench was built to permit high temperature and carburizing treatment of filaments. Experiments were carried out with benzene vapor [5] as a carburizing agent. It was noted that as carbon was dissolved in the rhenium [6], the electrical resistance of the filament increased and that by removing the benzene vapor and increasing the temperature the effect was reversed, i.e. carbon was removed. At the plutonium thermal ionization temperature of (nominally) 1700°C, the background could be removed by sustained heating but only after the carburization was significantly depleted. That is, removing the background depleted the carburization to such an extent that the filament produced only plutonium oxide ions and not metal ions [7]. By heating briefly after carburization at around 2000°C, however, the background depleted rapidly while sufficient carburization was maintained to allow production of metal ions. From these observations a procedure was developed which produced filaments with a background of less than one ion-count per second per mass position. These low-background filaments were produced by carburizing with benzene until the rate of resistance-increase slowed, taking the filament briefly to a higher temperature, and then immediately removing the filament from the

carburizing chamber. These three steps apparently accomplish the dissolving of carbon into the rhenium, removal of background-contributing absorbed organics, and prevention of significant re-absorption or adsorption of organics.

Because of differences in measurement systems a signal-to-background ratio may be more meaningful than a measured background rate in units of ion-counts per second (cps) per mass position. To put this background into perspective, an example of measurement of fallout plutonium in soil is given. Nominal values of 0.04 dpm ^{239}Pu per g and a ^{242}Pu/^{239}Pu ratio of 0.004 have been reported [8] for fallout in soil. Of the $3 \cdot 10^6$ atoms of ^{242}Pu in 1 g of soil, we would expect to collect 1500 ^{242}Pu ions over a 70-s collection period. A background of 1 cps per mass position would add 70 counts to the ^{242}Pu measurement which would thus produce about a 5% positive bias in measurement of the least abundant isotope, ^{242}Pu.

Sample purification and concentration

The sample solution to be placed on the filament must have high purity to reduce the chemical effects of the solution on the filament. For highest sensitivity, some final purification of separated plutonium will usually be needed. The mass spectrometer "V-type" filament [9] holds about 0.3 μl. The loading time becomes unreasonably long unless the sample volume to be loaded is reduced to a few μl. Thus both stringent purification and concentration measures are required. Ion exchange was the technique chosen to meet those requirements.

Ion exchange of plutonium(IV) provides an excellent purification from a very wide range of materials [10] and ion-exchange processes can be successfully miniaturized [11]. With this technique (miniaturized ion exchange) both purification and concentration requirements were achieved simultaneously. A general description of the ion-exchange purification and filament loading procedure is presented below.

Procedure. Adjust solution containing the separated sample plutonium to 2 M nitric acid and convert the plutonium to the tetravalent state with sodium nitrite. Adjust the HNO_3 concentration to 8 M and place the sample on a bed (0.2-cm diam., 6 cm high) of 100-200 mesh AG 1-X4 anion-exchange resin. Wash the resin bed with 3 ml of 8 M HNO_3 to remove almost all impurities; the uranium elution peak occurs at 0.5 ml of the 8 M HNO_3 wash. Then wash with 11 M HCl to remove thorium and to convert to a chloride system, more compatible with the rhenium filament [12]. Elute the plutonium with 100-μl aliquots of 1.2 M HCl. Nominally 95% of the plutonium is collected in a 200-μl fraction of eluate from the second and third 100-μl eluting aliquots.

Collect the 200 μl of eluate on a 1.5-cm diameter teflon disk and evaporate to 2—3 μl. The solution does not wet the disk and remains in a well-confined bead during evaporation. Use a fine drawn polyethylene pipet to transfer the sample from the disk to the filament. Add the sample solution in 0.3-μl aliquots and dry with a heat lamp between additions.

RESULTS AND DISCUSSION

The techniques which were developed for preparation of low-background filaments and for purification and concentration of the plutonium-containing solution were incorporated into a method for determination of isotopic composition of sub-picogram amounts of plutonium.

The method was tested with the 99.978% ^{239}Pu spike to show clearly the background in the minor isotope positions. Those data are presented in Table 1. A precise determination of the isotopic composition of the spike was accomplished by analyzing $^{239}PuO_2$ particles (the form supplied) that were directly loaded onto filaments. The average values of four particle analyses are listed in Table 1 as the true values and are in good agreement with the composition supplied with the spike material. An HCl solution of spike was prepared for tests 2—7 and was assayed for plutonium concentration by 2Π alpha proportional counting. Six equal aliquots of spike (0.43 pg per aliquot) were used. Three were loaded directly on filaments (tests 2—4) and three were processed as samples and then loaded on filaments (tests 5—7). Comparison of the measured minor isotopic (240, 241, and 242) compositions among tests 1—4 shows that less than 0.005 atom-% bias resulted from background. In tests 5—7, more representative of sample conditions, the sum of the ^{241}Pu and ^{242}Pu biases had an upper limit of <0.009 atom-%. Since the sum of ^{241}Pu and ^{242}Pu isotopic concentration in bomb debris fallout is about 0.9 atom-% and from nuclear reactors at least 0.4%, the tests show that the method described is clearly capable of revealing such compositional differences.

Additional tests of the method were made on a solution of plutonium

TABLE 1

Measured isotopic composition of ^{239}Pu at the sub-picogram level

Test No.	Isotopic Composition (atom-%)			
	239	240	241	242
"True" value[a]				
1	99.97975 ± 0.00016	0.01965 ± 0.00017	0.00018 ± 0.00002	0.00035 ± 0.000(
$0.43 \cdot 10^{-12}$ g of Spike direct-load				
2	99.9763 ± 0.0017	0.0212 ± 0.0016	0.0018 ± 0.0005	0.0006 ± 0.000:
3	99.9760 ± 0.0032	0.0184 ± 0.0026	0.0035 ± 0.0013	0.0020 ± 0.001:
4	99.9714 ± 0.0020	0.0235 ± 0.0018	0.0044 ± 0.0009	0.0007 ± 0.000:
$0.43 \cdot 10^{-12}$ g of Spike processed as sample				
5	99.9629 ± 0.0066	0.0282 ± 0.0054	0.0070 ± 0.0033	0.0018 ± 0.002:
6	99.9624 ± 0.0062	0.0291 ± 0.0055	0.0009 ± 0.0009	0.0075 ± 0.002:
7	99.9715 ± 0.0051	0.0234 ± 0.0048	0.0011 ± 0.0012	0.0040 ± 0.001(

[a] Average of 4 massive loads of spike.

TABLE 2

Measured isotopic composition of NBS-948 plutonium at the sub-picogram level

Test No.	Isotopic composition (atom-%)			
	239	240	241	242
NBS Certificate values[a]				
	91.648 ± 0.010	7.925 ± 0.010	0.394 ± 0.002	0.0331 ± 0.0003
Measured values from massive loads				
1	91.663 ± 0.011	7.911 ± 0.010	0.393 ± 0.002	0.0331 ± 0.0004
$0.38 \cdot 10^{-12}$ g of Spike direct-load				
2	91.6073 ± 0.0341	7.9582 ± 0.0312	0.3983 ± 0.0053	0.0362 ± 0.0016
3	91.6555 ± 0.0318	7.9184 ± 0.0314	0.3946 ± 0.0060	0.0314 ± 0.0018
4	91.6599 ± 0.0312	7.9059 ± 0.0309	0.3978 ± 0.0053	0.0364 ± 0.0016
$0.38 \cdot 10^{-12}$ g of Spike processed as sample				
5	91.7290 ± 0.0840	7.8224 ± 0.0832	0.4034 ± 0.0148	0.0452 ± 0.0046
6	91.7616 ± 0.1129	7.7847 ± 0.1089	0.4103 ± 0.0339	0.0434 ± 0.0060
7	91.6843 ± 0.952	7.8840 ± 0.0943	0.3946 ± 0.0168	0.0363 ± 0.0044

[a]These values are corrected for decay to 1st April 1976 from listed certificate values. Error is measurement error, and does not include uncertainty in calculation constants.

standard, NBS-948. Those data (Table 2) show the analysis perturbations on a representative plutonium isotopic composition. The NBS certificate isotopic composition values and an average of massive load analyses are listed in Table 2 for comparison with sub-picogram test results. Tests 2—7 were conducted in the same way as the previous ^{239}Pu tests. The direct-load tests, 2—4, show no significant bias. In tests 5—7 the low abundance isotopes, ^{241}Pu and ^{242}Pu, clearly show a positive bias. The larger uncertainties associated with the measured isotopic values of processed aliquots (tests 5—7) as compared to directly loaded aliquots (tests 2—4) reflect processing losses and thus fewer ions collected.

The test data of Tables 1 and 2 show that background is reduced to a level that would not interfere with the characterization of the isotopic composition of plutonium deposited in the environment from various sources. The chemical purification step yields a solution that permits isotopic composition measurements at sub-picogram levels with only a few percent bias at minor isotope abundance of about 0.4%.

This paper is based on work performed under U.S. Energy Research and Development Administration, Contract EY-76-C-06-1830.

REFERENCES

1 E. Hardy, Plutonium in Soil Northeast of the Nevada Test Site, Health Safety Lab. Q. Summ. Rep. HASL-306, (1976) I-51.
2 R. J. Dupzyk, R. D. Carver, and I. A. Dupzyk, Isotopic Analysis of Plutonium in Environmental Samples by Isotope Dilution Mass Spectrometry, Reference Methods for Marine Radioactivity Studies, International Atomic Energy Agency, Vienna, (1975) 87.
3 C. R. Lagergren and J. J. Stoffels, Int. J. Mass Spectrom. Ion Phys., 3 (1970) 429.
4 N. C. Fenner, J. Sci. Instrum., 41 (1964) 48.
5 M. H. Studier, J. Phys. Chem., 66(1962) 133.
6 J. E. Hughes, J. Less-Common Met., 1 (1959) 377.
7 A. N. Vol'skii and Ya. M. Sterlin, The Metallurgy of Plutonium, Israel Program for Scientific Translations, (1970) 61.
8 P. W. Krey and B. T. Krajewski, Plutonium Isotopic Ratios at Rocky Flats Plant, Health Safety Lab. Q. Summ. Rep., HASL 249, (1972) I-72.
9 J. A. McHugh, Int. J. Mass Spectrom. Ion Phys., 3 (1969) 267.
10 G. H. Coleman, The Radiochemistry of Plutonium, National Academy of Sciences, Nuclear Science Series, NAS-NS 3058, (1965) 92.
11 Fouad Tera and G. J. Wasserburg, Anal. Chem., 47 (1975) 2214.
12 K. B. Lebedev, Rhenium, Joint Publications Research Service, Washington, D.C., JPRS 23, 361, 1964, p. 7.

Analytica Chimica Acta, 91 (1977) 273—279

DETERMINATION OF PLATINUM IN ORES BY A COMBINED FIRE ASSAY—X-RAY FLUORESCENCE METHOD

R. J. COOMBES and A. CHOW

Chemistry Department, University of Manitoba

R. W. FLINT

Physics Department, University of Manitoba, Winnipeg, Manitoba R3T 2N2 (Canada)

(Received 28th September 1976)

SUMMARY

A combined fire assay—x-ray fluorescence procedure for the determination of platinum in ores is described. Silver beads obtained by cupellation in the classical fire assay process are flattened to constant thickness before placement in the x-ray beam. A standard plot of platinum—silver intensity ratio versus platinum concentration is used to measure the platinum content of ore samples.

Several ores and mattes have been analyzed for noble metals by x-ray fluorescence [1—3]. However, very little appears to have been done directly on silver beads obtained by cupellation using the classical fire assay process. Losev [4] dissolved the silver assay bead in dilute nitric acid, added tantalum as a comparison element, evaporated the solution, ignited the residue and ground it. The analytical lines used were platinum $L\alpha_1$ and tantalum $L\beta_1$ and $L\beta_2$. For concentrations less than 0.5% the bead was first treated with dilute sulfuric acid to dissolve the silver; the error quoted was 3—4%. Chow [5] developed a procedure for the determination of gold in silver beads; the beads were flattened and a constant area was exposed to the x-ray beam. Although the results were very promising for synthetic samples, ore samples were not analyzed.

The present paper reports an extension of this method to the determination of platinum in synthetic silver assay beads, and application of the method to ore samples. This work was part of a comparative study of methods for the determination of platinum in ores, and results are compared with previous analyses obtained from independent sources.

EXPERIMENTAL

Apparatus and instrumental conditions

A Lindberg Hevi-duty 20-kW electric furnace, magnesia cupels (Leonard Light Industries, Benoni, South Africa) and crucibles (A. P. Green Refractories,

Ontario) were used. The conditions for the x-ray fluorescence spectrometer (University of Manitoba Physics Dept.) are:

tube,	molybdenum,
voltage,	40 kV,
filament,	20 mA,
detector,	Kevex Si(Li) with an active area of 30 mm^2 and resolution of 195 eV full width at half maximum (FWHM) at 5.9 keV.
counting time,	8 min.

X-rays from the molybdenum tube are filtered (5 mm Mo foil) so as to be largely monochromatic, collimated and allowed to fall on the sample. The Si(Li) detector is placed immediately below the sample out of the path of the main beam, and operated at liquid nitrogen temperatures. The detector output signals are amplified and shaped for sorting by a 1024-channel pulse-height analyzer. The memory of the pulse-height analyzer may be continuously monitored by a display oscilloscope, which allows the entire range to be inspected at a single glance. The data are recorded in digital form as a teletype readout of the memory of the analyzer.

Reagents

Platinum solution (1 mg ml^{-1}). Pure platinum wire (1 g; Johnson, Matthey and Mallory) was dissolved in aqua regia. Nitrogen oxides were removed by repeated evaporations with concentrated hydrochloric acid. The solution was filtered into a 1-l flask and diluted to the mark with 0.1 M hydrochloric acid. The solution was standardized with thiophenol [6], and a second solution standardized spectrophotometrically [7] against the first, with calibrated glassware.

Palladium and gold solutions (1 mg ml^{-1}). The pure metals were dissolved in aqua regia, evaporated to dryness several times with concentrated hydrochloric acid and diluted with 0.1 M hydrochloric acid.

Rhodium solution (1 mg ml^{-1}). Sodium hexachlororhodate (0.5838 g; Alfa Inorganics) was dissolved in 100 ml of 0.1 M hydrochloric acid.

Iridium solution (1 mg ml^{-1}). Sodium chloroiridate (0.7292 g; Johnson, Matthey Chemicals Ltd., London) was dissolved in 100 ml of 0.1 M hydrochloric acid.

Silver nitrate solution (2 mg ml^{-1} and 20 mg ml^{-1}). Silver nitrate (0.3148 g and 3.148 g; Mallinckrodt, analytical reagent) was dissolved in 100 ml of doubly distilled, doubly de-ionized water.

Lead. 0.004-in foil (Matheson, Coleman and Bell) was used.

X-ray fluorescence of standard silver—platinum beads

Standard silver beads weighing approximately 11 mg and containing 0.2—4.2% platinum were prepared by salting lead boats and cupelling at 960°C with magnesia cupels. Blanks were also included. The cupels were heated for at least 10 min before use. The furnace door was kept closed for 5 min to allow the lead to melt, and then opened by placing a 0.6-cm steel

plate under the door. Under these conditions the driving of the lead occurred at a rate of about 1 g min^{-1}. When driving was complete, the furnace door was closed and cupellation finished for a further 5 min. Cupels were then slowly withdrawn from the furnace and allowed to cool. When cool, the beads were flattened between two steel blocks in order to present as large a surface area as possible to the x-ray beam. This was accomplished in two stages: after cupellation any adhering cupel material was carefully scraped away with a spatula and the beads flattened to approximately 0.5 mm; the beads were then annealed by heating in a porcelain crucible at red heat for 2—3 min, and finally flattened at a pressure of 10 tons with a hydraulic press. Bead thickness was constant at 0.10—0.12 mm; the diameters were 3.70—4.10 mm.

The beads were mounted on mylar foil (450 μg cm^{-2} thick) stretched over aluminum foil and held in position by vacuum grease. The holder was placed in the specimen chamber which was then evacuated. The sample made a 45° angle to the x-ray beam. Each bead was counted for 8 min; this was long enough to obtain 10% counting statistics for 0.18% platinum. Resolutions calculated for 9.44 keV (Pt $L\alpha_1$ peak) and 11.07 keV (Pt $L\beta_1$ peak) were 330 and 365 eV, respectively. Thus it was not possible to resolve $L\alpha_1$ and $L\alpha_2$ peaks nor $L\beta_1$ and $L\beta_2$ peaks. However, Pt $L\alpha$ and $L\beta$ peaks were easily resolved. Similar calculations show that $K\alpha_1$ and $K\alpha_2$ peaks of silver will appear as a single $K\alpha$ peak. This was also the case with the $K\beta$ peak. Ag $K\alpha$ and Ag $K\beta$ peaks were easily resolved.

A calibration curve was drawn of percentage platinum against Pt $L\alpha$/Ag $K\alpha$ intensity ratio by the method of least squares (Fig. 1). The concentration of platinum in the silver beads was calculated from the platinum added and the weight of the bead after cupellation. Blanks contributed a constant

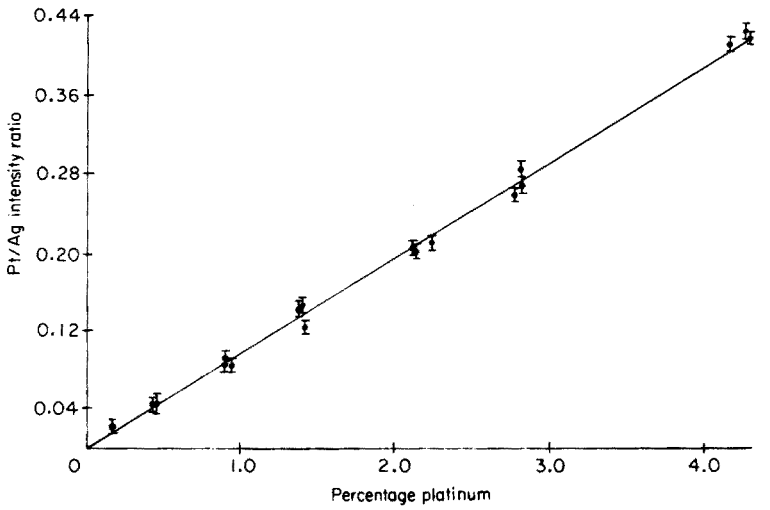

Fig. 1. X-ray fluorescence calibration curve for silver beads containing 0.18—4.2% platinum. Bars represent standard deviation at the 95% confidence level.

10 counts/8 min at the Pt Lα line, hence all platinum intensities were corrected by this amount. No correction was applied to the Ag Kα line.

RESULTS

The method was tested with synthetic fire assay samples prepared by salting a flux of 85 g PbO, 21.1 g Na_2CO_3, 4.5 g CaO, 15 g SiO_2 and 2 g of flour, contained in small polyethylene bags. The bags were placed in crucible pots, and after the flux has been dried and thoroughly mixed, the pots were placed in the furnace at 960°C. The furnace was heated at the maximum rate to 1200°C, and after 15 min at this temperature, the molten contents of the pots were poured into conical iron moulds. When cool, the lead buttons were broken off from the slags by gentle tapping with a hammer, and cupelled to silver beads. The beads were annealed, flattened and counted as described above. Recoveries are listed in Table 1. As was the case with standards, bead thickness was constant at 0.10—0.12 mm, and bead diameters were 3.40—3.90 mm.

Homogeneity of beads

To obtain quantitative results by an intensity ratio method, the platinum must be uniformly distributed throughout the silver matrix. To test the distribution, two beads — one at low concentration and one at high concentration — were chosen at random and both sides of the beads were counted 5 times for the same length of time. Results are shown in Table 2. Application of the Student 't' test for significance at the 95% confidence level shows that the averages for each bead are statistically the same. This indicates bead homogeneity and justifies the use of intensity ratios.

Interelement effects

It is necessary to determine the influence of iridium, gold, rhodium and palladium on the platinum—silver intensity ratio, since these metals are present in most platinum-bearing ores. Silver beads containing 100 μg Pt, 50 μg Pd, 10 μg Rh, 10 μg Au and 2 μg Ir, were prepared by salting lead boats and cupelling. These values represent the maximum amounts of each metal in

TABLE 1

X-ray fluorescence of synthetic fire assay samples

Pt added (μg)	20.1	40.2	60.3	200.1	400.2
Recovery (μg)	21.3[a]	38.6[a]	61.4[b]	206.2[a]	408.3[a]
S.d.[c]	1.8	3.3	6.8	15.6	27.9

[a] Average recovery from 5 beads.
[b] Average recovery from 4 beads.
[c] Values quoted at the 95% confidence level.

TABLE 2

Homogeneity of silver—platinum beads

Sample	Intensity ratio[a]	
	Side A	Side B
50.2 μg Pt	0.0451 ± 0.0017[b]	0.0447 ± 0.0020
480.3 μg Pt	0.4111 ± 0.0160	0.3951 ± 0.0119

[a] Side A: top side of bead. Side B: side in contact with cupel.
[b] Values at the 95% confidence level.

the platinum ores analyzed. The beads were counted in the usual way and compared with standard 100-μg platinum beads. The results are shown in Table 3. Comparison of absorption coefficients indicates no interference from the other noble metals.

Iridium and rhodium are not fully soluble in molten silver and hence are not uniformly distributed throughout the beads but appear as black specks on the surface. Both sides of the beads containing these metals were counted to determine if this had any effect on the platinum—silver ratio. Results appear in parentheses in Table 3.

Similarly it was shown that palladium and rhodium Kα lines do not interfere with the silver Kα line. This was expected because of the vast differences in the amounts of the elements present.

Analysis of ores

Ores for analysis were designated by name or number and originated from the Merensky Reef, South Africa. These ores, which had been crushed to pass through sieves of 100 and 200 mesh, had previously been analyzed for platinum metals and gold (see Table 4). The entire ore sample was placed on a large cellophane sheet and rolled or tumbled by lifting

TABLE 3

Comparison of standard 100-μg platinum beads with beads containing noble metal mixtures

Standard 100 μg platinum beads		Beads containing 100 μg Pt, 50 μg Pd, 10 μg Rh, 10 μg Au and 2 μg Ir	
% Pt	A[a]	% Pt	A[a]
0.886	0.0974	0.875	0.0977
0.939	0.0908	0.919	0.0951 (0.0986)
0.905	0.1039	0.892	0.1011 (0.0989)

[a] Intensity ratio divided by platinum concentration.

TABLE 4

Determination of platinum in ores by combined fire assay—x-ray fluorescence (Results are given as p.p.m. The errors are quoted at the 95% confidence level. The asterisked value was rejected at this level.)

	S4[a]	Float concentrate[a]	USBM 31[b]
	5.45	90.8	5.19
	4.54	92.0	8.26
	6.02	80.3*	6.88
	6.32	89.0	6.74
	4.97	90.6	6.08
	5.59	92.6	6.23
	4.29		7.04
			6.01
Average	5.31 ± 0.69	91.0 ± 1.7	6.55 ± 0.75
Previous analysis	5.23	82.6	4.9

[a]NIM Johannesburg, S. Africa. Previous analysis by combined fire assay—flame atomic absorption.
[b]United States Bureau of Mines, Reno, Nevada. The previous analysis value is the average result from 8 laboratories taking part in a 'round-robin' analysis. Methods of analysis included fire assay—flame atomic absorption, fire assay—emission spectrography and fire assay—spectrophotometry.

alternate corners of the sheet. After 25 min of mixing the ore was spread out evenly on the cellophane and marked off into 2.5-cm squares. The sample for assay was then obtained by taking small portions from each of the squares. The float concentrate and USBM 31 samples were roasted for 1 h at 700°C. Ore samples were added to small polyethylene bags containing the flux mentioned above. To ensure that the flux was not too basic, 10 g of SiO_2 was added to each ore. Silica (15 g) was used as a blank ore. Samples were fire-assayed and cupelled as described above. The cupellation beads so prepared were flattened and counted in the usual way. The results of the ore analyses are shown in Table 4. The weights taken of the ores designated S4 and USBM 31 were such that a minimum of 40 μg of platinum was determined. For the float concentrate, 1—2 g was taken.

CONCLUSION

X-ray fluorescence has been shown to be quantitative for platinum in the range studied. Acceptable results were obtained for S4 and the float concentrate, but the results for USBM 31 were high compared to previous independent analyses. Bead homogeneity was tested for USBM 31 by counting the opposite side of each bead. The result of this analysis was 6.36 ± 0.60 p.p.m., indicating bead homogeneity at the 95% confidence level.

Beads were also examined for lead. Lead peaks appear to the short wavelength side of platinum and hence may excite the platinum peaks, causing enhancement of the platinum—silver ratio. No evidence of lead was found. Also from experience with beads containing lead, more lead is usually present on the surface attached to the cupel, and so enhancement should be much higher on one side of the bead than on the other. This was not the case, and thus no satisfactory explanation can be given for the somewhat high results.

The low precision found with x-ray fluorescence spectrometry is in part due to the difficulty of preparing standards whose platinum content is known to a high degree of accuracy. Precision may be increased by using longer counting time or by using a crystal spectrometer and obtaining higher count rates in a shorter time.

X-ray fluorescence offers the advantages that the sample is not destroyed, speed of analysis compares favorably with other methods and very little sample preparation is required, thus keeping losses to a minimum. The fire assay procedure provides a method which concentrates the platinum up to 1000-fold and simultaneously removes the base metal matrix. Thus the combined fire assay—x-ray fluorescence method offers a rapid and reliable analysis for platinum in ores which may be applicable to several other matrices.

REFERENCES

1 A. Strasheim and F. T. Wybenga, Appl. Spectrosc., 18 (1964) 16.
2 B. G. Russell, B. T. Eddy, G. Beckman and T. W. Steele, J. S. Afr. Chem. Inst., Vol. XXV, 1972.
3 M. G. Bapat and F. E. Beamish, Anal. Lett., 2 (1969) 387.
4 N. F. Losev, Sb. Nauchn. Tr. Irkutsk. Gos. Nauchno-Issled. Inst. Redk. Met., 7 (1958) 25 (C.A. 53 (1959) 21417C).
5 A. Chow, Ph.D. Thesis, Toronto Univ., 1966.
6 J. E. Currah, W. A. McBryde, A. J. Cruikshank and F. E. Beamish, Ind. Eng. Chem. Anal. Ed., 18 (1946) 120.
7 G. H. Ayres and A. S. Meyer, Jr., Anal. Chem., 23 (1951) 299.

Analytica Chimica Acta, 91 (1977) 281—285

A NEW PROCEDURE FOR THE RECOVERY OF RUTHENIUM AND OSMIUM AFTER LEAD COLLECTION

A. DIAMANTATOS

J.C.I. Minerals Processing Research Laboratory, Knights 1413, Transvaal (South Africa)

(Received 22nd November 1976)

SUMMARY

A new scheme is proposed for the quantitative recovery of ruthenium and osmium collected in lead. The lead button is parted with perchloric acid in the presence of a little acetic acid, after heating at 160—180°C. Ruthenium remains totally undissolved; some osmium remains insoluble but some volatilizes and is collected in an alkaline solution. Platinum, palladium and rhodium are completely dissolved in the lead perchloric acid solution, and are removed by simple filtration. After fusion of the residue with sodium peroxide, the solution is combined with the alkaline osmium solution, and ruthenium and osmium oxides are distilled from a bromate—sulphuric acid medium, prior to their spectrophotometric determination. The method provides satisfactory recoveries, with relative standard deviations of 1.45% (Ru) and 6.3% (Os).

Early investigators [1, 2] have provided ample evidence that ruthenium and osmium are completely collected in the lead button obtained by the classical fire-assay fusion. Thiers et al. [1] used perchloric acid for dissolution of the button and succeeded in recovering the ruthenium quantitatively. They reported that when the lead perchlorate solution was heated at 205—210°C, ruthenium was partially distilled as the tetroxide whereas some ruthenium remained unattacked in the still. Osmium is quantitatively distilled as its tetroxide [2]. Beamish and van Loon [3] state that the above method [1] is at least as efficient as any other assay procedure and that the method provides a quantitative recovery of both ruthenium and osmium.

The present author showed recently [4] the suitability of perchloric acid for the separation of iridium from the platinum, palladium, rhodium and gold collected in lead. When the lead collector was parted with perchloric acid after heating at 160—180°C, all the platinum, palladium, rhodium and gold passed into solution whereas iridium metal remained completely unattacked. An x-ray fluorescence examination of this residue indicated that much of the ruthenium and some of the osmium were also present. The fact that ruthenium, like iridium, does not alloy with lead at high temperatures [5], suggested that ruthenium may remain totally unattacked by perchloric acid if the perchlorate solution is not boiled. During the disintegration of the lead button at 160—180°C, perchloric acid behaves as a non-oxidizing acid,

as can be seen by the evolution of hydrogen. It was therefore decided to investigate the behaviour of these two volatile noble metals under the above-mentioned parting conditions, and to examine the possibility of developing a procedure for their determination.

EXPERIMENTAL

Apparatus and reagents

The fire assay apparatus, the spectrophotometer and the lead flux were the same as described recently [4].

Standard copper—nickel matte contained 205 p.p.m. Ru, 19 p.p.m. Os, total noble metals 0.18%, 28.9% Cu, 48.2% Ni, 1.4% Fe, 22.4% S etc.

Recommended procedure

Mix thoroughly 2—60 g of the sample, as required, with 150—180 g of lead flux, and transfer to a suitable fireclay crucible. Fuse at 1200°C for 1 h and then pour the melt into a conical iron mould. After cooling, detach the lead button from the slag by tapping. (Re-fuse the slag if large quantities of ruthenium or osmium are present.) Place the button in 100 ml of 30% (w/v) sodium hydroxide solution, and boil to remove completely any adhering slag. Compress the button to a disc about 4 mm thick. Place the disc in a 1-l distillation flask connected to two 250-ml flasks containing 100 ml of water (trap) and 100 ml of 20% NaOH solution, respectively. (The distillation flask is fitted with a dropping funnel and air admission tube.) Introduce 300 ml of 70% perchloric acid and 30 ml of glacial acetic acid through the funnel and draw air through the apparatus (1—3 bubbles per second). Dissolve the lead by heating the still at 160—180°C; some osmium volatilizes and is absorbed in the alkaline solution. After completion of the dissolution, continue heating at a lower temperature (140—150°C) for another 15—20 min, then remove the flame and allow the solutions to cool. Dilute the lead perchlorate solution by introducing 200 ml of water, via the tap funnel, and mix well by increasing the bubbling rate. Disconnect the distillation apparatus, and reserve the alkaline receiving solution. Filter the diluted perchlorate solution through an asbestos filter pad into a Büchner flask under vacuum. Wash the filter with hot water and dry the asbestos pad in a zirconium crucible. Fuse with 10 g of sodium peroxide, cool and leach the melt with 200 ml of water in a 400-ml beaker. Combine the alkaline leach with the 100 ml of 20% sodium hydroxide solution, containing the volatilized osmium.

Transfer the combined solutions to a distillation train consisting of a 1-l still, fitted with a dropping funnel and air admission tube, and five 250-ml receivers. To each of the first four receivers add 100 ml of 6 M hydrochloric acid for the absorption of ruthenium tetroxide; to the fifth receiver add 25—30 ml of 10% (w/v) thiourea in 6 M hydrochloric acid for the absorption of osmium tetroxide. Connect the distillation train and draw air through as before. (The distillation and receiving flasks are connected by glass ball and

socket joints, held with spring clips.) Slowly add 50 ml of (1 + 1) sulphuric acid to the flask via the funnel, close the tap, and mix until the liquid is clear. Introduce 30 ml of aqueous 10% (w/v) sodium bromate solution through the funnel and close the tap again. Gradually heat the solution to boiling, and continue the distillation for 5—10 min after the pink osmium—thiourea colour has appeared in the final receiving flask. (There is no need to apply heat to each of the absorption flasks, since the contents of each receiver are heated to boiling by the steam issuing from the previous flask.) Remove the flame, disconnect the absorption flasks one at a time, starting from the distillation flask side, while air is still being drawn through the train.

Determine the osmium content by measuring the pink osmium—thiourea colour spectrophotometrically at 482 nm [6]. To determine ruthenium, combine the four hydrochloric acid receiving solutions in an 800-ml beaker, and evaporate to near dryness in the presence of a little sodium chloride. Dissolve the residue by boiling with 20 ml of 6 M hydrochloric acid and 3—4 drops of 100-vol. hydrogen peroxide for 2—3 min and then determine ruthenium spectrophotometrically by the thiourea method [7].

RESULTS AND DISCUSSION

The behaviour of ruthenium and osmium during the parting of the lead button

A sample (25 g) of the "standard" copper—nickel matte was leached with 300 ml of 11 M hydrochloric acid in presence of 100 g of ammonium chloride by boiling for about 2 h, to remove the bulk of the base metals; 300 ml of hot water were added and the diluted solution was boiled again for 10—15 min. The warm solution was filtered through an asbestos filter pad under vacuum, the insoluble residue containing the noble metals being washed with hot water. After drying, the residue was mixed with 180 g of the lead flux and the mixture fused at 1200°C for 1 h. The lead button obtained was parted in an 800-ml squat beaker with 300 ml of perchloric acid (70%), by heating at 160—180°C for 1 h. The perchlorate solution was cooled somewhat, diluted with 300 ml of water, stirred, boiled gently for a few minutes, and filtered through an asbestos filter pad under vacuum. The pad and residue were dried and fused with ca. 20 g of sodium peroxide in a zirconium crucible. The cake was leached with water and the alkaline slurry was transferred to a distillation flask, after diluting to about 400 ml with water. The bromate—sulphuric acid distillation [8] and spectrophotometric determinations of ruthenium [7] and osmium [6], were then carried out as described above.

The strong brown colour of ruthenium trichloride in the first two receivers (the other two act rather as traps), as well as the pink colour of the fifth receiving solution, indicated a high content of both metals in the unattacked residue; 5.056 mg of ruthenium and 0.225 mg of osmium were recovered compared to 5.125 and 0.475 mg, respectively, present in 25 g of the original

matte. These results indicate that while none of the ruthenium was apparently dissolved by the parting acid, almost half the osmium had been lost during the parting process.

The formation and volatilization of osmium tetroxide during the parting of the lead button were therefore investigated. To measure the loss of osmium directly, the lead button was dissolved in a distillation apparatus with two receiving flasks containing water and sodium hydroxide solution (20% w/v), respectively (see Experimental). The button was dissolved with 300 ml of 70% perchloric acid by heating at 160—180°C while air was gently drawn through the apparatus. After the parting, the osmium tetroxide which escaped was recovered by bromate—sulphuric acid distillation of the alkaline trap solution, as described in the recommended procedure. The pink colour of the osmium—thiourea complex appeared in the fifth receiver, whereas the first four hydrochloric acid solutions were absolutely colourless, confirming that no ruthenium had volatilized during the parting. Spectrophotometric measurement of the osmium—thiourea solution showed that 36.4% of the total osmium had been volatilized under the conditions of parting.

When the above procedure was repeated with a stream of nitrogen instead of air during the dissolution of the lead, it was found that 31.0% of the osmium present in the original matte had been volatilized. Once more, there was no apparent volatilization of ruthenium.

The effect of adding acetic acid to the perchloric acid used for the parting was then studied. This addition resulted in a milder dissolution, and might have prevented the partial oxidation and volatilization of osmium. A 50-g lead button, containing the precious metals of 25 g of "standard" matte, was dissolved in a 1-l beaker with 300 ml of perchloric acid (70%) and 30 ml of acetic acid (glacial) by heating at 160—180°C. To facilitate comparison, another 50-g button was simultaneously parted with 300 ml of perchloric acid only. After complete disintegration of the lead button, both solutions were diluted to approximately 600 ml with water and filtered through an asbestos pad, under vacuum. The filter, retaining the unattacked ruthenium, osmium and iridium, was dried, fused with sodium peroxide and leached with water. Both osmium and ruthenium were distilled by the bromate—sulphuric acid treatment, as described above, and determined spectrophotometrically [6, 7]. The results showed quantitative recovery of ruthenium in both cases. With regard to osmium, the sample treated with perchloric acid alone gave a result of 0.218 mg while the sample containing acetic acid gave a result of 0.350 mg. Thus even in the presence of acetic acid, 26.2% of the total osmium was dissolved and subsequently volatilized, while in the absence of acetic acid, 54.1% of the osmium was lost.

The above reduction of osmium losses on addition of some acetic acid, demanded a further experiment with more acetic acid in the parting mixture. This time the lead button was parted with 200 ml of perchloric acid and 200 ml of acetic acid. Complete dissolution of the button then required more

than 2 h instead of the usual 1 h, and from time to time more acetic acid had to be added to replace that which had evaporated. Analysis of the residue showed a recovery of 81% for osmium; thus even in the presence of large amounts of acetic acid, which cause a very slow attack of the button, 19% of the original osmium was still lost by volatilization.

This investigation has shown that for quantitative recovery of the osmium in the lead button, the parting treatment must be done in a distillation flask connected to a receiving flask containing a sodium hydroxide solution, to absorb the escaping osmium tetroxide. Of course, if a determination of osmium is not required, the parting can be done in a beaker, because ruthenium remains as a metallic residue. Here, the ruthenium was determined spectrophotometrically, but direct spectrographic analysis of the metallic residue would obviate the fusion of the residue and the distillation of the ruthenium. It is of interest that the present work suggests that osmium, like ruthenium and iridium, does not alloy with the lead on fusion, but is spread as a suspension in the fire-assay button.

Accuracy and precision

The accuracy and precision of the method were evaluated by analysing ten 5-g portions of the "standard" matte for ruthenium and osmium by the recommended procedure. The individual results, standard deviations (0.015 for Ru and 0.006 for Os) and relative standard deviations (1.45% for Ru and 6.3% for Os), confirmed the reliability of the proposed method in practical application.

REFERENCES

1 R. Thiers, W. Graydon and F. E. Beamish, Anal. Chem., 20 (1948) 831.
2 W. J. Allan and F. E. Beamish, Anal. Chem., 24 (1952) 1569.
3 F. E. Beamish and J. C. van Loon, Miner. Sci. Eng., 4 (4) (1972) 3.
4 A. Diamantatos, Anal. Chim. Acta, 90 (1977) 179.
5 H. Ste-C. Deville and J. S. Stas, Procès-verbaux, Comité International de Poids et Mésures, 2 (1877) 162.
6 E. B. Sandell, Ind. Eng. Chem. Anal. Ed., 16 (1944) 342.
7 G. H. Ayres and F. Young, Anal. Chem., 22 (1950) 1277.
8 W. R. Schoeller and A. R. Powell, The Analysis of Minerals and Ores of the Rarer Elements, Charles Griffin, London, 3rd edn., 1955.

Analytica Chimica Acta, 91 (1977) 287—294

METHOD FOR THE SEPARATION OF PLATINUM, PALLADIUM, RHODIUM, IRIDIUM AND GOLD BY SOLVENT EXTRACTION

A. DIAMANTATOS and A. A. VERBEEK

Department of Chemistry, University of Natal, Pietermaritzburg (South Africa)

(Received 20th December 1976)

SUMMARY

The use of diphenylthiourea in conjunction with potassium iodide or tin(II) chloride provides a systematic scheme for the extraction—separation of platinum, palladium, rhodium, iridium, and gold in hydrochloric acid solution. Gold is extracted initially into methyl isobutyl ketone from 6 M hydrochloric acid. Platinum and palladium are extracted simultaneously into chloroform as their diphenylthiourea complexes at the same acidity; the palladium is separated from platinum as its dimethylglyoxime complex in chloroform. Rhodium is separated from iridium by extracting its diphenylthiourea—tin(II) chloride complex into chloroform from 1—2 M hydrochloric acid. The proposed scheme, applied to several synthetic solutions containing varying amounts and ratios of the noble metals in hydrochloric acid, gives satisfactory recoveries; the average relative errors for Pt, Pd, Rh, Ir, and Au are 0.2, 0.3, 0.5, 1.1, and 0.4%, respectively.

The first application of diphenylthiourea as an extraction reagent for precious metals was reported by Geilmann and Neeb [1] who separated ruthenium from osmium. Their procedure involved the formation of the blue ruthenium complex in hot solution, its extraction into chloroform, and spectrophotometric measurement of ruthenium in this organic phase; osmium remained in the aqueous phase. Shul'man and Kosareva [2] reported the quantitative extraction of palladium(II) and ruthenium(IV) from 3 M HCl solutions heated to 60°C before extraction, by solutions of diphenylthiourea. Solutions of rhodium(III), platinum(IV) and iridium(IV) had to be heated to at least 100°C to achieve quantitative extraction. Copper(II) was quantitatively co-extracted, but only negligible amounts of nickel, cobalt, and iron were obtained in the organic phase. Palladium and iridium have been separated with this reagent. Vorob'eva et al. reported [3] that, of twelve extraction systems for the concentration of the noble metals, extraction with chloroform of the diphenylthiourea complexes was the most suitable. Their method involved preliminary treatment of the hydrochloric acid solution with 0.5 M tin(II) chloride in 6 M hydrochloric acid, the addition of 0.25 M diphenylthiourea in acetone, and boiling for 40 min before extraction with chloroform to achieve the simultaneous separation of platinum, palladium, rhodium, iridium, ruthenium, gold, and silver from nickel, iron, cobalt, and zinc (but not from copper). This extract was evaporated on powdered carbon and analysed spectrographically to determine the individual noble metals.

In view of the apparent potential utility of diphenylthiourea as an extractable complex-forming reagent, it was decided to extend the scope of application of this reagent in the separation and determination of the platinum-group metals. This paper describes the development of an integrated scheme for the separation of platinum, palladium, rhodium, iridium, and gold from hydrochloric acid solutions, by solvent extraction, mainly with diphenylthiourea in conjunction with either potassium iodide or tin(II) chloride at room temperature, to form chloroform-extractable complexes.

EXPERIMENTAL

Reagents and equipment

Standard solutions of the noble metals were prepared from Johnson-Matthey "Specpure" platinum sponge, palladium wire, gold foil, ammonium chlororhodite and ammonium chloroiridate respectively, by procedures described previously [4].

The reagent was a 0.5% (w/v) s-diphenylthiourea (Merck) solution in acetone.

A Zeiss model PMQ II spectrophotometer was used for the absorbance measurements.

Recommended procedure

Extraction of gold. Transfer the hydrochloric acid solution containing Pt, Pd, Rh, Ir and Au to a 250-ml separatory funnel. The final volume should be ca. 100 ml, and the final hydrochloric acid concentration should be ca. 6 M. Add 50 ml of methyl isobutyl ketone, previously shaken with an equal volume of 6 M hydrochloric acid containing ca. 5% (v/v) of nitric acid. Shake for 3—4 min and allow the phases to separate. Run off the aqueous phase into another 250-ml separatory funnel. Back-wash the gold extract twice with two 25-ml portions of 6 M hydrochloric acid and add these washings to the second funnel. Strip the co-extracted base metals from the organic phase, by shaking with three 25-ml portions of 0.5 M hydrochloric acid, and discard these aqueous fractions which contain Te, Fe, etc.

Simultaneous extraction of platinum and palladium. Gently shake the 6 M hydrochloric acid raffinate, obtained after the extraction of gold, which contains the platinum metals, with 50-ml portions of chloroform to remove the residual dissolved methyl isobutyl ketone. Discard this chloroform extract. To the aqueous phase add 10 ml of diphenylthiourea reagent solution, mix gently, and leave for 2—3 min. Add 0.5 g of potassium iodide dissolved in a minimum of water, mix, and leave for a further 15 min. Extract the platinum and palladium complexes simultaneously with successive 100-ml and 50-ml portions of chloroform, shaking for 5 min each time, and transfer the chloroform phases to a 400-ml beaker.

Extraction of rhodium. Run the aqueous phase obtained after the simultaneous extraction of Pt + Pd, into a 400-ml beaker and evaporate to dryness. To the dry residue add 10 ml of concentrated nitric acid, boil for 5 min, add 5 ml of concentrated hydrochloric acid, boil again, and evaporate to dryness. Decompose the residue completely by evaporating twice to dryness from a mixture of 9 parts of concentrated nitric acid and 1 part of 100-vol hydrogen peroxide. Convert the residue to chloro-complexes by boiling with 10 ml of concentrated hydrochloric acid and evaporating to dryness. Repeat the process with a second 10-ml portion of hydrochloric acid. Add 20 ml of 6 M HCl and 2—3 drops of 100-vol hydrogen peroxide, and boil for 2—3 min. Cool, transfer the solution to a 250-ml separatory funnel and dilute to approximately 100 ml in 1—2 M HCl. Add 10 ml of diphenylthiourea reagent solution and mix gently; after 5 min, add while swirling the funnel 1 ml of 20% tin(II) chloride solution in 6 M hydrochloric acid, and mix again. Leave for 20—30 min, and then extract the precipitated yellow rhodium complex with first 80 and then with 50 ml of a chloroform : acetone (3 : 2) mixture. Combine the two extracts in a 400-ml beaker for the subsequent determination of rhodium. Keep the aqueous phase for the determination of iridium as described below.

Extraction—separation of palladium and platinum. Evaporate the Pt + Pd chloroform extract on a steam bath while directing a gentle stream of air on to the solvent surface. To the dry residue add 20 ml of concentrated nitric acid, cover with a watch-glass, and boil gently to rinse the beaker wall with the refluxing acid. Cool somewhat, add 5 ml of concentrated hydrochloric acid, heat gently until the reaction ceases, and evaporate to dryness in the presence of sodium chloride (50 mg). Add 5 ml of perchloric acid (70%) and 3 ml of 18 M sulphuric acid, heat strongly, and evaporate to dryness. Cool, add 20 ml of concentrated hydrochloric acid, boil under cover for approximately 10 min, remove the watch-glass, and evaporate to dryness. Repeat this treatment with another 10-ml portion of hydrochloric acid. To the dry residue add 5 ml of concentrated hydrochloric acid and 2—3 drops of hydrogen peroxide (100 vol) and boil for 2—3 min. Cool, transfer the solution to a separatory funnel, and dilute to approximately 100 ml with water. (The solution prior to the palladium precipitation should be 0.1—0.6 M in HCl.) Add 2—3 drops of concentrated nitric acid and mix (to retain the platinum as Pt(IV)). Slowly, and while swirling, add 5 ml of ethanolic 1% dimethylglyoxime solution, mix, and leave for 45 min for the complex-forming reaction to proceed to completion. Extract the precipitated yellow palladium complex with 50, 50, and 25 ml of chloroform, shaking for 5 min each time. Combine the extracts in a 250-ml beaker for the subsequent spectrophotometric determination of palladium. Retain the aqueous phase for the determination of platinum.

Determination of gold. Transfer the gold—methyl isobutyl ketone extract to a 100-ml beaker and evaporate to dryness as described previously. Destroy the organic matter by evaporating twice to dryness after additions of 10 ml

of a mixture (9 + 1) of concentrated nitric acid and 100-vol hydrogen peroxide; finally, remove the last traces of the nitric acid by at least three evaporations with 10-ml portions of 12 M hydrochloric acid in the presence of a little sodium chloride. Dissolve the dried residue in 10 ml of 12 M hydrochloric acid containing a few drops of 100-vol hydrogen peroxide. Boil the solution for a few min to decompose the peroxides completely. Determine gold spectrophotometrically by the bromaurate method [5].

Determination of platinum. Determine spectrophotometrically, directly in the raffinate from the palladium extraction, by the tin(II) chloride method [6].

Determination of palladium. Evaporate the palladium—chloroform extract to dryness on a steam bath while blowing air on to the surface of the solvent. Destroy the yellow residue with 10 ml of a mixture (9 + 1) of concentrated nitric acid and 100-vol hydrogen peroxide and convert to a hydrochloric acid solution by boiling and evaporating with at least three small additions of the acid in the presence of a little sodium chloride, as described above for gold. Determine palladium spectrophotometrically with potassium bromide [7].

Determination of rhodium. Evaporate the rhodium—chloroform extract on a steam bath as described previously. Destroy the organic matter with the nitric acid—hydrogen peroxide mixture and convert the rhodium to its chlorocomplex as described for palladium. Determine rhodium spectrophotometrically by the tin(II) chloride method [8].

Determination of iridium. Evaporate the aqueous phase from the extraction of rhodium to dryness. Boil the residue with nitric acid and perchloric acids and again evaporate to dryness. Add 20 ml of 12 M hydrochloric acid and boil. Determine the iridium spectrophotometrically by the tin(II) chloride—hydrobromic acid method [9]. Alternatively, and preferably, separate iridium from the residual salts by extracting its 2-mercaptobenzothiazole complex in acetic acid medium into chloroform [10] and complete the determination spectrophotometrically by the above method.

DISCUSSION AND RESULTS

Extraction of gold

The extraction of gold(III) by methyl isobutyl ketone, which has been investigated thoroughly by several workers [11—14], appeared to be suitable for the desired extraction scheme; it offered the advantage not only of separating gold from the platinum metals, but also of co-extracting iron(III), chromium(VI), tellurium(IV), and other base metals which might be present in real samples. These co-extracted metals can be conveniently stripped from the solvent with 0.5 M hydrochloric acid.

The distribution ratio for gold in this extraction is very favourable, and only one extraction is necessary, but the ease of reduction of gold(III) to the metal necessitates the use of methyl isobutyl ketone which has been

shaken previously with 6 M hydrochloric acid containing 5% (by volume) of nitric acid, in order to eliminate the risk of such reduction by impurities (e.g. hexanol) in the solvent. This pretreatment also gave an apparently better phase separation.

Extraction of platinum and palladium

The extraction of platinum as a diphenylthiourea—iodide complex was investigated at several acidities between 0.25 and 6 M hydrochloric acid. Aliquots (100 ml) of a solution, each containing 1.002 mg of platinum, were treated with 10 ml of acetonic 0.5% diphenylthiourea solution. A yellow precipitate appeared in solutions that were at least 2 M in hydrochloric acid. In solutions of lower acidity only a white turbidity, resulting from the insolubility of the reagent, was noticed. After 3 min, 5 ml of aqueous 10% potassium iodide solution were added, and the solution was mixed gently and allowed to stand for 15 min before extraction of the precipitate with 80 ml and then with 50 ml of chloroform. Sharp phase separations were observed in all cases. The aqueous layers were analysed for unextracted platinum.

The results shown in Table 1 indicate that complete extraction of platinum was achieved from solutions which were at least 3 M in hydrochloric acid. It was decided to use 6 M acid, as this was the acidity of the solution after the extraction of gold, and more rapid coagulation of the diphenylthiourea precipitate occurred at the higher acidity.

The experiments were repeated, reversing the order of addition of reagents. The initial addition of potassium iodide resulted in a pink colouration, indicating the formation of the platinum—iodide complex; when diphenylthiourea was added, a yellow precipitate again appeared in the more acidic solutions and a white turbidity appeared in the less acidic solutions. Analysis of the aqueous phase, after its extraction with chloroform, again indicated complete recovery of platinum from solutions which had been at least 3 M in hydrochloric acid.

TABLE 1

Extraction of platinum—diphenylthiourea—iodide complex by chloroform
(In each case 1.002 mg of Pt was contained in the initial solution, 10 ml of 0.5% diphenylthiourea and 0.5 g KI were used in the precipitation, and the total volume of the aqueous phase extracted with $CHCl_3$ was 100 ml.)

Molarity of HCl	Pt unextracted (mg)	Pt extracted (%)
0.25	0.416	58.5
0.5	0.352	64.9
1	0.304	69.7
2	0.205	79.5
3—6	Not detected	>99.8

A series of solutions, each containing 0.504 mg of palladium, was treated similarly. Palladium could not be detected in the aqueous phase remaining after the extraction with chloroform, regardless of the order of addition of reagents, for all acidities between 0.25 and 6 M hydrochloric acid.

The presence of potassium iodide is not necessary for the extraction of palladium (which forms an extractable complex with diphenylthiourea alone), but is essential for the complete recovery of platinum under the conditions used. Shul'man and Kosareva [2] showed that palladium(II) but not platinum(IV) was extracted by chloroform after reaction with diphenylthiourea alone at 60°C. Much higher temperatures were used by these workers to form the extractable complexes of platinum(IV), rhodium and iridium. The present work confirmed that, at room temperature, even in the presence of potassium iodide, neither rhodium nor iridium was extracted in detectable quantities.

Separation of palladium from platinum

This separation was achieved by extraction of the dimethylglyoxime complex of palladium into chloroform from 0.5 M hydrochloric acid [15, 16]. The separation of this element from platinum occurs over a range of acidities from pH 2 up to 2 M hydrochloric acid without interference from lead, silver, copper, or nickel.

Extraction of rhodium and its separation from iridium

Shul'man and Kosareva [2] showed that both rhodium and iridium formed extractable complexes with diphenylthiourea when heated to at least 100°C during the complex formation. In this work, the use of tin(II) chloride in conjunction with diphenylthiourea gave yellow precipitates at room temperature in 1—6 M hydrochloric acid with rhodium but not with iridium. This provided a basis for the separation of these two elements.

The complex formed by rhodium was extractable into chloroform but the occasional formation of a rhodium-containing skin at the phase boundary made the use of this solvent undesirable. The metal could be completely extracted, without the formation of a boundary skin, with a chloroform—acetone mixture (3:2) after complex formation had been achieved by the use of 10 ml of diphenylthiourea and 1 ml of 20% tin(II) chloride in 6 M hydrochloric acid, and after standing for 20 min to complete the formation of the complex. Similar treatment of solutions of iridium confirmed that it was not extractable.

Effect of base metals (Cu, Ni, Fe, Cr, Te)

These metals, which are likely to be present in solutions obtained from real samples, could interfere in the spectrophotometric determinations of the precious metals, and their fate in the extraction scheme must be considered. The extraction of gold with methyl isobutyl ketone results in the co-extraction of iron(III), chromium(VI), and telluruim(IV) but these

are removed by stripping of the solvent with 0.5 M hydrochloric acid. Thus, only copper and nickel remain in the aqueous phase containing the platinum metals. Subsequently, copper is co-extracted with platinum and palladium as a diphenylthiourea complex. This base metal remains in the aqueous phase with platinum after the separation of palladium. Moderate amounts of copper, however, have no effect on the spectrophotometric measurement of platinum by the tin(II) chloride method [6] at 403 nm. Nickel remains in the final aqueous phase which contains only iridium of the original precious metals. The iridium—2-mercaptobenzothiazole extraction method [10], however, achieves complete separation of iridium from macro-quantities of this undesirable base metal.

Application of the scheme to synthetic solutions

To check the efficiency of the scheme, six solutions containing varying amounts and ratios of the five elements in hydrochloric acid were prepared from the standard solutions. These solutions were evaporated to dryness in the presence of a little sodium chloride, and the residues were dissolved in hydrochloric acid and hydrogen peroxide; the excesses of chlorine and peroxide were boiled off, and the resulting solutions treated as in the recommended procedure. The results shown in Table 2 indicate acceptable recoveries for each metal.

TABLE 2

Recoveries from synthetic solutions

mg	Pt	Pd	Rh	Ir	Au
Added	0.501	0.252	0.507	0.1006	0.101
Found	0.499	0.252	0.504	0.0977	0.101
Added	2.004	1.008	0.203	0.1006	0.101
Found	2.004	1.004	0.206	0.1026	0.100
Added	1.002	1.008	0.507	0.503	0.505
Found	1.006	1.008	0.510	0.508	0.502
Added	0.250	0.504	1.015	1.006	1.010
Found	0.248	0.506	1.012	1.002	1.016
Added	3.006	0.504	0.203	0.503	0.505
Found	3.005	0.504	0.203	0.501	0.505
Added	2.004	0.252	1.015	1.006	0.505
Found	2.004	0.254	1.012	1.005	0.505
Average relative difference (%)	0.2	0.3	0.5	1.1	0.4

REFERENCES

1 I. W. Geilmann and R. Neeb, Z. Anal. Chem., 152 (1956) 96; 156 (1957) 420.
2 V. M. Shul'man and L. A. Kosareva, Izv. Sib. Otd. Akad. Nauk, S.S.S.R., Ser. Khim. Nauk, 5 (1973) 137.

3 G. A. Vorob'eva, Yu. A. Zolotov, L. A. Izosenkova, A. V. Karyakin, L. I. Pavlenko, O. M. Petruklin, I. V. Seryakova, L. M. Simonova and V. N. Shevchenko, Zh. Anal. Khim., 29 (1947) 497.
4 A. Diamantatos, Anal. Chim. Acta, 66 (1973) 147.
5 W. A. E. McBryde and J. H. Yoe, Anal. Chem., 20 (1948) 1094.
6 E. B. Sandell, Colorimetric Determination of Traces of Metals, Interscience, New York, 1944.
7 A. Diamantatos, Anal. Chim. Acta, 63 (1973) 220.
8 G. H. Ayres, B. L. Tuffly and J. S. Forrester, Anal. Chem., 27 (1955) 1742.
9 S. S. Berman and W. A. E. McBryde, Analyst (London), 81 (1956) 566.
10 A. Diamantatos and A. A. Verbeek, Anal. Chim. Acta, 86 (1976) 169.
11 H. Goto, S. Suzuki, M. Saito and M. Kishimoto, Nippon Kagaku Zasshi, 85 (1964) 75.
12 F. W. E. Strelow, E. C. Feast, P. M. Mathews, C. T. C. Bothma and C. R. van Zyl, Anal. Chem., 38 (1966) 115.
13 S. L. Law and T. E. Green, Anal. Chem., 41 (1969) 1008.
14 N. Ichinose, Talanta, 18 (1971) 105.
15 R. S. Young, Analyst (London), 76 (1951) 49.
16 P. B. Mikhel'son and L. V. Kalabina, Zh. Anal. Khim., 24 (1969) 261.

Analytica Chimica Acta, 91 (1977) 295—302

OPTIMUM CONDITIONS OF MASKING

B. W. BUDESINSKY

Phelps Dodge Corporation, Morenci, Arizona 85540 (U.S.A.)

(Received 20th December 1976)

SUMMARY

The maximum of the function $\Psi_{MN} = \alpha_{M(Y)}^{-mq} \alpha_{N(Y)}^{np[H]^{iq-jn}}$ corresponds to the optimum acidity for masking of the metal ion N with a ligand Y in the presence of metal ion M; $M_mH_iL_n$ and $N_pH_jL_q$ are the complexes of M and N with the reagent ligand L, and $\alpha_{M(Y)}$ and $\alpha_{N(Y)}$ are the respective side-reaction coefficients of M and N with Y. The theoretical conditions were compared with practice for precipitation of uranyl oxinate, barium sulfate and calcium oxalate; complexation of iron(II) with 1,10-phenanthroline and aluminium with tiron; and uranyl thenoyltrifluoracetone and silver dithizone extraction. EDTA is used as masking reagent throughout. An extension of the theory to systems with several interfering cations and ligands is shown.

Several monographs [1—4] deal theoretically with the problem of masking with an excess of the masking reagent, with the intention of utilizing theory in the search for optimum conditions for reactions and analytical determinations. Recently [5], the side-reaction function Φ_M* was successfully used to determine optimum acidities of precipitation, complexation and extraction. A similar function was also suggested for reactions including interfering ions. However, the mathematics then became so complicated that the advantage of the approach was disputable. In this paper, the problem of interfering ions is solved on the basis of optimum masking conditions.

THEORETICAL

Optimum acidity

If $M_mH_iL_n$ and $N_pH_jL_q$ (H is the dissociable hydrogen) are the only compounds between the metal ion M, the interfering metal ion N and the ligand L, and if the system contains an excess of a masking reagent of ligand Y that masks ion N, then the total concentration of ion N is given by

$$c_N = (K\Psi_{MN})^{1/(np)} \quad (1)$$

where K is a constant depending on the composition of the above compounds,

* The original designation was Φ_H, but Φ_M is more correct.

their overall stability constants (or solubility products), their partition constants (in the case of extraction) and the total concentration c_M. The specific meaning of eqn. (1) in individual cases of analytical reactions is discussed below. The masking function Ψ_{MN} depends on acidity and is given by

$$\Psi_{MN} = \alpha_{M(Y)}^{-mq}\ \alpha_{N(Y)}^{np}\,[H]^{iq-jn} \tag{2}$$

where $\alpha_{M(Y)}$ and $\alpha_{N(Y)}$ are the corresponding side-reaction coefficients (Fig. 1).

The maximum of the function Ψ_{MN} in relation to pH is given by

$$\mathrm{d}\log \Psi_{MN}/\mathrm{d}pH = 0 \quad \text{and} \quad \mathrm{d}^2 \log \Psi_{MN}/\mathrm{d}pH^2 < 0 \tag{3ab}$$

i.e., after substitution from eqn. (2)

$$-mq\ \mathrm{d}\log \alpha_{M(Y)}/\mathrm{d}pH + np\ \mathrm{d}\log \alpha_{N(Y)}/\mathrm{d}pH + iq - jn = 0 \tag{4}$$

and

$$mq\ \mathrm{d}^2 \log \alpha_{M(Y)}/\mathrm{d}pH^2 > np\ \mathrm{d}^2 \log \alpha_{N(Y)}/\mathrm{d}pH^2 \tag{5}$$

Relationships (4) and (5) are useful in graphical calculation.

The most convenient way of establishing the maximum of the function $\log \Psi_{MN} = f(pH)$ is to perform iterations with eqn. (2), by introducing the values $pH_w = pH_0 + w\Delta pH$ (where $w = 1, 2, \ldots$ and ΔpH is the measure of precision; pH_0 is the optional starting value of pH). The first value of pH for which $\log \Psi_{MN(w)} < \log \Psi_{MN(w-1)}$ indicates the optimum value $pH_{opt} = pH_{w-1}$. According to eqn. (1), the maximum value of $\log \Psi_{MN}$ corresponds to the maximum value of c_N, and that represents the optimum condition of masking.

Masking in various reactions

Because the ion N is quantitatively masked by Y, all equations for calculation of the total concentration c_L are the same as when N is absent [5]. The side-reaction function [5] is

$$\Phi_M = [H]^i\ \alpha_{M(Y)}^{-m}\ \alpha_{L(H)}^{-n} \tag{6}$$

where the meaning of $\alpha_{L(H)}$ is explained in Fig. 1.

Precipitation. If the compound $M_mH_iL_n$ is quantitatively precipitated and the formation of $N_pH_jL_q$ masked, then eqn. (1) becomes

$$c_N = [(\beta_{min}^{\,q}/\beta_{pjq}^{\,n})\ (10^{-3}\, c_M)^{mq}\ \Psi_{MN}]^{1/(np)} \tag{7}$$

and, from [5],

$$c_L = [\beta_{min}\ \Phi_M^{-1}(10^{-3}\, c_M)^{-m}]^{1/n} + c_M^{\,n/m} \tag{8}$$

where c_M and c_L are the respective starting concentrations of M and L, and β_{min} and β_{pjq} are the solubility products of the above compounds. The logarithms of their values are always negative numbers and so cannot be confused with the overall stability constants (see Fig. 1).

Complexation. In the case of quantitative formation of the complex $M_mH_iL_n$ and total masking of the complex $N_pH_jL_q$ in the solution, eqn. (1) becomes

$$c_N = [(\beta_{min}{}^q/\beta_{pjq}{}^n)\,(m^q/p^n)\,10^{-3(mq+n)}\,c_M{}^{mq+n-q}\,\Psi_{MN}]^{1/(np)} \tag{9}$$

and, from [5]

$$c_L = [10^{3m}\,c_M{}^{1-m}\,(m\beta_{min}\,\Phi_M)^{-1}]^{1/n} + c_{Mn/m} \tag{10}$$

where β_{min} and β_{pjq} are the respective overall stability constants of the above complexes. The other symbols have the same meaning as above.

Extraction. If $M_mH_iL_n$ is extracted and the formation of $N_pH_jL_q$ avoided by masking, eqn. (1) becomes

$$c_N = \{(mP_{ML}\beta_{min})^q\,(10^3pP_{NL}\beta_{pjq})^{-n}\,(c_Ms_1)^{n-q}\,c_M{}^{mq}\,[1 - s_1(1 + 1/P_{ML})]^{mq}\,\Psi_{MN}\}^{1/(np)} \tag{11}$$

and, from [5]

$$s_xc_M(mP_{ML})^{-1}\,[c_{M(x)} - s_xc_M(1 + 1/P_{ML})]^{-m}\,[c_L - ns_xc_Mm^{-1}\,(1 + 1/P_{ML})]^{-n} = \beta_{min}\Phi_M \tag{12}$$

and

$$\sum_1^X s_x \geqslant 0.99 \tag{13}$$

where P_L, P_{ML}, P_{NL} are the respective partition coefficients of H_RL, $M_mH_iL_n$ and $N_pH_jL_q$; c_M, c_N and c_L are the total concentrations in both phases (the volumes of organic and aqueous phase are assumed equal); x designates the sequential number of extraction ($x = 1, 2, \ldots$); $c_{M(x)}$ is the total concentration of M during the x-th extraction ($c_{M(1)} = c_M$); X is the total number of extractions necessary to transfer at least 99% of M into the organic phase (see eqn. 13); s_x is the normalized parameter ($0 < s_x < 1$) to describe the progress of extraction.

With suitable optional values of c_L and c_M, iteration of eqn. (12) gives the number of extractions to satisfy eqn. (13). The value of $s_x + 0.01$, for which the left-hand side of eqn. (12) exceeds the right-hand side, determines the final value of s_x.

More complicated systems

If the system contains more masking ligands ($Y^1, Y^2, \ldots Y^U$) and more interfering metal ions ($N^1, N^2, \ldots N^V$), the masking function for each interfering metal ion has the form

$$\Psi_{MN^v} = [H]^{iq-jn}\,(\sum_1^U \alpha_{N(Y^u)})^{np}/(\sum_1^U \alpha_{M(Y^u)})^{mq} \tag{14}$$

where p, j, q can vary for each N^v. Again the condition $c_{Yu} \gg c_{N^v}$ must be

met for each masking ligand and interfering metal ion. The final optimum acidity can be calculated as an average value, or better as an optimum statistical value, taking into the account the possible concentration of each interfering element.

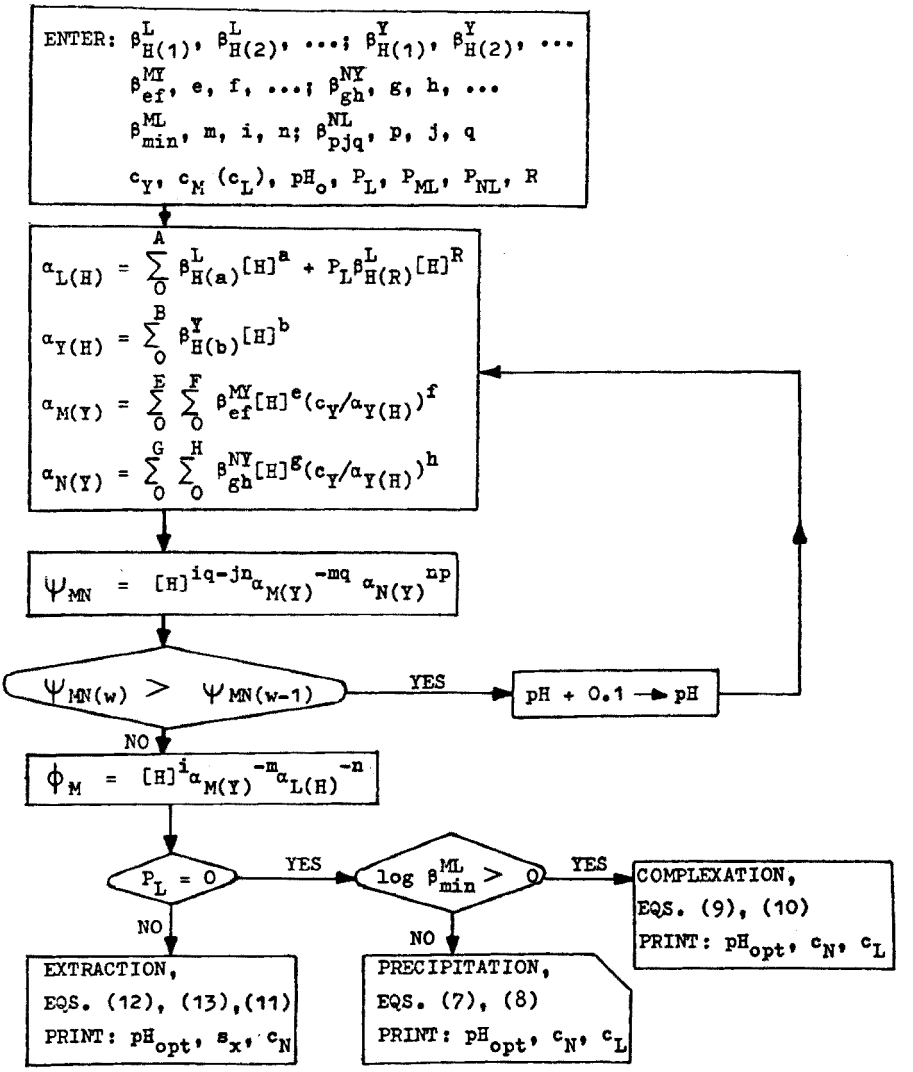

Fig. 1. Flow chart of the computer program for optimum masking in precipitation, complexation and extraction. The overall stability constants β corresponding to particular ligands or complexes are designated with superscripts L, Y, MY, NY, ML and NL; $\beta^{L}_{H(x)} = [H_xL]\,[H]^{-x}[L]^{-1}$, $\beta^{MY}_{ef} = [MH_eY_f]\,[M]^{-1}[H]^{-e}[Y]^{-f}$, $\beta^{ML}_{min} = [M_mH_iL_n]\,[M]^{-m}[H]^{-i}[L]^{-n}$, etc.

RESULTS AND DISCUSSION

The flow chart of all computations is given in Fig. 1. Optimum masking conditions for several precipitation and complexation reactions are given in Table 1. Masking for solvent extraction is shown in Table 2. The theory is compared with experimental conditions (further details can be found in each paper referred to) and reasonable agreement can be seen. Attention was given only to systems with EDTA and CDTA as masking reagents, because these systems have been fully described, which is not true for other systems, such as fluoride, cyanide, BAL etc.

The acidity optimum for masking (like the acidity optimum of formation of a particular complex [5]) does not depend on the concentrations of M, N and L and the stability constants of their complexes. It depends only on the complexation of M and N with the masking ligand (and the total concentration of the latter) and the composition of the complexes $M_mH_iL_n$ and $N_pH_jL_q$.

The shapes of several curves of the dependence $\log \Psi_{MN} = f(pH)$ are shown in Fig. 2. If $i > 0$, the curves usually exhibit a good maximum. If $i = 0$, the maximum is very flat with practically the same values of $\log \Psi_{MN}$ over an interval of 3—4 pH units. In these cases, it is useful to know the

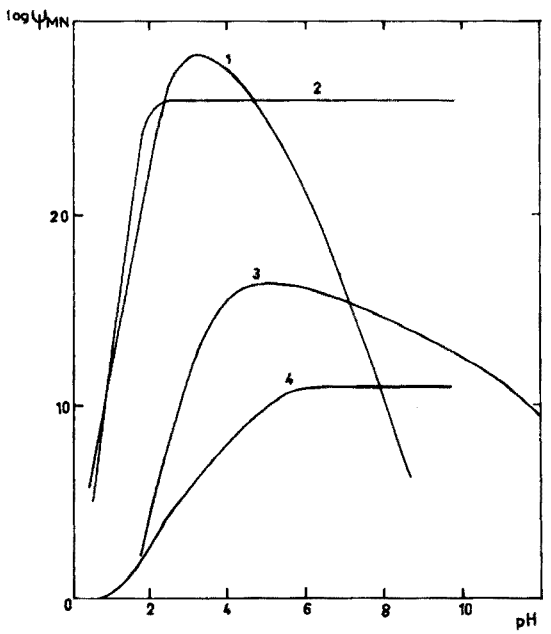

Fig. 2. The relationship $\log \Psi_{MN} = f(pH)$ in various systems of M—N—Y (m, i, n—p, j, q): (1) UO_2^{2+}—Fe^{3+}—CDTA (1, 1, 3—1, 0, 3); (2) Al^{3+}—Fe^{3+}—EDTA (1, 0, 3—1, 0, 3); (3) Ca^{2+}—Cu^{2+}—EDTA (1, 1, 3—1, 0, 2); (4) Ba^{2+}—Pb^{2+}—EDTA (1, 0, 1—1, 0, 1); $c_Y = 0.01$ M throughout.

TABLE 1

Optimum conditions of masking for precipitation and complexation[a]

N	p	j	q	$\log \Psi_{MN}$	$-\log \Phi_M$	pH_{opt}	c_N[b]	c_L[b]
Precipitation of calcium oxalate (CaC_2O_4)								
(c_M = 0.001 M, c_Y = 0.01 M EDTA, pH_{opt} = 4—5 [6])								
Cd^{2+}	1	0	1	5.89	1.39	4.7	1.0-3[c]	9.9-2
Cu^{2+}	1	0	1	8.19	1.39	4.7	1.0-3[c]	9.9-2
Fe^{2+}	1	0	1	3.59	1.39	4.7	4.9-5	9.9-2
La^{3+}	2	0	3	8.59	0.68	4.2	9.9-5	2.0-2
Mn^{2+}	1	0	1	3.43	1.39	4.7	1.0-3[c]	9.9-2
Ni^{2+}	1	0	1	7.99	1.39	4.7	1.0-3[c]	9.9-2
Pb^{2+}	1	0	1	7.71	1.39	4.7	1.0-3[c]	9.9-2
Th^{4+}	1	0	2	14.10	0.60	4.1	1.0-3[c]	1.7-2
Zn^{2+}	1	0	1	5.65	1.39	4.7	1.0-3[c]	9.9-2
Precipitation of uranyl oxinate (UO_2HOx_3)								
(c_M = 0.001 M, c_Y = 0.01 M EDTA, pH_{opt} = 5—9 [7])								
Al^{3+}	1	0	3	4.68	6.65	4.2	6.9-5	3.0-3
Ca^{2+}	1	0	2	—7.79	7.72	5.2	2.4-9	3.0-3
Cu^{2+}	1	0	2	16.84	7.93	5.3	1.0-3[c]	3.0-3
Fe^{3+}	1	0	3	30.48	6.65	4.2	1.0-3[c]	3.0-3
Pb^{2+}	1	0	2	15.40	7.93	5.3	1.0-3[c]	3.0-3
Zn^{2+}	1	0	2	9.22	7.93	5.3	1.0-3[c]	3.0-3
Precipitation of barium sulfate ($BaSO_4$)								
(c_M = 0.001 M, c_Y = 0.01 M EDTA, pH_{opt} = 4.5—5.0 [8])								
Ca^{2+}	1	0	1	2.74	2.29	7.0	6.6-9	2.2-2
Pb^{2+}	1	0	1	10.47	2.29	7.0	1.0-3[c]	2.2-2
Sr^{2+}	1	0	1	0.96	2.29	7.0	3.1-9	2.2-2
Complexation of iron(II) with 1,10-phenanthroline ($FePhen_3$)								
(c_M = $1.0 \cdot 10^{-5}$ M, c_Y = 0.01 M EDTA, pH_{opt} = 3—4 [9])								
Cd^{2+}	1	0	3	6.88	6.79	3.2	1.0-3[c]	1.8-4
Co^{2+}	1	0	3	6.28	6.79	3.2	1.0-3[c]	1.8-4
Cu^{2+}	1	0	3	13.78	6.79	3.2	1.0-3[c]	1.8-4
Fe^{3+}	1	0	3	32.68	6.79	3.2	1.0-3[c]	1.8-4
Hg^{2+}	1	0	3	22.76	6.79	3.2	1.0-3[c]	1.8-4
Mn^{2+}	1	0	3	—0.45	6.79	3.2	1.0-3[c]	1.8-4
Ni^{2+}	1	0	3	13.18	6.79	3.2	2.5-6	1.8-4
Pb^{2+}	1	0	3	12.34	6.79	3.2	1.0-3[c]	1.8-4
Tl^{3+}	1	0	3	70.78	6.79	3.2	1.0-6	1.8-4
Zn^{2+}	1	0	3	6.16	6.79	3.2	1.0-3[c]	1.8-4
Complexation of aluminium with tiron ($AlTir_2$)								
(c_M = $1.0 \cdot 10^{-5}$ M, c_Y = 0.01 M EDTA, pH_{opt} = 5—8 [10])								
Cd^{2+}	1	0	2	0.00	23.45	7.2	1.0-3[c]	2.7-2
Co^{2+}	1	0	2	—0.40	23.45	7.2	1.0-3[c]	2.7-2
Cu^{2+}	1	0	2	4.60	23.45	7.2	1.0-3[c]	2.7-2
Fe^{3+}	1	0	3	17.20	22.55	7.6	2.0-10	2.7-2
Ni^{2+}	1	0	2	4.20	23.45	7.2	1.0-3[c]	2.7-2
Pb^{2+}	1	0	2	3.64	23.45	7.2	1.0-3[c]	2.7-2
Zn^{2+}	1	0	2	—0.48	23.45	7.2	1.0-3[c]	2.7-2

[a]For the values of stability constants and solubility products used, see ref. 12.
[b]6.9-5 means the concentration $6.9 \cdot 10^{-5}$ M, etc.
[c]The value is limited by the concentration of EDTA.

TABLE 2

Optimum conditions of masking for extraction[a]

N	p	j	q	$\log \Psi_{MN}$	$-\log \Phi_M$	pH_{opt}	s_x	c_N[b]
Extraction of uranyl with thenoyltrifluoracetone in benzene (UO_2HTt_3)								
($c_M = 1.0 \cdot 10^{-5}$ M, $c_L = 0.1$ M, $c_Y = 0.01$ M EDTA, $pH_{opt} = 3.5$—8.0 [11])								
Al^{3+}	1	0	3	4.68	15.48	4.2	0.99	$1.0\text{-}3^c$
Ca^{2+}	1	0	2	−7.79	15.21	5.2	0.99	$1.0\text{-}3^c$
Ce^{3+}	1	0	3	3.44	15.48	4.2	0.99	$1.0\text{-}3^c$
Co^{2+}	1	0	2	9.37	15.21	5.3	0.99	$1.0\text{-}3^c$
Cu^{2+}	1	0	2	16.84	15.21	5.3	0.99	$1.0\text{-}3^c$
Fe^{3+}	1	0	3	30.48	15.48	4.2	0.99	$1.0\text{-}3^c$
Ga^{3+}	1	0	3	18.74	15.48	4.2	0.99	$1.0\text{-}3^c$
In^{3+}	1	0	3	31.34	15.48	4.2	0.99	$1.0\text{-}3^c$
La^{3+}	1	0	3	1.34	15.48	4.2	0.99	$1.0\text{-}3^c$
Mn^{2+}	1	0	2	2.59	15.21	5.3	0.99	$1.0\text{-}3^c$
Pb^{2+}	1	0	2	15.40	15.21	5.3	0.99	$1.0\text{-}3^c$
Sc^{3+}	1	0	3	30.59	15.48	4.2	0.99	$1.0\text{-}3^c$
Th^{4+}	1	0	4	26.79	15.84	3.9	0.99	$1.0\text{-}3^c$
U^{4+}	1	0	4	28.38	15.84	3.9	0.99	$1.0\text{-}3^c$
Y^{3+}	1	0	3	9.74	15.48	4.2	0.99	$1.0\text{-}3^c$
Zr^{4+}	1	0	4	39.39	15.84	3.9	0.99	$1.0\text{-}3^c$
Extraction of silver with dithizone in carbon tetrachloride (AgDz)								
($c_M = 1.0 \cdot 10^{-5}$ M, $c_L = 0.002$ M, $c_Y = 0.01$ M EDTA, $pH_{opt} = 4$ M—7.0 [11])								
Cd^{2+}	1	0	2	8.79	2.94	5.9	0.99	$1.0\text{-}3^c$
Co^{2+}	1	0	2	8.59	2.94	5.9	0.99	$1.0\text{-}3^c$
Cu^{2+}	1	0	2	11.10	2.94	5.9	0.99	$1.0\text{-}3^c$
Ga^{3+}	1	0	3	13.16	2.98	5.7	0.99	$1.0\text{-}3^c$
In^{3+}	1	0	3	17.36	2.98	5.7	0.99	$1.0\text{-}3^c$
Ni^{2+}	1	0	2	10.89	2.94	5.9	0.99	$1.0\text{-}3^c$
Zn^{2+}	1	0	2	8.60	2.94	5.9	0.99	$1.0\text{-}3^c$
Hg^{2+}	1	0	2	14.09	2.94	5.9	0.99	1.0-6

[a,b,c] See Table 1.

threshold of the maximum; this can be estimated on the basis of the relationship

$$\log \Psi_{MN(w)} \leqslant \log \Psi_{MN(w-1)} + 0.01 \qquad (15)$$

Tables 1 and 2 also show that the acidity optimum remains constant in a particular system of M, L, Y and different N if the values p, j, q are constant.

The use of just one masking reagent in eqn. (2) is sometimes an imperfect way of describing a system. At least, masking by metal hydrolysis should also be taken into account.

The masking function Ψ_{MN} together with the side-reaction function Φ_M represents a useful tool in theoretical descriptions of the reactions used in analytical chemistry. The optimum case occurs if both these functions reach their maximum values at the same acidity. The reaction system in

solution can be evaluated according to that. The masking function Ψ_{MN} does not specify what excess of c_N over c_M can be used. This is obvious from the equations for the calculation of c_N containing the stability constants (plus partition constants or solubility products) of compounds $M_mH_iL_n$ and $N_pH_jL_q$.

Finally, it should be emphasized that the problem does not lie in an inadequate theory of computation, but in our inadequate knowledge of the equilibria involved and their constants. With increasing complexity of calculation, the effect of errors in the determination of individual equilibrium constants becomes more significant and can lead to useless results.

In some simple cases, if the calculation is made separately and stepwise for pH_{opt}, Ψ_{MN}, Φ_M, s_x, c_N and c_L, even a personal calculator like HP-97, HP-67 (Hewlett-Packard) or SR-52 (Texas Instruments) can be used.

REFERENCES

1 A. Ringbom, Complexation in Analytical Chemistry, Interscience, New York, 1963.
2 W. B. Guenther, Chemical Equilibrium, Plenum, New York, 1976.
3 J. Inczédy, Analytical Applications of Complex Equilibria, Halsted Press, New York, 1976.
4 D. D. Perrin, Masking and Demasking of Chemical Reactions, Interscience, New York, 1970.
5 B. W. Budesinsky, Anal. Chim. Acta, 85 (1976) 117.
6 R. Přibil and L. Fiala, Chem. Listy, 46 (1952) 331.
7 R. N. Sen Sarma and A. K. Malik, Anal. Chim. Acta, 12 (1955) 329.
8 R. Přibil and D. Marincová, Chem. Listy, 46 (1952) 542.
9 F. Vydra and V. Marková, Z. Anal. Chem., 192 (1963) 347.
10 T. Yotsuyanagi, K. Goto and M. Nagayama, Nippon Kagaku Zasshi, 88 (1967) 1282.
11 J. Starý, Solvent Extraction of Metal Chelates, Pergamon, London, 1964.
12 L. G. Sillén and A. E. Martell, Stability Constants of Metal-Ion Complexes, The Chemical Society, Spec. Publ. 17, London, 1964; 2nd edn, Supplement No. 1, Spec. Publ. 25, 1971.

Analytica Chimica Acta, 91 (1977) 303—306

SPECTROPHOTOMETRIC DETERMINATION OF CYANIDE WITH γ-PICOLINE AND BARBITURIC ACID

SHIGERU NAGASHIMA

Department of Chemistry, Tokyo Metropolitan Industrial Technical Institute, Nishigaoka, Kita-ku, Tokyo (Japan)

(Received 1st November 1976)

SUMMARY

A spectrophotometric method for the determination of cyanide in water with a γ-picoline—barbituric acid reagent is described. Cyanide reacts with chloramine-T, and then the reagent is added to form a soluble violet-blue product, which is measured at 605 nm. Maximum absorbance is achieved within 5 min at 25 ± 1°C, and remains constant for about 30 min. This method is applicable to water samples containing 0—0.5 μg CN ml^{-1}. The reagent is stable for at least 3 weeks, if stored at about 10°C. The procedure can also be employed for the determination of thiocyanate.

Of the many methods for the spectrophotometric determination of cyanide based on the König reaction [1], the pyridine—pyrazolone method proposed by Epstein [2] and the pyridine—barbituric acid method of Asmus and Garschagen [3] have been generally used, since the carcinogenic properties of benzidine, which was used by Aldridge [4], became known. Although these two methods are very sensitive, they have the following defects: the pyridine—pyrazolone reagent is unstable and must be prepared daily; in the pyridine—barbituric acid method the color fades rapidly after maximum absorbance is reached.

Murty and Viswanathan [5] modified the method of Asmus and Garschagen by using bromine water instead of chloramine-T, and attempted to stabilize the developed color; but this procedure requires a lengthy heating time (40 min at 40°C). Lambert et al. [6] used a *N*-chlorosuccinimide—succinimide reagent instead of chloramine-T or bromine water, but this reagent is somewhat troublesome to prepare. Bark and Higson [7, 8] proposed a method with bromine water and pyridine—*p*-phenylenediamine reagent, and stated that the reagent was stable for 6 weeks; in fact the reagent must be prepared immediately before use.

In the present work, the color reactions of cyanide with several pyridine derivatives—barbituric acid reagents were examined. A relatively stable violet-blue product was formed when a γ-picoline—barbituric acid reagent was added to a cyanide solution which had been treated with chloramine-T. The γ-picoline—barbituric acid reagent was stable for at least 3 weeks, if stored at about 10°C.

EXPERIMENTAL

Apparatus and reagents

An Hitachi 124 double-beam spectrophotometer was used with 10-mm cells. Test tubes, 25 × 200 mm, fitted with ground stoppers, were used as reaction tubes.

All chemicals were of analytical-reagent grade. Deionized water was used throughout.

Standard cyanide solutions. Dissolve 2.50 g of potassium cyanide in water and dilute to exactly 1 l (1000 mg l^{-1}). Prepare working solutions by suitable dilution with water.

Buffer solution (pH 5.2). Dissolve 13.6 g of potassium dihydrogenphosphate and 0.28 g of disodium hydrogenphosphate in water and dilute to 1 l.

γ-Picoline—barbituric acid reagent. Place 3.0 g of barbituric acid and a small quantity of water in a 50-ml beaker. Add 15 ml of γ-picoline (4-methylpyridine) and 3 ml of concentrated hydrochloric acid (d = 1.18), while stirring to dissolve the acid. After cooling, dilute the mixture to 50 ml with water. The reagent obtained was light yellow.

Procedure

In a dried reaction tube, place 10.0 ml of sample solution containing less than 5 μg of cyanide. Add 5.0 ml of buffer solution and 0.25 ml of 1% (w/v) chloramine-T solution, stopper the tube and shake gently. After 1—2 min, add 3.0 ml of γ-picoline—barbituric acid reagent, stopper the tube again, mix, and keep the mixture at 25 ± 1°C for 5 min. Measure the absorbance at 605 nm against a reagent blank.

RESULTS AND DISCUSSION

Color development with pyridine derivative and barbituric acid

When pyridine is used [3], the color develops and fades rapidly. Several pyridine derivatives were therefore tested to replace pyridine. The color development was examined by the proposed procedure for a standard cyanide solution (5.0 μg CN^-/10 ml). Both α-picoline and β-picoline produced an orange-red color but the color formed with the β-picoline reagent faded rapidly. γ-Picoline, which formed a violet-blue color, was adopted because it gave a higher maximum absorbance than α-picoline. No color was developed with 2,6-lutidine.

Figure 1 shows the absorption spectra obtained by the proposed procedure with the γ-picoline—barbituric acid reagent. The wavelength of maximum absorption is ca. 605 nm.

The effect of time on color development was examined at 25 ± 1°C by varying the standing time after the addition of the γ-picoline—barbituric acid reagent. Maximum absorbance was achieved within 5 min, and the absorbance remained constant for about 30 min. The absorbance decreased

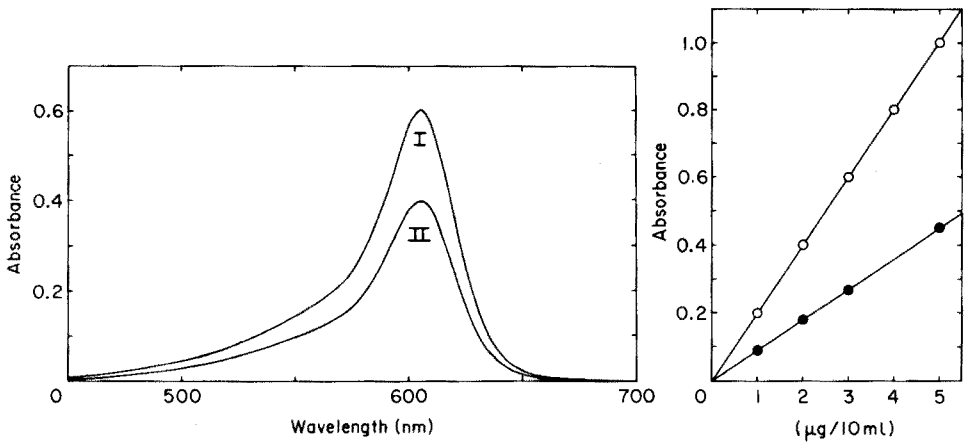

Fig. 1. Absorption spectra of the solution obtained by the proposed procedure with γ-picoline. CN^- taken: (I) 3.0 μg/10 ml, (II) 2.0 μg/10 ml. Reference: reagent blank.

Fig. 2. Calibration curves. (○) Cyanide, (●) thiocyanate. Reference: reagent blank.

by about 3% after 60 min and by about 7% after 120 min. These tests were made with 2.0 and 3.0 μg CN^-/10 ml.

Stability of the reagent

The γ-picoline—barbituric acid reagent was stored at about 10°C in a refrigerator, and the color development was examined by the proposed procedure over a period of time. The absorbance of the colored solutions obtained with the reagent stored for 3 weeks was almost the same as that with the newly prepared reagent. When the reagent was stored at room temperature, its color changed from light yellow to orange-yellow after about 7 days, and the colored solution obtained with this reagent was tinged with yellow.

Effect of experimental variables

According to Asmus and Garschagen [3], the amount of chloramine-T solution affects significantly the results of the pyridine—barbituric acid method. Thus, in the present work, the effect of varying the amount of the chloramine-T solution (0—1.0 ml) was examined. For 3 μg CN^-/10 ml, constant absorbance was obtained with 0.10—0.25 ml of the chloramine-T solution, but the absorbance decreased slightly when more than 0.5 ml was added. The amount of chloramine-T solution was therefore chosen as 0.25 ml.

The effect of standing time after the addition of the chloramine-T solution (0.25 ml) was tested. The absorbance did not change for standing times of 1—10 min.

The effect of the pH of the solution before the addition of the reagent solutions (chloramine-T and γ-picoline—barbituric acid reagent) was examined by varying the buffer solution of the proposed procedure. The absorbance was found to be constant in the pH range 3—9, but decreased remarkably above pH 9. As the sample solutions used for the cyanide determinations are ordinarily alkaline, a phosphate buffer solution (pH 5.2) was selected.

Effect of diverse ions

The effect of diverse ions was examined by using solutions containing 2.0 μg CN^- and various diverse ions. The results are shown in Table 1.

Calibration curves

As Table 1 shows, thiocyanate causes a significant positive error, and the error increases with increasing amount of thiocyanate. Standard thiocyanate solutions were therefore analyzed by the proposed procedure. Figure 2 shows the calibration curves obtained for thiocyanate solutions and cyanide solutions. Both show a good linear relationship.

TABLE 1

Effect of diverse ions on the determination of 2.0 μg CN^-/10 ml

Ion	Added as	Amount added (μg/10 ml)	CN^- found (μg)	Error (μg)
Cl^-	NaCl	1000	2.0	0.0
NO_2^-	$NaNO_2$	1000	2.0	0.0
NO_3^-	KNO_3	1000	2.0	0.0
SO_3^{2-}	Na_2SO_3	1000	1.9	−0.1
SO_4^{2-}	Na_2SO_4	1000	2.0	0.0
CH_3COO^-	$CH_3COONa \cdot 3\ H_2O$	1000	2.0	0.0
CNO^-	KCNO	1000	2.0	0.0
SCN^-	KSCN	2	2.9	+0.9
		5	4.3	+2.3
Fe^{3+}	$FeCl_3$	100	2.0	0.0
$Fe(CN)_6^{4-}$	$K_4[Fe(CN)_6] \cdot 3\ H_2O$	100	2.1	+0.1
$Fe(CN)_6^{3-}$	$K_3[Fe(CN)_6]$	100	2.1	+0.1

REFERENCES

1 W. König, J. Prakt. Chem., 69 (1904) 105.
2 J. Epstein, Anal. Chem., 19 (1947) 272.
3 E. Asmus and H. Garschagen, Fresenius' Z. Anal. Chem., 138 (1953) 414.
4 W. N. Aldridge, Analyst, 69 (1944) 262.
5 G. V. L. N. Murty and T. S. Viswanathan, Anal. Chim. Acta, 25 (1961) 293.
6 J. L. Lambert, J. Ramasamy and J. V. Paukstelis, Anal. Chem., 47 (1975) 916.
7 L. S. Bark and H. G. Higson, Talanta, 11 (1964) 471.
8 L. S. Bark and H. G. Higson, Talanta, 11 (1964) 621.

Analytica Chimica Acta, 91 (1977) 307—313

OBSERVATIONS ON THE REACTION BETWEEN NITRIC ACID AND BRUCINE

GIOVANNI PICCARDI and PAOLA CELLINI LEGITTIMO
Institute of Analytical Chemistry, University of Florence, 50121 Firenze (Italy)
(Received 19th July 1976)

SUMMARY

The reaction between nitric acid and brucine has been investigated by spectrophotometric and potentiometric methods. With cerium(IV) and dichromate the oxidation of brucine corresponds to two electrons per mole and the spectrum taken during oxidation is similar to that observed in the reaction with nitric acid. By studying the reaction of brucine with nitrous acid, and the effect of chloride ions, an interpretation of the oxidation reaction can be suggested and chemicals that interfere in practice can be indicated.

The nitrate—brucine reaction has long been known [1], but the quantitative potential of the reaction has been established only recently. Irreproducible results were obtained [2, 3] with a method that does not take into account uncontrolled heating during colour development. Other investigators [4—6] proposed the addition of the brucine reagent to a cold solution of a sample in sulphuric acid with subsequent transfer of the test tube to a bath of boiling water for 20 min. The aim of the present work was to investigate the reaction between brucine and nitrate in view of its application to the determination of nitrate in waters.

The effect of brucine and acid concentrations

In an attempt to obtain further information on the course of the reaction, the Jenkins—Medsker method [5] was simplified by omitting the addition of both sulphanilic acid and sodium chloride. For this purpose the reagent solution was prepared by dissolving brucine in 0.3 M hydrochloric acid.

The reaction between brucine and nitrate ions was studied in solutions of different sulphuric acid concentration. Figure 1 indicates that 60% sulphuric acid gives maximum colour development; the yellow colour does not form in solutions containing less than 40% sulphuric acid. In 60% H_2SO_4 the linearity of the calibration curve with $1 \cdot 10^{-5}$ mol of brucine covers the range 0—$2.5 \cdot 10^{-5}$ M nitrate (Fig. 2a, curve 1). With double or triple quantities of brucine the range of linearity is unchanged (Fig. 2a, curves 2 and 3). Obviously the range of linearity does not depend upon the ratio of reagents, but on the concentration of nitrate in solution. The

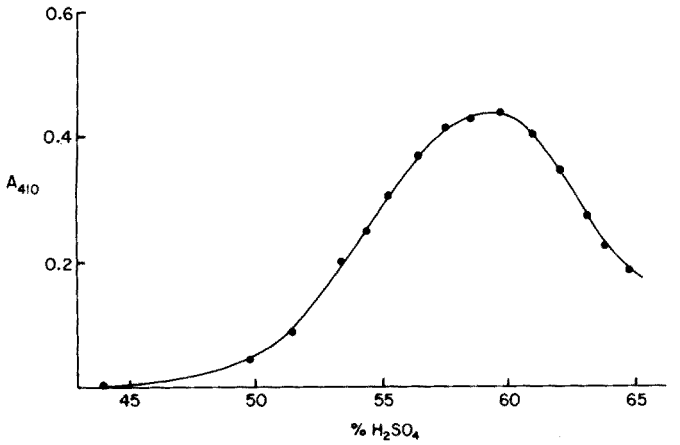

Fig. 1. Effect of H_2SO_4 concentration (w/w) on brucine—nitrate colour production. $1.25 \cdot 10^{-5}$ M NO_3^-; $5.7 \cdot 10^{-4}$ M brucine; $9.4 \cdot 10^{-2}$ M Cl^-.

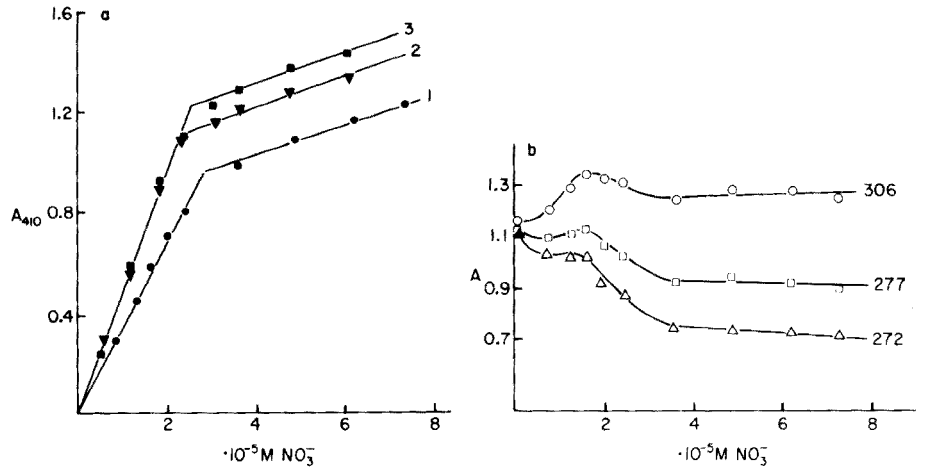

Fig. 2. Absorbance vs. nitrate concentration. (a) At 410 nm with brucine amounts 1. (•) $1 \cdot 10^{-5}$ mol; 2. (▾) $2 \cdot 10^{-5}$ mol; 3. (▪) $3 \cdot 10^{-5}$ mol. (b) In the u.v. range with $1 \cdot 10^{-5}$ mol brucine (5 ml of solution (a) diluted to 25 ml): (△) 272 nm, (□) 277 nm, (○) 306 nm.

concentration of nitrate ions in the reaction solution at the end of the linear portion of the calibration curve for the methods reported earlier [3—5] is close to $2.5 \cdot 10^{-5}$ M.

Further information about the reaction can be obtained from the ultraviolet spectra. A solution of brucine in 60% sulphuric acid shows three maxima, of almost the same molar absorptivity, at 272, 277 and 306 nm as shown by curve a of Fig. 3. The addition of nitrate modifies the spectrum and produces a band at 410 nm. The variation of absorbance with the quantity of nitrate ion at the three wavelengths is shown in Fig. 2(b). At the

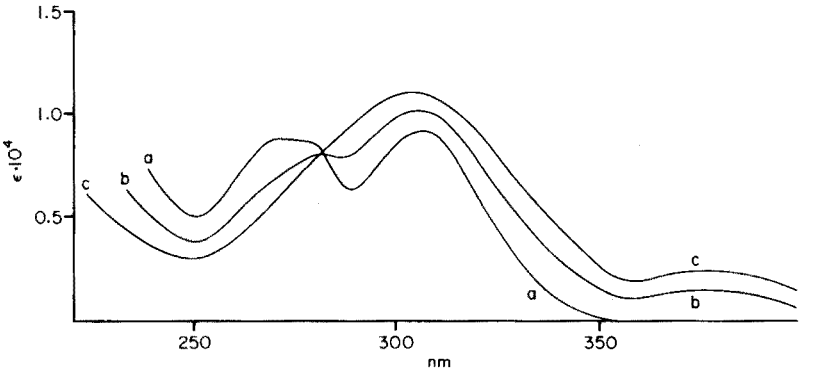

Fig. 3. Brucine spectra (a), at the end of linearity (b), at the maximum of A_{410} (c).

limit of linearity of A_{410} (ca. $5 \cdot 10^{-6}$ mol nitrate) the maxima at 272 and 277 nm are greatly reduced and that at 306 nm increases a little. The spectrum is shown by curve b in Fig. 3.

The colour of the brucine—nitrate reaction product increases up to about $2.5 \cdot 10^{-6}$ mol nitrate and then decreases as shown by Fig. 4(a). After the maximum, the 410-nm peak disappears and the background absorbance increases at higher wavelengths until it reaches a constant value. At $2.5 \cdot 10^{-6}$ mol the ultraviolet spectrum shows only one band at 306 nm (Fig. 3c). The complete disappearance of both maxima at 270 nm shows that brucine is no longer in solution. If all the brucine is converted to the yellow compound with a maximum at 410 nm it is possible to calculate that the molar absorptivity corresponds to $\epsilon = 2.5 \cdot 10^2$. The ratio of brucine to nitrogen is about 4:1. An analogous curve was found [7] for high nitrate concentrations

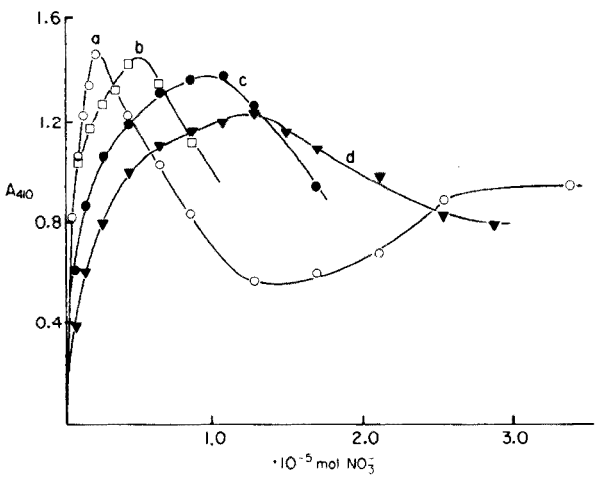

Fig. 4. Absorbance vs. HNO_3 mol in presence of (a) (○) 0.0; (b) (□) 3.0; (c) (●) 9.0; (d) (▼) $30 \cdot 10^{-6}$ mol sulphamic acid.

with the Jenkins—Medsker method [5], and the different molar ratio of brucine to nitrogen (2.5:1) found [5] must be ascribed to the presence of sulphanilic acid.

The addition of a substance which can destroy nitrites, e.g. sulphamic acid, to the brucine reagent modifies the 410-nm absorption as shown by Fig. 4, curves b—d. This is not produced by a kinetic phenomenon; all the measurements, after heating at 100°C for the 20 min recommended [6], reached an equilibrium value.

Reactions of brucine with oxidizing agents

In an attempt to interpret the reaction between brucine and nitrate, the behaviour of brucine with some oxidizing agents was examined. Brucine is partially oxidized in cold 60% sulphuric acid by cerium(IV) sulphate solution, giving first an orange and then a yellow compound. The reaction may be observed potentiometrically; the molar ratio of brucine to cerium, at the potential jump, is 1:2. In hot sulphuric acid it is not possible to obtain an equivalence point potentiometrically, because the cerium(IV) ions are involved in the subsequent oxidation of the organic substance. The spectral behaviour of the reaction between cerium and brucine is analogous to that of nitrates. In Fig. 5 the values reported were measured at four different wavelengths versus the quantity of oxidizing agent. The absorbance at 410 nm increases linearly to a molar ratio of brucine to cerium of 1:2, while the absorption bands at 272 and 277 nm decrease and vanish at the same molar ratio. At 410 nm the molar absorptivity of the oxidation product of brucine is about 2,500, which is the same as for the nitrate reaction. The points of the lower curve are all corrected for the absorption of cerium(III) ions produced during the reaction. The oxidation of brucine with potassium dichromate may also be followed potentiometrically; the oxidation corresponds to 2 electrons per mole. Potassium permanganate, potassium chlorate, and chlorine water also oxidize brucine with the formation of a yellow compound; this reaction is not quantitative, because even at low concentration the oxidative degradation begins.

Nitrites also react with brucine. In cold 60% sulphuric acid, in the absence of chlorides, the reaction instantaneously produces a pink colour that slowly changes to yellow. The ultraviolet and visible spectra show initially a strong decrease in the 272 and 277-nm peaks and the appearance of two peaks at 510 and 530 nm. At room temperature the two visible peaks are transformed slowly to one at 410 nm; one broad band at 290 nm also remains. In hot sulphuric acid the pink colour rapidly changes to yellow and the compound formed, with peaks at 306 and 410 nm is analogous to that formed in the reaction with nitrates. Figure 6 shows how the absorbance varies with the nitrite concentration for two different quantities of brucine. For both curves the inflection point corresponds to a concentration of about $2.5 \cdot 10^{-5}$ M, a value close to that for the reaction with nitrate. With increased nitrite the absorption at 410 nm increases and, as happens with

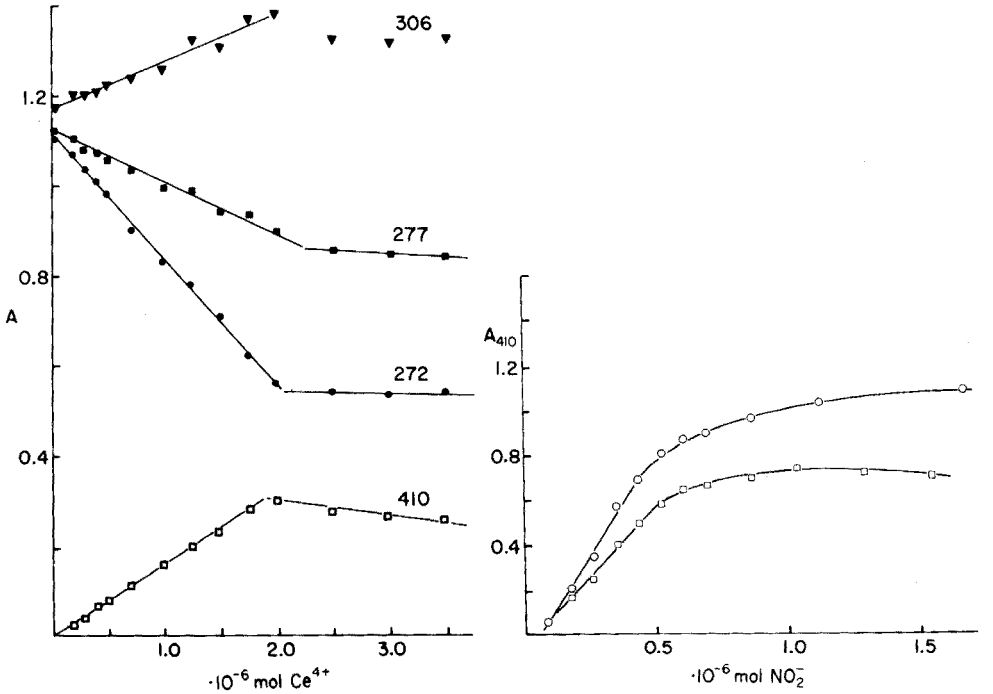

Fig. 5. Absorbance vs. cerium(IV) mol. (□) 410 nm, (●) 272 nm, (■) 277 nm, (▼) 306 nm. Brucine, $1 \cdot 10^{-6}$ mol (dilution 5 ml to 25 ml).

Fig. 6. Absorbance vs. HNO_2 mol. Brucine: (□) $5 \cdot 10^{-6}$ mol; (○) $1 \cdot 10^{-5}$ mol.

nitrate ions, reaches a maximum. In this case, however, at only $5 \cdot 10^{-6}$ moles, the absorbance reaches a value indicating the complete transformation of brucine into a yellow compound with the same spectroscopic properties as those of nitrate and cerium(IV).

The brucine—nitrate reaction

The reaction between nitrate and brucine does not take place instantaneously, but slowly in a hot solution and in the presence of chloride. The solution of brucine in 60% sulphuric acid does not react with relatively concentrated (1 M) nitric acid either in cold or hot solution but the addition of chloride to the hot solution instantaneously produces the yellow colour. The reactivity of nitrate in the presence of chloride may be ascribed to the known formation of oxidizing species e.g. nitrosyl and chlorine. Deno and co-workers [8] showed that in 60% sulphuric acid the nitrate ion is completely converted to nitric acid. The oxidation does not take place directly, but probably through an ion such as NO^+ [9]. Sandhu et al. [9] stated that brucine acts as a redox indicator in 2—3 M nitric acid, provided that urea is present. As is well known, urea reacts with nitrous acid,

forming nitrogen and carbon dioxide. A solution of nitrous acid plus nitric acid, without chloride ions, develops a yellow colour with an absorbance at 410 nm that is higher than that given by nitrite alone. The reaction takes place slowly in a hot solution; the heating produces the oxidizing agents, NO^+ and Cl_2. Brucine also reacts in a cold solution with nitrate and chloride provided that they are both converted previously, by heating, to the oxidizing species. The instantaneous reaction between brucine and nitrites can be explained in the same manner. Seel and Winkler [10] showed that, in 60% sulphuric acid, 90% of the nitrous acid is present as the NO^+ species. This is in agreement with the behaviour of sulphamic acid shown in Fig. 4. In this case, the range of linearity also decreases with increasing sulphamic acid concentration.

The quinoidal form of the yellow compound may be confirmed both by the electron number involved during the cerium(IV) and dichromate oxidation and by the discharge of colour by very mild reducing agents, e.g. SO_2. Moreover, a reversible change of colour (yellow to red) obtained on dilution suggests oxonium salt formation in sulphuric acid. The formation of bruciquinone may explain the red colour produced initially by several oxidizing agents in cold solution.

To employ the brucine method successfully for the determination of nitrate in water, it is essential to take into account some of the points made above. The yellow colour is an oxidation product; all oxidizing agents present react similarly with positive interference. Nitrite also interferes positively and must be destroyed previously with sulphamic acid, sulphanilic acid or urea.

The simultaneous addition of sulphanilic acid and brucine, as recommended in some papers, does not prevent the reaction between brucine and nitrous acid and the subsequent positive interference. Any excess of sulphamic acid or similar agents must not be present, because they lower the absorbance value.

EXPERIMENTAL

Reagents and equipment

All reagents were of analytical grade, dissolved in doubly distilled water. Every bottle of sulphuric acid was tested with brucine for nitric acid. Brucine solution was prepared by dissolving brucine sulphate heptahydrate in water or more usually in 0.3 M hydrochloric acid. Beckman DU Quartz and Uvispec SP 800 B recording spectrophotometers were used.

Procedure

Carefully transfer, by pipette, 6 ml of nitrate solution to a reaction test tube and add 10 ml of sulphuric acid solution (500 ml H_2SO_4 + 125 ml H_2O) and 1 ml of water or sulphamic acid solution. Place the tube in a cool water bath for at least 10 min and then add 0.5 ml of brucine reagent.

Mix thoroughly, and place the tube in a boiling water bath for exactly 20 min. Immerse the tube in a cold water bath for at least 15 min and read the absorbance value at 410 nm in 1-cm cells against a reagent blank.

REFERENCES

1 L. N. Winkler, Chem. Zentralbl., 23 (1899) 454; 25 (1901) 586.
2 A. E. Greenberg, J. R. Rossum, N. Moskowitz and P. A. Villarruz, J. Am. Water Works Assoc., 50 (1958) 821.
3 F. L. Fisher, R. E. Ibert and H. F. Beckman, Anal. Chem., 30 (1958) 1972.
4 H. Fadrus and J. Maly, Z. Anal. Chem., 202 (1964) 164.
5 D. Jenkins and L. L. Medsker, Anal. Chem., 36 (1964) 610.
6 Standard Methods for the Examination of Water and Sewage, 13th edn., American Public Health Association, New York, 1971.
7 J. G. Holty and H. S. Potworowski, Environ. Sci. Tech., 6 (1972) 835.
8 N. C. Deno, H. J. Peterson and E. Sacher, J. Phys. Chem., 65 (1961) 199.
9 S. S. Sandhu, S. C. S. Dhillon and D. Singh, Talanta, 13 (1966) 1702.
10 F. Seel and R. Winkler, Z. Phys. Chem. (Frankfurt), 25 (1960) 217.

Analytica Chimica Acta, 91 (1977) 315—324

EFFECT OF ELECTROLYTES ON LIQUID—LIQUID DISTRIBUTION AND KETO—ENOL TAUTOMERIC EQUILIBRIUM OF BENZOYLACETONE*

YASUKI YOSHIMURA and NOBUO SUZUKI

Department of Chemistry, Faculty of Science, Tohoku University, Aoba, Sendai 980 (Japan)

(Received 17th August 1976)

SUMMARY

The salt effect in solvent extraction of systems involving a β-diketone was investigated. The salting coefficients for the keto and enol tautomers of benzoylacetone in hydrochloric acid, sodium chloride, perchloric acid and sodium perchlorate solutions have been determined by liquid—liquid distribution and solubility measurements at 25°C. The values obtained by these methods agreed well. The salting coefficients for the keto tautomer were smaller than those for the enol tautomer in the respective electrolyte systems. A difference of the keto—enol tautomeric equilibrium in different aqueous electrolyte solutions may be explained by taking account of the activity coefficients of the tautomers in the aqueous electrolyte solutions. The distribution coefficient of the enol tautomer was also independent of the electrolytes when the activity coefficient was considered. The apparent change in the distribution ratios of benzoylacetone with electrolytes is caused by change of the activity coefficients of the respective tautomers in the aqueous electrolyte phases.

In a previous paper [1] the effect of solvents on the distribution of benzoylacetone (abbreviated BA) was studied; the distribution of BA was affected markedly by electrolytes in the aqueous phase. Even in liquid—liquid extraction systems involving metal chelates, such salt effects cannot be ignored. However, little is known about the salt effect in liquid—liquid extraction of non-electrolytes, such as organic reagents and their metal chelates. In an equilibrium or kinetic study of complicated extraction systems, quantitative treatment of the salt effect seems to be important. In this respect, a treatment of the salt effects on the distribution of a chelating agent itself may turn out to be simpler than the case involving metal chelates. It seems, at first, to be appropriate to study the influence of electrolytes on the distribution of the chelating agents themselves; this could provide fundamental information on salt effects in the extraction of metal chelates.

For β-diketones, which have been used widely as extractants for metal ions, few papers have dealt with the above problems [2, 3]. To clarify salt

*This paper is part of a doctoral thesis to be submitted by Y. Yoshimura to the Tohoku University.

effects on the distribution of β-diketones, it is necessary to examine the influence of several kinds of electrolyte on the distribution of the respective tautomers. In connection with the molecular structures or physical properties of the respective tautomers, the rôle of the electrolytes in the distribution of each of the tautomers is also of interest.

The purpose of this research was to clarify the behavior of BA in aqueous electrolyte solutions by both the liquid—liquid distribution and the solubility methods. The difference in the behavior of the tautomers of BA is discussed.

EXPERIMENTAL

Chemicals

BA was purified and dried as reported previously [1]. Sodium perchlorate was prepared by neutralizing perchloric acid with sodium carbonate, with subsequent recrystallization from water. The stock solution of sodium perchlorate was standardized gravimetrically by drying a 5-ml portion at ca. 80°C and by weighing as the anhydrous salt. Reagent-grade hydrochloric acid, perchloric acid, and sodium chloride were used without further purification. A stock solution (4 M) of sodium chloride was prepared by weighing sodium chloride dried for 2 h at ca. 120°C. The stock solutions of hydrochloric acid and perchloric acid were standardized by a similar gravimetric method after a 5-ml portion of the respective stock solutions had been neutralized (aqueous sodium hydroxide). n-Heptane was purified, dried [4] and distilled. Redistilled water was used.

Solubility measurement

The solubility of BA was determined with the apparatus shown in Fig. 1; BA (ca. 0.5 g) and ca. 150 ml of the desired aqueous electrolyte solution were placed in the apparatus, which was thermostated at 25 ± 0.2°C, and the mixture was stirred (magnetic stirrer) for ca. 72 h. The saturated solution was passed through a glass wool filter under pressure. A volume of the saturated solution suitable for the subsequent spectroscopic measurement was transferred by pipette to a 25-ml volumetric flask and diluted to the mark. The final concentration of electrolyte was adjusted to 0.1 M with the same electrolyte. The absorbance at 310 nm was measured; the concentration of BA was calculated from the molar absorptivity. The solubility of BA in terms of molarity was calculated by

$$S = C \times 25 \times 1/A \qquad (1)$$

where S and C denote the solubility and the concentration of BA, respectively and A indicates the volume (ml) of saturated solution taken. As shown in Table 1, equilibrium appears to be reached within ca. 24 h. However, all of the sample runs were equilibrated for ca. 72 h and the solubility measurements were made from 6 to 10 replicate samples. The relative deviation from the mean values was ±0.4%. To confirm equilibrium attainment, a

TABLE 1

Solubility of benzoylacetone in water at 25°C

Medium	Equilibration time (h)	Solubility S^0 ($\cdot 10^{-3}$ mol l^{-1})	Medium	Equilibration time (h)	Solubility S^0 ($\cdot 10^{-3}$ mol l^{-1})
10^{-4} M HCl	24	2.41_5	10^{-3} M HCl	24	2.41_5
	36	2.42_5		48	2.42_0
	48	2.40_6	10^{-4}M $HClO_4$	24	2.42_3
	56	2.43_0		40	2.40_8
	70	2.42_3		72	2.41_3
		Mean $2.41_8 \pm 0.00_6$			

sample was equilibrated for 24 h at 40°C and then for 72 h at 25°C. The solubility value obtained agreed within experimental error with that obtained when equilibrium was approached from undersaturation.

Determination of keto—enol tautomerism constants of BA in aqueous electrolyte solutions

To determine the tautomerism constants of BA in the aqueous electrolyte solutions, the molar absorptivities of BA at 310 nm in the aqueous electrolyte solutions were measured independently three times [1]. The absorption maximum at 310 nm in the aqueous solutions has been assigned to the enol tautomer of BA [5]. The wavelength at maximum absorption was not affected by the electrolytes. The tautomerism constant k'_{aq}, was calculated by

$$k'_{aq} = (1 - \epsilon/\epsilon_e)/(\epsilon/\epsilon_e) \quad (2)$$

where ϵ denotes the measured apparent molar absorptivity and ϵ_e the molar absorptivity of the enol tautomer at 310 nm. From the apparent ϵ of 5150 l mol^{-1} cm^{-1} [1] and the enol tautomer content of 34.1% in 0.001 M hydrochloric acid solution [6, 7], ϵ_e was estimated as 15100 l mol^{-1} cm^{-1}; s_r was within 1%.

The distribution ratios of BA between n-heptane and the aqueous electrolyte solutions were determined with the apparatus and procedure reported previously [1]; s_r for four determinations was within 1%. All experiments were carried out at 25 ± 0.3°C.

RESULTS

The solubility of BA in pure water is given in Table 1. Benzoylacetone is a weak acid (pK_a = 8.69 [8]) and partly dissociates in pure water. The aqueous solution was made slightly acidic to prevent this dissociation. Table 1 shows that equilibrium is attained within 24 h; the solubility is constant irrespective of small concentrations of acids and can be regarded as the solubility of BA in pure water.

The solubilities of BA in aqueous solutions of different electrolytes are given in Table 2. With the sodium chloride and sodium perchlorate systems, small amounts of hydrochloric or perchloric acid (0.001 M) were added to the respective aqueous electrolyte solutions; this condition was maintained throughout the solubility and distribution experiments.

The keto—enol tautomerism constants of BA in the aqueous electrolyte solutions, defined as the concentration ratio of keto to enol tautomers, are given in Table 3. The keto tautomer content increased with increased electrolyte concentration for all the electrolytes studied. N.m.r. spectrometry showed that the keto tautomer content of acetylacetone also increased with an increase in the concentration of sodium perchlorate [9].

The distribution ratios of BA between n-heptane and the aqueous electrolyte solutions are given in Table 4. n-Heptane was chosen because of its low water solubility and its high boiling point, factors expected to give high reproducibility in the distribution ratio measurements. From both the solubility and distribution ratio measurements, BA is apparently salted-in

TABLE 2

Solubility of benzoylacetone in aqueous electrolyte solutions at 25°C[a]

Electrolyte	Electrolyte concentration (mol l^{-1})			
	0.5	1.0	1.5	2.0
HCl	$2.47_1 \pm 0.00_7$	$2.52_8 \pm 0.01_0$	$2.62_0 \pm 0.00_4$	$2.73_8 \pm 0.00_6$
$HClO_4$	$3.39_9 \pm 0.01_0$	$4.48_7 \pm 0.01_2$	$5.72_2 \pm 0.01_7$	$7.27_2 \pm 0.01_3$
NaCl[b]	$2.05_4 \pm 0.00_5$	$1.63_9 \pm 0.01_0$	$1.39_4 \pm 0.00_3$	$1.13_6 \pm 0.00_4$
$NaClO_4$[c]	$2.78_5 \pm 0.01_0$	$2.99_5 \pm 0.00_3$	$3.13_5 \pm 0.00_8$	$3.25_9 \pm 0.01_1$

[a] $S(\cdot 10^{-3}$ mol $l^{-1})$, given as the mean value ± the relative deviation from 6—10 determinations.
[b] Contains 10^{-3} M HCl.
[c] Contains 10^{-3} M $HClO_4$.

TABLE 3

Tautomerism constant of benzoylacetone in aqueous electrolyte solutions at 25°C[a]

Electrolyte	Electrolyte concentration (mol l^{-1})				
	0.1	0.5	1.0	1.5	2.0
HCl	1.98 ± 0.03	2.03 ± 0.01	2.07 ± 0.02	2.09 ± 0.01	2.10 ± 0.01
$HClO_4$	2.00 ± 0.02	2.07 ± 0.01	2.20 ± 0.04	2.30 ± 0.02	2.38 ± 0.02
NaCl[b]	2.02 ± 0.01	2.14 ± 0.01	2.32 ± 0.01	2.46 ± 0.01	2.64 ± 0.02
$NaClO_4$[c]	2.01 ± 0.02	2.21 ± 0.02	2.45 ± 0.02	2.69 ± 0.02	2.95 ± 0.02

[a] Defined as a concentration ratio of keto to enol, calculated from the apparent molar absorptivity at 310 nm, and given as the mean value ± the relative deviation from 3 measurements.
[b,c] See footnotes to Table 2.

TABLE 4

Distribution ratio of benzoylacetone between n-heptane and aqueous electrolyte solution at 25 °C[a]

Electrolyte	Electrolyte concentration (mol l^{-1})				
	0.1	0.5	1.0	1.5	2.0
HCl	$98.8_0 \pm 0.4_0$	$98.0_0 \pm 0.2_9$	$95.9_9 \pm 0.4_0$	$93.2_5 \pm 0.3_5$	$89.2_6 \pm 0.4_4$
$HClO_4$	$91.4_2 \pm 0.2_6$	$72.6_0 \pm 0.0_8$	$55.0_7 \pm 0.1_6$	$43.3_1 \pm 0.1_0$	$34.7_8 \pm 0.1_9$
NaCl[b]	$101._7 \pm 0._3$	$117._9 \pm 0._4$	$148._4 \pm 0._4$	$179._3 \pm 1._3$	$212._0 \pm 0._9$
$NaClO_4$[c]	$96.0_9 \pm 0.1_4$	$87.1_1 \pm 0.3_1$	$81.5_9 \pm 0.2_7$	$76.8_4 \pm 0.3_3$	$74.7_8 \pm 0.6_3$

[a]Given as the mean value ± the relative deviation from 4 determinations; the initial concentration of BA in n-heptane phase was 0.0250 M.
[b,c]See footnotes to Table 2.

with hydrochloric acid, perchloric acid, and sodium perchlorate, and salted-out with sodium chloride. Similar behavior with perchloric acid and sodium perchlorate has been observed [2, 3].

To evaluate the salt effect on the distribution and solubility of each of the tautomers, their solubilities and distribution coefficients were estimated as follows. The apparent distribution coefficient, P'_e, of the enol tautomer between an aqueous electrolyte solution and n-heptane, in which the keto

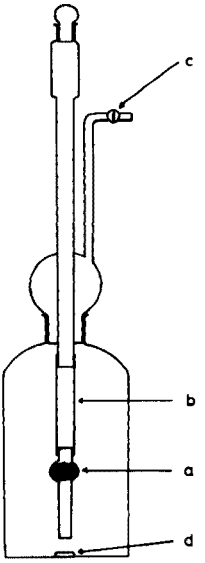

Fig. 1. Apparatus for solubility measurement. (a) Filter filled with glass wool. (b) Vinyl tube. (c) Stop-cock for injecting air. (d) Magnetic stirring bar.

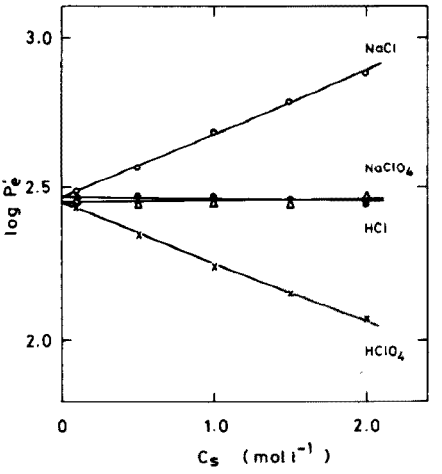

Fig. 2. Plot of logarithmic apparent distribution coefficient for enol tautomer of benzoylacetone between n-heptane and aqueous electrolyte solution (log P'_e) against concentration of electrolyte (C_S). Straight lines calculated by method of least squares.

tautomer can be neglected (by n.m.r. spectrometry), is calculated by

$$P'_e = D \times (1 + k'_{aq}) \quad (3)$$

where D indicates the overall distribution ratio of BA summarized in Table 4. The solubility of the enol tautomer in an aqueous electrolyte solution, S_e, and that of the keto tautomer, S_k, are calculated by the following equations, respectively

$$S_e = S/(1 + k'_{aq}) \quad (4)$$

$$S_k = S - S_e \quad (5)$$

In eqns. (4) and (5), S denotes the apparent solubility of BA in the aqueous electrolyte solutions given in Table 2, and it is assumed that the tautomerism constants given in Table 3 may also be adopted for saturated solutions of BA because of its relatively low solubility. It has not yet been confirmed whether BA is a mixture of two tautomers in the solid phase, but it can be assumed that the chemical potentials of the two tautomers in the solid phase are identical. On this assumption, it seems that the conception of solubility for each tautomer has a normal thermodynamic meaning as in a solution equilibrium, i.e. the chemical potential of a solute in the liquid phase is identical to that in its pure solid phase.

Generally, the activity coefficient, f_i, of non-electrolyte, i, in aqueous electrolyte solutions may be expressed [10] by

$$\log f_i = k_s C_s + k_i C_i \quad (6)$$

where C_s and C_i indicate the molar concentrations of electrolyte and non-electrolyte, respectively, and k_s and k_i are referred to as the salting coefficient and the non-electrolyte self-interaction coefficient, respectively. When C_i is low, the term $k_i C_i$ may be omitted. Therefore, the distribution coefficient can be related to the electrolyte concentration [11] by

$$\log P'_i = \log P_i - \log (f_i)_{org} + k_s C_s \quad (7)$$

where P'_i and P_i indicate the apparent distribution coefficient and the thermodynamic distribution coefficient of the non-electrolyte, respectively, and $(f_i)_{org}$ denotes the activity coefficient of the non-electrolyte in the organic phase. The plot of $\log P'_i$ vs. C_s should give a straight line with slope k_s provided that the $(f_i)_{org}$ is kept constant. Figure 2 shows that such a plot gives straight lines for the respective electrolytes in accordance with eqn. (7). The salting coefficients obtained by least squares analysis are listed in Table 5.

On the other hand, as the chemical potential of the non-electrolyte in saturated solution equals that of its pure solid phase, the solubility can be related to the electrolyte concentration [10] by

$$\log (S_i^0/S_i) = \log (f_i/f_i^0) = k_s C_s \quad (8)$$

TABLE 5

Salting coefficients (in l mol^{-1}) for the enol tautomer from distribution ratio determinations and for the keto ($k_{s(k)}$) and enol ($k_{s(e)}$) tautomers at 25°C from solubility measurements[a]

Electrolyte	$k_{s(e)}$[b]	$k_{s(k)}$[c]	$k_{s(e)}$[c]
HCl	−0.014 ± 0.005	−0.033 ± 0.002	−0.023 ± 0.004
$HClO_4$	−0.193 ± 0.009	−0.232 ± 0.006	−0.192 ± 0.003
NaCl	0.213 ± 0.010	0.151 ± 0.005	0.211 ± 0.007
$NaClO_4$	0.006 ± 0.007	−0.068 ± 0.005	0.015 ± 0.004

[a]Errors are given as the relative deviation of each experimental point from the straight line drawn by the method of least squares in Figs. 2 (for column 2) and 3 (for columns 3 and 4).
[b]From distribution ratio measurements.
[c]From solubility measurements.

and therefore,

$$\log S_i = \log S_i^0 - k_s C_s \tag{9}$$

where S_i^0 and f_i^0 denote the solubility and the activity coefficient of the non-electrolyte in pure water, respectively. Figure 3 shows that the plots of $\log S_i$ vs. C_s give straight lines for both the enol and keto tautomers in accordance with eqn. (9). The salting coefficients for these two tautomers are also listed in Table 5.

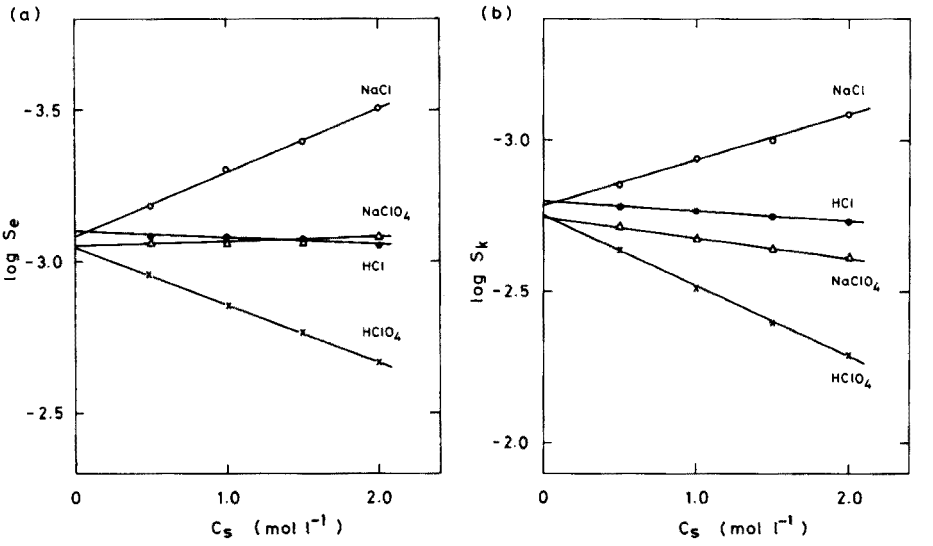

Fig. 3. Plot of logarithmic solubility for keto and enol tautomers of benzoylacetone in aqueous electrolyte solution (log S) against concentration of electrolyte (C_s). (a) For enol tautomer. (b) For keto tautomer. Straight lines are drawn by method of least squares.

DISCUSSION

Although various theoretical approaches have been tried to explain the salt effects, the McDevit—Long theory [12] seems to have been most widely applied [13]. The salting coefficient can be expressed [12] by

$$k_s = \bar{V}_i^0 \times (V_s - \bar{V}_s^0)/2.3\beta_0 RT \qquad (10)$$

where $\bar{V}_i^0$, V_s, $\bar{V}_s^0$, and β_0 indicate the partial molar volume of non-electrolyte at infinite dilution, the molar volume of pure (liquid) electrolyte, the partial molar volume of electrolyte at infinite dilution, and the compressibility of pure water, respectively. The term $(V_s - \bar{V}_s^0)$ is a measure of the electrostriction produced by the electrolyte. In this theory, the salting coefficient is expressed as a result of the effect of the electrolyte upon the internal pressure of the solvent, and thus on the energy required to create a hole for the non-electrolyte molecule. This theory predicts accurately not only the sequence of the salting coefficients for various electrolytes, but also the salting-in effect of large electrolytes such as perchloric acid (which gives a negative value for $(V_s - \bar{V}_s^0)$) but it predicts much higher values than the experimental ones for the salting coefficients [10, 12]. As shown in Table 5, the salting coefficients of the keto tautomer were lower than those of the enol tautomer for all the electrolytes studied. If eqn. (10) is valid for BA, the difference in the salting coefficients of two tautomers for a given electrolyte may be ascribed to the difference in $\bar{V}_i^0$ of two tautomers. Osugi et al. [14] estimated the molar volumes of the keto and enol tautomers of acetylacetone and ethyl acetoacetate to be 116.4, 102.6 and 126.5, 115.5 ml mol^{-1}, respectively. By analogy, the keto tautomer of BA will also have a larger volume than the enol tautomer, though data for the two tautomers of BA are not available. However, a discussion based on the volume contribution cannot give a clear explanation for the finding that, for the keto tautomer in comparison with the enol tautomer, perchloric acid causes a larger salting-in effect and sodium chloride causes a smaller salting-out effect. Essentially, the McDevit—Long theory [12] is only valid for non-polar non-electrolytes, i.e. in this theory, it is assumed that a non-polar non-electrolyte occupies a volume and that interactions between a non-polar non-electrolyte and its surroundings are identical in water and in aqueous electrolyte solution. It has been confirmed experimentally that a polar non-electrolyte exhibits a lower salting coefficient than a non-polar one for a given electrolyte; this has been predicted by electrostatic theories [10, 15]. Accordingly, the finding that the keto tautomer exhibits a lower salting coefficient than the enol tautomer can be understood by considering that the former is more polar than the latter. This assumption has also been discussed previously [1]. A trial calculation of a theoretical value of the salting coefficients by eqn. (10) cannot be made because $\bar{V}_i^0$ is unknown for these tautomers. However, the sequence of salting coefficients listed in Table 5 is NaCl > HCl ~ $NaClO_4$ > $HClO_4$, the same

order as $(V_s - \bar{V}_s^0)$ for all electrolytes. Thus, the salt effects on the respective tautomers of BA may be explained qualitatively by both the McDevit—Long theory and their polarity [10].

The sequence of the apparent molar absorptivities of BA at 310 nm (i.e. of the enol tautomer contents) $HCl > HClO_4 > NaCl > NaClO_4$ (cf. Table 3), clearly differs from the order of salting coefficient, $NaCl > HCl \sim NaClO_4 > HClO_4$, but agrees with the reversed order of the absolute value of difference between the salting coefficient of the keto tautomer and that of the enol tautomer ($|k_{s(k)} - k_{s(e)}|$) (cf. Table 5). As can be derived from eqn. (8), for a given electrolyte, the keto tautomer exhibiting the lower salting coefficient gives a lower activity coefficient in the same electrolyte solution than the enol tautomer exhibiting the higher salting coefficient. However, the lower the activity coefficient of the keto tautomer, the higher its content, i.e. the lower the enol tautomer content. For all electrolytes studied, the salting coefficients of the keto tautomer are lower than those of the enol tautomer; a decrease in the content of enol tautomer, i.e., an increase in the keto—enol tautomerism constants (cf. Table 3) therefore results. Furthermore, among the electrolytes, one giving a higher value of $|k_{s(k)} - k_{s(e)}|$ makes the activity coefficient of the keto tautomer, compared with the enol tautomer, lower than one giving a lower value of $|k_{s(k)} - k_{s(e)}|$. The content of enol tautomer in the former solution is therefore lower than that in the latter solution. Thus, a reasonable explanation is that the order of the enol tautomer content agrees with the reversed order of $|k_{s(k)} - k_{s(e)}|$. The overall effect of an electrolyte must be discussed from two standpoints; an effect on the ratio of the activity coefficients of the keto and enol tautomers, and an effect on the activity coefficient itself of each of the tautomers.

For the enol tautomer, the salting coefficients estimated from the distribution ratio measurement agree well with those from the solubility measurement for all the electrolytes studied (cf. Table 5). Accordingly, it can be concluded that a variation in the distribution ratio with electrolytes is caused by a change in the activity coefficients of the keto and enol tautomers in the aqueous phases. Figure 4 shows that the thermodynamic distribution coefficient of the enol tautomer and tautomerism constant applied activity coefficients corrections are nearly constant, independent of the electrolytes, as expected. The thermodynamic tautomerism constant, k_{aq}, was calculated from

$$k_{aq} = (f_k/f_e) \times k'_{aq} \tag{11}$$

where subscripts k and e denote the keto and enol tautomers of BA, respectively. Assuming that the activity coefficient of the enol tautomer in n-heptane is unity (which seems to be valid because a low initial concentration of BA (0.0250 M) and high distribution ratio results in virtually constant equilibrium concentration of BA in the organic phase), the thermodynamic distribution coefficient of the enol tautomer, P_e, is calculated by

$$P_e = P'_e/(f_e)_{aq} \tag{12}$$

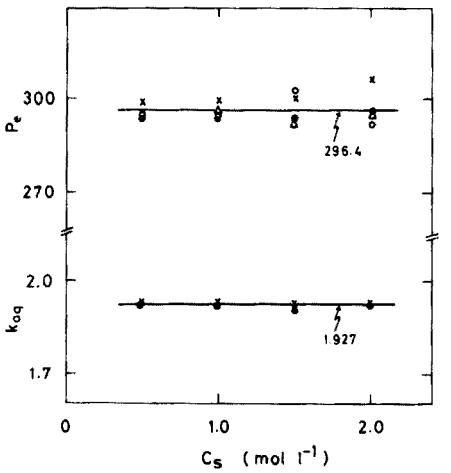

Fig. 4. Plot of thermodynamic distribution coefficient for enol tautomer (P_e) and tautomerism constant (k_{aq}) of benzoylacetone against concentration of electrolyte (C_s). Straight lines indicate mean values of all points. (○) NaCl, (●) HCl, (△) $NaClO_4$, (×) $HClO_4$.

The activity coefficients of the respective tautomers in the aqueous electrolyte solutions are obtained from eqn. (8) by assuming that their activity coefficients in pure water are unity; this is valid because of the low solubility of BA. The mean values of all data corrected for activity coefficient were 296.4 and 1.927 for the thermodynamic distribution coefficient of the enol tautomer and the thermodynamic tautomerism constant, respectively. These values agree satisfactorily with the distribution coefficient of the enol tautomer between n-heptane and water (291.2), and the tautomerism constant in water (1.93).

REFERENCES

1 Y. Yoshimura and N. Suzuki, Anal. Chim. Acta, 85 (1976) 383.
2 H. Johansson and J. Rydberg, Acta Chem. Scand., 23 (1969) 2797.
3 T. Sekine, Y. Hasegawa and N. Ihara, J. Inorg. Nucl. Chem., 35 (1973) 3968.
4 J. A. Riddick and W. B. Bunger, Techniques of Chemistry, Vol. VII, Organic Solvents, Wiley-Interscience, New York, 3rd edn., 1970, pp. 597—598.
5 R. A. Morton, A. Hassan and T. C. Calloway, J. Chem. Soc., (1934) 883.
6 M. L. Eidinoff, J. Am. Chem. Soc., 67 (1945) 2073.
7 M. Bergon and J. P. Calmon, Bull. Soc. Chim. Fr., (1972) 1020.
8 M. L. Eidinoff, J. Am. Chem. Soc., 67 (1945) 2072.
9 H. Watarai and N. Suzuki, unpublished data.
10 F. A. Long and W. F. McDevit, Chem. Rev., 51 (1952) 119.
11 J. G. Mason and I. Lipschitz, Talanta, 13 (1966) 1462.
12 W. F. McDevit and F. A. Long, J. Am. Chem. Soc., 74 (1952) 1773.
13 See e.g., E. Grunwald and A. F. Butler, J. Am. Chem. Soc., 82 (1960) 5647; N. C. Deno and C. H. Spink, J. Phys. Chem., 67 (1963) 1347; J. E. Gordon and R. L. Thorne, J. Phys. Chem., 71 (1967) 4390; R. Aveyard and R. Heselden, J. Chem. Soc., Faraday Trans 1, 71 (1975) 312.
14 J. Osugi, T. Mizukami and T. Tachibana, Nippon Kagaku Zasshi, 88 (1967) 721.
15 P. M. Gross, Chem. Rev., 13 (1933) 91.

Analytica Chimica Acta, 91 (1977) 325—329

Short Communication

DOSAGE SIMULTANÉ DU PLOMB ET DE L'ÉTAIN PAR POLAROGRAPHIE À TENSION ALTERNATIVE SURIMPOSÉE. APPLICATION AUX SOUDURES COMMERCIALES ÉTAIN PLOMB À AME DÉCAPANTE

A. M. SHAFIQUL ALAM et OLIVIER VITTORI

Laboratoire de Chimie Analytique III, 43, Bd du 11 Novembre 1918, 69621-Villeurbanne (France)

HÉLÈNE TERSIGNI* et GILLES COURTOIS

Service Central de Microanalyse, 2, rue Henry Dunant, 94320-Thiais (France)

(Reçu le 15 septembre 1976)

Le problème posé par le dosage simultané de plomb (II) et étain (IV) en milieu aqueux par polarographie n'a été jusqu'à présent résolu que par le biais d'une séparation préalable, sur résine échangeuse ou d'une complexation d'un des éléments. Dans le cas du plomb qui est réductible reversiblement dans la plupart des électrolytes supports usuels, le dosage polarographique est en règle générale simple et sensible. Le cas de Sn(IV) est plus ardu car Lingane [1] a montré qu'en milieu perchlorique l'espèce $Sn(H_2O)_6^{4+}$ n'est pas électroréductible, et seule la présence d'ions chlorure permet d'obtenir $SnCl_6^{2-}$ qui est électroactif selon

$$SnCl_6^{2-} + 2e \rightleftharpoons SnCl_4^{2-} + 2Cl^- \quad E_{\frac{1}{2}} : -0{,}25 \text{ V/ECS}$$

$$SnCl_6^{2-} + 4e \rightleftharpoons Sn^0 + 6Cl^- \quad E_{\frac{1}{2}} : -0{,}52 \text{ V/ECS.}$$

Il se trouve qu'il faut utiliser un milieu HCl 1 M—NH_4Cl 4 M et dans ce cas la vague du plomb est confondue avec la seconde de l'étain à −0,52 V/ECS.

Des tentatives nombreuses ont été effectuées dans divers milieux pour parvenir à utiliser la polarographie pour les mélanges plomb—etain, mais il faut mentionner aussi que des méthodes très classiques comme la précipitation [2], l'extraction liquide—liquide [3, 4] et la complexation [5] sont encore d'actualité. Des méthodes spectrales comme l'absorption atomique [6—8], la spectroscopie d'emission [9] et la fluorescence-x [10] sont aussi utilisées mais les sensibilités sont moyennes. Notons encore l'analyse par activation [12]. Souvent il y a couplage de plusieurs méthodes comme séparation sur résine puis spectrophotométrie ou electrochimie [11].

* Adresse présente: Division de Lyon du SCM, 43, Bd du 11 Novembre 1918, 69621-Villeurbanne (France)

De toutes ces techniques la moins coûteuse à performances égales est la polarographie d'autant qu'avec des soudures étain—plomb, malgré les dilutions dues à la mise en solution des échantillons les concentrations restent dans la gamme 10^{-3}—10^{-5} M. Des essais de dosage simultané ont déjà été réalisés par polarographie à radiofréquence [13], par oscillopolarographie dans HCl 6 M—HBr 6 M [14] et par polarographie à tension alternative surimposée (p.t.a.s.) dans H_3PO_4—HBr [15]. Cependant dans ces milieux très concentrès et acides le facteu séparation n'est pas très favorable et l'objet du présent article est de montrer qu'en choisissant un électrolyte support contenant de l'iodure d'ammonium, en milieu HCl 0,5 M, la séparation des pics de Sn et Pb, en p.t.a.s. est satisfaisante.

Partie Expérimentale

Electrolyte support. La préparation de l'électrolyte support requiert quelques précautions. Après pesée de la quantité convenable de NH_4I, le sel est dissous dans un minimum d'eau distillée préalablement désoxygénée par un courant d'azote (maintenu ensuite). Puis HCl est ajouté et nous complétons avec de l'eau jusqu'à la composition NH_4I 1 M—HCl 0,5 M. Ainsi préparé l'électrolyte support se conserve quelques jours sans jaunissement appréciable, du à l'apparition d'iode (complexe I_3^-), alors que sans précaution ce phénomène se développe en quelques minutes.

Solutions étalons. Les solutions sont réalisées à partir de nitrate de plomb (Merck) et d'étain en poudre à 99,99% (Prolabo). Dans ce dernier cas environ 120 mg d'étain sont attaqués à reflux par 6 ml d'HCl 6 M et 0,2 ml de H_2SO_4 18 M. Après dilution à 100ml en ajustant la concentration en HCl à 1 M la solution est 10^{-2} M en étain.

Soudures. Les soudures analysées sont à ame décapante et contiennent dans des canaux coaxiaux centraux de la résine naturelle (acide abietique et composés analogues) et un faible pourcentage d'agent décapant. Ces soudures sont donc débarassées de leur fraction organique par chauffage à reflux dans le méthanol pendant deux heures. Elles sont ensuite rincées puis séchées. La mise en solution des soudures se fait de façon analogue à celle de l'étain (attaque par HCl 6 M—H_2SO_4 18 M).

Appareillage. Les polarogrammes en p.t.a.s. sont obtenus avec l'ensemble PRG 3 Solea Tacussel. Le montage est à trois électrodes, référence au calomel saturée, auxiliaire de platine, indicatrice à goutte de mercure (capillaire de 20—40 μm de diamètre et débit moyen de 0,5 mg s^{-1}). Les valeurs des paramètres d'application de la p.t.a.s. sont: amplitude de la tension surimposée, 10 mV; fréquence 60 Hz; angle de déphasage avec la tension, 0°. La durée de vie de goutte est fixée à 3 s. Les ajouts dosés sont faits avec une micropipette Eppendorf de 10 μl.

Résultats et Discussion

Le domaine d'électroactivité de l'électrolyte support NH_4I 1 M—HCl 0,5 M est assez restreint. La plage de potentiel utilisable va de —0,45 V à —1,0

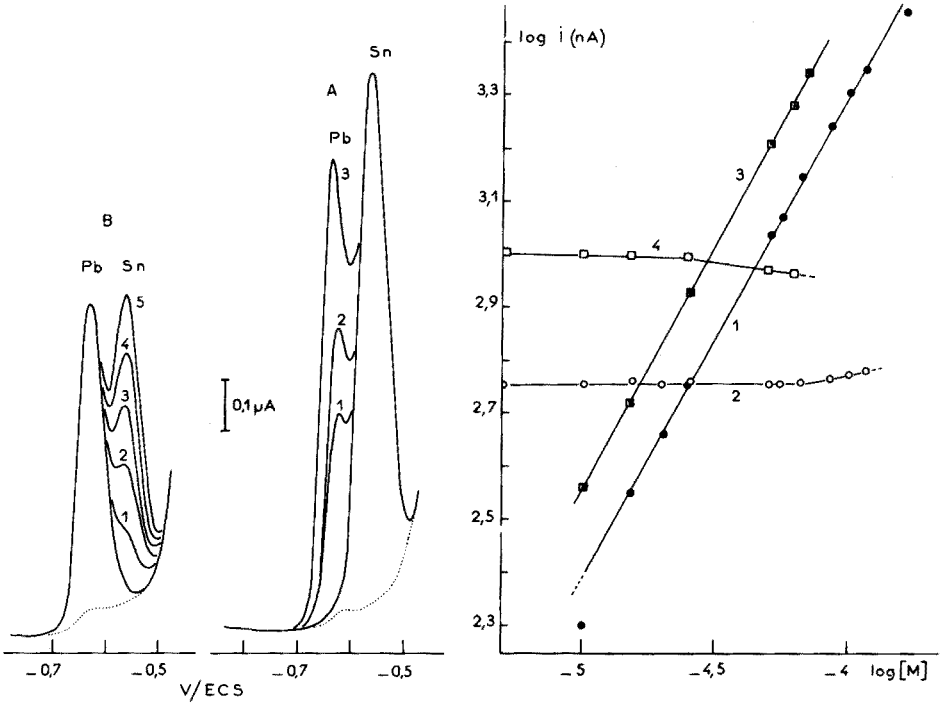

Fig. 1. Electrolyte support NH_4I 1 M—HCl 0,5 M. (A) Evolution du pic de plomb pour [Sn] = $5 \cdot 10^{-5}$ M avec [Pb] variable: 1, 10^{-5} M; 2, $1{,}5 \cdot 10^{-5}$ M; 3, $2{,}5 \cdot 10^{-5}$ M. (B) Evolution du pic de l'étain pour [Pb] = $1{,}5 \cdot 10^{-5}$ M avec [Sn] variable: $1{,}5 \cdot 10^{-6}$ M; 2, 10^{-5} M; 3, $1{,}5 \cdot 10^{-5}$ M; 4, $2 \cdot 10^{-5}$ M; 5, $2{,}5 \cdot 10^{-5}$ M.

Fig. 2. Droites d'étalonnage dans NH_4I 1 M—HCl 0,5 M. Courbes 1 et 2, Influence de la concentration croissante de Sn (•) sur la hauteur du pic du plomb (○); [Pb] = $1{,}5 \cdot 10^{-5}$ M. Courbes 3 et 4, Influence de la concentration croissante de Pb ▪ sur la hauteur du pic l'étain □; [Sn] = $5 \cdot 10^{-5}$ M.

V/ECS, zone dans laquelle le courant de base est suffisamment faible pour que l'analyse de traces soit possible. Les potentiels de pics de l'étain et du plomb sont alors respectivement —0,56 et —0,63 V/ECS, soit 70 mV d'écart et une séparation convenable en p.t.a.s. (Fig. 1).

A partir de solutions synthétiques à teneurs constantes en plomb, ou en étain, nous avons observé l'évolution des hauteurs de pics de l'autre élément, ajouté progressivement. L'accroissement du pic de l'espèce dont la concentration augmente, provoque un recouvrement partiel puis total du pic de l'autre rendant alors la mesure impossible. Nous remarquons que les dosages simultanés sont corrects si les rapports [Pb]: [Sn] vont de 5:1 à 1:5. De plus les rapports $i_{pic}/[M]$ (M = Pb ou Sn) sont à peu près constants lorsque [Pb] et [Sn] varient, et ils ne sont plus corrects lorsque les rapports des concentrations sont soit élevés, soit faibles. Ceci provient de la difficulté d'estimation

TABLEAU 1

Dosage simultané du plomb et de l'étain dans les soudures Sn—Pb (60—40). Electrolyte support NH_4I 1 M—HCl 0,5 M. (Quatre déterminations sur chaque échantillon)

Echantillon	Masse de l'échantillon (mg)	Sn		Pb	
		%	Ecart-type	%	Ecart-type
1	325,23	61,51	1,32	38,03	0,21
2	210,08	61,67	1,23	39,84	0,19
3	274,25	58,77	1,44		0,71

de la hauteur du pic chevauchant la base de l'élément majeur. La technique par ajouts dosés semble dans ce cas préférable à l'utilisation d'une droite d'étalonnage pré-établie car le rapport [Pb]: [Sn] est peu modifié. Nous n'avons pas ici recherché les limites de détection de Sn ou Pb séparément mais compte tenu de nos essais elles peuvent être raisonnablement estimées autour de 10^{-6} M pour Sn (0,1 p.p.m.) et pour Pb (0,02 p.p.m.); La Fig. 2 illustre ces résultats.

Application aux soudures étain-plomb. Après dissolution des échantillons dans HCl comme décrit précédemment l'électrolyte support est ajouté et le polarogramme tracé. Les concentrations en étain et plomb sont estimées par ajouts dosés à partir des solutions étalons. Le Tableau 1 résume quelques essais. Il est à remarquer que la somme des pourcentages n'est pas rigoureusement égale à 100% mais cela tient au fait que les teneurs sont calculées séparément pour chaque élément. Les soudures dont nous disposions titraient en théorie 60% Sn—40% Pb. Nos essais confirment ces teneurs. Toutefois les légers écarts enregistrés peuvent être imputés soit à une non homogénéité du fil, soit simplement aux diverses opérations du dosage pour un même essai.

Conclusion

Nous avons montré qu'un électrolyte support NH_4I 1 M—HCl 0,5 M, sous certaines conditions de préparation, se prêtait bien au dosage polarographique de Sn(IV) et Pb(II), en favorisant le facteur séparation (70 mV). Une application aux soudures industrielles Sn—Pb 40/60 à ame décapante montre que les résultats obtenus sont conformes aux pourcentages attendus pour des durées d'analyse modérées.

BIBLIOGRAPHIE

1 J. J. Lingane, J. Am. Chem. Soc., 67 (1945) 919.
2 A. F. Bogenshuetz et U. George, Metalloberflaech. Angew. Electrochem., 27 (1973) 160.
3 N. V. Stashkova, K. F. Borozhbitkaya, N. E. Pastukhova et E. V. Novikova, Opred. Mikroprimesei, 2 (1968) 37.

4 A. Hofer et B. Landl, Fresenius Z. Anal. Chem., 244 (1969) 103.
5 V. M. Bhuchar et A. K. Agrawal, Indian Stand. Inst. Bull., 26 (1974) 10.
6 B. Perry, Spectrovision, 25 (1971) 8.
7 T. M. Quarrell, R. J. W. Powell et H. J. Cluley, Analyst (London), 98 (1973) 443.
8 J. Seco, A. Gomez Coedo et M. T. Dorado Lopez, Rev. Met. (Madrid), 5 (1969) 602.
9 S. Alexandrov et N. Krasnobaeva, Acta Chim. (Budapest), 64 (1970) 11.
10 C. L. Fillmore, A. C. Eckert, Jr. et J. V. Scholle, Appl. Spectrosc., 23 (1969) 502.
11 N. A. Mymrik et A. Yu Chernysheva, Zh. Anal. Khim., 28 (1973) 2056.
12 V. N. Levkovskii, O. I. Artem'ev et G. E. Kovel'skaya, Zh. Anal. Khim., 29 (1974) 2199.
13 M. Harrisson, C. L. Roughton et B. Surfleet, Analyst (London), 95 (1970) 894.
14 L. S. Nadezhina, E. L. Grinzaid et E. G. Novakovskaya, Tr. Leningrad. Politekh. Inst., 304 (1970) 141.
15 L. I. Veselago, Zh. Anal. Khim., 24 (1969) 464.

Analytica Chimica Acta, 91 (1977) 331—334

Short Communication

DETERMINATION OF CROTONALDEHYDE IN ETHANOL BY DIFFERENTIAL PULSE POLAROGRAPHY

LISE-NETTE OPHEIM

Department of Chemistry, University of Oslo, Blindern, Oslo 3 (Norway)

(Received 6th September 1976)

In the production of ethanol from chemical pulp, crotonaldehyde (2-butenal) is formed from acetaldehyde by an aldol condensation reaction. As the pharmaceutical industries demand ethanol with low concentrations of unsaturated compounds, particularly crotonaldehyde, sensitive determinations of crotonaldehyde in ethanol are required. Crotonaldehyde may be determined by u.v. spectrometry, but the $n—\pi^*$ transition in the 360-nm region is weak, and only the $\pi—\pi^*$ transition in the 200-nm range is useful for low concentrations of crotonaldehyde. Gas chromatography is not very useful, as it is difficult to obtain adequate separation of crotonaldehyde from ethanol.

The electrochemistry of crotonaldehyde has been investigated [1, 2]. Barnes and Zuman [1] studied the electro-reduction of crotonaldehyde in Britton—Robinson buffers, and found that the protonated form is reduced in a one-electron step to form a radical which dimerizes and gives a 1,2-diol, while the unprotonated form is reduced to a radical anion, which is then protonated and reduced to crotyl alcohol.

In the work described here, the use of differential pulse polarography (d.p.p.) for the determination of trace impurities of crotonaldehyde in ethanol was examined.

Experimental

Polarograms were recorded with a PAR Model 174 Polarographic Analyzer. A Metrohm EA 427 Ag/AgCl(sat. KCl) electrode served as reference electrode, and a platinum coil as auxiliary electrode. Dissolved oxygen was removed from the solutions by bubbling argon through the cell for 10 min and passing it over the solution during the experiment. All experiments were performed at 25.0 ± 0.2° C.

The pH values were measured with a Metrohm EA 120 combination microelectrode and a Beckman H5 pH-meter. As the solutions contained 50% ethanol, the pH values are only relative values.

Samples of ethanol with various contaminations of crotonaldehyde were obtained from A/S Borregaard Industries Ltd., Sarpsborg.

Recommended procedure. For the reagent solution, mix equal volumes of 0.3 M tetramethylammonium bromide, 0.09 M potassium tetraborate and, 0.03 M potassium carbonate. Pipet 5 ml of the ethanol sample and 5 ml of the reagent solution into a polarographic cell, and remove dissolved air by bubbling argon (or oxygen-free nitrogen) through the cell for 10 min, and record the d.p. peak.

Results and discussion

Ethanol exhibits tensammetric peaks at potentials close to the reduction potential of crotonaldehyde in solutions of most common inorganic salts [3], and quaternary ammonium compounds are therefore recommended as supporting electrolytes in ethanolic solutions. With a 50% ethanolic solution, tensammetric peaks are obtained when tetraethylammonium hydroxide is used as supporting electrolyte, but not when tetramethylammonium bromide is used; tetramethylammonium bromide was therefore chosen. Typical differential pulse polarograms of crotonaldehyde in this medium are shown in Fig. 1.

The effect of pH on the peak potential and peak current of a 50% ethanolic solution containing 5 p.p.m. crotonaldehyde in Britton—Robinson buffers [4] is shown in Table 1. The variation of the peak current is similar to the variation of the d.c. diffusion current, reported by Barnes and Zuman [1]. In this medium, the equation of the peak potential of the first peak was found to be E_p (mV) = −900—60 pH, while in McIlvaine buffers [4] it was found to be E_p (mV) = −790—83 pH, which is in good agreement with the equation for the d.c. half-wave potential reported by Vadaszy and Cover [2]. Table 1 indicates that the pH ranges 2—4 or 9—11 should be best suited for analytical purposes. A better separation of the crotonaldehyde peak from the residual current was obtained at the higher pH (Fig. 1) and a borate buffer was therefore chosen.

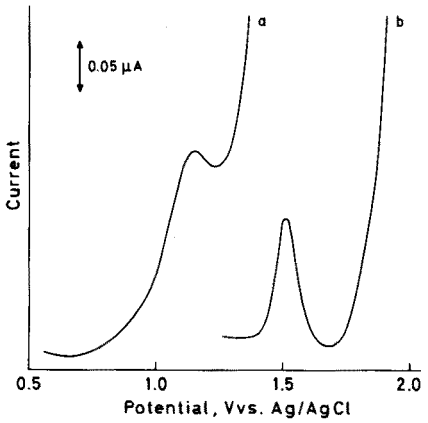

Fig. 1. Differential pulse polarograms of 0.5 p.p.m. crotonaldehyde in 50% ethanolic solution of 0.04 M tetramethylammonium bromide. (a) pH 3.7 (McIlvaine buffer); (b) pH 10.5 (Borax buffer).

TABLE 1

Effect of pH on differential pulse peak potential and peak current of 5 p.p.m. crotonaldehyde in 50% ethanolic solutions of Britton—Robinson buffers

pH	Peak 1		Peak 2	
	E_p(V vs. Ag/AgCl)	i_p(μA)	E_p(V vs. Ag/AgCl)	i_p(μA)
2.45	−1.045	2.08		
3.25	−1.080	1.95		
3.95	−1.130	1.89		
5.10	−1.210	1.13		
5.80	−1.250	0.49	−1.480	0.13
6.40	−1.270	0.13	−1.480	1.00
7.30			−1.470	1.35
7.90			−1.470	1.55
8.70			−1.470	1.55
9.70			−1.480	1.71
10.70			−1.510	1.87
11.80			−1.540	1.50
12.90			−1.550	1.00

Polarograms obtained by analyzing ethanol samples with various amounts of crotonaldehyde present, by the recommended procedure, showed that the d.p. peak current varies linearly with the concentration of crotonaldehyde within the range 0.07—70 p.p.m., which corresponds to 10^{-6} M—10^{-3} M.

The results of a few determinations of crotonaldehyde in ethanol samples are given in Table 2. The relatively poor precision obtained is most probably due to capillary noise at the high pH. Although the noise was slightly reduced by adding carbonate, it was still difficult to measure the peak heights reproducibly at the lower levels. Some of the samples were also analyzed in

TABLE 2

Determination of crotonaldehyde in ethanol samples

Sample	Differential pulse polarography				Independent value[b] (p.p.m.)
	pH 3.7		pH 10.5		
	p.p.m.[a]	s_r (%)	p.p.m.[a]	s_r (%)	
A			0.04		
B			0.06	20	0.05
C			0.15	25	0.13
D	0.73	20	0.23	10	0.24
E	0.85	5	0.74	10	
F	1.43		1.41	5	
G	11.6	5	10.8	5	8.9

[a]Mean of 5 determinations.
[b]Obtained by a gas chromatographic method.

McIlvaine buffer pH 3.7, as the capillary noise was negligible at this low pH. Because of the difficulties in drawing the baseline, only samples containing more than 0.5 p.p.m. could be analyzed in this medium, and no significant improvement in precision was observed.

The author thanks Dr. Walter Lund, University of Oslo, for valuable discussions, and Dr. Trond Rojahn, Research Department, Borregaard Industries Ltd. for the supply of samples and for useful information.

REFERENCES

1 D. Barnes and P. Zuman, J. Chem. Soc. (B), (1971) 1118.
2 R. Vadaszy and R. E. Cover, J. Electroanal. Chem. Interfacial Electrochem., 49 (1974) 433.
3 B. Breyer and S. Hacobian, Aust. J. Chem., 9 (1956) 7.
4 H. T. S. Britton, Hydrogen Ions, Vol. I, Chapman & Hall, London, 1955, pp. 356, 365.

Analytica Chimica Acta, 91 (1977) 335—338

Short Communication

APPLICATION OF A ROTATING DISC ELECTRODE AND A ROTATING CELL WITH STATIONARY ELECTRODE IN STRIPPING VOLTAMMETRY FOR THE DETERMINATION OF LEAD AND ZINC

F. VYDRA and T. V. NGHI

J. Heyrovský Institute of Physical Chemistry and Electrochemistry, Czechoslovak Academy of Sciences, Jilská 16, 110 00 Prague 1 (Czechoslovakia)

(Received 16th November 1976)

The accumulation of the species to be determined on the working electrode, i.e. preelectrolysis, is the most time-consuming step in electrochemical stripping analysis. Preelectrolysis, carried out under otherwise optimal conditions (suitable electrode, potential of electrolysis, etc.), is most effective if rapid transport of the analyzed material to the electrode is assured by an intensive flow of the electrolyte. Because only a small fraction of the required metal is deposited on the electrode (during a known time interval t_e), the conditions of preelectrolysis must be completely reproducible. In addition to electrochemical factors, the hydrodynamic conditions of preelectrolysis play an important rôle. Two basic types of hydrodynamic conditions can be chosen: a) a stationary working electrode in a stirred solution, where turbulent flow prevails; and b) a rotating disc electrode immersed in a suitable volume of electrolyte, where laminar flow prevails. In the first case, rapid movement of the electrolyte is achieved by mechanical or magnetic stirring or by rotation of the cell. In the second case, movement of the electrolyte is constant over a wide range provided that the rotation velocity is constant.

This communication describes a comparison of the application of a rotating disc electrode (RDE) and a stationary electrode combined with a rotating cell (ERC) in stripping voltammetry. The electrode material used was glassy carbon with a mercury film deposited simultaneously with the required metals during the preelectrolysis step [1].

Experimental

Apparatus and reagents. Stripping voltammetric curves were recorded with a three-electrode polarograph OH-102 (Radelkis, Hungary). The rotating disc electrode was constructed in this Institute [2]; the glassy carbon electrode (Le Carbon Loraine, France) had a diameter of 3 mm. The rotation velocity in all experiments (and during preelectrolysis) was 2200 r.p.m. A commercial ElectRoCell rotating cell (capacity 30 ml) constructed from polymethylmethacrylate for stripping voltammetry (McKee Pederson Inst., Danville, USA)

was used. The stationary electrode used with the rotating cell was made from glassy carbon and was of identical size to the RDE. The electrode was placed horizontally, and the active area was a disc of 3-mm diameter. Stirring involved periodic reversal of the cell rotation. During the preelectrolysis the electrode was immersed in a film (ca. 1-mm thick) of electrolyte on the cell wall. The stripping process was carried out with unstirred solutions, as in the case of the RDE.

Hydrochloric acid and lead(II) and zinc(II) salt solutions were prepared from Suprapur chemicals (E. Merck); other chemicals used were of reagent grade. Water was twice distilled from glass and quartz apparatus.

Procedure. The procedures and experimental conditions were chosen so as to obtain comparable results with respect to the influence of hydrodynamic conditions. Only the volumes of the test solutions differed, 50 ml for the RDE and 30 ml for the ElectRoCell. In both cases, dissolved oxygen was removed by a 2-min passage of pure nitrogen (0.5 l min^{-1}).

After the preelectrolysis at constant potential in the presence of a mercury(II) salt in the electrolyte, anodic dissolution of the amalgam was achieved by linearly decreasing the voltage at a rate of 25—100 mV s^{-1}.

Optimal conditions for the determination of lead and zinc

For the stripping voltammetric determination of lead, a 0.1 M HCl medium was found most suitable for both systems. The influence of the concentration of mercury(II) salt on the peak height has been studied [3]. In the hydrochloric acid medium, maximum peak heights were obtained when the mercury(II) concentration was about ten times higher than that of lead(II). At high lead(II) concentrations, the peak height was constant and independent of mercury(II) concentration. When electrodes of 3-mm diameter are used with a pre-electrolysis potential of —1.0 V, the conditions given in Table 1 are recommended. These optimal concentrations are the same for both the RDE and the ERC.

The optimal medium for the determination of zinc was found to be ammonium acetate (0.05 M, pH 6.0—6.5). Whether the RDE or the ERC is used, the conditions given in Table 2 are satisfactory when the preelectrolysis is carried out at —1.5 V.

TABLE 1

Optimal conditions for the determination of lead

[Pb], M	$[Hg^{2+}]$, M	t_e, min	mV s^{-1}
$5 \cdot 10^{-9}$—10^{-8}	$5 \cdot 10^{-6}$	20	100
10^{-8}—$5 \cdot 10^{-8}$	$5 \cdot 10^{-6}$	15	100
$5 \cdot 10^{-8}$—10^{-7}	$5 \cdot 10^{-6}$	10	50
10^{-7}—$5 \cdot 10^{-7}$	10^{-5}	5—7	50
$5 \cdot 10^{-6}$—10^{-6}	10^{-5}	3—5	50

TABLE 2

Optimal conditions for the determination of zinc

[Zn], M	$[Hg^{2+}]$, M	t_e, min	mV s^{-1}
10^{-7}—$5 \cdot 10^{-7}$	10^{-5}	15—18	100
$5 \cdot 10^{-7}$—10^{-6}	$3 \cdot 10^{-5}$	10—15	50
10^{-6}—$5 \cdot 10^{-5}$	$3 \cdot 10^{-5}$	5	50

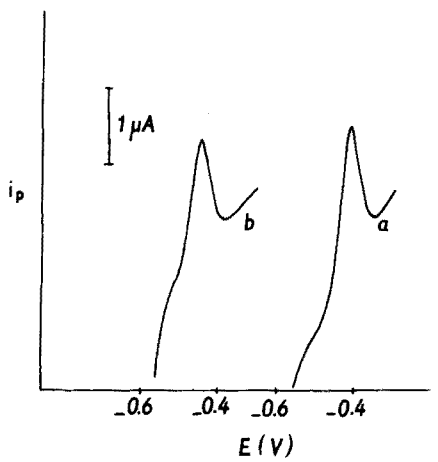

Fig. 1. (left) Anodic stripping voltammetric curves for lead obtained with the RDE (curve a) and ERC (curve b). $5 \cdot 10^{-9}$ M Pb^{2+}, $5 \cdot 10^{-6}$ M Hg^{2+}, 0.1 M HCl, $E_e = -1.2$ V, $t_e = 20$ min, $v = 100$ mV s^{-1}, (a) RDE $\omega = 2200$ r.p.m.

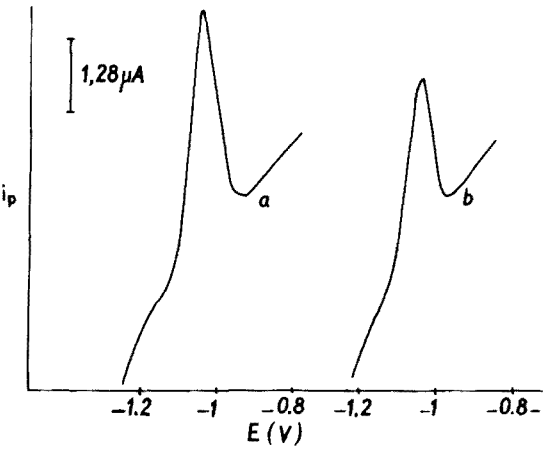

Fig. 2. (right) Anodic stripping voltammetric curves for zinc on the RDE (curve a) and ERC (curve b). 10^{-7} M Zn^{2+}, 10^{-5} M Hg^{2+}, 0.05 M $NH_4CH_3CO_2$ (pH 6.5) $E_e = -1.5$ V, $t_e = 18$ min, $v = 100$ mV s^{-1}, (a) RDE $\omega = 2200$ r.p.m.

For the above-mentioned conditions, the dependences of the maximum peak heights (i_p) on the concentration of lead or zinc are linear. The relative error of the determination lies in the range ± 3—7%. Typical stripping voltammograms of lead and zinc obtained under the given conditions with the RDE and ERC are presented in Figs. 1 and 2. The peak heights and shapes showed excellent reproducibility.

Influence of hydrodynamic conditions on the sensitivity of the determination

When the above conditions are carefully fulfilled, there is little difference between the results obtained with the RDE and ERC. It can therefore be concluded that these different arrangements of stirring and electrodes are equally acceptable in stripping voltammetry. However, when the RDE was applied, the results were more sensitive (ca. 30%) in all cases. This is illustrated by the calibration graphs for lead shown in Fig. 3.

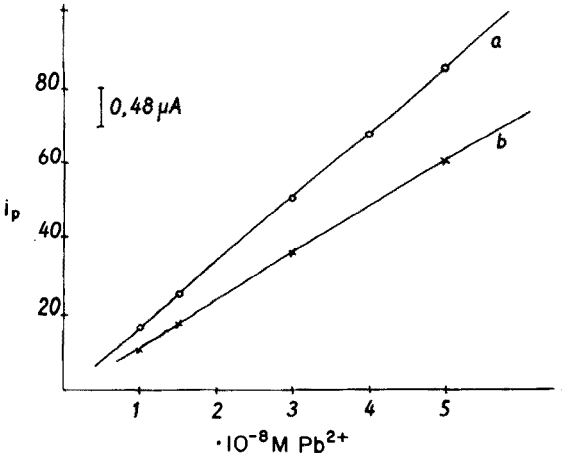

Fig. 3. Dependence of peak current (i_p) on concentration of lead. E_e = −1.0 V, t_e = 15 min, 0.1 M HCl, v = 50 mV s^{-1}, (a) RDE ω = 2200 r.p.m. (b) ERC.

From the point of view of routine analysis, the RDE is advantageous because the surface area of this electrode can be easily renewed by polishing as the electrode rotates.

REFERENCES

1 E. M. Roizenblat and Kh. Z. Brainina, Elektrokhimiya, 5 (1969) 369.
2 T. V. Nghi and F. Vydra, Anal. Chim. Acta, 80 (1975) 267.
3 L. Luong and F. Vydra, J. Electroanal. Chem. Interfacial Electrochem., 50 (1974) 379.

Analytica Chimica Acta, 91 (1977) 339—343

Short Communication

SPECIFIC CONDUCTANCE AND ALKALINITY DETERMINATIONS IN DILUTE NATURAL WATERS

M. P. BERTENSHAW

Department of Geology, Nottingham University, Nottingham, NG7 2RD (England)

(Received 4th November 1976)

In natural waters of around pH 7, alkalinity is primarily caused by hydrogencarbonate ions. The conventional procedure for alkalinity determinations is potentiometric titration with dilute acid [1, 2]; the pH is plotted against small increments of titrant, added in the region of pH 4.5. Many readings are required to plot the titration curve; equilibrium for each reading is obtained slowly, 30 min may be needed for a single titration, and the point of inflexion is often indistinct. If conductance instead of pH is followed in the titration, the plot against titrant volume is defined by two straight lines whose intersection marks the end-point. Only six points are required for such a plot; up to ten titrations per hour can be carried out accurately.

Most commercially available conductance bridges measure conductance over a very wide range, of which only a relatively small span is normally encountered in any one field of work. A non-linear calibration is necessary if conductance is to be read directly from the instrument. Both of these facilities are often provided at the expense of sensitivity. In addition, the instruments are cumbersome and usually require a mains supply. A compact, battery-operated bridge of high precision has therefore been designed to measure the range of conductance normally found in dilute natural waters.

Construction and operation of the conductance bridge

The apparatus included a conductivity cell, Wheatstone bridge and balance point detector. The bridge was supplied with alternating current to eliminate electrolysis in the cell.

A dip-cell with 1-cm^2 platinized electrodes about 1 cm apart was constructed as described by Vogel [3]. The bridge circuit (Fig. 1) incorporated a 100 Ω, 10-turn, linear potentiometer which could be read to ±0.1 Ω with a suitable dial. A capacitor, C, was fitted to compensate for the capacitance of the dip-cell, which was measured in distilled water with a capacitance bridge and was found to be ca. 0.01 μF. The resistance, R, could be changed (wafer switch) to make it similar to that of the dip-cell; 250 Ω, 500 Ω and 1000 Ω resistors were found adequate for a considerable range of waters. The output, D, incorporated a bridge rectifier (r.f. diodes) so that a d.c.

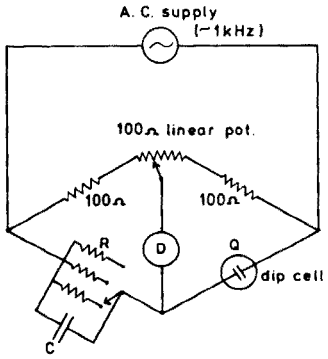

Fig. 1. Conductance bridge circuit.

meter could be used to detect the balance point, although headphones (impedance ca. 50 Ω) proved to be the most sensitive detector.

An a.c. supply, provided by an oscillator—amplifier circuit (Fig. 2), gave an output of 4.5 V at 1250 Hz from which 50-mA current could be drawn with a stability of 55 Hz over 3 h. Gold-band, "Hystab" 0.5 W resistors were used throughout; transistors were mounted on T.O.5 holders. The value of the resistance, G, in the oscillator stage depended on the gain of the transistor T.

The entire circuit was built into a metal case (190 × 120 × 60 mm) to which the negative terminal of a 9-V dry battery used to power the oscillator was earthed. The external controls comprised a 10-turn, graduated dial from which "bridge resistance" was read, a "range selector" switch for R, an "On/Off" switch, a socket for the connection of the dip-cell leads, and d.c. and a.c. output sockets for a detector.

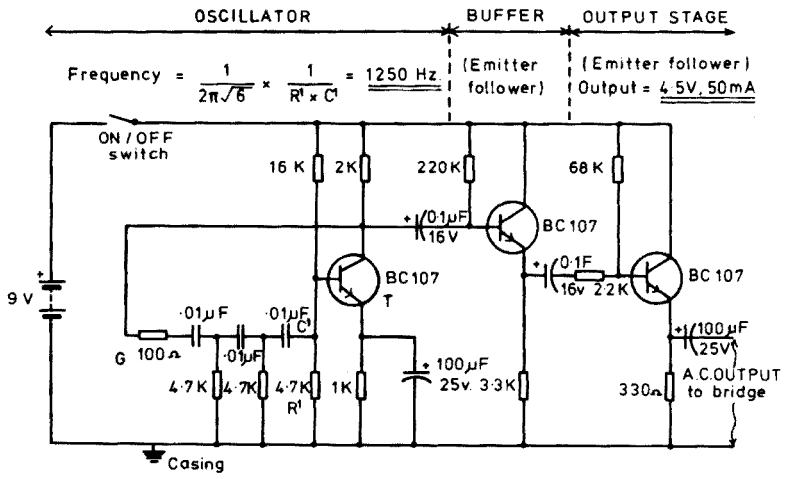

Fig. 2. Oscillator—amplifier circuit.

Cell conductivity (Ω^{-1}) was obtained from the measured bridge resistance, x, by the relationship

$$\text{Cell conductivity } (\Omega^{-1}) = \frac{(100 + x)}{(200 - x)} \cdot \frac{1}{R}$$

For convenience, a bridge resistance-cell conductivity conversion table was computed with R equal to 500 Ω. When R was set to 250 Ω or 500 Ω the cell conductivity read from the table was multiplied by a factor of 2 or 0.5 respectively.

The conductivities of solutions of potassium chloride, potassium nitrate and potassium hexacyanoferrate(II), each at concentrations of 0.005, 0.01 and 0.02 M, were measured at 25°C and compared with published values [4]. Three cell constants were derived for the three ranges. Specific conductance of any sample was obtained by multiplying the cell conductivity by the appropriate cell constant and range factor.

Conductometric titration for alkalinity

The dip-cell was immersed fully in 50.0 ml of sample in a 100-ml beaker, seated on a magnetic stirrer from which it was thermally insulated. Sulphuric acid (0.01639 N; 1 ml ≡ 1 mg HCO_3^-) previously standardized against sodium carbonate solution, was dispensed from a 25-ml burette in 2-ml aliquots up to the end-point, after which 1-ml increments were made. The bridge resistance at balance was noted for each increment of titrant; three readings were required on each side of the end-point.

Bridge resistances were converted to cell conductivities (as shown in Table 1) and plotted against titrant volume. The intersection of two straight lines marked the end-point clearly. Alkalinity expressed as p.p.m. of HCO_3^- was obtained by multiplying titrant volume at the end-point by 20.

Discussion

The derived cell constants differed slightly for each range, partly because of variations from the nominal values of the resistors. The constants are accurate to approximately ±0.5%. The precision of bridge resistance readings at balance is ±0.1 Ω, so that cell conductivity may be read to more than three significant figures. Hence, although the precision of specific conductance measurements is high, accuracy is limited by the accuracy with which cell constants are derived. High precision is required if chemical changes are to be followed through a titration, or if similar waters are to be compared.

TABLE 1

Specimen results of alkalinity titration

Titrant added (ml)	8.0	10.0	12.0	14.0	15.0	16.0
Bridge resistance (Ω)	64.9	63.9	63.0	66.1	75.5	83.7
Cell conductivity ($\Omega^{-1} \cdot 10^{-3}$)	2.44	2.41	2.38	2.48	2.82	3.16

Specific conductance measurements are useful [5] in estimating ionic strengths in dilute natural waters; the bridge may be modified to measure conductivity in solutions of any ionic strength by adjustment of the resistors in the circuit.

Alkalinity titrations should be executed without delay to avoid errors through changes in temperature or undesired carbon dioxide evolution. A delay of a few seconds occurs before readings may be made because of reaction time and mixing, but otherwise the response of the electrodes is instantaneous and independent of hydrodynamic effects.

Conductivity is fairly constant up to the end-point, after which it rises sharply. In contrast to the potentiometric method, readings near the end-point have no significance; the effects of dissociation and solubility of reaction products are therefore negligible.

To avoid excessive curvature of the plot through dilution, the titrant should be about five times stronger than the sample so that the volume of acid added, v, is small relative to the initial volume, V, on commencing the plot. A volume correction, achieved by multiplying conductivities by $(V + v)/V$, may be applied if better accuracy is required. To evaluate the accuracy and precision of the method, ten replicate analyses were performed on three independently prepared 200 p.p.m. HCO_3^- standards; this concentration is typical of waters issuing from carbonate rocks. The results shown in Table 2 demonstrate a high precision with standard deviations of 0.53—1.03 p.p.m. Volume correction does not alter the precision of the method, but volume-corrected analyses are ca. 1 p.p.m. higher and slightly more accurate. The overall low bias of the results may be attributed to the acidity of the "de-ionized" water with which the standards were made; the accuracy depends on the preparation of reliable hydrogencarbonate standards.

The technique is rapid and simple to operate in the field. It is preferable, however, to make conductivity measurements in a laboratory where temperature can be more carefully controlled; samples of limestone-derived water, collected in airtight polythene bottles with no air space remained unchanged for several days with respect to both conductivity and alkalinity.

TABLE 2

Results of analyses of 200 p.p.m. HCO_3^- standards

Standard	Without volume correction		With volume correction	
	Mean (p.p.m.)	s	Mean (p.p.m.)	s
A	197.2	1.03	198.2	0.79
B	195.8	0.63	197.6	0.70
C	196.1	0.74	197.5	0.53

Thanks are expressed to I. G. Cullis for assistance in the design and construction of the bridge, and to B. P. Atkin and P. K. Harvey for helpful advice. The work was carried out during the tenure of an N.E.R.C. studentship.

REFERENCES

1 I. Barnes, U.S. Geol. Survey Water-Supply Paper 1535-H (1964).
2 E. Brown, M. W. Skougstad and M. J. Fishman, U.S. Geol. Survey Techniques of Water-Resources Investigations, Book 5, Chapter A1, 1970, p. 41.
3 A. I. Vogel, A Text-book of Quantitative Inorganic Analysis, Longmans, London, 3rd edn., 1961, pp. 972, 975.
4 R. C. Weast (Ed.), Handbook of Chemistry and Physics, Chemical Rubber Company, Cleveland, 50th edn., 1970, p. D-121.
5 C. J. Lind, U.S. Geol. Surv., Prof. Paper 700-D, p. 272.

Analytica Chimica Acta, 91 (1977) 345–352

Short Communication

ULTRAHIGH-SPEED PHOTOGRAPHIC OBSERVATION OF THE ELECTRODE EROSION PROCESS IN SPARK DISCHARGE

TSUTOMU TAKAHASHI
National Research Institute for Metals, Tokyo (Japan)
TOKUNOSUKE NAKAJIMA
Japan Atomic Energy Research Institute, Ibaraki-Ken (Japan)
HIROSHI MATSUI
Industrial Research Institute of Kanagawa, Kanagawa-Ken (Japan)
SHOHEI ODA
Faculty of Engineering, University of Tokyo, Tokyo (Japan)
(Received 8th September 1976)

An ultrahigh-speed photographic observation of low-voltage spark discharges — the most frequently used method of spectrochemical excitation — is reported. High-speed techniques have been used previously to observe spark discharges. The methods used have involved an image converter tube [1], a Faraday shutter [2], a Kerr cell shutter [3, 4], a micro flash [5], and a rotating mirror camera [6]. In this research a rotating mirror camera was used to investigate fully the phenomena. The work was designed to examine (1) initial breakdown, (2) channel expansion, (3) vapour jet ejection, and (4) anodic and cathodic spot behavior.

Experimental

The camera used was a Nikkon model UHF-500C; the specifications are given in Table 1. A modular spark source (Shimadzu-Seisakusho) was used;

TABLE 1

Specifications of UHF-500C camera

Maximum framing rate: higher than 500,000 frames/s
Minimum exposure time per frame: less than 0.4 μs
Brightness of image: max. f/8
Picture frame size: 15 × 5 mm
Number of frames photographed: continuously 600 frames
Film used: standard 35-mm film
Length of film loaded at a time: 2000 mm (effective 1000 mm)
Driving of rotating mirror by turbine (with air or nitrogen gas)
Driving of drum by a.c. series motor

the circuit diagram is shown in Fig. 1. The source conditions and oscillograms of the discharge current are shown in Fig. 2. Figure 3 (A) shows the oscillogram of the igniter for the circuit marked (⨯) in Fig. 1; for the circuit marked (∧∧∧) in Fig. 1, the current oscillogram is indicated in Fig. 3 (B).

Argon and air atmospheres were used. The cathodes were pure copper with a steel disc; the anodes were pure copper with a graphite rod (6 mm diam. 90° cone). The optical layout is shown in Fig. 4. The crossmark and relay lens were set as for editing a movie picture. The interference filter (515.0 nm, half-width 5.0) passed only a particular wavelength for copper.

Results and discussion

Figure 5 (A) shows that, before complete breakdown, a plasma channel is formed between the electrode gap and becomes slightly luminous; within 10—20 μs the channel disappears and a complete breakdown occurs 10—20 μs later. These photographs prove that there is a statistically large time lag before sparking. Apparenly, the modular source used as the impulse voltage generator

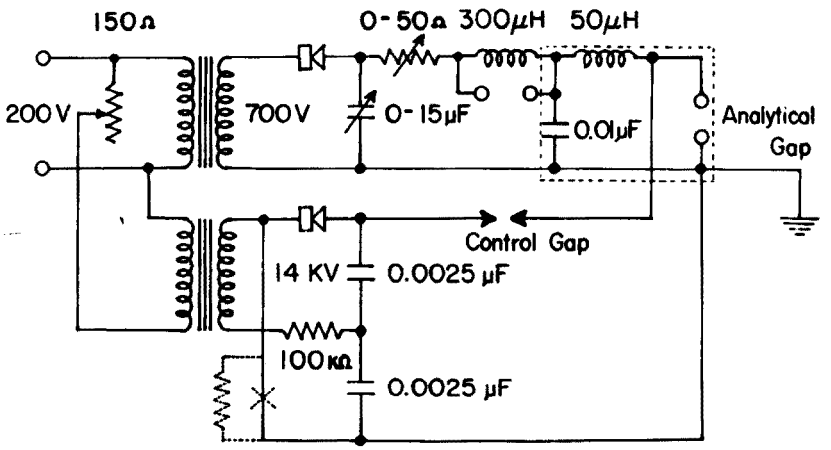

Fig. 1. Circuit diagram of Modular Source.

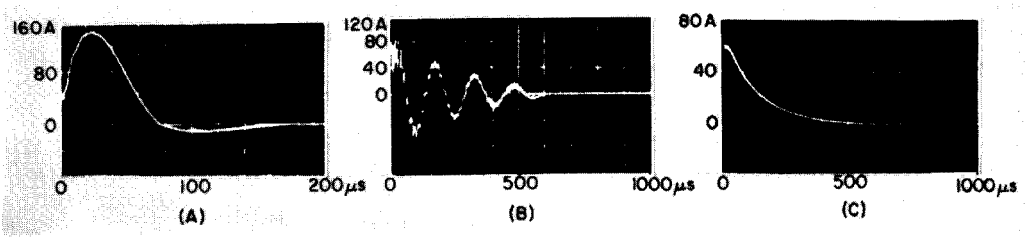

Fig. 2. Discharge conditions and their current oscillograms. (A) Critically damped discharge; C = 6 μF; L = 50 μH; R = 3 Ω; V = 1 kV. (B) Oscillating discharge; C = 2 μF; L = 350 μH; R = 0; V = 1 kV. (C) Overdamped discharge; C = 10 μF; L = 50 μH; R = 5; V = 1 kV.

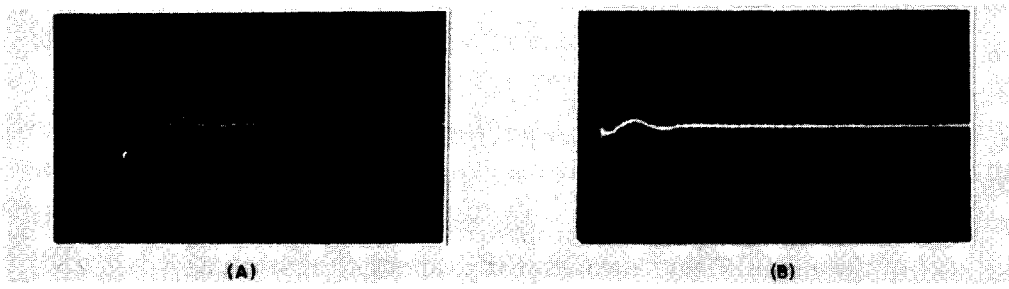

Fig. 3. Current oscillograms of igniter. (A) Unidirectional condition. (B) Oscillating condition.

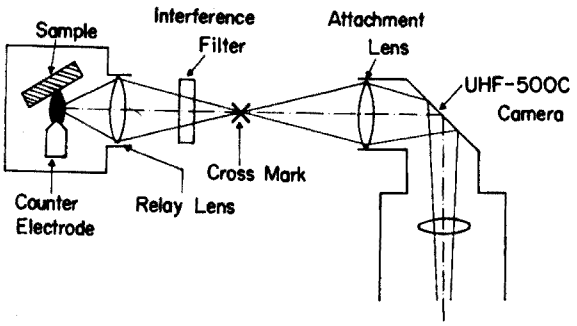

Fig. 4. Optical layout.

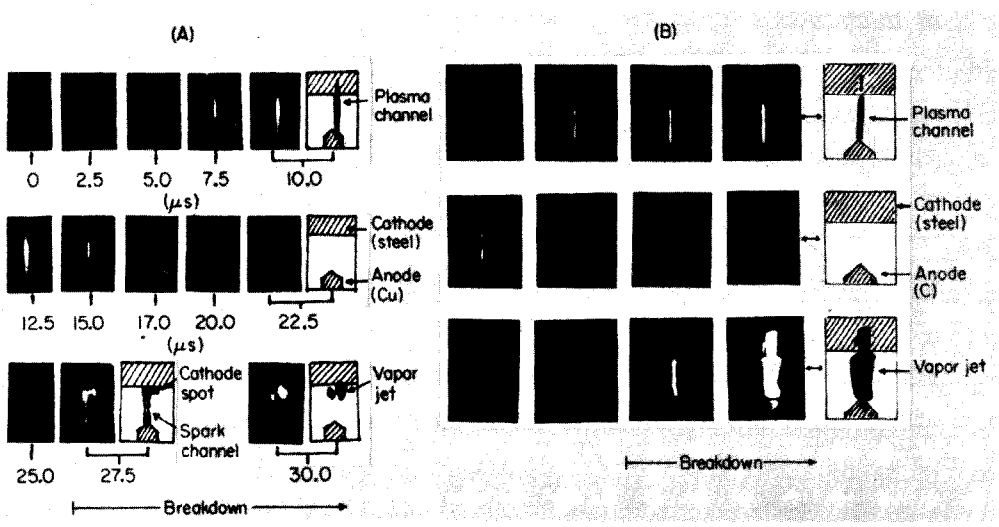

Fig. 5. (A) Initial breakdown phenomena; overdamped discharge (Fig. 2C); argon at 20 l min^{-1}. (B) Initial breakdown phenomena and channel expansion; critically damped discharge (Fig. 2A); air atmosphere.

does not provide a high overvoltage. During the initial breakdown, neither a cathode nor an anode signal can be recognized, but after complete breakdown, both cathode and anode signals are observed (Fig. 5). During the initial breakdown, the channel characteristics are straight and thin.

In an argon atmosphere, vapor jets from cathode and anode can be observed for an oscillating discharge by the igniter. However, when the igniter is unidirectional, the first frame is recognized only as shown in Fig. 6. During main spark discharge in an argon atmosphere, there is erosion of the cathode but not of the anode. Figure 7 shows that a vapor jet can be observed under

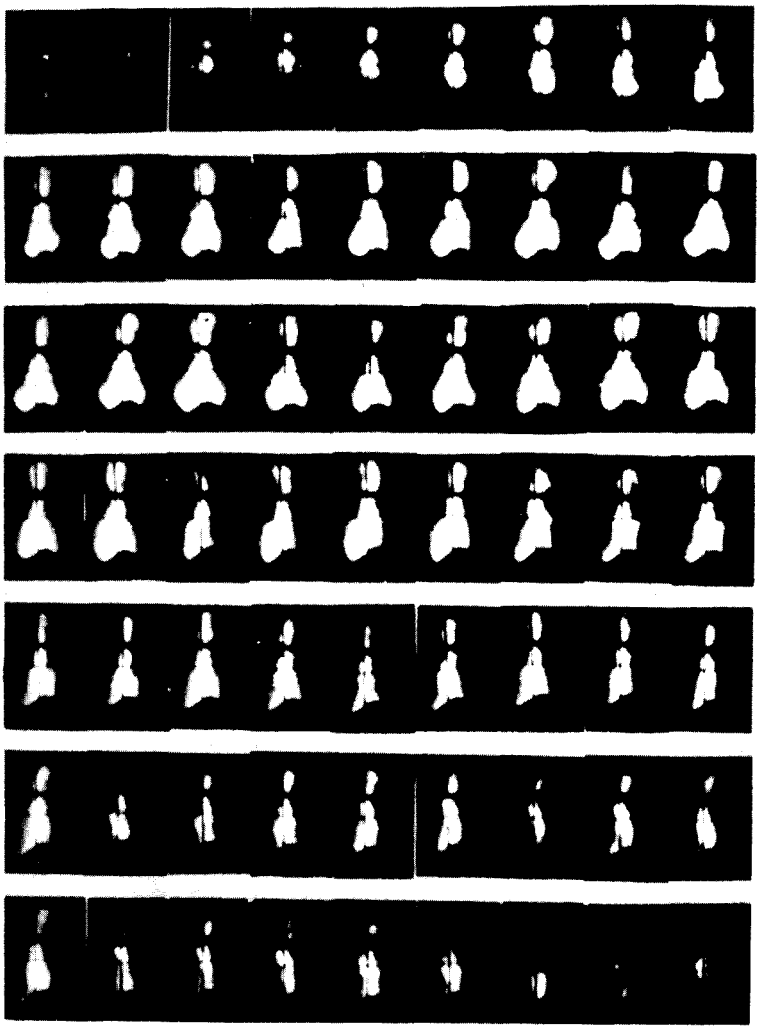

Fig. 6. Intermittent eruption of vapor jet and its speed. Exposure, 0.8 μs; frame delay, 2.5 μs; atmosphere, argon at 20 l min^{-1}; filter, 515.0 nm; electrode, Cu—Cu.

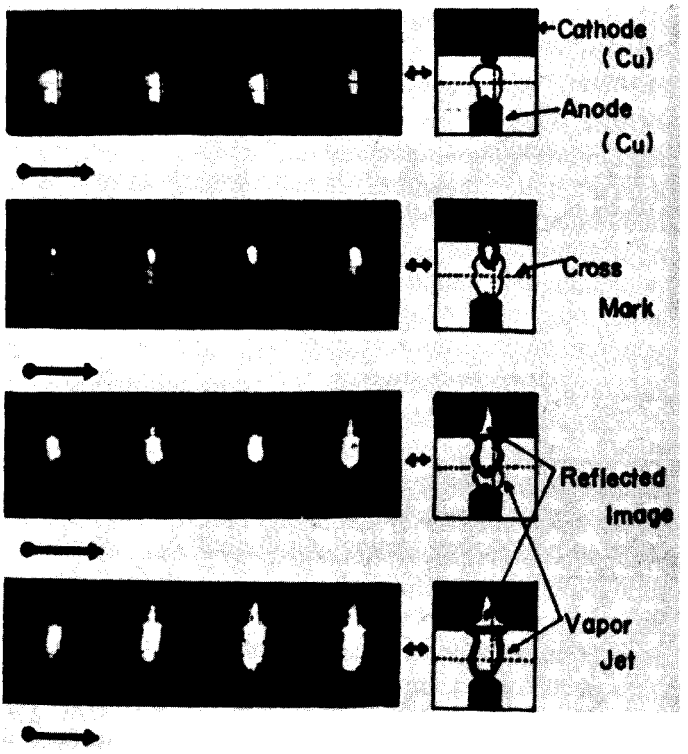

Fig. 7. Oscillating discharge. Conditions as for Fig. 6 except that no filter was used.

oscillating discharge conditions only when the electrode is negative; in Fig. 7 frames 1—3 were taken at a late period of the second cycle whereas frames 4—16 were taken early in the third cycle. In contrast, in an air atmosphere, erosion can be observed on both the cathode and the anode, and the plasma has a mushroom shape (Fig. 8). The reason for this phenomenon is not clear.

The speed of the vapor jet during the main discharge is ca. $2 \cdot 10^4$ cm s^{-1} measured from Fig. 6. In most cases of low-voltage spark discharge, the speed of the jet was estimated as $1—3 \cdot 10^4$ cm s^{-1}, not exceeding the speed of sound, but the speed has been reported [1] as ca. 10^5 cm s^{-1}. The reason for the difference is not clear; the increasing rate of the current or the peak current value should be smaller than reported earlier.

Figures 6 and 9 indicate that the main discharge jets are intermittent eruptions from the cathode. In the later period of pulse duration (Fig. 9), the intermittent eruption of vapor can be observed clearly; its interval is 10—12 μs. This interval is independent of the cathode material, the value being the same in photographs obtained for the steel cathode. A parasitic oscillation is superimposed on the main discharge current. The period of this oscillation is ca. 10—12 μs (Fig. 9), which is essentially the same as the interval of intermittent

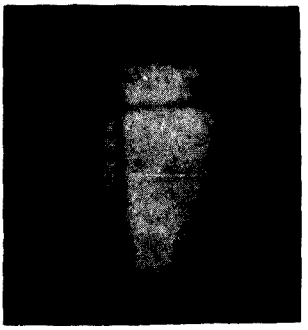

Fig. 8. Discharge in air. Exposure, 0.8 μs.

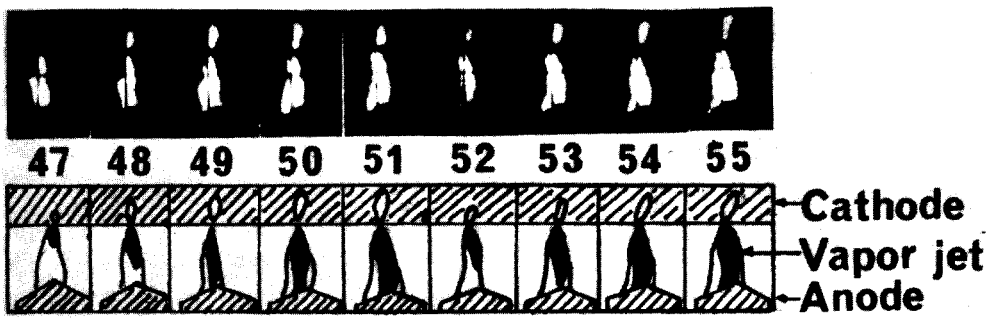

Fig. 9. The sequence taken at a later period of Fig. 6.

eruption; the parasitic oscillation is caused by the resonating circuit (see Fig. 1, inside the dotted line).

When diffuse burns are used many cathode spots can be observed (Fig. 10A) and these increase as the current increases. The energy involved is dispersed (Fig. 10A) so that erosion of the cathode decreases. In condensed burns (Fig. 10B), only one cathode spot appears, the energy is concentrated on this spot, and there is extensive erosion. Figure 11 shows the crater formed after twelve discharges on the surface of a copper cathode under critically damped discharge conditions (900 V, 30 μF, 10 Ω, 50 μH). Thirteen or fourteen craters could be seen, using a microscope, on the surface of the copper cathode. Apparently, one crater is made by one pulse discharge on a condensed burn.

The speed of channel expansion was calculated to be 710 ms^{-1} which is higher than the speed of sound; a cylindrical channel was assumed (Fig. 5B). This result coincides with that of Mandel'shtam [5].

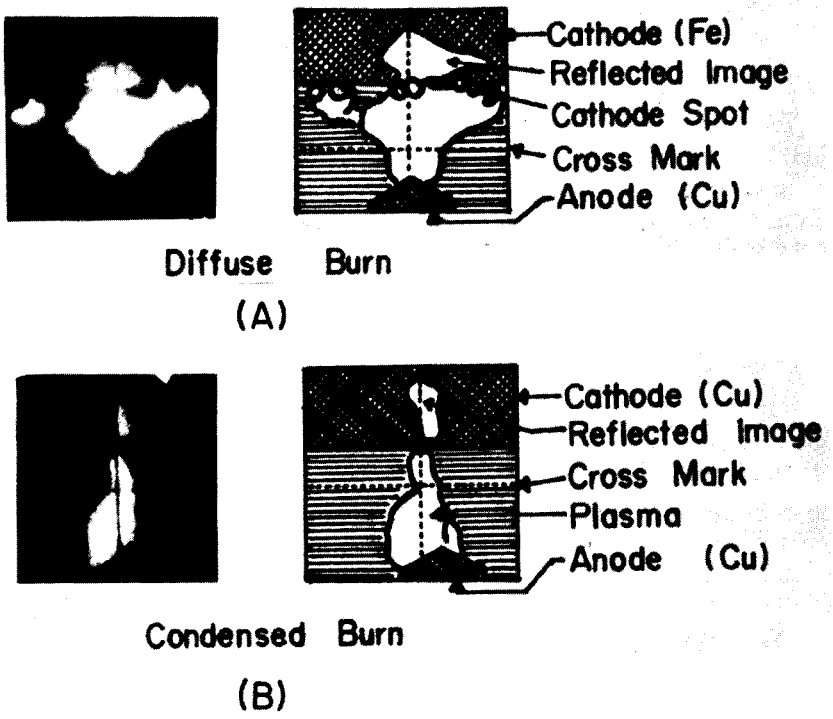

Fig. 10. Diffuse burn (A) and condensed burn (B). Exposure, 0.8 μs.

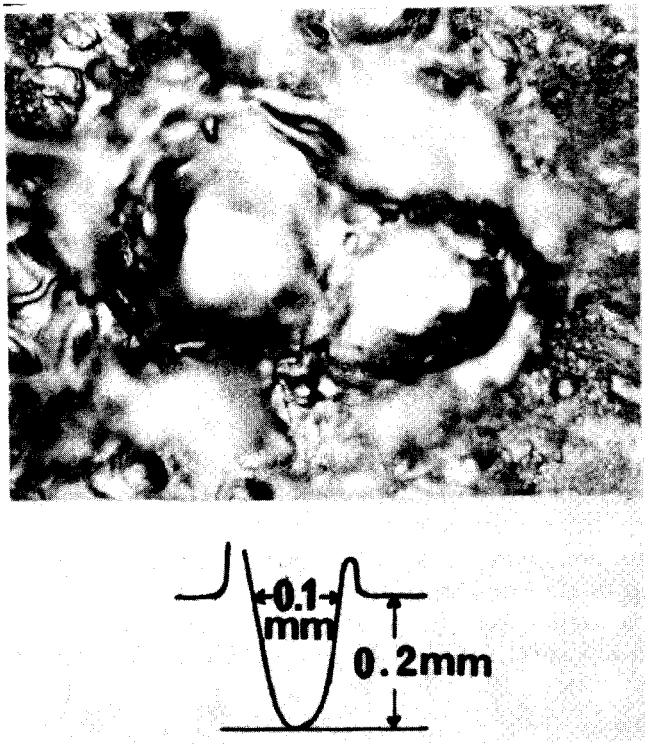

Fig. 11. Discharge trace of copper cathode in argon atmosphere (× 400).

The authors thank Dr. Shoichiro Yoshida (Nikkon) and Dr. Kenjiro Tohyama (Shimadzu Seisakusho) and members of the light-source research group for assistance.

REFERENCES

1 C. M. Cundall and J. D. Craggs, Spectrochim. Acta, 7 (1955) 149.
2 V. Grackov and V. Hermoch, Chekh. Fiz. Zh. 13 (1963) 509.
3 H. Fisher and W. B. Rüppel, Appl. Opt. 3 (1964) 769.
4. H. Fisher and C. C. Gallagher, Appl. Opt., 4 (1965) 1151.
5 L. Mandelsh'tam, Spectrochim. Acta, 15 (1959) 255.
6 R. H. Scott and A. Strasheim, Spectrochim. Acta B, 25 (1970) 311.

Analytica Chimica Acta, 91 (1977) 353—356

Short Communication

COPPER DETERMINATION IN STANDARD MATERIALS BY NEUTRON ACTIVATION AND SRAFION NMRR ANION-EXCHANGE RESIN

ERNEST S. GLADNEY

Los Alamos Scientific Laboratory, P.O. Box 1663, Los Alamos, N.M. 87545 (U.S.A.)

(Received 15th November 1976)

Several recent articles have described the use of Srafion NMRR anion-exchange resin for the quantitative separation of noble metals [1—3], silver [4], and mercury [5] from complex matrices. This resin is selective for the d^8-electron configuration characteristic of noble metal complexes in chloride solutions. However, in attempts to employ this resin for air particulate and fly ash analyses, a serious problem with retention of ^{64}Cu ($t_{\frac{1}{2}}$ = 12.9 h) was encountered. This caused a severe loss of sensitivity for the low-energy γ-rays from ^{109}Pd, ^{197}Pt and ^{199}Au because of increased Compton background from 511-keV annihilation radiation. An investigation by Muzzarelli and Rocchetti [6] has shown that several cations, including copper, are at least partially absorbed on Srafion NMRR under certain conditions. Strelow [7] suggested that the halide ion concentration might be the controlling variable for copper retention on anion-exchange resins. The present communication reports results of a study of halide ion effects on Srafion NMRR and demonstrates the use of this resin for the determination of copper in standard reference materials.

Effect of halide ion on copper retention

Copper retention on Srafion NMRR as a function of the halide ion concentration was studied with radioactive ^{64}Cu as a tracer. The separation procedure was similar to that described by Nadkarni and Morrison [1]. Fusions of non-irradiated fly ash with tracer added were performed in nickel crucibles. The fusion cakes were dissolved with hydrochloric, hydrobromic or hydriodic acids. These solutions were boiled to destroy residual peroxides, adjusted to pH 1.5 with ammonia solution, and eluted through a column (10 × 1.5 cm) of Srafion NMRR at a rate of 1 ml min^{-1}. The resin was counted directly on a Ge(Li) detector; the 511-keV annihilation radiation from ^{64}Cu was used to assess the copper retention.

The concentrations of chloride, bromide and iodide were varied from 0.05 M to 5.0 M by adding different amounts of distilled water to the dissolved melts. The copper retention was similar for chloride and bromide; the results for bromide are shown in Fig. 1. This was not unexpected since the chemistry of halo-complexes of divalent copper, palladium and platinum are

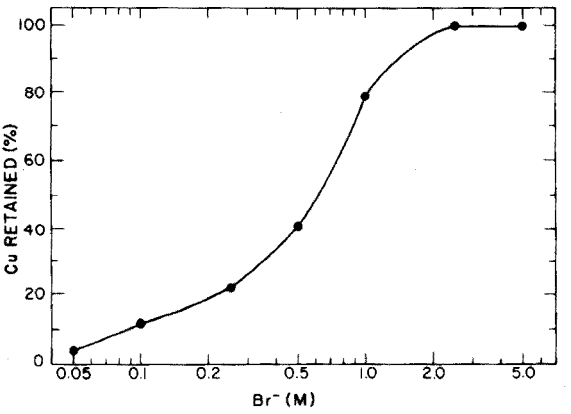

Fig. 1. Copper retention on Srafion NMRR resin as a function of the bromide concentration.

similar [8]. Increasing halide concentration stabilizes the halo—copper complex and increases retention on Srafion NMRR. Under the conditions reported [1] the final chloride concentration in the dissolved melts is ca. 2.5 M, which results in ca. 100% of the copper being retained on the resin (Fig. 1) and thus leads to a severe interference with the measurement of the short-lived noble metal isotopes in some matrices. This is in sharp contrast to the copper retention of 1% recently suggested [9]. The current results suggest that this problem may be controlled to a degree by minimizing the amount of hydrochloric acid used in the dissolution of the melt and by reducing chloride concentration in the final solution by large scale dilution. Nadkarni and Morrison [10] have also reported the removal of copper before ion exchange by solvent extraction of the copper—neocuproine complex into chloroform.

The copper retention with hydriodic acid was quantitative over the entire range of iodide concentrations studied. This suggested that a suitable procedure could be developed to exploit this resin for the determination of copper.

Experimental

For the measurement of copper in various standard matrices, 100-mg samples were encapsulated in polyethylene vials and irradiated for 5 min in a thermal neutron flux of $5 \cdot 10^{12}$ n $cm^{-2} s^{-1}$ at the Los Alamos Omega West Reactor. After cooling for a few hours, the samples were transferred to nickel crucibles and those with significant organic content were ashed at 500°C for 10 min. Both rocks and ashes were fused in a mixture (5 : 2) of sodium peroxide : sodium hydroxide [1]. After cooling, the melts were dissolved in 40 ml of 8 M hydrochloric acid and diluted to 100 ml with distilled water. Following boiling and pH adjustment (pH 1—2), 5 ml of saturated potassium iodide solution was added. These reagents were substituted for hydriodic acid for economic reasons when tracer studies revealed similar copper retention. The samples were eluted through a short resin column (5 × 1 cm) at flow rates

of 2—6 ml min^{-1}. The columns were washed with 20 ml of 0.05 M hydrochloric acid and the 511-keV annihilation radiation from ^{64}Cu was measured on a large Ge(Li) detector for 5 min. These analyses were standardized by the simultaneous irradiation of weighed quantities of copper sulfate. Less than 5-mg amounts were employed to minimize the self-shielding of copper during irradiation. The copper sulfate was dissolved directly in the 8 M hydrochloric acid solution and treated in the same manner as the samples.

Results and discussion

The results of analyses of standard materials are given in Table 1. The good agreement between the present experimental values and the certified (NBS) or accepted average values (USGS) demonstrates the utility of this technique.

TABLE 1

Copper concentrations in standard materials

Material	This work, ppm $\bar{x} \pm s$	Accepted values, ppm
NBS Fly Ash No. 1633	136 ± 6	128 ± 5[a]
NBS Coal No. 1632	17 ± 1	18 ± 2[a]
NBS Orchard Leaves No. 1571	13 ± 1	12 ± 1[a]
NBS Bovine Liver No. 1577	183 ± 8	193 ± 10[a]
USGS G-2	10 ± 2	11.7 [11]
USGS PCC-1	13 ± 3	11.3 [11]
USGS BCR-1	15 ± 2	18.4 [11]
USGS AGV-1	56 ± 4	59 [11]
Kodak TEG-50-A	48 ± 2	49 ± 5 [12]

[a]National Bureau of Standards Certified Values.

Precisions of ±10% or better can be expected. The average difference between the present results and the accepted values is 9% of the certified value. The detection limit for irradiations and counting times, each of 5 min, is ca. 10 ng of copper. This may be enhanced by two orders of magnitude, if desired, by extending both the irradiation and counting times to 60 min. However, the short irradiation and counting times, and the rapid chemical separation, give the advantage of rapid turn around and higher sample through-put.

The counting procedure is nearly free of interference. Only very weak lines from ^{56}Mn and ^{24}Na were detected. The radiochemical purity of the 511-keV line was checked by following the half-life for several days. Deviations from the accepted ^{64}Cu half-life were not observed.

I thank Ken Apt for his interest, and the staff of the Omega West Reactor for assistance with the irradiations. This work was performed under the auspices of the U.S. Energy Research and Development Administration.

REFERENCES

1 R. A. Nadkarni and G. H. Morrison, Anal. Chem., 46 (1974) 232.
2 L. L. Sundberg, Anal. Chem., 47 (1975) 2037.
3 E. S. Gladney and K. E. Apt, Anal. Chem., 47 (1975) 1484.
4 R. A. Nadkarni and G. H. Morrison, Anal. Chem., 47 (1975) 2285.
5 S. L. Law, Science, 174 (1971) 285.
6 R. A. A. Muzzarelli and R. Rocchetti, Anal. Chim. Acta, 70 (1974) 465.
7 F. W. E. Strelow, Anal. Chem., 32 (1960) 1185.
8 F. A. Cotton and G. Wilkinson, Advanced Inorganic Chemistry, John Wiley, New York, 2nd edn., 1966, pp. 903, 1029—1031.
9 R. A. Nadkarni, private communication (1976).
10 R. A. Nadkarni and G. H. Morrison, presented at the Modern Trends in Activation Analysis Conference, Munich, Germany, Sept. 1976.
11 F. J. Flanagan, Geochim. Cosmochim. Acta, 37 (1973) 1189.
12 D. H. Anderson, J. J. Murphy and W. W. White, Anal. Chem., 48 (1976) 116.

Analytica Chimica Acta, 91 (1977) 357—358

Short Communication

DETERMINATION OF THORIUM AND URANIUM IN CERIUM COMPOUNDS BY EPITHERMAL NEUTRON ACTIVATION ANALYSIS

E. STEINNES

Institutt for Atomenergi, Isotope Laboratories, Kjeller (Norway)

(Received 12th November 1976)

Thorium is a common impurity in cerium compounds because of the similar chemical properties of the two elements. Although the theoretical sensitivity of a thorium determination via 27.8-d ^{233}Pa is very high, applications of neutron activation analysis to the determination of thorium in cerium matrices have been few [1, 2], possibly because of the erratic behaviour of the carrier-free ^{233}Pa activity often observed in radiochemical separations. Neutron activation also offers a very high sensitivity if 2.35-d ^{239}Np is employed for the determination of uranium, but here again the difficulty associated with a carrier-free activity in radiochemical separations may explain why the determination of uranium in cerium compounds has not yet been reported.

If a Ge(Li) detector is used, thorium and uranium in cerium matrices can be determined without chemical separations, especially if activation is done with epithermal neutrons. The feasibility of epithermal irradiation in the determination of these elements by instrumental activation analysis has previously been demonstrated in the case of silicate rocks [3]. The gain in sensitivity obtained for the measurement of ^{233}Pa in the presence of the major matrix activity ^{141}Ce corresponds to a factor of 10 if the irradiation is performed at a reactor position with $R_{Cd}^{Au} = 3.0$ [4]. In the case of ^{239}Np, the corresponding advantage factor is as high as 30.

Experimental

Samples of about 100 mg were wrapped in 30 × 30-mm aluminium foil for irradiation. Standards were prepared by evaporating aliquots of dilute solutions carefully on the same sort of aluminium sheets. About 5 μg of Th and 5 μg of U were used as standards. Cylindrical cadmium boxes (1.0 mm thick, 20 mm i.d. and 12 mm internal height) were used for irradiation in the JEEP II reactor (Kjeller, Norway), at a position with a thermal neutron flux of $1.5 \cdot 10^{13}$ n cm^{-2} s^{-1} and $R_{Cd}^{Au} = 2.9$. After a delay of 6 d following irradiation for 20 h, when the activity of 33.4-h ^{143}Ce had decayed to a negligible level, samples and standards were subjected to γ-spectrometry with a 35-cm^3 Ge(Li) detector coupled to a multichannel analyzer (System

resolution 2.3 keV FWHM for the 1332-keV γ-ray of ^{60}Co). Peak areas were evaluated by the method of Covell [5]; 2, 3 and 4 channels, respectively, on either side of the channel containing the greatest number of counts were included and the average of the three peak area values thus obtained was taken. The 279-keV peak of ^{239}Np and 311-keV peak of ^{233}Pa were used for the determination of uranium and thorium, respectively.

Results and discussion

The test samples used were three different qualities of analytical-grade cerium compounds and a technical grade cerium oxide sample. Results are given in Table 1. It appears that thorium concentrations of the order of 50 p.p.m. can be determined in cerium matrices with a precision of 3—4%. At thorium concentrations of 0.1% or more, a precision of about 1% may be obtained. The limit of detection for thorium is about 1 p.p.m. after epithermal activation, compared with 10 p.p.m. by activation in the same flux without cadmium cover, or with 15 p.p.m. in a pure thermal neutron flux. The sensitivity for thorium determination would not be improved by further delay between irradiation and counting, since the half-life of the major interfering nuclide ^{141}Ce is similar to that of ^{233}Pa.

The limit of detection for uranium in high-purity cerium matrices also appears to be about 1 p.p.m. by instrumental activation analysis with epithermal neutrons. In this case, an improvement in sensitivity of a factor of 30 is observed relative to that obtained by irradiation in the same flux without cadmium cover. In comparison with activation in a purely thermal neutron flux, the epithermal activation technique yields an improvement of a factor of 120 for uranium in cerium matrices, as far as the purely instrumental analysis is concerned.

TABLE 1

Determination of thorium and uranium in some samples of cerium(IV) compounds

Sample	p.p.m. Th		p.p.m. U
	Mean value[a]	s_r%	
$Ce(SO_4)_2$, p.a.	60.7	3.2	<1
CeO_2, p.a. I	47.4	4.4	<1
CeO_2, p.a. II	44.5	3.7	<1
CeO_2, technical grade	1564	0.9	—

[a]Mean of 6 separate determinations.

REFERENCES

1 G. W. Smith and D. M. Mongan, Int. J. Appl. Radiat. Isot., 16 (1965) 81.
2 J. Op de Beeck, Anal. Chim. Acta, 40 (1968) 221.
3 A. O. Brunfelt and E. Steinnes, Anal. Chim. Acta, 48 (1969) 13.
4 E. Steinnes, in A. O. Brunfelt and E. Steinnes (Eds.), Activation Analysis in Geochemistry and Cosmochemistry, Universitetsforlaget, Oslo, 1971, p. 113.
5 D. Covell, Anal. Chem., 31 (1959) 1785.

Analytica Chimica Acta, 91 (1977) 359—363

Short Communication

EXTRACTION OF GLUTARIC AND SUCCINIC ACIDS BY TRI-ISOOCTYLAMINE

A. S. VIEUX and N. RUTAGENGUA

Laboratoire de Chimie analytique, Université Nationale du Zaïre, Campus de Kinshasa (Zaïre)

(Received 4th October 1976)

The equilibria involved in the extraction of dicarboxylic acids by long-chain alkylamines remain open to question. The conclusions reached regarding the neutralization of one or both of the carboxyl groups are divergent; according to Bullock et al. [1] only the neutral salt of oxalic acid is formed, while Lipovskii and Kuzina [2] assumed that the formation of the neutral salt occurs only when the ratio amine/acid is very high; otherwise, the compound formed corresponds to the bioxalate. Our previous conclusions [3] followed the latter view [2]. Results for the extraction of glutaric acid and some complementary experimental data on the extraction of succinic acid are now reported. Numerous factors seem to govern the extraction behaviour of carboxylic acids [4].

Chemical data were obtained by the methods used previously [3]. Investigations were undertaken of the influence of the diluent for some of the undissociated solvents used more commonly in extraction by alkylamines, e.g. benzene, xylene, 1,2-dichloroethane, 1,2-dichlorobenzene, and chloroform.

Experimental

The reagents, extraction procedures, apparatus and analytical methods were the same as previously described [3]. Characteristics reported for glutaric acid are: pK_{a_1}, 4.32; pK_{a_2}, 5.46 [5]; molecular weight, 132.12; b.p., 304.5°C; d., 1.429; aqueous solubility (20°C), 64 g/100 g [6]. High solubility is reported in alcohol, and diethyl ether. Solubility in benzene is negligible [5]. The equilibria between aqueous glutaric acid solutions and chloroform, 1,2-dichlorobenzene, and 1,2-dichloroethane have shown that acid extraction by the organic diluent occurs; the organic phase acidity was 0.120 M in chloroform for aqueous 3 M glutaric acid and 0.003 M in 1,2-dichloroethane and 1,2-dichlorobenzene. Correction for free acid extraction was made when necessary.

Results and discussion

Figure 1 gives the results for tri-isooctylamine plus aqueous 0.25 M and 0.5 M glutaric and succinic acids, obtained by the isomolar series method. The results of the distribution of glutaric acid between the two phases are presented in Fig. 2 as logarithmic plots of the acid distribution coefficient vs. the amount of amine in the organic phase at equilibrium. The data on the influence of aqueous acid concentration are given in Fig. 3.

The results from the method of isomolar series (Fig. 1) give unambiguous corroboration of our previous results [3]. The stoichiometric composition of the compounds indicates that acidic salt formation occurs with the overall formula $R_3N(COOH)_2(CH_2)_n$ with $n = 2$ or 3, respectively, for succinic and glutaric acids. The method of isomolar series is suitable and accurate for such studies; the results agree with previous data for extraction with long-chain alkylamines [7–9].

The absence of any inflexion point on the curves of Fig. 1 gives further

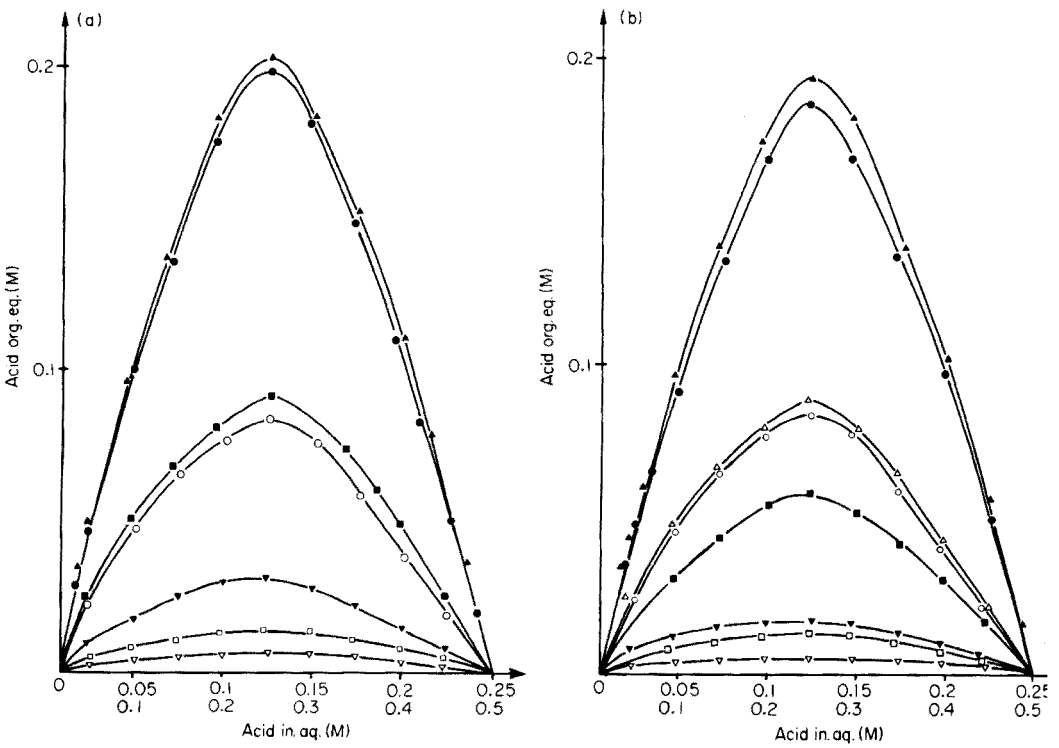

Fig. 1. Relation of acid concentration in the equilibrated organic phase (org. eq.) to the initial acid concentration in the aqueous phase (init. aq.). (a) TIOA + 0.25 M $(CH_2)_3(COOH)_2$ in xylene ▽, benzene □, chloroform ○, 1,2-dichloroethane △; TIOA + 0.50 M $(CH_2)_3(COOH)_2$ in xylene ▼, benzene ■, chloroform ●, 1,2-dichloroethane ▲. (b) TIOA + 0.25 M $(CH_2)_2(COOH)_2$ in xylene ▽, benzene □, chloroform ○, 1,2-dichloroethane △; TIOA + 0.50 M $(CH_2)_2(COOH)_2$ in xylene ▼, benzene ■, chloroform ●, 1,2-dichloroethane ▲.

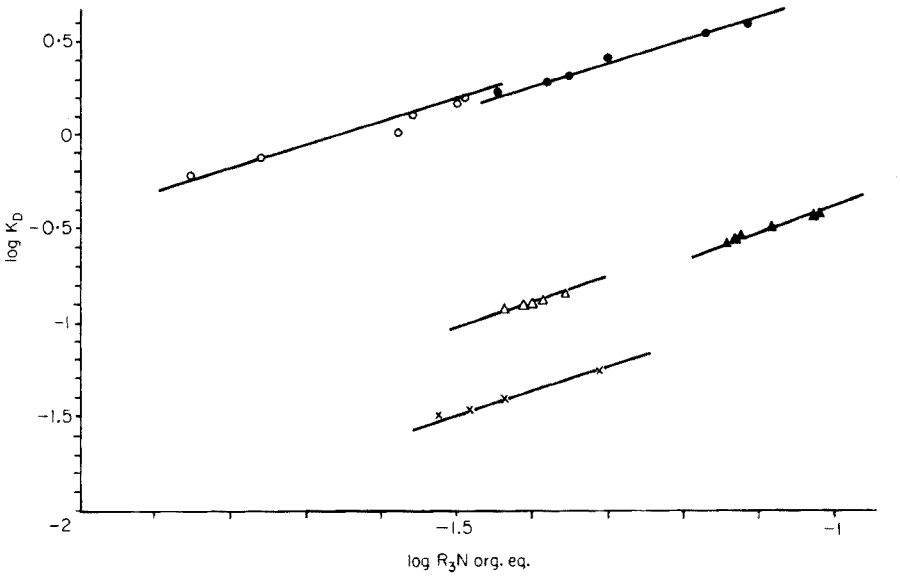

Fig. 2. Logarithmic plots of the distribution coefficients of the organic acid vs. the amount of tri-isooctylamine in the organic phase at equilibrium. In $CHCl_3$, $R_3N_{init.}$ = 0.05 M (○), $R_3N_{init.}$ = 0.1 M (●). In 1,2-dichlorobenzene, $R_3N_{init.}$ = 0.05 M (△), $R_3N_{init.}$ = 0.1 M (▲). In C_6H_6, $R_3N_{init.}$ = 0.05 M (×).

evidence that the neutralization reaction involves only one carboxyl group, thus excluding formation of the neutral salts. The ease of neutralization of the amine appears to depend on solvent influence. Aqueous acid concentrations corresponding to complete neutralization of the amine solution are summarized as follows:

For 0.1 M R_3N in benzene, 2.203 M; in 1,2-dichlorobenzene, 1.11 M; and in chloroform, 0.498 M.

For 0.05 M R_3N in benzene, 1.12 M; in 1,2-dichlorobenzene, 0.85 M; in chloroform, 0.395 M.

Ease of extraction appears to follow the sequence: benzene < 1,2-dichlorobenzene < chloroform, implying that the diluents are not inert but interact through both long-range coulombic effects and chemical bonding with the extracted species, as suggested by different authors [10, 11].

The extracted species appear, from the close to unit value obtained for the slope of the curves in log–log plots of the acid distribution coefficients vs. the amount of amine in the organic phase at equilibrium, mainly as undissociated ion pairs.

As glutaric acid is highly soluble in water, a wide range of initial aqueous acid concentrations could be investigated. However, the relatively low value of the distribution coefficient limited the range of investigations to an initial high molar ratio of amine to initial concentration of acid in the aqueous phase. Consequently, as pointed out [3] for the first three homologous

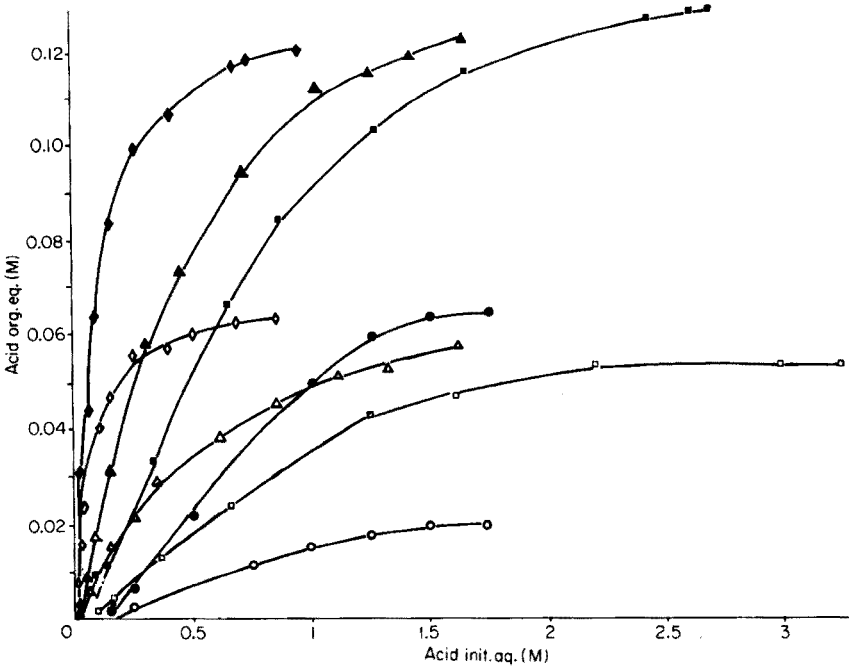

Fig. 3. Distribution of glutaric acid between an aqueous solution and a solution of tri-isooctylamine in various diluents. Xylene (○), C_6H_6 (□), $CHCl_3$ (◇) and 1,2-dichlorobenzene (△) with $R_3N_{init.}$ = 0.05 M; xylene (●) C_6H_6 (■), $CHCl_3$ (◆) and 1,2-dichlorobenzene (▲) with $R_3N_{init.}$ = 0.1 M.

dicarboxylic acids, it can be assumed that, in the range of concentrations considered, the interaction between tri-isooctylamine and glutaric acid leads to the formation of the hydrogenoglutarate of tri-isooctylamine, without excluding the possibility of the formation of neutral salts for higher molar ratios of amine: organic acid content. For the acids studied, the formation of an organic precipitate occurs only in the extraction of oxalic acid.

Comparison of distribution coefficients indicates that extraction with glutaric and malonic acids is preferable to succinic acid, excluding the effect of molecular dimension noticed by Pagel and McLafferty [4] in the extraction of acids by tributylphosphate. Higher aqueous solubility seems to be followed by better extraction. This would suggest that the structure of the acid in aqueous solution influences the extraction. It was noticed that substituted succinic acid solutions contain internal hydrogen bonds; this feature was not apparent for malonic acid solutions [12]. Explanations regarding aqueous dicarboxylic acid solutions as a function of an even number of carbon atoms have been given [13]. The possibility of intermolecular hydrogen bonding [4] could also account for the differences obtained in extraction.

REFERENCES

1 J. I. Bullock, S. S. Choi, D. A. Goodrick, D. C. Tuck and E. G. Woodhouse, J. Phys. Chem., 68 (1964) 2687.
2 A. A. Lipovskii and M. G. Kuzina, Radiokhim., 10 (1968) 175.
3 A. S. Vieux, N. Rutagengwa, J. B. Rulinda and A. Balikungeri, Anal. Chim. Acta, 68 (1974) 415.
4 A. Pagel and F. W. McLafferty, Anal. Chem., 20 (1948) 272.
5 Handbook of Chemistry and Physics, 50th edn., CRC, Cleveland, 44128C-359 (1969—1970).
6 L. S. Ralph, The Systematic Identification of Organic Compounds, 4th edn., Wiley, New York, 1962.
7 V. S. Smelov and A. V. Strakhova, Radiokhim., 5 (1963) 509.
8 V. V. Fomin, R. N. Maslova and L. L. Zaitseva, Zh. Neorg. Khim., 5 (1960) 1383.
9 A. S. Kertes and A. Beck, J. Chem. Soc., (1961) 1926.
10 R. M. Diamond, in Solvent Extraction Chemistry, North-Holland, Amsterdam, 1967, p. 349.
11 W. Muller, G. Duyckaerts and J. Fuger, in H. A. C. McKay, T. V. Healy, I. L. Jenkins and A. Naylor, Solvent Extraction Chemistry of Metals, Macmillan, London, 1965, p. 233.
12 D. Chapman, D. R. Lloyd and R. H. Prince, J. Chem. Soc., (1964) 550.
13 A. W. Ralston, Fatty Acids and Their Derivatives, J. Wiley, New York, 1948.

Analytica Chimica Acta, 91 (1977) 365—368

Short Communication

THE DETERMINATION OF 1,6-HEXAMETHYLENE DIISOCYANATE IN PAINT HARDENERS BY HIGH-PRESSURE LIQUID CHROMATOGRAPHY

G. B. COX and K. SUGDEN

Laboratory of the Government Chemist, Cornwall House, Stamford Street, London SE1 9NQ (England)

(Received 22nd November 1976)

Diisocyanates are added to the hardener in some two-component paint sprays to give the finished product good weather resistance and colour retention. Such paints have many applications, particularly in the vehicle industry. Aromatic diisocyanates were employed initially, but more recently the addition of aliphatic compounds such as 1,6-hexamethylene diisocyanate, which gives rise to finishes with improved lasting properties, has been adopted. Methods for the determination of diisocyanates, which may be toxic when inhaled, are required: Dunlap et al. [1] described a procedure for their determination in working atmospheres which employs conversion of the isocyanates to stable urea derivatives and subsequent gradient-elution high-pressure liquid chromatography on a pellicular silica gel. In the procedure described in this communication that method is modified to allow the determination of 1,6-hexamethylene diisocyanate in paint hardeners themselves, with the advantage that gradient programming of the solvent during the analysis is not required.

Experimental

Chromatographic apparatus and conditions. The liquid chromatograph comprised a Varian Series 4100 constant flow pump, a stopped-flow injection system, and a Cecil Instruments CE 212 ultraviolet monitor as detector. LiChrosorb Si60 (5 μm average particle size, BDH Chemicals Ltd), heated under reflux with 2 M hydrochloric acid for 4 h, was filtered, washed with water and acetone, and dried for 15 h at 200 °C. A stainless steel column (25 cm × 5 mm i.d.) was packed with the treated silica by a high-pressure slurry technique [2]. The mobile phase was 10% ethanol in 2,2,4-trimethylpentane at a flow rate of 1.1 ml min^{-1}. The column effluent was monitored at 275 nm.

Preparation of N-(4-nitrophenylmethyl)-N-propylamine (nitro reagent). *N*-(4-Nitrophenylmethyl)-*N*-propylamine hydrochloride (3 g), prepared by the method of Keller et al. [3], was dissolved in 300 ml of water. The free amine, precipitated by the addition of 330 ml of aqueous 1 M sodium hydroxide, was extracted with 4 × 50 ml of dichloromethane. The extracts were combined, made up to 250 ml, and dried over sodium sulphate.

Preparation of standard urea derivatives. Solutions containing 0.6, 0.36, 0.24, 0.12 and 0.06% (w/v) of 1,6-hexamethylene diisocyanate were made up in dry dichloromethane; to 1 ml of each solution, 25 ml of the nitro reagent solution was added. After the mixtures had been stirred for 60 min, they were evaporated to near dryness (rotary evaporator). The residues were diluted to 10 ml in calibrated flasks with dry dichloromethane.

Preparation of sample derivatives. Between 0.2 and 0.5 g of sample, weighed accurately, was dissolved in a small volume of dry dichloromethane. To this solution was added 25 ml of nitro reagent solution and the mixture was stirred for 60 min, evaporated, and made up to 10 ml as for the above standard solutions.

Results and discussion

The diisocyanates most commonly found in paints are toluene diisocyanate, 4,4′-diphenylmethane diisocyanate and 1,6-hexamethylene diisocyanate. The concentration of the two aromatic diisocyanates in paints has been determined for some time in this Laboratory by a modification of a method [4] that involves the formation of the corresponding ethyl urethanes with ethanol, followed by direct analysis by reversed-phase liquid chromatography with ultraviolet detection. As the urethane derived from 1,6-hexamethylene diisocyanate does not absorb u.v. radiation appreciably, such a procedure is not applicable. For similar reasons the procedure described recently for toluene diisocyanate [5] would also be unsuitable. This problem is effectively eliminated by the preparation of a u.v.-absorbing urea [1], as reported for determinations of isocyanates in working atmospheres.

Chromatography of the bis-(*N*-(4-nitrophenylmethyl)-*N*-propylurea) derivative was carried out initially on an octadecyl bonded phase packing but this approach was abandoned as components from some hardeners interfered. A column packed with silica gel of 5-μm particle size gave an adequate separation of all the components; because of the higher efficiency (and therefore peak capacity) of this column compared with the column packed with pellicular silica [1], the chromatography could be carried out under constant mobile phase composition rather than by a gradient elution procedure. This represents a considerable advantage; the analysis can be performed with simpler and less expensive equipment. However, a number of components with retention times considerably in excess of the urea are present (Fig. 1). Such compounds are possibly non-volatile components of the paint hardener as they do not appear in the chromatograms for working atmospheres [1]; they could be eluted rapidly from the column by a "step gradient" to a polar mobile phase to reduce the analysis time if necessary.

Initial investigation showed the presence in the hardeners tested of substances, other than free 1,6-hexamethylene diisocyanate, which reacted with the nitro reagent. In consequence, a large excess of the reagent was necessary for quantitative analysis. The concentration of 1,6-hexamethylene diisocyanate in the samples was calculated by measurement of the chromatographic peak

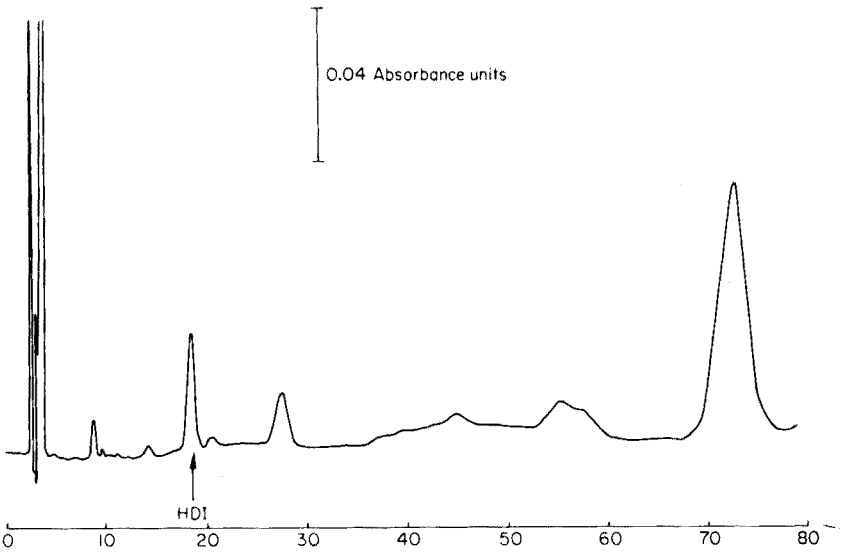

Fig. 1. Chromatogram of the dichloromethane extract of a hardener spiked with 0.60% HDI.

height after calibration of the detector response at 275 nm with the standard urea solutions. This response was rectilinear with urea concentration over the range tested. The maximum point of this range corresponded to 1.2% of the diisocyanate in 0.5 g of paint hardener. The recovery of isocyanate from a commercial hardener was determined by spiking with 1,6-hexamethylene diisocyanate at nine different concentrations ranging from 0.09% to 1.14%; yields ranging from 92 to 108% (mean, 99%; s = 5.7) were obtained. A typical chromatogram is illustrated in Fig 1. Toluene, xylene and ethylene glycol ethers may be used as solvents in paint hardeners; solutions of these compounds in dichloromethane (10% v/v) did not interfere with the chromatography of the diisocyanate derivative.

Commercial hardeners analysed by this method gave satisfactory replicate values in the range 0.26—0.30% of 1,6-hexamethylene diisocyanate. This diisocyanate was not detected in two of the commercial samples; the lower limit of detection (0.05% in these cases) was governed not by the detector noise but by the extent of overlap of adjacent chromatographic peaks from other materials present. Where no interference arose, the detection limit (expressed as three times the baseline noise, for a sample size of 0.5 g) was 0.01%.

We thank D. A. Bagon of the HSE Occupational Medicine and Hygiene Laboratories, Cricklewood for carrying out some of the practical work, and the Health and Safety Executive for sponsoring the development of this work.

REFERENCES

1 K. L. Dunlap, R. L. Sandridge and J. Keller, Anal. Chem., 48 (1976) 497.
2 G. B. Cox, C. R. Loscombe, M. J. Slucutt, K. Sugden and J. A. Upfield, J. Chromatogr., 117 (1976) 269.
3 J. Keller, K. L. Dunlap and R. L. Sandridge, Anal. Chem., 46 (1974) 1845.
4 D. M. Heinekey, private communication.
5 P. McFadyen, J. Chromatogr., 123 (1976) 468.

Analytica Chimica Acta, 91 (1977) 369—372

Short Communication

SOME PROBLEMS IN THE DETERMINATION OF BENZENE VAPOUR

C. W. KEEP and S. TERRY

Applied Chemistry Division, AERE Harwell, Didcot, Oxon. (England)

(Received 29th November 1976)

During a study [1] of the formation of carbon deposits on nickel heated in a hydrocarbon, a carbon and hydrogen mass balance deficit, which could be accounted for only by incorrect analysis for some reaction product, was discovered. The carbon : hydrogen mole ratio of the mass deficit was 1 : 1. Various features suggested that the determination of benzene might be in error, because of sorption on the walls of experimental vessels. This report describes an investigation of the errors involved in the sampling and determination of benzene.

Experimental

Gas Analysis. All gas analyses were conducted with a Perkin Elmer F30 gas chromatograph fitted with twin columns of Porapak Q (length 6 ft.) and flame ionization detectors. This was calibrated for benzene by injection of known aliquots of benzene and benzene—acetone mixtures. To work within the linear range of the detector, it is often necessary to dilute gas samples with helium. Samples, taken from the experimental apparatus at pressures below atmospheric, were diluted by pressurizing in steel vessels to 400 p.s.i.g. with helium.

Apparatus. The glass apparatus used has been described previously [1].

Method and results

Initially it was not clear whether sorption of benzene was occurring on the glass walls of the apparatus or the steel walls of the sampling vessels. Gas mixtures containing known concentrations of benzene were admitted to the sampling vessels and/or to the apparatus. By re-sampling and analysis, different methods of pretreatment of the sample vessels and glass surfaces were compared. The benzene mixtures of known concentration were admitted via an expansion bulb to various parts of the apparatus before sampling in a steel vessel by a procedure identical to that used in the hydrocarbon/nickel experiments.

Benzene mixtures. The benzene mixtures of known concentration were prepared by passing helium through a bubbler immersed in benzene and then through a stainless steel pressure vessel. The bubbler was maintained

at constant temperature in the range 10—17°C, and the steel vessel at 20°C. The helium flow was maintained overnight, to enable the benzene distribution between gas and walls to attain a steady state. The benzene concentration was determined from the benzene saturated vapour pressure at the bubbler temperature; the helium was at atmospheric pressure. This mixture was further diluted, to obtain a benzene concentration similar to that found in the previous experiments, by pressurizing with helium to about 400 p.s.i., at constant vessel temperature. The concentrations of benzene in these mixtures, as determined by chromatography, were a little higher than expected, possibly because of droplet entrainment in the bubbler.

Pretreatment of vessel and glass surfaces. To determine the benzene sorption in the steel sample vessel, the vessel was heated to 525 K, with continuous evacuation overnight to below 10^{-5} mm Hg, and then allowed to cool to room temperature while still evacuated. This treatment should have removed benzene or other materials from the vessel surface. Gas was transferred to this vessel, and analysed. The results are shown in Fig. 1 (solid circles). Measurements in which the steel vessel was used as received from a previous analysis for benzene, with no cleaning treatment, are also shown in Fig. 1 (open circles). Here the analysis of the starting gas and of the sample agree; this was still the case when the vessel surface was cleaned by prolonged evacuation before use. The fractional partial pressure loss is greater at lower partial pressures of benzene.

Benzene sorption on the glass surface of the apparatus was investigated in two experiments. In the first, the furnace tube was heated overnight at 975 K under vacuum. The benzene mixture was then admitted, and allowed to remain in contact with the hot glass for 1 h (a time comparable to the

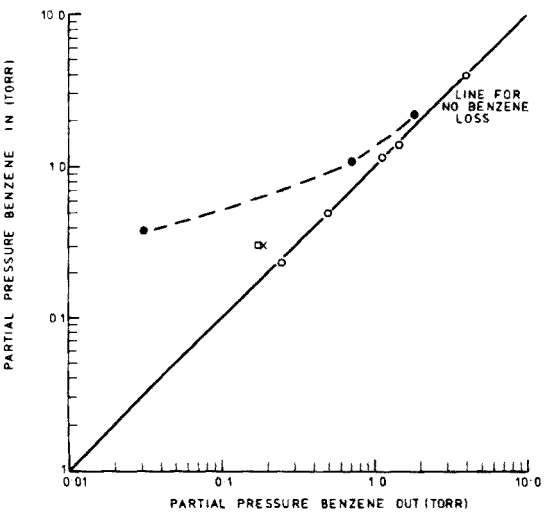

Fig. 1. Benzene sorption on glass surfaces and steel sample vessels. The line is for no benzene loss. • Vessel preheated to 525 K. ○ Vessel conditioned with benzene. □ Glass heated to 450 K. X Vessel after use with CO_2/CO mixtures.

exposure in the hydrocarbon/nickel experiments [1]). The gas was then sampled by means of a conditioned steel sampling vessel. The results showed that there was no benzene sorption or reaction in the furnace. In the second experiment, the glass walls of the apparatus were degassed by heating to about 450 K with a hair-dryer for 1 h, with the rig under vacuum. It was allowed to cool; the benzene mixture was admitted, and again sampled with a conditioned vessel. The result given in Fig. 1 (square) demonstrates that benzene was sorbed on the clean walls; the concentration was only about 50% of that expected.

The steel sampling vessels are generally used for removing CO_2/CO samples from high pressure loops. In a final experiment, a sampling vessel was taken from this application, and used to sample a benzene gas mixture, without any intermediate treatment. The result, plotted as a cross in Fig. 1, demonstrates that benzene was also sorbed on the surface of this vessel, but to a lesser extent than on the steel surface cleaned by heating to 525 K.

Discussion

The loss in benzene fractional partial pressure with the sampling vessels preheated to 525 K is greatest at low partial pressures of benzene. The calculated amounts of benzene lost are shown in Table 1; the amount of benzene lost, essentially constant at $2.6 \cdot 10^{-6}$ mol, is independent of the benzene partial pressure within the range studied. (As the internal geometrical surface area of the pressure vessel is 230 cm^2, the loss is $1.13 \cdot 10^{-8}$ mol cm^{-2}.)

After the sampling vessel had been used for an analysis in which more than $2.6 \cdot 10^{-6}$ mol of benzene was present in the gas phase, subsequent analysis with the same sample vessel showed no further sorption, even after evacuation overnight before use. This suggests that a fast, Langmuir-type sorption, which levels out at $1.13 \cdot 10^{-8}$ mol cm^{-2}, occurs with a very slow desorption rate at room temperature.

It also appears that there is a constant loss of benzene in steel vessels used without heat pretreatment after analysis of CO_2 mixtures; this loss is estimated (see Table 1) to be $3.9 \cdot 10^{-9}$ mol cm^{-2}. The surface complexes

TABLE 1

Loss of benzene through sorption processes

Pretreatment	Benzene lost (mol)	Initial benzene partial pressure (Torr)	Vessel surface area (cm^2)
Preheated at 525 K	$2.5 \cdot 10^{-6}$	0.38	230
	$2.6 \cdot 10^{-6}$	2.23	230
	$2.7 \cdot 10^{-6}$	1.10	230
New steel pressure vessel	$8.9 \cdot 10^{-7}$	0.31	230
Glass preheated to 450 K	$1.3 \cdot 10^{-6}$	0.31	220

formed on the steel by the CO_2/CO mixtures presumably occupy ca. 70% of the surface sites available for benzene sorption.

Sorption of benzene occurs on glass walls at room temperature, but not at 975 K. This shows that cracking of benzene is negligible at this temperature. Glass walls at room temperature can be "conditioned" in the same way as the steel vessel, as no loss was found in the experiments with a "conditioned" steel container. In the glass equipment, the amount of benzene sorbed per unit geometrical surface area was about 50% of that sorbed on the steel.

From a practical point of view, it is therefore important that equipment and sample containers should be conditioned for use with benzene. If "clean" vessels must be used, errors will be minimized if relatively high partial pressures in the mixture to be analysed, and vessels with the highest volume-to-surface area ratio (i.e. spherical containers), are used.

The authors thank Mr. H. A. Prior, Mr. E. E. Jackson and Mr. A. R. Trowell for useful discussions, and Dr. J. K. Linacre for critical assessment of this report.

REFERENCE

1 C. W. Keep, R. T. K. Baker and J. France, J. Catal., in press.

Analytica Chimica Acta, 91 (1977) 373—374

Short Communication

SPECTROPHOTOMETRIC DETERMINATION OF NITRATE IN WATER IN THE $\mu g\ l^{-1}$ RANGE

YULIN L. TAN

Health and Safety Laboratory, U.S. Energy Research and Development Administration, New York, NY 10014 (U.S.A.)

(Received 10th November 1976)

The biological importance of nitrogen in living organisms has been well recognized and the determination of nitrate or oxides of nitrogen is one of the primary steps for environmental studies concerning air and water pollution, sanitation and public health. Considerable work has been done in this area [1—4]. However, the published procedures are either not sensitive enough for low nitrate levels or require sophisticated instrumentation. Thus, for relatively unpolluted environmental samples with low nitrate contents, only "less than" values have been reported.

For studies of precipitation samples in this laboratory, a sensitive procedure for nitrate determination has been developed. The method is based on nitration of 2,6-dimethylphenol and spectrophotometric measurement of the product. The nitration conditions and extraction procedures have been optimized. A linear relationship between absorbance and nitrate concentration has been obtained. The interference of nitrite and chloride was removed by using sulfamic acid and mercury(II) sulfate, respectively.

Experimental

Apparatus and reagents. A Beckman DK spectrophotometer was used with matched 1-cm cells. All chemicals were of reagent grade.

Procedure. Pipet 25 ml of sample into a 125-ml Erlenmeyer flask with stopper. Add 40 ml of concentrated sulfuric acid slowly from a buret. Mix, place the flask in a cold water bath and cool to room temperature. Add 0.1 ml of aqueous 5% (w/v) sulfamic acid reagent, 0.1 ml of 5% (w/v) mercury(II) sulfate reagent in 10% (v/v) sulfuric acid, and 1 ml, by pipet, of 1% (w/v) 2,6-dimethylphenol reagent in glacial acetic acid. Mix well and incubate the flask in a 30°C water bath for 15 min. Transfer the reaction mixture to a 250-ml Teflon-stoppered separatory funnel. Wash the flask and dilute the solution with 100 ml of ice-cold deionized water. Extract the 2, 6-dimethyl-4-nitrophenol into 10 ml of toluene. Shake the mixture for 1 min, discard the lower aqueous layer, wash the toluene extract with 10 ml of water, and discard the wash solution. The last step should be carried out with special care

and precision, to avoid diluting the final solution or losing the sample. Convert the phenol to phenoxide by adding 5 ml, by pipet, of 2M NaOH. Shake the funnel for 1 min and wait for the phases to separate. Rinse the funnel stem with a few drops of aqueous alkaline extract, then collect the extract and record its spectrum from 600 to 400 nm.

Results and discussion

The typical spectrum of 2,6-dimethyl-4-nitrophenoxide in the reaction mixture is shown in Fig. 1. The absorbance of this phenoxide is taken as the difference of the absorbance at the 428-nm peak and the plateau absorbance in the 560—520 nm range. The plateau absorbance is thought to be contributed by the residual turbidity of the solution and varies very slightly from solution to solution. A linear relationship was observed between absorbance and nitrate concentration over the range 0—900 $\mu g\ l^{-1}$. The lowest reliable determination is at 50 $\mu g\ l^{-1}$ with a calibration absorbance of 0.11 ± 0.01. Lower levels could be detected, but less reliably because of instrumental limitations. The accuracy of the method is ± 15 $\mu g\ l^{-1}$ or ± 5% whichever the higher.

The amount of sulfamic acid and mercury(II) sulfate used prevents the interference of nitrite and chloride, respectively, up to 50 mg l^{-1}. For higher levels of nitrite and chloride, the amount of sulfamic acid and mercury(II) sulfate could be increased proportionally.

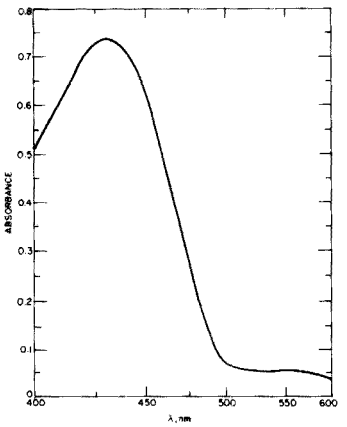

Fig. 1. Spectrum of 2,6-dimethyl-4-nitrophenoxide.

REFERENCES

1 W. D. Ross, G. W. Buttler, T. G. Duff, W. R. Rehg, M. T. Wininger and R. T. Sievers, J. Chromatogr., 112 (1975) 719.
2 B. K. Afghan and J. F. Ryan, Anal. Chem., 47 (1975) 2347.
3 A. M. Hartley and R. I. Asai, Anal. Chem., 35 (1963) 1207.
4 D. W. W. Andrews, Analyst (London), 89 (1964) 730.

Analytica Chimica Acta, 91 (1977) 375—377

Short Communication

SPECTROPHOTOMETRIC DETERMINATION OF PHOSPHORUS IN PHOSPHOSILICATE GLASS

EIICHI KITAZUME, NORIO SHIBATA and NORIKAZU HASHIMOTO
Central Research Laboratory, Hitachi Ltd., Kokubunji, Tokyo (Japan)
(Received 24th September 1976)

The determination of phosphorus based on the molybdenum blue reaction continues to be widely used because it is sensitive and convenient. However, silicon, arsenic and germanium also react to form blue compounds. To avoid interference, these elements must be separated in advance. Murphy and Riley [1] used antimony, as potassium antimonyl tartrate, to increase the reduction rate. Recently, Going et al. [2, 3] reported on the mechanism of formation of molybdoantimonylphosphoric acid and the negligible effect of silicate. As the effect of silicon is not completely understood, the interference of silicon on phosphorus determination in phosphosilicate glass has been studied. A reliable determination is proposed, and the effects of arsenic and germanium are reported.

Experimental

Apparatus and reagents. A Hitachi model 333 spectrophotometer was used with 1-cm cells. All solutions were prepared from analytical-reagent grade chemicals, except for potassium antimonyl tartrate, and deionized water. A mixed reagent was prepared as described by Going et al. [2] except for potassium antimonyl tartrate. For the mixed reagent, 2.12 g of sodium molybdate was dissolved in 150 ml of water, 20.8 ml of concentrated sulfuric acid was added, and the mixture was cooled to room temperature; 0.334 g of potassium antimonyl tartrate (recrystallized twice to reduce the impurity content) was then added and the solution was diluted to 250 ml. Ascorbic acid (1%) was freshly prepared.

Procedure. A phosphosilicate glass (PSG) sample deposited on a silicon wafer was weighed and placed in a 100-ml platinum evaporating dish. Next, 5 ml of hydrofluoric acid (5%) and 1 ml of perchloric acid were added. After the PSG film had dissolved, the silicon wafer was removed from the solution, washed, dried and reweighed. The solution was heated to fumes of perchloric acid, cooled slightly, transferred to a 10-ml standard flask, and diluted to 10 ml with water. A suitable aliquot was pipetted and neutralized with NaOH; 0.5 ml of the mixed reagent and 0.2 ml of ascorbic acid solution were added, and the solution was diluted with water to 5 ml. After 10 min, the absorbance

was measured against water at 710 nm.

To examine the effects of coexisting silicon, arsenic and germanium, a given amount of each was added, and phosphorus was then determined with the mixed reagent as above.

Results and discussion

The areas representing the conditions under which the molybdenum blue reaction takes place are shown in Figs. 1 [4] and 2. The molybdenum blue reaction is considered to occur when the sample becomes blue more intensely than the blank. A molybdenum blue reaction does not occur or the reaction rate is very small for silicon and germanium for Fig. 2. Figure 3 shows the effects of arsenic and silicon on absorbance. Arsenic(III) and especially arsenic(V) affect the determination of phosphorus even in low concentrations. However, silicon does not interfere, even when it exists in concentrations a thousand times that of phosphorus. The results obtained for PSG films are shown in Table 1.

These experiments demonstrated that the procedure is suitable for the determination of phosphorus in silicate glasses, such as PSG. Perchloric acid

TABLE 1

Determination of phosphorus in PSG film
(Results are given as μg; each value shows the amount of phosphorus in a 1 ml aliquot of 2.515 mg of PSG film dissolved in 200 ml of sample solution.)

Sample	1	2	3	4	5	*s*	R.s.d. (%)
Found	1.37	1.40	1.36	1.35	1.41	±0.026	±1.9

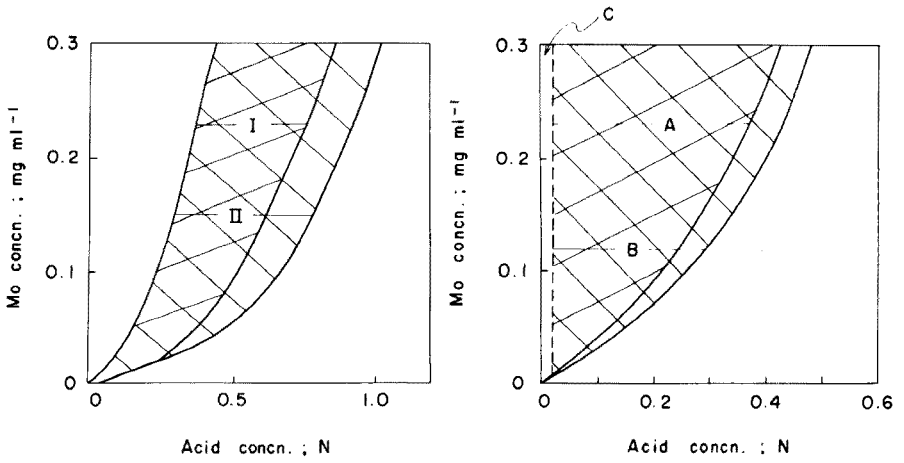

Fig. 1. Molybdenum blue reaction area with tin(II) chloride as reducing agent. I, Si (0.2 μg ml^{-1}) or Ge (0.3 μg ml^{-1}); II, P (0.1 μg ml^{-1}) or As(V) (0.3μg ml^{-1}) [4].

Fig. 2. Molybdenum blue reaction area by the proposed method. (A) As(V) (0.2 μg ml^{-1}); (B) P (0.2 μg ml^{-1}); (C) Precipitation area for reduction of MoO_4^{2-}.

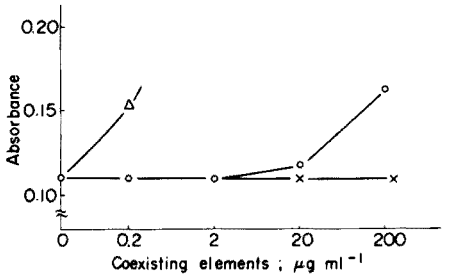

Fig. 3. Effect of As(III), As(V) and Si on the determination of 0.2 μg P ml^{-1}. (○) As(III); (△) As(V); (×) Si.

was used instead of sulfuric acid when the solution was heated to eliminate silicon as SiF_4 to avoid polymerization of orthophosphoric acid.

The authors are grateful to Dr. Naoyuki Nagashima, Mr. Hideaki Suzuki, and Mr. Mituo Hayashi for valuable technical discussions and to Mr. Yuji Yatuda for preparation of the samples.

REFERENCES

1 J. Murphy and J. P. Riley, Anal. Chim. Acta, 27 (1962) 31.
2 J. E. Going and S. J. Eisenreich, Anal. Chim. Acta, 70 (1974) 95.
3 J. Going, S. Wenzel and J. Thompson, Microchem. J., 20 (1975) 126.
4 H. Levine and I. J. Powe, Anal. Chem., 27 (1955) 258.

Analytica Chimica Acta, 91 (1977) 379—383

Short Communication

THE MICRODETERMINATION OF NICKEL, COBALT AND ZINC BY REFLECTANCE SPECTROMETRY

R. REISFELD, H. HARNIK, S. LEVI and W. J. LEVENE*

Department of Inorganic and Analytical Chemistry, The Hebrew University of Jerusalem, Jerusalem (Israel)

(Received 2nd December 1976)

Spot test papers for semi-quantitative determinations of nickel, cobalt and zinc are available, but more exact and more sensitive determinations are desirable. In the present work, the techniques developed previously for mercury(II) [1], lead(II) [2], copper(II) [3], nitrite, sulphate and phosphate [4] are extended to nickel(II), cobalt (II) and zinc(II); the ions are determined by measuring the diffuse reflectance spectra of their coloured complexes precipitated on filter cards. In each case linear expressions are obtained relating the Kubelka—Munk function [5], $F(R) = (1 - R)^2/2R$, of the diffuse reflectance, R, at the appropriate wavelength, to the concentration, C (ppm), within certain ranges.

Nickel(II). For the range 8—320 ppm, the reagent used is an aqueous solution of the sodium salt of dimethylglyoxime; this gives more uniform spots than the alcoholic solution normally used [6]. In the range 1—12 ppm, rubeanic acid [6] is preferable. Urea is added to the test solution to optimize the pH.

Cobalt(II). Simple tests may be performed at concentrations of 1—20 ppm with 1-nitroso-2-naphthol [6] dissolved in aqueous alkaline solution. Cobalt in the range 2—250 ppm may be determined with the same reagent dissolved in alcohol. In this range the precision and sensitivity of the test are enhanced when the reagent is used in 50% acetic acid solution; but this enhancement is obtained at the expense of reduced stability of both the reagent and the test spots.

Zinc(II). Aqueous dithizone was found to be a satisfactory reagent for zinc(II) determinations; the standard technique [6] with CCl_4 solutions of this reagent does not give stable spots on filter paper. The reagent is not, however, specific for zinc.

Experimental

Reagents. I. Alcoholic 0.5% (w/v) rubeanic acid (B.D.H.) solution was prepared by heating to 40—50°C.

*Present address: Electro-Optical Industry, Ltd., Rehovoth, Israel.

II. Aqueous 2.85% (w/v) sodium dimethylglyoximate (Baker) solution was used.
III. Aqueous 0.05% (w/v) 1-nitroso-2-naphthol (Fluka) solution was adjusted to pH 11 with KOH.
IV. 1-Nitroso-2-naphthol (1.00 g) was dissolved in 50 ml of glacial acetic acid, and diluted to 100 ml with water.
V. Alcoholic 2% (w/v) 1-nitroso-2-naphthol solution was prepared by refluxing for 1 h.
VI. Aqueous 0.08% (w/v) dithizone (Eastman-Kodak) solution was adjusted to ca. pH 12 with KOH.

All chemicals were of analytical-reagent grade, and triply distilled water was used throughout.

Test solutions. Stock solutions of $NiSO_4 \cdot 6H_2O$ (600 ppm), $CoSO_4 \cdot 7H_2O$ (500 ppm), $ZnSO_4 \cdot 7H_2O$ (500 ppm) were used.

Tests for interfering ions. The stock solutions used contained 10,000 ppm of $Fe(NO_3)_3$, 1000 ppm of $CuSO_4 \cdot 5H_2O$ or $CoSO_4 \cdot 7H_2O$, or 100 ppm of $UO_2(NO_3)_2 \cdot 6H_2O$, $NiSO_4 \cdot 6H_2O$, $Pb(NO_3)_2$, $AgNO_3$, $CrCl_3 \cdot 6H_2O$, $Ba(NO_3)_2$, $FeSO_4 \cdot 7H_2O$, $HgCl_2$, $MgSO_4 \cdot 7H_2O$, $MnSO_4 \cdot 4H_2O$, or $Cd(NO_3)_2 \cdot 4H_2O$.

Procedure. The experimental procedure has been described [1]. Drops of reactants were applied from microsyringes (7 μl). Diffuse reflectance measurements were made with a Fast Scanning Spectrocolorimeter Model SCF-1 (Israel Electro-Optical Industry, Ltd.). The test specimens were prepared on Whatman 120 filter card strips with 18 spots per strip. Sufficient accuracy was generally obtained by taking the average reflectance of 2 spots for each measurement, so that 9 measurements could be made on each strip. The photographs reproduced here were multiple exposures on Polaroid film from a camera mounted on the oscilloscope of the instrument, which presents the spectral reflectance curve.

The standard drying time of the spots on the filter card was 10 min at 40—50° C. In the reaction between nickel and rubeanic acid, the spots developed slowly, and drying for 20 min was required at the second stage (after the addition of the drop of test solution).

Interference of different ions was tested by comparing the reflectance spectra of test spots made from solutions of (a) the tested ion alone, (b) the suspected interfering ion alone, and (c) an appropriate mixture of the two.

In the tests for nickel with reagent I, there were interferences from Cu(II), Co(II), Fe(II) and Fe(III) in 10-ppm concentrations. In the tests with reagent II, interferences were found from Cu(II) (200 ppm), Co(II) (200 ppm) and Fe(III) (500 ppm). With reagent II, masking of interference by Cu(II) or Co(II) by dipping the formed spots on the filter paper into aqueous 3% ammonia [6] was satisfactory for concentrations up to 1000 ppm of the interfering ion. Masking of Fe(III) by adding enough sodium tartrate and sodium fluoride to saturate the test solution, was satisfactory for up to 10 000 ppm of Fe(III) with reagent II.

In the determination of cobalt, Cu(II), Fe(II), Fe(III) and UO_2(II) interfered at 50-ppm levels with reagents IV and V. With reagent III, Cu(II), Fe(II) and Fe(III) interfered at the 10-ppm level, but UO_2(II) interfered only above 500 ppm. With reagent I, Cu(II) and Ni(II) interfered at the 10-ppm level, whereas Fe(III) interfered only above 100 ppm.

For the determination of zinc with reagent VI, all the heavy metal ions tested interfered at the 10-ppm level, except for Mn(II) which did not interfere up to 100 ppm.

Results

Table 1 summarizes the experimental conditions and results. Figures 1—3 show spectra as seen on the oscilloscope for the various tests. In Figs. 1 and 2, the upper curves relate to the lower concentrations of test ion in the solution.

TABLE 1

Summary of experimental conditions and results

Reagent	Ni(II)[a]		Zn(II)[c]			
	I[d]	II	VI			
Range (ppm)	1—12	8—320	1—40			
Precision (ppm)	±0.85	±6.3	±1.4			
Equation: $10^3 \times F(R) =$	$4.80C +$ 0.907	$2.06C +$ 0.674	$13.24C +$ 53.4			
Wavelength (nm)	570	545	570			
Reagent stability (d)	3	30	>7			
Spot stability (d)	20	30	20			
Reagent	**Co(II)[b]**					
	III	IV		V		I[e]
Range (ppm)	1—20	2—50	50—250	2—50	50—250	5—120
Precision (ppm)	±0.42	±0.7	±6	±2	±12.5	±2
Equation: $10^3 \times F(R) =$	$6.76C +$ 8.92	$2.77C +$ 2.77	$1.71C +$ 85.0	$1.24C +$ 15.2	$0.707C +$ 43.3	$0.252C +$ 2.65
Wavelength (nm)	500	550		570		500
Reagent stability (d)	2	1		30		3
Spot stability (d)	>10	(1h)		3—4		20

[a] 1—320 ppm corresponds to $7 \cdot 10^{-9}$—$2.25 \cdot 10^{-6}$ g in a drop. [b] 1—250 ppm corresponds to $7 \cdot 10^{-9}$—$2.1 \cdot 10^{-6}$ g in a drop. [c] 1—40 ppm corresponds to $7 \cdot 10^{-9}$—$2.8 \cdot 10^{-7}$ g in a drop. [d] Solid urea was dissolved to give 2% (w/v) in the test solution. [e] Solid sodium acetate was dissolved to give 6% (w/v) in the test solution.

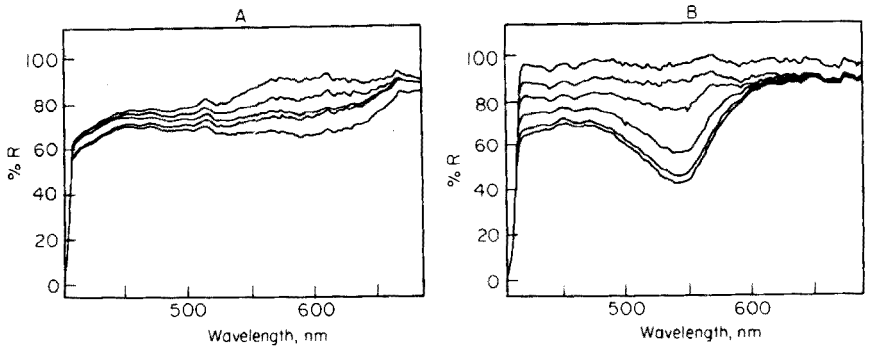

Fig. 1. Diffuse reflectance spectra for nickel. (A) With reagent I; successive curves downward relate to instrument calibration ($MgCO_3$ block), and solutions containing 0, 3, 8, 12 and 20 ppm Ni^{2+}. (B) With reagent II; successive curves downward relate to instrument calibration and solutions containing 0, 20, 75, 150 and 200 ppm Ni^{2+}.

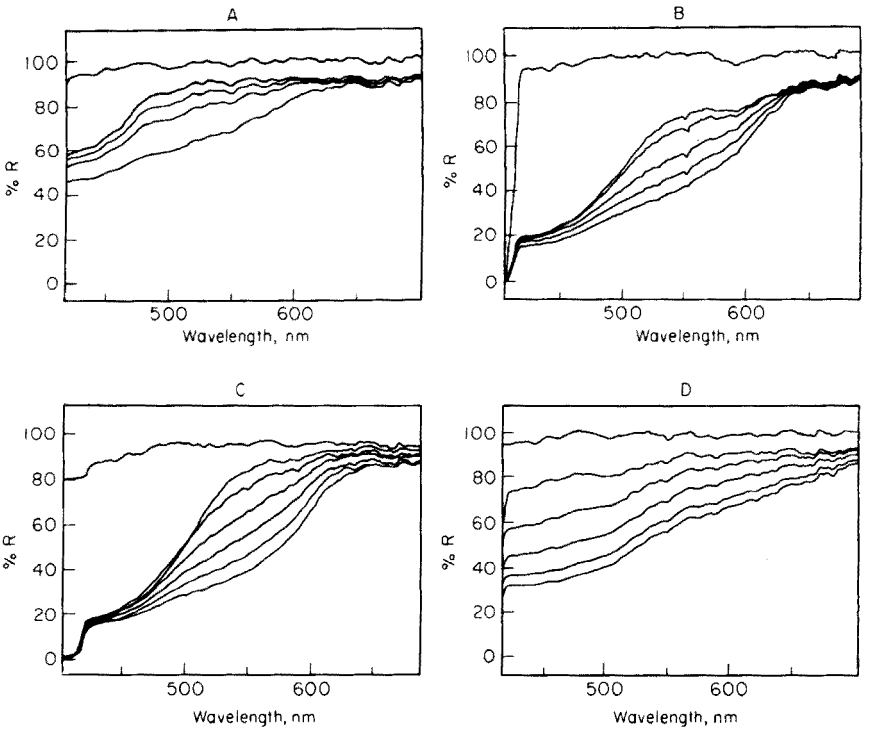

Fig. 2. Diffuse reflectance spectra for cobalt. (A) With reagent III; successive curves downward relate to instrument calibration and solutions containing 0, 2, 5 and 20 ppm Co^{2+}. (B) With reagent IV; successive curves downward relate to instrument calibration and solutions containing 0, 10, 50, 100 and 200 ppm Co^{2+}. (C) With reagent V; the curves (downward) relate to instrument calibration and solutions containing 0, 5, 20, 50, 100 and 200 ppm Co^{2+}. (D) With reagent I; the curves (downward) relate to instrument calibration and solutions containing 0, 30, 100, 225 and 300 ppm Co^{2+}.

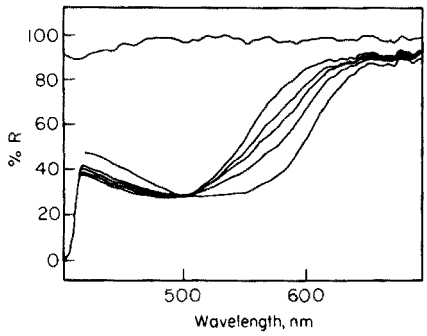

Fig. 3. Diffuse reflectance spectra for the zinc test with reagent VI. Successive curves downward relate to instrument calibration and solutions containing 0, 5, 10, 20 and 50 ppm Zn^{2+}.

Figure 3 shows an isosbestic point; to the right of this point the upper curves relate to the weakest solution. In each case the top curve is the 100% test line of the instrument.

The graphs relating the Kubelka—Munk expression to concentration are summarized in Table 1 as a computer-calculated best fit. For cobalt, with reagents IV and V (columns 5—8), it was necessary to use different equations for the branches of the curve below and above a knee. The precision mentioned in the Table is the standard deviation of the points measured from this equation; each point was the average of two measurements. Manganese(II) which usually interferes in the sulphide determination of zinc does not interfere with the present test.

Conclusions

The detection limits quoted here for Co(II), Ni(II) and Zn(II) are lower than those found in the literature for spot tests. The tests have been extended to make them quantitative, with standard deviations as low as 2.5% at the 20-ppm level.

REFERENCES

1 R. Reisfeld, E. Greenberg and W. J. Levene, Anal. Chim. Acta, 74 (1975) 253.
2 R. Reisfeld, S. Levi, E. Greenberg and W. J. Levene, Anal. Chim. Acta, 76 (1975) 477.
3 R. Reisfeld, S. Levi, E. Greenberg and W. J. Levene, Anal. Chim. Acta, 79 (1975) 326.
4 R. Reisfeld, S. Levi and W. J. Levene, Anal. Chim. Acta, 84 (1976) 135.
5 G. Kortum, Reflectance Spectroscopy, Springer-Verlag, Berlin, 1969.
6 F. Feigl, Spot Tests in Inorganic Analysis, Elsevier, Amsterdam, 1958.

Analytica Chimica Acta, 91 (1977) 385—387

Short Communication

EXTRACTION—SPECTROPHOTOMETRIC DETERMINATION OF PHOSPHATE AS THE METHYLENE BLUE MOLYBDOPHOSPHATE

TSUTOMU MATSUO, JUNICHI SHIDA and WAICHIRO KURIHARA

Department of Applied Chemistry, Faculty of Engineering, Yamagata University, Jonan-4 Yonezawa 992 (Japan)

(Received 4th August 1976)

Most methods for determining traces of phosphorus are based on the absorption spectrophotometry in solution of phosphate as yellow phosphomolybdic acid, or as the blue reduction products in aqueous or organic media. Kirkbright et al. [1] have reported a method based on the formation of a complex between rhodamine B and molybdophosphoric acid. Golkowska and Pszonicki [2] have studied the composition and properties of the ion-association complex of rhodamine B with silicomolybdic acid, and used this method for the determination of silicon. The indirect determination of germanium [3] and tantalum [4], based on extraction of heteropoly molybdates with methyl isobutyl ketone (MIBK) [5], by atomic absorption spectrometry has been studied. In the method for the spectrophotometric determination of phosphorus described here, the absorbance of the ion-association complex formed between molybdophosphate and methylene blue is measured after its extraction into MIBK.

Experimental

Apparatus and reagents. An Hitachi—Perkin-Elmer Model 139 spectrophotometer with 10-mm glass cells was used. All the chemicals were of analytical-reagent grade. Water was deionized and distilled.

Standard phosphate solution (31 μg P ml^{-1}). Dissolve 0.1361 g of potassium dihydrogenphosphate in water and dilute to 1 l. This solution was diluted as required to 1.55 μg P ml^{-1} with water.

Molybdate solution (0.1 M). Dissolve 17.7 g of ammonium molybdate tetrahydrate in water and dilute to 1 l.

Methylene blue solution ($2 \cdot 10^{-3}$ M). Dissolve 0.747 g of methylene blue (C.I. 922) in water and dilute to 1 l. Stock solutions (1 μg ml^{-1}) of diverse ions were prepared by dissolution of their salts in water or dilute hydrochloric acid.

Procedure. Place a sample solution containing less than 8 μg P in a 100-ml separatory funnel, and add 8 ml of 5 M nitric acid and 10 ml of 0.1 M molybdate solution. Then, add 2 ml of $2 \cdot 10^{-3}$ M methylene blue and dilute

with water to 50 ml. Mix well. Extract vigorously with 10.0 ml of MIBK for 5 min. Allow the phases to separate for 5 min, remove the aqueous phase, add 25 ml of 2 M nitric acid and shake for 5 min. Separate the phases and measure the absorbance of the MIBK extract at 655 nm in 10-mm glass cells. Take a reagent blank through the complete procedure to obtain the net absorbance for the sample.

Results and discussion

The spectra of the complex in MIBK are shown in Fig. 1; there are shoulders at 610—630 nm and an absorption maximum at 655 nm.

Effect of reaction variables. The optimum acidity of the aqueous solution for the extraction of methylene blue molybdophosphate with MIBK was found to be 0.7—0.9 M nitric acid. The absorbance decreased gradually over the range 0.9—1.8 M HNO_3. The reproducibility was poor below 0.6 M nitric acid because of precipitation. A concentration of 0.8 M nitric acid in the initial solution was chosen as the optimum.

The effect of ammonium molybdate on the extraction of methylene blue molybdophosphate was studied; the absorbance increased when up to 7 ml of 0.1 M ammonium molybdate was used, but then remained constant for up to 20 ml of the reagent; 10 ml of the molybdate solution was used in further work. As shown in Fig. 2, a constant absorbance was obtained when 1.5—2.5 ml of $2 \cdot 10^{-3}$ M methylene blue solution was added; 2 ml of this solution was used in further work.

The nitric acid concentration in the washing solution for the extraction of the excess of methylene blue reagent from the MIBK extract was not very important. The absorbances were the same when the acidity was 1—4 M,

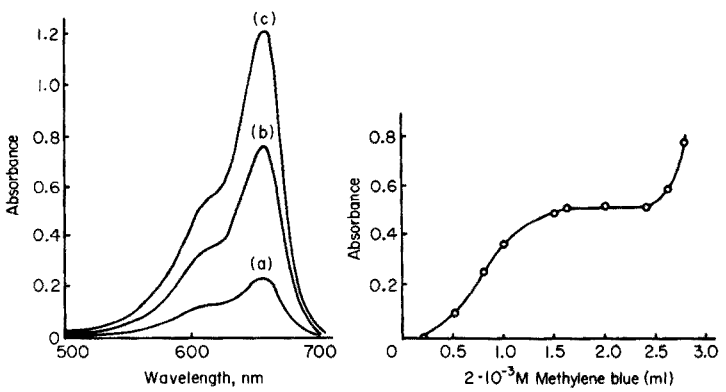

Fig. 1. Absorption spectra of (a) 1.55 μg P, (b) 4.65 μg P, (c) 7.75 μg P. [Mo] = $2 \cdot 10^{-2}$ M, [MB] = $8 \cdot 10^{-5}$ M. Reference: reagent blank. MB = methylene blue.

Fig. 2. Effect of methylene blue concentration. 3.1 μg P. [Mo] = $2 \cdot 10^{-2}$ M. Reference: reagent blank, 655 nm.

measured against reagent blanks. Washing only once for 5 min with 25 ml of 2 M nitric acid was sufficient to remove the excess of methylene blue.

Calibration. The calibration graph was linear in the range 0.8—8 μg of phosphorus. The molar absorptivity of methylene blue molybdophosphate was $4.8 \cdot 10^4$ l mol^{-1} cm^{-1} (at 655 nm).

No change in absorbance was observed for at least 2 h in the MIBK extract.

Effect of diverse ions. The effect of diverse ions on the absorbance produced from 3.1 μg of phosphorus by the recommended procedure was investigated. An ion was considered not to interfere when the error in the absorbance was less than 4% for the test solutions compared with the standards. The following ions did not interfere at 1000-fold (weight) amounts: Ag, Al, Ba, Ca, Cd, Ce(IV), Co(II), Cu(II), Fe(III), Hg(II), La, Mg, Mn(II), Ni, Sn(IV), Sr, Th, Zn, Zr, Cl^-, Br^- and SO_4^{2-}. Less than 5-fold V(V), 10-fold Si(IV), Cr(VI), and 100-fold ClO_4^- did not interfere. As(V) and Ge(IV) caused errors of 41.1% and 8.5%, respectively, even when present only in weights equal to that of phosphorus. Arsenic, germanium and silicon, which form heteropoly acids like phosphorus, interfered seriously. Vanadium(V) caused positive errors while chromium caused negative errors.

REFERENCES

1 G. F. Kirkbright, R. Narayanaswamy and T. S. West, Anal. Chem., 43 (1971) 1434.
2 A. Golkowska and L. Pszonicki, Talanta, 20 (1973) 749.
3 T. Matsuo, J. Shida and S. Kudo, Bunseki Kagaku, 22 (1973) 1009.
4 T. Matsuo, J. Shida and S. Kudo, Bull. Chem. Soc. Jpn., 46 (1973) 3595.
5 H. Kitagawa and N. Shibata, Bunseki Kagaku, 8 (1959) 302.

Analytica Chimica Acta, 91 (1977) 389—392

Short Communication

EXTRACTION OF MOLYBDOARSENIC ACID WITH HIGH-MOLECULAR-WEIGHT AMINES

N. A. IVANOV and N. G. TODOROVA
Institute of Chemical Technology, Sofia-1156 (Bulgaria)
(Received 1st November 1976)

The extraction of molybdoarsenic acid and its reduced forms with oxygen-containing solvents has been widely studied and applied [1, 2]. Interest in this problem is connected with the extraction—photometric determination of arsenic itself and also with the inhibitory influence of arsenic on the determination of phosphorus and silicon. Solutions of high-molecular-weight amines in organic solvents extract heteropoly complexes efficiently [1, 3], but this type of extraction has not been applied to the separation, concentration or investigation of arsenic heteropoly compounds.

Experimental

Solutions and equipment. A standard solution of arsenate (10^{-2} M) and a molybdate solution (0.2 M) were prepared from $Na_2HAsO_4 \cdot 7H_2O$ and $(NH_4)_6Mo_7O_{24} \cdot 2H_2O$, p.a., respectively. Solutions (0.1 M and 10^{-2} M) of di-(2-ethylhexyl)amine (DEHA), dinonylamine (DNA) and diisooctylamylamine (DIOAA) in 1,2-dichloroethane were standardized by means of two-phase potentiometric titrations.

Absorbances were measured with an SF-4A spectrophotometer and 1-cm silica cells.

Procedure. Mix the required quantities of molybdate, acid, and arsenate consecutively in a graduated flask (50 or 100-ml) and dilute to volume with water. After 10—15 min shake an aliquot of the solution (10—75 ml) vigorously in a separatory funnel for ca. 1 min with 10 or 5 ml of the extractant. Measure the absorption of the aqueous solution or extract at 400 nm against water or dichloroethane, and in the u.v. region against the corresponding nitrate—molybdate solutions or extracts in the absence of arsenic.

The molybdenum concentration in the organic phase was determined by the rhodanide method after re-extraction with a base.

Results and discussion

The extraction system is characterized by the high stability of the heteropoly complexes to precipitation and reduction in the organic phase.

In the visible region, the absorbance in aqueous solutions of the

molybdoarsenate complexes (Fig. 1) is close to zero; with the extracts the absorbance is considerable. This unusual effect is obviously complex in character and is connected both with the stabilization of the heteropoly ions in the extract and with the gradual conversion to the β-modification [4]. Arsenic was extracted completely under the conditions of Fig. 1, as proved by two-fold extraction with photometric checking of both phases, at an HNO_3:Mo ratio of ca. 10 and an amine concentration exceeding $5 \cdot 10^{-3}$ M (Fig. 1, curves 1, 2). The u.v. spectra of the extracts in the absence of arsenic, and the chemical analysis data, showed that the quantity of isopolymolybdate extracted is commensurate with that of the heteropoly complex.

Figure 2 shows the curves for the organic phase saturated consecutively with arsenate and molybdate.

The expected maximal absorbance for the extracts, at a constant molybdate concentration of $7.2 \cdot 10^{-3}$ M, with complete binding and extraction of molybdenum as $AsMo_{12}O_{40}^{3-}$, should be 1.33 (2×0.665; Fig. 1, curves 1, 2) corresponding to $6 \cdot 10^{-4}$ M arsenate. Part of the molybdenum, however, is extracted as isopolymolybdate, while another part (MoO_2, etc.) does not react with arsenic. The real maximal absorbance is, therefore, 0.595, corresponding to an arsenate concentration of $2.67 \cdot 10^{-4}$ M (Fig. 2, curve 1). The effective concentration of molybdenum, capable of heteropoly complex formation, can be expressed by means of the factor $F = 0.595/1.330 = 0.446$. Its significance for the series is $3.22 \cdot 10^{-3}$ M ($7.2 \cdot 10^{-3} \times 0.446$) and the Mo:As ratio in the extracted complexes is correspondingly 12.0 ($3.22 \cdot 10^{-3}/2.67 \cdot 10^{-4}$). With a constant arsenate concentration of $5 \cdot 10^{-4}$ M (Fig. 2, curve 2), the maximal absorbance (0.665) corresponds to $8.3 \cdot 10^{-3}$ M molybdate. From the above-established factor for molybdenum, a value of 12.3 ($8.3 \cdot 10^{-3} \times 0.446 = 3 \cdot 10^{-4}$) is obtained for the ratio Mo:As in the extracted complexes of this series.

The confirmation of the ratio Mo:As = 12 shows that the extraction does not involve a change in the composition of the heteropoly ions. The identical behaviour of secondary and tertiary amines (Fig. 3) and other major considerations [5] confirm the anion-exchange mechanism of the extraction:

$$H_3AsMo_{12}O_{40} + 3BH \cdot NO_{3_{org}} = (BH)_3AsMo_{12}O_{40_{org}} + 3HNO_3$$

where BH^+ is the protonated cation of the amine salt.

The predominant form of molybdenum in aqueous solutions under the conditions used is octamolybdate — $H_4Mo_8O_{26}$ [4, 6, 7] while the compound extracted with amines is $(BH)_2Mo_4O_{13}$. The quantity of Mo in the organic phase should increase with an increase in the concentration of the free extractant ($BH \cdot NO_3$), as confirmed by the analytical data for the extracts (Table 1).

In accordance with the prevailing concepts [4, 6] for the heteropoly complex formation in the aqueous phase, the total reaction may be expressed as:

$$H_3AsO_4 + \tfrac{3}{2}H_4Mo_8O_{26} + 3BH \cdot NO_{3_{org}} = BH \cdot AsMo_{12}O_{40_{org}} + 3HNO_3 + 3H_2O$$

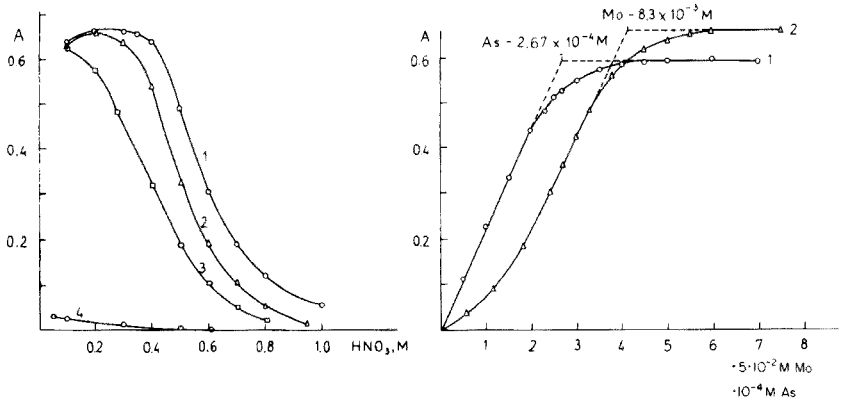

Fig. 1. Effect of HNO_3 on absorbance and extraction of molybdoarsenic complexes. Curves 1, 2, 3 — Extracts in dichloroethane with 10^{-2} M, $5 \cdot 10^{-3}$ M, 10^{-3} M DEHA, respectively. Curve 4, aqueous solution. $2 \cdot 10^{-2}$ M Mo; $3 \cdot 10^{-4}$ M AsO_4^{3-}; 1-cm cells; 400 nm; volume of phases, 10 ml.

Fig. 2. Determination of molar ratio Mo:As in extracted complexes. Extractant, 10^{-2} M DEHA in dichloroethane. (1) Saturation with arsenate; $7.2 \cdot 10^{-3}$ M Mo, $8.2 \cdot 10^{-2}$ M HNO_3 (2) Saturation with molybdate: $3 \cdot 10^{-4}$ M AsO_4^{3-}; HNO_3:Mo = 10. 1-cm cells; 400 nm; volume of phases, 10 ml.

TABLE 1

Chemical composition of extract
(Aqueous phases: $3 \cdot 10^{-4}$ M AsO_4^{3-}, 0.2 M HNO_3, $2 \cdot 10^{-2}$ M Mo)

DEHA ($\cdot 10^{-3}$ M)	Extn. As (%)	Mo_{org} ($\cdot 10^{-3}$ M)		Amine (%) bound with		
		Total	Unbound	$AsMo_{12}O_{40}^{3-}$	$Mo_4O_{13}^{2-}$	NO_3^-
1.5	75.0	3.60	0.55	50	19	31
5.0	100.0	5.02	1.42	18	14	68

The conventional equilibrium constant can be calculated from the curve of saturation with arsenate (Fig. 2, curve 1), taking into account the factor for molybdenum as well as the participation of the amine and the acid in the afore-mentioned side reactions. The following value was obtained:
$K'_{ex} = 9.1 \pm 1.35 \cdot 10^9$; $\log K'_{ex} = 9.96 \pm 0.13$.

Extractive—photometric determination of arsenic

The change in the optical properties and the stabilization of dodecamolybdoarsenate during its extraction with amine makes possible a simple and sensitive determination of arsenic without reduction of the heteropoly complex. The optimal conditions of the determination at 400 nm (1-cm cells) are: volume of phase, 10 ml; Mo, $2 \cdot 10^{-2}$M; HNO_3, 0.2 M; amine, 10^{-2}M in dichloroethane; As(V), 2.5—25 μg ml^{-1} of organic phase ($\epsilon_{400} = 2.25 \cdot 10^3$ l mol^{-1} cm^{-1}). The

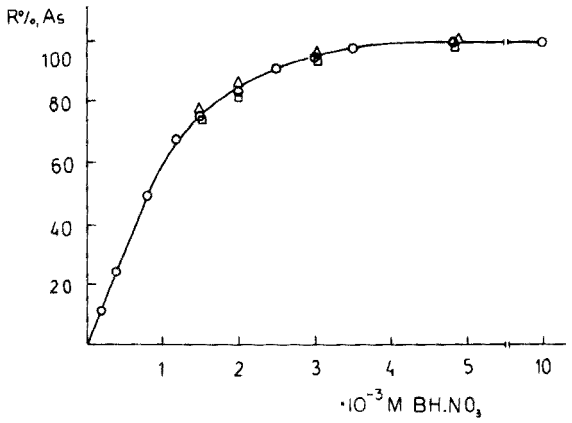

Fig. 3. Effect of concentration and type of amine on extraction of the heteropoly complexes. $3 \cdot 10^{-4}$ M AsO_4^{3-}; $2 \cdot 10^{-2}$ M Mo; 0.2 M HNO_3. ○-DEHA, △-DNA, □-DIOAA.

relative standard deviation is ca. 2.5%. The extraction concentration increases the sensitivity of the determination by one order.

Procedure. Place 50 ml of the solution containing 0.25—2.5 μg ml^{-1} of As(V) in a separatory funnel. Add 5.0 ml of 2 M HNO_3 and 5.0 ml of 0.2 M molybdate. After 10—15 min, add 5.0 ml of a 10^{-2} M solution of amine in dichloroethane, and extract. Because of the possible presence of traces of PO_4^{3-}, SiO_3^{2-} and AsO_4^{3-} in the reagents, a blank measurement by extraction of the acid and molybdate solution in 50 ml of water is essential.

The absorption of the extracts is maximal ($\epsilon_{312} = 1.74 \cdot 10^4$) in the u.v. region of the spectrum, but the concentration conditions of the determination are restricted because of the interfering effect of the reagents (amine, $2—2.5 \cdot 10^{-4}$ M; Mo, ca. 10^{-3} M; HNO_3, ca. 10^{-2} M). Beer's Law is observed in the range 0.3—3 μg As ml^{-1} of organic phase. The maximal sensitivity of the determination with a tenfold extraction concentration is 0.04 μg As ml^{-1} of initial solution, with a relative standard deviation of 15%.

REFERENCES

1 I. P. Alimarin, F. P. Sudakov and V. I. Kalitina, Usp. Khim., 34 (1965) 1368.
2 F. Umland, A. Janssen, D. Thierig and G. Wünsch, Theorie und Praktische von Komplexbildern, Akad. Verlag, Frankfurt am Main, 1971.
3 R. Kollar, V. Plichou and I. Saulnier, Anal. Chim. Acta, 30 (1970) 457.
4 A. Halasz and E. Pungor, Talanta, 18 (1971) 557, 569, 577.
5 V. S. Smith, Extraction with Amines, Atomizdat, Moscow, 1970.
6 A. Ringbom, B. E. Ahlers and S. Sitonen, Anal. Chim. Acta, 20 (1969) 78.
7 J. D. H. Strickland, J. Am. Chem. Soc., 74 (1952) 862.

Analytica Chimica Acta, 91 (1977) 393—396

Short Communication

DETERMINATION OF NITRILOTRIACETIC ACID IN DETERGENT FORMULATIONS

LEO HARJU and ROLF SARA
Department of Chemistry, Åbo Akademi, Åbo (Finland)
(Received 9th November 1976)

Phosphorus compounds in detergent formulations were partly replaced by nitrilotriacetic acid (NTA) about 1969 to reduce eutrophication phenomena. Shortly afterwards the use of NTA was banned in several countries but it is still used in some detergents, e.g. in Finland. NTA is a considerably stronger complexing agent than the phosphates and thus a very efficient water softener. Because of this strong complexing ability, it can be expected that NTA will affect the heavy metal balance in our water systems.

The present communication reports a direct application of earlier work [1], where NTA was titrated spectrophotometrically with copper(II) solution and equilibrium constants were determined for the system. Among the many methods devised for the determination of NTA in detergents and natural waters, the method of Clinckemaille [2] is relevant; he titrated NTA visually with copper(II) solution with chrome azurol S as indicator.

Experimental

The spectrophotometric titrations were made with a Coleman model 46 spectrophotometer equipped with a quartz flow cell. Titrant was added from a Metrohm E 457 microburet. The sample solutions of the detergents were stirred for ca. 30 min before the titrations. The heavy metal content of the commercial detergents was checked spectrographically and was found to be less than 0.001%.

NTA and EDTA (Fluka AG; pro analysi) were used. Pentasodium tripolyphosphate ($Na_5P_3O_{10}$), tetrasodium pyrophosphate ($Na_4P_2O_7$), trisodium orthophosphate (Na_3PO_4) and hexasodium metaphosphate ($(NaPO_3)_6$) were of technical grade (Turun Saippua Oy).

Conditional constants

To estimate the possibilities of determining NTA in the presence of different phosphorus compounds, the conditional constants of their copper(II) complexes were calculated for different pH values. The results are plotted in Fig. 1; the values of the conditional constants of Cu—EDTA complexes are also included. The conditional constants indicate that NTA can be titrated

quantitatively as the 1:1 chelate without interference from phosphate compounds. The difference in the constants exceeds 3 logarithmic units over almost the entire pH range. In this work most titrations were carried out at pH 5.3 (acetate buffer); this resulted in simpler titration curves because 1:1 chelates are formed predominantly below pH ca. 7. The optimal range for the formation of 1:2 Cu—NTA chelates is pH 8—11.

Orthophosphate forms very weak complexes with copper(II) ions [3] and does not interfere in the determination of NTA.

Spectrophotometric titrations

The copper—NTA chelates absorb very strongly in the u.v. region, and 270 nm was chosen as the analytical wavelength.

First the interference of different phosphate compounds on the determination of NTA was studied by titrating a mixture of NTA and several phosphate ions with copper(II) solution (Fig. 2). A sharp break was obtained at the equivalence point for NTA. The phosphate compounds did not interfere, as predicted from the conditional constants. A linear regression method was used to evaluate the equivalence volume; the absorbance values were first corrected for the change in volume of the sample solution and the best straight lines were calculated before and after the end-point by the method of least squares. Titration points close to the end-point were omitted. The

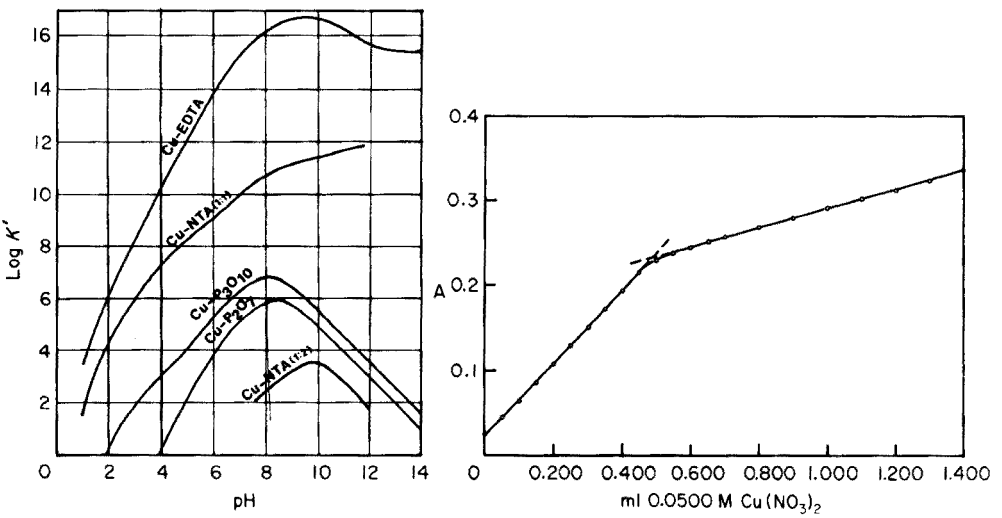

Fig. 1. Conditional constants for the Cu—NTA [1, 4], Cu—EDTA [3], Cu—P_3O_{10} [5] and Cu—P_2O_7 [5] systems as a function of pH.

Fig. 2. Spectrophotometric titration of 6.39 mg of NTA in the presence of tripolyphosphate (25 mg), diphosphate (10 mg), metaphosphate (10 mg) and orthophosphate (10 mg). The equivalence volume is 0.492 ml corresponding to 6.32 mg of Na_3NTA. pH 5.3 (0.1 M acetate). Initial volume, 100 ml; 270 nm; slit, 0.4 mm.

first linear part of the curve (slope 0.425) corresponds to the formation of Cu—NTA chelates, and the second to the formation of Cu—phosphate compounds.

A commercial detergent was titrated; according to the manufacturer, this contained 10% NTA, and other ingredients were different phosphorus compounds, synthetic tensides, perborates, sodium hydrogen carbonate and sodium silicate. The curve (Fig. 3) showed a break at a consumption of 0.335 ml (for 49.1 mg of detergent) which gives 8.8% NTA (calculated as Na_3NTA) in the formulation. The agreement is satisfactory for a technical product. A series of five determinations of NTA in this detergent gave the results 8.75, 8.64, 8.75, 8.82 and 8.80%; the mean value was 8.75 ± 0.07%.

Figure 4 (Curve A) shows the titration of the same detergent (10% NTA) at pH 9.7; here the buffer capacity of the detergent is used. The shape of the curve is typical for the titration of NTA with Cu(II) at this pH. The rounded curvature at the 1:2 equivalence point and the sharp break at the 1:1 equivalence point provide good evidence for the occurrence of NTA in the detergent formulation.

The effect of EDTA on the determination of NTA was also studied. Figure 4 (Curve B) shows a titration where EDTA was added to the commercial detergent containing 10% NTA. As can be expected from the conditional constants ($K'_{Cu-EDTA} = 10^{13.0}$ and $K'_{Cu-NTA} = 10^{8.5}$ at pH 5.5), EDTA and NTA can be titrated successively. Two breaks are obtained, giving the equivalence volumes of EDTA and NTA, respectively.

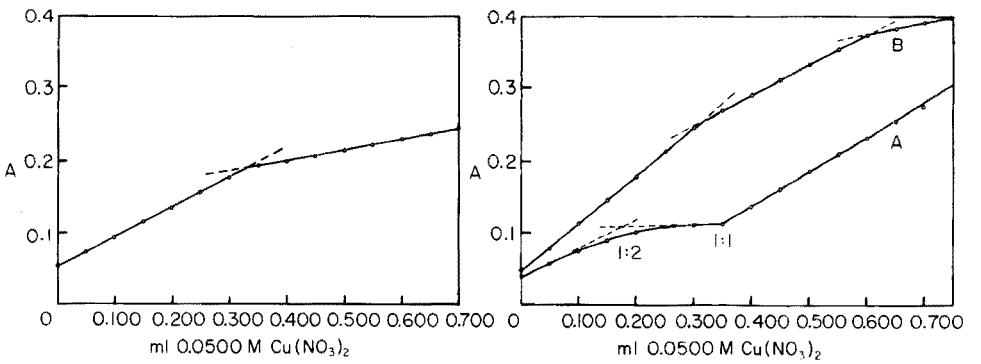

Fig. 3. Spectrophotometric titration of NTA in a sample (49.1 mg) of commercial detergent containing 10% NTA. The equivalence volume was 0.335 ml, corresponding to 4.3 mg of Na_3NTA. Conditions as for Fig. 2.

Fig. 4. Spectrophotometric titrations of the commercial detergent (10% NTA). Curve A. Titration at pH ≈ 9.7; the equivalence volume for 50.5 mg of sample is 0.347 ml (as 1:1 chelate). Initial volume, 50 ml; 310 nm. Curve B. Titration in presence of 5.70 mg of EDTA; the equivalence points for 45.0 mg of sample are at 0.299 ml and 0.597 ml, corresponding to 5.68 mg of Na_4EDTA and 3.83 mg of Na_3NTA. pH, 5.3; initial volume, 100 ml; 270 nm.

Discussion

A copper(II) solution was chosen as titrant because the equilibrium constants of the Cu—NTA and Cu—phosphate systems are well known and the method of analysis thus can be based on theoretical calculations. Other metal ion solutions can of course be used for the same purpose.

The result obtained, 8.8%, for the detergent was somewhat lower than given by the manufacturer but the agreement is still satisfactory. Other commercial detergents containing 0.5% and 2.5% NTA were analysed with satisfactory accuracy by the proposed method.

The conditional constants show that in the pH range of natural waters, NTA will most probably increase the mobility of copper(II) ions because of its strong complexing ability. This is also true for other heavy metals.

REFERENCES

1 L. Harju and R. Sara, Anal. Chim. Acta, 73 (1974) 129.
2 G. G. Clinckemaille, Anal. Chim. Acta, 43 (1968) 520.
3 A. Ringbom, Complexation in Analytical Chemistry, Wiley-Interscience, New York 1963.
4 L. Harju, Suom. Kemistil., B 46 (1973) 199.
5 A. Johansson and E. Wänninen, Talanta, 10 (1963) 769.

Analytica Chimica Acta, 91 (1977) 397—398

Short Communication

ANALYSIS OF AMERICIUM ARSENIDE

W. BARTSCHER

European Institute for Transuranium Elements (EURATOM), P.O. Box 2266, D-7500 Karlsruhe (Federal Republic of Germany)

(Received 28th October 1976)

Studies of electronic configuration in actinide compounds involve simple binary products, e.g. arsenides, which crystallize in a NaCl-type lattice. To check the composition of these compounds, precise determinations of the main constituents are needed. Since only milligram amounts of sample material are available, the methods applied must be sensitive and, to keep the radiation load as low as possible for the operator, they should be rapid.

In the case of americium arsenide, an EDTA titration of americium [1] meets these requirements. This method is rapid and arsenic does not interfere. A similar simple procedure for the determination of arsenic was therefore sought. The distillation method [2] is too lengthy. Precipitation by calcium hypophosphite followed by titration with cerium(IV) sulfate [3] promised to be both rapid and sensitive; but, in agreement with Smales and Pate [4], the results found were 5—10% low. Finally the well known titration with bromate after reduction with hydrazine sulfate [5] was found not to suffer interference from americium.

Procedure

Transfer 5—10 mg of the sample material to a 50-ml volumetric flask containing 5 ml of 7 M nitric acid. Close the flask immediately after introduction of the sample. For the absorption of any hydrogen arsenide, leave the solution for 24 h. No heating is necessary. Dilute the solution to the mark, and pipette a 10-ml aliquot into a 50-ml beaker. Add 3 ml of 18 M sulfuric acid and heat the solution to fumes. After cooling, add 100 mg of hydrazine sulfate, taking care that no salt touches the wall of the beaker. Again heat the

TABLE 1

Reduction step and influence of gadolinium

As added	As found (mg)	s (μg)	No. of results
1.000 mg As(III)	0.9960	1.7	7
1.000 mg As(V)	0.9953	2.0	4
1.000 mg As(V) + 6 mg Gd	0.9942	0.6	2

solution to strong fumes for 10 min. After cooling, dilute the solution to about 10 ml, add 1 ml of 10% potassium bromide solution, and insert a combined platinum—calomel electrode. Titrate with $5 \cdot 10^{-3}$ M potassium bromate solution from a burette graduated to 10^{-3} ml. The end-point is marked by a sharp potential shift of about 150 mV (1 ml of 0.005 M $KBrO_3$ corresponds to 0.1873 mg As).

Titrate the americium with EDTA in another 5-ml aliquot [1].

Results

The reduction step of the method was checked by determining known amounts of As(III) and As(V) as in the above procedure. The As(III) solution was prepared by dissolution of arsenic trioxide in sodium hydroxide solution; the As(V) solution was obtained by evaporating one part of this solution with nitric acid and dilution to the original volume. Gadolinium was taken as a substitute for americium in the preliminary experiments. The results are reported in Table 1. No significant differences in the results and the standard deviations between the three series are detectable. Thus the reduction is complete and gadolinium does not interfere. From all results, a standard deviation of 1.7 μg As with 10 degrees of freedom was calculated. There is a 98% probability that the results are low with respect to the added quantity, the most probable difference being 4.3 μg which corresponds to 0.43%. All further values were therefore corrected for this difference.

Table 2 shows the results and the confidence limits (68% level) for the analysis of four americium arsenide samples, which had been prepared at different temperatures [6]. The results for low temperatures of preparation are close to 100%; for higher temperatures the differences increase. This might be due to oxidation, as problems of sealing the preparation apparatus become more important with higher temperature.

TABLE 2

Analysis of americium arsenide

Preparation temp. (°C)	Am found (%)	As found (%)	Total (%)
600	76.85 ± 0.22	22.89 ± 0.11	99.74 ± 0.25
850	77.06 ± 0.19	22.71 ± 0.10	99.77 ± 0.21
1100	75.87 ± 0.21	22.43 ± 0.11	98.30 ± 0.24
1200	76.08 ± 0.18	22.34 ± 0.10	98.42 ± 0.21

REFERENCES

1 K. Buijs and W. Bartscher, Anal. Chim. Acta, 88 (1977) 403.
2 J. C. Bartlet, M. Wood and R. A. Chapman, Anal. Chem., 24 (1952) 1821.
3 O. P. Case. Anal. Chem., 20 (1948) 902.
4 A. A. Smales and B. D. Pate, Anal. Chem., 24 (1952) 717.
5 W. Fresenius and G. Jander, Handbuch der Analytischen Chemie, Bd. V aγ, Springer Verlag, Berlin, 1951, p. 128.
6 J. P. Charvillat, U. Benedict, D. Damian and W. Müller, Radiochem. Radioanal. Lett., 20 (1975) 371.

Analytica Chimica Acta, 91 (1977) 399—402

Short Communication

NAPHTHIDINES AS INDICATORS IN TITRATIONS WITH CERIUM (IV) SULPHATE

H. SANKE GOWDA and R. SHAKUNTHALA

Department of Post-graduate Studies and Research in Chemistry, University of Mysore, Manasa Gangotri, Mysore 570006 (India)

(Received 24th August 1976)

Straka and Oesper [1] proposed naphthidine as indicator for the titration of iron (II) with dichromate. Belcher et al. [2—5] studied systematically the indicator properties of naphthidines, and proposed naphthidine (N), naphthidinesulphonic acid (NS), 3,3′-dimethylnaphthidine (DMN), 3,3′-dimethylnaphthidinedisulphonic acid (DMNS) and naphthidinedisulphonic acid (NDS) in the titration of iron (II) with dichromate. NS and DMNS indicators were stated to be of no value in the titration of iron (II) with cerium(IV) sulphate as the end-points were very sluggish even in the presence of phosphoric acid [4]. The present communication reports optimum conditions for the use of N, NDS and DMNS indicators in cerimetry; DMN was found to be of no use.

Experimental

Reagents. Solutions (0.2% w/v) of N, NDS and DMNS were prepared as described by Belcher et al. [4, 5]. Approximately 0.05 N solutions of hydroquinone [6, 7], molybdenum(V) [8] and uranium(IV) [9] were prepared and standardised against cerium(IV) sulphate by the accepted methods. Other working solutions were made by suitable dilution of the standardized stock solutions. Solutions of iron(II) ammonium sulphate, cerium(IV) sulphate and ferroin were prepared by the usual procedures.

Determination of the formal redox potentials of N and NDS. Equimolar vanadate—vanadyl potentiopoised solutions were prepared by the method of Smith and Banick [10]; 10 ml of each of the six potentiopoised solutions in 0.1—2.5 M sulphuric acid were placed in 20-ml test tubes, and 0.2 ml of 0.2% N or NDS was added to each solution and mixed thoroughly. The potential of the solution in which a complete colour change was effected was interpolated with the potential of the next lower solution in which the pink colour of the oxidized form of the indicator was barely perceptible. A mid-point interpolation was taken to establish the formal redox potential.

Titration of 0.05—0.005 M iron(II). Iron(II) solution (20 ml), 0.2 ml of N, NDS or DMNS solution, 4 ml of syrupy phosphoric acid (d. 1.75) and 2 ml of 1 N oxalic acid solution (no oxalic acid for NDS) were mixed and diluted

to 40 ml with enough sulphuric or hydrochloric acid to give 1 M acid at the end point. The mixture was titrated with cerium(IV) sulphate solution to the appearance of a red or red-violet colour. In the titration of 0.005 M iron(II), 2 ml of syrupy phosphoric acid, 1 ml of 1 N oxalic acid and 0.1 ml of the indicator were used.

Titration of 0.05—0.005 N hydroquinone. Hydroquinone solution (20 ml) and 0.2 ml (0.1 ml in the titration of 0.005 N) of N, NDS or DMNS were mixed and diluted to 40 ml with enough sulphuric or hydrochloric acid to keep the overall acidity 1 N at the end-point. The mixture was titrated with cerium(IV) solution to the appearance of a red colour.

Titration of 0.05—0.005 N molybdenum(V) or uranium(IV). The sample solution (20 ml), indicator and sulphuric or hydrochloric acid were mixed as described for hydroquinone, and the titration was started. Syrupy phosphoric acid (2ml) was added and the titration continued to a red or red-violet colour. Phosphoric acid should be added near the end-point in the titration of uranium (IV). In the titration of 0.005 N molybdenum(V) or uranium(IV), 1 ml of syrupy phosphoric acid and 0.1 ml of the indicator were used.

Results and Discussion

Determination of the formal redox potential of N and NDS. Belcher et al. [4] determined the formal redox potentials of DMN and DMNS by the method of Crawford and Bishop [11] which failed to give the formal redox potentials of N and NDS [3]. The potentiopoised method [10] used here showed the formal redox potential of N in 0.2 M sulphuric acid to be 922 mV and of NDS in 2.15 M sulphuric acid to be 1064 mV.

Titration of iron(II). The results obtained with the different indicators are shown in Table 1. When 0.1 ml of the N, NDS or DMNS solution was used, a pink colour was obtained almost immediately with 0.05 ml of 0.02 M cerium (IV) sulphate in 25 ml of 1.0—3.0 N sulphuric acid solutions. At higher acidities, the oxidation of the indicators is retarded. Iron(III) forms a red colour with N and DMNS but not with NDS in sulphuric acid medium. Phosphoric acid inhibits the oxidation of the indicators by cerium(IV) slightly, whereas oxalic acid catalyses this oxidation. The reduction of the oxidized form of the indicators by iron(II) in sulphuric acid medium is slow; phosphoric and oxalic acids appear to catalyse this reduction, the combined effect being greater than that of either acid alone. The effect increases with increasing concentration of phosphoric and oxalic acids.

N and DMNS give sharp and correct end-points in the titration of 0.05 M iron(II), from parrot green through yellow-brown to red, in 1—2 N sulphuric or hydrochloric acid solution containing 3—8 ml of syrupy phosphoric acid and 1.0—4.0 ml of 1 N oxalic acid in a total volume of 60 ml. The red colour is stable for 5—10 min, and can be reversed in 1—3 min by a drop of iron(II). Overtitration occurs with more than 4 ml of 1 N oxalic acid. Premature sluggish end-points are obtained with more than 8 ml of syrupy phosphoric acid or more than 2 N sulphuric or hydrochloric acid. NDS gives a sharp

TABLE 1

Titration of iron(II), hydroquinone, molybdenum(V) and uranium(IV) with cerium(IV) solution in presence of N, NDS and DMNS indicators

Reductant taken (mg)	Reductant found (mg)			Reductant taken (mg)	Reductant found (mg)		
	N	NDS	DMNS		N	NDS	DMNS
Iron(II)				*Molybdenum(V)*			
38.50	38.60	38.40	38.60	60.80	60.60	60.60	60.60
27.40	27.20	27.20	27.20	36.60	36.40	36.40	36.40
5.26	5.24	5.24	5.24	8.44	8.42	8.42	8.42
3.82	3.82	3.80	3.82	4.84	4.84	4.84	4.84
Hydroquinone				*Uranium(IV)*			
21.20	21.20	21.20	21.20	52.60	52.60	52.60	52.60
12.20	12.20	12.00	12.20	28.40	28.50	28.50	28.50
4.44	4.42	4.42	4.42	10.28	10.26	10.26	10.26
2.86	2.86	2.86	2.86	5.87	5.86	5.86	5.86

reversible colour change from parrot green to pink at the equivalence point in 1—3 N sulphuric or hydrochloric acid solution containing 2—8 ml of syrupy phosphoric acid or 1—2 drops of 1 N oxalic acid in a total volume of 60 ml. The end-point colour is stable for 1—3 min with phosphoric acid and 30—45 s with oxalic acid. Higher concentrations of the mineral acids give sluggish premature end-points.

In the titration of 0.005 M iron(II), all three indicators give sharp colour changes from almost colourless to pink in 1.0—1.5 N sulphuric or hydrochloric acid containing 0.5—5 ml of syrupy phosphoric acid and 0.5—3 ml of 1 N oxalic acid (no oxalic acid for NDS) in a total volume of 60 ml. Higher acidities cause premature end-points.

Influence of indicator concentration. At least 0.1 ml of 0.2% N, NDS or DMNS solution is necessary in a total volume of 60 ml, but more than 0.4 ml gives sluggish end-points. The indicator correction is almost negligible in the titration of 0.05 M iron(II). In the titration of iron(II), NDS is superior to DMNS and N, because the end-points are sharper and more reversible, no oxalic acid is needed, and a wider range of sulphuric or hydrochloric acid is permissible.

Titration of hydroquinone. N, NDS and DMNS give sharp end-points in the titration of 0.05 N hydroquinone in 1—5 N sulphuric acid or in 1—2 N hydrochloric acid media in a total volume of 60 ml. The colour changes from yellowish-brown through brown to red. The red colour of NDS and DMNS can be reversed immediately by a drop of hydroquinone while that of N can be reversed in about 20—60 s in 1—5 N sulphuric acid. The end-point with N and DMNS in 1 N sulphuric acid is stable for 8 min and that with NDS for about 1 min. Sluggish premature end-points are obtained with more than 5 N sulphuric acid, whereas overtitration occurs with more than 2 N hydrochloric acid.

In the titration of 0.005 N hydroquinone, NDS and DMNS give sharp colour changes from almost colourless to pink under the above conditions of acidity.

The pink colours of N and DMNS are stable for 3—5 min and that of NDS for 40 s. The behaviour of the indicators at higher acidities is similar to that described above. In this titration, DMNS provides the best sensitivity and clearest end-point.

Titration of molybdenum(V). The reaction between cerium(IV) and molybdenum(V) induces the reaction between molybdenum(V) and the oxidized indicator. Although this induction occurs without phosphoric acid, it is marked only when phosphoric acid is present; the reaction becomes slow at high acidities, causing sluggish premature end-points. In the titration of 0.05—0.005 N molybdenum(V), N, NDS and DMNS give sharp end-points from almost colourless to pink in 1—2 N [1—1.5 N for 0.005 N Mo(V)] sulphuric or hydrochloric acid solutions containing 1.0—3.0 ml of syrupy phosphoric acid in a total volume of 60 ml. The end-points with N and DMNS are stable for 10—15 min and that with NDS for about 2 min. Of the three indicators, NDS gives the sharpest reversible end-points.

Titration of uranium(IV). When 1.0—4.0 ml of syrupy phosphoric acid is added to 40 ml of 1—2 N sulphuric acid containing 20 ml of 0.05 N uranium (IV), a white precipitate develops after 2—5 min, and the titration results are erratic. If the phosphoric acid is added near the end-point (after 98% titration), turbidity is not observed and correct results are obtained. The colour change from green to pink is sharp. Higher concentrations of sulphuric and phosphoric acids give sluggish premature end-points. The end-point with N and DMNS is stable for 9 min and that with NDS for 45 s. All three indicators are satisfactory in the titration of 0.005 N uranium(IV) solution in 1.0—1.5 N sulphuric acid solution containing 0.5—3.0 ml of syrupy phosphoric acid added near the end-point. In this titration NDS is superior to N and DMNS because it gives sharper reversible end-points.

In all the titrations tested, the results presented in Table 1 compare favourably with those obtained with ferroin indicator.

The authors thank Dr. W. I. Stephen, Department of Chemistry, University of Birmingham, for the supply of pure N, NDS and DMNS indicators.

REFERENCES

1 L.E. Straka and R. E. Oesper, Ind. Eng. Chem. Anal. Ed., 6 (1934) 405.
2 R. Belcher and A. J. Nutten, J. Chem. Soc., (1951) 548.
3 R. Belcher, A. J. Nutten and W. I. Stephen, J. Chem. Soc., (1951) 1520, 3444; (1952) 2438.
4 R. Belcher, A. J. Nutten and W. I. Stephen, J. Chem. Soc., (1952) 1269, 3857.
5 R. Belcher, S. J. Lyle and W. I. Stephen, J. Chem. Soc., (1958) 3243,4454.
6 G. G. Rao and T. P. Sastri, Z. Anal. Chem., 163 (1958) 263.
7 N. H. Furman and J. H. Wallace, J. Am. Chem. Soc., 52 (1930) 1443.
8 N. H. Furman and W. M. Murray, J. Am. Chem. Soc., 58 (1936) 1689.
9 C. W. Sill and H. E. Peterson, Anal. Chem., 24 (1952) 1175.
10 G. F. Smith and W. M. Banick, Jr., Talanta 2 (1959) 348.
11 E. Bishop and A. B. Crawford, J. Royal Tech. Coll. Glasgow, 5 (1950) 52.

Analytica Chimica Acta, 91 (1977) 403—405

Short Communication

EFFECT OF VOLATILITY AND ADSORPTION DURING DRY ASHING ON DETERMINATION OF CHROMIUM IN BIOLOGICAL MATERIALS

JORMA KUMPULAINEN

Department of Food Chemistry and Technology, University of Helsinki, 00710 Helsinki 71 (Finland)

(Received 2nd December 1976)

The essential rôle of trace chromium as a nutrient has been demonstrated [1—5]; reliable determinations of the chromium content of biological materials are therefore necessary to estimate daily chromium intakes and the chromium nutritional status in man. Numerous methods are available for chromium on a macro scale, but its determination in biological samples has been very unreliable [4, 6, 7], partly because of the very low concentrations of chromium in most biological materials.

Attempts have been made to resolve the causes of the analytical errors. Chromium may be lost as volatile organic complex(es) during dry ashing [9, 10], but not all investigators have confirmed this hypothesis [8, 11, 12]. Cary and Allaway [11] have reported that chromium is lost during dry ashing by fusion or adsorption on the wall of the digestion crucible. Jones et al. [12] have shown that adsorption may cause serious errors when mineral acids other than concentrated sulphuric acid are used for dissolution of the ash after dry ashing. However, Jones et al. used very small sample weights (0.03 g), and their results are not directly applicable to normal chromium determinations, for which the sample weights are usually 1—2 g.

The aim of the present study was to establish if the volatility or adsorption of chromium from brewer's yeast during dry ashing can cause serious errors when the sample weights are 1—3 g (on a wet basis) and common mineral acids are used for dissolution of the ash. Brewer's yeast was chosen as the sample because it is rich both in total chromium and in the most biologically active organic chromium complexes [1, 4, 12], and is easy to label with a radioactive isotope.

Experimental

Yeast production and sample preparation. Sabouraud's medium containing 2% (w/v) Bactopeptone and 5% (w/v) dextrose in 2 l of water was sterilized in an Erlenmeyer flask by autoclaving. A yeast culture (*S. carlsbergensis*) grown in 200 ml of Sabouraud's medium was added to the flask. Then 0.2 mg of chromium chloride and 0.2 mCi of $^{51}CrCl_3 \cdot 6\ H_2O$

were added to the medium and incubated for 7 d at 20°C under agitation. Three days after the incubation the glucose concentration was adjusted to 5% (w/v). The yeast cells were separated by centrifugation and washed with 3 × 800 ml of water.

Activity measurements and dry ashing. Weighed samples (1.1—3.3 g on a wet basis) were placed in 4 × 3.5-cm porcelain crucibles (Haldenwanger, Berlin, 79 MF-6) which had been rinsed with hot 10% HCl and twice with distilled water. The γ-activity of the crucibles was measured with a γ-scintillation counter. The counting time of the background activity was 1000 min.

The samples were carefully ashed over a flame and ignited in a muffle furnace overnight at 550°C. After dry ashing the γ-activity of the crucibles was measured.

Dissolution of the ash. After dry ashing, the ash was dissolved with concentrated nitric, sulphuric or perchloric acid or 6 M hydrochloric acid. The ash was dissolved completely in 2 ml of acid by heating. In addition, the crucibles were rinsed with 3 × 2 ml of water. The γ-activity of the crucibles was again measured.

Results and discussion

Table 1 shows the results obtained for the recovery of ^{51}Cr after dry ashing and the adsorption of ^{51}Cr on the crucible walls after dissolution of the ash in the acids. Clearly, the volatility of chromium during dry ashing was negligible. Adsorption of ^{51}Cr on the crucible walls was also of little importance, even when concentrated nitric acid was used for dissolution of ash.

The results of this study agree well with those of Jones et al. [12] with regard to the volatility of chromium during dry ashing and to the order of extraction efficiency of chromium with the mineral acids. However, the degree of chromium adsorption obtained here differs greatly from that obtained by Jones et al. [12]; the differences are obviously due to different sample weights. The samples used by Jones et al. weighed only 30 mg, which corresponds to 30 ng of chromium when the chromium content of the

TABLE 1

Recovery of ^{51}Cr from yeast after dry ashing and residual ^{51}Cr in porcelain crucibles after dissolution of ash in acids

Code of crucible	No. of crucibles	Mean sample weight (wet), g	Mean recovery (% ± *s*)	Acid used	Mean ^{51}Cr retained (% ± *s*)
A	3	3.3	98.2 ± 0.1	6 M HCl	0.4 ± 1.0
B	4	1.8	97.1 ± 2.6	14 M HNO_3	2.1 ± 2.1
C	3	1.8	98.1 ± 1.9	18 M H_2SO_4	0.2 ± 0.1
D	4	1.1	98.5 ± 1.3	72% $HClO_4$	0.4 ± 0.5

yeast is 1 p.p.m. Thus the degree of chromium adsorption can be assumed to be much greater than in the present study, in which the sample weights were 10—20 times larger. The chromium content of the yeast was 0.8 p.p.m. based on the γ-activity measurements.

These results should be applicable to most biological materials, since brewer's yeast is rich in organic chromium complexes.

REFERENCES

1 W. Mertz, Physiol. Rev., 49 (1969) 163.
2 H. A. Schroeder, Am. J. Clin. Nutr., 21 (1968) 230.
3 W. Mertz and E. E. Cornatzer (Ed.), Newer Trace Elements in Nutrition, Dekker, New York, 1971, p. 438.
4 W. Mertz, E. W. Toepfer, E. E. Roginski and M. M. Polansky, Fed. Proc., 33 (1974) 3275.
5 W. Mertz, Nutr. Rev., 33 (1975) 129.
6 R. M. Parr, Paper presented at chromium workshop, University of Missouri, May 1—2 (1974) Columbia, Mo.
7 J. Kumpulainen and P. Koivistoinen, Acta Agric. Scand., 27 (1976) 000.
8 J. J. Christensen, P. A. Hearty and R. M. Izatt, J. Agric. Food Chem., 24 (1976) 811.
9 W. Wolf, W. Mertz and R. Masironi, J. Agric. Food Chem., 22 (1974) 1037.
10 D. Behne, P. Brätter, H. Gessner, G. Hube, W. Mertz and U. Rösik, Z. Anal. Chem., 278 (1976) 269.
11 E. E. Cary and W. H. Allaway, J. Agric. Food Chem., 19 (1971) 1159.
12 G. B. Jones, R. A. Buckley and C. S. Chandler, Anal. Chim. Acta, 80 (1975) 389.

Analytica Chimica Acta, 91 (1977) 407—410

Short Communication

THE USE OF SILK AND ANIMAL HAIRS AS STANDARDS FOR HAIR ANALYSIS

J. F. ALDER, C. A. PANKHURST, A. J. SAMUEL and T. S. WEST*
Chemistry Department, Imperial College, London SW7 2AY (England)
(Received 14th January 1977)

For the simultaneous determination of trace metals in human hair [1—3], an analytical reference material, containing elements in concentrations similar to those normally present in that matrix, is required. At present no substance which fulfils the requirements of a reference material, viz. homogeneity, well-defined elemental concentration, and elements in the correct concentration range, is available. The aim of this work was to make a preliminary assessment of the suitability of silk as a reference material for this purpose and to investigate the possibility of doping this matrix to the required elemental levels.

Human hair is inhomogeneous and there are variations over individuals and populations [4]; it cannot therefore be used as a reference material unless artificially homogenized. Hair has ion-exchange properties [5, 6] and these could possibly be exploited to produce a homogeneous level of metal concentrations, but because hair is so variable a matrix a more uniform substance on which to base such a reference material was sought.

Spun silk has many attractive features as a base material. The part of natural silk used for spinning (i.e. tyrosine), is a protein and similar in nature to wool keratin, although it contains no sulphur. It has ion-exchange properties [7], can be handled like human hair, and was therefore considered to offer the best starting point for the preparation of an artificial reference material.

Experimental

Apparatus and materials. The silk samples were ashed and atomized in an HGA 70 graphite furnace (Perkin-Elmer) and examined by atomic absorption with a Hilger-Watts D330 monochromator (Rank Hilger) and a Servoscribe recorder. All reagents were of high-purity grade; the silk was untreated woven tissue, 1 oz./sq. yd. Pongees 504 (Pongees Ltd., St. Martins-le-Grand, London EC1A 4DY).

*Present address: The Macaulay Institute for Soil Research, Craigiebuckler, Aberdeen, AB9 2QJ, Scotland.

Doping procedure. The aim was to dope the silk with Cu, Ag, Co, Ni, and Pb to the levels normally found in human hair. This was achieved by preliminary washing and pre-treatment of the silk followed by soaking in a solution of the metals, washing, and drying.

A piece of silk about 100 mm × 100 mm, was washed in ethanol for 30 min to remove grease and dirt, rinsed with water, and soaked for 120 min in 0.1 M HNO_3 to extract metals. After rinsing with water, the silk was soaked for 120 min in metal salt solutions ($CuSO_4$, $AgNO_3$, $Pb(NO_3)_2$, $CoCl_2$, $NiCl_2$) at room temperature, removed and allowed to drain. The material was then soaked in 3 × 100-ml aliquots of water to remove the unbound salt solution and allowed to dry in air.

Analytical procedure. The metal content of the silk strands was determined by carbon furnace atomic absorption spectrometry. Two procedures were employed: the silk sample (ca. 100 μg) was weighed and introduced into the furnace with a solids injector. The sample was ashed and then atomized at about 2500°C. The absorption signal was referred to a calibration curve obtained with pure aqueous standard solutions of the metal. Alternatively, a larger portion of the silk (ca. 200 mg) was dissolved in 5 ml of 46% (w/v) sulphuric acid and the solution was made up to 10.0 ml with water in a graduated flask. An aliquot (10 μl) of this solution was then introduced into the furnace, ashed, and atomized. The amount of metal in the silk was determined by adding known amounts of metal solution directly into the furnace along with the silk solution prior to ashing. Both the wet and dry ashing procedures have been found satisfactory [3] in previous work on the analysis of human hair. The results obtained are shown in Table 1.

Animal hair. Hairs from a domestic dog and cat were analysed by the dry ashing method used for the silk. The dog hair was analysed along its length (1-cm sections) for silicon. The cat hairs were analysed for silicon and copper. The results are summarized in Fig. 1.

Discussion

The aim of this work was to establish whether silk could be used as a standard material in hair analysis and whether the levels of metal in silk could be increased, by doping, to those normally found in human hair. The concentration of Cu, Ag, and Pb in silk could be modified; the results for Co and Ni were poor, probably because the levels were near the limit of detection of the method. Iron is present naturally in silk at the levels found normally in hair (ca. 20 p.p.m.) and modification was not necessary. The wet and dry ash results for Cu, Ag and Fe were in reasonable agreement with each other, but for Co and Ni agreement was poor. The results for copper showed that doping increased the level of the metal in silk and improved the uniformity of the distribution. For silver however, the level decreased on soaking and the relative standard deviation increased. It should be emphasised that the standard deviation obtained for the dry ash results reflects not only imprecision in the analytical method but also the uniformity

TABLE 1

Analysis of silk before and after doping

Metal	Level in hair (p.p.m.)	Sample	Soak soln. concn. (p.p.m.)	Method of analysis[a]	Found (p.p.m.)	s^b
Cu	<250	1	natural[c]	dry	17.2	8.4
		2	100	dry	47.7	11.4
		2	100	wet	49.4	12.4
		3	100	wet	38.3	12.8
		3	100	dry	34.4	4.5
Ag	<2	1	natural[c]	wet	2.9	0.6
		2	0.01	dry	1.4	0.6
		3	0.01	wet	1.9	0.8
Co	<0.6	1	natural[c]	wet	1.5	0.3
		2	0.005	dry	0.9	0.4
		3	0.005	dry	1.2	0.5
		4	0.005	wet	0.3	0.1
		5	0.005	wet	0.4	0.2
		6	0.01	dry	1.0	0.5
Ni	<10	1	natural[c]	dry	2.2	0.8
		2	0.001	dry	3.0	1.3
		3	0.001	wet	0.5	0.1
		4	0.001	wet	0.4	0.1
		5	0.005	dry	2.1	1.4
		6	0.005	wet	0.5	0.1
		7	0.005	wet	0.6	0.1
Fe	<100	1	natural[c]	dry	22.2	4.0
		2	natural[c]	wet	24.9	3.3
Pb	<100	1	natural[c]	dry	1.2	0.5
		2	10	dry	3.3	1.6
		3	100	dry	3.9	2.5

[a] For Cu, Ag, Co, Ni, Fe, the programme was: ash at 1100°C, 30 s; atomize at 2500°C. For Pb: ash at 750°C, 30 s; atomize at 2500°C.
[b] Standard deviation obtained from 10 replicate results.
[c] Analysis of the silk after ethanol wash and water rinse but without doping.

of the distribution of metal over the silk fibres. The precision of the wet results was poor because the concentrations in the solutions analysed were often near the limit of detection.

The one major physical difference between the silk used and hair was that the silk, from untreated woven cloth, consisted of many very fine fibres. Handling the silk in 1-cm lengths was very difficult; skilful and careful manipulation by the operator was necessary. After introduction into the carbon tube, the silk tended to unwind on heating; poor melting and ashing often occurred. This is reflected in the poor precision for the dry ash results.

Analytica Chimica Acta, 91 (1977) 411—415

Short Communication

LOSS OF TIN FROM AQUEOUS SOLUTIONS DURING STORAGE

ERNEST S. GLADNEY and WILLIAM E. GOODE

Los Alamos Scientific Laboratory, P.O. Box 1663, Los Alamos, New Mexico 87545 (U.S.A.)

(Received 1st November 1976)

The environmental chemistry of tin has received little attention, largely because of the lack of sufficiently sensitive analytical techniques for its measurement at ambient levels. The development of hydride generation methods coupled with atomic absorption [1, 2] has made the study of this element feasible; at least one laboratory has undertaken a comprehensive study of tin in the environment [3]. Since these procedures involve the measurement of tin in aqueous solutions, the potential loss of tin during storage must be investigated. Many metals of environmental interest have a limited shelf life in solution, e.g. cadmium [4, 5], lead [5, 6], mercury [7, 9], zinc [5, 9], chromium [10] and selenium [11]. Vijan and Chan [3] investigated the loss of tin from aqueous solution in glass and polyethylene containers and the use of hydrochloric and nitric acids as preservatives. Their observations of rapid tin loss under certain circumstances prompted this examination of the problem in greater depth; radioactive ^{113}Sn was used as a tracer rather than the hydride generation system [3].

Experimental

The containers examined were 500-ml bottles with screw caps. Six different types were investigated: borosilicate glass, linear polyethylene, Teflon, polyvinylchloride, polypropylene and polycarbonate. All adsorption experiments were conducted in bottles soaked in nitric acid for ca. 24 h and then rinsed with distilled water.

^{113}Sn ($t_{1/2}$ = 115 d) of high specific activity was used to prepare solutions in water, 0.05 M and 0.5 M sulfuric acid, 0.1 M and 1.0 M nitric acid, and 0.1 M and 1.0 M hydrochloric acid. Several containers were also investigated with aqueous 0.05% solutions of potassium dichromate, potassium permanganate and potassium persulfate; these chemicals are excellent preservatives for small quantities of mercury [12]. All solutions and containers were studied at levels of 1 ppb of tin. All samples were stored in the dark at room temperature. Counting aliquots (1 ml) were taken with plastic micropipets and transferred to 20-ml glass scintillation counting vials. These samples were taken daily during the first week and at weekly intervals thereafter for 60 d.

Since ^{113}Sn decays by electron capture to ^{113m}In ($t_{1/2}$ = 100 min) with only a weak γ-branch (1.8 %), the 393-keV γ-ray from the decay of ^{113m}In was used to monitor the tin concentration. Following the collection of counting aliquots, a 24-h delay was employed so that decay equilibrium could be re-established prior to counting. Thus no assumption need be made about the chemistry of radio-indium in the initial containers. The radiotracer was counted at the surface of a vertically mounted 55-cm^3 Ge(Li) detector (FWHM, 1.8 keV at 1332 keV) coupled with a linear amplifier and 4096-channel pulse-height analyzer. All data were reduced on line. For such a simple γ-ray spectrum as emitted by ^{113m}In, a NaI(Tl) detector would normally have been used; however, contamination of the ^{113}Sn with one or more additional activities precluded this approach.

Results and discussion

The fraction of the original tin retained in solution at the end of the storage period (60 d) is shown in Table 1 for aqueous and acid solutions at the 1 ppb tin level. The three acids are excellent preservatives at either 0.1 M or 1.0 M for up to 60 d in all the containers investigated. Loss rates of tin from aqueous solutions are shown in Fig. 1. The rates of loss in polyvinylchloride, teflon and polypropylene are similar to that in polyethylene; for simplicity they are not shown. Glass is an especially poor choice of container; there is an overnight loss of almost 80% of the tin. Most of the plastics exhibit less than 10% loss during the first week of storage.

The results of a limited experiment conducted at a higher tin concentration (1 ppm) are shown in Table 2; the rate of loss for aqueous solutions is plotted in Fig. 2. The rate curves for polyethylene and polycarbonate resemble that of glass; polypropylene and polyvinylchloride are similar to that shown for Teflon. The rapid, quantitative loss from aqueous solution observed at this higher tin concentration is similar to that observed for the 1 ppb solutions (Fig. 1). The behavior of the 0.1 M hydrochloric acid solutions is not understood. The expected reduction in loss from solution at higher elemental concentration was not observed for several solutions; the behavior in four of the plastic containers warrants further investigation.

Three popular preservatives in dilute solution for low concentrations of mercury [12] have also been investigated; as shown in Table 3 and Fig. 3, large quantities of tin were lost from each type of container in the presence of each of these oxidants.

Conclusions

Aqueous solutions of tin require an acid preservative at 0.1 M concentration if the solutions are to be stored. Acidification is effective in preventing the loss of tin for at least 60 d. If solutions are to be analyzed within 24 h after collection, several plastic containers may be used without preservation; however, glass must be avoided unless dilute acid is added. Some oxidizing agents did not prevent the loss of tin.

TABLE 1

Tin retention at the 1 ppb level in various solutions and containers

Solution	Container	% in solution at 60 d	Solution	Container	% in solution at 60 d
Water	G[a]	4 ± 4	1.0 M H_2SO_4	G	103 ± 5
	PE[b]	40 ± 3		PE	103 ± 5
	T[c]	38 ± 3		T	104 ± 5
	PP[d]	55 ± 4		PP	109 ± 5
	PVC[e]	66 ± 4		PVC	97 ± 5
	PC[f]	17 ± 6		PC	95 ± 5
0.1 M H_2SO_4	G	98 ± 5	1.0 M HNO_3	G	98 ± 5
	PE	100 ± 5		PE	102 ± 5
	T	98 ± 5		T	95 ± 5
	PP	107 ± 5		PP	94 ± 5
	PVC	101 ± 5		PVC	99 ± 5
	PC	102 ± 5		PC	102 ± 5
0.1 M HNO_3	G	100 ± 5	1.0 M HCl	G	102 ± 5
	PE	98 ± 5		PE	101 ± 5
	T	91 ± 5		T	100 ± 5
	PP	96 ± 5		PP	100 ± 5
	PVC	100 ± 5		PVC	103 ± 5
	PC	98 ± 5		PC	104 ± 5
0.1 M HCl	G	101 ± 5			
	PE	98 ± 5			
	T	91 ± 5			
	PP	96 ± 5			
	PVC	96 ± 5			
	PC	94 ± 5			

[a]Glass. [b]Polyethylene. [c]Teflon. [d]Polypropylene. [e]Polyvinylchloride. [f]Polycarbonate.

TABLE 2

Tin retention at the 1 ppm level in two solutions and 6 containers

Solution	Container	% in solution at 60 d	Solution	Container	% in solution at 60 d
Water	G	1 ± 1	0.1 M HCl	G	95 ± 5
	PE	1 ± 1		PE	64 ± 4
	T	2 ± 2		T	79 ± 4
	PP	3 ± 3		PP	76 ± 4
	PVC	2 ± 2		PVC	44 ± 3
	PC	1 ± 1		PC	96 ± 5

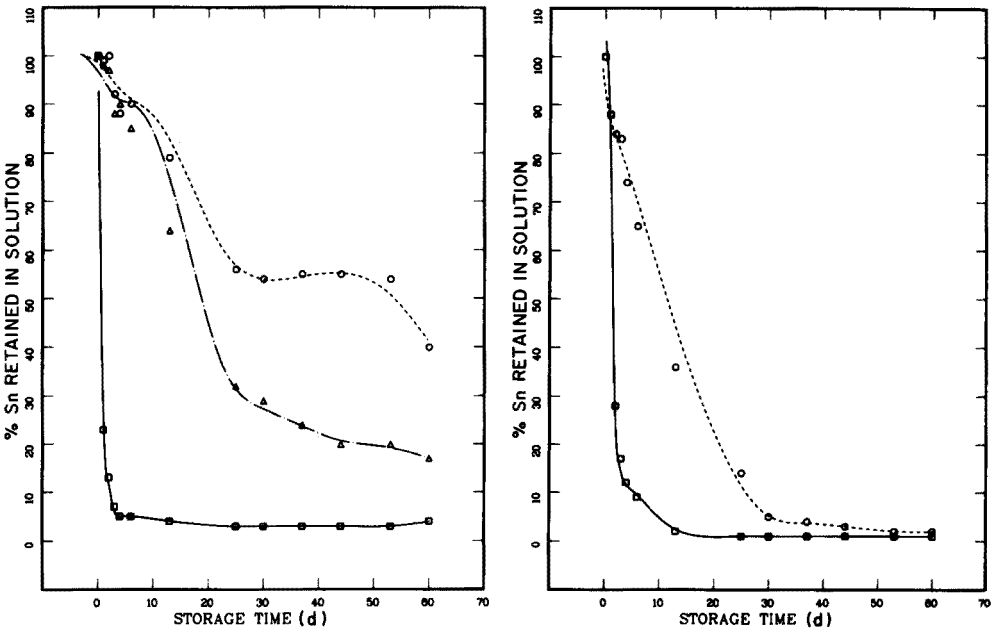

Fig. 1. Rate of loss of tin from 1 ppb solutions stored in glass (□), polyethylene (○) and polycarbonate (△) containers.

Fig. 2. Rate of loss of tin from 1 ppm solutions stored in glass (□) and Teflon (○) containers.

TABLE 3

Effect of common preservatives on tin retention at the 1 ppb level

Preservative	Container	% in solution at 60 d	Preservative	Container	% in solution at 60 d
$K_2Cr_2O_7$	G	28 ± 5	$KMnO_4$	G	52 ± 5
	PE	18 ± 3		PE	77 ± 4
	T	9 ± 4			
	PP	56 ± 5	$K_2S_2O_8$	G	4 ± 4
	PVC	47 ± 5		PE	4 ± 4

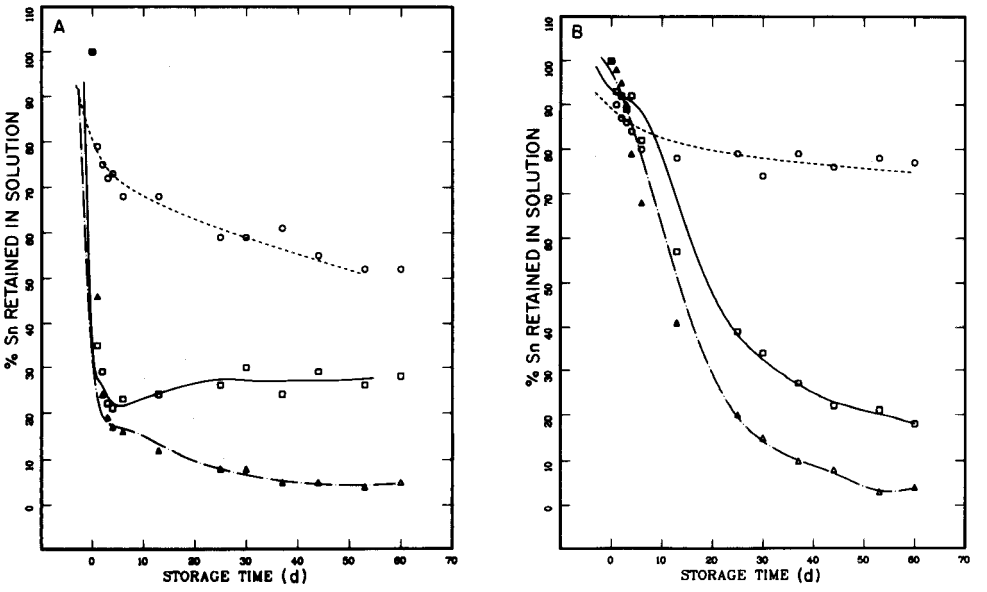

Fig. 3. Rate of loss of tin from 1 ppb solutions stored in containers utilizing dichromate (□), permanganate (○) and persulfate (△) as preservatives. A. Glass. B. Polyethylene.

We thank Gloria Martinez and Dianne Baldonado for assistance with the counting and appreciate Dr. Vijan's willingness to make copies of his slides available. This work was performed under the auspices of the U.S. Energy Research and Development Administration.

REFERENCES

1 K. C. Thompson and D. R. Thomerson, Analyst, 99 (1974) 595.
2 F. J. Schmidt, J. L. Royer and S. M. Muir, Anal. Lett., 8 (1975) 123.
3 P. N. Vijan and C. Y. Chan, A Semi-Automated Method for the Determination of Trace Amounts of Tin, presented at Pittsburgh Conference on Analytical Chemistry and Applied Spectroscopy, Cleveland, Ohio, March, 1976.
4 W. G. King, J. M. Rodriguez and C. M. Wai, Anal. Chem., 46 (1974)771.
5 A. W. Stuempler, Anal. Chem., 45 (1973) 2251.
6 H. J. Issaq and W. L. Zielinski, Anal. Chem., 46 (1974) 1328.
7 P. Benes and I. Rajman, Collect. Czech. Chem. Commun., 34 (1969) 1375.
8 R. V. Coyne and J. A. Collins, Anal. Chem., 44 (1972) 1093.
9 Y. Dokiya, H. Ashikawa, S. Yamazaki and K. Fuwa, Spectrosc. Lett., 7 (1974) 551.
10 A. D. Shendrikar and P. W. West, Anal. Chim. Acta, 72 (1974) 91.
11 A. D. Shendrikar and P. W. West, Anal. Chim. Acta, 74 (1975) 189.
12 P. Avotins and E. A. Jenne, J. Environ. Qual., 4 (1975) 515.

Analytica Chimica Acta, 91 (1977) 417—420

Short Communication

DETERMINATION OF CARBON IN ORGANIC-CONTAINING MATERIALS WITH A LECO IR-12 CARBON DETERMINATOR

B. A. SWINEHART

Research and Development Laboratory, Corning Glass Works, Sullivan Park, Corning, New York 14830 (U.S.A.)

(Received 16th December 1976)

The determination of carbon in organic substances is normally done with commercial CHN analyzers, but certain sample characteristics may occasionally make it impractical to use such instrumentation. An example occurred during development of an automotive catalyst support system for emissions control [1] when it became necessary to determine the organic extrusion aids. In this system, the inorganic components — comprising approximately 97% of the total batch — were blended with methyl cellulose and diglycol stearate. Attempts were made to use a CHN analyzer for quality control of the organic components, but the combination of discrete particles and small sample size resulted in an unacceptably poor precision. Consequently, a new procedure with a Leco IR-12 Automatic Carbon Determinator (Leco, St. Joseph, Michigan) was developed.

This communication summarizes the procedural modifications that permit the Leco equipment to be used on relatively non-volatile organic compounds.

Principle of method. The sample is loaded into a ceramic crucible along with a metal combustion accelerator (usually copper or iron) and placed in the quartz combustion chamber of the induction furnace. The sample is ignited in an oxygen atmosphere, and the carbon is converted to a mixture of carbon monoxide and carbon dioxide. This gas mixture is dried, passed through a heated platinum catalyst to convert carbon monoxide to carbon dioxide and transported to the detector cell for measurement. The reaction zone is confined primarily to the heated crucible; thus any carbon-containing material that escapes from the crucible and collects on the quartz tube may not be completely burned. This is generally not a problem with metals and refractories because the carbon is in a non-volatile form such as a carbide or carbonate, but with organic materials, pyrolysis rather than complete combustion may occur. Thus the determination of carbon in organic materials with the Leco Determinator will depend on the sample being confined to the crucible until combustion is complete.

Methods of achieving complete combustion

Position of sample in crucible. For the analysis of metals, the combustion accelerator should be layered evenly over the bottom of the crucible and the sample placed on top of this layer. With organic-containing materials this procedure almost always results in incomplete recovery of the carbon. In an induction furnace the heat is generated in the metal accelerator and transferred to the sample. If the sample is on top, the pyrolysis products are free to escape directly into the oxygen atmosphere. If, however, the sample is placed on the bottom and covered with accelerator, the pyrolysis products must diffuse through a layer of molten metal. Consequently, this was the first procedural modification adopted, and in some cases it is the only change needed to achieve quantitative recovery of carbon. For example, primary standard potassium hydrogenphthalate (47.0% C) was successfully analyzed (46.9% C found) simply by covering with iron chip accelerator.

Sample considerations. Sample size, degree of subdivision, and extent of dilution must be considered. The infrared detector cell in the IR-12 is capable of measuring up to about 90 mg of carbon dioxide, which corresponds to about 25 mg of carbon in the sample. However, to avoid saturation of the detector and to minimize the possibility of producing explosive mixtures of oxygen and unknown pyrolysis fragments a sample containing not more than 5 mg of carbon should be taken.

Subdividing the sample helps to avoid localized eruptions that often occur when single large pieces of sample are ignited. Sample dilution is another effective way of controlling the reaction. Localized concentrations of carbon-containing materials can be avoided simply by mixing the sample with a non-carbon-containing substance. Granular copper accelerator or powdered silica are convenient and effective diluents.

When metals are analyzed with the Leco IR-12 an open crucible is usually employed, although a crucible cover is supplied for certain applications. The cover is a doughnut-shaped ceramic disc that covers about three fourths of the crucible; it deflects the oxygen stream from the supply jet directed onto the crucible and provides a barrier that slows down the escape of reaction products from the melt. Both of these functions are often desirable during analysis of organic substances.

Selected applications

Automotive catalyst support system. The development of an automotive catalyst support system required the determination of the total organic content of a mixture consisting of approximately 97% inorganic materials, such as clay, talc, and alumina, and 3% organic extrusion aids (methyl cellulose and diglycol stearate).

In testing the feasibility of analyzing organic materials with the Leco equipment, it was first demonstrated that essentially complete recovery of the carbon (46.9% found) in primary standard-grade potassium hydrogenphthalate could be achieved. Methyl cellulose, however, is not a standard material. The carbon content of the commercial product varies with the number of

methoxyl groups substituted on the glucose units. The degree of substitution for Methocel MC (Dow Chemical Company) may vary from 1.64 to 1.92 and result in a carbon content ranging from 50.1% to 50.9%. A given lot of methyl cellulose was found to contain 3.6% water and, consequently, had an expected carbon content of from 48.3% to 49.1%. The value of 48.8% found was in excellent agreement. Finally, after a synthetic standard of clay, talc, alumina, 3% methyl cellulose and 0.5% diglycol stearate having a calculated carbon content of 1.76% had been analyzed and found to contain 1.74% carbon, it was concluded that the Leco IR-12 could be successfully applied to automotive catalyst support formulations.

The precision of the method was estimated by repetitively analyzing a plant sample batched to contain a total of 2.41% carbon. Table 1 indicates a 95% confidence interval of $\pm$ 0.04_5% carbon for duplicate analyses. The technique described was routinely used to ensure proper batch formulation and to evaluate mixing procedures for dry blends of the batch ingredients.

Miscellaneous applications. Extension of the method to other organic-containing samples was examined. For example, it takes less than 5 min to determine the loading of column packings used in gas—liquid chromatography. Results on several stationary phases frequently used in this laboratory are presented in Table 2. The examples were selected to illustrate the wide range of carbon contents that can be handled and to demonstrate versatility with respect to type of polymer (e.g., silicone, polyalkylene oxide, hydrocarbon and polyester).

The feasibility of determining components separated by thin-layer chromatography (t.l.c.) was also demonstrated. Thus, a mixture of 66 μg of itaconic acid and 60 μg citric acid was separated on a t.l.c. plate (silica gel G on aluminum foil) with the butyl acetate—acetic acid—water system [2]. After separation the spots were located on a test strip by a spray containing 0.2% bromophenol blue in ethanol. The plate to be analyzed was not sprayed but the positions corresponding to those on the test plate were cut out and analyzed for % C. The calculated recoveries (64 μg of itaconic acid and 68 μg of citric acid) were considered acceptable. The major inconvenience in this application is the restricted number of acceptable commercial plates. Thus, it is not possible to use plastic-backed plates and the coating itself must be

TABLE 1

Estimate of precision for determination of % carbon in automotive catalyst support formulation

Carbon content, % batched	2.41
Number of determinations	16
Range, % C	2.38—2.49
Mean, % C	2.45
Standard deviation	0.030
Variance	0.00093
95% confidence interval, duplicates	0.04_5

TABLE 2

Use of % carbon to establish loading of stationary phases on gas-liquid chromatography packings

Material	% C		% Loading calculated
	Expected	Found	
Silicone Gum Rubber SE-30	32.4	33.0	—
Carbowax 20M	54.5	53.5	—
0.5% SE-30 on glass beads	0.16	0.19	0.59
10% SE-30 on Gas Chrom Z	3.24	3.30	10.2
10% Carbowax 20M on Chromosorb W	5.45	5.60	10.3
9.1% Apiezon L on Hylon P	7.80	8.05	9.4
12% HI-EFF 1B on Gas Chrom Z	6.12	6.06	11.9

free of organic binders and fluorescent indicators. In addition, it is essential to run carbon blanks on the developed plate to ensure removal of high-boiling solvents.

REFERENCES

1 I. M. Lachman and R. M. Lewis, U. S. Patent 3885977 (1975).
2 G. Zweig and J. Sherma (Eds.), Handbook of Chromatography, Vol. I, CRC Press, Cleveland, Ohio, 1972, p.470.

Analytica Chimica Acta, 91 (1977) 421—423

Short Communication

PREPARATION OF STANDARD GERMANIUM SOLUTION

SHIGERU SHIMOMURA, HIROMU SAKURAI, HIDEYOSHI MORITA and YOSHIKI MINO

Faculty of Pharmaceutical Sciences, University of Tokushima, Tokushima, 770 (Japan)

MASATOSHI INOUE

Osaka Pharmaceutical College, Matsubara-shi, Osaka, 580 (Japan)

(Received 15th November 1976)

Standard germanium solutions can be prepared from germanium dioxide or germanium metal. In papers [1—7] dealing with atomic absorption spectrometry and other methods for germanium, germanium dioxide has generally been used, probably because of its high stability in air. Germanium has not been used, because the metal adsorbs carbon dioxide and water from air, forming a surface film of germanium oxides with liberation of hydrogen when this metal is heated [8].

Germanium dioxide can be dissolved in fused alkali [1] or in dilute alkaline solution [2—7] for the preparation of standard solutions. However, it was found here that the commercially available germanium dioxide could not be dissolved completely in 1 M sodium hydroxide.

Polymorphism in germanium dioxide is well known [8]. The hexagonal modification — often called the soluble form — dissolves in cold water (4 g l^{-1}); the tetragonal (insoluble) form, dissolves only in fused alkali. Presumably, the latter insoluble form affects the preparation of standard solutions if alkali fusion is not used.

This communication reports a simple procedure for the preparation of standard germanium solutions, without foreign materials, from commercially available germanium dioxide, based on the chemical properties of the polymorphic germanium dioxide.

Experimental

Equipment and chemicals. A Rigakudenki Rotaflex x-ray diffractometer (RU-200) equipped with both graphite bent-monochromator and scintillation counter was used. The working conditions were: x-ray source Cu-Kα; voltage 40 kV; current 150 mA; count range 80,000 cps or 2,000 cps; angle range $2\theta = 4°$ (interplanar spacing, $d = 22.09$ Å)—$60°$ ($d = 1.542$ Å). The insoluble form of germanium dioxide was determined by the method of Alexander and Klug [9] from counts at the strongest angle, 28.6°. Centrifugation was done at 3,000 r.p.m. (5 min).

Germanium dioxide was obtained from Wako Pure Chemical Industries (Japan) and Merck (Germany). All other reagents were of special grade.

Results and discussion

The x-ray diffraction patterns of germanium dioxide are shown in Fig. 1. The samples are a commercial product (A), the component insoluble in 1 M sodium hydroxide (B), and the component soluble in water (C). The x-ray diffraction pattern of (A) can be superimposed on the joint diffraction patterns of (B) and (C). The patterns of (B) and (C) correspond to the insoluble and soluble forms of germanium dioxide, respectively (American Society for Testing and Materials Card 9-379, tetragonal, and Card 4-0497, hexagonal). The strong peak of the insoluble form at 28.6° could not be detected in sample (C), which was obtained by the procedure described below, even when (C) was measured at higher sensitivity.

The germanium dioxides obtained from two companies were analyzed by the x-ray powder diffraction method. A few percent of the insoluble form was found in all lots investigated; one lot contained 2.8% of the insoluble form. It is, therefore, very difficult to dissolve completely the commercial germanium dioxide in water or in dilute alkaline solution without alkali fusion.

These observations enabled a simple procedure to be developed for the preparation of standard germanium solutions from commercial germanium dioxide, in which the soluble form was isolated.

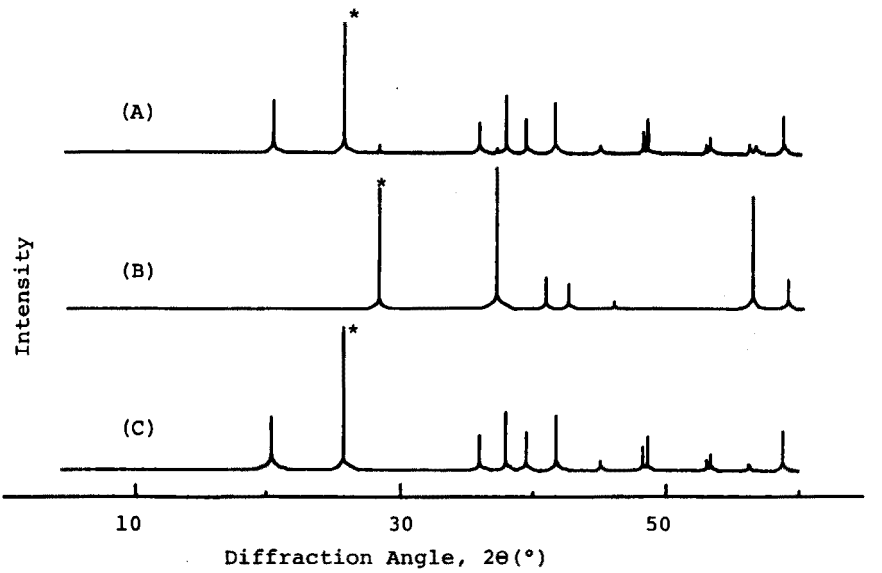

Fig. 1. X-ray diffraction patterns of germanium dioxide. (A) Commercial product. (B) Component which could not be dissolved in 1 M sodium hydroxide, insoluble form. (C) Component dissolved in water, soluble form. The strongest lines (asterisked) are shown as half of the original peak height.

Recommended procedure. Dissolve ca. 1 g of the commercial product as much as possible in about 100 ml of boiling deionized water. Remove the insoluble fraction by centrifugation, and evaporate the supernatant liquid to dryness to constant weight. This isolated powder is the soluble form. Prepare a 500-p.p.m. standard germanium solution by dissolving 0.360 g of the isolated soluble form of germanium dioxide in an appropriate amount of hot deionized water, and diluting the solution to 500 ml with deionized water after cooling.

Such standard solutions, without any additions, are stable for periods exceeding a year in a stoppered glass flask. Consequently, this solution is suitable as a stock solution, especially in studies on interference phenomena.

REFERENCES

1 R. Jakubiec and D. F. Boltz, Anal. Chem., 41 (1969) 78.
2 D. J. Johnson, T. S. West and R. M. Dagnall, Anal. Chim. Acta, 67 (1973) 79.
3 E. N. Pollock, At. Absorpt. Newsl., 10 (1971) 77.
4 R. M. Dagnall, G. F. Kirkbright, T. S. West and R. Wood, Analyst, 95 (1970) 425.
5 M. Yanagisawa, M. Suzuki and T. Takeuchi, Anal. Chim. Acta, 46 (1969) 152.
6 R. M. Dagnall, K. C. Thompson and T. S. West, Anal. Chim. Acta, 41 (1968) 551.
7 R. E. Popham and W. G. Schrenk, Spectrochim. Acta, Part B, 23 (1968) 543.
8 R. G. Rochow, in J. C. Bailer et al. (Eds.), Comprehensive Inorganic Chemistry, Vol. 2, Pergamon Press, Oxford, 1973, pp. 8, 27.
9 L. E. Alexander and H. P. Klug, X-Ray Diffraction Procedures (2nd edn.), J. Wiley, New York, 1974, p. 532.

Analytica Chimica Acta, 91 (1977) 425—430

Book Reviews

C. F. Simpson (Ed.), *Practical High Performance Liquid Chromatography*, Heyden, London, 1976, x + 315 pp., price U.S. $18.50, £9.30.

The use of high performance liquid chromatography (h.p.l.c.) has expanded rapidly in the past few years. This book contains contributions from many of the best known names in the field. It includes expanded versions of lectures given at the Chemical Society's School on h.p.l.c. held at Sussex University in 1975, and covers the theoretical background, techniques and practical use of the method. With the exception of a chapter on bioaffinity chromatography, most of the material has been published previously in books on liquid chromatography.

The book will be of interest both to practising liquid chromatographers and to newcomers in the field, although the latter would be well advised to avoid initially the theoretical chapters and concentrate on the practical section. One particularly useful chapter covers a series of simple experiments designed to highlight the factors which control liquid chromatographic separations. This chapter should help new chromatographers to avoid many of the pitfalls found by his predecessors.

Each chapter is well referenced, although these cannot be completely up-to-date, and the editor has managed to avoid too much duplication or contradiction between the various contributors. Altogether, the book is well presented, and it is a useful addition to the literature on liquid chromatography.

I. Jane

I. M. Kolthoff and P. J. Elving (Eds.), *Treatise on Analytical Chemistry, Part II, Volume 15 — Organic Analysis II, Functional Groups*, J. Wiley, New York, 1976, xxi + 409 pp., price U.S. $34.95, £20.00.

This volume upholds the general standards set by earlier parts of this Treatise, which aims to provide a complete and definitive source of information designed to stimulate fundamental research. This volume follows closely (in terms of subject matter, but not in time) on the heels of volume 13, which presented, in 1966, the hard core of the mainstream functional groups. This volume deals with some of the less common groups; the principal contributors are J. G. Baldinus and R. F. Muraca.

The first chapter, by Baldinus, deals with sulphur-based functions other than divalent functions (thiols, sulphides, disulphides, polysulphides and thiophenes were treated in volume 13 by J. H. Karchmer). This is the best chapter in the book, presenting in 159 pages some 582 references (more,

because author's afterthoughts, giving rise to the 152, 152a, 152b type of system, have been allowed to stand by the editors). The coverage is up to 1975. The two least satisfactory chapters follow — an odd little chapter by Muraca (35 references, 15 pp.) on the detection of nitrogen in samples, and a chapter on amines (193 references, 72 pp.) by Critchfield and Ruch, which could have been (and probably was) written in 1965. The final three chapters, all by Muraca, deal with diazonium groups (320 references, 95 pp.), diazo groups (111 references, 37 pp.), and azo groups (485 references, 116 pp.). Although there is the odd reference to work published in 1970, these chapters are based solidly on the literature of the mid-sixties.

There is an adequate index (not so carefully proof-read as the rest of the book, although there is a reference on p. 493 of the main text to work published in 1383). At present prices this book is good value, and dedicated Functional Groupers (Siggia's term!) will want to acquire it, if only for the comprehensive coverage it gives. But after waiting for so long, it is disappointing that the coverage is not more up-to-date.

D. M. W. Anderson

T. S. Ma and V. Horak, *Microscale Manipulations in Chemistry*, J. Wiley, New York, 1976, pp. xiii + 488, price U.S. $33, £19.40.

Microchemistry, although mainly practised by analytical and organic chemists, is wide ranging, being concerned with the principles and methods of using minimal amounts of material to obtain the required chemical information. It is therefore not surprising that many omissions can be noted, or that a reviewer should disagree with the balance of the material included.

Techniques are described and well illustrated for the manipulation of gaseous, solid, liquid and solution samples, and for sample collection, purification, transfer and storage. The book is not concerned primarily with microanalysis although many such determinations are referred to and/or referenced. Much of the material on chromatographic methods, e.g. an elementary account of the selection of solvents for t.l.c., could have been omitted, as such information is readily available; the space freed could then have been devoted to expansion of the sections on micro electrochemical and spectroscopic methods. The 18 pages devoted to a list of captions to illustrations and addresses for supply houses could be put to better use. An index of 44 pages is hard to justify, and 12 blank pages excluding end leaves indicates a lack of production control.

The collection of much interesting and diverse material into a single volume will be helpful to practising chemists and to students. The main criticism concerns the gross waste of expensive, potentially useful space.

D. Thorburn Burns

T. S. West (Ed.), *International Review of Science, Physical Chemistry Series 2, Vol. 13, Analytical Chemistry, Part 2*, Butterworths, London, 1976, 271 pp., price £13.45.

This volume contains seven reviews on widely diverse topics in analytical chemistry. In general, the reviews cover the period 1969—73, and the authors have had varying degrees of success in dealing with the problems of providing enough background information for the subsequent developments to make sense to the general reader, and then selecting from the massive recent literature only those references which report significant work. The balance is excellent in the chapters devoted to isotope dilution analysis (N. Saito), electron probe microanalysis (H. Malissa, Jr.) and infrared spectroscopy (D. M. W. Anderson). The review of ion-selective electrodes is less successful in giving a true picture of the current state-of-the-art, as must any review which attempts to deal with 373 references in the space of 15 pages.

The review of complexiметry (R. Přibil) is useful, for much information — not available compactly elsewhere — is given on complexones other than EDTA. The chapter also serves as a reminder that some chemistry can still be involved in analysis. This review and the review on electrophoresis (J. O. N. Hinckley) — which is marred by some atrocious terminology — tend to be quite general rather than concentrated on recent events. The review on ultramicroanalysis (I. L. Marr and G. Tolg) is good, but rather long, perhaps because of the old problem of defining where microanalysis ends and trace analysis starts.

Reviews are essential for an appreciation of what is happening over the wide field of analytical chemistry; the topics treated here have been selected well. The price of this volume is very reasonable. Perhaps the sole major criticism is the time lag between the most up-to-date references cited and the publication of the book.

A. M. G. Macdonald

Zygmunt Marczenko, *Spectrophotometric Determination of Elements*, Ellis Horwood—Halsted Press—J. Wiley, London, 1976, xi + 643 pp., price £19.50, U.S. $42.90.

This book can perhaps best be described as the poor man's Sandell. The layout of the text is proclaimedly similar to that of Sandell, and it is, therefore, with Sandell that it must be compared. The new book has advantages: obviously it is far more up-to-date, it gives extensive coverage to Russian and East European literature, and it deals with non-metals as well as metals. It also has disadvantages: it is less authoritative, less detailed, and much less satisfactory in providing warnings of pitfalls for the unwary analyst. The disadvantages are, of course, largely inevitable given the bulk of new spectro-

photometric methods published in the period 1958—1974 (the date of the latest reference in this book). However, it is disappointing to see just how much of all this 17 years of research effort has been wasted. The traditional methods of spectrophotometric analysis with the traditional reagents remain virtually intact. Details of a new method are appended here and there, but overall the recommended procedures are similar to those given by Sandell (1959) or Charlot (1962). Amongst all the original literature, there must be, somewhere, better first-choice methods than thiocyanate for iron and uranium, dithiol for molybdenum, dithizone for lead, mercury, silver and copper (!), etc. Given the essential cheapness of spectrophotometric methods — the best of them require no more preparation of samples than much more instrumentally sophisticated methods — it is a distinct disappointment that a really new book on spectrophotometric analysis must still be awaited by the analytical world.

Harold F. Walton (Ed.), *Ion-Exchange Chromatography*, Dowden, Hutchinson and Ross, Stroudsburg, Pa. (distributed by Halsted Press — J. Wiley), 1976, xviii + 440 pp., price £18.65, U.S. $33.30.

This excellently produced book contains the full texts of 48 original papers ranging from Samuelson's classic work on ion-exchange chromatography in 1939 to reports on ligand-exchange chromatography in 1973. It is intended to provide a survey of notable landmarks in the development of the technique. Professor Walton has selected the papers well, providing abbreviated translations into English where necessary, and his linking narrative leads the reader gently from one critical advance to the next. The papers are divided under twelve headings, covering theory and the most important areas of application to inorganic and organic analysis.

There are two main reasons for welcoming this book, which is one of a series dealing with different areas of analytical chemistry. First, the really important personal contributions to any area of science tend nowadays to vanish into the glut of material which *should* be read or taught or learned, and these books serve as reminders that the men with ideas remain the most vital factor in scientific advance. Secondly, the original literature is so large that really skilled guides are needed to bring meaning to its study. This type of book serves as a useful complement to the textbooks available on ion-exchange chromatography; and perhaps libraries which cannot afford the original journals will be able to afford these selected readings. One wonders, rather sadly, how books of this nature will appear in 30—40 years time if microfiche publication of original manuscripts becomes widespread.

Ivor L. Simmons and Galen W. Ewing (Eds.), *Progress in Analytical Chemistry, Vol. 8*, Plenum Press, New York, 1976, viii + 336 pp., price U.S. $18.00.

This volume — the Proceedings of the Eastern Analytical Symposium held in New York in October, 1975 — contains only 14 original papers, reproduced from typescripts. These form rather a mixed bag; five deal with applications of a.a.s., four with aspects of gas chromatography, and four with assorted spectrometric techniques. There is also a *cri de coeur* from an environmental chemist for analytical help. It is difficult to justify the cost of the book, or to suggest any good reason for buying it.

J. F. Combs, R. W. Sims and F. Martin (Eds.), *Analysis Instrumentation, Vol. 14*, Instrument Society of America, Pittsburg (distributed by J. Wiley), 1976, 125 pp., price U.S. $16.50, £9.75.

This paperback contains 20 of the 26 papers read at the 22nd ISA Symposium held in San Francisco in May, 1976. The papers deal with instrumentation for monitoring SO_2, NO, NO_2, H_2S and HCl in air, with analyzers for waste waters and process streams, with combustibles analyzers, and with analytical microprocessor systems. A careful scrutiny of several of these papers should be mandatory for those who retain undiminished faith in the efficacy and reliability of black boxes in practical situations. It is of interest that not only chemists have problems with microprocessors — some engineers are also feeling obsolescent.

K. Macek, I. M. Hals, J. Kopecký, V. Schwarz, J. Gasparič and J. Churáček (Eds.), *Bibliography of Paper and Thin-Layer Chromatography, 1970—1973, and Survey of Applications*, Elsevier, Amsterdam, 1976, xviii + 744 pp., price DFl 200, U.S. $76.95.

This book forms Supplementary Volume No. 6 of the Journal of Chromatography; the literature coverage presented follows directly on that for 1966—1969, published in 1972 as Supplementary Volume No. 2. Earlier bibliographies published by Macek and his co-editors now cover the literature continuously back to 1944. All practising chromatographers must be deeply grateful to Macek and the staunch band of fellow Czechoslovaks who have assisted him in these successive enterprises for so long.

The present volume covers the literature to the middle of 1973 and lists 5601 references. These simply give the details of authors' names, title of the paper, and the journal reference (with, in some cases, the appropriate Chemical Abstracts reference). The success of this book lies in the simple but com-

prehensive way in which the references are classified subject-wise, and in the amount of cross-referencing provided. Even the indexing supplied is meticulous in detail: the Author Index and Subject Index occupy 84 pp. and 196 pp., respectively.

This is a publication of high quality. The main points at issue — price and outdatedness — have been raised recently in connection with companion volumes. The price places these books beyond the pocket of private individuals; presumably the sales to libraries are still adequate to make the publication of these bibliographies a worthwhile financial proposition. Would more than twice as many copies be sold if the price were halved? For a book that appears to be destined to heavy handling in libraries the thin paper cover is inadequate. More serious scientifically, however, is the time-lag reflected between the publication date (May, 1976) and the most recent reference cited (mid-1973). Three years out-of-date is much too long. The publication, annually, of smaller books priced to sell more widely and containing material published not more than 12—24 months previously is something that the authors and publishers should strive to achieve.

J. Korýta, J. Dvořák and V. Boháčková, *Lehrbuch der Elekrochemie*, Springer-Verlag, Wien, 1976, xv + 348 pp., price DM 145,--.

This book is based on the second edition of the Czechoslovakian text which appeared in 1975. It is intended to provide a base for studies of specialized monographs and the original literature, but there are neither practical sections nor discussions of applications.

The five chapters deal with equilibria in electrolytes, transport processes, equilibria in heterogeneous electrochemical systems, membranes and bioelectrochemistry, and processes in heterogeneous systems. Compared with the first edition, the treatment of equilibria in homogeneous and heterogeneous systems has been condensed, the discussion of transport processes has been revised, and a new chapter on membrane and bio processes has been introduced. The general treatment is clear and good, and the book is very well produced. An English translation of the first edition appeared in 1970; an English translation of this extensively revised edition would be very welcome.

ANALYTICA CHIMICA ACTA, VOL. 91 (1977)

AUTHOR INDEX

ANALYTICA CHIMICA ACTA, VOL. 91 (1977)

SUBJECT INDEX

OURNAL OF CHROMATOGRAPHY
3IOMEDICAL APPLICATIONS

n international journal devoted to new developments and advances in omedical applications of chromatography and electrophoresis.

Aims and Scope

The journal will publish papers dealing with the following aspects:
- developments in, and applications of chromatographic and electrophoretic techniques related to clinical diagnosis (including the publication of normal values).
- screening and profiling procedures with special reference to metabolic disorders.
- results from basic medical research with direct consequences in clinical practice.
- combinations of chromatographic and electrophoretic methods with other physico-chemical techniques such as mass spectrometry.

Furthermore, the journal will encourage contributions that give new information concerning the composition of tissues and body fluids. Manuscripts dealing with drug and metabolic levels, with special reference to blood, urine and other body fluids, particularly when related to therapy, are welcome. Also acceptable are papers describing new chromatographic and electrophoretic techniques devoted to clinical toxicology, and the determination of toxic levels of commonly used pharmaceuticals, but excluding toxicological studies per se. Chromatographic and electrophoretic studies on environmental hazards will be considered for publication, providing they are directly related to clinical analysis.

Types of Contributions

Original papers
Short communications
Review articles (following a preliminary agreement with the editor).
Information regarding new instrumentation, chromatographic and electrophoretic materials and accessories, forthcoming events, etc., which will be published in the News Section.
Reviews of books within the scope of the journal.

Publication Schedule

The JOURNAL OF CHROMATOGRAPHY, BIOMEDICAL APPLICATIONS will be published bimonthly, six issues per year constituting one volume. The first issue is scheduled to appear in January 1977.

Subscription Information

The journal will form an integral part of the Journal of Chromatography. However, it can be subscribed to separately. The subscription price for Volume 1 is US $47.75/Dfl. 124.00. including postage.

Journals are automatically sent by air to the U.S.A. and Canada at no extra cost, and to Japan, Australia and New Zealand with a small additional postal charge.

ELSEVIER SCIENTIFIC PUBLISHING COMPANY
P.O. Box 211, Amsterdam, The Netherlands,

(continued from inside page of cover)

(continued from page 4 of cover)

Short Communications

PRINTED IN THE NETHERLANDS

VOL. 91 No. 2 ANALYTICA CHIMICA ACTA JULY 1977

CONTENTS

(continued on inside page of the cover)